EPA-450/4-86-016b

Evaluation of Short-Term Long-Range Transport Models
Volume II. Appendices A through E

by

A. J. Policastro, M. Wastag, L. Coke
Argonne National Laboratory
Argonne, Illinois 60439

R. A. Carhart
University of Illinois
Chicago, Illinois 60680

W. E. Dunn
University of Illinois
Urbana, Illinois 61801

IAG No. DW 89930807

EPA Project Officer: Norman C. Possiel

Prepared for

U.S. ENVIRONMENTAL PROTECTION AGENCY
Office of Air and Radiation
Office of Air Quality Planning and Standards
Source Receptor Analysis Branch
Research Triangle Park, NC 27711

October 1986

U.S. Environmental Protection Agency
Region 5, Library (PPL-16)
230 S. Dearborn Street, Room 1670
Chicago, IL 60604

Disclaimer

This report has been reviewed by The Office of Air Quality Planning and Standards, U. S. Environmental Protection Agency, and has been approved for publication. Mention of trade names or commercial products is not intended to constitute endorsement or recommendation for use.

TABLE OF CONTENTS

VOLUME II - APPENDICES

TABLE OF CONTENTS iii
LIST OF FIGURES vii
LIST OF TABLES. xxiii

APPENDIX A APCA PAPER/HARTFORD MEETING/OCTOBER 1983. . . . . A-1

APPENDIX B CHOICE OF MODEL-SPECIFIC INPUTS

INTRODUCTION. B-1

PART I: DATA BASE SELECTION AND INPUT PARAMETERS FOR THE MTDDIS MODEL B-1

Oklahoma Tracer Study. B-1
Savannah River Plant Krypton-85 Study. B-2

Source Information B-2
Meteorological Information B-2
Spatial and Temporal Grids B-3
Model-Specific Options B-5

PART II: DATA BASE SELECTION AND INPUT PARAMETERS FOR THE ARRPA MODEL. B-5

Oklahoma Tracer Study. B-5

Source Information B-5
Meteorological Information B-6
Spatial and Temporal Grids B-6
Model-Specific Options B-6

Savannah River Plant Krypton-85 Study. B-7

PART III: DESCRIPTION OF MESOPAC CHANGES AND OPTIONS. B-7

PART IV: DATA BASE SELECTION AND INPUT PARAMETERS FOR THE MESOPAC II WIND FIELD MODEL B-9

Description of MESOPAC II Options. B-10

PART V: DATA BASE SELECTION AND INPUT PARAMETERS FOR THE MESOPUFF, MESOPLUME, MSPUFF, AND MESOPUFF II MODELS . . B-13

Introduction B-13
Computational Considerations B-13
Decision Points. B-14

PART VI: DESCRIPTION OF RTM-II CHANGES AND OPTIONS B-16

TABLE OF CONTENTS (CONTINUED)

PART VII: DESCRIPTION OF RADM CHANGES AND OPTIONS B-17

APPENDIX C DESCRIPTION OF CODE MODIFICATIONS REQUIRED FOR THE EIGHT MODELS

INTRODUCTION. C-1

C.1. DESCRIPTION OF MTDDIS MODIFICATIONS C-1
C.2. DESCRIPTION OF ARRPA MODIFICATIONS. C-3
C.3. DESCRIPTION OF MESOPAC (METEOROLOGICAL PREPROCESSOR) MODIFICATIONS C-6
C.4. DESCRIPTION OF MESOPUFF MODIFICATIONS C-7
C.5. DESCRIPTION OF MESOPLUME MODIFICATIONS. C-9
C.6. DESCRIPTION OF MSPACK (METEOROLGICAL PREPROCESSOR) MODIFICATIONS C-11
C.7. DESCRIPTION OF MSPUFF MODIFICATIONS C-11
C.8. DESCRIPTION OF MESOPAC II (METEOROLOGICAL PREPROCESSOR) MODIFICATIONS C-13
C.9. DESCRIPTION OF MESOPUFF II MODIFICATIONS. C-17
C.10. RTM-II MODIFICATIONS (OKLAHOMA ONLY). C-18
C.11. DESCRIPTION OF RADM MODIFICATIONS C-20

APPENDIX D COMPLETE STATISTICAL COMPARISONS OF THE EIGHT MODELS WITH THE OKLAHOMA AND SAVANNAH RIVER PLANT DATA BASES

INTRODUCTION. D-1

PART I: TABULAR LISTING OF THE PREDICTED AND OBSERVED GROUND-LEVEL CONCENTRATIONS FOR EACH OF THE SRP AND OKLAHOMA DATA SETS D-2

PART II: PRESENTATION OF COMPLETE AMS STATISTICS RESULTS FOR THE OKLAHOMA AND SRP DATA SETS. D-23

APPENDIX E COMPLETE GRAPHICAL COMPARISONS OF THE EIGHT MODELS WITH THE OKLAHOMA AND SAVANNAH RIVER PLANT DATA BASES

INTRODUCTION. E-1

1. LOCATION OF AIR SAMPLERS AND SITE MAP FOR OKLAHOMA EXPERIMENTS E-3

2. EVIDENCE OF LOW-LYING NOCTURNAL JET DURING THE OKLAHOMA STUDY. E-7

3. ISOPLETH PLOTS OF PREDICTED GROUND-LEVEL CONCENTATIONS FOR THE OKLAHOMA EXPERIMENTS. E-18

4. SUMMARY GRAPHICAL PLOTS COMPARING MODEL PREDICTIONS AND FIELD DATA AT OKLAHOMA. E-103

TABLE OF CONTENTS (CONTINUED)

5. LOCATION OF AIR SAMPLERS AND SITE MAP FOR SAVANNAH RIVER EXPERIMENT. E-132

6. SKETCHES OF PREDICTED AND OBSERVED GROUND-LEVEL CONCENTRATIONS FOR TWO SAVANNAH RIVER PLANT EXPERIMENTS SUBCASES 4B AND 6C . E-134

7. SUMMARY GRAPHICAL PLOTS COMPARING MODEL PREDICTIONS AND FIELD DATA AT SAVANNAH RIVER PLANT. E-143

LIST OF FIGURES

Figure		Page
E-1	Location of the sequential air samplers (BATS) and aircraft sampling path at 100 km from the Oklahoma tracer release site .	E-4
E-2	Location of sequential samplers (BATS), LASL samplers, and aircraft sampling flight path at 600 km from the Oklahoma tracer release site	E-5
E-3	Location of significant source, weather and receptor sites for Oklahoma Experiment	E-6
E-4	Wind speed profiles from KTVY tower for July 8-9, 1980 for Oklahoma experiment	E-10
E-5	Wind speeds at 266 and 444 meters at KTVY tower for July 8-9, 1980 for Oklahoma experiment.	E-11
E-6	Wind speeds at 10, 24, 45, 89 and 177 meters at KTVY tower for July 8-9, 1980 for Oklahoma experiment.	E-12
E-7	Wind speeds at 10, 45, 177 and 444 meters at KTVY tower for July 8-9, 1980 for Oklahoma experiment.	E-13
E-8	Wind speed profiles from Tinker Air Force Base for July 8-9, 1980 for Oklahoma experiment.	E-14
E-9	Wind speed soundings from Monett, Missouri on July 8, 1980 at 18Z and on July 9, 1980 at 00Z, 06Z and 12Z for Oklahoma experiment.	E-15
E-10	Wind speed soundings from Topeka, Kansas on July 8, 1980 at 18Z and on July 9, 1980 at 00Z, 06Z and 12Z for Oklahoma experiment	E-16
E-11	Wind speed soundings at Omaha, Nebraska on July 8, 1980 at 18Z and on July 9, 1980 at 00Z, 06Z and 12Z for Oklahoma experiment	E-17
E-12	Isopleth plot of ground-level concentrations for the Oklahoma experiment of July 8, 1980 (2100 to 2145 GMT) ... (left) MESOPUFF predictions, (right) MESOPLUME predictions.	E-19
E-13	Isopleth plot of ground-level concentrations for the Oklahoma experiment of July 8, 1980 (2100 to 2145 GMT) ... (left) MSPUFF predictions, (right) MESOPUFF II predictions.	E-20
E-14	Isopleth plot of ground-level concentrations for the Oklahoma experiment of July 8, 1980 (2100 to 2145 GMT) ... (left) ARRPA predictions, (right) RTM-II predictions.	E-21

LIST OF FIGURES (CONTINUED)

Figure		Page
E-15	Isopleth plot of ground-level concentrations for the Oklahoma experiment of July 8, 1980 (2100 to 2145 GMT) ... RADM predictions	E-22
E-16	Isopleth plot of ground-level concentrations for the Oklahoma experiment of July 8, 1980 (2145 to 2230 GMT) ... (left) MESOPUFF predictions, (right) MESOPLUME predictions.	E-23
E-17	Isopleth plot of ground-level concentrations for the Oklahoma experiment of July 8, 1980 (2145 to 2230 GMT) ... (left) MSPUFF predictions, (right) MESOPUFF II predictions.	E-24
E-18	Isopleth plot of ground-level concentrations for the Oklahoma experiment of July 8, 1980 (2145 to 2230 GMT) ... (left) ARRPA predictions, (right) RTM-II predictions.	E-25
E-19	Isopleth plot of ground-level concentrations for the Oklahoma experiment of July 8, 1980 (2145 to 2230 GMT) ... RADM predictions	E-26
E-20	Isopleth plot of ground-level concentrations for the Oklahoma experiment of July 8, 1980 (2230 to 2315 GMT) ... (left) MESOPUFF predictions, (right) MESOPLUME predictions.	E-27
E-21	Isopleth plot of ground-level concentrations for the Oklahoma experiment of July 8, 1980 (2230 to 2315 GMT) ... (left) MSPUFF predictions, (right) MESOPUFF II predictions	E-28
E-22	Isopleth plot of ground-level concentrations for the Oklahoma experiment of July 8, 1980 (2230 to 2315 GMT) ... (left) ARRPA predictions, (right) RTM-II predictions.	E-29
E-23	Isopleth plot of ground-level concentrations for the Oklahoma experiment of July 8, 1980 (2230 to 2315 GMT) ... RADM predictions	E-30
E-24	Isopleth plot of ground-level concentrations for the Oklahoma experiment of July 8, 1980 (2315 to 0000 GMT) ... (left) MESOPUFF predictions, (right) MESOPLUME predictions	E-31
E-25	Isopleth plot of ground-level concentrations for the Oklahoma experiment of July 8, 1980 (2315 to 0000 GMT) ... (left) MSPUFF predictions, (right) MESOPUFF II predictions	E-32
E-26	Isopleth plot of ground-level concentrations for the Oklahoma experiment of July 8, 1980 (2315 to 0000 GMT) ... (left) ARRPA predictions, (right) RTM-II predictions.	E-33

LIST OF FIGURES (CONTINUED)

Figure		Page
E-27	Isopleth plot of ground-level concentrations for the Oklahoma experiment of July 8, 1980 (2315 to 0000 GMT) ... RADM predictions	E-34
E-28	Isopleth plot of ground-level concentrations for the Oklahoma experiment of July 9, 1980 (0000 to 0045 GMT) ... (left) MESOPUFF predictions, (right) MESOPLUME predictions	E-35
E-29	Isopleth plot of ground-level concentrations for the Oklahoma experiment of July 9, 1980 (0000 to 0045 GMT) ... (left) MSPUFF predictions, (right) MESOPUFF II predictions	E-36
E-30	Isopleth plot of ground-level concentrations for the Oklahoma experiment of July 9, 1980 (0000 to 0045 GMT) ... (left) ARRPA predictions, (right) RTM-II predictions.	E-37
E-31	Isopleth plot of ground-level concentrations for the Oklahoma experiment of July 9, 1980 (0000 to 0045 GMT) ... RADM predictions	E-38
E-32	Isopleth plot of ground-level concentrations for the Oklahoma experiment of July 9, 1980 (0045 to 0130 GMT) ... (left) MESOPUFF predictions, (right) MESOPLUME predictions	E-39
E-33	Isopleth plot of ground-level concentrations for the Oklahoma experiment of July 9, 1980 (0045 to 0130 GMT) ... (left) MSPUFF predictions, (right) MESOPUFF II predictions	E-40
E-34	Isopleth plot of ground-level concentrations for the Oklahoma experiment of July 9, 1980 (0045 to 0130 GMT) ... (left) ARRPA predictions, (right) RTM-II predictions	E-41
E-35	Isopleth plot of ground-level concentrations for the Oklahoma experiment of July 9, 1980 (0045 to 0130 GMT) ... RADM predictions	E-42
E-36	Isopleth plot of ground-level concentrations for the Oklahoma experiment of July 9, 1980 (0130 to 0215 GMT) ... (left) MESOPUFF predictions, (right) MESOPLUME predictions	E-43
E-37	Isopleth plot of ground-level concentrations for the Oklahoma experiment of July 9, 1980 (0130 to 0215 GMT) ... (left) MSPUFF predictions, (right) MESOPUFF II predictions	E-44
E-38	Isopleth plot of ground-level concentrations for the Oklahoma experiment of July 9, 1980 (0130 to 0215 GMT) ... (left) ARRPA predictions, (right) RTM-II predictions	E-45

LIST OF FIGURES (CONTINUED)

Figure		Page
E-39	Isopleth plot of ground-level concentrations for the Oklahoma experiment of July 9, 1980 (0130 to 0215 GMT) ... RADM predictions	E-46
E-40	Isopleth plot of ground-level concentrations for the Oklahoma experiment of July 9, 1980 (0800 to 1100 GMT) ... (left) MESOPUFF predictions, (right) MESOPLUME predictions	E-47
E-41	Isopleth plot of ground-level concentrations for the Oklahoma experiment of July 9, 1980 (0800 to 1100 GMT) ... (left) MSPUFF predictions, (right) MESOPUFF II predictions	E-48
E-42	Isopleth plot of ground-level concentrations for the Oklahoma experiment of July 9, 1980 (0800 to 1100 GMT) ... (left) ARRPA predictions, (right) RTM-II predictions	E-49
E-43	Isopleth plot of ground-level concentrations for the Oklahoma experiment of July 9, 1980 (0800 to 1100 GMT) ... RADM predictions	E-50
E-44	Isopleth plot of ground-level concentrations for the Oklahoma experiment of July 9, 1980 (1100 to 1400 GMT) ... (left) MESOPUFF predictions, (right) MESOPLUME predictions	E-51
E-45	Isopleth plot of ground-level concentrations for the Oklahoma experiment of July 9, 1980 (1100 to 1400 GMT) ... (left) MSPUFF predictions, (right) MESOPUFF II predictions	E-52
E-46	Isopleth plot of ground-level concentrations for the Oklahoma experiment of July 9, 1980 (1100 to 1400 GMT) ... (left) ARRPA predictions, (right) RTM-II predictions	E-53
E-47	Isopleth plot of ground-level concentrations for the Oklahoma experiment of July 9, 1980 (1100 to 1400 GMT) ... RADM predictions	E-54
E-48	Isopleth plot of ground-level concentrations for the Oklahoma experiment of July 9, 1980 (1400 to 1700 GMT) ... (left) MESOPUFF predictions, (right) MESOPLUME predictions.	E-55
E-49	Isopleth plot of ground-level concentrations for the Oklahoma experiment of July 9, 1980 (1400 to 1700 GMT) ... (left) MSPUFF predictions, (right) MESOPUFF II predictions	E-56
E-50	Isopleth plot of ground-level concentrations for the Oklahoma experiment of July 9, 1980 (1400 to 1700 GMT) ... (left) ARRPA predictions, (right) RTM-II predictions	E-57

LIST OF FIGURES (CONTINUED)

Figure		Page
E-51	Isopleth plot of ground-level concentrations for the Oklahoma experiment of July 9, 1980 (1400 to 1700 GMT) ... RADM predictions	E-58
E-52	Isopleth plot of ground-level concentrations for the Oklahoma experiment of July 9, 1980 (1700 to 2000 GMT) ... (left) MESOPUFF predictions, (right) MESOPLUME predictions	E-59
E-53	Isopleth plot of ground-level concentrations for the Oklahoma experiment of July 9, 1980 (1700 to 2000 GMT) ... (left) MSPUFF predictions, (right) MESOPUFF II predictions	E-60
E-54	Isopleth plot of ground-level concentrations for the Oklahoma experiment of July 9, 1980 (1700 to 2000 GMT) ... (left) ARRPA predictions, (right) RTM-II predictions	E-61
E-55	Isopleth plot of ground-level concentrations for the Oklahoma experiment of July 9, 1980 (1700 to 2000 GMT) ... RADM predictions	E-62
E-56	Isopleth plot of ground-level concentrations for the Oklahoma experiment of July 9, 1980 (2000 to 2300 GMT) ... (left) MESOPUFF predictions, (right) MESOPLUME predictions	E-63
E-57	Isopleth plot of ground-level concentrations for the Oklahoma experiment of July 9, 1980 (2000 to 2300 GMT) ... (left) MSPUFF predictions, (right) MESOPUFF II predictions	E-64
E-58	Isopleth plot of ground-level concentrations for the Oklahoma experiment of July 9, 1980 (2000 to 2300 GMT) ... (left) ARRPA predictions, (right) RTM-II predictions	E-65
E-59	Isopleth plot of ground-level concentrations for the Oklahoma experiment of July 9, 1980 (2000 to 2300 GMT) ... RADM predictions	E-66
E-60	Isopleth plot of ground-level concentrations for the Oklahoma experiment of July 9, 1980 (2300 to 0200 GMT) ... (left) MESOPUFF predictions, (right) MESOPLUME predictions	E-67
E-61	Isopleth plot of ground-level concentrations for the Oklahoma experiment of July 9, 1980 (2300 to 0200 GMT) ... (left) MSPUFF predictions, (right) MESOPUFF II predictions	E-68
E-62	Isopleth plot of ground-level concentrations for the Oklahoma experiment of July 9, 1980 (2300 to 0200 GMT) ... (left) ARRPA predictions, (right) RTM-II predictions	E-69

LIST OF FIGURES (CONTINUED)

Figure		Page
E-63	Isopleth plot of ground-level concentrations for the Oklahoma experiment of July 9, 1980 (2300 to 0200 GMT) ... RADM predictions	E-70
E-64	Isopleth plot of ground-level concentrations for the Oklahoma experiment of July 11, 1980 (2200 to 2245 GMT) ... (left) MESOPUFF predictions, (right) MESOPLUME predictions	E-71
E-65	Isopleth plot of ground-level concentrations for the Oklahoma experiment of July 11, 1980 (2200 to 2245 GMT) ... (left) MSPUFF predictions, (right) MESOPUFF II predictions	E-72
E-66	Isopleth plot of ground-level concentrations for the Oklahoma experiment of July 11, 1980 (2200 to 2245 GMT) ... (left) ARRPA predictions, (right) RTM-II predictions	E-73
E-67	Isopleth plot of ground-level concentrations for the Oklahoma experiment of July 11, 1980 (2200 to 2245 GMT) ... RADM predictions	E-74
E-68	Isopleth plot of ground-level concentrations for the Oklahoma experiment of July 11, 1980 (2245 to 2330 GMT) ... (left) MESOPUFF predictions, (right) MESOPLUME predictions	E-75
E-69	Isopleth plot of ground-level concentrations for the Oklahoma experiment of July 11, 1980 (2245 to 2330 GMT) ... (left) MSPUFF predictions, (right) MESOPUFF II predictions	E-76
E-70	Isopleth plot of ground-level concentrations for the Oklahoma experiment of July 11, 1980 (2245 to 2330 GMT) ... (left) ARRPA predictions, (right) RTM-II predictions	E-77
E-71	Isopleth plot of ground-level concentrations for the Oklahoma experiment of July 11, 1980 (2245 to 2330 GMT) ... RADM predictions	E-78
E-72	Isopleth plot of ground-level concentrations for the Oklahoma experiment of July 11, 1980 (2330 to 0015 GMT) ... (left) MESOPUFF predictions, (right) MESOPLUME predictions	E-79
E-73	Isopleth plot of ground-level concentrations for the Oklahoma experiment of July 11, 1980 (2330 to 0015 GMT) ... (left) MSPUFF predictions, (right) MESOPUFF II predictions	E-80
E-74	Isopleth plot of ground-level concentrations for the Oklahoma experiment of July 11, 1980 (2330 to 0015 GMT) ... (left) ARRPA predictions, (right) RTM-II predictions	E-81

LIST OF FIGURES (CONTINUED)

Figure		Page
E-75	Isopleth plot of ground-level concentrations for the Oklahoma experiment of July 11, 1980 (2330 to 0015 GMT) ... RADM predictions	E-82
E-76	Isopleth plot of ground-level concentrations for the Oklahoma experiment of July 12, 1980 (0015 to 0100 GMT) ... (left) MESOPUFF predictions, (right) MESOPLUME predictions	E-83
E-77	Isopleth plot of ground-level concentrations for the Oklahoma experiment of July 12, 1980 (0015 to 0100 GMT) ... (left) MSPUFF predictions, (right) MESOPUFF II predictions	E-84
E-78	Isopleth plot of ground-level concentrations for the Oklahoma experiment of July 12, 1980 (0015 to 0100 GMT) ... (left) ARRPA predictions, (right) RTM-II predictions	E-85
E-79	Isopleth plot of ground-level concentrations for the Oklahoma experiment of July 12, 1980 (0015 to 0100 GMT) ... RADM predictions	E-86
E-80	Isopleth plot of ground-level concentrations for the Oklahoma experiment of July 12, 1980 (0100 to 0145 GMT) ... (left) MESOPUFF predictions, (right) MESOPLUME predictions	E-87
E-81	Isopleth plot of ground-level concentrations for the Oklahoma experiment of July 12, 1980 (0100 to 0145 GMT) ... (left) MSPUFF predictions, (right) MESOPUFF II predictions	E-88
E-82	Isopleth plot of ground-level concentrations for the Oklahoma experiment of July 12, 1980 (0100 to 0145 GMT) ... (left) ARRPA predictions, (right) RTM-II predictions	E-89
E-83	Isopleth plot of ground-level concentrations for the Oklahoma experiment of July 12, 1980 (0100 to 0145 GMT) ... RADM predictions	E-90
E-84	Isopleth plot of ground-level concentrations for the Oklahoma experiment of July 12, 1980 (0145 to 0230 GMT) ... (left) MESOPUFF predictions, (right) MESOPLUME predictions	E-91
E-85	Isopleth plot of ground-level concentrations for the Oklahoma experiment of July 12, 1980 (0145 to 0230 GMT) ... (left) MSPUFF predictions, (right) MESOPUFF II predictions	E-92
E-86	Isopleth plot of ground-level concentrations for the Oklahoma experiment of July 12, 1980 (0145 to 0230 GMT) ... (left) ARRPA predictions, (right) RTM-II predictions	E-93

LIST OF FIGURES (CONTINUED)

Figure		Page
E-87	Isopleth plot of ground-level concentrations for the Oklahoma experiment of July 12, 1980 (0145 to 0230 GMT) ... RADM predictions	E-94
E-88	Isopleth plot of ground-level concentrations for the Oklahoma experiment of July 12, 1980 (0230 to 0315 GMT) ... (left) MESOPUFF predictions, (right) MESOPLUME predictions	E-95
E-89	Isopleth plot of ground-level concentrations for the Oklahoma experiment of July 12, 1980 (0230 to 0315 GMT) ... (left) MSPUFF predictions, (right) MESOPUFF II predictions	E-96
E-90	Isopleth plot of ground-level concentrations for the Oklahoma experiment of July 12, 1980 (0230 to 0315 GMT) ... (left) ARRPA predictions, (right) RTM-II predictions	E-97
E-91	Isopleth plot of ground-level concentrations for the Oklahoma experiment of July 12, 1980 (0230 to 0315 GMT) ... RADM predictions	E-98
E-92	Isopleth plot of ground-level concentrations for the Oklahoma experiment of July 12, 1980 (0315 to 0400 GMT) ... (left) MESOPUFF predictions, (right) MESOPLUME predictions	E-99
E-93	Isopleth plot of ground-level concentrations for the Oklahoma experiment of July 12, 1980 (0315 to 0400 GMT) ... (left) MSPUFF predictions, (right) MESOPUFF II predictions	E-100
E-94	Isopleth plot of ground-level concentrations for the Oklahoma experiment of July 12, 1980 (0315 to 0400 GMT) ... (left) ARRPA predictions, (right) RTM-II predictions	E-101
E-95	Isopleth plot of ground-level concentrations for the Oklahoma experiment of July 12, 1980 (0315 to 0400 GMT) ... RADM predictions	E-102
E-96	Frequency distribution of predicted and observed concentrations at Oklahoma for MESOPUFF based on points paired in space and time ... (top) concentration range: 0 - 100 parts per 10^{15}, (bottom) concentration range: 100 - 1000 parts per 10^{15}	E-104
E-97	Frequency distribution of residuals at Oklahoma for MESOPUFF based on points paired in space and time ... (top) residual range: -100 to 100 parts per 10^{15}, (bottom) residual range: -1000 to 1000 parts per 10^{15}.	E-105
E-98	Scatter plot of predicted and observed averaged concentrations at Oklahoma for MESOPUFF ... points paired in space and time .	E-106

LIST OF FIGURES (CONTINUED)

Figure		Page
E-99	Scatter plot of average of observed and predicted concentrations versus residuals at Oklahoma for MESOPUFF ... points paired in space and time	E-106
E-100	Cumulative frequency distributions of MESOPUFF predictions and observed concentrations at Oklahoma based on points paired in space and time.	E-107
E-101	Frequency distribution of predicted and observed concentrations at Oklahoma for MESOPLUME based on points paired in space and time ... (top) concentration range: 0 - 100 parts per 10^{15}, (bottom) concentration range: 100 - 1000 parts per 10^{15}. . . .	E-108
E-102	Frequency distribution of residuals at Oklahoma for MESOPLUME based on points paired in space and time ... (top) residual range: -100 to 100 parts per 10^{15}, (bottom) residual range: -1000 to 1000 parts per 10^{15}.	E-109
E-103	Scatter plot of predicted and observed averaged concentrations at Oklahoma for MESOPLUME ... points paired in space and time.	E-110
E-104	Scatter plot of average of observed and predicted concentrations versus residuals at Oklahoma for MESOPLUME ... points paired in space and time	E-110
E-105	Cumulative frequency distributions of MESOPLUME predictions and observed concentrations at Oklahoma based on points paired in space and time.	E-111
E-106	Frequency distribution of predicted and observed concentrations at Oklahoma for MSPUFF based on points paired in space and time ... (top) concentration range: 0 - 100 parts per 10^{15}, (bottom) concentration range: 100 - 1000 parts per 10^{15}	E-112
E-107	Frequency distribution of residuals at Oklahoma for MSPUFF based on points paired in space and time ... (top) residual range: -100 to 100 parts per 10^{15}, (bottom) residual range: -1000 to 1000 parts per 10^{15}.	E-113
E-108	Scatter plot of predicted and observed averaged concentrations at Oklahoma for MSPUFF ... points paired in space and time . .	E-114
E-109	Scatter plot of average of observed and predicted concentrations versus residuals at Oklahoma for MSPUFF ... points paired in space and time	E-114
E-110	Cumulative frequency distributions of MSPUFF predictions and observed concentrations at Oklahoma based on points paired in space and time.	E-115

LIST OF FIGURES (CONTINUED)

Figure		Page
E-111	Frequency distribution of predicted and observed concentrations at Oklahoma for MESOPUFF II based on points paired in space and time ... (top) concentration range: 0 - 100 parts per 10^{15}, (bottom) concentration range: 100 - 1000 parts per 10^{15}	E-116
E-112	Frequency distribution of residuals at Oklahoma for MESOPUFF II based on points paired in space and time ... (top) residual range: -100 to 100 parts per 10^{15}, (bottom) residual range: -1000 to 1000 parts per 10^{15}.	E-117
E-113	Scatter plot of predicted and observed averaged concentrations at Oklahoma for MESOPUFF II ... points paired in space and time.	E-118
E-114	Scatter plot of average of observed and predicted concentrations versus residuals at Oklahoma for MESOPUFF II ... points paired in space and time	E-118
E-115	Cumulative frequency distributions of MESOPUFF II predictions and observed concentrations at Oklahoma based on points paired in space and time	E-119
E-116	Frequency distribution of predicted and observed concentrations at Oklahoma for ARRPA based on points paired in space and time ... (top) concentration range: 0 - 100 parts per 10^{15}, (bottom) concentration range: 100 - 1000 parts per 10^{15}	E-120
E-117	Frequency distribution of residuals at Oklahoma for ARRPA based on points paired in space and time ... (top) residual range: -100 to 100 parts per 10^{15}, (bottom) residual range: -1000 to 1000 parts per 10^{15}	E-121
E-118	Scatter plot of predicted and observed averaged concentrations at Oklahoma for ARRPA ... points paired in space and time . . .	E-122
E-119	Scatter plot of average of observed and predicted concentrations versus residuals at Oklahoma for ARRPA ... points paired in space and time	E-122
E-120	Cumulative frequency distributions of ARRPA predictions and observed concentrations at Oklahoma based on points paired in space and time.	E-123
E-121	Frequency distribution of predicted and observed concentrations at Oklahoma for RTM-II based on points paired in space and time ... (top) concentration range: 0 - 100 parts per 10^{15}, (bottom) concentration range: 100 - 1000 parts per 10^{15}	E-124

LIST OF FIGURES (CONTINUED)

Figure		Page
E-122	Frequency distribution of residuals at Oklahoma for RTM-II based on points paired in space and time ... (top) residual range: -100 to 100 parts per 10^{15}, (bottom) residual range: -1000 to 1000 parts per 10^{15}.	E-125
E-123	Scatter plot of predicted and observed averaged concentrations at Oklahoma for RTM-II ... points paired in space and time . .	E-126
E-124	Scatter plot of average of observed and predicted concentrations versus residuals at Oklahoma for RTM-II ... points paired in space and time	E-126
E-125	Cumulative frequency distributions of RTM-II predictions and observed concentrations at Oklahoma based on points paired in space and time.	E-127
E-126	Frequency distribution of predicted and observed concentrations at Oklahoma for RADM based on points paired in space and time ... (top) concentration range: 0 - 100 parts per 10^{15}, (bottom) concentration range: 100 -1000 parts per 10^{15}.	E-128
E-127	Frequency distribution of residuals at Oklahoma for RADM based on points paired in space and time ... (top) residual range: -100 to 100 parts per 10^{15}, (bottom) residual range: -1000 to 1000 parts per 10^{15}	E-129
E-128	Scatter plot of predicted and observed averaged concentrations at Oklahoma for RADM ... points paired in space and time . . .	E-130
E-129	Scatter plot of average of observed and predicted concentrations versus residuals at Oklahoma for RADM ... points paired in space and time.	E-130
E-130	Cumulative frequency distributions of RADM predictions and observed concentrations at Oklahoma based on points paired in space and time.	E-131
E-131	Location of significant source, weather and receptors sites for Savannah River Plant Experiment	E-133
E-132	Comparison of 10-hour averages of predicted plume and observed data (in pCi/m^3) for Savannah River Plant experiment of November 18-19, 1976 (2200 to 0800 GMT) ... (top) MESOPUFF predictions, (bottom) MESOPLUME predictions	E-135
E-133	Comparison of 10-hour averages of predicted plume and observed data (in pCi/m^3) for Savannah River Plant experiment of November 18-19, 1976 (2200 to 0800 GMT) ... (top) MSPUFF predictions, (bottom) MESOPUFF II predictions	E-136

LIST OF FIGURES (CONTINUED)

Figure		Page
E-134	Comparison of 10-hour averages of predicted plume and observed data (in pCi/m^3) for Savannah River Plant experiment of November 18-19, 1976 (2200 to 0800 GMT) ... (top) MTDDIS predictions, (bottom) RTM-II predictions.	E-137
E-135	Comparison of 10-hour averages of predicted plume and observed data (in pCi/m^3) for Savannah River Plant experiment of November 18-19, 1976 (2200 to 0800 GMT) ... RADM predictions .	E-138
E-136	Comparison of 10-hour averages of predicted plume and observed data (in pCi/m^3) for Savannah River Plant experiment of February 17-18, 1977 (2200 to 0800 GMT) ... (top) MESOPUFF predictions, (bottom) MESOPLUME predictions	E-139
E-137	Comparison of 10-hour averages of predicted plume and observed data (in pCi/m^3) for Savannah River Plant experiment of February 17-18, 1977 (2200 to 0800 GMT) ... (top) MSPUFF predictions, (bottom) MESOPUFF II predictions	E-140
E-138	Comparison of 10-hour averages of predicted plume and observed data (in pCi/m^3) for Savannah River Plant experiment of February 17-18, 1977 (2200 to 0800 GMT) ... (top) MTDDIS predictions, (bottom) RTM-II predictions.	E-141
E-139	Comparison of 10-hour averages of predicted plume and observed data (in pCi/m^3) for Savannah River Plant experiment of February 17-18, 1977 (2200 to 0800 GMT) ... RADM predictions .	E-142
E-140	Frequency distribution of predicted and observed concentrations at Savannah River Plant for MESOPUFF based on points paired in space and time ... (top) concentration range: 0 - 100 pCi/m^3, (bottom) concentration range: 100 - 1000 pCi/m^3	E-144
E-141	Frequency distribution of residuals at Savannah River Plant for MESOPUFF based on points paired in space and time ... (top) residual range: -100 to 100 pCi/m^3, (bottom) residual range: -1000 to 1000 pCi/m^3	E-145
E-142	Scatter plot of predicted and observed averaged concentrations at Savannah River Plant for MESOPUFF ... points paired in space and time.	E-146
E-143	Scatter plot of average of observed and predicted concentrations versus residuals at Savannah River Plant for MESOPUFF ... points paired in space and time.	E-146
E-144	Cumulative frequency distributions of MESOPUFF predictions and observed concentrations at Savannah River Plant based on points paired in space and time.	E-147

LIST OF FIGURES (CONTINUED)

Figure		Page
E-145	Frequency distribution of predicted and observed concentrations at Savannah River Plant for MESOPLUME based on points paired in space and time ... (top) concentration range: 0 - 100 pCi/m^3, (bottom) concentration range: 100 - 1000 pCi/m^3	E-148
E-146	Frequency distribution of residuals at Savannah River Plant for MESOPLUME based on points paired in space and time ... (top) residual range: -100 to 100 pCi/m^3, (bottom) residual range: -1000 to 1000 pCi/m^3.	E-149
E-147	Scatter plot of predicted and observed averaged concentrations at Savannah River Plant for MESOPLUME ... points paired in space and time.	E-150
E-148	Scatter plot of average of observed and predicted concentrations versus residuals at Savannah River Plant for MESOPLUME ... points paired in space and time	E-150
E-149	Cumulative frequency distributions of MESOPLUME predictions and observed concentrations at Savannah River Plant based on points paired in space and time.	E-151
E-150	Frequency distribution of predicted and observed concentrations at Savannah River Plant for MSPUFF based on points paired in space and time ... (top) concentration range: 0 - 100 pCi/m^3, (bottom) concentration range: 100 - 1000 pCi/m^3	E-152
E-151	Frequency distribution of residuals at Savannah River Plant for MSPUFF based on points paired in space and time ... (top) residual range: -100 to 100 pCi/m^3, (bottom) residual range: -1000 to 1000 pCi/m^3.	E-153
E-152	Scatter plot of predicted and observed averaged concentrations at Savannah River Plant for MSPUFF ... points paired in space and time.	E-154
E-153	Scatter plot of average of observed and predicted concentrations versus residuals at Savannah River Plant for MSPUFF ... points paired in space and time.	E-154
E-154	Cumulative frequency distributions of MSPUFF predictions and observed concentrations at Savannah River Plant based on points paired in space and time.	E-155
E-155	Frequency distribution of predicted and observed concentrations at Savannah River Plant for MESOPUFF II based on points paired in space and time ... (top) concentration range: 0 - 100 pCi/m^3, (bottom) concentration range: 100 - 1000 pCi/m^3	E-156

LIST OF FIGURES (CONTINUED)

Figure		Page
E-156	Frequency distribution of residuals at Savannah River Plant for MESOPUFF II based on points paired in space and time ... (top) residual range: -100 to 100 pCi/m^3, (bottom) residual range: -1000 to 1000 pCi/m^3.	E-157
E-157	Scatter plot of predicted and observed averaged concentrations at Savannah River Plant for MESOPUFF II ... points paired in space and time.	E-158
E-158	Scatter plot of average of observed and predicted concentrations versus residuals at Savannah River Plant for MESOPUFF II ... points paired in space and time	E-158
E-159	Cumulative frequency distributions of MESOPUFF II predictions and observed concentrations at Savannah River Plant based on points paired in space and time	E-159
E-160	Frequency distribution of predicted and observed concentrations at Savannah River Plant for MTDDIS based on points paired in space and time ... (top) concentration range: 0 - 100 pCi/m^3, (bottom) concentration range: 100 - 1000 pCi/m^3	E-160
E-161	Frequency distribution of residuals at Savannah River Plant for MTDDIS based on points paired in space and time ... (top) residual range: -100 to 100 pCi/m^3, (bottom) residual range: -1000 to 1000 pCi/m^3.	E-161
E-162	Scatter plot of predicted and observed averaged concentrations at Savannah River Plant for MTDDIS ... points paired in space and time.	E-162
E-163	Scatter plot of average of observed and predicted concentrations versus residuals at Savannah River Plant for MTDDIS ... points paired in space and time.	E-162
E-164	Cumulative frequency distributions of MTDDIS predictions and observed concentrations at Savannah River Plant based on points paired in space and time.	E-163
E-165	Frequency distribution of predicted and observed concentrations at Savannah River Plant for RTM-II based on points paired in space and time ... (top) concentration range: 0 - 100 pCi/m^3, (bottom) concentration range: 100 - 1000 pCi/m^3	E-164
E-166	Frequency distribution of residuals at Savannah River Plant for RTM-II based on points paired in space and time ... (top) residual range: -100 to 100 pCi/m^3, (bottom) residual range: -1000 to 1000 pCi/m^3.	E-165

LIST OF FIGURES (CONTINUED)

Figure		Page
E-167	Scatter plot of predicted and observed averaged concentrations at Savannah River Plant for RTM-II ... points paired in space and time.	E-166
E-168	Scatter plot of average of observed and predicted concentrations versus residuals at Savannah River Plant for RTM-II ... points paired in space and time.	E-166
E-169	Cumulative frequency distributions of RTM-II predictions and observed concentrations at Savannah River Plant based on points paired in space and time.	E-167
E-170	Frequency distribution of predicted and observed concentrations at Savannah River Plant for RADM based on points paired in space and time ... (top) concentration range: 0 - 100 pCi/m^3, (bottom) concentration range: 100 - 1000 pCi/m^3	E-168
E-171	Frequency distribution of residuals at Savannah River Plant for RADM based on points paired in space and time ... (top) residual range: -100 to 100 pCi/m^3, (bottom) residual range: -1000 to 1000 pCi/m^3.	E-169
E-172	Scatter plot of predicted and observed averaged concentrations at Savannah River Plant for RADM ... points paired in space and time.	E-170
E-173	Scatter plot of average of observed and predicted concentrations versus residuals at Savannah River Plant for RADM ... points paired in space and time.	E-170
E-174	Cumulative frequency distributions of RADM predictions and observed concentrations at Savannah River Plant based on points paired in space and time.	E-171

LIST OF TABLES

Table		Page
D-1	Statistical Dataset (A-1) for Oklahoma Data.	D-24
D-2	Statistical Dataset (A-2) for Oklahoma Data	D-25
D-3	Statistical Dataset (A-4A) for Oklahoma Data.	D-26
D-4	Statistical Dataset (B-1) for Oklahoma Data	D-27
D-5	Statistical Dataset (B-3) for Oklahoma Data	D-29
D-6	Statistical Dataset (A-1) for Savannah River Plant Data. . . .	D-30
D-7	Statistical Dataset (A-2) for Savannah River Plant Data	D-31
D-8	Statistical Dataset (A-4A) for Savannah River Plant Data. . . .	D-32
D-9	Statistical Dataset (B-1) for Savannah River Plant Data	D-33
D-10	Statistical Dataset (B-3) for Savannah River Plant Data	D-36

APPENDIX A

APCA PAPER/HARTFORD MEETING/OCTOBER 1983
(REF. 23)

EVALUATION OF TWO SHORT-TERM LONG-RANGE TRANSPORT MODELS WITH FIELD DATA

Anthony J. Policastro,
Michael Wastag, and Jack D. Shannon
Argonne National Laboratory
Argonne, Illinois

Richard Carhart
University of Illinois at Chicago

William Dunn
University of Illinois at Urbana

The performance of two short-term long-range transport models, RTM-II and MESOPUFF, are evaluated with data from Krypton-85 releases. The RTM-II model employs a finite-difference method of plume dispersion, whereas MESOPUFF uses a variable-trajectory Lagrangian puff approach. In this evaluation a preprocessor, MESOPAC, produces for both models the wind field and mixing height as a function of time. Krypton-85 is a conservative tracer so only the transport and dispersion components of the models are tested. Fifteen datasets covering between one and twelve 10-hr periods are used for model testing. Thirteen samplers within 144 km of the tracer release points provide 10-hr averages of Kr-85 concentrations.

Both models typically show errors of 20 to 40° in the direction of the predicted plume (predictions usually clockwise relative to observed) along with an underprediction in plume spread. Predicted concentration decay with distance tends to be only within an order of magnitude of the data, even when errors in orientation are ignored. Graphical comparisons and performance statistics are unfavorable when points are paired in space and time. Model errors are most likely due to (a) the single-layer wind field analysis from twice-daily rawinsondes in MESOPAC (inadequately treating the diurnal cycles of mixing depth and vertical shear in the horizontal wind, as well as not treating meandering), and (b) an underprediction of small-scale processes by both models. The commonly used performance statistics do not permit the separation of directionality and dispersion effects. Methods of evaluating the ground patterns of the predicted plume and observed data need to be developed to supplement point-by-point model evaluations.

Introduction

In the March 1980 Federal Register,[1] the U.S. EPA published a request for submission of long-range transport models for possible inclusion in the next revision of EPA's "Guidelines on Air Quality Models." Seven models have been accepted as candidates for consideration: RTM-II,[2] MESOPUFF,[3,4] MESOPUFF-II,[5] MESOPLUME,[6] RADM,[7] MTDDIS,[8] and ARRPA.[9] These models predict short-term averages (3, 12, 24 hrs) of SO_2, sulfates, and particulates over distances of 20-1000 km from single or multiple sources. ANL is presently under contract with EPA to evaluate the performance of these models with field data. A important component in the evaluation is the use of the AMS-recommended statistics[10] coupled with supplementary graphical methods to quantify and interpret the performance of the models. Data bases used to test the models will largely represent single sources in which concentrations above background can be detected over mesoscale distances. The major application of the models in the EPA regulatory framework is for PSD analyses for Class I areas. Long-range transport models are required in calculations made at distances beyond about 50 km, the limits of applicability of straight-line Gaussian models.

This paper presents the early results of this model evaluation program. Two models, RTM-II and MESOPUFF, are tested here with tracer plume data taken at the Savannah River Plant during the period 1976-1977. Since our work represents a regulatory evaluation of models, rather than a scientific evaluation of the modeling concepts, those models are to be applied as indicated in the user's manuals for these models. Only data specifically required by the model are to be used.

Brief Descriptions of MESOPUFF and RTM-II

MESOPUFF is a variable trajectory Gaussian puff superposition model. A preprocessor to MESOPUFF called MESOPAC employs twice-daily rawinsonde soundings to provide a gridded field of winds (u,v), mixing heights, and Pasquill-Gifford-Turner (PGT) stability classes on an hour-by-hour basis. MESOPAC provides only a single-layer wind field; i.e., u and v are constant with height but vary in the horizontal plane and with time. Winds and mixing heights are first computed (twice daily) at each rawinsonde station; from those values, $1/r^2$-interpolation in space and linear interpolation in time is used to compute the winds and mixing heights at any grid point (x, y) at any hour in the day. PGT stability classes are a function of wind speed and mixing height at each grid point. The file of gridded winds, mixing heights, and PGT stability classes is then used by MESOPUFF to compute the dispersion of the plume.

In MESOPUFF, the emission is divided into a sequence of puffs emitted continually over time. The Gaussian puffs are advected by the wind and dispersed using σ_y and σ_z values similar to those of Turner[11] up to 100 km and based on the values presented by Heffter[12] beyond 100 km. At each hour, the contribution of each puff to the concentration at each sampler is determined.

RTM-II uses a puff-on-grid hybrid technique. The emission is released as a series of puffs and these puffs are transported and dispersed using a Gaussian puff formulation. When a puff expands to the size of either dimension of a grid cell (Δx, Δy or Δz = mixing height), the puff is integrated into the grid system and is dispersed as part of the finite-

difference solution to the convective-diffusion equation. The numerical scheme used is from Boris and Book.[13] This method is characterized by a two-stage, flux-corrected transport algorithm in which a correction of pollutant fluxes in the second stage counteracts the numerical diffusion arising from the first stage. Horizontal eddy diffusivities are parameterized in the model using a formula proposed by Smagorinsky,[14] where $K_H = K_x = K_y = \eta|Def|$, η is an empirical constant based on scale considerations, and $|Def|$ is the magnitude of the velocity deformation tensor. The horizontal diffusivities are constrained by maximum and minimum values chosen from regional-scale field studies.

There is no single wind-field model recommended by the developers, Systems Applications Inc. (SAI), for the RTM-II model. Several wind field models are available from them; however, for an application to the Savannah River Plant ^{85}Kr data, SAI recommended the use of MESOPAC. Thus, MESOPAC provided the fields of wind and mixing height for both MESOPUFF and RTM-II in the present study.

The Savannah River Plant ^{85}Kr Data Base

Krypton-85 is a noble gas which is released to the atmosphere during the chemical separation of nuclear fuel from target material at the Savannah River Plant (SRP) in Aiken, South Carolina.[15] The release comes from two 62-km stacks located 4 km apart. The release is strongly time-dependent as illustrated in Figure 1 for March 1976. Background measurements at the site indicated a level of 16 PCi/m^3; any measurement below that value was treated as 16 PCi/m^3. The location of air samplers on the ground around the source is sketched in Figure 2. The nearest sampler was 28 km from the stacks and the farthest was 144 km. Twice-daily samples representing 10-hr averages were used in this study for the testing of models. The terrain around the SRP consists of gently rolling hills. Four rawinsonde stations located in South Carolina and Georgia provide upper-air data to be used in the model evaluation. Meteorological data from a network of towers and ground stations in the area were available but could not be accepted as input by the models, according to the protocol established for the evaluation.

Since the Krypton-85 emission is a conservative tracer, the chemical conversion and wet and dry deposition submodels were inoperative. Only the transport and diffusion components of the models were evaluated.

Table 1 lists the time periods over which 10-hr samples were collected as well as the time periods over which plume dispersion calculations were made. The fifteen datasets listed were also the "standard" datasets used in the Model Validation Workshop[16,17] held in Hilton Head, South Carolina in November 1980. At least three datasets are available for each season of the year. Each dataset represented roughly 2-6 days of between one to twelve 10-hr sampling periods. In general, 1-1½ days of plume transport calculations were made in advance of the start of ground sampling measurements to assure that the plume had been sufficiently transported downwind.

Method of Preparation of Model Predictions

A rectangular coordinate grid surrounding the four rawinsonde stations was set up (see Figure 2) for MESOPAC predictions of winds, mixing heights, and PGT stability classes. This grid spanned 320 km by 540 km with grid spacing $\Delta X = \Delta Y = 10$ km. Computations of plume dispersion were made over

the smaller grid given in Figure 2, which was 270 km by 290 km and a subgrid of the larger meteorological grid.

Standard options were chosen in applying both models. However, engineering judgment was required in two areas. First, a choice had to be made as to how MESOPAC was to represent the single-layer time-dependent winds. Personal communications[18,19] with the ERT and SAI model developers elicited the common recommendation to average winds (u, v components) from the ground to 1500 m at times 00Z and 12Z. Second, for RTM-II, dispersion coefficients had to be chosen. The model developers recommended[18] a choice of $\eta = 2 \times 10^8$ m^2 with lower and upper limits on K_H of 100 and 3.3×10^4 m^2/s, respectively, based on the expected time of travel and lateral spreading of the plume. Guidance for such choices came from SAI's interpretation of regional scale studies by Randerson.[20,21]

General Discussion of Results

The fifteen datasets used for model predictions encompass sixty-five 10-hr averaging periods. Comparison of RTM-II and MESOPUFF ground patterns and observations at samplers revealed the following division of these 65 cases (for MESOPUFF)

- 10 cases appear well-predicted
- 17 cases reveal a predicted plume that is rotated 20-45° clockwise from the observations
- 5 cases reveal a predicted plume that is counterclockwise of the observations
- 7 cases had predicted plumes directed approximately 180° from observed data
- 10 cases had plumes predicted to be too narrow and located between two samplers. A greater predicted plume spread would have improved model performance
- 16 cases were such that no decision on model performance could be made because both modeled and actual plumes (apparently) passed between sensors.

Results for RTM-II revealed a similar division of cases. MESOPUFF generally provided higher surface concentrations but in a narrower plume than RTM-II and both predicted plumes did not spread out sufficiently. Figure 3 shows the rotation problem as illustrated in Case 4B for RTM-II. The figure presents measured 10-hr averaged concentrations (above background) at each sampler (in PCi/m^3) and numerical values of the predicted plume concentrations within the outlined plume. For sampler 6, 200 PCi/m^3 represents the predicted concentration and 1 PCi/m^3 represents the observed concentration. A noticeable rotation of the predicted plume approximately 45° clockwise relative to the data is noted. Determination of winds in MESOPAC through averaging u and v components to 1500 m seems to be partly the cause. For this nighttime period (2200-0800 hr GMT), the plume is not likely to be more than two stack heights high (~150 m) rather than 1500 m. Since nocturnal planetary boundary layer winds usually rotate clockwise with height (Ekman spiral effect), it is not surprising that our 1500 m average winds direct the plume clockwise of observations. One

might suggest a 1500 m averaging of winds for 12Z and 150 m averaging for 00Z. However, that choice leads to too low a wind speed at night for transport of the plume puffs already diffused aloft. There appears to be no good solution within the present framework of MESOPAC. In MESOPUFF-II (which includes new version of MESOPAC), two wind fields are created. The first provides a wind field for the mixing layer (say from ground to 1500 m in the day and up to 100 m at night) and a second wind field from the mixing layer to some fixed upper level, say the 750 or 850 mb level. The concept of two vertically averaged wind fields that are essentially uncoupled may be a better method to handle nocturnal wind shear. MESOPUFF-II will be tested with these data in the near future. Clearly, predictions of short-term averages at the lower end of the mesoscale range requires a very good wind-field model for accurate location predictions.

The second major problem identified in the model/data comparisons is the lack by both models of sufficient lateral spreading. The problem of insufficient lateral spreading is illustrated in Figure 4 for Case 6C for RTM-II. Greater plume spread would provide better predictions for samplers 9 and 6. For very short-term averages (2-3 hrs), such small spreading should be due to inadequate treatment of small-scale processes i.e., too small σ_y perhaps. For 24-hr averages, too small a lateral spreading would most likely be due to wind shear and plume meander, i.e., inadequate resolution in the meteorological preprocessor. For 10-hr averages as in the present case, we have a combination of both deficiencies. Concerning small-scale processes, the use of the Turner σ_y curves out to 100 km does not provide sufficient spreading, especially under stable conditions. The Turner σ's are more applicable in the range up to 20-30 km. For RTM-II, the value of η and the lower bound to K_H were probably too small for the present problem. Conversations with the developers indicated that the location of the four rawinsondes outside the plume computational grid leads to smooth streamlines for the interpolated winds passing through the plume grid. As a result, the velocity deformation will be small leading to a small K_H computed for each time step. As a result, the plume spreading will not be as large as otherwise expected. Internal model calculations of K_H may be leading to values at or below the specified lower bound for K_H. Higher values of η and the lower bound for K_H appear to be in order for this case. Unfortunately, no tested methodology is presently available from the model developers to implement the necessary engineering judgment required in the choice of K_H.

Discussion of Graphical and Statistical Comparisons

In order to provide a more systematic and objective means of evaluating model performance, a set of graphical and statistical comparisons were prepared for the two models. All comparisons of predictions and observed data are made with values above background. Most of the comparisons paired predicted and observed values in space and time. Evaluation of the model/data comparisons in this manner represents the most stringent test of model performance. Considering the modeling difficulties in predicting the correct plume location, it is to be expected that scatter plots of observed and predicted concentrations will be poor (see Figures 5 and 6). Numerous points lie on the axes indicating that either a predicted or observed value was zero. A threshold analysis was used to eliminate points that had both predicted and observed values of zero at a receptor. Note that MESOPUFF has more points on the axes indicative of a thinner plume that is less likely to be present at a receptor.

A frequency histogram of observed and predicted concentrations is given in Figure 7 for MESOPUFF. Although the agreement is reasonable, it should be noted that (a) this is a comparison unpaired in space and time, (b) the large frequency of occurrence in the range 0-10 PCi/m^3 is due to the large number of small values including zeroes in the 0-10 PCi/m^3 range, and (c) approximately 15% of the concentrations exceeding 100 PCi/m^3 are unplotted and are beyond the right side of the graph. These graphs indicate that unpaired statistics should indicate a much more successful model than statistics paired in space and time. Figure 8 presents the frequency histogram of residuals (observed minus predicted values) for MESOPUFF. This graph represents points paired in space and time. The RTM-II plot was similar. The large frequency for concentrations between 0-10 PCi/m^3 is a little deceiving: it represents many observations that were 1, 2, 3 or so in magnitude but with predictions of zero. Moreover, 25% of the residuals are beyond the flanks of the graph. Figure 9 presents the cumulative frequency distribution of predicted and observed concentrations for MESOPUFF, RTM-II, and observations. The large cumulative frequency for 1 PCi/m^3 is not surprising, considering the many pairs where predicted or observed were zero. In this graph, a triplet of points was considered in formulating cumulative frequency curves only if two of the entries (MESOPUFF predicted, RTM-II predicted, observed) were nonzero. The large number of zeroes for MESOPUFF predictions (follows from a thin predicted plume) explains the fact that it has the highest value for cumulative frequency at 1 PCi/m^3. The relative agreement in frequency of predicted and observed values above 100 PCi/m^3 is surprising.

A statistical evaluation of the model/data comparisons was carried out using a subset of the AMS statistics. No formal recommendation was given by AMS on the appropriate statistics for the evaluation of long-range transport models. Suggestions of possible statistics from which an evaluator can choose were made. Presented in Table 2 are several statistics based on a dataset of points for each model paired in space and time. The statistical dataset used as a basis for Table 1 was developed by (a) a threshold analysis eliminating predicted/observed pairs where both values were less than 20 PCi/m^3, (b) an analysis to eliminate outliers using Chauvenet's principle (5 prediction/observation pairs were eliminated from RTM-II and 2 from MESOPUFF), and (c) elimination of any predicted/observed pair from the statistical dataset of one model if the corresponding pair was not present in the statistical dataset from the other model. In (c), we were assured of having the same grouping of observations for both models. Similar choices were made in the Hilton Head Model Validation Workshop.[16] Results in Table 2 reveal poor performance by both models with a better performance with the data by RTM-II. The low correlation coefficients reveal no linear correlation between predicted and observed data; the poor statistical performance of the models is not surprising considering that the predicted plumes are not in the right position with respect to the data. Point by point paired comparisons will necessarily look poor. The application of unpaired statistics to these model/data comparisons is presently being undertaken. The use of unpaired statistics has some merit in a regulatory sense, much less so in a scientific sense.

Conclusions

Five major conclusions may be drawn from the present study.

1. Errors often exist in the direction of the predicted plume. We believe these errors are largely due to the oversimplifications made in

the wind field model MESOPAC. The use of a multi-layer wind field model would appear to be more appropriate.

2. A tendency to underpredict horizontal spreading is evident. This error is probably due to a combination of insufficient plume spread on an hour-by-hour basis and insufficient meander caused by inadequacies in the meteorological preprocessor.

3. The predicted pattern of ground-level concentrations is within an order of magnitude of the data in terms of concentration as a function of distance from the source, only if one is willing to ignore the plume rotation problem.

4. Model performance statistics are poor when points are paired in space and time, due to the errors in predicted plume orientation. Preparation of unpaired statistics are planned for future work as such statistics can be valuable in a regulatory evaluation.

5. The commonly used AMS performance statistics do not permit the separation of the effects of errors of directionality and dispersion. Methods to evaluate statistically the correctness of the ground concentration pattern irrespective of point by point performance are being examined.

Acknowledgments

The authors' research has been funded by the Office of Air Quality Planning and Standards of the U.S. EPA. The authors would like to thank Mr. Doug Stewart and Mr. Ralph Morris of SAI and Dr. Joseph Scire of ERT for their assistance in clarifying the details of development and operation of the RTM-II and MESOPUFF models respectively. We also appreciate the help of Dr. Alan Weber of the Savannah River Laboratory who clarified for us details of the ^{85}Kr experiment and the application of the AMS statistics as used in the Hilton Head Model Validation Workshop.

References

1. Federal Register, "Guidelines on Air Quality Models," 45:20157-20158 (March 27, 1980).

2. M. Yocke, R. Morris, M. Liu, "Revised user's guide to the Regional Transport Model," Publication No. 82120. Systems Applications, Inc., San Rafael, California (April 1982).

3. C.W. Benkley, A. Bass, "User's guide to MESOPUFF (Mesoscale Puff) Model," Environmental Research and Technology, Inc., Concord, Massachusetts, September 1979.

4. C.W. Benkley, A. Bass, "Development of mesoscale air quality simulation models. Volume 6. User's guide to MESOPAC (Mesoscale Meteorology Package)." EPA-600/7-79-XXX, Environmental Research and Technology, Inc., Concord, Massachusetts, September 1979.

5. J. Scire, Environmental Research and Technology, Inc., Concord, Massachusetts, private communication (1983).

6. C.W. Benkley and A. Bass, "Development of mesoscale air quality simulation models. Volume 2. User's guide to MESOPLUME (mesoscale plume segment) model," EPA-600/7-79-XXX, Environmental Research and Technology, Inc., Concord, Massachusetts, September 1979.

7. D.I. Austin, A.W. Bealer, W.R. Goodin. "Random-Walk Advection and Dispersion Model (RADM)," Dames & Moore, Inc., Los Angeles, California, December 1981.

8. I.T. Wang, T.L. Waldron, "User's guide for MTDDIS, Mesoscale Transport, Diffusion, and Deposition Model for Industrial Sources, Report EMSC6062.1UG(R2), Rockwell International, Inc., Creve Coeur, Missouri, December 1980.

9. S.F. Mueller, R.J. Valente, T.L. Crawford, A.J. Sparks, L.S. Gautney, Jr., "Description of the air resources regional pollution assessment (ARRPA) model, Tennessee Valley Authority, Muscle Shoals, Alabama, May 1983.

10. D.G. Fox. "Judging air quality model performance. A summary of the AMS workshop on dispersion model performance. Woods Hole, Mass., 8-11 September 1980." Bulletin American Meteorological Society, 62:599-609 (May 1981).

11. D.B. Turner, Workshop of atmospheric dispersion estimates, U.S. Dept. of H.E.W. Public Health Service, Pub. 999-AP-26, 88 p, (1970).

12. J.L. Heffter. The variations of horizontal diffusion parameters with time for travel periods of one hour or longer. J. Appl. Meteor. 4:153-156 (1965).

13. J.P. Boris, D.L. Book. "Flux-corrected transport - I. SHASTA, a fluid transport algorithm that works." J. Computational Physics 11:38-69 (1973).

14. J. Smagorinsky, General circulation experiments with the primitive equations: I. The basic experiment. Mon. Wea. Rev. 91:99-164 (1963).

15. Air Resources Laboratories. Silver Spring, Maryland. "Measured weekly and twice-daily Krypton-85 surface air concentrations within 150 km of the Savannah River Plant (March 1975 through September 1977) - final report," NOAA technical memorandum ERL ARL-80, (Jan. 1980).

16. M. Buckner, Compiler. "Proceedings of the First SRL Model Validation Workshop (November 19-21, 1980 at Hilton Head, South Carolina)," Report DP-1597, Savannah River Laboratory, Aiken, South Carolina (Oct. 1981).

17. A.H. Weber, M.R. Buckner, J.H. Weber, "Statistical performance of several mesoscale atmospheric dispersion models," J. Appl. Meteorology, 21:1633-1644 (Nov. 1982).

18. J. Scire, Environmental Research and Technology. Concord, Massachusetts, personal communication (July 1983).

19. R. Morris. Systems Applications, Inc. San Rafael, California. Personal communication (July 1983).

20. M.K. Liu, D.R. Durran, "The development of a regional air pollution model and its application to the Northern Great Plains," EPA-908/1-77-001, Systems Applications, Inc., San Rafael, California (July 1977).

21. D. Randerson, "Temporal changes in horizontal diffusion parameters of a single nuclear debris cloud," J. Appl. Meteor. 11:670-673 (1972).

Table 1. Sample Collection Periods and Model Calculational Periods for 10-Hour Samples

Case No.	Sample Collection Periods				Model Calculation Periods			
	Start		End		Start		End	
	Hr	Date	Hr	Date	Hr	Date	Hr	Date
1.	2200	10-05-76	1200	10-06-76	0000	10-05-76	0000	10-07-76
2.	2200	10-14-76	1200	10-16-76	0000	10-14-76	0000	10-17-76
3.	0900	10-29-76	0700	10-30-76	1200	10-28-76	1200	10-30-76
4.	1000	11-18-76	0800	11-20-76	1200	11-17-76	1200	11-20-76
5.	1000	02-02-77	0800	02-04-77	1200	02-01-77	1200	02-04-77
6.	2200	02-16-77	0800	02-19-77	1200	02-15-77	1200	02-19-77
7.	1000	02-22-77	0800	02-23-77	1200	02-21-77	1200	02-23-77
8.	2200	04-05-77	0800	04-09-77	1200	04-04-77	1200	04-09-77
9.	1000	04-11-77	0800	04-16-77	1200	04-10-77	1200	04-16-77
10.	2200	04-17-77	2000	04-22-77	0000	04-17-77	0000	04-23-77
11.	0900	04-27-77	0700	04-29-77	1200	04-26-77	1200	04-29-77
12.	0900	07-11-77	0900	07-12-77	1200	07-10-77	1200	07-12-77
13.	0900	07-15-77	0700	07-16-77	1200	07-14-77	1200	07-16-77
14.	0900	07-18-77	0900	07-20-77	1200	07-17-77	1200	07-21-77
15.	0900	07-25-77	0700	07-27-77	1200	07-24-77	1200	07-27-77

Table 2. Summary of Performance Statistics for MESOPUFF AND RTM-II models (threshold = 20.0 PCi/m^3)

	Mean		Bias (Average)	Standard Dev. of Residuals	Pearson's R
	Obs	Pred.			
MESOPUFF	119 ± 192[a]	141 ± 313[a]	-22 (-90,46)[b]	382 (339,438)[c]	-0.09
RTM-II	119 ± 192[a]	130 ± 248[a]	-10 (-64,44)[b]	298 (265,343)[c]	0.10

[a]Represents one standard deviation from the mean.

[b]Represents confidence limits using one-sample t-test.

[c]Represents confidence limits using chi-square test.

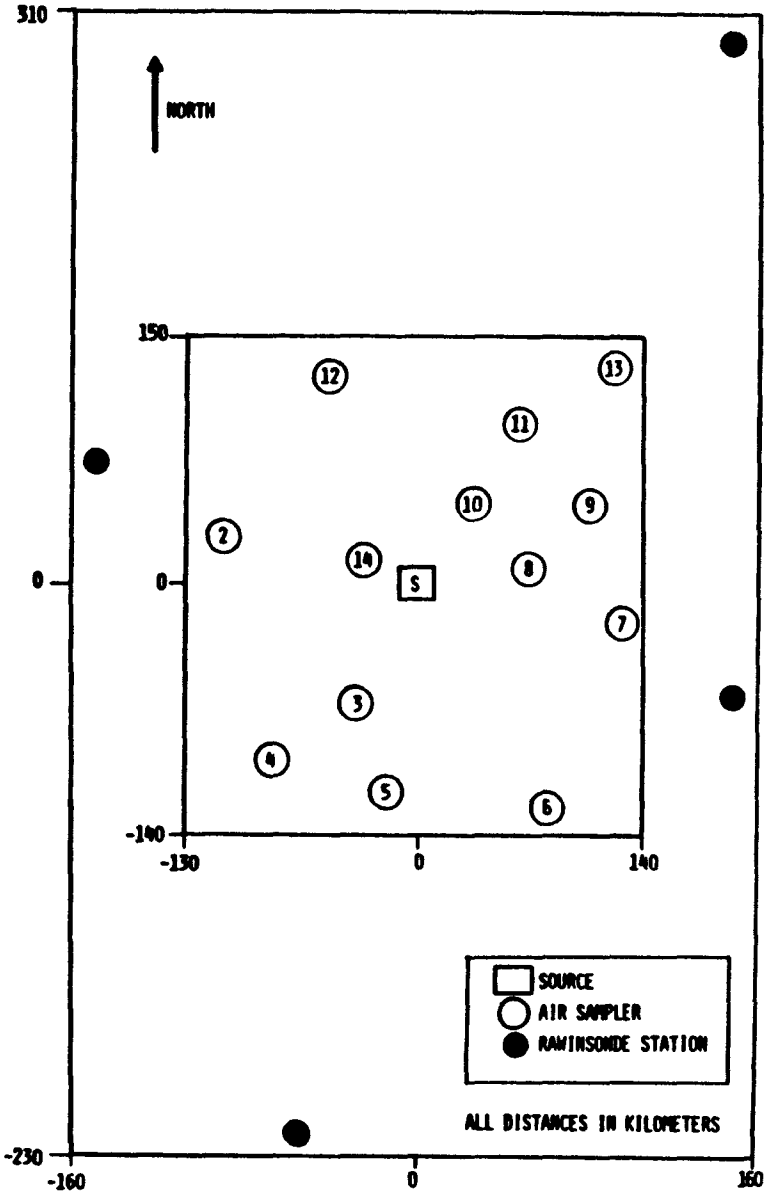

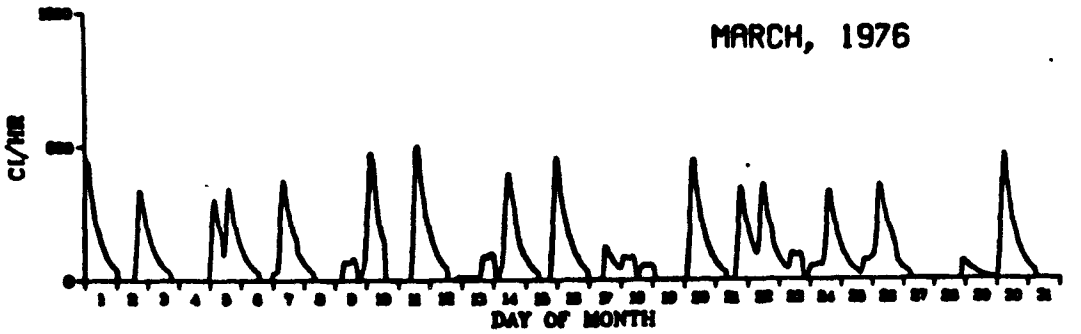

Figure 1. (above) Krypton-85 release rate for March, 1976 (adapted from (15)).

Figure 2. (left) Sketch of vicinity of Savannah River Plant site including the stacks, the 13 receptors, four rawinsonde stations, and the extent of meteorological and plume computational grids.

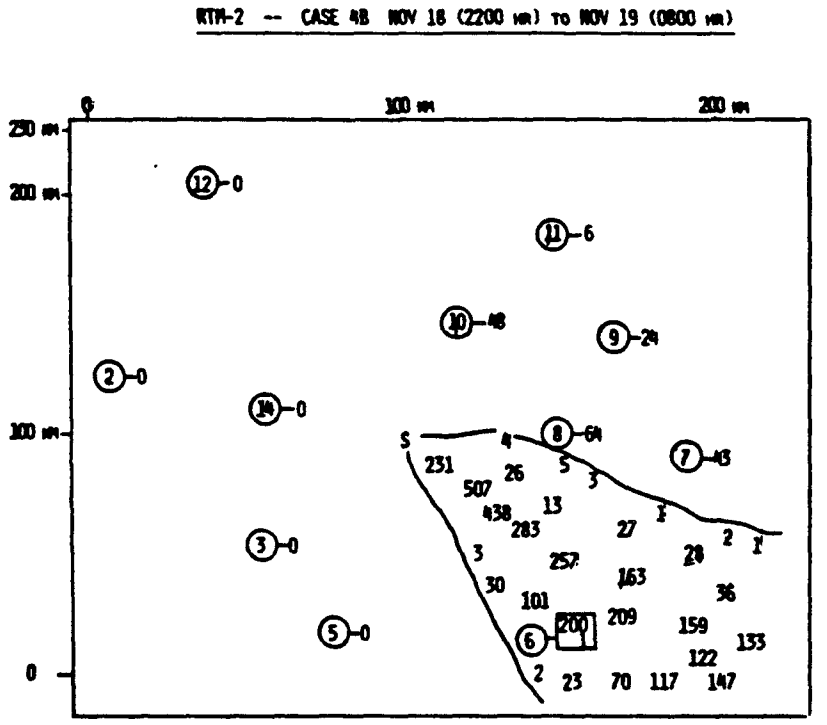

Figure 3. Comparison of 10-hour averages of predicted plume and observed data (in PCi/m^3) for RTM-II on November 18-19, 1976 (2200 Hr to 0800 Hr GMT).

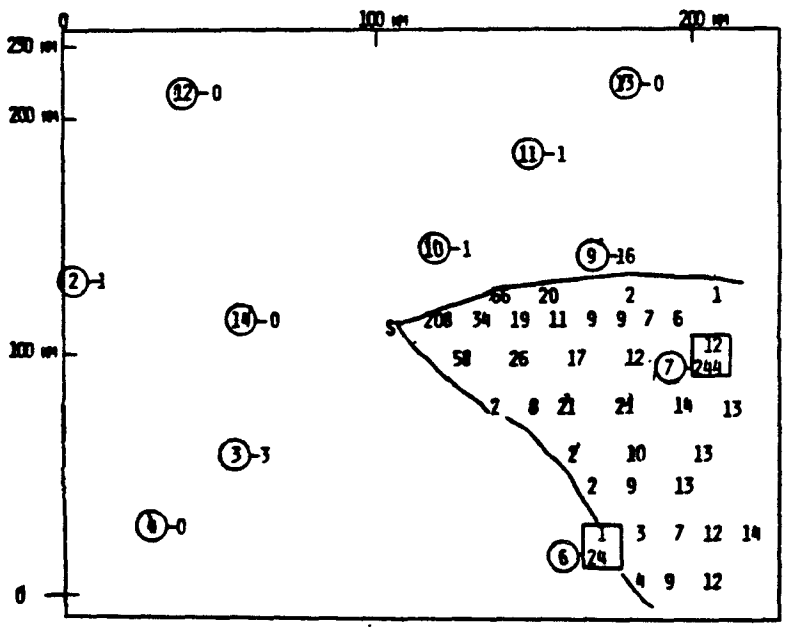

Figure 4. Comparison of 10-hour averages of predicted plume and observed data (in PCi/m^3) for RTM-II on February 17-18 (2200 Hr to 0800 Hr GMT).

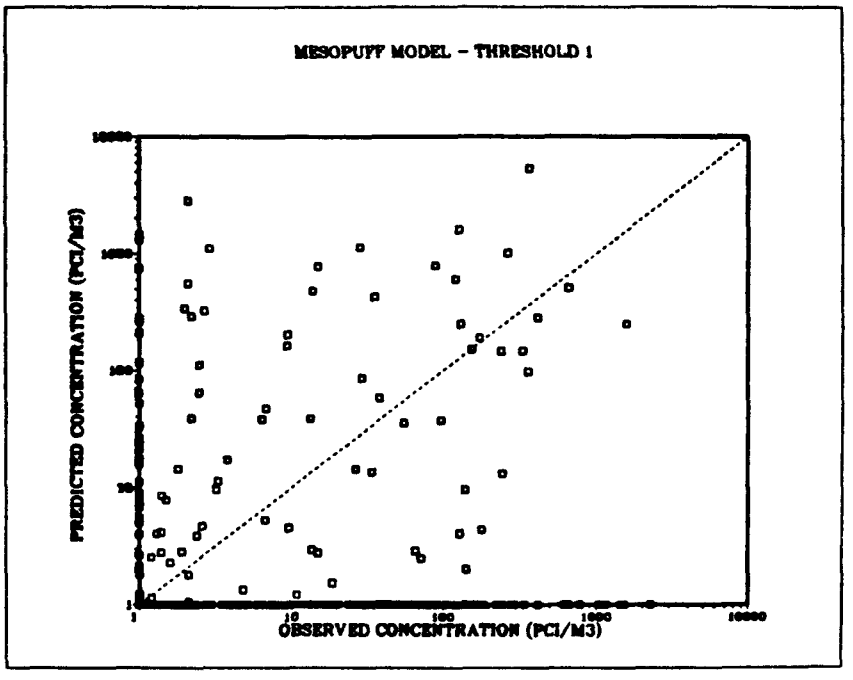

Figure 5. Scatter plots of predicted and observed 10-hr averaged concentrations for MESOPUFF ... Threshold 1 points only.

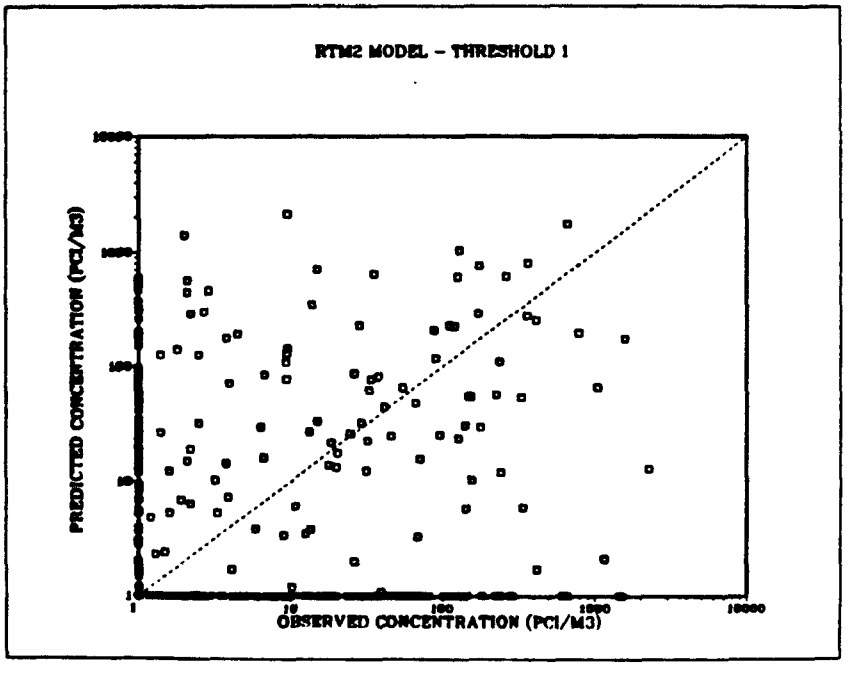

Figure 6. Scatter plots of predicted and observed 10-hr averaged concentrations for RTM-II ... Threshold 1 points only.

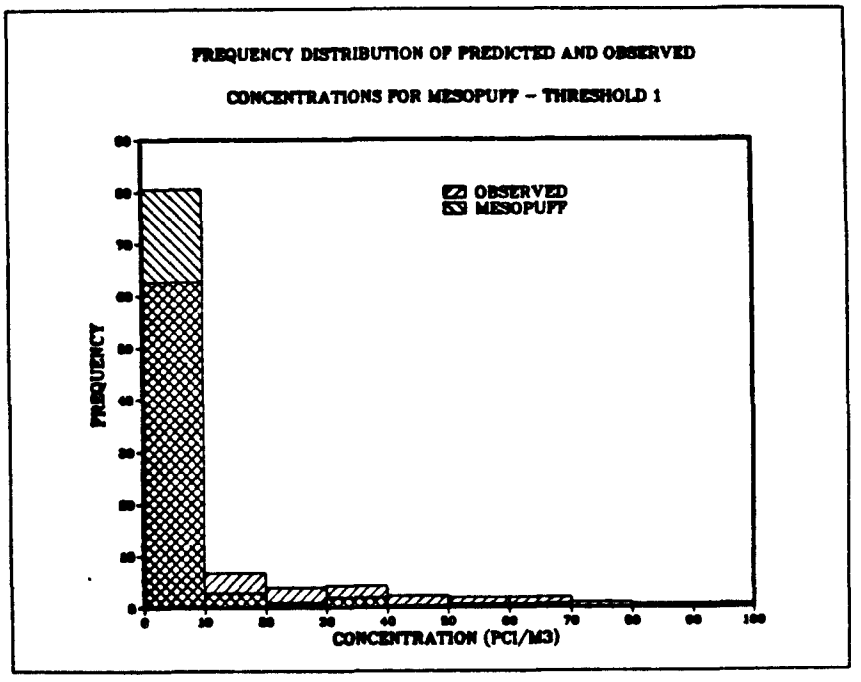

Figure 7. Frequency distribution of predicted and observed concentrations for MESOPUFF ... Threshold 1 points only.

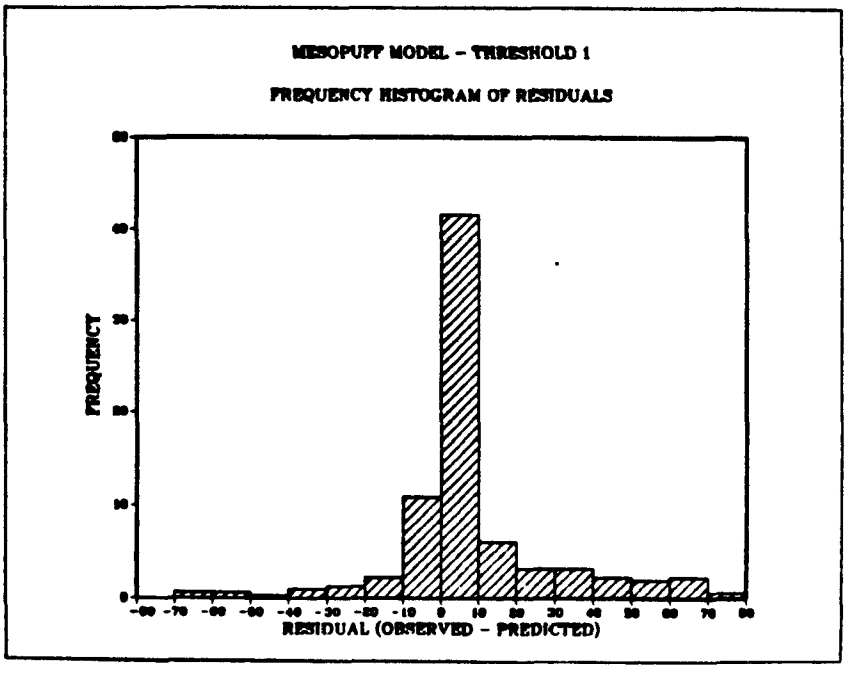

Figure 8. Frequency distribution of residuals for MESOPUFF ...Threshold 1 points only.

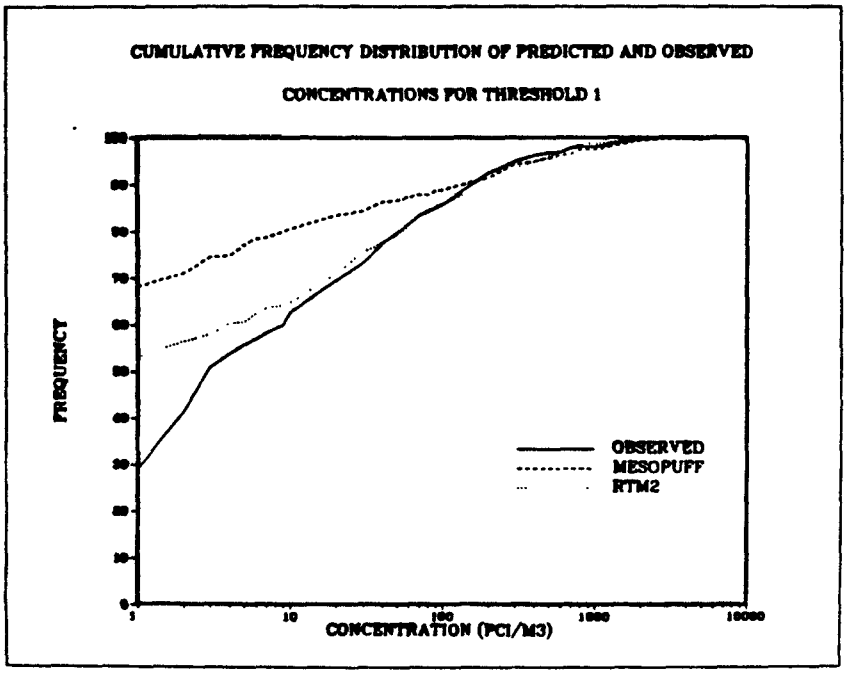

Figure 9. Cumulative frequency distribution of predicted (from MESOPUFF and RMT-II) and observed concentrations ... Threshold 1 points only.

APPENDIX B

CHOICE OF MODEL-SPECIFIC INPUTS*

* Reprinted from "Evaluation of Eight Short-Term Long-Range Transport Models with Field Data, Task I Report: Preparation of Input for Eight Long-Range Transport Models" by A.J. Policastro, M. Wastag, L. Coke, R.A. Carhart, and W.E. Dunn. Prepared by Argonne National Laboratory, Argonne, Illinois, and the University of Illinois at Chicago and Champaign-Urbana, for U.S. Environmental Protection Agency, Office of Air Quality Planning and Standards, Research Triangle Park, NC, January 1985.

INTRODUCTION

Two data bases have been employed in the evaluation of the 8 models; a discussion of these data bases has already been presented in Chapters 3 and 4. This appendix focuses on the model-specific considerations that apply to the Oklahoma tracer study and the Savannah River Plant (SRP) krypton-85 study. While every reasonable effort has been made to utilize exactly the same data base for all models, inherent differences in each model require unique decisions by the user. This appendix treats these issues. As a general rule, codes were modified when feasible to employ all data that were available, and the input parameters have been prepared to anticipate these changes. In some cases, parts of the codes were not relevant to these field cases and were not used; such an example is the chemical conversion and depletion associated with non-passive tracers. Also, choice of control parameters varied among models. The treatment of these issues is now presented for each model.

PART I: DATA BASE SELECTION AND INPUT PARAMETERS FOR THE MTDDIS MODEL

Oklahoma tracer study

The MTDDIS model was developed to handle only elevated releases from industrial stacks. An assumption was made that the single layer wind field is determined from wind speeds and directions at the effective height of release. The precise elevation used to compute the wind speeds and directions is important since surface data are extrapolated to that height using profile laws. The Oklahoma tracer was released from a 1-meter source elevation having effectly no updraft velocity. Since this source height does not represent an elevated source, the model was judged to be inapplicable and therefore no predictions of the Oklahoma study are included in this report. Clearly, 1-m level winds do not represent the wind speeds and directions of released puffs as they travel mesoscale distances. The ANL version of the MTDDIS computer code is, however, capable of running not only the SRP data sets but also the Oklahoma data sets.

Savannah River Plant Krypton-85 Study

Source Information

The source information for the SRP data is only available as an effective single source that has a highly variable emission rate. MTDDIS, like most long range transport models, was designed to predict concentrations from sources having a constant emission rate specified by a single input value. This problem was solved as with the other models by modifying the code to permit the reading of hourly-averaged values for the emission rate. Note, however, that additional changes were required to implement the variable rate in concentration calculations; these modifications are described in Appendix C.

Meteorological Information

MTDDIS originally permitted up to 10 surface stations to be used for meteorological input. As detailed in Chapter 4, meteorological data at SRP were modified when possible to simulate TDF-14 meteorological tapes in an effort to include all available data. The SRP study includes up to 26 surface WBANs, counting the simulated surface stations. The MTDDIS codes were modified to accommodate the additional meteorological station input.

Special considerations were required for the surface data obtained from the meteorological towers. The MTDDIS model requires input of 10-m level wind speeds and directions. Power-law formulas based on stability class are used to derive winds at elevated levels. The simulated data were measured at varying levels. Where 10-m level wind speeds were missing, they were estimated from the next highest available level by applying the 1/7-power law and extrapolating down to the 10-m level. However, recognizing that the 1/7-power law is representative of only neutral stability, provisions were made within the MTDDIS code to re-adjust the 10-m value so that the measured tower reading would be consistent with the stability-dependent power law internal to MTDDIS. This process was crucial for the 62-m level winds measured at the SRP station closest to the source. The code modifications to accomplish this are discussed in more detail in Appendix B.

The modelers' data base for the SRP study contains all available observed data relevant to the 15 selected cases. The support to extract the pertinent data for MTDDIS was included in the master preprocessor developed by ANL. The resulting output files for surface stations (including simulated WBANs) and emission rates become inputs to the MTDDIS codes.

MTDDIS also requires morning and afternoon mixing heights. The model allows input of a dual set of values, one set for user-analyzed values and another set from NCC mixing heights as supplied by NWS. Since most users would not have the expertise to analyze the meteorology, an objective method was preferred. Both inputs were set to the NCC values so that the model would default to NCC mixing heights. The NCC mixing height tape was selected from the available site nearest to the impact area (Charleston, South Carolina).

Spatial and Temporal Grids

The original MTDDIS code was designed to predict the impact for a 24-hour period corresponding to one full calendar day in the local time zone, consistent with the recording of NCC and TDF-14 tapes. The MTDDIS preprocessor code was designed to read 4 contiguous 24-hour periods of meteorological data along with the corresponding morning and afternoon mixing heights. Three morning and four afternoon mixing heights were required by the preprocessor to generate the prediction for a single impact day. These mixing heights were subsequently used with the remaining meteorological data to generate hourly mixing height values using a model-specific algorithm. If the impact day number is labeled day I, the 4-day scenario would be as illustrated below:

Day No.	Surface Data	Mixing Heights	Usage/function
I-2	used as cushion	afternoon only	buffer
I-1	for trajectory computation.	(both morning and afternoon)	trajectory carry-over, (may influence day I)
I	trajectories	both	impact day
I+1	used as cushion	both	buffer

The 15 release periods and corresponding sampling periods are shown in Table 3-6. The single impact day limitation was too restrictive for these cases, and therefore the code was extended to accommodate the larger time periods. As an example, the sample collection period for case number 1 was from 2200 hours GMT on 10-05-76 through 1200 hours on 10-06-76. Since MTDDIS operates using calendar days in Local Standard Time (LST), the MTDDIS modeling period would be from 0000 Hours LST on 10-05-76 through 2300 hours LST on 10-06-76. The extended model scenario fitting this impact period is illustrated as follows:

Day No.	Surface Data	Mixing Heights	Usage/function
10-03-76	used as cushion	afternoon only	buffer
10-04-76	(for computing trajectories)	(morning and afternoon)	trajectory carry-over, (may influence day I)
10-05-76	trajectories	both	impact day
10-06-76	trajectories	both	impact day
10-07-76	used as cushion	both	buffer

MTDDIS distinguishes between the impact region and the region for the meteorological data by permitting an independent specification of each. The spatial grid for concentration calculations was selected as 22 x 24 with a 10 kilometer spacing in both coordinates. Within this grid system, the source at the Savannah River Plant was by definition at the coordinates (11,12). This rectangular grid for concentration predictions is the Mercator projection of the geographical region encompassing the samplers and most of the WBANs. A somewhat larger region was selected for trajectory calculations to encompass all the surface stations.

MTDDIS requires input of the surface roughness at each surface station. The surface roughness at each meteorological station as required by MTDDIS was determined from land use data by using the 0.5 degree grid as discussed below in the description of MESOPAC-II.

WBAN station elevations are also required by MTDDIS. For all but the simulated stations, these values were part of the recorded data. The remaining simulated stations were derived from tower sites. Their elevations were available from a previous SRL study and were obtained through a private communication with Mal Pendergast of the Savannah River Laboratory. The

simulated on-site data was an exception since it was derived from a composite of readings taken from seven various site locations. The effective elevation in this case was taken as the mean value of the seven elevations.

Model-specific Options

The default values for wind velocity profile exponents and wind direction shear coefficients were used. The rationale is that, typically, most users would not have the local values and could not readily obtain them.

MTDDIS provides for user input of deposition-related parameters such as pollutant deposition velocity and half-life. Since krypton-85 tracer is a passive tracer, no deposition should occur. The half-life of krypton-85 is over 10 years, so for practical purposes the depletion due to decay can be disabled. To eliminate the effects, a special option flag was added to the code, and internal logic was added to make the code suppress deposition when the flag is set to a non-zero value. This new feature maintains upward-compatibility while providing the proper simulation for a passive tracer. When the flag is non-zero, deposition-related parameters have no effect regardless of their input values.

PART II: DATA BASE SELECTION AND INPUT PARAMETERS FOR THE ARRPA MODEL

Oklahoma Tracer Study

Source Information

The source information has already been discussed in previous sections. Only one minor modification was necessary for the ARRPA code, this being to permit the input of an hourly emission rate to handle the limited 3-hour source used at Oklahoma. The same hourly rate for emission described above for the MTDDIS model was incorporated into the ARRPA model so that zeroes would be read in for the emission rate before and after the release periods, and the computed average rate would be read in during the three-hour release period.

Meteorological Information

The ARRPA model provides a fully self-contained procedure for meteorological data. The NWS Boundary Layer Model is used to generate the meteorology for the eastern two-thirds of the United States. This region easily contains all of the relevant data for the Oklahoma study. The sample case provided by TVA actually contained the data required for the Oklahoma study of July 1980 and the TVA Meteorological Data Preprocessor Program (MDPP) had already been run successfully to replicate that data in the course of testing a sample case. Therefore, all of the meteorological data required by ARRPA were generated by running the MDPP program.

Spatial and Temporal Grids

July 8 Tracer Release: The first tracer release began at 1900 GMT on July 8, 1980. The start time for meteorological data was selected to be 0500 GMT (0000 CDT) on July 8. Data were measured at the 600 km samplers until 1900 GMT on July 11. To bracket the data, the computation continued through 2300 GMT on July 11. The emission rate was set to zero outside the 3-hour release interval.

July 11 Tracer Release: The second tracer release began at 1900 GMT and continued with a steady emission rate until 2200 GMT on July 11. The sampling was limited to the 100 km arc in this case, and ended at 0400 GMT July 12. To bracket the data, the computation started at 0000 GMT on July 11 and continued through 2300 GMT July 12. The emission rate was set to zero outside the 3-hour release interval.

Model-Specific Options

The ARRPA model was designed to compute the effects of chemical conversion and deposition for sulfur dioxide and sulfate compounds, whereas the Oklahoma tracer study used a passive perflourocarbon PMCH. In order to adjust for these factors, it was necessary to disable the ARRPA features

pertaining to chemical activity and deposition. The PMCH was treated as passive sulfur dioxide and the sulfate emission rate was set to zero. As previously noted, the code was modified to permit an hourly emission rate, and this feature allowed the 3-hour release period to be simulated.

The receptor grid was selected to include the samplers and also to be compatibile for comparison with other model predictions. Initially, a large grid of approximately 800 x 1000 kilometers with a 20 km grid spacing was used, making a 41 x 51 mesh. The lower southwest corner of the grid was taken as 34.34° N, 100.34° W; the top and bottom grid latitudes are 41.53° N and 34.34° N, respectively. The intent of choosing a large grid initially was to avoid any preconception about the plume transport and model predictions.

Savannah River Plant Krypton-85 study

Since the ARRPA model uses the NWS BLM tape for meteorological data, and since the BLM model was not fully operational at the time the 15 SRP experiments were performed (1976-77), ARRPA could not be run with the SRP data.

PART III: DESCRIPTION OF MESOPAC CHANGES AND OPTIONS

The MESOPAC model developed by ERT is a meteorological preprocessor used to provide wind, stability class and mixing height fields for two ERT long-range transport models: MESOPUFF and MESOPLUME. In the previous ANL/EPA evaluation with the krypton-85 data from the Savannah River Plant (see Ref. 23), the MESOPAC model was used to provide input data for both MESOPUFF and RTM-II. In addition, for RTM-II, MESOPAC was modified to incorporate the methods commonly used by SAI for providing horizontal diffusion coefficient and "region top" fields on the computational grid. The horizontal diffusion coefficients were computed as an empirical constant (obtained from scale considerations) multiplied by the deformation of the wind field, and the region top was set equal to the mixing height plus 100 m at each grid point.

The key assumption made in applying the preprocessor, agreed upon by both Mr. Doug Stewart of SAI and Mr. Joe Scire of ERT, was that the wind components to be supplied to MESOPAC would be obtained from the rawinsonde soundings by averaging the reported wind components between the ground and 1500 m MSL. In this integration, the wind measurements at each level are assumed to represent values half way to the next higher and next lower levels. Wind speed, direction and temperature data at a minimum of three levels between the ground and 1500 m are required for a sounding to be considered valid. (MESOPAC does not utilize surface wind data from weather stations; it relies solely on rawinsonde data). During the SRP runs, for most hours, all four rawinsonde stations reported valid data at the required minimum of three levels up to 1500 m MSL. For a small number of hours, only three stations reported valid data, and for only one or two hours were there as few as two stations reporting. MESOPAC handles missing data internally within the code as opposed to MESOPAC II, which requires replacement data (interpolated or translated from nearby stations) to be input for all missing data.

For the Oklahoma experiment, all hours between 12Z on July 7, 1980, and 12Z on July 12, 1980, have data reported for 5 of the 8 rawinsonde sites. At both Oklahoma City and Topeka one of the required soundings was missing (not the same hour at each site). At Salem, Illinois, however, only three of the 11 soundings required were reported.

The 15 Savannah River Plant cases were run with MESOPAC as the meteorological preprocessor providing input to the MESOPLUME model. The two Oklahoma study cases were processed by MESOPAC for MESOPUFF and MESOPLUME. The RTM-II model were given input meteorological data processed by ERT's MESOPAC II model for the two Oklahoma cases.

MESOPAC was run on a 33 by 56 grid for the 15 Savannah River Plant datasets (320 km in the E-W direction and 550 km in the N-S) direction. For the two Oklahoma datasets it was run on a 51 by 41 grid (1000 km in the E-W direction and 800 km in the N-S direction). The grid locations representing the source, samplers and meteorological data sites for both regions were provided using an extension of UTM coordinates for zone 17 (centered at 81.00° W longitude) over the full region for the Savannah River Plant and an extension of UTM coordinates for zone 15 (centered at 93.00° W longitude) over the full region for Oklahoma.

The transformation of wind components from the earth's surface to the UTM system were examined to see if any significant corrections needed to be made to the measured upper air data before input to any of the preprocessor models. Changes resulting from the transformation were compared with the errors inherent in the upper air wind. It was determined that such changes would not be required.

In MESOPAC the option to modify the interpolated wind field to make it divergence-free was not exercised: the time-interpolation option was selected as sinusoidal and maximum afternoon mixing heights were constrained to occur at 2100 GMT (1700 EST) for the Savannah River Plant cases and at 2200 GMT (1700 CST) for Oklahoma.

PART IV: DATA BASE SELECTION AND INPUT PARAMETERS FOR THE MESOPAC II WIND FIELD MODEL

Description of MESOPAC II Options

The MESOPAC II preprocessor is a later version of the MESOPAC wind field preprocessor. MESOPAC is the wind field preprocessor that was used earlier (Ref. 23) by ANL to run MESOPUFF and RTM-II with the Savannah River Plant krypton-85 data base. MESOPAC II has been adopted as the meteorological wind field and mixing height preprocessor for use with MESOPUFF II, RTM-II (Oklahoma study only), and RADM. The model developers of RTM-II and RADM have recommended this choice, since they do not have a meteorological preprocessor with adequate documentation available in a form suitable for use by third parties.

MESOPAC II accepts both rawinsonde and surface station data in standard NCC format, and also reads and processes precipitation data from an NCC tape. Precipitation data are not used in the Oklahoma and SRP computer runs of the models since both data bases involve the dispersion of passive tracers. The following list details the available choices and the decisions made in preparing this preprocessor for use with the Oklahoma and SRP data bases.

(1) Statements have been added to the code to allow the preprocessor to produce wind field data and mixing height data in a format suitable for RADM and RTM-II. The preprocessor's output was already in suitable format for MESOPUFF II.

(2) Changes have been made in dimension statements to accommodate the computational grids selected for both the Oklahoma (41 by 51) and Savannah River (33 by 56) experiments. The preprocessor was originally set up to accommodate at most an array of 40 by 40 grid points.

(3) The READ56 preprocessor of MESOPAC II has been bypassed; this preprocessor reads TDF5600 NCC rawinsonde tapes by using a comprehensive preprocessor (developed by ANL) to provide input to MESOPAC II identical to that which READ56 produces. In handling missing soundings at any station, the next-nearest sounding has been transferred to the station's location for that hour. This is done because MESOPAC II requires twice-daily data from every station. The following READ56 options have been adopted and applied to each rawinsonde sounding:

(a) If both the height and pressure fields were missing, the level was discarded. If either, but not both, were missing, the missing one was supplied by interpolation based on the one present. If, however, either wind data or temperature data were missing at the level, then it was discarded unless it was a mandatory level. The general policy has been to avoid double-interpolation on a level unless it was a mandatory level.

(b) If pressure and height were present and either wind data or temperature data were missing at a level, the missing data was supplied by interpolation between adjacent levels

(c) If the above two decision processes resulted in elimination of a mandatory pressure level, or if a mandatory pressure level was missing altogether, all of the data for the mandatory level were supplied by interpolation on bracketing levels.

(d) The rawinsonde soundings were processed up to and including the 700 mb mandatory level. Under most conditions this occurs at about 3000 m above MSL.

Land use categories at grid points have been obtained from the nearest value recorded on a 0.5 degree grid in both latitude and longitude[55]. The MESOPAC II preprocessor has a default table associating land use categories with average annual roughness heights taken from this report (see Table B-1). The preprocessor was modified to allow use of the seasonal variations presented in Ref. 55.

The surface wind speed height option in MESOPAC II was set to the default of 10 m, which is the actual measurement height at the surface stations. Default values have also been selected for the following variables:

(a) The Von Karman constant -- 0.4

(b) Control variables for input of friction velocity constants -- 4.7 for gamma and 1100 for A (Eqn. 2-21 in User's Guide).

(c) Control variables for input of mixing height constants -- 1.41 for B, 0.15 for E, 200m for the stepsize in z, 0.0010 deg. K/m for the minimum potential temperature lapse rate and 2400 for N. (Eqns. 2-24 through 2-27 in User's Guide).

(d) Control variables for input of wind field variables -- RADIUS=99 grid units, ILWF=2 (vertically averaged winds from ground to mixing height) and IUWF=4 (upper-layer winds averaged from mixing height to 700 mb).

(e) The default table for the reduction factor for solar radiation based on tenths of total opaque sky cover was used as follows:

TENTHS TOSC	FACTOR
0	1.00
1	0.91
2	0.84
3	0.79
4	0.75
5	0.72
6	0.68
7	0.62
8	0.53
9	0.41
10	0.23

(f) Heat flux constant at each grid point -- 0.3 (Eqn. 2-2 of User's Manual)

Table B-1. Surface Roughnesses for Different Land Use Types (in cm)

CAT	SPRING	SUMMER	FALL	WINTER	Description
1	3.	20.	0.5	0.1	Cropland and pasture
2	25.	30.	20.	10.	Cropland, woodland and grazing land
3	2.	5.	0.5	0.05	Irrigated crops
4	90.	90.	90.	90.	Grazed forest and woodland
5	100.	100.	100.	100.	Ungrazed forest and woodland
6	5.	10.	1.	0.1	Subhumid grassland & semiarid grazing land
7	20.	20.	20.	10.	Open woodland grazed
8	30.	30.	30.	15.	Desert shrubland
9	20.	20.	20.	5.	Swamp
10	50.	50.	50.	40.	Marshland
11	100.	100.	100.	100.	Metropolitan city
12	0.01	0.01	0.01	0.02	Lake or ocean

As originally written, the code read the surface data for each station from the appropriate NCC tape in CD-144 format on a different unit. With the ANL-developed preprocessor, the model is provided with surface data in this format. However, with up to 27 surface stations, 27 files would have to be opened at once to run MESOPAC II. This was beyond the capabilities of many computer systems, and of the Ridge computer in particular, which has a limit of opening 19 files at one time. Consequently, all of the surface station data were written for a single hour in sequence in one file in CD-144 format, and the preprocessor was modified to read the records sequentially instead of from separate units.

PART V: DATA BASE SELECTION AND INPUT PARAMETERS FOR THE MESOPUFF, MESOPLUME, MSPUFF, AND MESOPUFF II MODELS

Introduction

The input parameters and input streams for the MESOPUFF, MESOPLUME, and MESOPUFF II models were similar, which may be expected since all three models were developed by the same firm, Environmental Research and Technology (ERT). The MSPUFF model, developed by the North Dakota Department of Health, is based on the MESOPUFF model and likewise, has a similar input stream. Since these four models have a common input parameter list, only one discussion is needed to examine the variables chosen as input to the models.

Computational Considerations

The computational grid was laid out identically for all four models. The Savannah River Plant plume calculations were performed over a 28 X 30 grid with a grid spacing of 10 km, whereas the Oklahoma predictions were made over a 41 X 41 grid with a grid spacing of 20 km. The models all have a basic computational time step of one hour with predicted concentrations presented as averages over one hour periods. Concentrations were predicted at all grid nodal points as well as at pre-selected non-gridded receptor locations.

Decision Points

The following is a list of the most important user decisions made in the choice of input to the models.

(a) All meteorological input values such as wind speed, mixing height and stability fields were updated every hour (basic time step),

(b) Any chemical transformation such as conversion of sulfur dioxide to sulfuric acid and removal of pollutants by dry and/or wet deposition was turned off by an appropriate choice of model input parameters,

(c) A Gaussian vertical concentration distribution was assumed for each puff for MESOPUFF, MSPUFF, and MESOPUFF II with reflection terms considered when appropriate. The other choice of instantaneous vertical mixing of the puffs through the mixed layer was not chosen. This decision was not expected to be a significant one anyway since the closest sampler to the source was a distant 28 km at SRP and 91 km at Oklahoma. Vertical mixing through the mixed layer is expected by then, so either choice should yield essentially equivalent results at the receptors,

(d) For MESOPLUME, the plume has a vertical Gaussian distribution with no constraining lid,

(e) The horizontal and vertical dispersion coefficients that are dependent on PGT stability class are assigned the default values contained in the code, and

(f) For MESOPUFF, MSPUFF and MESOPUFF II, the following scheme was used to determine the number of puffs emitted per hour (puff release rate) and the number of times per hour that puffs would be sampled by the sampling function. These two decisions represent one of the more difficult challenges to the user in setting up model inputs. The methodology used was based on the following observation obtained from model computer runs. It was seen that when adjacent puff centerpoints were separated by 2 sigma-y, then computed concentrations differed by no more than ±2% from concentrations as computed by the models in the limit as puff separation distances go to zero.

The first step was to determine a sigma-y from Turner's curves for stability class F. The sigma-y value is to be evaluated at the distance from the source to the nearest non-gridded receptor. The nearest non-gridded receptor to the source at the Savannah River Plant is 28 km, whereas, the nearest receptor to the Oklahoma source is 91 km. Thus, the sigma-y values were 0.78 km for SRP and 1.9 km for Oklahoma.

The second step was to determine how many puffs to release per hour so that, based on the maximum wind speed for that case, the distance between puff centerpoints was less than two times sigma-y. This procedure insures that adjacent puffs would grow wide enough by the time they reached the first non-gridded receptor to provide enough overlap to simulate a continuous plume.

The puff sampling rate was then chosen manually for each case such that the product of the sampling rate (a model input) and the puff release rate (a model input) was equal to the total number of puffs released per hour as determined from step two. There was an extra degree of freedom here that was up to the user to define. For example, assume that in step two, it was found that 15 puffs per hour was sufficient to cause puff overlapping at the nearest receptor. The sampling rate could be chosen to be 3 samplings per hour with a puff release rate of 5 puffs per hour. Or, the sampling rate could be 5 with a puff release rate of 3. The product of the two should be equal to 15. It does not make much difference with respect to the predicted concentration which value was chosen for the sampling rate or release rate. It has been suggested that the user choose a smaller factor for the puff sampling rate to help minimize computer execution time.

This methodology is not the only way to choose the sampling and release rates. Another way (maybe not the best way) is through trial and error by actually running various combinations of the two parameters until the user finds a pair that gives unchanged predictions as compared to a run with a large number of puffs released per hour (and one sampling rate per hour). The above described in the previous paragraph is believed to be a good way to determine a starting pair of values for the sampling and release rates. It should be emphasized that this methodology requires an estimate of the maximum wind speed that occurs for a given run. This estimate requires execution of the wind field model (MESOPAC, MESOPAC II, or MSPACK). That output was required before specifications of those two parameters. The choices made for

all four models are presented in Table 4-2. As seen from the table, MSPUFF was run with a larger puff release and sampling rate than MESOPUFF, MESOPUFF II, and MESOPLUME. Mr. Steve Weber of the North Dakota Department of Health suggested changes in these parameters since the Oklahoma and SRP data bases were different in temporal and spatial scales from the common application of the model in North Dakota. Suggested were 10 puffs/hr and 10 samplings per hour for the SRP runs and 25 puffs/hr and 25 samplings per hour for the Oklahoma cases. Larger parameter values were recommended for Oklahoma due to the short 3-hour period of release and the short 45-min averaging period for measured ground-level concentrations at the 100-km arc. The combination of 25 puffs/hr and 25 samplings per hour represents nearly the maximum number of puffs that may be contained in the grid at one time. For SRP, the combination of 10 puffs/hr and 110 samplings/hr may still lead to some inaccuracy for samplers in the near field region of the plume.

PART VI: DESCRIPTION OF RTM-II CHANGES AND OPTIONS

This model was included as part of the earlier ANL/EPA study of two long-range transport models and was run for the 15 Savannah River Plant cases (Ref. 20). In this phase of our study of long-range transport models, RTM-II was run for the two Oklahoma tracer experiments. For the new data there were four changes from our previous choices and procedures.

First, the array sizes for the computational grid were modified to accommodate the new grid dimensions used for Oklahoma. The model was not run on the full meteorological grid, and required no buffering of points on the boundary. To include the source and all of the sampler locations required a grid of 35 (x) by 33 (y) with the 20 km grid spacing. This grid runs 640 km north of the source, 600 km east of the source, and 80 km west of the source. No advantage was gained by enlarging the grid farther for this model.

Second, whereas MESOPAC was previously used as the meteorological preprocessor for the Savannah River Plant runs, MESOPAC II was employed for the Oklahoma experiment, as suggested by Mr. Douglas Stewart of SAI. This means that there was an influence of surface wind measurements (in addition to rawinsonde measurements) on the input wind field for the model. With MESOPAC,

only rawinsonde wind measurements averaged over the lowest 1500 meters above sea level entered the computation of the wind field. In running MESOPAC II to obtain RTM-II input, the default option was selected of providing winds averaged from the ground to the mixing height. (For the Savannah River runs, a constant height of 1500 m was used.)

The source has been given dummy exit conditions of 1 m/s exit velocity, a 1 m radius and 45 deg. C exit temperature, with a stack height of 1 m. It was represented as a point source. This insures that a plume rise value is calculated without causing numerical difficulty during model runs. However, immediately after the plume rise was calculated in the code, it was reset to 1 m, which is the actual release height into the prevailing wind. (In the Savannah River Plant cases, the actual exit conditions for the stacks were used.)

Finally, the formula for the horizontal diffusion coefficient used in the application of RTM-II leads to a grid-sized dependent value that varies as the square of the grid interval. Consequently, this coefficient was increased by a factor of four since the grid interval at Oklahoma was 20 km, while that at the Savannah River Plant was 10 km.

PART VII: DESCRIPTION OF RADM CHANGES AND OPTIONS

The RADM model of Dames and Moore, Inc. is a random walk advection and diffusion model for predicting mesoscale transport of air pollutants on an episodic time scale. The model requires surface wind speeds and mixing heights as data input on a meteorological grid. We have chosen this grid to be the same as for the other models for the Savannah River Plant and Oklahoma data bases.

Since the User's Manual was essentially an internal Dames and Moore, Inc. document, and is not intended to present all of the information that an unfamiliar user would need to run the model, a number of decisions and changes had to be made in consultation with Dames and Moore personnel. The most significant problem was the unavailability of the usual meteorological preprocessing programs for providing a wind field and location-dependent mixing heights required as input for RADM. The model developers have

recommended the use of MESOPAC II to provide this input to their model for both the Oklahoma and SRP data bases. MESOPAC II represents a wind field and mixing height model that corresponds most closely to procedures commonly used by Dames and Moore, Inc. for RADM. MESOPAC II was modified at ANL to provide the gridded surface winds required by RADM. RADM extrapolates winds as a function of height internally from the surface wind field. The procedure for processing surface station data and rawinsonde data is discussed in the section on MESOPAC II. The maximum of 8 wind levels between 0 and 1500 m above ground were selected for wind extrapolation to insure the fullest representation of differential transport with height.

Since topographic input data were used only to compute solar radiation values, and considering that the topography for both experiments was reasonably regular, it was decided not to supply topographic data, although it was permitted as one of the available options in RADM. On the other hand, surface roughness values were being supplied at every grid point rather than using a single default average value for all points. The default value of the atmospheric transmission coefficient has been adopted (0.65).

The choice of the initial parcel mass has been based on the User's Manual recommendation that this mass be taken as equal to (total mass released during travel time to the boundary)/5000. Receptor sizes have also been chosen in agreement with User's Manual recommendations with respect to grid intervals at each site.

Other choices that have been made include (a) specification of zero values for pollutant decay rates, deposition height and deposition velocities in order to disable the sections of the code that allow net loss of tracer, (b) specification of the maximum number of parcels contained in the grid as 8500, (c) choice of the default 1000 m maximum horizontal separation and 50 m vertical separation for parcel lumping, (d) selection of 6500 (the default) as the number of parcels that survive after lumping, and (e) choice of 5 as the maximum number of parcels that can be lumped into one.

The RADM computer code was modified to produce concentrations at a regular grid of receptors in order to facilitate model intercomparisons. Array sizes for the meteorological grid have been altered to accommodate the 33 by 56 grid at the Savannah River Plant site and the 41 by 51 grid used for the Oklahoma experiments. The same computational grids as selected for

MESOPUFF II were used, both of which are somewhat smaller than the meteorological grids.

APPENDIX C

DESCRIPTION OF CODE MODIFICATIONS REQUIRED FOR THE EIGHT MODELS*

* Reprinted from "Evaluation of Eight Short-Term Long-Range Transport Models with Field Data, Task II Report: Preparation of Test Cases and Proposed Statistical/Graphical Evaluation Methods (Revised)" by A.J. Policastro, M. Wastag, L. Coke, R.A. Carhart, and W.E. Dunn. Prepared by Argonne National Laboratory, Argonne, Illinois, and the University of Illinois at Chicago and Champaign-Urbana, for U.S. Environmental Protection Agency, Office of Air Quality Planning and Standards, Research Triangle Park, NC, July 1985.

INTRODUCTION

This appendix provides a summary for each model of the changes to the computer codes that were required for application to the Oklahoma and SRP data bases. Each model consists of a meteorological preprocessor and a plume dispersion algorithm that are run in sequence. Table 4-1 provided a summary of the meteorological data needs of each model along with the name of the meteorological preprocessor it requires for the Oklahoma and SRP sites.

Previous work[23] by ANL/UI for the EPA involved the application of MESOPUFF and RTM-II to the SRP data base. No further discussion of those two models with that data base will be given here. Also, one model, ARRPA, can be applied only to the Oklahoma data base. The specialized meteorological preprocessor to the ARRPA model cannot be run for periods earlier than 1978. In addition, a second model, MTDDIS, could be applied only to the SRP data base. The RTM-II Model has employed the MESOPAC meteorological preprocessor for the SRP data base. On the recommendations of the model developers (and within the bounds of the user's manual), a different meteorological preprocessor (MESOPAC II) was used for the Oklahoma cases.

C.1. DESCRIPTION OF MTDDIS MODIFICATIONS

The MTDDIS model consists of three codes, AMMXHT, JHTO, and CONMAP, all of which utilize some FORTRAN IV language features not supported in FORTRAN 77. AMMHXT is a preprocessor program which combines meteorological data from selected sites as extracted from a TDF-14 meteorological tape. It also generates hourly mixing heights from a mixing height tape input based upon algorithms that perform interpolation using the available meteorological data. Information describing the emission sources is also processed by AMMHXT. All data required to make the actual model predictions, except for user input options, are passed by AMMHXT to subsequent programs by means of diskfile transfers. JHTO performs the actual trajectory calculations using the processed meteorological data provided from the output of AMMXHT. Subsequently, JHTO passes data for post-processing analysis to the CONMAP program. The CONMAP program produces concentration output which the user can interpret, including a trajectory plot which is designed for output to a

standard printer.

ANL/UI made three classes of changes to the codes received from Rockwell International, Inc. The first class was to make the codes operational on the ANL Ridge computer, which supports the ANSI X3.9-1978 standard FORTRAN 77 language. The primary objective at that time was that a test case supplied by the modelers could be reproduced as a check that the model was successfully ported. Changes of this type consisted primarily of converting non-standard ENCODE and DECODE statements to internal file conversion methods supported in FORTRAN 77, and conversion of input/output statements to open and close disk files.

The second class of changes was to modify the codes to make them applicable to some special and unique features of the SRP tracer study and to support the use of the modelers' data base as the source of meteorological and emission data. The original AMMXHT program provided support for decoding the character-type data from TDF-14 tape format meteorological data files into usable numeric form. That code version was required to run the benchmark case with its TDF-14 tape data. However, after the benchmark case validation, a different program version was required to access the modelers' data base in order to run the 15 SRP data sets. To assure validity of the working code, a special utility program was written to convert the test case input to the same format that ANL's master preprocessor would produce, then the converted test case was rerun to confirm the new code.

This second class of changes also included support to extend the impact period from one day to a maximum of 5 days, and to extend the maximum number of surface stations from 10 to 26. Many changes in array dimensions were made throughout the codes for these extensions. The logic design was modified in places such as DO loops and some loop algorithms were necessarily redesigned. The modified version also readjusts of wind speed and direction at the 6 simulated tower sites at SRP by employing the actual measurement height in conjunction with the MTDDIS stability-dependent profile laws. The purpose of this readjustment was to correct for the 1/7-power law used in the modelers' data base so that the stability-dependent profile laws within MTDDIS return the actual reference height values. The last step was to add support for features such as time-dependent emission rate and suppression of deposition effects. Fortuitously, these features could be added without sacrificing

upward compatibility, so the final code versions could reproduce the test case as well as all the study cases.

A third (and unexpected) class of changes was required to correct code bugs and logic errors when anomalous results were discovered from examination of the predictions. This last category of changes was by far the most time-consuming because the anomalies often occurred in a subtle way, making it necessary to investigate and thoroughly understand the intended logic of algorithms within the codes. Since the original programmer was not available for consultation, special effort was required from both ANL and Dr. I-Tung Wang of Rockwell International to resolve the problems. Moreover, EPA guidelines for the project did not permit ANL to disclose model/data comparisons to the model developers for the purpose of code checking; as a result, some coding bugs were necessarily resolved by ANL without further assistance. Special measures were employed to insure that all bugs were resolved in the final version by running the codes under debug-testing environments including WATFIV, by inserting and studying internal diagnostic tests within the codes, and by comparing all aspects of the program outputs with actual data. Note, however, that all changes made in the course of debugging were corrections of coding logic only - the MTDDIS model itself remained unaltered. All coding changes were carefully documented in order to record every modification made in the source codes.

C.2. DESCRIPTION OF ARRPA MODIFICATIONS

The ARRPA model consists of 4 programs: HEIGHT, MDPP, ARRPA, and ANALYSIS. Each code was modified to some degree in order to allow the model to properly handle the two Oklahoma datasets. One modification made throughout the set of codes was the expansion of the array of possible receptors for which ground-level concentrations were computed. In order to encompass the large grid of receptors at Oklahoma plus those required by the pattern interpretation method, it was necessary to expand array dimensions to allow up to 2091 receptors as required by a 41 x 51 receptor grid. All arrays associated with receptors were therefore extended from a dimension of 100 to 2091 (this change was not relevant to MDPP). Of this 41 x 51 receptor grid, predictions on a subset, 34 x 34, will be used to compare with other models by

means of the pattern comparison and graphical methods.

The benchmark case provided by TVA was reproduced exactly from the codes supplied after making only a few minor changes to adjust for compiler differences. The revised set of codes have been compiled successfully at ANL on a variety of machines and compilers, including both FORTRAN IV and FORTRAN 77. Users should have little difficulty transporting the codes to a system supporting either language. The code-specific changes are presented below for each program.

The HEIGHT code supplied by TVA was designed to input receptor heights relative to mean sea level and generate the x and y grid points. For the Oklahoma datasets, it was necessary to determine the surface elevations for (a) a rectangular mesh of receptor points generated by ANL/UI to assist in interpreting results later, and for (b) x and y coordinates corresponding to ground-level measurement locations in the experiment. Although the meteorological grid employed by the Boundary Layer Model (BLM) meteorological preprocessor is on a fixed 80 km by 80 km grid, plume predictions can be made on a much finer grid using those predicted meteorological data. The HEIGHT code contains the elevations for each BLM grid point for use in the GRDPTS interpolation subroutine and for use in the code that generates grid coordinates from user input specifications on size and spacing. A simple modification was made to the HEIGHT program to make it generate all receptor mean sea level heights by means of interpolation from known BLM grid point values. In this way, receptor elevations would be compatible with BLM grid point elevations. External input of receptor elevations could have led to inconsistencies between receptor heights and other heights internally defined in the code. The new code version generates the rectangular grid, interpolates to obtain all needed receptor heights, and writes the receptor coordinates to a file which is compatible as input to the revised ARRPA code.

The MDPP code is designed to read meteorological data from a tape file prepared by TVA containing predictions taken from the National Weather Service Boundary Layer Model (BLM). The MDPP code extracts data according to the start and end times specified on user input cards and writes a new data file representing the selected time interval; this MDPP output subsequently becomes the meteorological input data to the ARRPA code. Ideally, only the data required to make a given prediction is extracted, because the data file may

become quite large. However, under circumstances where data are missing, the original MDPP code could miss the exit test. This can happen because the exit test is not performed during interpolation to fill in missing hours. The test in the code compares the current hour read from the BLM data on unit 1 to the user-specified end time, and the processing terminates only if the two were exactly equal. Therefore, if BLM data were missing, the interpolation section of the code could read past the end time without the test being carried out, and from that point the end test could never be met until the end of file was processed. This problem was rectified by simply modifying the test condition. The revised code tests whether the hour associated with the latest BLM data record is either strictly equal to or greater than the final hour of data requested. This modification will have no effect on the actual predictions, but it may in some cases reduce peripheral storage requirements for the unit 2 output file created by the MDPP code.

The ARRPA code was modified to disable the effects of both wet and dry deposition so that the passive perflourocarbon tracer could be simulated correctly. ARRPA was designed to compute concentrations of sulfur dioxide and sulfates as separate quantities. Only one quantity is required for the tracer, so the sulfur dioxide quantity was chosen to represent the tracer. The sulfate emission rate, QSO4, was set to zero in the user input data. Additionally, the deposition velocities for both compounds, VDSO2 and VDSO4, were initialized to zero in the Block DATA statement. Wet and dry deposition computation switches were set to OFF by the user input on unit 5. Consequently, the passive tracer is properly represented in terms of the sulfur dioxide variable in the modified code.

In the Oklahoma experiments, the tracer was released steadily over a 3-hour period and then shut off. The original code assumed a constant emission rate as specified by the input variable QSO2. The code was modified to implement a time-dependent source by introducing the function QSO2FN. The function provides a release rate for each hour of the run. In the modified code, each initial plume segment released from the source now contains an amount of tracer according to the release rate assignment QSO21(1) = QSO2FN(hour), instead of QSO21(1) = QSO2. A user may define a new QSO2FN routine as any arbitrary function as he wishes for each run, but the version suitable for the Oklahoma data base is coded to return the constant rate QSO2

during the three-hour time interval of release and zero at all other times. The user specifies the hour, day, and year that the non-zero emission is to start and end; as part of model input this specification is made as one additional unit 5 card. This input could also include the variable QSO2, which is now taken as the emission level during the release interval. The additional emissions input is passed to the function QSO2FN via the /ONOFF/ COMMON block in the revised code.

Several other small changes were made to the ARRPA code. The functions ARCOS and ARSIN were renamed to the generic FORTRAN 77 standard names, ACOS and ASIN, respectively, so that the code would be portable to systems using FORTRAN 77. A provision was added to allow the user to input receptor coordinates directly from a file on unit 3. This input option is selected by setting the variable ITYPE to 2 on the user input card. When ITYPE=2, the code reads in the receptor data using list-directed input compatible with the output generated by the revised HEIGHT code. This makes it convenient to enter arbitrary receptor coordinates for up to 2091 receptors without being limited to the existing grid generation algorithms in the ARRPA code. Some additions were made to SUBROUTINE CHIGAU to prevent division overflow in computing CSUM2 in case either QOU or QOU1 is small.

The only major changes to the ANALYSIS program were the array dimension changes noted previously. However, the concentration data from the ARRPA output on unit 14 which was being read on unit 1 by ANALYSIS was changed to unit 14 for consistency, so that both codes refer to the same unit number. Also, the grid points are now printed to show both linear ordering and coordinate x-y numbering. These changes have no effect on the actual predictions.

C.3. DESCRIPTION OF MESOPAC (METEOROLOGICAL PREPROCESSOR) MODIFICATIONS

The MESOPAC preprocessor required very few modifications in order to enable that code to run under ANSI standard FORTRAN 77. The only necessary changes to assure compatibility with ANSI standard FORTRAN 77 were the insertion of the OPEN statements that define the input/output files.

MESOPAC dimension statements in the code were then expanded to enable the

code to run with the Savannah River Plant and Oklahoma meteorological grids. Arrays such as U,V, and H were dimensioned large enough to handle both the 33 x 56 Savannah River Plant meteorological grid and the 51 x 41 Oklahoma meteorological grid.

Correct operation of the MESOPAC code on the Ridge 32 minicomputer was assumed by running Case No. 1 (of the 15 total) of the Savannah River Plant and comparing the predictions with earlier results done on the IBM mainframe. A benchmark case provided by ERT, Inc. had already been run successfully on the IBM mainframe with excellent agreement with the output provided by ERT.

Logic was added in MAIN and SUBROUTINE NEWMET so that the user would have the option to output only a portion of the meteorological grid to the unformatted disk file via logical unit 2. (This is the file that is input into the MESOPUFF and MESOPLUME models.) The READ statement in MAIN for user input card number 6 was modified to read in four additional variables, ISTART, ISTOP, JSTART, and JSTOP. These variables define the extent of the meteorological subgrid in the x any y directions that is required for output. These values default to the full meteorological grid defined by IMAX and JMAX if left blank or zero. The WRITE statements in SUBROUTINE NEWMET that print out the meteorological grid variables were modified to incorporate the subgrid delineation variables, ISTART, ISTOP, JSTART, and JSTOP. Two integer switches were added to permit on option of suppressing the mixing height and/or stability class output files. These files are large and are not required for examination in all runs. This option helps maximize the utilization of the 142 Mb disk on the Ridge computer.

C.4. DESCRIPTION OF MESOPUFF MODIFICATIONS

The MESOPUFF Model was run previously for the fifteen Savannah River Plant datasets on the IBM mainframe at Argonne. In order to make the model operational on the Ridge 32 mini-computer with its FORTRAN 77 compiler, a few coding changes were required. The major change involved the editing of the user input routine, INPARM, and the file manager routine, FILMAN.

Standard ANSI FORTRAN does not allow input in the form of a NAMELIST, so

all the input statements in SUBROUTINE INPARM had to be rewritten using list-directed READs with FORMAT statements that describe the data input stream. Statements were added after every READ statement in SUBROUTINE INPARM to verify that input variables were within reasonable ranges and to set them equal to default values if the user did not supply them in the input stream. Statements were also added to output the input stream to a line printer in order to facilitate the checking of input variables. In this way, the intent of the NAMELIST statement could be preserved.

The direct access READ and WRITE statements in SUBROUTINE FILMAN had to be edited to conform to ANSI standard FORTRAN 77. The argument list of a direct access READ and WRITE statement requires more information in ANSI standard FORTRAN 77 than was provided. For example, READ (50'1) had to be changed to READ (UNIT=50,REC=1) and WRITE (15'INUMB) was changed to WRITE (UNIT=15,REC=INUMB). Although the file-management system will not be used, the corrections were needed to achieve an error free compilation. Also, OPEN statements were added to define and direct the input and output flow.

The model had to be further modified to accept the Oklahoma datasets. Every array such as XMET, YMET, U, V and HHM, dealing with the meteorological, computational, and receptor grids in MESOPUFF had to be assigned new dimensions in order to handle the 51 x 41 Oklahoma grid. The dimensions of the arrays, XRES and YRES, pertaining to receptors that were not part of the grid, had to be increased also because the number of receptor locations employed in the Oklahoma experiment exceeded the number allowed for in the code as received by ANL.

Modifications were made to SUBROUTINE WRITER to obtain the predicted concentrations in units of parts per 10^{15} for receptors located at both grid and non-grid positions. These results are then written to a disk file to be used later as input into the statistical and graphical programs.

An error routine had to be added to correct underflow conditions that were created on the Ridge with calls to the FORTRAN exponentiation function EXP. The calculated exponent was often beyond the lower limit for real numbers on the Ridge and an underflow error would be produced. The error routine corrects this problem by setting the EXP function value to zero.

The benchmark case provided for the MESOPUFF Model was run and checked on

the IBM mainframe at Argonne in the summer of 1983 with excellent agreement between ANL predictions and the ERT prepared computer run. The model was checked out on the Ridge 32 with that benchmark case as well as with the first of the 15 SRP datasets. The output from the Ridge run matched the IBM output for these two cases with only very minor differences in the output caused by the differences in accuracy of the floating point arithmetic between the two machines.

Care was taken in all the modifications made so that the MESOPUFF Model would be entirely in ANSI standard FORTRAN 77. In this way, the model would be easily transportable, and could be implemented in its current form on virtually any computer.

C.5. DESCRIPTION OF MESOPLUME MODIFICATIONS

The MESOPLUME benchmark case provided with the code from ERT, Inc. was run and checked on the Ridge computer to verify that the code was operating properly on the Ridge. The output produced on the Ridge matched the output of the same case listed in the user's manual with minor differences in the results that could be accounted for by differences in the accuracy of the floating point arithmetic between the two machines used to generate the runs.

Standard ANSI FORTRAN does not allow input in the form of a NAMELIST, so all the input statements in SUBROUTINE INPARM had to be rewritten using list directed READs with FORMAT statements that describe the data input stream. Statements were added after every READ statement in SUBROUTINE INPARM to verify that input variables were within reasonable ranges. Logic was also added to set parameters equal to default values if the user did not supply them in the input stream. Statements were also added to transmit the input stream to the line printer to facilitate the checking of input variables. In this way, the intent of the NAMELIST statement could be preserved.

The direct access READ and WRITE statements in SUBROUTINE FILMAN had to be edited to conform to standard ANSI FORTRAN. The argument list of a direct access READ and WRITE statement requires more information in ANSI FORTRAN than was provided. For example, READ (50'1) had to be changed to READ (UNIT = 50, REC = 1) and WRITE (15'INUMB) was changed to WRITE (UNIT=15,REC=INUMB).

Although the file management system set up in MESOPLUME is not useful in the present application to the SRP and Oklahoma datasets, changes were required, in any case, to achieve an error-free compilation. Also, OPEN statements were added to define and direct the input and output flow.

A major modification that had to be made to the MESOPLUME Model in application to the Savannah River Plant and Oklahoma datasets was the redimensioning of all arrays associated with the meteorological, computational, and sampling grids. Arrays such as U, V, HHM, and MSTAB were dimensioned large enough to handle both the 33 x 56 Savannah River Plant grid for the 15 SRP cases and the 51 x 41 for application to the Oklahoma grid. The arrays that contained information at receptors that were not at grid locations, such as XRES and YRES, had to be expanded in order to handle a greater number of receptors than was originally set up in the code.

MESOPLUME was altered to accept hourly input of the source emission rate by switching the definition of the emission rate array element, EMISS(2), with the definition of the emission factor array, ECYCLE (2,N) where N could vary between 24 and 168 depending upon the dataset. The original array EMISS(2) represented constant emission rates for SO_2 and SO_4 respectively. For SRP and Oklahoma, EMISS(1) = 1.0 representing the tracer and EMISS(2) = 0.0. The array ECYCLE(2,I) provided hourly emission rates. Emission rates are given by ECYCLE(1,I) with I=1,N where N is the number of hours in the run. Zero emission rates were given for SO_4 by means of ECYCLE(2,J) = 0.0 where J=1,N. ECYCLE has the emission rates read into it on an hourly basis from the user input stream before the start of the run. The dimension of the array ECYCLE was suitably determined so that it could handle the total number of hours for any run.

Statements were added to SUBROUTINE WRITER to convert the predicted concentrations at the grid and non-grid receptors into proper units for comparison with observations. These predicted concentrations are converted to pico-curies/cubic meter for the Savannah River Plant and to parts per 10^{15} for Oklahoma. They are then written out to a disk file for later processing by the statistical and graphical programs.

An error routine had to be added to correct underflow conditions that were created by the Ridge with calls to the FORTRAN exponentiation function EXP. The calculated exponent was often beyond the lower limit for real

numbers on the Ridge and an underflow error would be produced. The error routine would correct this problem by setting the EXP function value to zero.

Care was taken in all the modifications made so that the MESOPLUME Model would be in ANSI FORTRAN 77. In this way, the model could be easily transportable and could be easily implemented on virtually any computer.

C.6. DESCRIPTION OF MSPACK (METEOROLOGICAL PREPROCESSOR) MODIFICATIONS

A major modification that had to be made to the MSPACK meteorological preprocessor in application to the Savannah River Plant and Oklahoma datasets was the re-dimensioning of all arrays associated with the meteorological grid. Arrays such as U, V and H were dimensioned large enough to handle both the 33 x 56 SRP grid and the 51 x 41 Oklahoma grid.

In addition, statements were added to MSPACK that would produce a subgrid, if desired, of the predicted meteorological variables as input into MSPUFF if the meteorological grid is chosen to be smaller in MSPUFF than it is in MSPACK. The READ statement in MAIN for user input card number 6 was modified to read in four additional variables, ISTART, ISTOP, JSTART, and JSTOP. These variables define the extent of the meteorological subgrid in the x and y directions. These values default to the full meteorological grid defined by IMAX and JMAX if left blank or zero. The WRITE statements in SUBROUTINE WMET that print out the meteorological grid variables were modified to incorporate the subgrid delineation variables, ISTART, ISTOP, and JSTART, and JSTOP.

A benchmark case provided by North Dakota Department of Health was run successfully on the Ridge minicomputer. Model predictions were very close to those presented in the user's manual for the same case with differences attributable to the accuracy of the floating point arithmetic between the two machines.

C.7. DESCRIPTION OF MSPUFF MODIFICATIONS

The same benchmark case used to verify the operation of MSPACK was used

to test the operation of MSPUFF on the Ridge minicomputer. Predictions agreed with the values in the user's manual within differences due to floating point operations on the different computers.

ANSI standard FORTRAN 77 does not allow input in the form of a NAMELIST, so all the input statements in SUBROUTINE INPARM in MSPUFF had to be rewritten using list-directed READs with FORMAT statements that describe the data input stream. Statements were added after every READ statement in SUBROUTINE INPARM to verify that input variables were within reasonable ranges and to set them equal to default values if the user did not supply them in the input stream. Statements were also added to transmit the input stream to a line printer in order to facilitate the checking of input variables. In this way, the intent of the NAMELIST statement could be preserved.

The direct access READ and WRITE statements in SUBROUTINE FILMAN had to be edited to conform to ANSI standard FORTRAN 77. The argument list of a direct access READ and WRITE statement requires more information in standard FORTRAN than was provided. For example, READ (50'1) had to be changed to READ (UNIT=50,REC=1) and WRITE (15'INUMB) was changed to WRITE (UNIT=15,REC=INUMB). Although the file management system in MSPUFF will not be used, corrections were needed to achieve an error-free compilation. Also, OPEN statements were added to define and direct the input and output flow.

The MSPUFF Model also had to be modified to accept the Savannah River Plant and Oklahoma datasets. Every array, such as U, V and HHM, dealing with the meteorological, computational and sampling grids in MSPUFF had to be assigned larger dimensions in order to handle both the 33 x 56 Savannah River Plant and the 51 x 41 Oklahoma grids.

MSPUFF was altered to accept hourly input of the source emission rate by switching the definition of the emission rate array element, EMISS(2), with the definition of the emission factor array, ECYCLE(2,N) where N could vary between 24 and 168 depending upon the datasets. The original array EMISS(2) represented constant emission rates for SO_2 and SO_4 respectively. For SRP and Oklahoma, EMISS(1) = 1.0 representing the tracer and EMISS(2) = 0.0. The array ECYCLE(2,I) provided hourly emission rates. Emission rates for the tracer are given by ECYCLE(1,I) with I=1,N where N is the number of hours in the run. Zero emission rates were given for SO_4 by means of ECYCLE(2,J) = 0.0 where J=1,N. ECYCLE has the emission rates read into it on an hourly basis

from the user input stream before the start of the run. The dimension of the array ECYCLE were determined so that it could handle the total number of hours for any run.

Statements were added to SUBROUTINE WRITER to obtain the predicted concentrations at the grid and non-grid receptors. These predicted concentrations were converted to pico-curies/cubic meter for Savannah River Plant and parts per 10^{15} for Oklahoma. These are then written out to a disk file for later processing by the statistical and graphical programs. Also, SUBROUTINEs TOPLOT and RDAY were added to convert predicted concentrations for all receptors at grid points to the units given aboves, and to write them out to a second disk file for later processing.

An error routine had to be added to correct underflow conditions that were created on the Ridge with calls to the FORTRAN exponentiation function EXP. The calculated exponent was often beyond the lower limit for real numbers on the Ridge and an underflow error would be produced. The error routine would correct this problem by setting the EXP function value to zero. MSPACK did not require this routine; only MSPUFF needed this modification.

Care was taken in all the modifications made so that the MSPACK preprocessor and the MSPUFF Model would be entirely in standard ANSI FORTRAN 77. In this way, the preprocessor and the model would be easily transportable and could be implemented on virtually any computer.

C.8. DESCRIPTION OF MESOPAC II (METEOROLOGICAL PREPROCESSOR) MODIFICATIONS

A MESOPAC II benchmark case provided by ERT, Inc. was run on the Ridge computer to verify that the code was working properly. The output produced on the Ridge matched the output listed in the user's manual with minor differences that could be explained by the differences in floating point arithmetic between the two machines.

The first type of modification made to MESOPAC II permitted the code to run in ANSI standard FORTRAN 77, rather than in FORTRAN IV as originally provided. OPEN statements were inserted for all input and output files, and

the handling of character and logical data was changed.

Several FORTRAN IV variable type declaration statements had to be changed. Standard ANSI FORTRAN 77 does not allow initialization of a variable on the same line that declares the type of the variable or the dimension of an array. DATA and assignment statements were used to modify the lines as required.

Constants like XMIN and XMAX had to be reassigned new values because the original assignment statements had numerical values that were either too small or too large to fit the numerical range of the Ridge. XMAX was set equal to -10^{-25} instead of -10^{-75} and XMIN was set equal to 10^{25} instead of 10^{75}.

The READ statement for the CD144 meteorological data was altered so it would not contain the array, IPREC, in the input list. Both krypton-85 and perfluorocarbons are passive tracers, and precipitation data (as an example) are not used. The FORMAT of the READ statement for SUBROUTINE GETDAT was thereby modified because the data file is being provided to the model in a more compact form (due to fewer variables being read in) than the CD144 format used by the NCC.

The dimensions of all arrays representing data on the meteorological grid were changed from 40 x 40 to 51 x 56. The minimum required dimensions where 51 x 41 for the Oklahoma datasets and 33 x 56 for the Savannah River Plant datasets. The number of surface stations permitted (25) and the number of upper air stations permitted (10) in the original code, as well as the number of levels in each sounding permitted (79) were all adequate for the Oklahoma data. That data base has 24 surface stations, 8 upper air stations and no more that 38 levels in any single sounding. The Savannah River Plant datasets have 26 surface stations, 4 upper air stations and no more than 30 levels in any single sounding, so the dimension of arrays relating to surface stations had to be increased to 26.

In the code as originally supplied by ERT, the hourly data for each surface station was read in on a separate unit (or "file number"). The data for each upper air station was also read in on a separate unit. Thus, one would have to open more than 24+8=32 units to run the Oklahoma cases, and 26+4=30 units to run the Savannah River Plant cases. The Ridge has a limit of 19 on the number of simultaneous units (or "files") that can be opened. A

separate unit was maintained for each of the upper air stations, but all of the surface station data (CD144 format) was combined into a single file, with all available stations for a single hour occurring together.

A set of 10 integer switches was installed to allow for subsets of the massive gridded output data from MESOPAC II to be printed out. For most runs only values of two wind components and of the mixing height need to be shown. The code, as supplied, also prints out hourly gridded values at grid points of two other wind components, the surface wind speed, the boundary layer height, the friction velocity, the convective velocity scale, the Monin-Obukhov length and the PGT stability class. This massive output would be wasteful and difficult to process, especially considering the large grids being used. With the switches, a variety of printed output options can be selected. In addition, a section has been added to the code, applicable mainly to the Savannah River Plant data cases (which span all four seasons), that computes the surface roughness lengths as a function of season from the available values of the land-use category.

A section of code was installed in subroutine OUTHR to provide hourly meteorological data at the grid points for RTM-II and RADM. The required grid values are written out in binary files with unformatted WRITE statements to save machine storage space. The nature of these files for RTM-II for the Oklahoma datasets (provided on a 34 x 34 grid that is a subset of the full meteorological grid) is as follows:

(i) Layer 1 wind components are written to the MDF file, having been computed as an average from the ground up through the mixing height.

(ii) The exposure class is also written to the MDF file. Exposure class is closely related to PGT stability class, and is computed from it and the wind speed.

(iii) The horizontal diffusion coefficient is written to the HDFSN file. It is computed as a constant BETA times the "deformation" of the wind field, but is constrained to lie between specified maximum and minimum values, KHMAX and KHMIN. For the Oklahoma cases, the values of BETA, KHMAX and KHMIN were multiplied by $(20km/10km)^2 = 4$, since the relationship between wind field

deformation and K_H supposed to be proportional to the square of the grid step size. The grid size is 20 km for the Oklahoma cases and 10 km for the SRP cases; in this way, values for the SRP cases determined in the earlier model validation work (Ref. 18), are being adjusted for the Oklahoma site.

(iv) The mixing height is written to the MIXHT file.

(v) The region top is computed as the maximum mixing height over the grid at the current hour plus 100m, and is written to the RGNTP file.

The files that are computed and written to disk for the RADM Model are the following:

(i) Grid values (51 x 41 for Oklahoma and 33 x 56 for SRP) of the lower layer wind components are written to the file RADMWF, having been computed as an average from the ground up through the mixing height.

(ii) Grid values (51 x 41 for Oklahoma and 33 x 56 for SRP) of the mixing height are written to the file RADMHTM. These values are used also as a reference height for the computation of "surface" wind values. The code as supplied by Dames & Moore uses a single reference height, but this has been modified to use a gridded reference height set equal to half of the mixing height at each grid point. The discussion of the computation of "surface" wind values is given in Part XI.

(iii) Grid values (51 x 41 for Oklahoma and 33 x 56 for SRP) of the surface roughness length are written to a file denoted RADMHTR.

(iv) Average values of cloud ceiling, the potential temperature gradient in both the mixing layer and in the inversion, the total opaque sky cover, the PGT stability class, and the surface temperature are written to various diskfiles.

C.9. DESCRIPTION OF MESOPUFF II MODIFICATIONS

The MESOPUFF II benchmark case provided by ERT, Inc. was run on the Ridge computer to verify that the code was working properly. The output produced on the Ridge matched the output listed in the user's manual with minor differences that could be explained by the differences in floating point arithmetic between the two machines used to generate the runs.

All MESOPUFF II revisions sent from ERT, Inc. through EPA during the past year were included in the code with a test run made to insure an error free run after each set of additions was implemented. Three revisions were sent in October 1984, February 1985, and May 1985.

A major modification that had to be made to the MESOPUFF II Model in application to the Savannah River Plant and Oklahoma datasets was the redimensioning of all arrays associated with the meteorological, computational and sampling grids. Arrays such as US, VS, UUP, and VUP were dimensioned large enough to handle both the 33 x 56 Savannah River Plant grid and the 51 x 41 Oklahoma grid. The arrays that contained the CD144 meteorological data had to be re-dimensioned to accept all the surface stations. Arrays such as PAMT, TEMPK and IRH were enlarged to handle the 26 surface stations for the Savannah River Plant datasets.

Several FORTRAN variable type declaration statements had to be changed. Standard ANSI FORTRAN 77 does not allow initialization of a variable on the same line that declares the type of the variable or the dimension of the array. DATA statements and assignment statements were used to modify the lines where needed.

The constant, DMIN2, used in MAIN, SUBROUTINE WET, and SUBROUTINE FINDOZ had to be reassigned the value of 10^{30} because the original assignment of 10^{50} was beyond the computer's numerical range. Likewise, the constants, XMIN and XMAX, in SUBROUTINE OUT had to be reassigned numerical values with exponents +30 and -30, respectively, instead of +75 and -75.

MESOPUFF II was altered to accept an hourly input of the source emission rate by expanding the emission rate array, EMIS. EMIS is now a two-dimensional array with the first index representing the pollutant (only the first index is used for SRP and Oklahoma, representing the tracer) and the second

index indicating the particular hour in the day. Input subroutine INPARM was modified to read in the source emission rate on an hour by hour basis. Every statement in the code containing the variable, EMIS, was modified to account for the new index.

Statements were added in MAIN to convert the units of the predicted concentrations at both the grid and non-grid receptors. As noted in Chapter 1, the predicted concentrations were converted to pico-curies/cubic meter in the Savannah River Plant computer runs and to parts per 10^{15} in the Oklahoma computer runs. These predicted concentrations are then written to a disk file for later processing by the statistical and graphical programs.

An error routine had to be added to correct underflow conditions that were created on the Ridge with calls to the FORTRAN exponentiation function EXP. The calculated exponent was often beyond the lower limit for real numbers on the Ridge and an underflow error would be produced. The error routine would correct this problem by setting the EXP function value to zero. Care was taken in all the modifications made so that the MESOPUFF II code would be in ANSI standard FORTRAN 77. In this way, the model would be easily transportable and could be easily implemented on virtually any computer.

C.10. RTM-II MODIFICATIONS (OKLAHOMA ONLY)

In order to run the RTM-II model on the Ridge computer, a number of changes had to be made. Differences between the ANSI standard FORTRAN IV language in which the code was provided by SAI and the ANSI standard FORTRAN 77 language available on the Ridge had to be resolved. This included adding OPEN statements for input and output files. It also required changing how character and logical variables were treated.

The first Savannah River Plant case (previously run on the IBM mainframe) was rerun on the Ridge computer to verify that the model was properly modified to run on this computer. Predictions were compared to those obtained on the IBM mainframe during the summer of 1983. The small differences noted were consistent with the differences between the IBM mainframe and the Ridge mini-computer in single precision arithmetical accuracy.

Proper units were obtained for output concentrations as indicated in Chapter 1. For the Savannah River Plant datasets, the relative factor of 10^{-6} (conversion factor between micro- and pico-curies) between input and output units required no changes to the emissions as read in or to the concentrations provided as output except for proper labeling. For the Oklahoma datasets, the simplest way to achieve proper output concentration units was simply to multiply emission rates by the factor 9.03×10^5 immediately after they were read in. Printed labels were changed accordingly.

Labeling of a variety of output records had to be changed to correspond to the type of tracer and other information peculiar to the Oklahoma data base.

The other major changes that had to be made to this model in order to produce predictions for the Oklahoma cases related to an expansion of the original dimensions of the grid arrays in the model. As originally supplied, the dimensions of all grid arrays were 30 x 30. To apply the model to the Savannah River Plant krypton-85 experiment, the computational grid size was increased to 33 x 56, employing an externally-read grid step of 10 km along both axes. For the Oklahoma runs, the computational grid size was changed to 34 x 34, with an externally-read grid step set of 20 km along both axes. These dimensions are smaller than used for the meteorological grid, which is 51 x 41, but sufficient for this model to include the source and all receptor locations. In this model one does not need to leave a computational "cushion" around the edges of the active region (as required by MESOPUFF, MESOPUFF II, MESOPLUME, and MSPUFF) in order to obtain accurate results for receptors near the boundary of the computational grid.

The gridded quantities whose dimensions required expansion included the following:

X-component of the average wind
Y-component of the average wind
Mixing height
Stability class or "exposure class"
Horizontal diffusion coefficient
Region top
Rain (not used)

Boundary conditions

Lower and upper layer concentrations

One significant prior change that was made in RTM-II in order to prepare the earlier SRP predictions, was to add logic for handling time-dependent emissions in the model. As supplied by SAI, the model could only handle the same hourly pattern of emissions for every day in a given run, whereas the emissions data for both data bases had time-dependent emissions that did not have the same daily pattern.

C.11. DESCRIPTION OF RADM MODIFICATIONS

As supplied to EPA by Dames & Moore, Inc., this code was not written in ANSI standard FORTRAN IV. It relied heavily on "banking" of common blocks and other types of data, which is similar to using INCLUDE statements in FORTRAN IV. Use of this programming method is available at some installations, but is not standard. These statements had to be commented out and COMMON blocks added. Also, it was necessary to add OPEN statements for each of the 7 input files and 3 output files required by the model. As with the other models, the handling of character and logical data had to be altered to meet the ANSI standard for FORTRAN 77.

The dimensions of the arrays containing meteorological and surface type data in grid form were modified to accommodate the values of 33 x 56 for the Savannah River Plant datasets, and to 51 x 41 for the Oklahoma data. This makes the full meteorological region available as a computational region for RADM, thus avoiding any bias of results due to boundary effects. The model allows for specification of 150 receptors. In the Oklahoma study, there are 54 active receptors, while in the Savannah River study there are only 13. No change in the size of receptor-related arrays was necessary. Obviously, with a single source for each data base, there was no need to increase the available size of arrays relating to source characteristics, since RADM allows for 150 sources. This model has been provided to EPA with documentation more appropriate for internal use by Dames & Moore, Inc., than by external users. In particular, the input meteorological data files are not documented, because the model is supposed to be used in conjunction with meteorological

models available within Dames & Moore, Inc. Although these meteorological preprocessor codes have inputs that are documented in the RADM User's Manual, their output, which constitutes input for RADM, is not documented. The format of these files had to be determined from the code itself, and verified with Dames & Moore personnel. Dames & Moore, Inc. was unwilling to release any version of their wind field and mixing height preprocessor programs, DEPTH, WNDSRF, and WIND3D. They cited that their versions of these programs had not been released by their quality assurance department. The RADM representatives recommended the use of MESOPAC II predictions as gridded hourly input meteorological data for RADM.

The meteorological data in grid form that RADM requires on an hourly basis are the two wind components and the mixing height. A surface wind field modified by upper air data is typically used for RADM. In this sense, the wind field includes the influence of winds aloft. On a one-time basis, the user also has to supply grid values of roughness heights and surface elevations for the site of interest. The surface elevations are used only to determine solar insolation, and did not need to be supplied in the Oklahoma and SRP cases. MESOPAC II has been altered to supply the modified surface winds on an output file named RADMWF, the mixing heights on a file RADMHTM, and the surface roughness values on an output file named RADMHTR. These files are all unformatted binary files which saves disk space. The corresponding READ statements for each of these files has been modified to read the unformatted files properly.

Instead of only supplying actual surface winds to RADM (which would utilize only CD144 surface weather data), MESOPAC II has been programmed to provide the lower-level (Layer 1) wind field for RADM for use as the modified wind field. The Layer 1 field was obtained by averaging the wind, from the ground to the mixing height at each grid point. The RADM model has also been changed to utilize half of the mixing height at each grid point as the reference height for the wind field, instead of relying on a single reference height for the entire meteorological grid, as originally coded. This method of obtaining the wind field for input to RADM was felt to be consistent with the usual way Dames and Moore, Inc. applies one of their three wind models in that the modified surface wind includes the true surface wind data but suitably adjusted by upper air data. It should be recognized that the actual

surface wind data (unaltered by upper air data) is being used directly to develop Pasquill stability classes in RADM. As a result, two wind fields were output from MESOPAC II for RADM input: the modified surface winds for plume transport and the true surface wind data for Pasquill stability class determination.

Subroutine CONCEN in RADM is called from the MAIN program during the main time loop to provide both (a) instantaneous concentrations for the puffs at the end of each time step, and (b) average concentration values (measured from some user-specified input time) at each of the grid points receptors specified to the code. This feature is retained to provide predictions at the non-grid receptors, both for the Savannah River Plant and Oklahoma datasets. However, based on the needs of the current model evaluation work, hourly average concentration values are required both at the non-grid receptors and for points on the fixed grid of receptors (34 by 34 for Oklahoma and 22 by 24 for SRP). Statements were added to the RADM code to average the instantaneous concentrations computed at the end of each time step for the purpose of obtaining hourly average concentration predictions at the non-grid receptors.

For the purpose of obtaining hourly averaged concentrations at the prediction grids noted above, a new subroutine GCONC was introduced, which is a very similar to the CONCEN routine. It is called just after CONCEN in the program MAIN. It provides hourly averaged concentrations on the 34 x 34 grid for the Oklahoma datasets and on the 22 x 24 grid for the Savannah River Plant datasets. Thus, hourly averaged concentrations at grid locations are now printed out by the code at hourly intervals along with instantaneous and hourly-averaged values at the non-grid receptors.

APPENDIX D

COMPLETE STATISTICAL COMPARISONS OF THE EIGHT MODELS WITH THE OKLAHOMA AND SAVANNAH RIVER PLANT DATA BASES

INTRODUCTION

This appendix provides the complete results of the application of the AMS statistics to the predicted/observed pairs obtained from the model/data comparisons. Listed first are the actual predictions and observations for each of the 15 Savannah River Plant data sets and the two Oklahoma data sets. They are presented in tabular form and are helpful in gaining an appreciation of the differences that can occur among the models for the same receptor during the same averaging period. The Savannah River Plant tables are presented first followed by the Oklahoma tables. A brief legend is provided on the next two pages to guide the reader in his interpretation of the tables. These tables were used in the preparation of the analyses using the AMS statistics.

Following the tabular list of model predictions and data values are the complete AMS statistical tables for the Oklahoma and SRP sites. The A and B tables are presented first for the Oklahoma and then the SRP data sets. Note that the B-1 tables were not presented in Chapter 5 yet are presented here for the reader who wishes to examine the performance of the models on a receptor-by-receptor basis. Some of the results from the A-1 and B-1 tables should be treated with caution since the number of pairs that were used in preparing those statistics were not large.

This appendix is divided into two parts. Part I presents the tabular listing of the predictions for each of the models and the observations from each of the Oklahoma and SRP data sets. Part II provides a complete presentation of the AMS statistical results.

Part I: Tabular Listing of the Predicted and Observed Ground-level Concentrations for each of the SRP and Oklahoma Data Sets.

Receptor Identification Number

Sampling Starting Time

Duration (hrs) of Sampling

Observed Concentrations

Day, Month, Year, Julian Date

Case Identification

Model Predictions

Note: PUFF1 indicates MESOPUFF
PLUME indicates MESOPLUME
PUFF2 indicates MESOPUFF II

DD	MM	YY	JUL	SI	HOUR	DUR	OBS	PUFF1	PLUME	MSPUFF	PUFF2	MTDDIS	ARRPA	RTM2	RADM
CASE 1-A				ID Ø1 RECP Ø7 GR Ø1											
5	1Ø	76	279	2	22ØØ	14.Ø	172.8	19Ø.2	159.5	Ø.	237.3	49.Ø	Ø.	294.9	7.7
5	1Ø	76	279	5	22ØØ	14.Ø	1.Ø	Ø.	Ø.	Ø.	Ø.	Ø.1	Ø.	Ø.	Ø.
5	1Ø	76	279	6	22ØØ	14.Ø	1.4	Ø.	Ø.	Ø.	Ø.	Ø.	Ø.	Ø.	Ø.
5	1Ø	76	279	1Ø	22ØØ	14.Ø	Ø.	Ø.	Ø.	156.7	19.7	Ø.	Ø.	Ø.	Ø.
5	1Ø	76	279	11	22ØØ	14.Ø	Ø.	Ø.	Ø.	5Ø4.9	16.8	Ø.	Ø.	Ø.	Ø.
5	1Ø	76	279	12	22ØØ	14.Ø	36Ø.Ø	97.7	156.Ø	129.3	85.9	Ø.2	Ø.	28Ø.1	Ø.
5	1Ø	76	279	14	22ØØ	14.Ø	659.9	5Ø9.9	389.2	Ø.	24.7	341.3	Ø.	1756.4	453Ø.5
CASE 2-A				ID Ø2 RECP 12 GR Ø3											
14	1Ø	76	288	2	22ØØ	15.Ø	Ø.7	Ø.	Ø.	Ø.	Ø.	Ø.	Ø.	Ø.	Ø.
14	1Ø	76	288	3	23ØØ	13.Ø	2.Ø	Ø.	Ø.	Ø.	Ø.	Ø.9	Ø.	Ø.	Ø.
14	1Ø	76	288	4	22ØØ	14.Ø	Ø.	Ø.	Ø.	Ø.	Ø.	Ø.	Ø.	Ø.	Ø.
14	1Ø	76	288	5	22ØØ	14.Ø	Ø.	Ø.	Ø.	Ø.	Ø.	Ø.3	Ø.	Ø.	Ø.
14	1Ø	76	288	6	22ØØ	14.Ø	Ø.9	4.Ø	Ø.	Ø.	21.4	1.8	Ø.	76.4	Ø.
14	1Ø	76	288	7	22ØØ	15.Ø	Ø.	277.8	388.3	262.5	614.5	13.6	Ø.	312.1	Ø.
14	1Ø	76	288	9	22ØØ	14.Ø	Ø.	1321.7	923.8	Ø.	Ø.	1Ø.1	Ø.	338.1	Ø.
14	1Ø	76	288	1Ø	22ØØ	13.Ø	31.6	Ø.	Ø.	Ø.	Ø.	11.7	Ø.	12.5	Ø.
14	1Ø	76	288	11	2155	14.Ø	Ø.	Ø.	Ø.	Ø.	Ø.	1.2	Ø.	Ø.1	Ø.
14	1Ø	76	288	12	22ØØ	14.Ø	Ø.	Ø.	Ø.	Ø.	Ø.	Ø.	Ø.	Ø.	Ø.
14	1Ø	76	288	13	21ØØ	15.Ø	Ø.	Ø.3	Ø.	Ø.	Ø.	Ø.	Ø.	Ø.2	Ø.
14	1Ø	76	288	14	2225	14.Ø	Ø.	Ø.	Ø.	Ø.	Ø.	1.5	Ø.	Ø.	Ø.

Note: Case 1-A indicates SRP Case 1 - Event A
Case 2-A indicates SRP Case 2 - Event A
Case 2-B indicates SRP Case 2 - Event B
.
.
.
Case 15-D indicates SRP Case 15 - Event D
Case 20-A indicates OKL Exp 1 (100 km arc) - Event A
.
.
.
Case 20-G indicates OKL Exp 1 (100 km arc) - Event G
Case 30-A indicates OKL Exp 1 (600 km arc) - Event A
.
.
.
Case 30-F indicates OKL Exp 1 (600 km arc) - Event F
Case 40-A indicates OKL Exp 2 (100 km arc) - Event A
.
.
.
Case 40-H indicates OKL Exp 2 (100 km arc) - Event H

DD MM YY	JUL	SI	HOUR	DUR	OBS	PUFF1	PLUME	MSPUFF	PUFF2	MTDDIS	ARRPA	RTM2	RADM
CASE 1-A ID 01 RECP 07 GR 01													
5 10 76	279	2	2200	14.0	172.8	190.2	159.5	0.	237.3	49.0	0.	294.9	7.7
5 10 76	279	5	2200	14.0	1.0	0.	0.	0.	0.	0.1	0.	0.	0.
5 10 76	279	6	2200	14.0	1.4	0.	0.	0.	0.	0.	0.	0.	0.
5 10 76	279	10	2200	14.0	0.	0.	0.	156.7	19.7	0.	0.	0.	0.
5 10 76	279	11	2200	14.0	0.	0.	0.	504.9	16.8	0.	0.	0.	0.
5 10 76	279	12	2200	14.0	360.0	97.7	156.0	129.3	85.9	0.2	0.	280.1	0.
5 10 76	279	14	2200	14.0	659.9	509.9	389.2	0.	24.7	341.3	0.	1756.4	4530.5
CASE 2-A ID 02 RECP 12 GR 03													
14 10 76	288	2	2200	15.0	0.7	0.	0.	0.	0.	0.	0.	0.	0.
14 10 76	288	3	2300	13.0	2.0	0.	0.	0.	0.	0.9	0.	0.	0.
14 10 76	288	4	2200	14.0	0.	0.	0.	0.	0.	0.	0.	0.	0.
14 10 76	288	5	2200	14.0	0.	0.	0.	0.	0.	0.3	0.	0.	0.
14 10 76	288	6	2200	14.0	0.9	4.0	0.	0.	21.4	1.8	0.	76.4	0.
14 10 76	288	7	2200	15.0	0.	277.8	388.3	262.5	614.5	13.6	0.	312.1	0.
14 10 76	288	9	2200	14.0	0.	1321.7	923.8	0.	0.	10.1	0.	338.1	0.
14 10 76	288	10	2200	13.0	31.6	0.	0.	0.	0.	11.7	0.	12.5	0.
14 10 76	288	11	2155	14.0	0.	0.	0.	0.	0.	1.2	0.	0.1	0.
14 10 76	288	12	2200	14.0	0.	0.	0.	0.	0.	0.	0.	0.	0.
14 10 76	288	13	2100	15.0	0.	0.3	0.	0.	0.	0.	0.	0.2	0.
14 10 76	288	14	2225	14.0	0.	0.	0.	0.	0.	1.5	0.	0.	0.
CASE 2-B ID 02 RECP 11													
15 10 76	289	2	1300	8.0	0.	0.	0.	0.	0.	0.3	0.	0.	0.
15 10 76	289	3	1200	7.0	0.	0.	0.	0.	0.	11.8	0.	0.	0.
15 10 76	289	4	1300	8.0	1.1	0.	0.	0.	0.	0.8	0.	0.	0.
15 10 76	289	5	1300	8.0	4.2	0.	0.	0.	2.6	7.6	0.	0.	0.
15 10 76	289	6	1300	8.0	0.	0.	0.	0.	3.2	52.3	0.	0.	0.
15 10 76	289	7	1300	8.0	1.0	0.	0.	0.	0.	377.1	0.	0.6	0.
15 10 76	289	8	1345	7.3	33.0	0.	0.	176.3	456.5	897.6	0.	62.5	0.
15 10 76	289	9	1300	7.9	28.4	1128.4	309.9	0.	0.	289.2	0.	230.6	0.
15 10 76	289	10	1200	9.0	20.6	0.	0.	0.	0.	179.5	0.	17.7	0.
15 10 76	289	12	1300	8.0	0.	0.	0.	0.	0.	0.3	0.	0.	0.
15 10 76	289	13	1315	7.2	1.6	2.3	39.0	0.	0.	13.1	0.	12.3	0.
CASE 2-C ID 02 RECP 01													
15 10 76	289	9	2200	14.0	175.4	0.	0.	0.	154.5	39.8	0.	766.0	0.
CASE 3-A ID 03 RECP 09 GR 02													
29 10 76	303	2	900	10.0	178.7	4.4	22.1	17.1	0.	0.	0.	29.6	0.
29 10 76	303	3	900	10.0	0.	0.	0.	0.	0.	0.5	0.	0.	0.
29 10 76	303	4	900	10.0	0.2	0.	0.	0.	0.	0.	0.	0.	0.
29 10 76	303	5	900	10.0	0.	0.	0.	0.	0.	0.	0.	0.	0.
29 10 76	303	6	900	10.0	0.	0.	0.	0.	0.	0.	0.	0.	0.
20 10 76	303	7	900	10.0	0.	0.	0.	0.	0.	0.	0.	0.	0.
29 10 76	303	9	900	10.0	0.	0.	0.	0.	0.	0.	0.	0.	0.
29 10 76	303	10	900	10.0	0.	0.	0.	0.	0.	0.	0.	0.	0.
29 10 76	303	14	900	10.0	331.0	146.9	245.7	212.6	0.	3.1	0.	54.2	0.
CASE 3-B ID 03 RECP 08													
29 10 76	303	2	2100	10.0	141.6	2.0	3.7	0.	0.1	0.3	0.	30.6	0.
29 10 76	303	3	2100	10.0	2.4	0.	0.	0.	0.	1.7	0.	0.	0.
29 10 76	303	4	2100	10.0	0.	0.	0.	0.	0.	0.	0.	0.	0.
29 10 76	303	5	2100	10.0	19.0	0.	0.	0.	0.	0.1	0.	0.	0.
29 10 76	303	6	2100	10.0	0.	0.	0.	0.	0.	0.	0.	0.	0.
29 10 76	303	10	2100	10.0	0.	0.	0.	0.	0.	14.9	0.	0.	0.
29 10 76	303	12	2100	10.0	0.	64.2	70.5	87.9	15.3	0.	0.	41.5	0.
29 10 76	303	14	2100	10.0	226.5	0.	0.	0.	24.5	70.7	0.	57.1	0.
CASE 4-A ID 04 RECP 11 GR 04													
18 11 76	323	2	1000	10.0	1.1	0.	0.	0.	0.	0.	0.	0.	0.
18 11 76	323	3	1000	10.0	7.9	0.	0.	0.	0.	0.	0.	0.	0.
18 11 76	323	4	1000	10.0	1.9	0.	0.	0.	0.	0.	0.	0.	0.
18 11 76	323	6	1000	10.0	10.2	0.	0.	0.	0.	0.	0.	1.2	0.
18 11 76	323	7	1000	10.0	4.3	0.	0.	0.	0.	0.	0.	0.	0.
18 11 76	323	8	1000	10.0	3.6	0.	0.	0.	0.	16.0	0.	0.	0.
18 11 76	323	10	1000	10.0	1.2	0.	0.	0.	0.	0.	0.	0.	0.
18 11 76	323	11	1430	5.5	0.	0.	0.	0.	0.	0.	0.	0.	0.
18 11 76	323	12	1000	10.0	0.1	0.	0.	0.	0.	0.	0.	0.	0.
18 11 76	323	13	1000	10.0	0.1	0.	0.	0.	0.	0.	0.	0.	0.
18 11 76	323	14	1000	10.0	1.3	0.	0.	0.	0.	0.	0.	0.	0.

DD MM YY	JUL	SI	HOUR	DUR	OBS	PUFF1	PLUME	MSPUFF	PUFF2	MTDDIS	ARRPA	RTM2	RADM
CASE 4-B ID 04 RECP 12													
18 11 76	323	2	2200	10.0	0.	0.	0.	0.	0.	0.	0.	0.	0.
18 11 76	323	3	2200	10.0	0.	0.	0.	0.	0.	0.	0.	0.	0.
18 11 76	323	4	2200	10.0	0.	0.	0.	0.	0.	0.	0.	0.	0.
18 11 76	323	5	2200	10.0	0.	0.	0.	0.	0.	0.	0.	0.	0.
18 11 76	323	6	2200	10.0	0.6	118.5	1.1	140.4	0.	0.	0.	200.4	0.
18 11 76	323	7	2200	10.0	43.0	0.	0.	0.	48.8	11.0	0.	0.	0.
18 11 76	323	8	2200	10.0	64.0	0.	0.	0.	25.3	121.6	0.	0.	134.7
18 11 76	323	9	2200	10.0	23.9	0.	0.	0.	0.	20.9	0.	0.	0.
18 11 76	323	10	2200	10.0	48.0	0.	0.	0.	0.	26.5	0.	0.	0.
18 11 76	323	11	2200	10.0	5.9	0.	0.	0.	0.	1.2	0.	0.	0.
18 11 76	323	12	2200	10.0	0.	0.	0.	0.	0.	0.	0.	0.	0.
18 11 76	323	14	2200	10.0	0.	0.	0.	0.	0.	0.	0.	0.	0.
CASE 4-C ID 04 RECP 11													
19 11 76	324	2	1000	10.0	0.	0.	0.	0.	0.	0.	0.	0.	0.
19 11 76	324	3	1000	10.0	0.	0.	0.	0.	0.	0.	0.	0.	0.
19 11 76	324	4	1000	10.0	0.1	0.	0.	0.	0.	0.	0.	0.	0.
19 11 76	324	5	1000	10.0	2.8	0.	0.	0.	0.	0.	0.	0.	0.
19 11 76	324	6	1000	10.0	0.	0.	0.	0.	0.	0.1	0.	0.	0.
19 11 76	324	8	1000	10.0	238.9	146.4	192.6	170.4	296.5	755.8	0.	110.0	377.0
19 11 76	324	10	1000	10.0	0.9	0.	0.	0.	0.	22.7	0.	0.	0.
19 11 76	324	11	1000	10.0	0.	0.	0.	0.	0.	46.3	0.	0.	0.
19 11 76	324	12	1000	10.0	0.	0.	0.	0.	0.	0.	0.	0.	0.
19 11 76	324	13	1000	10.0	1.3	0.	0.	0.	0.	72.8	0.	0.	0.
19 11 76	324	14	1000	10.0	0.	0.	0.	0.	0.	0.	0.	0.	0.
CASE 4-D ID 04 RECP 09													
19 11 76	324	2	2200	10.0	0.	0.	0.	0.	0.	0.	0.	0.	0.
19 11 76	324	3	2200	10.0	0.	0.	0.	0.	0.	0.	0.	0.	0.
19 11 76	324	4	2200	10.0	0.	0.	0.	0.	0.	0.	0.	0.	0.
19 11 76	324	5	2200	10.0	0.	0.	0.	0.	0.	0.	0.	0.	0.
19 11 76	324	9	2200	10.0	10.8	0.	0.	0.	0.	68.0	0.	0.	0.
19 11 76	324	11	2200	10.0	0.	0.	0.	0.	0.	7.2	0.	0.	0.
19 11 76	324	12	2200	10.0	0.	0.	0.	0.	0.	0.	0.	0.	0.
19 11 76	324	13	2200	10.0	0.	0.	0.	0.	0.	17.6	0.	0.	0.
19 11 76	324	14	2200	10.0	0.	0.	0.	0.	0.	0.	0.	0.	0.
CASE 5-A ID 05 RECP 06 GR 04													
2 2 77	33	2	1000	10.0	1.7	0.	0.	0.	0.	0.	0.	0.	0.
2 2 77	33	3	1200	9.9	0.	8.9	20.8	0.	0.	15.6	0.	261.1	0.
2 2 77	33	4	1000	10.0	0.	0.	0.	0.	0.	0.	0.	0.4	0.
2 2 77	33	5	1000	10.0	0.	0.2	38.8	0.	0.	0.	0.	15.2	0.
2 2 77	33	11	1000	10.0	0.	0.	0.	0.	0.	0.	0.	0.	0.
2 2 77	33	14	1000	10.0	101.7	0.	0.	0.	157.9	58.2	0.	0.1	285.8
CASE 5-B ID 05 RECP 06													
2 2 77	33	2	2200	10.0	12.8	0.	0.	0.	1.8	0.5	0.	0.	0.
2 2 77	33	4	2200	10.0	0.	0.	0.	0.	0.	0.1	0.	6.9	0.
2 2 77	33	5	2200	10.0	0.	0.	99.8	0.	0.	0.	0.	3.9	0.
2 2 77	33	11	2200	10.0	0.	26.8	56.4	0.	16.9	0.	0.	66.4	0.
2 2 77	33	13	2145	10.0	5.9	0.1	0.	0.	4.7	0.	0.	3.8	0.
2 2 77	33	14	2200	10.0	1.4	8.5	18.4	0.	17.4	51.2	0.	125.7	11.4
CASE 5-C ID 05 RECP 07													
3 2 77	34	2	1000	10.0	1.2	0.	0.	0.	0.	153.1	0.	0.	0.
3 2 77	34	3	1000	10.0	0.	0.	0.	0.	0.	5.2	0.	0.	0.
3 2 77	34	4	1000	10.0	0.	0.	0.	0.	0.	1.7	0.	0.	0.
3 2 77	34	5	1000	10.0	0.	0.	0.	0.	0.	0.4	0.	0.	0.
3 2 77	34	11	1000	10.0	0.	1453.8	852.9	0.	20.0	2.5	0.	592.8	0.
3 2 77	34	13	1000	10.0	0.	751.8	339.9	0.	2.5	0.2	0.	507.6	0.
3 2 77	34	14	1000	10.0	417.6	0.	0.	0.	0.	1911.0	0.	1.7	1195.4
CASE 5-D ID 05 RECP 06													
3 2 77	34	2	2200	10.0	2.3	0.	0.	0.	0.	23.6	0.	0.	0.
3 2 77	34	3	2200	10.0	0.1	0.	0.	0.	0.	5.5	0.	0.	0.
3 2 77	34	4	2200	10.0	0.	0.	0.	0.	0.	0.8	0.	0.	0.
3 2 77	34	5	2200	10.0	0.	0.	0.	0.	0.	0.2	0.	0.	0.
3 2 77	34	13	2145	10.0	82.4	0.	0.	0.	1.1	0.4	0.	0.	152.1
3 2 77	34	14	2200	10.0	71.2	0.	0.	0.	0.	87.3	0.	0.	390.0

DD MM YY	JUL	SI	HOUR	DUR	OBS	PUFF1	PLUME	MSPUFF	PUFF2	MTODIS	ARRPA	RTM2	RADM
CASE 6-A ID 06 RECP 11 GR 05													
16 2 77	47	2	2200	10.0	0.	0.	0.	0.	0.	0.	0.	0.	0.
16 2 77	47	3	2200	10.0	0.	0.	0.	0.	0.	0.	0.	0.	0.
16 2 77	47	4	2200	10.0	0.	0.	0.	0.	0.	0.	0.	0.	0.
16 2 77	47	5	2200	10.0	0.	0.	0.	0.	0.	0.	0.	0.	0.
16 2 77	47	6	2200	10.0	35.5	426.7	520.5	0.	0.	2.7	0.	651.1	0.
16 2 77	47	7	2200	10.0	0.	0.	0.	0.	0.	0.	0.	0.	0.
16 2 77	47	9	2200	10.0	0.	0.	0.	0.	0.	0.	0.	0.	0.
16 2 77	47	11	2200	10.0	0.1	0.	0.	0.	0.	0.	0.	0.	0.
16 2 77	47	12	2200	10.0	0.	0.	0.	0.	0.	0.	0.	0.	0.
16 2 77	47	13	2145	10.0	0.	0.	0.	0.	0.	0.	0.	0.	0.
16 2 77	47	14	2200	10.0	0.	0.	0.	0.	0.	0.	0.	0.	0.
CASE 6-B ID 06 RECP 12													
17 2 77	48	2	1000	11.0	0.	0.	0.	0.	0.	0.	0.	0.	0.
17 2 77	48	3	1000	10.0	0.	0.	0.	0.	0.	1.3	0.	0.	0.
17 2 77	48	4	1000	10.0	0.	0.	0.	0.	0.	0.	0.	0.	0.
17 2 77	48	5	1000	10.0	56.0	0.	0.	0.	0.	14.3	0.	0.	0.
17 2 77	48	6	1000	10.0	38.0	57.9	129.3	0.	18.7	782.4	0.	82.3	1119.5
17 2 77	48	7	1000	10.0	0.	0.	0.	0.	27.5	1.9	0.	0.	0.
17 2 77	48	8	1000	10.0	9.1	0.	0.	0.	12.6	1.4	0.	0.	0.
17 2 77	48	9	1000	10.0	0.	0.	0.	0.	0.	0.	0.	0.	0.
17 2 77	48	10	1000	10.0	0.	0.	0.	0.	0.	0.	0.	0.	0.
17 2 77	48	12	1000	10.0	0.	0.	0.	0.	0.	0.	0.	0.	0.
17 2 77	48	13	945	10.0	0.	0.	0.	0.	0.	0.	0.	0.	0.
17 2 77	48	14	1000	10.0	0.	0.	0.	0.	0.	0.	0.	0.	0.
CASE 6-C ID 06 RECP 11													
17 2 77	48	2	2200	10.0	1.3	0.	0.	0.	0.	0.	0.	0.	0.
17 2 77	48	3	2200	10.0	2.2	0.	0.	0.	0.	0.3	0.	0.	0.
17 2 77	48	4	2200	10.0	0.	0.	0.	0.	0.	0.	0.	0.	0.
17 2 77	48	6	2200	10.0	23.8	0.	0.	0.	0.	73.0	0.	0.5	0.
17 2 77	48	7	2200	10.0	243.9	13.3	21.8	3.2	8.7	7.6	0.	12.0	22.6
17 2 77	48	9	2200	10.0	15.9	0.	0.	0.	7.7	0.4	0.	0.	147.0
17 2 77	48	10	2200	10.0	0.8	0.	0.	0.	0.	0.8	0.	0.	0.
17 2 77	48	11	2200	10.0	0.6	0.	0.	0.	0.	0.	0.	0.	0.
17 2 77	48	12	2200	10.0	0.	0.	0.	0.	0.	0.	0.	0.	0.
17 2 77	48	13	2200	10.0	0.	0.	0.	0.	0.	0.	0.	0.	0.
17 2 77	48	14	2200	10.0	0.	0.	0.	0.	0.	0.1	0.	0.	0.
CASE 6-D ID 06 RECP 12													
18 2 77	49	2	1000	10.0	0.	0.	0.	0.	0.	10.6	0.	0.	0.
18 2 77	49	3	1000	10.0	0.	0.	0.	0.	0.	33.1	0.	0.	0.
18 2 77	49	4	1000	10.0	0.	0.	0.	0.	0.	6.1	0.	0.	0.
18 2 77	49	5	1000	10.0	0.	0.	0.	0.	0.	23.1	0.	0.	0.
18 2 77	49	6	1000	10.0	7.3	0.	0.	0.	0.	97.8	0.	0.	0.
18 2 77	49	7	1000	10.0	33.2	0.	0.	465.9	193.6	279.0	0.	0.	0.
18 2 77	49	8	1000	10.0	9.5	0.	0.	2171.1	179.9	286.1	0.	78.4	56.6
18 2 77	49	9	1000	10.0	126.5	1602.9	1089.9	0.	20.5	307.5	0.	613.3	431.9
18 2 77	49	10	1000	10.0	149.1	0.	0.	0.	49.9	537.2	0.	55.9	92.1
18 2 77	49	11	1000	10.0	242.3	0.	0.	0.	176.0	265.8	0.	0.5	29.5
18 2 77	49	12	1000	10.0	0.	0.	0.	0.	0.	67.4	0.	0.	0.
18 2 77	49	14	1000	10.0	0.	0.	0.	0.	0.	79.0	0.	0.	0.
CASE 6-E ID 06 RECP 07													
18 2 77	49	2	2200	10.0	2.4	0.	0.	0.	0.	0.3	0.	0.	0.
18 2 77	49	6	2200	10.0	0.	0.	0.	0.	0.	2.0	0.	0.	0.
18 2 77	49	7	2200	10.0	1.3	0.	0.	0.	203.1	10.2	0.	0.	209.9
18 2 77	49	8	2200	10.0	0.3	0.	0.	491.3	313.4	10.2	0.	34.3	282.1
18 2 77	49	9	2200	10.0	33.9	13.6	34.2	0.	0.	27.4	0.	77.7	0.
18 2 77	49	10	2200	10.0	107.9	0.	0.	0.	0.	121.1	0.	0.	0.
18 2 77	49	14	2200	10.0	0.	0.	0.	0.	0.	1.5	0.	0.	0.

DD	MM	YY	JUL	SI	HOUR	DUR	OBS	PUFF1	PLUME	MSPUFF	PUFF2	MTDDIS	ARRPA	RTM2	RADM
CASE 7-A			ID 07		RECP 13		GR 02								
22	2	77	53	2	1000	10.0	2.2	0.	0.	0.	0.	0.	0.	0.	0.
22	2	77	53	3	1000	10.0	0.	0.	0.	0.	0.	0.	0.	0.	0.
22	2	77	53	4	1000	10.0	0.	0.	0.	0.	0.	0.	0.	0.	0.
22	2	77	53	5	1000	10.0	0.	0.	0.	0.	0.	0.	0.	0.	0.
22	2	77	53	6	1000	10.0	0.	0.	0.	0.	0.	0.2	0.	0.	0.
22	2	77	53	7	1000	10.0	32.2	0.	0.	0.1	2.8	18.4	0.	22.4	8.4
22	2	77	53	8	1000	10.0	24.8	0.	2.8	0.	0.	13.5	0.	26.0	0.
22	2	77	53	9	1000	8.0	6.7	5.3	7.1	0.	11.0	109.9	0.	16.3	59.9
22	2	77	53	10	1000	10.0	292.1	0.	0.	0.	43.9	277.9	0.	0.8	2077.2
22	2	77	53	11	1000	10.0	661.2	0.	0.	0.	0.	208.4	0.	0.	328.6
22	2	77	53	12	1000	10.0	0.	0.	0.	0.	0.	0.1	0.	0.	0.
22	2	77	53	13	945	10.0	46.9	0.	0.	0.	0.	134.4	0.	0.	2.8
22	2	77	53	14	1000	10.0	0.	0.	0.	0.	0.	0.1	0.	0.	0.
CASE 7-B			ID 07		RECP 12										
22	2	77	53	2	2200	10.0	0.	0.	0.	0.	0.	0.	0.	0.	0.
22	2	77	53	3	2200	10.0	0.	0.	0.	0.	0.	0.	0.	0.	0.
22	2	77	53	5	2200	10.0	0.	0.	0.	0.	0.	0.	0.	0.	0.
22	2	77	53	6	2200	10.0	0.	0.	0.	0.	0.	0.	0.	0.	0.
22	2	77	53	7	2200	10.0	0.	0.	0.	0.	0.	0.2	0.	0.	0.
22	2	77	53	8	2200	10.0	0.	0.	0.	0.	0.	0.1	0.	0.	0.
22	2	77	53	9	2000	10.0	0.	0.	0.	0.	0.	2.9	0.	0.	0.
22	2	77	53	10	2200	10.0	7.9	0.	0.	0.	0.	0.7	0.	0.	0.
22	2	77	53	11	2200	10.0	3.5	0.	0.	0.	0.	19.3	0.	0.	0.
22	2	77	53	12	2200	10.0	0.	0.	0.	0.	0.	0.	0.	0.	0.
22	2	77	53	13	2145	10.0	0.9	0.	0.	0.	0.	32.8	0.	0.	0.
22	2	77	53	14	2200	10.0	0.	0.	0.	0.	0.	0.	0.	0.	0.
CASE 8-A			ID 08		RECP 08		GR 07								
5	4	77	95	3	2200	10.0	0.	0.	0.	0.	0.	0.	0.	0.	0.
5	4	77	95	4	2200	10.0	0.	0.	0.	0.	0.	0.	0.	0.	0.
5	4	77	95	5	2200	10.0	0.8	0.	0.	0.	0.	0.	0.	0.	0.
5	4	77	95	8	2200	10.0	2.2	0.	0.	0.	0.	0.	0.	6.4	0.
5	4	77	95	11	2200	10.0	0.	0.	0.	0.	0.	0.	0.	0.	0.
5	4	77	95	12	2200	34.0	0.	0.	0.	0.	0.	0.	0.	0.	0.
5	4	77	95	13	2115	10.0	0.	0.	0.	0.	0.	0.	0.	0.	0.
5	4	77	95	14	2200	10.0	0.1	0.	0.	0.	0.	0.	0.	0.	0.
CASE 8-B			ID 08		RECP 10										
6	4	77	96	2	1000	10.0	0.	0.	0.	0.	0.	0.	0.	0.	0.
6	4	77	96	4	1000	10.0	0.	0.	0.	0.	0.	0.	0.	0.	0.
6	4	77	96	5	1000	10.0	0.	0.	0.	0.	0.	0.	0.	0.	0.
6	4	77	96	6	1000	10.0	0.	0.	0.	0.	0.	0.	0.	0.3	0.
6	4	77	96	7	1000	10.0	184.1	0.	0.	0.	0.	296.5	0.	1.0	0.
6	4	77	96	8	1000	10.0	615.5	0.	0.	0.	8.4	1190.8	0.	0.5	0.
6	4	77	96	10	1000	10.0	0.1	0.	0.	0.	0.	2.4	0.	0.	0.
6	4	77	96	11	1000	10.0	0.	0.	0.	0.	0.	0.	0.	0.	0.
6	4	77	96	13	915	10.0	0.	0.	0.	0.	0.	0.	0.	0.	0.
6	4	77	96	14	1400	6.0	0.	0.	0.	0.	0.	0.	0.	0.	0.
CASE 8-C			ID 08		RECP 08										
6	4	77	96	3	2200	10.0	0.	0.	0.	0.	0.	0.	0.	0.	0.
6	4	77	96	4	2200	10.0	0.	0.	0.	0.	0.	0.	0.	0.	0.
6	4	77	96	6	2200	10.0	0.	0.	0.	0.	119.3	0.	0.	0.	1132.1
6	4	77	96	7	2200	10.0	127.7	4.1	0.	0.	0.	319.6	0.	23.5	0.
6	4	77	96	8	2200	10.0	156.9	0.	0.	0.	0.	96.0	0.	10.3	0.
6	4	77	96	10	2200	10.0	0.	0.	0.	0.	0.	0.	0.	0.	0.
6	4	77	96	13	2115	10.0	0.	0.	0.	0.	0.	0.	0.	0.	0.
6	4	77	96	14	2200	10.0	0.	0.	0.	0.	0.	0.	0.	0.	0.
CASE 8-D			ID 08		RECP 12										
7	4	77	97	2	1000	10.0	0.	0.	0.	0.	0.	0.	0.	0.	0.
7	4	77	97	3	1000	10.0	0.	0.	0.	0.	0.	0.2	0.	0.	0.
7	4	77	97	4	1000	10.0	0.	0.	0.	0.	0.	0.	0.	0.	0.
7	4	77	97	6	1000	10.0	2.2	38.8	42.6	4.5	0.	14.8	0.	18.9	31.2
7	4	77	97	7	1000	10.0	49.6	0.	0.	0.	0.	96.8	0.	0.	0.
7	4	77	97	8	1000	10.0	17.8	0.	0.	0.	0.	57.4	0.	0.	0.
7	4	77	97	9	1000	10.0	0.6	0.	0.	0.	0.	8.2	0.	0.	0.
7	4	77	97	10	1000	10.0	39.7	0.	0.	0.	101.1	3.7	0.	0.	191.4
7	4	77	97	11	1000	10.0	8.3	0.	0.	0.	0.	0.5	0.	0.	0.
7	4	77	97	12	1000	10.0	0.	0.	0.	0.	0.	0.	0.	0.	0.
7	4	77	97	13	915	10.0	0.	0.	0.	0.	0.	0.5	0.	0.	0.
7	4	77	97	14	1000	10.0	0.	0.	0.	0.	0.	50.3	0.	0.	0.

DD	MM	YY	JUL	SI	HOUR	DUR	OBS	PUFF1	PLUME	MSPUFF	PUFF2	MTDDIS	ARRPA	RTM2	RADM
CASE 8-E			ID 08 RECP 07												
7	4	77	97	3	2200	10.0	0.	0.	0.	0.	0.	0.2	0.	0.	0.
7	4	77	97	4	2200	10.0	0.	0.	0.	0.	0.	0.	0.	0.	0.
7	4	77	97	5	2200	10.0	0.	0.	0.	0.	0.	0.1	0.	0.	0.
7	4	77	97	10	2200	10.0	146.6	0.	0.	0.	0.	382.0	0.	0.	0.
7	4	77	97	12	2200	10.0	0.	0.	0.	0.	0.	0.3	0.	0.	0.
7	4	77	97	13	2115	10.0	19.8	0.	0.	0.	15.0	54.3	0.	0.	0.
7	4	77	97	14	2200	10.0	0.	0.	0.	0.	0.	1.0	0.	0.	0.
CASE 8-F			ID 08 RECP 10												
8	4	77	98	2	1000	10.0	0.	0.	0.	0.	0.	0.	0.	0.	0.
8	4	77	98	3	1000	10.0	0.	0.	0.	0.	0.	0.	0.	0.	0.
8	4	77	98	4	1000	10.0	0.	0.	0.	0.	0.	0.	0.	0.	0.
8	4	77	98	5	1000	10.0	0.	0.	0.	0.	0.	0.	0.	0.	0.
8	4	77	98	6	1000	10.0	0.	0.	0.	16.0	0.	0.1	0.	0.	0.
8	4	77	98	7	1000	10.0	18.2	0.	0.	0.	239.9	28.9	0.	0.1	226.6
8	4	77	98	9	1000	10.0	52.7	0.	0.	0.	0.	79.0	0.	0.	0.
8	4	77	98	10	1000	10.0	36.6	0.	0.	0.	0.	11.0	0.	0.	0.
8	4	77	98	12	1000	10.0	0.	0.	0.	0.	0.	0.3	0.	0.	0.
8	4	77	98	14	1000	10.0	0.	0.	0.	0.	0.	0.1	0.	0.	0.
CASE 8-G			ID 08 RECP 06												
8	4	77	98	3	2200	10.0	0.	0.	0.	0.	0.	0.	0.	0.	0.
8	4	77	98	4	2200	10.0	0.	0.	0.	0.	0.	0.	0.	0.	0.
8	4	77	98	8	2200	10.0	52.1	0.	0.	0.	0.	2.6	0.	0.	0.
8	4	77	98	9	2200	10.0	0.	0.	0.	0.	0.	5.1	0.	0.	0.
8	4	77	98	10	2200	10.0	0.	0.	0.	0.	0.	0.7	0.	0.	0.
8	4	77	98	12	2200	10.0	0.	0.	0.	0.	0.	0.1	0.	0.	0.
CASE 9-A			ID 09 RECP 13 GR 10												
11	4	77	101	2	1000	10.0	0.	0.	0.	0.	0.	0.	0.	0.	0.
11	4	77	101	3	1000	10.0	0.	11.2	0.	0.	0.	0.	0.	475.3	0.
11	4	77	101	4	1000	10.0	0.2	0.	0.	0.	0.	0.	0.	76.2	0.
11	4	77	101	5	1000	10.0	4.5	0.	0.	0.	0.	0.	0.	192.7	0.
11	4	77	101	6	1000	10.0	0.	1.1	0.	0.	0.	0.	0.	2.8	0.
11	4	77	101	7	1000	10.0	0.	0.	0.	0.	1.5	7.6	0.	1.5	0.
11	4	77	101	8	1000	10.0	9.6	4.5	0.	0.	2359.6	285.9	0.	144.8	187.2
11	4	77	101	9	1000	10.0	279.9	0.	0.	0.	52.4	287.1	0.	0.1	251.5
11	4	77	101	10	1000	10.0	182.8	0.	0.	0.	1183.5	659.5	0.	0.	63.7
11	4	77	101	11	1000	10.0	30.6	0.	0.	0.	42.6	615.6	0.	0.	304.1
11	4	77	101	12	1000	10.0	0.	0.	0.	0.	0.	1.0	0.	0.	0.
11	4	77	101	13	915	10.0	130.5	0.	0.	0.	0.1	77.8	0.	0.	0.
11	4	77	101	14	1000	10.0	0.	0.	0.	0.	57.9	0.6	0.	27.0	0.
CASE 9-B			ID 09 RECP 10												
11	4	77	101	2	2200	10.0	0.	33.4	0.	0.	4.5	0.2	0.	187.1	0.
11	4	77	101	5	2200	10.0	0.	17.7	45.0	0.	0.7	0.	0.	41.5	0.
11	4	77	101	6	2200	10.0	0.	7.5	0.	0.	0.7	0.	0.	14.2	0.
11	4	77	101	8	2200	10.0	0.7	2.7	0.	0.	767.1	53.6	0.	48.4	84.1
11	4	77	101	9	2200	10.0	39.3	0.	0.	0.	142.6	70.2	0.	1.1	1502.9
11	4	77	101	10	2200	10.0	41.4	0.2	0.	0.	375.7	185.7	0.	44.5	69.6
11	4	77	101	11	2200	10.0	77.6	0.	0.	0.	136.5	99.2	0.	0.	39.8
11	4	77	101	12	2200	10.0	0.	0.	0.	0.	13.3	5.3	0.	2.0	0.
11	4	77	101	13	2115	10.0	44.3	0.	0.	0.	23.0	34.8	0.	0.	0.
11	4	77	101	14	2200	10.0	0.	209.8	2476.8	0.	44.8	5.6	0.	537.7	0.
CASE 9-C			ID 09 RECP 09												
12	4	77	102	3	1000	10.0	0.6	209.2	152.2	0.	38.1	0.3	0.	370.6	0.
12	4	77	102	4	1000	10.0	0.1	262.2	792.5	0.	6.7	0.	0.	179.3	0.
12	4	77	102	5	1000	10.0	0.	83.3	3.2	0.	14.4	0.1	0.	47.6	0.
12	4	77	102	6	1000	10.0	0.	5.4	0.	0.	22.4	0.4	0.	12.0	0.
12	4	77	102	7	1000	10.0	1.4	2.8	0.	0.	83.1	19.7	0.	26.3	0.
12	4	77	102	9	1000	10.0	0.9	1.8	0.	0.	109.1	106.7	0.	33.1	0.
12	4	77	102	11	1000	10.0	2.8	0.	0.	0.	67.3	178.4	0.	0.	264.1
12	4	77	102	12	1000	10.0	0.	0.	0.	0.	19.6	10.7	0.	0.	0.
12	4	77	102	13	915	10.0	15.9	0.	0.	0.	20.3	288.0	0.	0.	175.7

DD	MM	YY	JUL	SI	HOUR	DUR	OBS	PUFF1	PLUME	MSPUFF	PUFF2	MTDDIS	ARRPA	RTM2	RADM
CASE 9-D				ID 09 RECP 08											
12	4	77	102	3	2200	10.0	3.2	9.6	4.5	0.	51.6	0.2	0.	10.3	0.
12	4	77	102	4	2200	10.0	3.3	11.3	17.7	0.	20.6	0.	0.	5.3	0.
12	4	77	102	6	2200	10.0	0.	0.1	0.	0.	17.0	0.2	0.	0.	0.
12	4	77	102	7	2200	10.0	1.0	0.3	0.	0.	40.9	3.6	0.	0.	0.
12	4	77	102	10	2200	10.0	0.8	21.8	0.	0.	145.3	7.8	0.	19.2	0.
12	4	77	102	11	2200	10.0	1.3	4.1	0.	0.	70.0	18.5	0.	2.3	245.5
12	4	77	102	13	2115	10.0	2.1	0.1	0.	0.	23.3	25.5	0.	0.	225.0
12	4	77	102	14	2200	10.0	2.0	339.7	26.6	0.	1833.2	1.9	0.	1401.8	20.2
CASE 9-E				ID 09 RECP 10											
13	4	77	103	2	1000	10.0	1.8	14.4	34.5	0.	137.3	0.1	0.	140.6	0.
13	4	77	103	3	1000	10.0	1.4	4.2	5.6	0.	43.8	0.	0.	0.	0.
13	4	77	103	4	1000	10.0	0.8	2.1	0.6	0.	35.9	0.	0.	0.	0.
13	4	77	103	5	1000	10.0	2.1	1.1	0.8	0.	21.8	0.	0.	0.	0.
13	4	77	103	6	1000	10.0	0.	0.2	0.7	0.	8.6	0.	0.	0.	0.
13	4	77	103	7	1000	10.0	0.8	1.2	1.2	0.	10.6	0.	0.	0.	0.
13	4	77	103	8	1000	10.0	0.8	5.1	3.8	0.	26.0	12.0	0.	0.	0.
13	4	77	103	11	1000	10.0	138.5	9.6	0.	0.	24.5	42.2	0.	0.	0.
13	4	77	103	13	915	10.0	65.5	2.9	0.	0.	9.9	1.7	0.	0.	243.6
13	4	77	103	14	1000	10.0	2.1	2837.9	1252.9	0.2	136.2	2.7	0.	451.4	0.
CASE 9-F				ID 09 RECP 09											
13	4	77	103	2	2200	10.0	2.1	1.8	0.	71.1	51.5	0.4	0.	15.1	0.
13	4	77	103	3	2200	10.0	0.4	0.4	0.	0.	16.3	0.1	0.	0.	0.
13	4	77	103	4	2200	10.0	0.	0.2	0.	0.	12.7	0.	0.	0.	0.
13	4	77	103	6	2200	10.0	0.	0.	0.	0.	4.6	0.	0.	0.	0.
13	4	77	103	7	2200	10.0	1.0	0.2	0.3	0.	7.9	0.2	0.	0.	0.
13	4	77	103	9	2200	10.0	0.6	0.7	1.0	0.	14.5	4.0	0.	0.	0.
13	4	77	103	12	2200	10.0	9.5	201.9	174.8	45.8	89.1	9.6	0.	130.9	0.
13	4	77	103	13	2115	10.0	4.8	1.3	0.	0.	13.5	3.1	0.	0.	155.6
13	4	77	103	14	2200	10.0	18.6	1.5	0.9	5.4	45.9	81.4	0.	21.7	0.
CASE 9-G				ID 09 RECP 12											
14	4	77	104	3	1000	10.0	0.	0.	0.	2.8	8.8	0.2	0.	0.	0.
14	4	77	104	4	1300	7.0	0.	0.	0.	1.0	7.3	0.	0.	0.	0.
14	4	77	104	5	1000	10.0	0.	0.	0.	0.2	5.0	0.	0.	0.	0.
14	4	77	104	6	1000	10.0	0.	0.	0.	0.	3.1	0.1	0.	0.	0.
14	4	77	104	7	1000	6.0	0.	0.	0.	0.	5.3	3.8	0.	0.	0.
14	4	77	104	8	1000	10.0	0.	0.	0.	1.0	9.0	11.0	0.	0.	0.
14	4	77	104	9	1000	10.0	0.	0.1	0.	0.2	9.4	27.1	0.	0.	0.
14	4	77	104	10	1000	10.0	0.8	0.	0.	11.0	16.0	49.6	0.	0.	4.7
14	4	77	104	11	1000	10.0	1.2	2.6	0.	1.5	14.8	68.8	0.	0.7	0.6
14	4	77	104	12	1000	10.0	1.2	1.1	0.	47.5	58.4	12.7	0.	4.8	0.
14	4	77	104	13	915	10.0	2.4	3.9	0.	0.	10.5	41.1	0.	1.0	0.
14	4	77	104	14	1000	10.0	0.	0.	0.	36.8	22.0	5.3	0.	0.	0.
CASE 9-H				ID 09 RECP 11											
14	4	77	104	2	2200	10.0	1.5	0.	0.	16.8	27.7	0.2	0.	0.	0.
14	4	77	104	4	2200	10.0	0.	0.	0.	0.6	0.1	0.	0.	0.	0.
14	4	77	104	5	2200	10.0	5.1	0.	0.	0.1	0.	0.1	0.	0.	0.
14	4	77	104	6	2200	10.0	0.	0.	0.	0.	0.	0.2	0.	0.	0.
14	4	77	104	7	2200	10.0	0.	0.	0.	0.	0.	3.7	0.	0.	0.
14	4	77	104	8	2200	10.0	0.6	0.	0.	0.9	0.2	5.2	0.	0.	0.
14	4	77	104	10	2200	10.0	339.6	0.	0.	5.7	2.4	9.3	0.	5.9	73.7
14	4	77	104	11	2200	10.0	4.9	0.4	0.	3.0	1.3	16.0	0.	0.	178.8
14	4	77	104	12	2200	10.0	2.2	0.	0.	30.6	49.7	2.1	0.	0.	0.
14	4	77	104	13	2115	10.0	1.9	2.8	0.	0.6	0.5	16.0	0.	6.9	0.
14	4	77	104	14	2200	10.0	1.5	0.	0.	1282.4	7.7	1.4	0.	2.4	0.
CASE 9-I				ID 09 RECP 12											
15	4	77	105	3	1000	10.0	1.7	0.	0.	1.6	3.5	1.2	0.	0.3	0.
15	4	77	105	4	1000	10.0	0.	0.	0.	2.2	2.5	0.4	0.	0.	0.
15	4	77	105	5	1000	10.0	0.	0.	0.	0.6	0.9	0.7	0.	0.	0.
15	4	77	105	6	1000	10.0	0.	0.	0.	0.3	0.2	1.8	0.	0.	0.
15	4	77	105	7	1000	10.0	96.3	37.5	25.1	0.9	0.4	24.4	0.	25.3	0.
15	4	77	105	8	1000	10.0	120.5	607.4	320.5	2.2	6.1	282.9	0.	226.7	2546.1
15	4	77	105	9	1000	10.0	142.8	0.	0.	2.4	1.3	45.8	0.	5.8	0.
15	4	77	105	10	1000	10.0	18.0	0.	0.	5.3	6.4	149.9	0.	14.0	1890.6
15	4	77	105	11	1000	10.0	30.5	0.	0.	4.9	3.3	34.0	0.	0.	263.2
15	4	77	105	12	1000	10.0	0.5	0.	0.	12.3	26.7	5.7	0.	0.	0.
15	4	77	105	13	915	10.0	0.	0.	0.	2.8	1.0	40.5	0.	0.	11.0
15	4	77	105	14	1000	10.0	0.1	0.	0.	5.3	13.3	3.8	0.	0.9	0.

DD	MM	YY	JUL	SI	HOUR	DUR	OBS	PUFF1	PLUME	MSPUFF	PUFF2	MTDDIS	ARRPA	RTM2	RADM
CASE 9-J				ID 09 RECP 10											
15	4	77	105	3	2200	10.0	0.	0.	0.	8.1	8.0	0.6	0.	27.8	0.
15	4	77	105	4	2200	10.0	0.2	0.	0.	11.3	6.1	0.2	0.	1.2	0.
15	4	77	105	6	2200	10.0	0.	0.	0.	1.3	5.2	1.4	0.	1.5	0.
15	4	77	105	8	2200	10.0	26.6	14.4	108.7	3.9	43.7	52.1	0.	87.8	1295.1
15	4	77	105	9	2200	10.0	9.1	0.	0.1	5.0	4.9	18.7	0.	3.4	21.6
15	4	77	105	10	2200	10.0	1.1	0.	0.	5.2	11.6	14.4	0.	0.3	0.
15	4	77	105	11	2200	10.0	0.	0.	0.	6.0	7.0	7.8	0.	0.	193.6
15	4	77	105	12	2200	10.0	0.	0.	0.	4.5	16.6	1.0	0.	0.	0.
15	4	77	105	13	2115	10.0	0.	0.	0.	5.6	3.2	4.6	0.	0.	137.5
15	4	77	105	14	2200	10.0	20.2	0.	0.	13.3	15.3	5.0	0.	13.4	565.7
CASE 10-A				ID 10 RECP 01 GR 10											
17	4	77	107	14	2200	10.0	1039.9	0.	0.	0.	145.5	119.4	0.	65.8	46384.1
CASE 10-B				ID 10 RECP 11											
18	4	77	108	2	1000	10.0	63.4	0.	0.	0.7	458.7	370.5	0.	0.9	1268.7
18	4	77	108	3	1000	10.0	0.1	0.	0.	154.0	74.9	41.7	0.	0.	0.
18	4	77	108	4	1000	10.0	0.	0.	0.	13.5	15.2	20.0	0.	0.	0.
18	4	77	108	5	1000	10.0	1.1	0.	0.	157.5	0.1	8.7	0.	0.	0.
18	4	77	108	6	1000	10.0	0.	0.	0.	190.5	0.	3.7	0.	0.	0.
18	4	77	108	7	1000	10.0	3.5	0.6	0.	48.1	0.	4.5	0.	0.	0.
18	4	77	108	8	1000	10.0	2.6	4.7	7.2	169.8	0.	15.4	0.	0.3	0.
18	4	77	108	9	1000	10.0	0.6	52.5	148.5	20.2	0.	7.7	0.	24.6	0.
18	4	77	108	11	1000	22.0	2.5	111.0	371.0	5.5	0.	13.7	0.	126.6	0.
18	4	77	108	12	1000	10.0	69.2	0.	0.	0.	0.9	117.7	0.	3.3	0.
18	4	77	108	13	915	12.0	0.	115.6	303.6	0.	0.	3.9	0.	93.6	0.
CASE 10-C				ID 10 RECP 06											
18	4	77	108	2	2200	10.0	2.1	0.	0.	5.3	330.3	166.5	0.	0.	76.6
18	4	77	108	3	2200	10.0	0.	0.	0.	17.0	2.1	11.9	0.	0.	0.
18	4	77	108	4	2200	10.0	0.	0.	0.	2.6	3.8	8.4	0.	0.	0.
18	4	77	108	5	2200	10.0	0.9	0.	0.	9.5	0.	2.7	0.	0.	0.
18	4	77	108	10	2200	10.0	0.	0.	0.	209.5	0.	18.2	0.	78.7	0.
18	4	77	108	13	2115	10.0	1.7	0.	0.	85.8	0.	1.5	0.	0.4	0.
CASE 10-D				ID 10 RECP 11											
19	4	77	109	2	1000	10.0	0.1	0.	0.	0.1	0.	114.8	0.	0.	16.4
19	4	77	109	3	1000	10.0	0.	0.	0.	0.3	0.	23.7	0.	0.	0.
19	4	77	109	5	1000	10.0	0.	0.	0.	0.1	0.	8.7	0.	0.	0.
19	4	77	109	7	1000	10.0	0.	0.	0.	112.7	0.	5.8	0.	0.	0.
19	4	77	109	8	1000	10.0	0.1	0.	0.	349.8	544.7	18.5	0.	9.4	1119.2
19	4	77	109	9	1000	10.0	91.2	0.	8.0	777.6	174.3	15.1	0.	118.3	22.4
19	4	77	109	10	1000	10.0	129.4	248.5	3298.5	582.2	174.0	124.3	0.	1044.9	716.2
19	4	77	109	11	1000	27.0	14.0	479.3	1603.2	405.5	221.9	43.5	0.	355.3	0.
19	4	77	109	12	1000	10.0	5.2	0.	0.	1.0	144.0	659.1	0.	0.	0.
19	4	77	109	13	915	10.0	263.6	1012.5	866.9	166.3	0.	13.0	0.	620.9	0.
19	4	77	109	14	1000	10.0	0.	0.	0.	1.1	0.	104.1	0.	0.6	0.
CASE 10-E				ID 10 RECP 09											
19	4	77	109	2	2200	10.0	1.2	0.	0.	1.3	5.6	37.2	0.	0.	0.
19	4	77	109	3	2200	10.0	0.	0.	0.	1.4	0.	13.4	0.	0.	0.
19	4	77	109	4	2200	10.0	0.	0.	0.	0.6	0.	9.1	0.	0.	0.
19	4	77	109	7	2200	10.0	0.	0.	0.	51.4	0.3	10.4	0.	0.	0.
19	4	77	109	8	2200	10.0	0.5	0.	0.	102.2	68.7	76.8	0.	0.	116.6
19	4	77	109	9	2200	10.0	1.4	0.	0.	401.8	740.7	60.1	0.	0.2	34.4
19	4	77	109	12	2200	10.0	1.7	0.	0.	62.6	125.8	116.1	0.	0.	0.
19	4	77	109	13	2115	10.0	9.4	161.8	115.9	166.5	122.8	56.5	0.	108.9	0.
19	4	77	109	14	2200	10.0	1.6	0.	0.	1037.8	12.2	43.4	0.	5.3	104.4
CASE 10-F				ID 10 RECP 12											
20	4	77	110	2	1000	10.0	0.	0.	0.	2327.2	5.4	24.4	0.	3.0	0.
20	4	77	110	3	1000	10.0	0.	0.	0.	14.2	0.	2.0	0.	0.	0.
20	4	77	110	4	1000	10.0	0.	0.	0.	7.7	0.	0.2	0.	0.	0.
20	4	77	110	5	1000	10.0	0.	0.	0.	4.8	0.	0.3	0.	0.	0.
20	4	77	110	6	1000	10.0	0.	0.	0.	3.1	0.	1.2	0.	0.	0.
20	4	77	110	7	1000	10.0	0.	0.	0.	6.1	0.3	21.4	0.	0.	0.
20	4	77	110	8	1000	10.0	0.	0.	0.	16.8	7.8	39.6	0.	0.	0.
20	4	77	110	9	1000	10.0	0.3	0.	0.	15.5	25.8	61.6	0.	0.	320.0
20	4	77	110	10	1000	10.0	1436.2	0.	0.	52.2	107.8	83.1	0.	0.	166.9
20	4	77	110	12	1000	10.0	0.2	6.8	142.4	148.0	137.7	10.7	0.	28.6	140.4
20	4	77	110	13	915	10.0	0.8	0.	0.	13.0	46.9	39.4	0.	2.8	0.
20	4	77	110	14	1000	10.0	9.6	0.	0.	3581.6	197.5	2628.9	0.	2153.5	0.

DD	MM	YY	JUL	SI	HOUR	DUR	OBS	PUFF1	PLUME	MSPUFF	PUFF2	MTDDIS	ARRPA	RTM2	RADM
CASE 10-G ID 10 RECP 09															
20	4	77	110	2	2200	10.0	0.5	0.	0.	0.	0.	109.4	0.	0.	0.
20	4	77	110	3	2200	10.0	0.	0.	0.	0.	0.	0.8	0.	0.	0.
20	4	77	110	4	2200	10.0	0.	0.	0.	0.	0.	0.2	0.	0.	0.
20	4	77	110	6	2200	10.0	0.3	0.	0.	0.	0.	0.3	0.	0.	0.
20	4	77	110	7	2200	10.0	0.	0.	0.	0.	0.	2.6	0.	0.	0.
20	4	77	110	9	2200	10.0	0.	0.	0.	0.	0.	6.3	0.	0.	0.
20	4	77	110	11	2200	10.0	1.8	0.	0.	0.	0.	8.7	0.	0.	149.0
20	4	77	110	12	2200	10.0	71.6	2.5	0.	47.3	373.3	76.0	0.	15.8	1405.9
20	4	77	110	13	2115	10.0	9.0	0.	0.	0.	0.	6.9	0.	0.	4.5
CASE 10-H ID 10 RECP 13															
21	4	77	111	2	1000	10.0	0.	0.	0.	0.	0.	251.6	0.	0.	0.
21	4	77	111	3	1000	10.0	0.	0.	0.	0.	0.	4.0	0.	0.	0.
21	4	77	111	4	1000	10.0	1.9	0.	0.	0.	0.	2.1	0.	0.	0.
21	4	77	111	5	1000	10.0	0.	0.	0.	0.	0.	1.5	0.	0.	0.
21	4	77	111	6	1000	10.0	0.	0.	0.	0.	0.	1.3	0.	0.	0.
21	4	77	111	7	1000	10.0	0.	0.	0.	0.	0.	5.7	0.	0.	0.
21	4	77	111	8	920	10.0	0.	0.	0.	0.	0.	9.7	0.	0.	0.
21	4	77	111	9	1000	10.0	0.	0.	0.	0.	0.	14.9	0.	0.	0.
21	4	77	111	10	1000	10.0	0.1	0.	0.	0.	0.	20.2	0.	0.	0.
21	4	77	111	11	1000	10.0	0.	0.	0.	0.	0.	27.0	0.	0.	0.
21	4	77	111	12	1000	10.0	2.1	557.4	1207.9	85.5	797.1	58.3	0.	567.9	2380.9
21	4	77	111	13	915	10.0	0.5	0.	0.	0.	0.	25.3	0.	0.	0.
21	4	77	111	14	1000	10.0	781.2	0.	0.	0.	0.	2863.3	0.	196.8	83.1
CASE 10-I ID 10 RECP 10															
21	4	77	111	2	2200	10.0	0.	0.	0.	0.	0.	76.0	0.	0.	0.
21	4	77	111	3	2200	10.0	0.9	0.	0.	0.	0.	0.3	0.	0.	0.
21	4	77	111	6	2200	10.0	0.	0.	0.	0.	0.	0.1	0.	0.	0.
21	4	77	111	7	2200	10.0	0.	0.	0.	0.	0.	0.3	0.	0.	0.
21	4	77	111	8	2200	10.0	0.	0.	0.	0.	0.	0.6	0.	0.	0.
21	4	77	111	9	2200	10.0	0.	0.	0.	0.	0.	0.8	0.	0.	0.
21	4	77	111	10	2200	10.0	0.	0.	0.	0.	0.	1.2	0.	0.	0.
21	4	77	111	12	2200	10.0	0.	5.5	2.4	149.3	47.1	31.6	0.	12.6	0.
21	4	77	111	13	2115	10.0	0.	0.	0.	0.	0.	1.5	0.	0.	0.
21	4	77	111	14	2200	10.0	3.8	0.	0.	0.	0.	194.1	0.	177.7	0.
CASE 10-J ID 10 RECP 12															
22	4	77	112	2	1000	10.0	0.	0.	0.	0.	0.	130.5	0.	0.	0.
22	4	77	112	3	1000	10.0	0.	0.	0.	0.	0.	0.1	0.	0.	0.
22	4	77	112	4	1000	10.0	0.	0.	0.	0.	0.	0.1	0.	0.	0.
22	4	77	112	5	1000	10.0	0.3	0.	0.	0.	0.	0.	0.	0.	0.
22	4	77	112	6	1000	10.0	0.	0.	0.	0.	0.	0.	0.	0.	0.
22	4	77	112	7	1000	10.0	0.	0.	0.	0.	0.	0.	0.	0.	0.
22	4	77	112	8	1000	10.0	0.	0.	0.	0.	0.	0.1	0.	0.	0.
22	4	77	112	9	1000	10.0	0.	0.	0.	0.	0.	0.1	0.	0.	0.
22	4	77	112	11	1000	10.0	0.	0.	0.	0.	0.	0.2	0.	0.	0.
22	4	77	112	12	1000	10.0	46.2	0.	8.4	0.	18.4	20.7	0.	24.7	230.6
22	4	77	112	13	915	10.0	0.	0.	0.	0.	0.	0.1	0.	0.	0.
22	4	77	112	14	1000	10.0	1152.3	0.	0.	0.	165.2	672.9	0.	2.1	190.5
CASE 11-A ID 11 RECP 13 GR 04															
27	4	77	117	2	900	10.0	0.	0.	0.	0.	0.	0.	0.	0.	0.
27	4	77	117	3	900	12.0	0.	0.	0.	0.	0.	0.	0.	0.	0.
27	4	77	117	4	900	10.0	0.	0.	0.	0.	0.	0.	0.	0.	0.
27	4	77	117	5	830	10.0	0.	0.	0.	0.	0.	0.	0.	0.	0.
27	4	77	117	6	900	10.0	0.	0.	0.1	8.9	18.8	17.8	0.	96.5	63.6
27	4	77	117	7	900	10.0	67.0	0.	0.	0.	0.	99.5	0.	0.	0.
27	4	77	117	8	900	22.0	10.8	1.2	0.	0.	0.	20.6	0.	6.1	0.
27	4	77	117	9	900	10.0	0.	0.	0.	0.	0.	0.7	0.	0.	0.
27	4	77	117	10	900	10.0	0.	0.	0.	0.	0.	0.	0.	0.	0.
27	4	77	117	11	900	10.0	0.	0.	0.	0.	0.	0.	0.	0.	0.
27	4	77	117	12	900	10.0	0.	0.	0.	0.	0.	0.	0.	0.	0.
27	4	77	117	13	815	10.0	0.	0.	0.	0.	0.	0.	0.	0.	0.
27	4	77	117	14	900	10.0	0.	0.	0.	0.	0.	0.	0.	0.	0.

DD	MM	YY	JUL	SI	HOUR	DUR	OBS	PUFF1	PLUME	MSPUFF	PUFF2	MTDDIS	ARRPA	RTM2	RADM
CASE 11-B ID 11 RECP 08															
27	4	77	117	2	2100	10.0	0.	0.	0.	0.	0.	0.	0.	0.	0.
27	4	77	117	3	2345	10.0	0.	0.	0.	0.	0.	0.	0.	0.	0.
27	4	77	117	6	2100	10.0	0.	0.	0.	0.	6.1	2.6	0.	0.	13.9
27	4	77	117	9	2100	10.0	25.0	0.	0.	0.	0.	57.9	0.	0.	0.
27	4	77	117	10	2100	10.0	2.0	0.	0.	0.	0.	3.0	0.	0.	0.
27	4	77	117	11	2100	10.0	0.2	0.	0.	0.	0.	0.5	0.	0.	0.
27	4	77	117	12	2100	10.0	0.	0.	0.	0.	0.	0.	0.	0.	0.
27	4	77	117	14	2100	10.0	0.	0.	0.	0.	0.	0.	0.	0.	0.
CASE 11-C ID 11 RECP 10															
28	4	77	118	2	1200	7.0	0.	0.	0.	0.	0.	0.	0.	0.	0.
28	4	77	118	4	900	10.0	0.	0.	0.	0.	0.	0.	0.	0.	0.
28	4	77	118	5	900	10.0	2.3	0.	0.	0.	0.	0.	0.	0.	0.
28	4	77	118	6	900	10.0	0.	0.	0.	0.	0.	0.	0.	0.	0.
28	4	77	118	7	900	10.0	411.4	282.2	320.5	825.8	0.	172.5	0.	256.4	0.
28	4	77	118	8	900	10.0	1557.6	249.9	312.2	169.9	0.	1959.0	0.	175.5	0.
28	4	77	118	9	900	10.0	116.5	0.	0.	0.	0.	125.6	0.	0.	0.
28	4	77	118	10	900	10.0	0.	0.	0.	0.	0.	0.	0.	0.	0.
28	4	77	118	12	900	10.0	0.	0.	0.	0.	0.	0.	0.	0.	0.
28	4	77	118	13	815	10.0	0.	0.	0.	0.	0.	6.1	0.	0.	0.
CASE 11-D ID 11 RECP 12															
28	4	77	118	2	2100	10.0	2.3	0.	0.	0.	0.	0.	0.	0.	0.
28	4	77	118	3	2100	10.0	1.2	0.	0.	0.	0.	0.	0.	0.	0.
28	4	77	118	4	2100	10.0	0.	0.	0.	0.	0.	0.	0.	0.	0.
28	4	77	118	5	2100	10.0	0.	0.	0.	0.	0.	0.	0.	0.	0.
28	4	77	118	6	2100	10.0	0.	0.	0.	0.	0.	0.	0.	0.	0.
28	4	77	118	7	2100	10.0	12.6	0.5	0.	32.4	178.7	120.8	0.	3.5	413.8
28	4	77	118	8	2100	10.0	13.4	38.6	24.6	122.3	115.4	327.9	0.	27.0	232.1
28	4	77	118	9	2100	10.0	55.2	35.3	21.5	0.	0.	416.9	0.	65.8	0.
28	4	77	118	11	2100	10.0	0.	0.	0.	0.	0.	4.8	0.	0.	0.
28	4	77	118	12	2100	10.0	0.	0.	0.	0.	0.	0.	0.	0.	0.
28	4	77	118	13	2015	10.0	1.6	0.	0.	0.	0.	13.3	0.	0.	0.
28	14	77	118	14	2100	10.0	0.	0.	0.	0.	0.	0.	0.	0.	0.
CASE 12-A ID 12 RECP 12 GR 02															
11	7	77	192	2	900	10.0	0.	0.	0.	0.	0.	0.	0.	0.	0.
11	7	77	192	3	900	10.0	0.	0.	0.	0.	0.	0.1	0.	0.	0.
11	7	77	192	4	900	10.0	0.	0.	0.	0.	0.	0.	0.	0.	0.
11	7	77	192	5	900	10.0	0.	0.	0.	0.	0.	0.	0.	0.	0.
11	7	77	192	7	900	10.0	2.9	1106.1	644.8	0.	84.7	199.5	0.	462.9	0.
11	7	77	192	8	900	10.0	15.1	777.6	484.7	0.	2064.6	741.8	0.	711.4	0.
11	7	77	192	9	900	10.0	111.3	0.2	0.	0.3	1452.5	171.6	0.	229.9	0.
11	7	77	192	10	900	10.0	27.4	0.	0.	2347.3	0.	21.2	0.	0.2	0.
11	7	77	192	11	900	10.0	0.	0.	0.	213.1	0.	8.4	0.	5.5	0.
11	7	77	192	12	900	10.0	0.	0.	0.	0.	0.	0.	0.	0.	0.
11	7	77	192	13	830	10.0	0.	1.0	0.	19.6	0.	3.3	0.	16.7	0.
11	7	77	192	14	900	10.0	0.	0.	0.	0.	0.	0.2	0.	0.	0.
CASE 12-B ID 12 RECP 11															
11	7	77	192	2	2100	10.0	0.	0.	0.	0.	0.	0.2	0.	0.	0.
11	7	77	192	3	2100	10.0	0.	0.	0.	0.	0.	0.7	0.	0.	0.
11	7	77	192	5	2100	10.0	1.0	0.	0.	0.	0.	0.2	0.	0.	0.
11	17	77	192	6	1600	15.0	0.	0.	0.	0.	0.	2.8	0.	0.	0.
11	7	77	192	7	2100	10.0	0.	0.4	0.7	0.	79.9	75.6	0.	9.2	1168.6
11	7	77	192	8	2100	10.0	0.	0.	1.3	17.0	444.2	153.3	0.	8.3	175.6
11	7	77	192	9	2100	10.0	2.5	64.3	17.8	198.2	256.0	105.0	0.	31.9	0.
11	7	77	192	11	2100	10.0	6.4	38.1	4.0	90.7	73.8	113.8	0.	29.8	0.
11	7	77	192	12	2100	10.0	0.	0.	0.	0.	0.	1.4	0.	0.	0.
11	7	77	192	13	2045	10.0	29.2	85.7	55.3	24.9	42.2	22.6	0.	32.4	0.
11	7	77	192	14	2100	10.0	0.	0.	0.	0.	0.	5.4	0.	0.	0.

DD	MM	YY	JUL	SI	HOUR	DUR	OBS	PUFF1	PLUME	MSPUFF	PUFF2	MTDDIS	ARRPA	RTM2	RADM
CASE 13-A ID 13 RECP 11 GR 02															
15	7	77	196	2	900	10.0	0.5	0.	0.2	0.	2.0	8.5	0.	0.	0.
15	7	77	196	3	900	10.0	0.	0.	0.	0.	0.	3.7	0.	0.	0.
15	7	77	196	4	900	10.0	0.	0.	0.	0.	0.	0.	0.	0.	0.
15	7	77	196	5	900	10.0	0.	0.	0.	0.	0.	0.	0.	0.	0.
15	7	77	196	7	900	10.0	0.	0.	0.	0.	0.	0.	0.	0.	0.
15	7	77	196	9	900	10.0	0.	0.	0.	0.	0.	0.1	0.	0.	0.
15	7	77	196	10	900	10.0	223.1	0.	0.	0.	0.	36.7	0.	0.	0.
15	7	77	196	11	900	10.0	12.2	0.	0.	0.	0.	0.8	0.	0.	0.
15	7	77	196	12	900	10.0	2.7	0.	0.	0.	0.	6.9	0.	0.	0.
15	7	77	196	13	845	10.0	0.	0.	0.	0.	0.	0.	0.	0.	0.
15	7	77	196	14	900	10.0	26.5	0.	0.4	0.	15.9	267.8	0.	2.0	21.6
CASE 13-B ID 13 RECP 09															
15	7	77	196	2	2200	10.0	0.	16.1	5.7	0.	7.4	54.5	0.	27.9	0.
15	7	77	196	3	2100	10.0	0.2	0.	0.	0.	0.	2.0	0.	0.	0.
15	7	77	196	4	2100	10.0	0.	0.	0.	0.	0.	0.5	0.	0.	0.
15	7	77	196	7	2100	10.0	9.5	0.	0.	0.	0.	0.	0.	0.	0.
15	7	77	196	8	2100	10.0	0.	0.	0.	0.	0.	0.2	0.	0.	0.
15	7	77	196	10	2100	10.0	2.4	0.	0.	0.	0.	2.8	0.	0.	0.
15	7	77	196	11	2100	10.0	0.5	0.	0.	0.	0.	0.4	0.	0.	0.
15	7	77	196	12	2100	10.0	6.5	0.	0.	0.	0.4	16.4	0.	0.	0.
15	7	77	196	14	2100	10.0	1.5	7.9	6.3	0.	0.	115.0	0.	1.0	18.2
CASE 14-A ID 14 RECP 12 GR 05															
18	7	77	199	2	900	10.0	0.	0.	0.	0.	0.	0.	0.	0.	0.
18	7	77	199	3	900	10.0	0.	0.	0.	0.	0.	0.	0.	0.	0.
18	7	77	199	4	900	10.0	0.	0.	0.	0.	0.	0.	0.	0.	0.
18	7	77	199	5	900	10.0	0.	0.	0.	0.	0.	0.	0.	0.	0.
18	7	77	199	7	900	10.0	0.	0.	0.	0.	0.	0.	0.	0.	0.
18	7	77	199	8	900	10.0	0.	0.	0.	0.	0.	0.	0.	0.	0.
18	7	77	199	9	900	10.0	0.	0.	0.	0.	0.	0.	0.	0.	0.
18	7	77	199	10	900	10.0	0.	0.	0.	0.	0.	0.	0.	0.	0.
18	7	77	199	11	1200	7.0	0.	0.	0.	0.	0.	0.	0.	0.	0.
18	7	77	199	12	900	10.0	0.	0.	0.	0.	0.	0.	0.	0.	0.
18	7	77	199	13	1300	5.8	0.1	0.	0.	0.	0.	0.	0.	0.	0.
18	7	77	199	14	900	10.0	20.1	0.	0.	0.	0.	0.	0.	0.	0.
CASE 14-B ID 14 RECP 09															
18	7	77	199	2	2100	10.0	0.	0.	0.	0.	0.	0.	0.	0.	0.
18	7	77	199	3	2100	10.0	0.	0.	0.	0.	0.	0.	0.	0.	0.
18	7	77	199	4	2100	10.0	0.	0.	0.	0.	0.	0.	0.	0.	0.
18	7	77	199	7	2100	10.0	0.	0.	0.	0.	0.	0.	0.	0.	0.
18	7	77	199	9	2100	10.0	0.	0.	0.	0.	0.	0.	0.	0.	0.
18	7	77	199	10	2100	10.0	0.	0.	0.	0.	0.	0.	0.	0.	0.
18	7	77	199	12	2100	10.0	0.	0.	0.	0.	0.	0.	0.	0.	0.
18	7	77	199	13	2030	10.0	17.2	0.	0.	0.	0.	0.	0.	0.	0.
18	7	77	199	14	2100	10.0	0.	0.	0.	0.	0.	0.	0.	0.7	0.
CASE 14-C ID 14 RECP 11															
19	7	77	200	2	900	10.0	0.	0.	0.	0.	0.	0.	0.	0.	0.
19	7	77	200	3	900	10.0	0.	0.	0.	0.	0.	0.	0.	0.	0.
19	7	77	200	5	900	10.0	0.	0.	0.	0.	0.	0.	0.	0.	0.
19	7	77	200	7	900	10.0	0.	0.	0.	0.	0.	0.	0.	0.	0.
19	7	77	200	8	900	10.0	2.1	0.	0.	0.	0.	0.	0.	0.	0.
19	7	77	200	9	900	10.0	0.	0.	0.	0.	0.	0.	0.	0.	0.
19	7	77	200	10	900	10.0	2259.6	0.	0.	0.	0.	52.3	0.	12.8	0.
19	7	77	200	11	900	10.0	1509.1	0.	0.	0.	0.	0.4	0.	0.7	0.
19	7	77	200	12	900	10.0	0.	0.	0.8	605.9	0.	5.2	0.	86.5	0.
19	7	77	200	13	830	12.0	0.	0.	0.	0.	0.	0.	0.	0.	0.
19	7	77	200	14	900	10.0	0.	0.	0.	0.	0.	79.0	0.	153.2	0.

DD	MM	YY	JUL	SI	HOUR	DUR	OBS	PUFF1	PLUME	MSPUFF	PUFF2	MTDDIS	ARRPA	RTM2	RADM
CASE 14-D				ID 14 RECP 06											
19	7	77	200	2	2100	10.0	0.	0.	0.	0.	0.	0.3	0.	0.	0.
19	7	77	200	3	2100	10.0	0.	0.	0.	0.	0.	0.	0.	0.	0.
19	7	77	200	4	2100	10.0	0.	0.	0.	0.	0.	0.	0.	0.	0.
19	7	77	200	5	2100	10.0	0.	0.	0.	0.	0.	0.	0.	0.	0.
19	7	77	200	10	2100	10.0	66.4	0.	0.	0.	80.6	254.4	0.	48.5	180.9
19	7	77	200	14	2100	10.0	0.	0.	0.	0.	0.	10.0	0.	0.	0.
CASE 14-E				ID 14 RECP 10											
20	7	77	201	3	900	10.0	0.	0.	0.	0.	0.	0.	0.	0.	0.
20	7	77	201	5	900	10.0	0.	0.	0.	0.	0.	0.	0.	0.	0.
20	7	77	201	7	900	10.0	0.	0.	0.	0.	0.	0.2	0.	0.	0.
20	7	77	201	8	900	10.0	0.	0.	0.	0.	0.	1.0	0.	0.	0.
20	7	77	201	9	900	5.0	0.1	0.	0.	0.	0.	10.4	0.	53.8	0.
20	7	77	201	10	900	10.0	4.0	0.	0.	0.	0.	27.4	0.	71.5	0.
20	7	77	201	11	900	8.5	2.2	291.0	717.5	0.	46.9	119.6	0.	292.0	2.5
20	7	77	201	12	900	10.0	0.	0.	0.	0.4	0.	21.9	0.	0.	0.
20	7	77	201	13	830	10.0	6.8	47.4	178.0	0.	36.1	119.3	0.	85.4	0.
20	7	77	201	14	900	9.3	0.	0.	0.	0.	0.	0.3	0.	0.	0.
CASE 15-A				ID 15 RECP 10 GR 04											
25	7	77	206	3	900	10.0	0.	0.	0.	0.	0.	0.	0.	0.	0.
25	7	77	206	4	900	10.0	0.	0.	0.	0.	0.	0.	0.	0.	0.
25	7	77	206	5	900	10.0	0.	0.	0.	0.	0.	0.	0.	0.	0.
25	7	77	206	7	900	10.0	0.	0.	0.	0.	0.	0.	0.	0.	0.
25	7	77	206	8	900	10.0	0.	0.	0.	549.1	0.	1.3	0.	0.	0.
25	7	77	206	10	900	10.0	365.9	5308.8	2294.7	0.	0.5	578.7	0.	807.7	68.0
25	7	77	206	11	900	10.0	88.6	787.0	447.9	0.	0.	9.5	0.	209.1	6.3
25	7	77	206	12	900	10.0	0.7	0.	0.	0.	0.	0.	0.	0.	0.
25	7	77	206	13	830	10.0	153.4	151.6	112.9	0.	0.	0.	0.	54.7	0.
25	7	77	206	14	900	10.0	0.	0.	0.	0.	0.	0.	0.	1.7	0.
CASE 15-B				ID 15 RECP 09											
25	7	77	206	3	2100	10.0	0.	0.	0.	0.	0.	0.	0.	0.	0.
25	7	77	206	4	2100	10.0	2.1	0.	0.	0.	0.	0.	0.	0.	0.
25	7	77	206	7	2100	10.0	0.	0.	0.	1199.4	0.	0.	0.	0.	0.
25	7	77	206	8	2100	10.0	0.	0.	0.	263.5	0.	6.9	0.	0.1	0.
25	7	77	206	9	2100	10.0	2.7	323.5	504.7	0.	431.4	119.2	0.	305.5	834.4
25	7	77	206	10	2100	10.0	13.7	2.9	17.2	0.	73.4	1381.7	0.	3.8	173.0
25	7	77	206	11	2100	10.0	15.1	2.8	14.3	0.	141.1	620.0	0.	33.2	117.2
25	7	77	206	12	2100	10.0	0.	0.	0.	0.	0.	0.	0.	0.	0.
25	7	77	206	14	2100	10.0	9.6	0.	0.	0.	0.	0.	0.	0.	0.
CASE 15-C				ID 15 RECP 10											
26	7	77	207	3	900	10.0	0.	0.	0.	0.	0.	0.	0.	0.	0.
26	7	77	207	4	900	10.0	0.	0.	0.	0.	0.	0.	0.	0.	0.
26	7	77	207	5	900	10.0	0.	0.	0.	0.	0.	0.	0.	0.	0.
26	7	77	207	7	900	10.0	0.	0.	0.	81.8	0.	0.4	0.	5.3	0.
26	7	77	207	8	900	10.0	0.	24.6	28.5	200.6	0.	6.5	0.	60.4	0.
26	7	77	207	9	900	10.0	0.	0.	0.3	0.	14.3	69.2	0.	22.7	0.
26	7	77	207	10	900	10.0	55.7	0.	0.	0.	29.4	512.5	0.	0.1	2.1
26	7	77	207	11	900	10.0	59.2	0.	0.	0.	113.8	615.9	0.	0.	472.3
26	7	77	207	12	900	10.0	0.	0.	0.	0.	0.	0.1	0.	0.	0.
26	7	77	207	13	830	10.0	38.5	0.	0.	0.	512.6	664.1	0.	0.	113.7
CASE 15-D				ID 15 RECP 11											
26	7	77	207	3	2100	10.0	0.	0.	0.	0.	0.	1.6	0.	0.	19.2
26	7	77	207	4	2100	10.0	0.	0.	0.	0.	0.	0.2	0.	0.	0.
26	7	77	207	5	2100	10.0	0.	0.	0.	0.	0.	0.4	0.	0.	0.
26	7	77	207	7	2100	10.0	0.	0.	0.	0.	12.1	22.6	0.	0.	0.
26	7	77	207	8	2100	10.0	1.0	0.	0.	0.	17.7	72.4	0.	3.7	285.1
26	7	77	207	9	2100	10.0	3.8	17.4	31.2	0.	127.5	167.9	0.	14.4	186.1
26	7	77	207	10	2100	10.0	3.9	0.	0.	0.	28.4	121.8	0.	7.3	0.
26	7	77	207	11	2100	10.0	4.1	0.	0.	0.	118.4	266.4	0.	1.7	123.1
26	7	77	207	12	2100	10.0	14.2	0.	0.	0.	2.4	17.2	0.	0.	0.
26	7	77	207	13	2030	10.0	3.0	0.	0.	0.	148.1	304.0	0.	0.5	547.7
26	7	77	207	14	2100	10.0	0.5	0.	0.	0.	1.2	11.8	0.	0.	0.

DD	MM	YY	JUL	SI	HOUR	DUR	OBS	PUFF1	PLUME	MSPUFF	PUFF2	MTDDIS	ARRPA	RTM2	RADM
CASE 20-A			ID 20		RECP 09		GR 07								
8	7	80	190112	2100		0.75	0.1	90.3	323.5	403.8	0.	0.	0.	0.	0.
8	7	80	190113	2100		0.75	1.0	408.3	922.6	2114.1	0.	0.	0.	0.	0.
8	7	80	190114	2100		0.75	1.7	1554.7	2793.2	5701.7	0.	0.	0.	0.	0.
8	7	80	190115	2100		0.75	1.9	2361.5	4846.5	2853.7	0.	0.	0.	0.	0.
8	7	80	190116	2100		0.75	0.	1892.0	5136.4	719.0	0.	0.	0.	0.	0.
8	7	80	190118	2100		0.75	0.	378.6	2453.6	0.	0.	0.	0.	0.	0.
8	7	80	190119	2100		0.75	0.	32.1	809.4	0.	0.	0.	0.	0.	0.
8	7	80	190120	2100		0.75	0.7	0.	144.3	0.	0.	0.	0.	0.	0.
8	7	80	190122	2100		0.75	2.7	0.	0.	0.	11.4	0.	0.	0.	0.
CASE 20-B			ID 20		RECP 10										
8	7	80	190112	2145		0.75	647.0	624.7	756.8	6553.6	0.	0.	0.	26.2	0.
8	7	80	190113	2145		0.75	1297.0	1629.4	1782.9	12667.7	0.	0.	0.	368.5	0.
8	7	80	190114	2145		0.75	917.0	3622.8	3975.5	11333.9	0.	0.	0.	324.0	0.
8	7	80	190115	2145		0.75	757.0	3881.2	5031.2	2937.3	0.	0.	0.3	253.3	37.7
8	7	80	190116	2145		0.75	1107.0	2705.5	4341.1	547.5	0.	0.	3.5	202.8	308.2
8	7	80	190118	2145		0.75	287.0	375.5	1411.6	0.	121.1	0.	0.	281.7	1851.0
8	7	80	190119	2145		0.75	127.0	23.0	380.8	0.	322.2	0.	0.	355.7	1419.0
8	7	80	190120	2145		0.75	13.0	0.	48.1	0.	533.3	0.	0.	388.6	1103.9
8	7	80	190121	2145		0.75	24.1	0.	0.	0.	468.7	0.	0.	41.4	857.3
8	7	80	190122	2145		0.75	2.7	0.	0.	0.	1937.6	0.	3515.3	34.7	3417.9
CASE 20-C			ID 20		RECP 10										
8	7	80	190112	2230		0.75	3997.0	1514.0	1451.7	13179.3	0.	0.	0.1	69.0	0.
8	7	80	190113	2230		0.75	5897.0	2893.2	2859.5	16899.1	0.	0.	1.5	622.5	0.
8	7	80	190114	2230		0.75	4667.0	4646.1	6648.8	10296.8	0.	0.	18.3	561.4	0.
8	7	80	190115	2230		0.75	2727.0	4006.8	4787.4	1996.7	0.	0.	93.9	464.4	37.7
8	7	80	190116	2230		0.75	2807.0	2533.6	3538.7	307.8	0.	0.	316.7	395.1	370.3
8	7	80	190118	2230		0.75	2097.0	276.0	645.5	0.	234.1	0.	1229.9	536.8	3419.2
8	7	80	190119	2230		0.75	557.0	12.3	111.0	0.	800.7	0.	1502.4	626.2	4563.4
8	7	80	190120	2230		0.75	212.0	0.	0.	0.	1682.2	0.	1463.3	662.8	5159.5
8	7	80	190121	2230		0.75	0.6	0.	0.	0.	1825.1	0.	1345.7	139.9	4604.4
8	7	80	190122	2230		0.75	1.1	0.	0.	0.	3274.6	0.	3926.7	134.6	7711.1
CASE 20-D			ID 20		RECP 10										
8	7	80	190112	2315		0.75	2837.0	2758.3	2408.4	20280.8	0.	0.	0.3	128.5	0.
8	7	80	190113	2315		0.75	2737.0	4199.5	4152.2	14808.4	0.	0.	4.4	762.0	0.
8	7	80	190114	2315		0.75	1647.0	4624.5	10813.3	2590.4	0.	0.	54.9	712.4	0.
8	7	80	190115	2315		0.75	1257.0	2738.2	4115.2	32.0	0.	0.	280.7	633.3	0.
8	7	80	190116	2315		0.75	997.0	1376.2	2729.1	0.	0.	0.	939.7	576.9	186.4
8	7	80	190118	2315		0.75	337.0	79.9	155.0	0.	339.0	0.	3689.7	765.3	4704.6
8	7	80	190119	2315		0.75	47.0	0.	0.	0.	1435.5	0.	4507.2	811.5	9433.4
8	7	80	190120	2315		0.75	11.0	0.	0.	0.	3446.7	0.	4389.9	822.5	12167.0
8	7	80	190121	2315		0.75	0.	0.	0.	0.	4069.0	0.	4037.1	295.6	11241.3
8	7	80	190122	2315		0.75	0.4	0.	0.	0.	4022.3	0.	1234.3	299.5	12879.5
CASE 20-E			ID 20		RECP 10										
9	7	80	191112		0	0.75	2167.0	3631.1	418.5	11175.7	0.	0.	979.6	468.0	0.
9	7	80	191113		0	0.75	497.0	4075.1	815.7	4545.5	0.	0.	3207.3	1566.0	0.
9	7	80	191114		0	0.75	179.0	2939.9	490.2	234.1	0.	0.	8114.7	1543.8	0.
9	7	80	191115		0	0.75	85.0	1188.9	0.	0.	4.4	0.	10242.3	1450.9	0.
9	7	80	191116		0	0.75	87.0	473.4	0.	0.	75.6	0.	7598.0	1359.2	59.9
9	7	80	191118		0	0.75	0.	0.	0.	0.	1639.8	0.	2300.7	1419.9	2690.8
9	7	80	191119		0	0.75	0.	0.	0.	0.	2881.8	0.	1208.8	1530.2	5460.4
9	7	80	191120		0	0.75	0.8	0.	0.	0.	3642.2	0.	503.5	1535.6	7606.8
9	7	80	191121		0	0.75	0.	0.	0.	0.	3243.6	0.	230.8	650.0	8027.3
9	7	80	191122		0	0.75	0.8	0.	0.	0.	1160.8	0.	2.9	589.3	5260.7
CASE 20-F			ID 20		RECP 10										
9	7	80	191112		45	0.75	40.0	1338.3	139.5	3726.0	0.	0.	746.4	648.5	0.
9	7	80	191113		45	0.75	1.0	1498.2	271.9	1515.2	5.9	0.	1127.0	1402.3	0.
9	7	80	191114		45	0.75	1.0	1084.8	163.4	78.0	114.6	0.	2960.3	1390.3	43.7
9	7	80	191115		45	0.75	1.5	443.9	0.	0.	643.9	0.	3638.6	1348.4	282.4
9	7	80	191116		45	0.75	6.0	175.1	0.	0.	1299.1	0.	2615.9	1308.5	899.2
9	7	80	191118		45	0.75	0.	0.	0.	0.	2891.0	0.	767.9	1324.4	4502.4
9	7	80	191119		45	0.75	0.	0.	0.	0.	2734.2	0.	403.0	1374.3	5993.9
9	7	80	191120		45	0.75	1.5	0.	0.	0.	2128.6	0.	168.2	1332.5	5953.8
9	7	80	191121		45	0.75	0.1	0.	0.	0.	1578.4	0.	77.0	695.1	4581.3
9	7	80	191122		45	0.75	0.7	0.	0.	0.	413.8	0.	0.9	704.6	1843.2

DD	MM	YY	JUL	SI	HOUR	DUR	OBS	PUFF1	PLUME	MSPUFF	PUFF2	MTDDIS	ARRPA	RTM2	RADM
CASE 20-G			ID 20		RECP 09										
9	7	80	191112		130	0.75	1.6	127.9	0.	0.8	58.6	0.	419.9	715.0	474.9
9	7	80	191114		130	0.75	2.0	104.8	0.	0.	925.2	0.	255.4	1186.6	2075.6
9	7	80	191115		130	0.75	1.8	47.6	0.	0.	1639.8	0.	224.5	1174.1	2751.6
9	7	80	191116		130	0.75	0.	17.3	0.	0.	2078.9	0.	83.3	1164.8	2877.6
9	7	80	191118		130	0.75	0.	0.	0.	0.	2494.9	0.	1.1	1156.7	4321.4
9	7	80	191119		130	0.75	0.	0.	0.	0.	1831.6	0.	0.1	1170.2	4502.3
9	7	80	191120		130	0.75	1.1	0.	0.	0.	926.1	0.	0.3	1180.9	3514.1
9	7	80	191121		130	0.75	0.	0.	0.	0.	501.5	0.	0.1	661.2	1942.0
9	7	80	191122		130	0.75	2.5	0.	0.	0.	26.9	0.	0.	727.3	89.6
CASE 30-A			ID 30		RECP 32	GR 06									
9	7	80	191600		800	3.00	0.	0.	0.	0.	0.	0.	0.	0.	0.
9	7	80	191601		800	3.00	0.	0.	0.	0.	0.	0.	0.	0.	0.
9	7	80	191602		800	3.00	0.6	0.	0.	0.	0.	0.	0.	0.	0.
9	7	80	191603		800	3.00	0.7	0.	0.	0.	0.	0.	0.	0.	0.
9	7	80	191604		800	3.00	0.	0.	0.	0.	0.	0.	0.	0.	0.
9	7	80	191606		800	3.00	14.2	0.	0.	0.	0.	0.	0.	0.	0.
9	7	80	191607		800	3.00	0.2	0.	0.	0.	0.	0.	0.	0.	0.
9	7	80	191609		800	3.00	624.0	0.	0.	0.	0.	0.	0.	0.	0.
9	7	80	191610		800	3.00	1277.0	0.	0.	0.	0.	0.	0.	0.	0.
9	7	80	191611		800	3.00	1007.0	0.	0.	0.	0.	0.	0.	0.	0.
9	7	80	191612		800	3.00	897.0	0.	0.	0.	0.	0.	0.	0.	0.
9	7	80	191613		800	3.00	977.0	0.	0.	0.	0.	0.	0.	0.	0.
9	7	80	191615		800	3.00	13.0	0.4	0.	0.	0.	0.	9.6	0.	0.
9	7	80	191616		800	3.00	1.8	0.1	0.	0.	0.	0.	0.	0.	0.
9	7	80	191617		800	3.00	0.	0.5	0.	0.	0.	0.	0.	0.	0.
9	7	80	191618		800	3.00	0.	3.2	0.	0.1	0.	0.	0.	0.	0.
9	7	80	191619		800	3.00	0.	0.2	0.	5.2	0.	0.	0.	0.	0.
9	7	80	191620		800	3.00	0.	1.0	0.	150.2	0.	0.	0.	0.	0.
9	7	80	191623		800	3.00	0.	0.	0.	492.0	0.	0.	0.	0.	0.
9	7	80	191624		800	3.00	0.	0.	0.	185.9	0.	0.	0.	0.	0.
9	7	80	191625		800	3.00	0.	0.	0.	98.5	0.	0.	0.	0.	0.
9	7	80	191626		800	3.00	0.	0.	0.	3.3	0.	0.	0.	0.	0.
9	7	80	191628		800	3.00	0.	0.	0.	0.	0.	0.	0.	0.	0.
9	7	80	191629		800	3.00	0.	0.	0.	0.	0.	0.	0.	0.	0.
9	7	80	191630		800	3.00	0.	0.	0.	0.	0.	0.	0.	0.	0.
9	7	80	191631		800	3.00	0.	0.	0.	0.	0.	0.	0.	0.	0.
9	7	80	191632		800	3.00	0.	0.	0.	0.	0.	0.	0.	0.	0.
9	7	80	191633		800	3.00	0.	0.	0.	0.	0.	0.	0.	0.	0.
9	7	80	191634		800	3.00	0.4	0.	0.	0.	0.	0.	0.	0.	0.
9	7	80	191635		800	3.00	0.	0.	0.	0.	0.	0.	0.	0.	0.
9	7	80	191636		800	3.00	0.	0.	0.	0.	0.	0.	0.	0.	0.
9	7	80	191637		800	3.00	0.	0.	0.	0.	0.	0.	0.	0.	0.

DD	MM	YY	JUL	SI	HOUR	DUR	OBS	PUFF1	PLUME	MSPUFF	PUFF2	MTDDIS	ARRPA	RTM2	RADM
CASE 30-B ID 30 RECP 34															
9	7	80	191600	1100	3.00		0.	0.	0.	0.	0.	0.	0.	0.	0.
9	7	80	191601	1100	3.00		0.	0.	0.	0.	0.	0.	0.	0.	0.
9	7	80	191602	1100	3.00		0.5	0.	0.	0.	0.	0.	0.	0.	0.
9	7	80	191603	1100	3.00		0.	0.	0.	0.	0.	0.	0.	0.	0.
9	7	80	191604	1100	3.00		0.	0.	0.	0.	0.	0.	0.	0.	0.
9	7	80	191606	1100	3.00		7.5	0.	0.	0.	0.	0.	0.	0.	0.
9	7	80	191607	1100	3.00		0.	0.	0.	0.	0.	0.	0.	0.	0.
9	7	80	191609	1100	3.00		60.0	0.	0.	0.	0.	0.	0.	0.	0.
9	7	80	191610	1100	3.00		817.0	0.	0.	0.	0.	0.	0.	0.	0.
9	7	80	191611	1100	3.00		527.0	0.	0.	0.	0.	0.	0.	0.	0.
9	7	80	191612	1100	3.00		183.0	0.	0.	0.	0.	0.	0.	0.	0.
9	7	80	191613	1100	3.00		497.0	0.	0.	0.	0.	0.	0.	0.	0.
9	7	80	191615	1100	3.00		0.	12.6	30.7	0.	0.	0.	25.0	0.	0.
9	7	80	191616	1100	3.00		0.	19.9	33.0	0.	0.	0.	57.5	0.	0.
9	7	80	191617	1100	3.00		0.	72.0	103.8	0.	0.	0.	903.5	0.	0.
9	7	80	191618	1100	3.00		0.	270.7	389.3	0.	0.	0.	2449.2	0.	0.
9	7	80	191619	1100	3.00		0.	289.2	442.0	1.7	0.	0.	444.7	0.	0.
9	7	80	191620	1100	3.00		0.	485.6	658.5	53.8	0.	0.	0.2	0.	0.
9	7	80	191623	1100	3.00		0.	48.5	109.6	590.6	0.	0.	0.	0.	0.
9	7	80	191624	1100	3.00		0.	6.0	11.6	813.2	0.	0.	0.	0.	0.
9	7	80	191625	1100	3.00		0.	0.3	0.	577.3	0.	0.	0.	0.	0.
9	7	80	191626	1100	3.00		0.	0.	0.	278.1	0.	0.	0.	0.	0.
9	7	80	191627	1100	3.00		0.	0.	0.	221.2	0.	0.	0.	0.	0.
9	7	80	191628	1100	3.00		0.	0.	0.	4.7	0.	0.	0.	0.	0.
9	7	80	191629	1100	3.00		0.	0.	0.	0.7	0.	0.	0.	0.	0.
9	7	80	191630	1100	3.00		0.	0.	0.	0.	0.	0.	0.	0.	0.
9	7	80	191631	1100	3.00		0.3	0.	0.	0.	0.	0.	0.	0.	0.
9	7	80	191632	1100	3.00		0.	0.	0.	0.	0.	0.	0.	0.	0.
9	7	80	191633	1100	3.00		0.	0.	0.	0.	0.	0.	0.	0.	0.
9	7	80	191634	1100	3.00		0.	0.	0.	0.	0.	0.	0.	0.	0.
9	7	80	191635	1100	3.00		0.	0.	0.	0.	0.	0.	0.	0.	0.
9	7	80	191636	1100	3.00		0.	0.	0.	0.	0.	0.	0.	0.	0.
9	7	80	191637	1100	3.00		0.	0.	0.	0.	0.	0.	0.	0.	0.
9	7	80	191638	1100	3.00		0.	0.	0.	0.	0.	0.	0.	0.	0.
CASE 30-C ID 30 RECP 32															
9	7	80	191600	1400	3.00		0.	0.	0.	0.	0.	0.	0.	0.	0.
9	7	80	191601	1400	3.00		0.	0.	0.	0.	0.	0.	0.	0.	0.
9	7	80	191602	1400	3.00		0.1	0.	0.	0.	0.	0.	0.	0.	0.
9	7	80	191603	1400	3.00		0.	0.	0.	0.	0.	0.	0.	0.	0.
9	7	80	191604	1400	3.00		0.	0.	0.	0.	0.	0.	0.	0.	0.
9	7	80	191606	1400	3.00		0.	0.	0.	0.	0.	0.	0.	0.	0.
9	7	80	191609	1400	3.00		0.9	0.	0.	0.	0.	0.	0.	0.	0.
9	7	80	191610	1400	3.00		23.0	0.	0.	0.	0.4	0.	0.	0.	0.
9	7	80	191611	1400	3.00		161.0	0.	0.	0.	4.1	0.	0.	0.	0.
9	7	80	191612	1400	3.00		96.0	0.	0.	0.	13.4	0.	0.	0.1	0.
9	7	80	191613	1400	3.00		347.0	0.	0.	0.	10.9	0.	0.	0.	0.
9	7	80	191615	1400	3.00		1.5	0.	0.	0.	113.4	0.	0.	1.3	0.
9	7	80	191616	1400	3.00		1.3	3.1	4.2	0.	103.9	0.	0.1	1.8	0.
9	7	80	191617	1400	3.00		0.	51.5	53.4	0.	139.2	0.	308.1	1.1	0.
9	7	80	191618	1400	3.00		0.	203.6	185.4	0.	158.9	0.	888.7	2.3	0.
9	7	80	191619	1400	3.00		0.	482.6	423.8	0.6	69.1	0.	574.7	1.0	0.
9	7	80	191620	1400	3.00		0.	745.8	509.2	17.9	27.1	0.	0.5	2.1	0.
9	7	80	191623	1400	3.00		0.	245.5	206.1	196.9	0.	0.	0.	0.1	0.
9	7	80	191624	1400	3.00		0.	145.7	168.6	271.1	0.	0.	0.	0.	0.
9	7	80	191625	1400	3.00		0.	28.9	4.7	192.4	0.	0.	0.	0.	0.
9	7	80	191626	1400	3.00		0.	0.	0.	94.5	0.	0.	0.	0.	0.
9	7	80	191627	1400	3.00		0.	0.	0.	75.4	0.	0.	0.	0.	0.
9	7	80	191628	1400	3.00		0.	0.	0.	2.6	0.	0.	0.	0.	0.
9	7	80	191629	1400	3.00		0.	0.	0.	0.5	0.	0.	0.	0.	0.
9	7	80	191631	1400	3.00		0.	0.	0.	0.	0.	0.	0.	0.	0.
9	7	80	191632	1400	3.00		0.	0.	0.	0.	0.	0.	0.	0.	0.
9	7	80	191633	1400	3.00		0.	0.	0.	0.	0.	0.	0.	0.	0.
9	7	80	191634	1400	3.00		0.	0.	0.	0.	0.	0.	0.	0.	0.
9	7	80	191635	1400	3.00		0.	0.	0.	0.	0.	0.	0.	0.	0.
9	7	80	191636	1400	3.00		0.	0.	0.	0.	0.	0.	0.	0.	0.
9	7	80	191637	1400	3.00		0.	0.	0.	0.	0.	0.	0.	0.	0.
9	7	80	191638	1400	3.00		0.	0.	0.	0.	0.	0.	0.	0.	0.

DD	MM	YY	JUL	SI	HOUR	DUR	OBS	PUFF1	PLUME	MSPUFF	PUFF2	MTDDIS	ARRPA	RTM2	RADM
CASE 30-D				ID 30	RECP 32										
9	7	80	191600		1700	3.00	0.	0.	0.	0.	0.	0.	0.	0.	0.
9	7	80	191601		1700	3.00	0.	0.	0.	0.	0.	0.	0.	0.	0.
9	7	80	191602		1700	3.00	0.	0.	0.	0.	0.	0.	0.	0.	0.
9	7	80	191603		1700	3.00	0.	0.	0.	0.	0.	0.	0.	0.	0.
9	7	80	191604		1700	3.00	0.	0.	0.	0.	0.	0.	0.	0.	0.
9	7	80	191605		1700	3.00	0.	0.	0.	0.	0.	0.	0.	0.	0.
9	7	80	191606		1700	3.00	0.	0.	0.	0.	0.	0.	0.	0.	0.
9	7	80	191607		1700	3.00	0.	0.	0.	0.	0.	0.	0.	0.	0.
9	7	80	191609		1700	3.00	0.2	0.	0.	0.	0.	0.	0.	0.	0.
9	7	80	191610		1700	3.00	0.	0.	0.	0.	0.	0.	0.	0.	0.
9	7	80	191611		1700	3.00	25.0	0.	0.	0.	0.	0.	0.	0.	0.
9	7	80	191612		1700	3.00	29.0	0.	0.	0.	0.	0.	0.	0.	0.
9	7	80	191613		1700	3.00	63.0	0.	0.	0.	0.3	0.	0.	0.	0.
9	7	80	191615		1700	3.00	8.0	0.	0.	0.	18.3	0.	0.	0.9	0.
9	7	80	191616		1700	3.00	3.4	0.	0.	0.	42.0	0.	0.	1.4	8.7
9	7	80	191617		1700	3.00	0.	17.2	17.8	0.	110.5	0.	102.7	2.5	285.7
9	7	80	191619		1700	3.00	0.	178.9	141.3	0.2	118.0	0.	191.6	2.7	0.
9	7	80	191620		1700	3.00	0.	269.1	169.7	6.0	32.1	0.	0.2	1.3	0.
9	7	80	191623		1700	3.00	0.	110.4	68.7	65.6	0.	0.	0.	0.3	0.
9	7	80	191624		1700	3.00	0.	116.8	56.2	90.4	0.	0.	0.	0.2	0.
9	7	80	191625		1700	3.00	0.	17.6	1.6	64.1	0.	0.	0.	0.1	0.
9	7	80	191627		1700	3.00	0.	0.	0.	25.1	0.	0.	0.	0.	0.
9	7	80	191628		1700	3.00	0.	0.	0.	0.9	0.	0.	0.	0.	0.
9	7	80	191629		1700	3.00	0.	0.	0.	0.2	0.	0.	0.	0.	0.
9	7	80	191630		1700	3.00	0.	0.	0.	0.	0.	0.	0.	0.	0.
9	7	80	191631		1700	3.00	0.	0.	0.	0.	0.	0.	0.	0.	0.
9	7	80	191632		1700	3.00	0.	0.	0.	0.	0.	0.	0.	0.	0.
9	7	80	191633		1700	3.00	0.	0.	0.	0.	0.	0.	0.	0.	0.
9	7	80	191634		1700	3.00	0.	0.	0.	0.	0.	0.	0.	0.	0.
9	7	80	191636		1700	3.00	0.	0.	0.	0.	0.	0.	0.	0.	0.
9	7	80	191637		1700	3.00	0.	0.	0.	0.	0.	0.	0.	0.	0.
9	7	80	191638		1700	3.00	0.	0.	0.	0.	0.	0.	0.	0.	0.
CASE 30-E				ID 30	RECP 33										
9	7	80	191600		2000	3.00	0.	0.	0.	0.	0.	0.	0.	0.	0.
9	7	80	191601		2000	3.00	0.	0.	0.	0.	0.	0.	0.	0.	0.
9	7	80	191602		2000	3.00	0.	0.	0.	0.	0.	0.	0.	0.	0.
9	7	80	191603		2000	3.00	0.1	0.	0.	0.	0.	0.	0.	0.	0.
9	7	80	191604		2000	3.00	0.	0.	0.	0.	0.	0.	0.	0.	0.
9	7	80	191605		2000	3.00	0.	0.	0.	0.	0.	0.	0.	0.	0.
9	7	80	191606		2000	3.00	0.	0.	0.	0.	0.	0.	0.	0.	0.
9	7	80	191607		2000	3.00	0.	0.	0.	0.	0.	0.	0.	0.	0.
9	7	80	191609		2000	3.00	0.	0.	0.	0.	0.	0.	0.	0.	0.
9	7	80	191610		2000	3.00	0.6	0.	0.	0.	0.	0.	0.	0.	0.
9	7	80	191611		2000	3.00	2.3	0.	0.	0.	0.	0.	0.	0.	0.
9	7	80	191612		2000	3.00	1.1	0.	0.	0.	0.	0.	0.	0.	0.
9	7	80	191615		2000	3.00	3.4	0.	0.	0.	0.	0.	0.	0.	0.
9	7	80	191616		2000	3.00	2.7	0.	0.	0.	0.	0.	0.	0.	0.
9	7	80	191617		2000	3.00	0.2	5.7	5.9	0.	36.8	0.	34.2	0.8	95.2
9	7	80	191619		2000	3.00	0.	59.6	47.1	0.1	39.3	0.	63.9	0.9	0.
9	7	80	191620		2000	3.00	0.	89.7	56.6	2.0	10.7	0.	0.1	0.4	0.
9	7	80	191623		2000	3.00	0.	36.8	22.9	21.9	0.	0.	0.	0.1	0.
9	7	80	191624		2000	3.00	0.	40.5	18.7	30.1	0.	0.	0.	0.1	0.
9	7	80	191625		2000	3.00	0.	5.9	0.5	21.4	0.	0.	0.	0.	0.
9	7	80	191626		2000	3.00	0.	0.1	0.	10.5	0.	0.	0.	0.	0.
9	7	80	191627		2000	3.00	0.	0.	0.	8.4	0.	0.	0.	0.	0.
9	7	80	191628		2000	3.00	0.	0.	0.	0.3	0.	0.	0.	0.	0.
9	7	80	191629		2000	3.00	0.	0.	0.	0.1	0.	0.	0.	0.	0.
9	7	80	191630		2000	3.00	0.	0.	0.	0.	0.	0.	0.	0.	0.
9	7	80	191631		2000	3.00	0.1	0.	0.	0.	0.	0.	0.	0.	0.
9	7	80	191632		2000	3.00	0.	0.	0.	0.	0.	0.	0.	0.	0.
9	7	80	191633		2000	3.00	0.	0.	0.	0.	0.	0.	0.	0.	0.
9	7	80	191634		2000	3.00	0.	0.	0.	0.	0.	0.	0.	0.	0.
9	7	80	191635		2000	3.00	0.	0.	0.	0.	0.	0.	0.	0.	0.
9	7	80	191636		2000	3.00	0.	0.	0.	0.	0.	0.	0.	0.	0.
9	7	80	191637		2000	3.00	0.	0.	0.	0.	0.	0.	0.	0.	0.
9	7	80	191638		2000	3.00	0.	0.	0.	0.	0.	0.	0.	0.	0.

DD	MM	YY	JUL	SI	HOUR	DUR	OBS	PUFF1	PLUME	MSPUFF	PUFF2	MTDDIS	ARRPA	RTM2	RADM
CASE 30-F			ID 30		RECP 30										
9	7	80	191601	2300	3.00		0.	0.	0.	0.	0.	0.	0.	0.	0.
9	7	80	191602	2300	3.00		0.	0.	0.	0.	0.	0.	0.	0.	0.
9	7	80	191604	2300	3.00		0.	0.	0.	0.	0.	0.	0.	0.	0.
9	7	80	191605	2300	3.00		0.	0.	0.	0.	0.	0.	0.	0.	0.
9	7	80	191606	2300	3.00		0.	0.	0.	0.	0.	0.	0.	0.	0.
9	7	80	191607	2300	3.00		0.2	0.	0.	0.	0.	0.	0.	0.	0.
9	7	80	191609	2300	3.00		0.	0.	0.	0.	0.	0.	0.	0.	0.
9	7	80	191610	2300	3.00		0.	0.	0.	0.	0.	0.	0.	0.	0.
9	7	80	191611	2300	3.00		0.	0.	0.	0.	0.	0.	0.	0.	0.
9	7	80	191612	2300	3.00		0.	0.	0.	0.	0.	0.	0.	0.	0.
9	7	80	191615	2300	3.00		0.	0.	0.	0.	0.	0.	0.	0.	0.
9	7	80	191616	2300	3.00		0.	0.	0.	0.	0.	0.	0.	0.	0.
9	7	80	191617	2300	3.00		0.	1.9	2.0	0.	12.3	0.	11.4	0.3	31.7
9	7	80	191619	2300	3.00		0.	19.9	15.7	0.	13.1	0.	21.3	0.3	0.
9	7	80	191620	2300	3.00		0.	29.9	18.9	0.7	3.6	0.	0.	0.1	0.
9	7	80	191623	2300	3.00		0.	12.3	7.6	7.3	0.	0.	0.	0.	0.
9	7	80	191624	2300	3.00		0.	13.5	6.2	10.0	0.	0.	0.	0.	0.
9	7	80	191625	2300	3.00		0.	2.0	0.2	7.1	0.	0.	0.	0.	0.
9	7	80	191627	2300	3.00		0.	0.	0.	2.8	0.	0.	0.	0.	0.
9	7	80	191628	2300	3.00		0.	0.	0.	0.1	0.	0.	0.	0.	0.
9	7	80	191629	2300	3.00		0.	0.	0.	0.	0.	0.	0.	0.	0.
9	7	80	191630	2300	3.00		0.	0.	0.	0.	0.	0.	0.	0.	0.
9	7	80	191631	2300	3.00		0.	0.	0.	0.	0.	0.	0.	0.	0.
9	7	80	191632	2300	3.00		0.	0.	0.	0.	0.	0.	0.	0.	0.
9	7	80	191633	2300	3.00		0.	0.	0.	0.	0.	0.	0.	0.	0.
9	7	80	191634	2300	3.00		0.	0.	0.	0.	0.	0.	0.	0.	0.
9	7	80	191635	2300	3.00		0.	0.	0.	0.	0.	0.	0.	0.	0.
9	7	80	191636	2300	3.00		0.	0.	0.	0.	0.	0.	0.	0.	0.
9	7	80	191637	2300	3.00		0.	0.	0.	0.	0.	0.	0.	0.	0.
9	7	80	191638	2300	3.00		0.	0.	0.	0.	0.	0.	0.	0.	0.
CASE 40-A			ID 40		RECP 16	GR 08									
11	7	80	193114	2200	0.75		0.6	26.8	34.1	0.	0.	0.	0.	0.	0.
11	7	80	193115	2200	0.75		0.	105.0	139.9	0.	0.	0.	0.	0.	0.
11	7	80	193116	2200	0.75		0.8	181.6	273.4	3.1	0.	0.	0.	0.	0.
11	7	80	193117	2200	0.75		0.	280.0	470.4	40.3	0.4	0.	0.	0.	0.
11	7	80	193118	2200	0.75		1.5	304.1	584.8	179.5	0.9	0.	0.	0.	0.
11	7	80	193119	2200	0.75		0.	158.9	502.0	157.4	0.	0.	0.	0.	0.
11	7	80	193120	2200	0.75		1.2	53.3	272.6	73.4	0.	0.	0.	0.	0.
11	7	80	193121	2200	0.75		0.5	18.7	138.4	23.2	0.	0.	0.	0.	0.
11	7	80	193122	2200	0.75		7.0	12.9	58.9	117.8	0.	0.	0.	0.	0.
11	7	80	193123	2200	0.75		1.0	0.	0.	0.	0.	0.	0.	0.	0.
11	7	80	193124	2200	0.75		5.2	0.	0.	0.	0.	0.	0.	0.	0.
11	7	80	193126	2200	0.75		0.5	0.	0.	0.	0.	0.	0.	0.	0.
11	7	80	193127	2200	0.75		0.	0.	0.	0.	0.	0.	0.	0.	0.
11	7	80	193128	2200	0.75		0.	0.	0.	0.	0.	0.	0.	0.	0.
11	7	80	193129	2200	0.75		0.	0.	0.	0.	0.	0.	0.	0.	0.
11	7	80	193130	2200	0.75		0.	0.	0.	0.	0.	0.	0.	0.	0.
CASE 40-B			ID 40		RECP 16										
11	7	80	193114	2245	0.75		35.0	114.5	106.0	0.	0.4	0.	0.1	118.9	2.0
11	7	80	193115	2245	0.75		47.0	275.5	299.0	13.9	20.0	0.	0.6	91.5	92.9
11	7	80	193116	2245	0.75		107.0	364.1	447.7	117.3	62.8	0.	3.6	69.5	255.6
11	7	80	193117	2245	0.75		9.0	396.7	554.5	502.9	176.0	0.	17.0	61.0	356.9
11	7	80	193118	2245	0.75		72.0	320.1	508.5	1230.2	298.5	0.	45.0	75.5	407.8
11	7	80	193119	2245	0.75		37.0	161.2	321.5	1366.7	174.3	0.	93.5	114.0	210.7
11	7	80	193120	2245	0.75		35.0	51.2	220.9	748.9	55.3	0.	0.	128.2	37.0
11	7	80	193121	2245	0.75		124.0	18.6	88.7	323.3	16.7	0.	0.	1.7	5.6
11	7	80	193122	2245	0.75		297.0	4.3	19.6	126.0	14.8	0.	395.5	1.0	3.0
11	7	80	193123	2245	0.75		216.0	0.	0.	0.	0.	0.	336.9	1.5	0.
11	7	80	193124	2245	0.75		53.0	0.	0.	0.	0.	0.	256.4	2.5	0.
11	7	80	193126	2245	0.75		0.9	0.	0.	0.	0.	0.	0.	2.6	0.
11	7	80	193127	2245	0.75		0.	0.	0.	0.	0.	0.	0.	0.	0.
11	7	80	193128	2245	0.75		0.	0.	0.	0.	0.	0.	0.	0.	0.
11	7	80	193129	2245	0.75		0.	0.	0.	0.	0.	0.	0.	0.	0.
11	7	80	193130	2245	0.75		0.	0.	0.	0.	0.	0.	0.	0.	0.

DD	MM	YY	JUL	SI	HOUR	DUR	OBS	PUFF1	PLUME	MSPUFF	PUFF2	MTDDIS	ARRPA	RTM2	RADM
CASE 40-C				ID 40	RECP 16										
11	7	80	193114	2330		0.75	267.0	227.1	126.2	0.	1.0	0.	3.5	225.9	16.0
11	7	80	193115	2330		0.75	277.0	406.2	704.0	62.4	56.1	0.	5.5	183.0	264.8
11	7	80	193116	2330		0.75	238.0	453.3	640.1	306.5	171.5	0.	23.4	148.4	772.2
11	7	80	193117	2330		0.75	177.0	403.6	414.4	1010.7	419.9	0.	80.1	126.3	1080.4
11	7	80	193118	2330		0.75	256.0	266.8	313.6	1988.1	618.7	0.	162.9	150.1	1157.3
11	7	80	193119	2330		0.75	327.0	124.3	154.2	1953.4	393.2	0.	262.5	212.0	703.6
11	7	80	193120	2330		0.75	299.0	36.1	130.0	969.4	137.2	0.	204.0	235.8	170.1
11	7	80	193121	2330		0.75	357.0	12.6	42.5	405.8	48.8	0.	195.7	11.1	36.5
11	7	80	193122	2330		0.75	197.0	0.	0.	90.7	16.9	0.	493.3	10.6	4.6
11	7	80	193123	2330		0.75	142.0	0.	0.	0.	0.	0.	375.3	14.3	0.
11	7	80	193124	2330		0.75	73.0	0.	0.	0.	0.	0.	273.7	20.6	0.
11	7	80	193126	2330		0.75	11.0	0.	0.	0.	0.	0.	1.4	17.8	0.
11	7	80	193127	2330		0.75	0.	0.	0.	0.	0.	0.	0.1	0.4	0.
11	7	80	193128	2330		0.75	0.	0.	0.	0.	0.	0.	0.	0.6	0.
11	7	80	193129	2330		0.75	0.	0.	0.	0.	0.	0.	0.	0.9	0.
11	7	80	193130	2330		0.75	0.	0.	0.	0.	0.	0.	0.	0.	0.
CASE 40-D				ID 40	RECP 15										
12	7	80	194114		15	0.75	175.0	364.6	94.9	0.	1.8	0.	10.2	321.1	42.2
12	7	80	194115		15	0.75	187.0	497.1	1355.0	145.4	108.3	0.	14.6	274.6	515.6
12	7	80	194116		15	0.75	139.0	449.1	850.6	570.6	326.2	0.	59.6	236.5	1549.8
12	7	80	194117		15	0.75	87.0	300.9	50.3	1563.7	732.3	0.	189.3	196.1	2170.4
12	7	80	194118		15	0.75	213.0	144.1	0.	2453.3	961.2	0.	353.8	223.8	2248.5
12	7	80	194120		15	0.75	233.0	7.8	0.	734.6	245.9	0.	612.1	322.9	399.1
12	7	80	194121		15	0.75	123.0	0.7	0.	270.6	96.2	0.	587.0	28.0	92.7
12	7	80	194122		15	0.75	97.0	0.	0.	11.9	6.2	0.	293.4	28.8	4.8
12	7	80	194123		15	0.75	43.0	0.	0.	0.	0.	0.	115.2	38.4	0.
12	7	80	194124		15	0.75	30.0	0.	0.	0.	0.	0.	52.0	54.2	0.
12	7	80	194126		15	0.75	4.9	0.	0.	0.	0.	0.	4.2	45.8	0.
12	7	80	194127		15	0.75	0.	0.	0.	0.	0.	0.	0.3	1.3	0.
12	7	80	194128		15	0.75	0.	0.	0.	0.	0.	0.	0.1	1.9	0.
12	7	80	194129		15	0.75	0.	0.	0.	0.	0.	0.	0.	2.6	0.
12	7	80	194130		15	0.75	0.	0.	0.	0.	0.	0.	0.	0.	0.
CASE 40-E				ID 40	RECP 14										
12	7	80	194114		100	0.75	62.0	354.7	0.	0.	59.3	0.	26.1	210.8	167.6
12	7	80	194116		100	0.75	65.0	324.9	33.4	855.2	726.3	0.	455.7	217.2	1672.0
12	7	80	194117		100	0.75	47.0	164.3	0.	1857.9	935.5	0.	998.5	140.9	2009.1
12	7	80	194118		100	0.75	96.0	57.8	0.	2315.2	680.8	0.	1306.1	149.4	1646.9
12	7	80	194120		100	0.75	63.0	0.	0.	436.8	96.8	0.	725.0	177.2	148.2
12	7	80	194121		100	0.75	39.0	0.	0.	129.2	38.8	0.	461.7	47.9	26.1
12	7	80	194122		100	0.75	37.0	0.	0.	0.	0.	0.	63.5	56.5	0.
12	7	80	194123		100	0.75	17.0	0.	0.	0.	0.	0.	13.7	67.9	0.
12	7	80	194124		100	0.75	22.0	0.	0.	0.	0.	0.	4.7	84.8	0.
12	7	80	194126		100	0.75	0.5	0.	0.	0.	0.	0.	0.2	48.2	0.
12	7	80	194127		100	0.75	0.	0.	0.	0.	0.	0.	0.	2.5	0.
12	7	80	194128		100	0.75	0.	0.	0.	0.	0.	0.	0.	4.5	0.
12	7	80	194129		100	0.75	0.	0.	0.	0.	0.	0.	0.	7.3	0.
12	7	80	194130		100	0.75	0.	0.	0.	0.	0.	0.	0.	0.	0.
CASE 40-F				ID 40	RECP 14										
12	7	80	194114		145	0.75	34.0	126.9	0.	0.	395.1	0.	8.7	157.2	936.7
12	7	80	194115		145	0.75	0.	152.5	8.3	114.9	734.0	0.	49.3	158.7	1450.4
12	7	80	194116		145	0.75	22.0	122.4	11.1	376.0	734.4	0.	151.9	159.5	1746.9
12	7	80	194117		145	0.75	25.0	61.2	0.	772.4	559.7	0.	332.8	120.6	1468.1
12	7	80	194118		145	0.75	46.0	20.8	0.	929.1	304.4	0.	435.4	125.5	763.9
12	7	80	194120		145	0.75	27.0	0.	0.	226.0	38.6	0.	310.6	141.2	51.6
12	7	80	194121		145	0.75	18.0	0.	0.	71.8	14.6	0.	183.2	46.7	8.7
12	7	80	194122		145	0.75	17.0	0.	0.	0.	0.	0.	21.2	56.5	0.
12	7	80	194124		145	0.75	6.3	0.	0.	0.	0.	0.	1.6	80.7	0.
12	7	80	194126		145	0.75	0.1	0.	0.	0.	0.	0.	0.1	40.3	0.
12	7	80	194127		145	0.75	0.	0.	0.	0.	0.	0.	0.	1.5	0.
12	7	80	194128		145	0.75	0.	0.	0.	0.	0.	0.	0.	3.1	0.
12	7	80	194129		145	0.75	0.	0.	0.	0.	0.	0.	0.	5.7	0.
12	7	80	194130		145	0.75	0.	0.	0.	0.	0.	0.	0.	0.	0.

DD	MM	YY	JUL	SI	HOUR	DUR	OBS	PUFF1	PLUME	MSPUFF	PUFF2	MTDDIS	ARRPA	RTM2	RADM
CASE 40-G				ID 40	RECP 14										
12	7	80	194114	230		0.75	10.0	8.7	0.	0.	555.9	0.	0.	119.7	1140.8
12	7	80	194115	230		0.75	0.	14.0	0.	26.7	714.6	0.	0.	120.0	1393.0
12	7	80	194116	230		0.75	6.5	14.1	0.	91.0	544.4	0.	0.	120.4	1320.5
12	7	80	194117	230		0.75	9.0	6.4	0.	153.1	261.0	0.	0.	99.0	808.1
12	7	80	194118	230		0.75	21.0	1.5	0.	157.4	79.6	0.	0.	102.2	214.9
12	7	80	194120	230		0.75	20.0	0.	0.	80.4	6.3	0.	68.9	112.2	2.2
12	7	80	194121	230		0.75	8.0	0.	0.	28.8	1.7	0.	29.3	41.5	0.
12	7	80	194123	230		0.75	3.0	0.	0.	0.	0.	0.	0.	61.9	0.
12	7	80	194124	230		0.75	2.5	0.	0.	0.	0.	0.	0.	73.4	0.
12	7	80	194126	230		0.75	0.1	0.	0.	0.	0.	0.	0.	31.0	0.
12	7	80	194127	230		0.75	0.	0.	0.	0.	0.	0.	0.	0.9	0.
12	7	80	194128	230		0.75	0.	0.	0.	0.	0.	0.	0.	2.2	0.
12	7	80	194129	230		0.75	0.	0.	0.	0.	0.	0.	0.	4.3	0.
12	7	80	194130	230		0.75	0.	0.	0.	0.	0.	0.	0.	0.	0.
CASE 40-H				ID 40	RECP 14										
12	7	80	194114	315		0.75	2.4	0.	0.	0.	541.9	0.	0.	98.3	780.0
12	7	80	194115	315		0.75	0.	0.	0.	0.	329.3	0.	0.	99.0	731.0
12	7	80	194116	315		0.75	2.3	0.	0.	0.	156.3	0.	0.	100.0	392.9
12	7	80	194118	315		0.75	7.0	0.	0.	0.	6.5	0.	0.	79.7	0.
12	7	80	194120	315		0.75	4.7	0.	0.	0.	0.	0.	0.	90.0	0.
12	7	80	194121	315		0.75	0.	0.	0.	0.	0.	0.	0.	32.1	0.
12	7	80	194122	315		0.75	2.0	0.	0.	0.	0.	0.	0.	46.9	0.
12	7	80	194123	315		0.75	0.	0.	0.	0.	0.	0.	0.	54.2	0.
12	7	80	194124	315		0.75	2.4	0.	0.	0.	0.	0.	0.	62.8	0.
12	7	80	194126	315		0.75	0.3	0.	0.	0.	0.	0.	0.	20.3	0.
12	7	80	194127	315		0.75	0.	0.	0.	0.	0.	0.	0.	0.7	0.
12	7	80	194128	315		0.75	0.	0.	0.	0.	0.	0.	0.	1.7	0.
12	7	80	194129	315		0.75	0.	0.	0.	0.	0.	0.	0.	3.3	0.
12	7	80	194130	315		0.75	0.	0.	0.	0.	0.	0.	0.	0.	0.

Part II: Presentation of Complete AMS Statistics Results for the Oklahoma and SRP Data Sets.

Table D-1. Statistical Dataset (A-1) for Oklahoma Data

MODEL	NUMBER OF EVENTS	AVERAGE OBSERVED VALUE	AVERAGE DIFFERENCE* (OBS-PRED)	STANDARD DEVIATION OF RESIDUALS*	MAXIMUM FREQUENCY DIFFERENCE
MESOPUFF	21	753.1	-437.9	1023.6	0.29
			(-903.8, 28.1)	(783.1,1478.2)	(0.420)
MESOPLUME	21	753.1	-836.1	2181.4	0.24
			(-1829.1, 156.9)	(1668.9,3150.0)	(0.420)
MSPUFF	21	753.1	-3130.1	4955.8	0.33
			(-5386.1, -874.2)	(3791.5,7156.5)	(0.420)
MESOPUFF II	21	753.1	-363.9	1171.0	0.29
			(-896.9, 169.2)	(895.9,1691.0)	(0.420)
RTM-II	21	753.1	404.6	1322.5	0.24
			(-197.4, 1006.6)	(1011.8,1909.8)	(0.420)
RADM	21	753.1	-1756.1	2740.5	0.33
			(-3003.6, -508.6)	(2096.6,3957.4)	(0.420)
ARRPA	21	753.1	-827.2	2024.0	0.33
			(-1748.5, 94.2)	(1548.5,2922.8)	(0.420)

* 95 PERCENT CONFIDENCE INTERVAL IN PARENTHESES.

Table D-2. Statistical Dataset (A-2) for Oklahoma Data.

MODEL	NUMBER OF DATA PAIRS	AVERAGE OBSERVED VALUE	AVERAGE DIFFERENCE* (OBS-PRED)	FRACTION OF POSITIVE RESIDUALS (OBS > PRED)	STANDARD DEVIATION OF RESIDUALS*	ROOT MEAN SQUARE ERROR	AVERAGE ABSOLUTE RESIDUAL	PEARSON CORR. COEFF.	SPEARMAN CORR. COEFF.	KENDALL CORR. COEFF.	VARIANCE COMPARISON* (OBS/PRED)
MESOPUFF	35	828.4	192.9	0.69	608.1	629.7	393.7	0.91	0.17	0.10	1.171
			(-16.0, 401.9)		(491.3, 797.7)						(0.591, 2.321)
MESOPLUME	34	852.8	-143.3	0.56	1343.1	1330.9	667.7	0.81	0.27	0.17	0.440
			(-612.0, 325.5)		(1082.1, 1770.2)						(0.220, 0.881)
MSPUFF	38	763.0	-887.4	0.50	3354.3	3426.8	1268.3	0.86	0.24	0.15	0.101
			(-1990.1, 215.4)		(2731.9, 4344.1)						(0.053, 0.195)
MESOPUFF II	31	935.3	166.1	0.61	1961.2	1936.4	1153.6	0.07	0.30	0.19	1.329
			(-553.3, 885.5)		(1567.2, 2621.5)						(0.641, 2.756)
RTM-II	37	783.6	433.1	0.54	1107.0	1174.7	599.1	0.71	0.39	0.28	5.985
			(64.0, 802.3)		(899.3, 1439.5)						(3.081,11.624)
RADM	28	1035.5	-1145.6	0.64	4427.5	4496.1	2368.6	-.05	0.32	0.19	0.153
			(-2862.4, 571.2)		(3500.7, 6027.2)						(0.071, 0.330)
ARRPA	33	878.6	-829.1	0.42	2230.8	2348.0	1466.2	0.57	0.37	0.28	0.305
			(-1620.3, -37.9)		(1791.8, 2954.7)						(0.151, 0.618)

* 95 PERCENT CONFIDENCE INTERVAL IN PARENTHESES.

Table D-3. Statistical Dataset (A-4A) for Oklahoma Data.

MODEL	NUMBER OF DATA PAIRS	AVERAGE OBSERVED VALUE	AVERAGE PREDICTED VALUE	DIFFERENCE OF AVERAGES* (OBS-PRED)	DIFFERENCE OF MEDIANS* (OBS-PRED)	VARIANCE COMPARISON* (OBS/PRED)	MAXIMUM FREQUENCY DIFFERENCE
MESOPUFF	25	1809.7	2617.6	-807.9	-1448.5	1.341	0.48
				(-1548.9, -66.9)	(-1716.6, -221.2)	(0.591, 3.045)	(0.385)
MESOPLUME	25	1809.7	3231.5	-1421.8	-1536.2	0.367	0.40
				(-2511.3, -332.3)	(-2235.5, -174.7)	(0.161, 0.832)	(0.385)
MSPUFF	25	1809.7	6347.0	-4537.3	-1680.3	0.060	0.60
				(-6940.9,-2133.7)	(-5296.6, -989.7)	(0.027, 0.137)	(0.385)
MESOPUFF II	25	1809.7	2230.4	-420.7	-680.6	2.042	0.44
				(-1105.3, 263.8)	(-1120.6, -35.2)	(0.899, 4.635)	(0.385)
RTM-II	25	1809.7	1234.3	575.4	-67.4	27.887	0.40
				(-9.3, 1160.0)	(-269.6, 772.6)	(12.284,63.305)	(0.385)
RADM	25	1809.7	5894.0	-4084.3	-3447.6	0.232	0.64
				(-5391.0,-2777.7)	(-4512.5,-2507.4)	(0.102, 0.527)	(0.385)
ARRPA	25	1809.7	3183.5	-1373.9	-1358.9	0.337	0.40
				(-2498.5, -249.2)	(-1991.9, -232.9)	(0.149, 0.765)	(0.385)

* 95 PERCENT CONFIDENCE INTERVAL IN PARENTHESES.

Table D-4. Statistical Dataset (B-1) for Oklahoma Data.

MODEL	SITE	NUMBER OF DATA PAIRS	AVERAGE OBSERVED VALUE	AVERAGE DIFFERENCE (OBS-PRED)	STANDARD DEVIATION OF RESIDUALS
MESOPUFF	114	15	533.4	-786.7	1142.1
MESOPUFF	115	13	410.9	-828.9	993.5
MESOPUFF	116	15	372.3	-366.5	587.7
MESOPUFF	118	12	286.1	100.7	569.9
MESOPUFF	120	15	61.5	51.6	97.5
MESOPUFF	121	10	69.4	64.4	108.6
MESOPUFF	122	14	47.5	46.3	90.1

MODEL	SITE	NUMBER OF DATA PAIRS	AVERAGE OBSERVED VALUE	AVERAGE DIFFERENCE (OBS-PRED)	STANDARD DEVIATION OF RESIDUALS
MESOPLUME	114	15	533.4	-1149.7	2470.3
MESOPLUME	115	12	445.2	-1328.7	1773.7
MESOPLUME	116	14	398.9	-886.9	1525.0
MESOPLUME	118	12	286.1	-219.9	926.2
MESOPLUME	120	15	61.5	7.1	136.9
MESOPLUME	121	10	69.4	42.5	114.9
MESOPLUME	122	14	47.5	41.9	89.9

MODEL	SITE	NUMBER OF DATA PAIRS	AVERAGE OBSERVED VALUE	AVERAGE DIFFERENCE (OBS-PRED)	STANDARD DEVIATION OF RESIDUALS
MSPUFF	114	15	533.4	-1482.3	3170.7
MSPUFF	115	12	445.2	-236.7	1140.9
MSPUFF	116	14	398.9	120.8	823.8
MSPUFF	118	11	312.1	-529.0	1289.6
MSPUFF	120	15	61.5	-156.4	277.4
MSPUFF	121	10	69.4	-55.8	70.9
MSPUFF	122	14	47.5	22.8	64.7

MODEL	SITE	NUMBER OF DATA PAIRS	AVERAGE OBSERVED VALUE	AVERAGE DIFFERENCE (OBS-PRED)	STANDARD DEVIATION OF RESIDUALS
MESOPUFF II	114	15	533.4	360.4	1339.1
MESOPUFF II	115	13	410.9	84.0	1072.9
MESOPUFF II	116	14	398.9	-42.2	1155.8
MESOPUFF II	118	14	245.3	-516.9	1182.7
MESOPUFF II	120	15	61.5	-801.1	1289.5
MESOPUFF II	121	13	53.4	-862.2	1408.0
MESOPUFF II	122	14	47.5	-730.0	1381.6

Table D-4 (Continued). Statistical Dataset (B-1) for Oklahoma Data.

MODEL	SITE	NUMBER OF DATA PAIRS	AVERAGE OBSERVED VALUE	AVERAGE DIFFERENCE (OBS-PRED)	STANDARD DEVIATION OF RESIDUALS
RTM-II	114	15	533.4	68.7	1289.9
RTM-II	115	13	410.9	-69.9	949.6
RTM-II	116	14	398.9	-33.9	942.6
RTM-II	118	14	245.3	-211.3	740.8
RTM-II	120	15	61.5	-417.2	541.8
RTM-II	121	14	49.6	-142.7	317.6
RTM-II	122	14	47.5	-144.7	317.9

MODEL	SITE	NUMBER OF DATA PAIRS	AVERAGE OBSERVED VALUE	AVERAGE DIFFERENCE (OBS-PRED)	STANDARD DEVIATION OF RESIDUALS
RADM	114	15	533.4	186.4	1510.4
RADM	115	13	410.9	-170.4	1331.9
RADM	116	14	398.9	-487.6	1321.9
RADM	118	14	245.3	-1749.7	1632.0
RADM	120	15	61.5	-2359.4	3738.0
RADM	121	13	53.4	-2363.8	3707.4
RADM	122	14	47.5	-2182.1	3937.2

MODEL	SITE	NUMBER OF DATA PAIRS	AVERAGE OBSERVED VALUE	AVERAGE DIFFERENCE (OBS-PRED)	STANDARD DEVIATION OF RESIDUALS
ARRPA	114	15	533.4	-230.1	2619.8
ARRPA	115	11	485.7	-837.1	3425.0
ARRPA	116	14	398.9	-476.2	2282.3
ARRPA	118	14	245.3	-489.9	1117.8
ARRPA	120	15	61.5	-501.5	1131.5
ARRPA	121	13	53.4	-496.4	1133.8
ARRPA	122	14	47.5	-663.0	1337.4

Table D-5. Statistical Dataset (B-3) for Oklahoma Data.

MODEL	NUMBER OF DATA PAIRS	AVERAGE OBSERVED VALUE	AVERAGE DIFFERENCE* (OBS-PRED)	FRACTION OF POSITIVE RESIDUALS (OBS > PRED)	STANDARD DEVIATION OF RESIDUALS*	ROOT MEAN SQUARE ERROR	AVERAGE ABSOLUTE RESIDUAL	PEARSON CORR. COEFF.	SPEARMAN CORR. COEFF.	KENDALL CORR. COEFF.	VARIANCE COMPARISON* (OBS/PRED)	MAXIMUM FREQUENCY DIFFERENCE
MESOPUFF	224	243.4	-116.0	0.54	673.9	682.3	290.4	0.68	0.13	0.08	0.65	0.09
			(-204.7, -27.3)		(616.7, 742.9)						(0.50, 0.84)	(0.13)
MESOPLUME	216	252.4	-191.3	0.61	1049.5	1064.4	389.2	0.57	0.07	0.04	0.33	0.19
			(-331.9, -50.6)		(958.9,1159.1)						(0.25, 0.43)	(0.13)
MSPUFF	230	237.1	-538.5	0.52	2201.5	2261.8	708.5	0.75	0.08	0.04	0.07	0.15
			(-824.5, -252.6)		(2016.8,2423.5)						(0.05, 0.09)	(0.13)
MESOPUFF II	203	268.6	-97.0	0.59	1176.3	1177.4	587.1	-0.14	-0.20	-0.14	0.90	0.16
			(-259.7, 65.6)		(1071.8,1303.4)						(0.68, 1.18)	(0.13)
RTM-II	228	239.1	7.4	0.41	781.6	779.9	355.0	0.12	0.24	0.17	3.23	0.18
			(-94.6, 109.4)		(715.8, 860.8)						(2.49, 4.19)	(0.13)
RADM	192	284.0	-721.9	0.61	2428.3	2527.3	1205.3	-0.11	-0.10	-0.06	0.12	0.24
			(-1067.2, -376.7)		(2207.0,2699.0)						(0.09, 0.16)	(0.14)
ARRPA	208	262.1	-207.5	0.58	1539.0	1549.3	640.2	-0.05	0.08	0.06	0.33	0.16
			(-417.8, 2.7)		(1403.8,1703.1)						(0.25, 0.43)	(0.13)

* 95 PERCENT CONFIDENCE INTERVAL IN PARENTHESES.

Table D-6. Statistical Dataset (A-1) for Savannah River Plant Data.

MODEL	NUMBER OF EVENTS	AVERAGE OBSERVED VALUE	AVERAGE DIFFERENCE* (OBS-PRED)	STANDARD DEVIATION OF RESIDUALS*	MAXIMUM FREQUENCY DIFFERENCE
MESOPUFF	63	228.4	-104.0	903.5	0.30
			(-331.5, 123.6)	(768.3,1096.5)	(0.242)
MESOPLUME	63	228.4	-87.5	744.5	0.37
			(-275.0, 100.0)	(633.1, 903.6)	(0.242)
MSPUFF	63	228.4	-54.2	616.9	0.46
			(-209.6, 101.1)	(524.6, 748.7)	(0.242)
MESOPUFF II	63	228.4	-26.1	644.3	0.21
			(-188.3, 136.2)	(547.9, 782.0)	(0.242)
MTDDIS	63	228.4	-168.0	531.2	0.27
			(-301.8, -34.2)	(451.7, 644.6)	(0.242)
RTM-II	63	228.4	-27.3	489.6	0.19
			(-150.6, 96.0)	(416.4, 594.2)	(0.242)
RADM	63	228.4	-247.8	853.0	,0.29
			(-462.6, -32.9)	(725.3,1035.2)	(0.242)

* 95 PERCENT CONFIDENCE INTERVAL IN PARENTHESES.

Table D-7. Statistical Dataset (A-2) for Savannah River Plant Data.

MODEL	NUMBER OF DATA PAIRS	AVERAGE OBSERVED VALUE	AVERAGE DIFFERENCE* (OBS-PRED)	FRACTION OF POSITIVE RESIDUALS (OBS > PRED)	STANDARD DEVIATION OF RESIDUALS*	ROOT MEAN SQUARE ERROR	AVERAGE ABSOLUTE RESIDUAL	PEARSON CORR. COEFF.	SPEARMAN CORR. COEFF.	KENDALL CORR. COEFF.	VARIANCE COMPARISON* (OBS/PRED)
MESOPUFF	13	621.3	-596.2	0.15	967.0	1103.9	724.8	0.80	0.76	0.56	0.262
			(-1180.6, -11.9)		(693.4, 1596.2)						(0.080, 0.862)
MESOPLUME	13	621.3	-409.2	0.15	611.6	716.1	577.2	0.76	0.61	0.49	0.612
			(-778.8, -39.6)		(438.5, 1009.6)						(0.186, 2.011)
MSPUFF	13	621.3	-470.7	0.15	913.9	996.3	640.2	0.60	0.76	0.62	0.419
			(-1023.0, 81.5)		(655.3, 1508.6)						(0.128, 1.378)
MESOPUFF II	13	621.3	-123.7	0.23	676.0	661.2	492.5	0.59	0.77	0.62	0.974
			(-532.2, 284.8)		(484.7, 1115.9)						(0.296, 3.199)
MTDDIS	13	621.3	-161.7	0.31	656.6	651.2	443.8	0.66	0.70	0.51	0.795
			(-558.4, 235.1)		(470.8, 1083.8)						(0.242, 2.612)
RTM-II	13	621.3	-48.9	0.23	650.0	626.4	507.0	0.51	0.64	0.49	2.156
			(-441.7, 343.8)		(466.1, 1072.9)						(0.656, 7.084)
RADM	13	621.3	-3955.6	0.31	12427.2	12577.8	4152.3	0.25	0.70	0.53	0.003
			(-11465.2,3554.1)		(8910.7,20513.5)						(0.001, 0.011)

* 95 PERCENT CONFIDENCE INTERVAL IN PARENTHESES.

Table D-8. Statistical Dataset (A-4A) for Savannah River Plant Data.

MODEL	NUMBER OF DATA PAIRS	AVERAGE OBSERVED VALUE	AVERAGE PREDICTED VALUE	DIFFERENCE OF AVERAGES* (OBS-PRED)	DIFFERENCE OF MEDIANS* (OBS-PRED)	VARIANCE COMPARISON* (OBS/PRED)	MAXIMUM FREQUENCY DIFFERENCE
MESOPUFF	25	643.7	926.2	-282.5	-191.5	0.250	0.24
				(-778.0, 213.0)	(-363.5, 77.4)	(0.110, 0.569)	(0.385)
MESOPLUME	25	643.7	909.3	-265.6	-278.9	0.504	0.36
				(-645.0, 113.9)	(-437.6, -8.9)	(0.222, 1.144)	(0.385)
MSPUFF	25	643.7	858.7	-215.0	-139.0	0.398	0.20
				(-628.9, 198.9)	(-281.8, 110.8)	(0.175, 0.903)	(0.385)
MESOPUFF II	25	643.7	700.3	-56.6	-90.6	0.814	0.20
				(-384.6, 271.3)	(-201.9, 116.5)	(0.359, 1.848)	(0.385)
TDDIS	25	643.7	925.4	-281.7	-293.6	0.619	0.48
				(-636.9, 73.5)	(-401.9, -46.1)	(0.273, 1.406)	(0.385)
RTM-II	25	643.7	666.8	-23.2	-171.8	1.357	0.32
				(-312.6, 266.3)	(-245.6, 71.0)	(0.598, 3.080)	(0.385)
RADM	25	643.7	3043.8	-2400.1	-766.2	0.004	0.48
				(-6153.6, 1353.5)	(-905.0, -150.5)	(0.002, 0.008)	(0.385)

* 95 PERCENT CONFIDENCE INTERVAL IN PARENTHESES.

Table D-9. Statistical Dataset (B-1) for Savannah River Plant Data.

MODEL	SITE	NUMBER OF DATA PAIRS	AVERAGE OBSERVED VALUE	AVERAGE DIFFERENCE (OBS-PRED)	STANDARD DEVIATION OF RESIDUALS
MESOPUFF	2	24	24.8	13.8	47.2
MESOPUFF	3	16	1.5	-13.7	52.2
MESOPUFF	4	12	1.0	-22.0	75.7
MESOPUFF	5	17	5.9	-0.1	26.0
MESOPUFF	6	15	8.0	-36.0	103.5
MESOPUFF	7	24	56.1	-15.9	248.7
MESOPUFF	8	29	103.1	38.4	322.3
MESOPUFF	9	30	45.3	-107.0	418.3
MESOPUFF	10	35	173.1	13.6	969.6
MESOPUFF	11	30	97.5	-9.4	443.9
MESOPUFF	12	19	31.3	-18.1	153.5
MESOPUFF	13	34	28.3	-40.6	186.3
MESOPUFF	14	27	181.5	31.1	664.9

MODEL.	SITE	NUMBER OF DATA PAIRS	AVERAGE OBSERVED VALUE	AVERAGE DIFFERENCE (OBS-PRED)	STANDARD DEVIATION OF RESIDUALS
MESOPLUME	2	23	25.8	16.0	44.3
MESOPLUME	3	15	1.6	-10.6	39.5
MESOPLUME	4	11	1.1	-72.6	238.8
MESOPLUME	5	18	5.6	-4.8	31.3
MESOPLUME	6	12	10.0	-47.8	140.9
MESOPLUME	7	24	56.1	-2.4	172.8
MESOPLUME	8	30	99.7	50.1	272.8
MESOPLUME	9	30	45.3	-58.0	275.7
MESOPLUME	10	35	173.1	12.8	791.2
MESOPLUME	11	30	97.5	-38.1	484.0
MESOPLUME	12	20	29.7	-58.5	280.2
MESOPLUME	13	32	30.0	-32.8	141.0
MESOPLUME	14	27	181.5	17.9	651.5

MODEL	SITE	NUMBER OF DATA PAIRS	AVERAGE OBSERVED VALUE	AVERAGE DIFFERENCE (OBS-PRED)	STANDARD DEVIATION OF RESIDUALS
MSPUFF	2	23	25.8	-80.2	493.3
MSPUFF	3	20	1.2	-8.8	34.6
MSPUFF	4	18	0.7	-1.5	4.6
MSPUFF	5	18	5.6	-4.0	40.5
MSPUFF	6	16	7.5	-15.3	61.0
MSPUFF	7	28	48.1	-62.3	266.0
MSPUFF	8	34	87.9	-58.5	484.9
MSPUFF	9	29	46.8	-2.2	174.4
MSPUFF	10	37	163.7	72.5	600.2
MSPUFF	11	31	94.4	54.5	325.6
MSPUFF	12	22	27.0	-39.3	148.2
MSPUFF	13	33	29.1	14.4	54.0
MSPUFF	14	28	175.1	-45.5	841.7

Table D-9 (Continued). Statistical Dataset (B-1) for Savannah River Plant Data.

MODEL	SITE	NUMBER OF DATA PAIRS	AVERAGE OBSERVED VALUE	AVERAGE DIFFERENCE (OBS-PRED)	STANDARD DEVIATION OF RESIDUALS
MESOPUFF II	2	25	23.8	-27.0	116.1
MESOPUFF II	3	17	1.4	-13.1	23.3
MESOPUFF II	4	17	0.7	-5.8	9.7
MESOPUFF II	5	18	5.6	3.1	15.4
MESOPUFF II	6	22	5.5	-5.9	28.9
MESOPUFF II	7	30	44.9	-16.6	168.9
MESOPUFF II	8	31	96.4	-154.1	664.1
MESOPUFF II	9	30	45.3	-79.7	296.8
MESOPUFF II	10	36	168.3	100.2	479.9
MESOPUFF II	11	32	91.4	50.4	298.1
MESOPUFF II	12	22	27.0	-64.9	192.8
MESOPUFF II	13	33	29.1	-2.3	109.7
MESOPUFF II	14	29	169.0	67.7	478.2

MODEL	SITE	NUMBER OF DATA PAIRS	AVERAGE OBSERVED VALUE	AVERAGE DIFFERENCE (OBS-PRED)	STANDARD DEVIATION OF RESIDUALS
MTDDIS	2	32	18.6	-30.9	98.0
MTDDIS	3	35	0.7	-4.6	10.2
MTDDIS	4	24	0.5	-1.6	4.9
MTDDIS	5	25	4.0	1.3	10.8
MTDDIS	6	28	4.3	-33.6	141.1
MTDDIS	7	38	35.4	-24.2	105.2
MTDDIS	8	40	74.7	-115.3	216.8
MTDDIS	9	39	34.8	-40.5	88.5
MTDDIS	10	39	155.3	3.8	500.7
MTDDIS	11	37	79.1	-15.2	318.1
MTDDIS	12	32	18.6	-21.3	135.4
MTDDIS	13	40	24.0	-29.5	129.9
MTDDIS	14	43	114.0	-115.8	583.6

MODEL	SITE	NUMBER OF DATA PAIRS	AVERAGE OBSERVED VALUE	AVERAGE DIFFERENCE (OBS-PRED)	STANDARD DEVIATION OF RESIDUALS
RTM-II	2	25	23.8	-5.4	67.1
RTM-II	3	17	1.4	-65.9	149.6
RTM-II	4	13	0.9	-19.8	52.3
RTM-II	5	18	5.6	-11.1	49.1
RTM-II	6	16	7.5	-64.9	157.0
RTM-II	7	26	51.8	7.1	133.6
RTM-II	8	31	96.4	37.1	306.7
RTM-II	9	30	45.3	-53.2	174.9
RTM-II	10	36	168.3	105.9	480.6
RTM-II	11	32	91.4	37.8	328.4
RTM-II	12	21	28.3	-28.8	130.8
RTM-II	13	34	28.3	-17.3	116.1
RTM-II	14	32	153.2	-72.2	597.3

Table D-9 (Continued). Statistical Dataset (B-1) for Savannah River Plant Data.

MODEL	SITE	NUMBER OF DATA PAIRS	AVERAGE OBSERVED VALUE	AVERAGE DIFFERENCE (OBS-PRED)	STANDARD DEVIATION OF RESIDUALS
RADM	2	22	27.0	-35.2	268.2
RADM	3	15	1.6	0.3	5.7
RADM	4	11	1.1	1.1	1.1
RADM	5	14	7.2	7.2	14.8
RADM	6	13	9.2	-172.3	415.6
RADM	7	23	58.5	-30.6	292.3
RADM	8	29	103.1	-134.5	637.3
RADM	9	28	48.5	-87.6	331.1
RADM	10	35	173.1	8.2	643.6
RADM	11	29	100.9	7.1	327.4
RADM	12	17	34.9	-209.6	655.8
RADM	13	32	30.0	-25.3	133.3
RADM	14	26	188.5	-1880.7	8903.3

Table D-10. Statistical Dataset (B-3) for Savannah River Plant Data.

MODEL	NUMBER OF DATA PAIRS	AVERAGE OBSERVED VALUE	AVERAGE DIFFERENCE* (OBS-PRED)	FRACTION OF POSITIVE RESIDUALS (OBS > PRED)	STANDARD DEVIATION OF RESIDUALS*	ROOT MEAN SQUARE ERROR	AVERAGE ABSOLUTE RESIDUAL	PEARSON CORR. COEFF.	SPEARMAN CORR. COEFF.	KENDALL CORR. COEFF.	VARIANCE COMPARISON* (OBS/PRED)	MAXIMUM FREQUENCY DIFFERENCE
MESOPUFF	312	70.5	-12.4	0.74	442.6	442.1	132.3	0.07	-0.08	-0.06	0.34	0.39
			(-61.7, 37.0)		(410.4, 480.4)						(0.27, 0.43)	(0.11)
MESOPLUME	307	71.6	-12.9	0.78	394.1	393.6	133.7	0.05	-0.04	-0.04	0.50	0.46
			(-57.3, 31.4)		(365.1, 428.0)						(0.40, 0.62)	(0.11)
MSPUFF	337	65.2	-10.2	0.70	395.4	395.0	129.4	-0.02	-0.30	-0.23	0.48	0.33
			(-52.7, 32.2)		(367.6, 427.8)						(0.38, 0.59)	(0.10)
MESOPUFF II	342	64.3	-8.9	0.53	329.2	328.8	117.9	-0.01	0.01	0.00	0.83	0.09
			(-44.0, 26.1)		(306.2, 355.9)						(0.67, 1.03)	(0.10)
MTDDIS	452	48.6	-36.4	0.28	269.7	271.8	86.9	0.35	0.43	0.31	0.53	0.24
			(-61.4, -11.4)		(253.1, 288.5)						(0.44, 0.64)	(0.09)
RTM-II	331	66.4	-4.5	0.63	297.7	297.3	109.9	0.09	0.05	0.03	1.06	0.20
			(-36.8, 27.7)		(276.6, 322.3)						(0.86, 1.32)	(0.11)
RADM	294	74.8	-213.4	0.74	2681.4	2685.3	324.0	0.25	0.21	0.16	0.01	0.43
			(-521.4, 94.7)		(2480.5,2917.6)						(0.01, 0.01)	(0.11)

* 95 PERCENT CONFIDENCE INTERVAL IN PARENTHESES.

APPENDIX E

COMPLETE GRAPHICAL COMPARISONS OF THE EIGHT MODELS WITH THE OKLAHOMA AND SAVANNAH RIVER PLANT DATA BASES

INTRODUCTION

This appendix provides a summary of the graphs prepared as part of the model evaluation process. This appendix is divided into seven parts:

Part 1. This section provides the location of air samplers and a site map for the Oklahoma experiments.

Part 2. This section provides several plots illustrating the evidence of a low-lying nocturnal jet during the two Oklahoma experiments.

Part 3. This section provides isopleth plots of the predicted ground-level concentrations of perfluorocarbon tracer for each averaging period for the two Oklahoma experiments. An explanation of how to interpret the plots is contained in Chapter 5.

Part 4. This section provides summary graphical plots of model performance for each of the seven models and the Oklahoma data base. The graph types included are:

* scatter plots of predicted and observed concentrations (points paired in space and time)

* scatter plots of residual versus average of observed and predicted concentrations (points paired in space and time),

* frequency distribution of predicted and observed concentrations (points paired in space and time, then unpaired for preparation of histogram)

* frequency histogram of residuals (points paired in space and time), and

* cumulative frequency distribution of predicted and observed concentrations (points paired in space and time, then unpaired for preparation of cumulative frequency plots).

Part 5. This section provides a plot of the air samplers and a site map for the Savannah River Plant experiments.

Part 6. This section provides sketches of the model predictions and measured data for each of the seven models for Cases 4B and 6C. Similar graphs are available for each of the data sets and averaging periods (65 in total) for each of the seven models. Space limitations preclude presentation of all 455 graphs (65 x 7). Cases 4B and 6C present the highlights of the complete set of graphs.

Part 7. This section presents summary graphs of model performance for each of the seven models and Savannah River Plant data base. The graph types included are:

* scatter plots of predicted and observed concentrations (points paired in space and time),

* scatter plots of residual versus average of observed and predicted concentrations (points paired in space and time),

* frequency distribution of predicted and observed concentrations (points paired in space and time, then unpaired for preparation of histogram),

* frequency histogram of residuals (points paired in space and time), and

* cumulative frequency distribution of predicted and observed concentrations (points paired in space and time, then unpaired for preparation of cumulative frequency plots).

1. LOCATION OF AIR SAMPLERS AND SITE MAP FOR OKLAHOMA EXPERIMENT

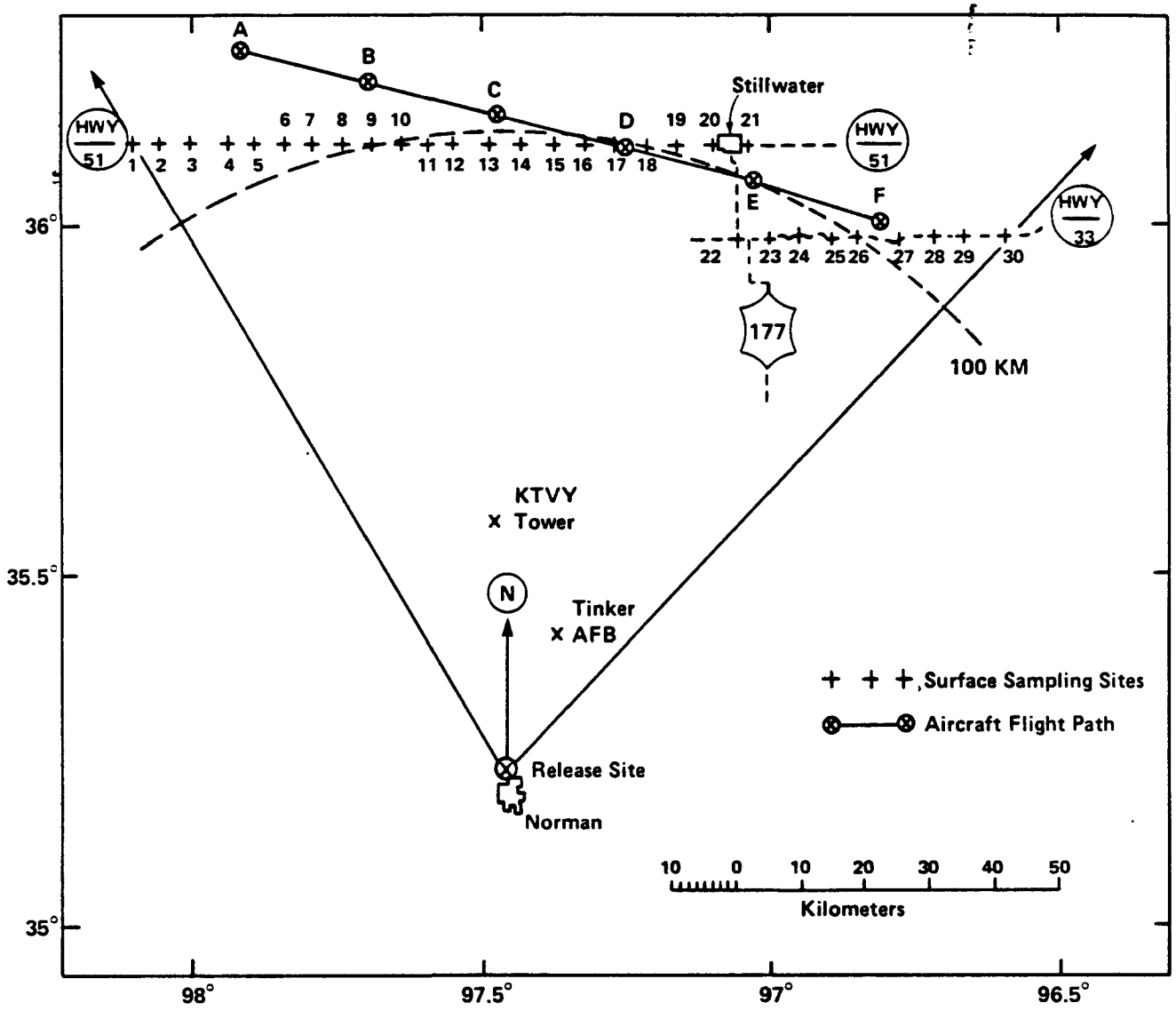

Figure E-1. Location of the sequential air samplers (BATS) and aircraft sampling path at 100 km from the Oklahoma tracer release site.

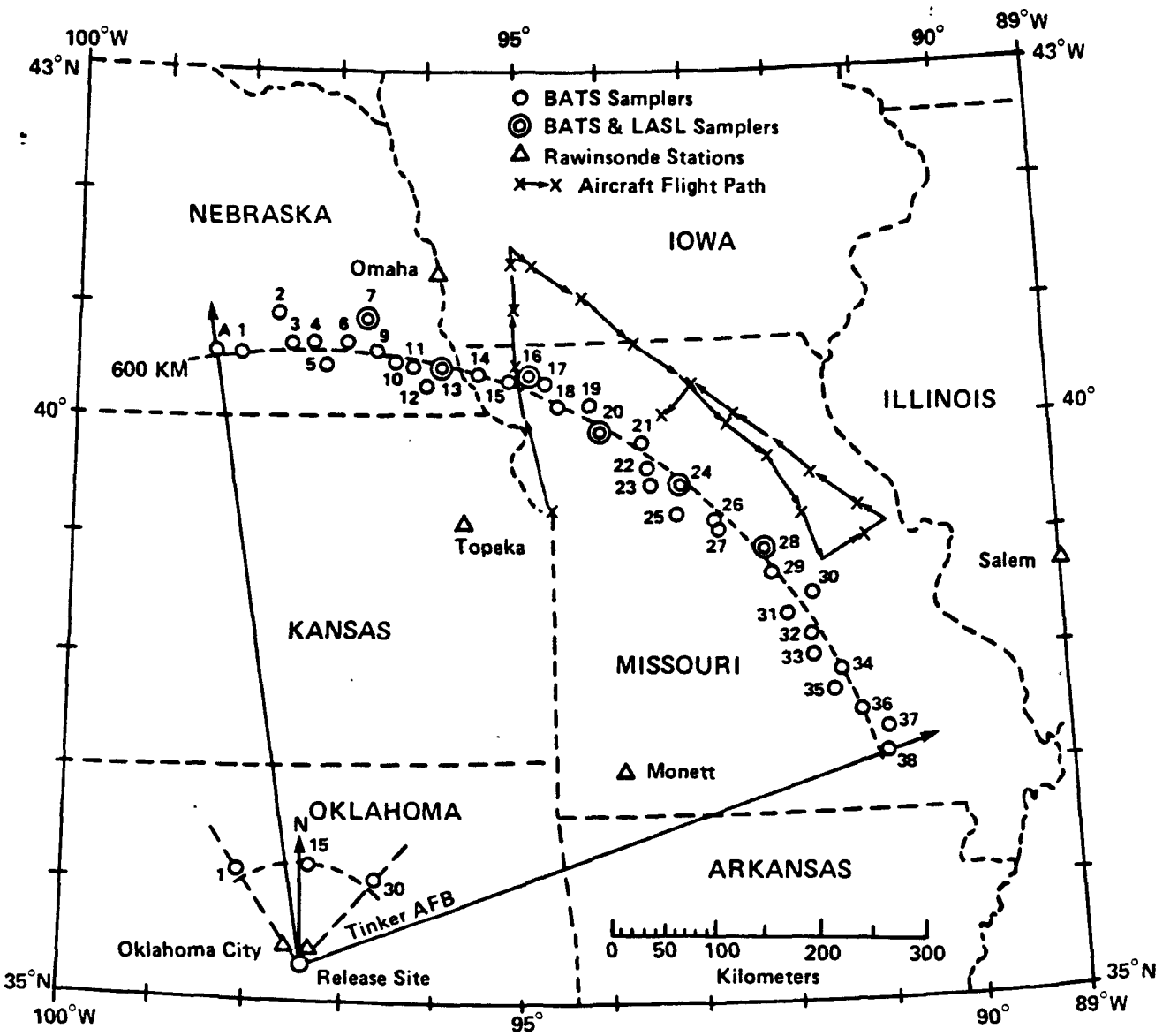

Figure E-2. Location of sequential samplers (BATS), LASL samplers, and aircraft sampling flight path at 600 km from the Oklahoma tracer release site.

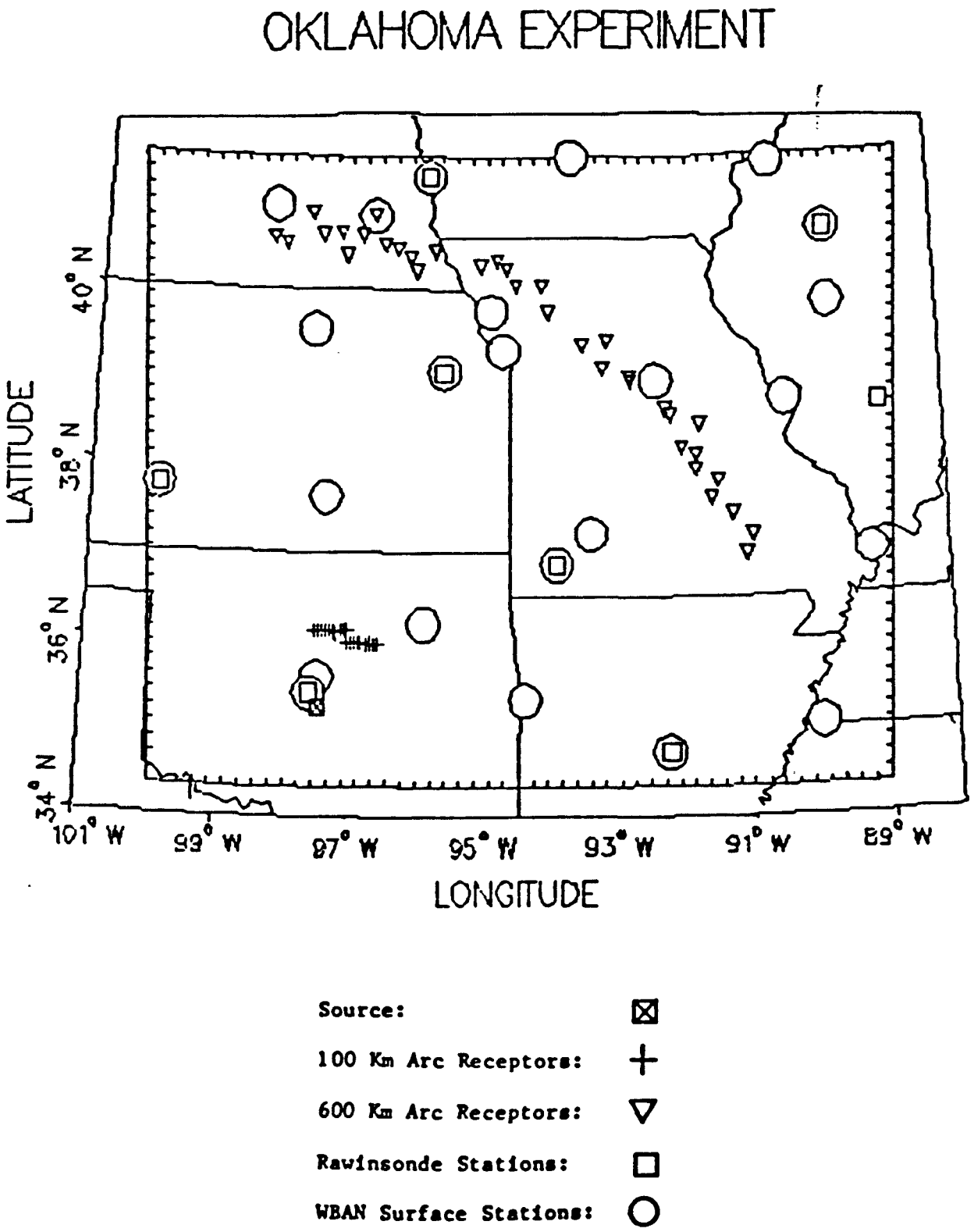

Figure E-3. Location of significant source, weather and receptor sites for Oklahoma Experiment.

2. EVIDENCE OF LOW-LYING NOCTURNAL JET DURING THE OKLAHOMA STUDY

Evidence of a Low-Lying Nocturnal Jet During the Oklahoma Study

During the night of July 8-9 1980, an elevated nocturnal jet appears to have developed over the study region. On the south end of the region, the jet seems to have started about 0000 GMT on July 9 (6 PM CST, July 8) and at the north end of the region sometime between 0000 GMT and 0600 GMT on July 9 (6 PM to midnight CST, July 8). The jet led to about a doubling of the average wind speeds from a range of 8-12 m/s to a range of 16-24 m/s, with the higher values occurring in the northern half of the region. The jet appeared to occupy a layer between about 600 m MSL and 1000 m MSL in the southern half of the region; it was present at least up to 1000 m above the 600 m MSL elevation in the northern half. The jet persisted at least until 1200 GMT on July 9 (6 AM CST).

Evidence may be seen of the nocturnal jet in the attached graphs plotted from the available tower and rawinsonde data. A summary of the main conclusions that can be reached from an examination of the graphs follows:

KTVY TOWER (plotted period: 1800 GMT July 8 - 0200 GMT July 9)

The tower had measurements at levels up to 444 m above ground (794 m MSL). The measurements show a definite increase in winds from 0000 GMT - 0200 GMT on July 9 for elevations above 100 m (450 m MSL). Wind speeds averaging 5 m/s increased to 10-14 m/s on average.

TINKER AIR FORCE BASE SOUNDINGS (plotted period: 1700 GMT, July 8 - 0300 GMT, July 9)

Seven soundings were made during this period. They show the jet from 2100 GMT on July 8 through 0300 GMT on July 9 at elevations above 600 m MSL. Average winds of 6 m/s aloft become 12 m/s, with winds of 16 m/s occurring at 0300 GMT on July 9. These elevated winds can be seen from 600 m MSL to 900 m MSL.

MONETT, MISSOURI RAWINSONDE STATION (plotted period: 1800 GMT, July 8 - 1200 GMT, July 9)

In addition to the 0000 and 1200 GMT regular soundings on July 9, this station took special soundings at 1800 GMT on July 8 and at 0600 GMT on July 9. The nocturnal jet is apparent in the 0600 GMT and 1200 GMT soundings for July 9 at elevations above 600 m MSL; it appears clearly

between 600 m MSL and 1000 m MSL. Average winds of 8 m/s increase to 12-16 m/s. These winds persist through 1200 GMT on July 9. (Thus, the jet was present at midnight and 6 AM CST, but not at 6PM on July 8. The tower data confirm this because the tower winds only start to show the increase at 6 PM CST.)

TOPEKA, KANSAS RAWINSONDE STATION (plotted period: 1800 GMT, July 8 - 1200 GMT, July 9)

Again, the 1800 GMT (for July 8) and the 0000 GMT (for July 9) soundings do not reveal the jet but the 0600 and 1200 GMT (for July 9) soundings do show its presence. The jet lies between 600 and 1400 m MSL, and is present at higher levels at 1200 GMT on July 9. Average winds of 8-10 m/s aloft increase to 20-24 m/s. The jet is clearly stronger at this more northerly reporting station.

OMAHA, NEBRASKA RAWINSONDE STATION (plotted period: 1800 GMT, July 8 - 1200 GMT, July 9)

This is the most northern of the rawinsonde stations. The systematic behavior of the data agrees largely with the Topeka, Kansas station but the 0600 GMT sounding on July 9 shows less of an increase in winds due to the nocturnal jet.

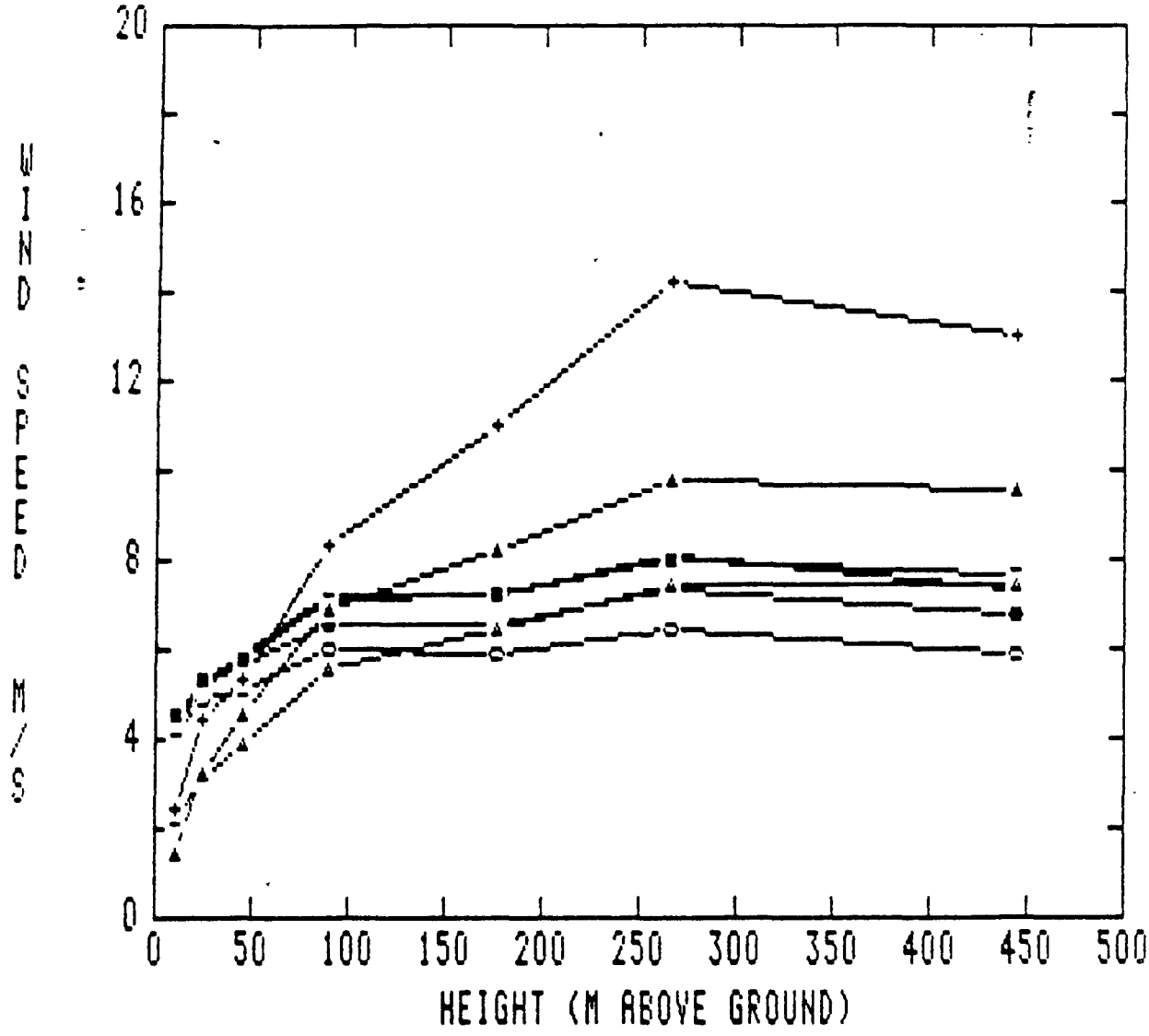

July 8-9, 1980, wind speed profiles from KTVY tower

1900-2000 GMT
2000-2100 GMT
2100-2200 GMT
2200-2300 GMT
2300-0000 GMT
0000-0100 GMT
0100-0200 GMT

Add 350 m to convert to m MSL

Figure E-4. Wind speed profiles from KTVY tower for July 8-9, 1980 for Oklahoma experiment.

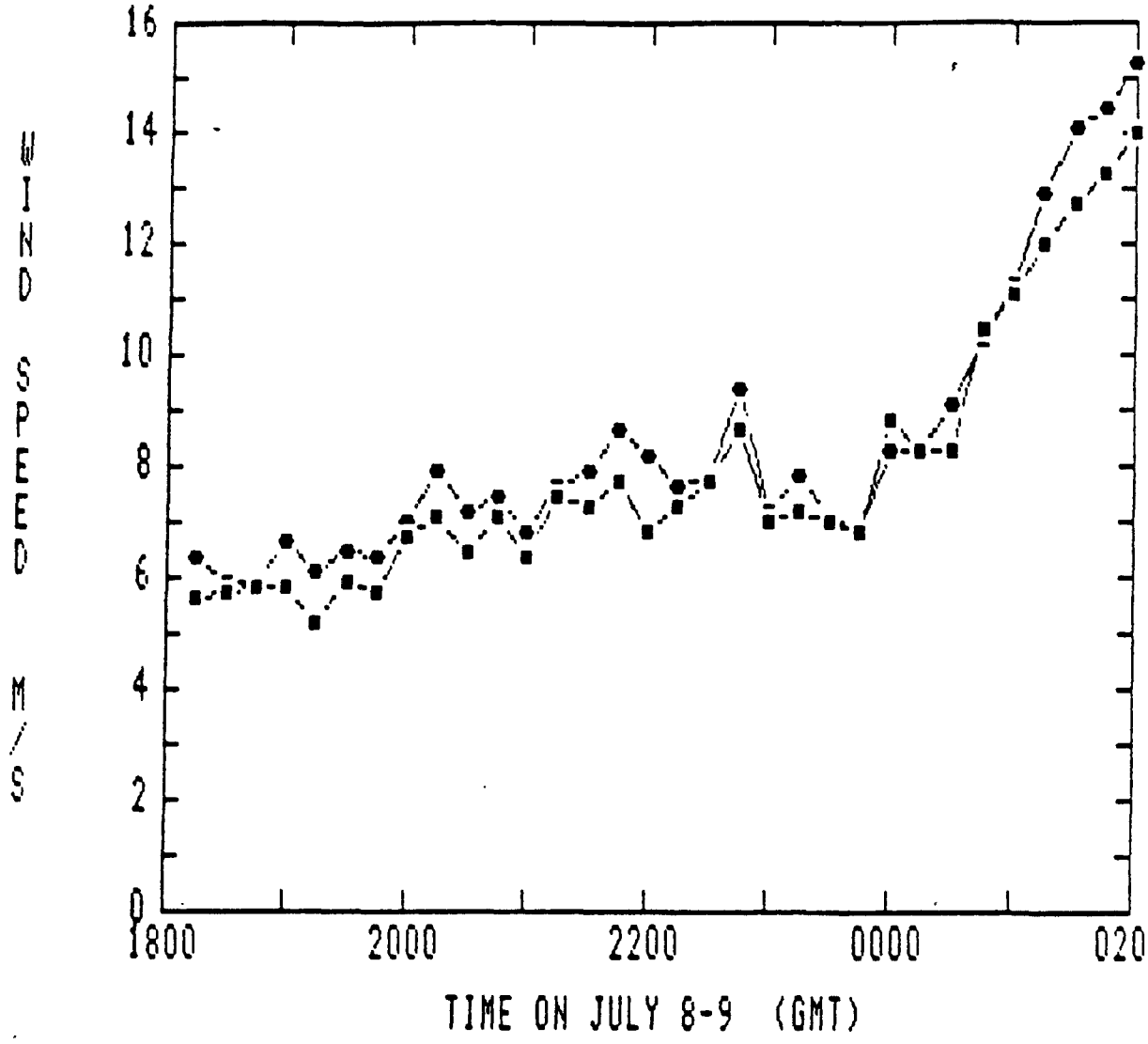

July 8-9, 1980, wind speeds at 266 and 444 m at KTVY

266 m above ground (616 m MSL)

444 m above ground (794 m MSL)

Note 266 m is a little stronger than 444 m

Figure E-5. Wind speeds at 266 and 444 meters at KTVY tower for July 8-9, 1980 for Oklahoma experiment.

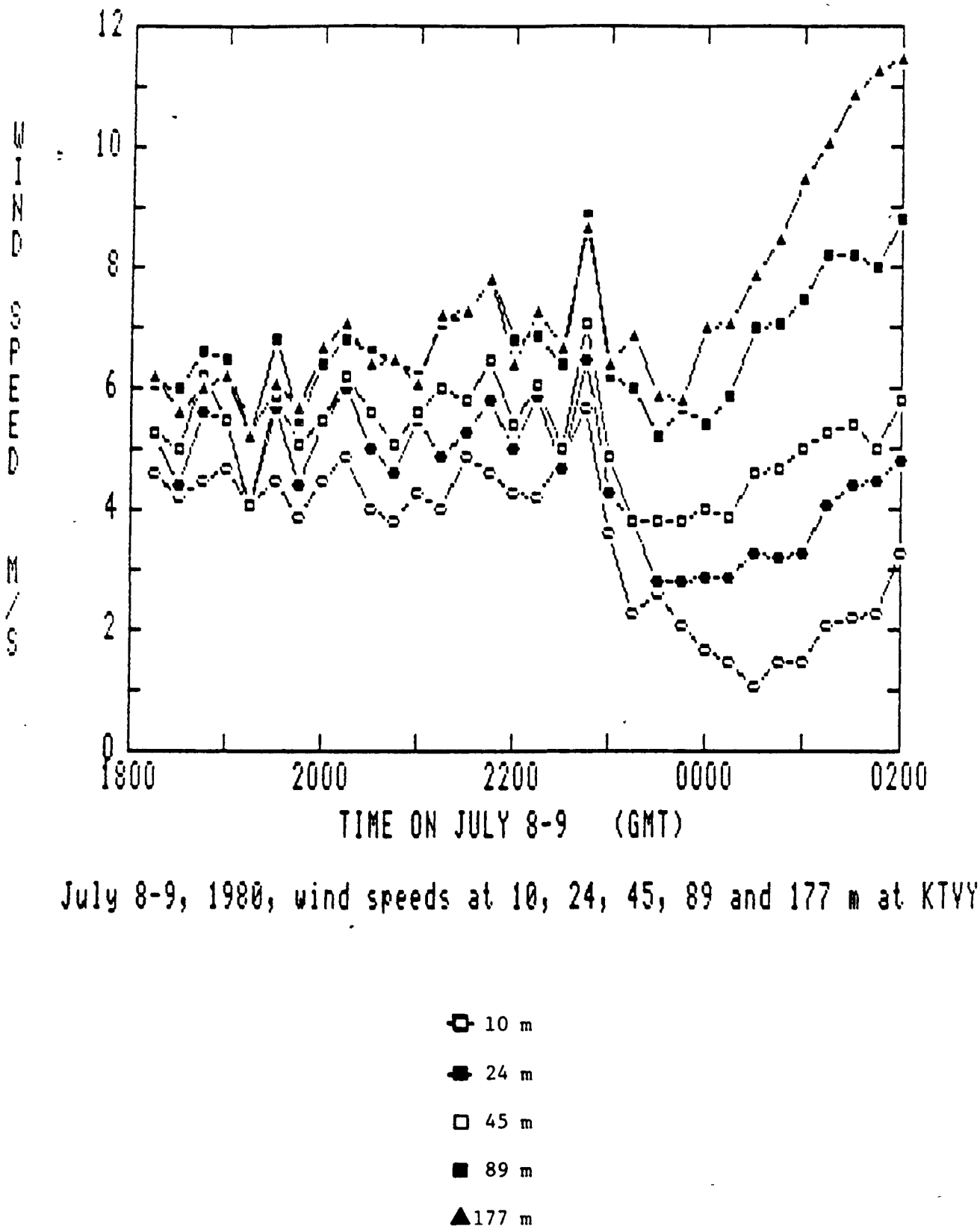

Figure E-6. Wind speeds at 10, 24, 45, 89 and 177 meters at KTVY tower for July 8-9, 1980 for Oklahoma experiment.

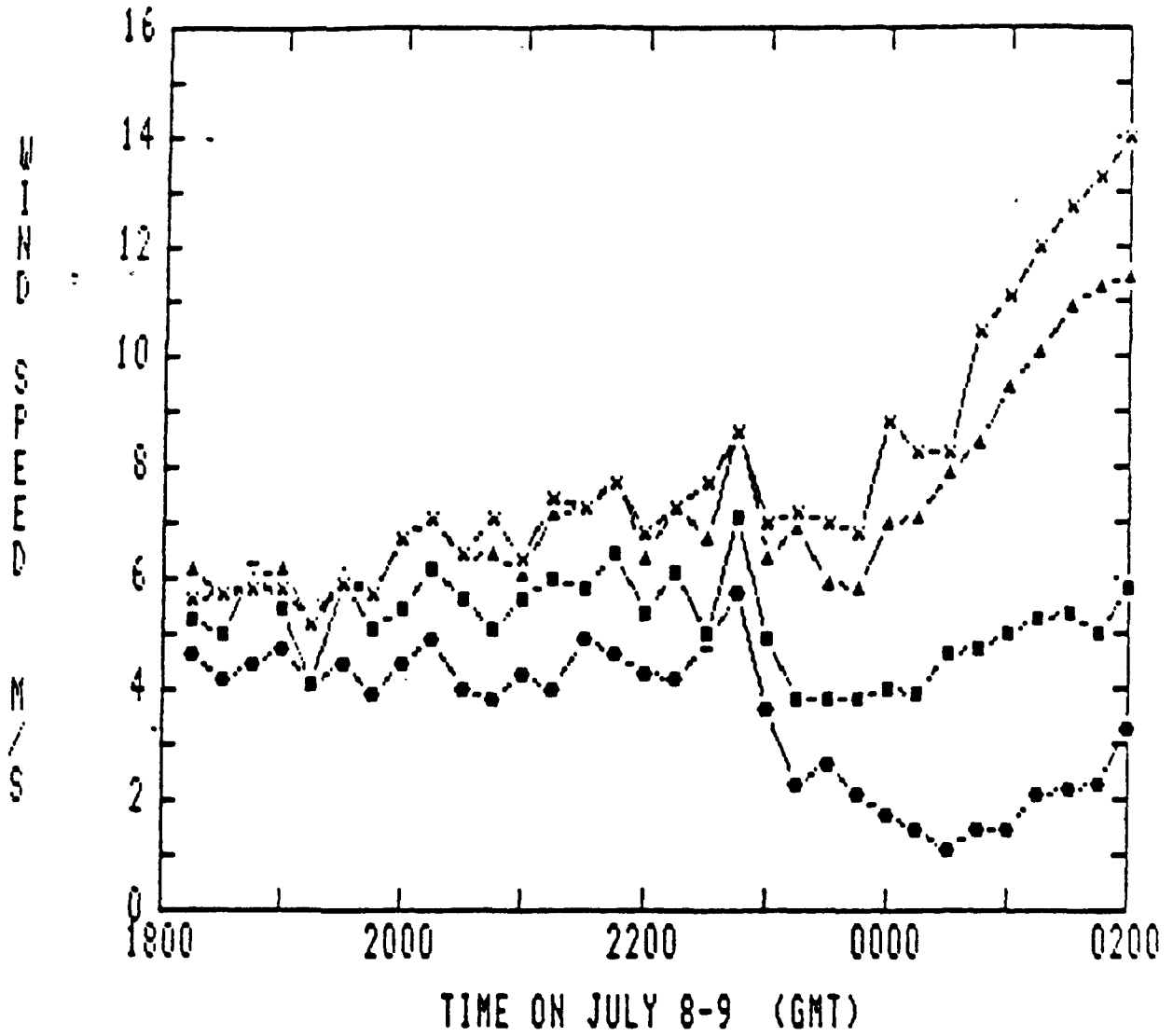

July 8-9, 1980, wind speeds at 10, 45, 177 and 444 m at KTVY

10 m

45 m

177 m

X 444 m

Surface winds do drop at 2300-0100 GMT, but seem to pick up by 0200 GMT

Figure E-7. Wind speeds at 10, 45, 177 and 444 meters at KTVY tower for July 8-9, 1980 for Oklahoma experiment.

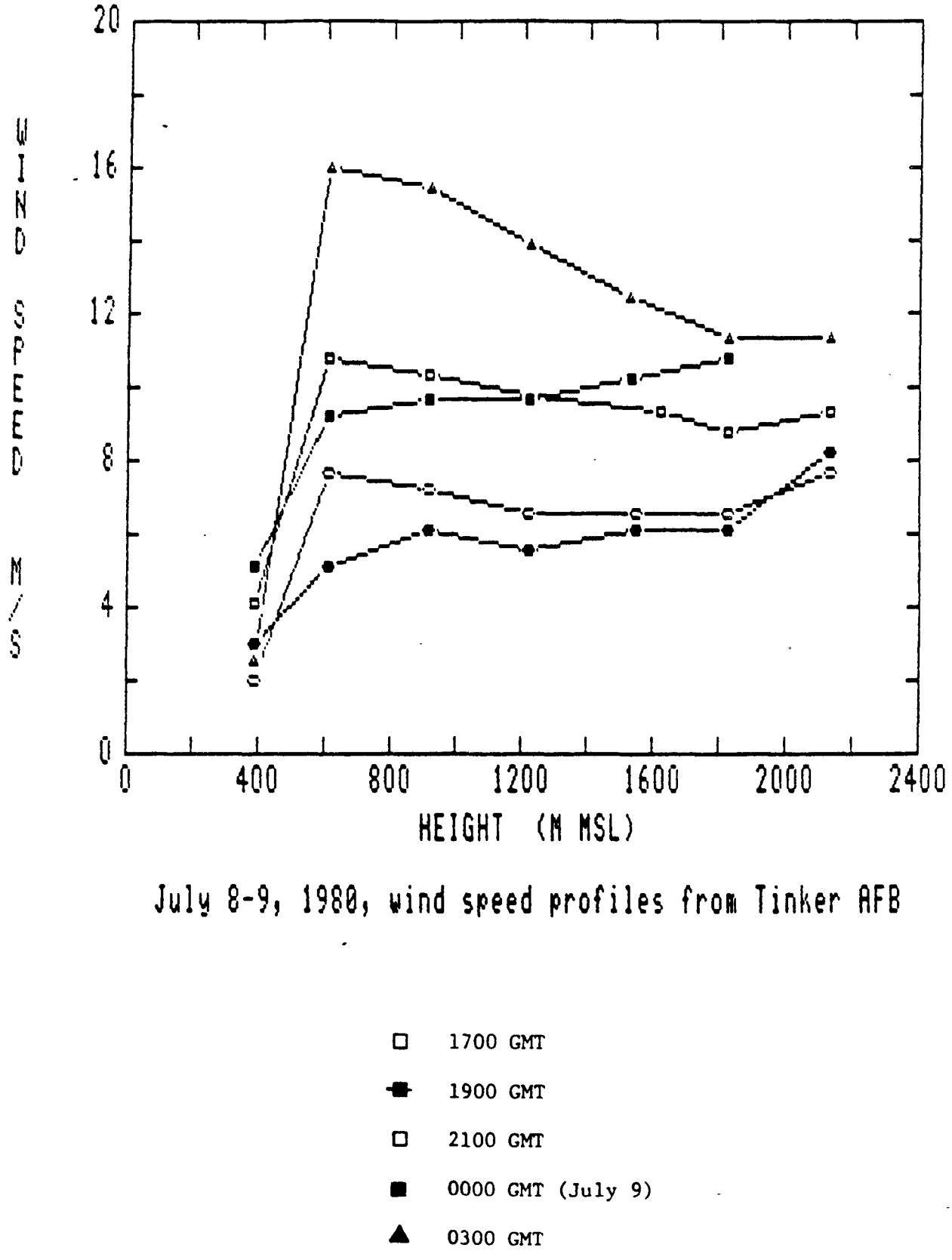

Figure E-8. Wind speed profiles from Tinker Air Force Base for July 8-9, 1980 for Oklahoma experiment.

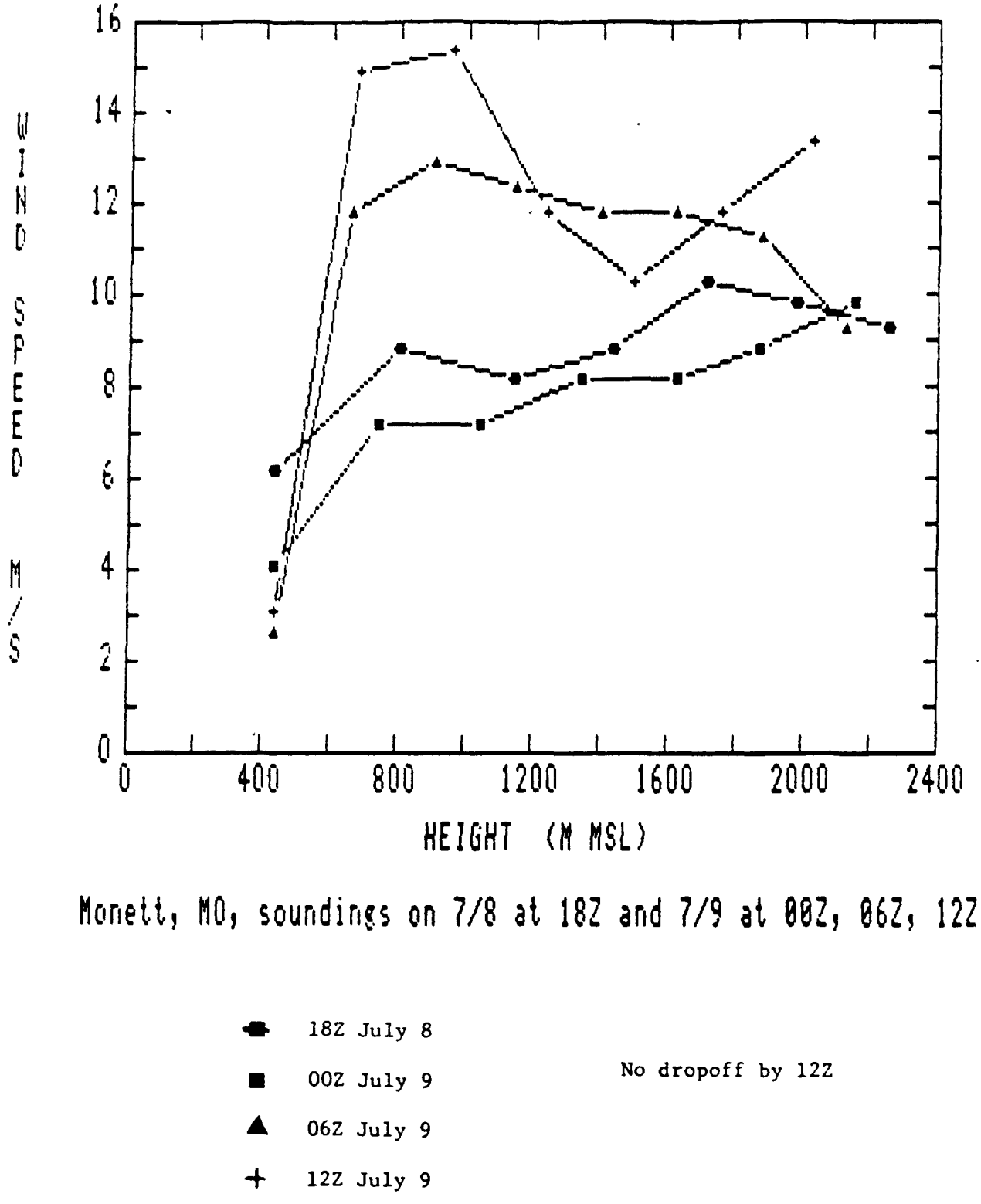

Figure E-9. Wind speed soundings from Monett, Missouri on July 8, 1980 at 18Z and on July 9, 1980 at 00Z, 06Z and 12Z for Oklahoma experiment.

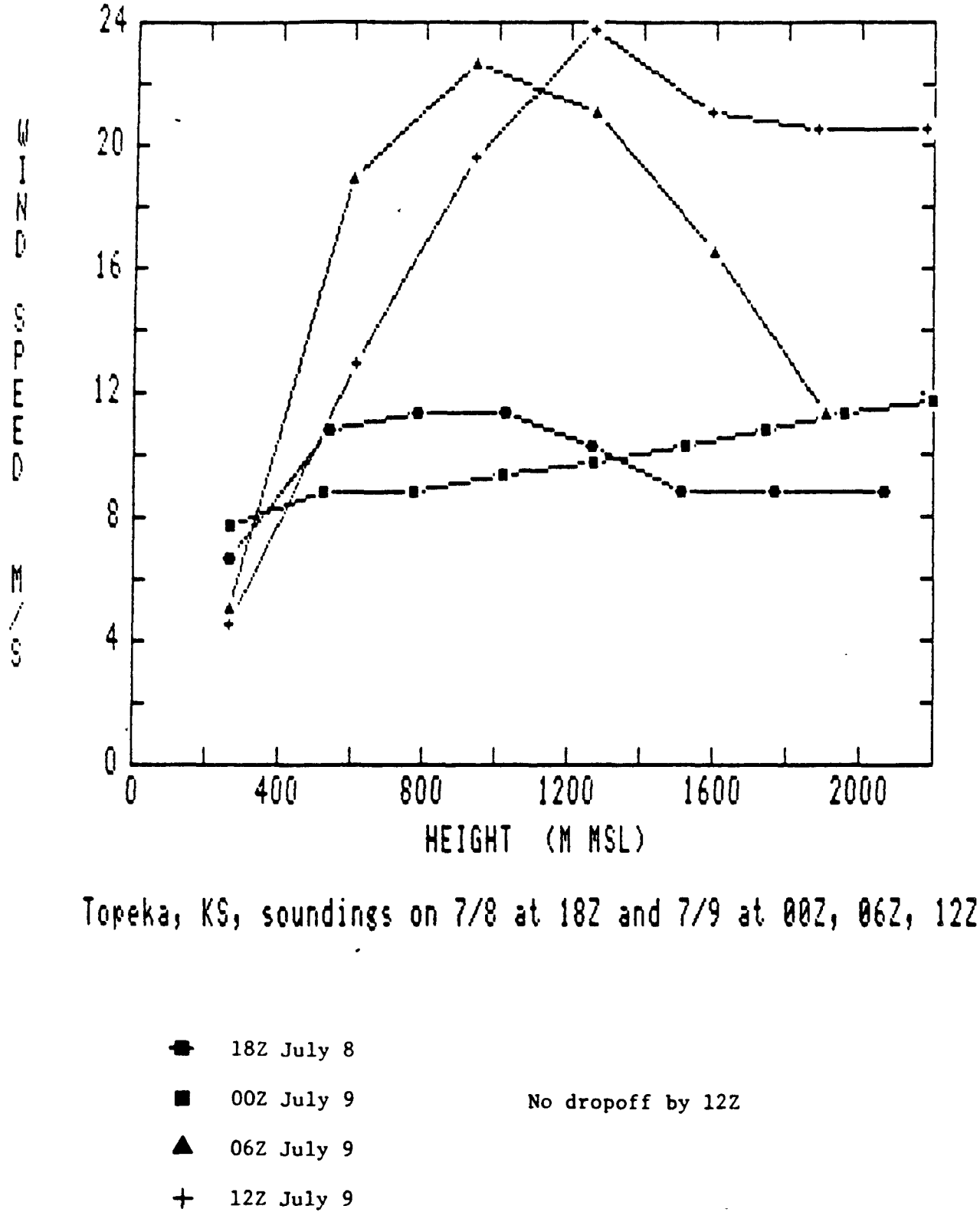

Figure E-10. Wind speed soundings from Topeka, Kansas on July 8, 1980 at 18Z and on July 9, 1980 at 00Z, 06Z and 12Z for Oklahoma experiment.

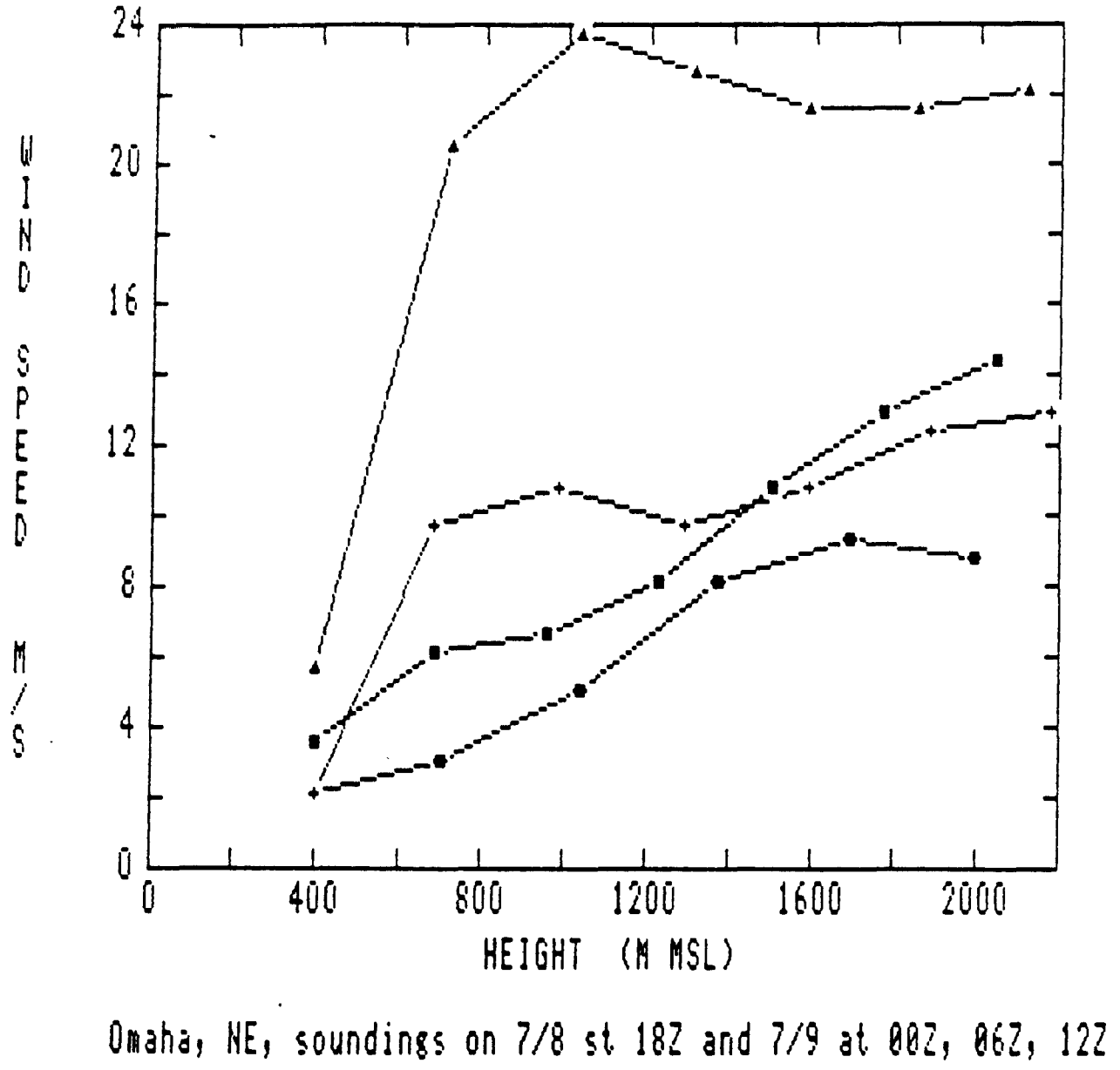

18Z July 8

00Z July 9

06Z July 9

12Z July 9 Note how these dropped off

Figure E-11. Wind speed soundings at Omaha, Nebraska on July 8, 1980 at 18Z and on July 9, 1980 at 00Z, 06Z and 12Z for Oklahoma experiment.

3. ISOPLETH PLOTS OF PREDICTED GROUND-LEVEL CONCENTRATIONS FOR THE OKLAHOMA EXPERIMENTS

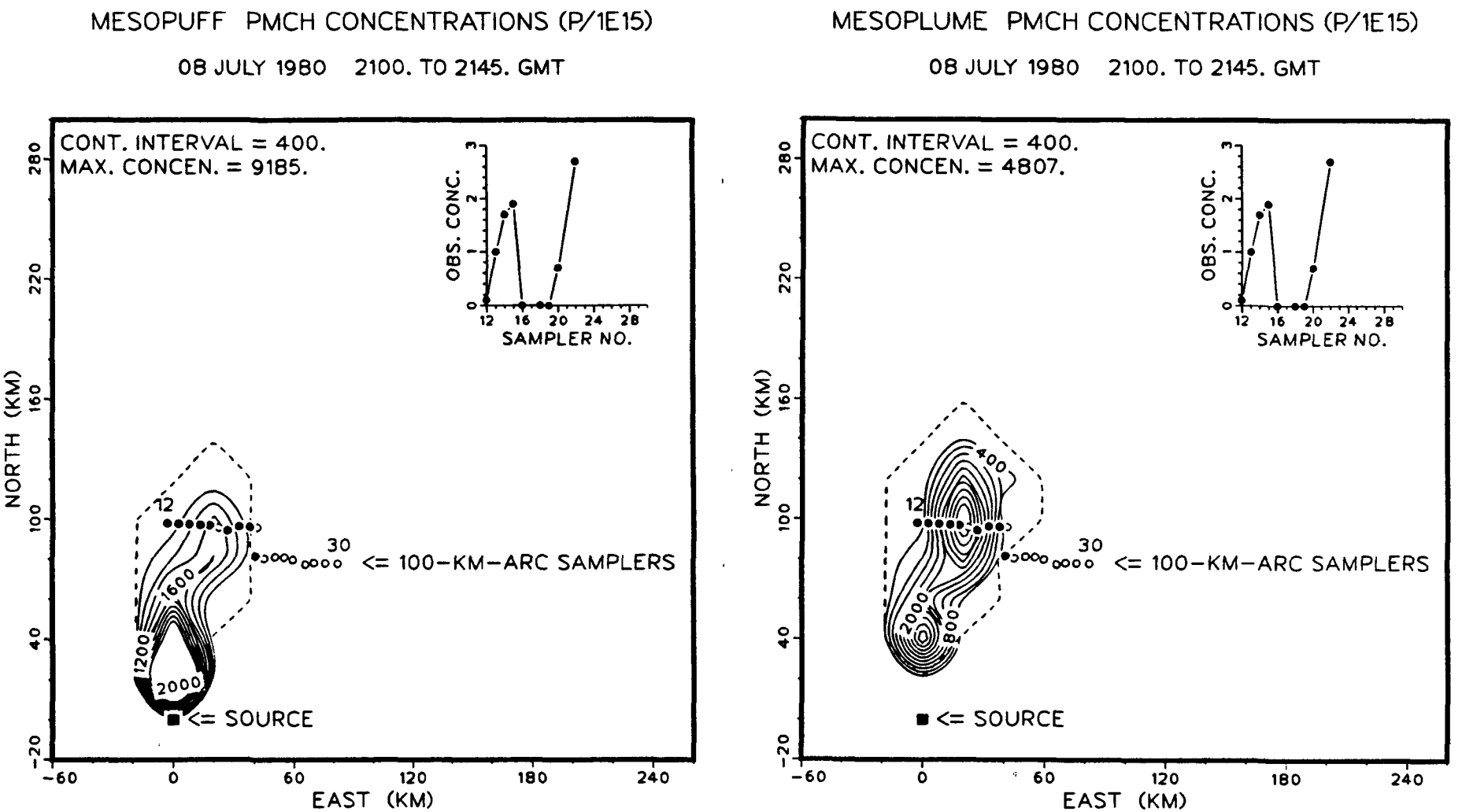

Figure E-12. Isopleth plot of ground-level concentrations for the Oklahoma experiment of July 8, 1980 (2100 to 2145 GMT) ... (left) MESOPUFF predictions, (right) MESOPLUME predictions.

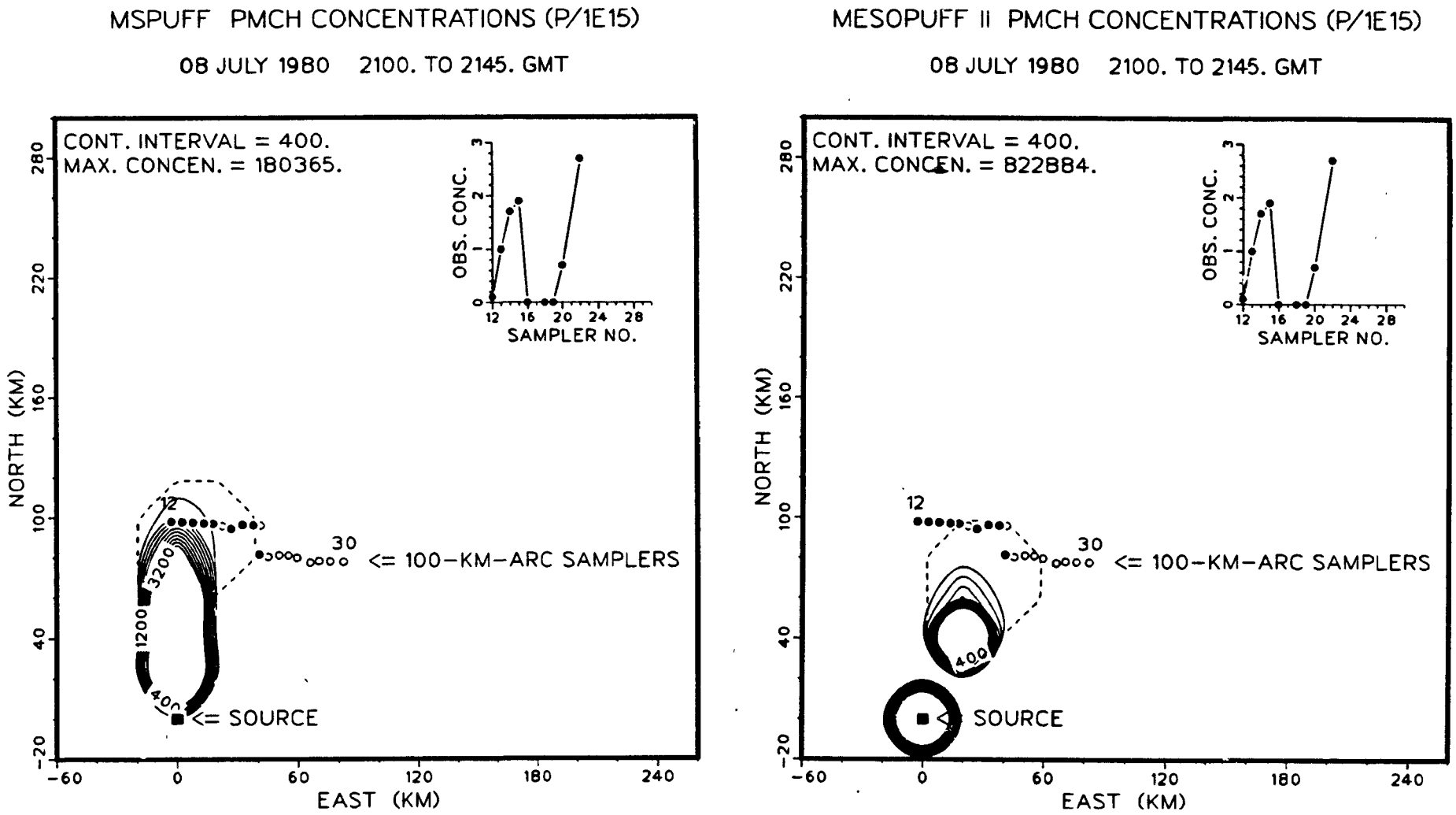

Figure E-13. Isopleth plot of ground-level concentrations for the Oklahoma experiment of July 8, 1980 (2100 to 2145 GMT) ... (left) MSPUFF predictions, (right) MESOPUFF II predictions.

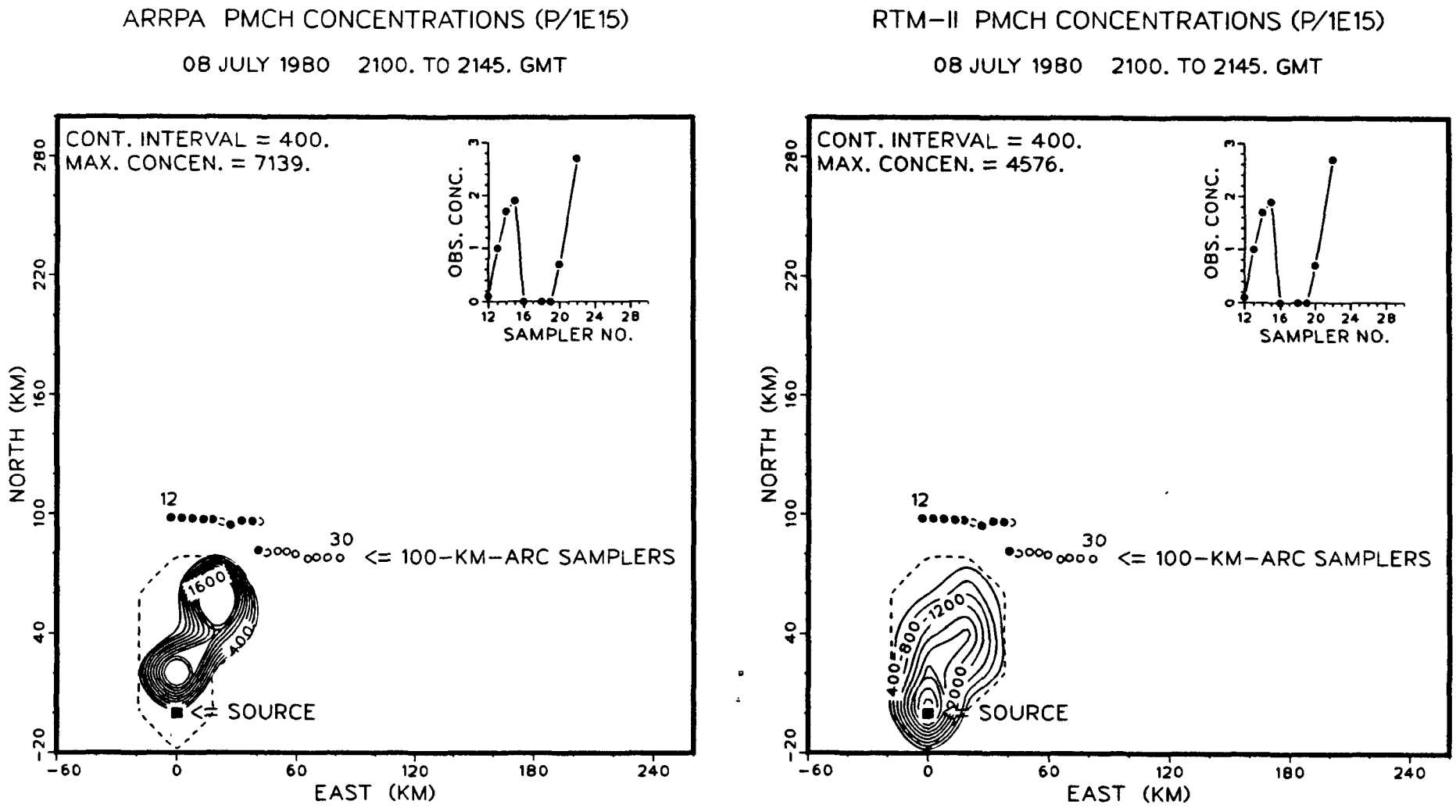

Figure E-14. Isopleth plot of ground-level concentrations for the Oklahoma experiment of July 8, 1980 (2100 to 2145 GMT) ... (left) ARRPA predictions, (right) RTM-II predictions.

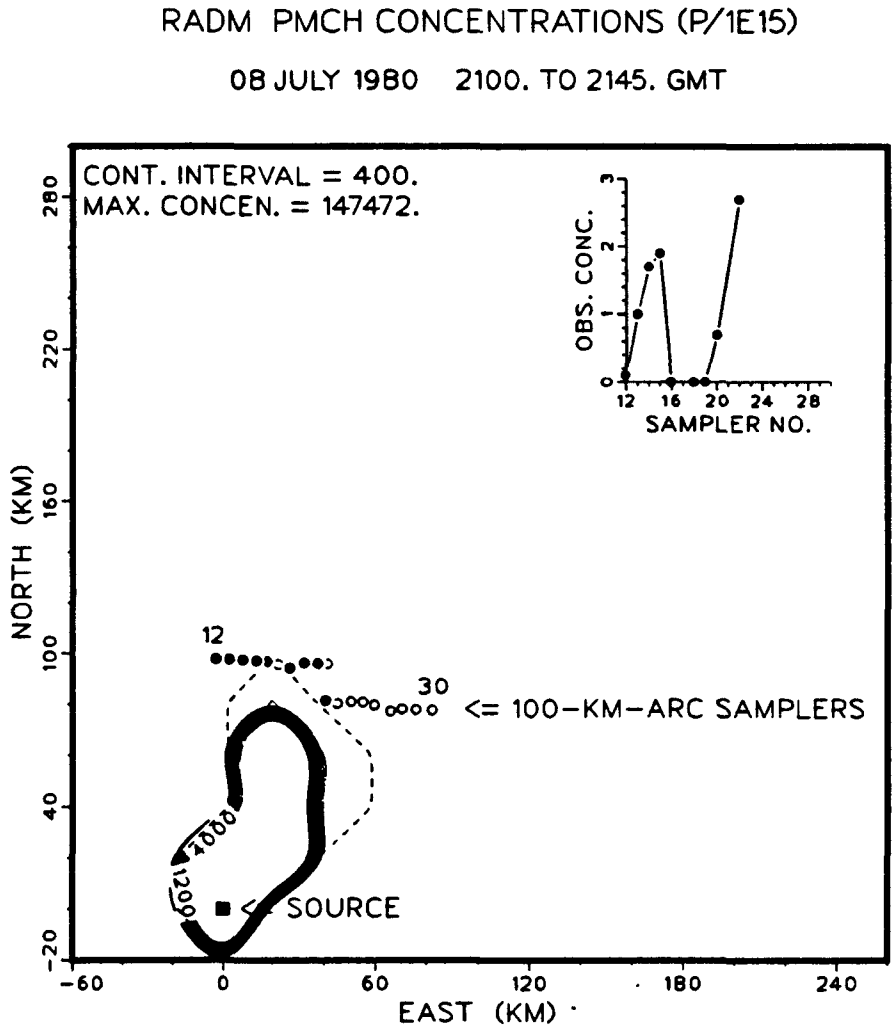

Figure E-15. Isopleth plot of ground-level concentrations for the Oklahoma experiment of July 8, 1980 (2100 to 2145 GMT) ... RADM predictions.

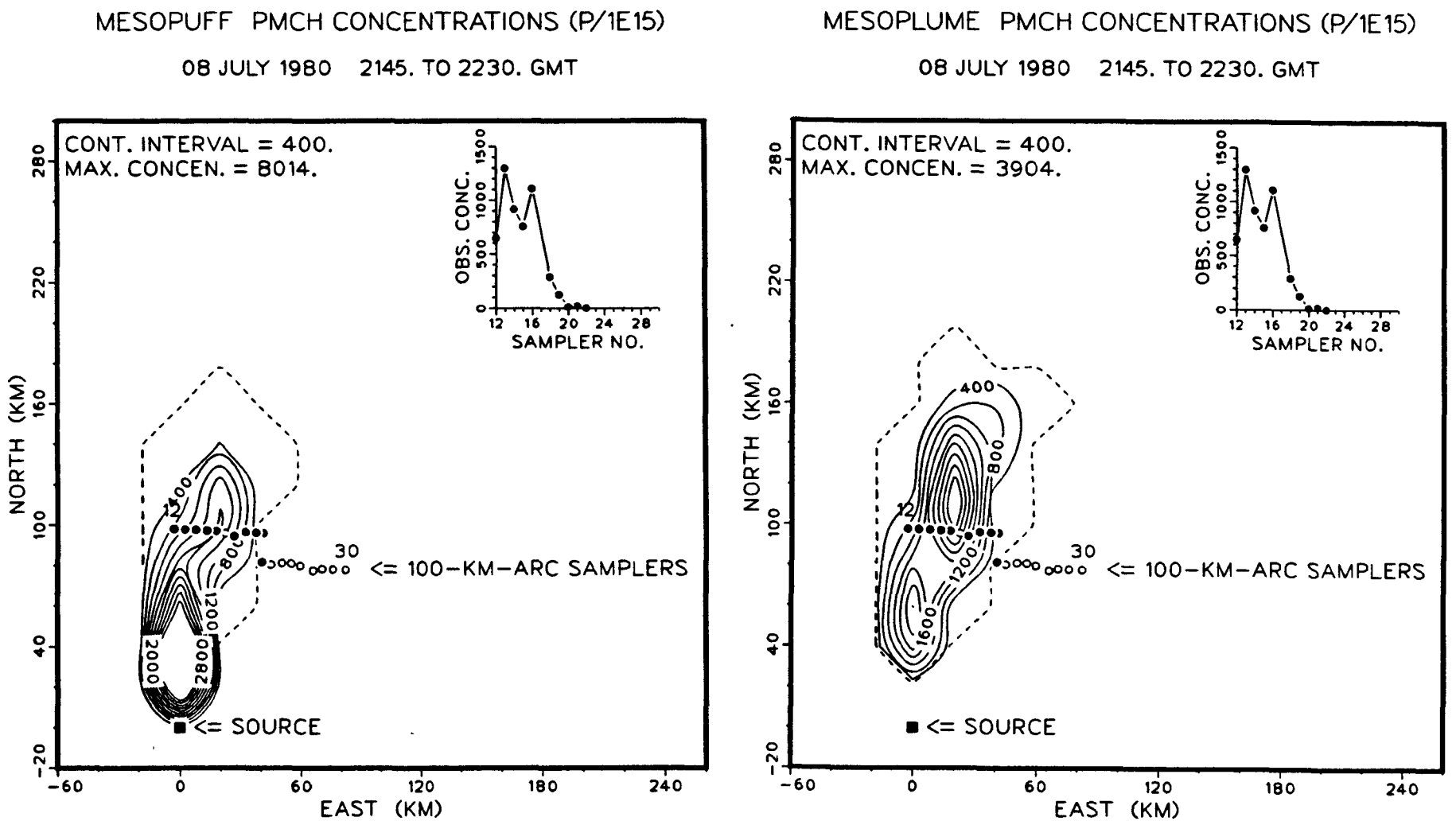

Figure E-16. Isopleth plot of ground-level concentrations for the Oklahoma experiment of July 8, 1980 (2145 to 2230 GMT) ... (left) MESOPUFF predictions, (right) MESOPLUME predictions.

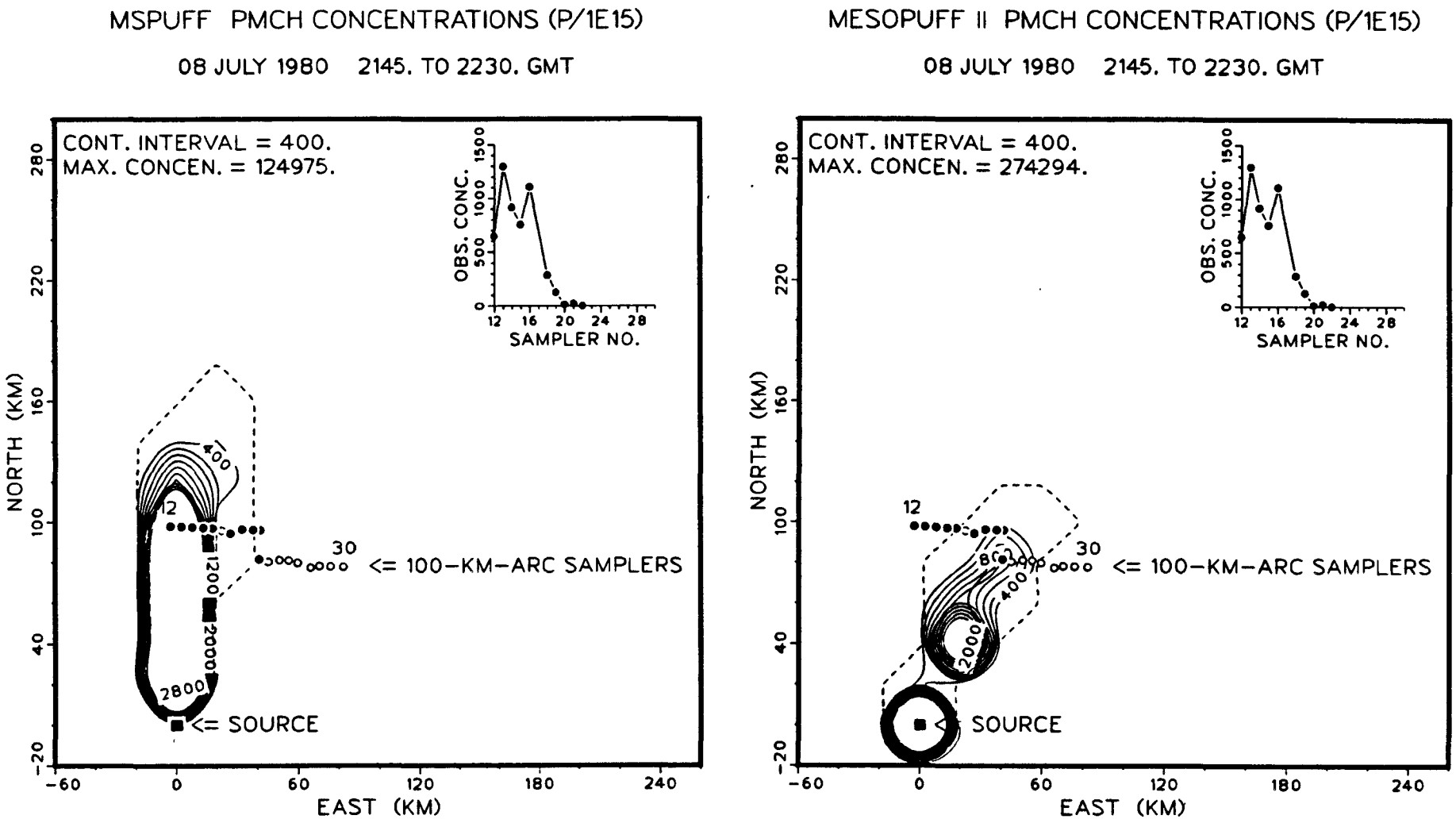

Figure E-17. Isopleth plot of ground-level concentrations for the Oklahoma experiment of July 8, 1980 (2145 to 2230 GMT) ... (left) MSPUFF predictions, (right) MESOPUFF II predictions.

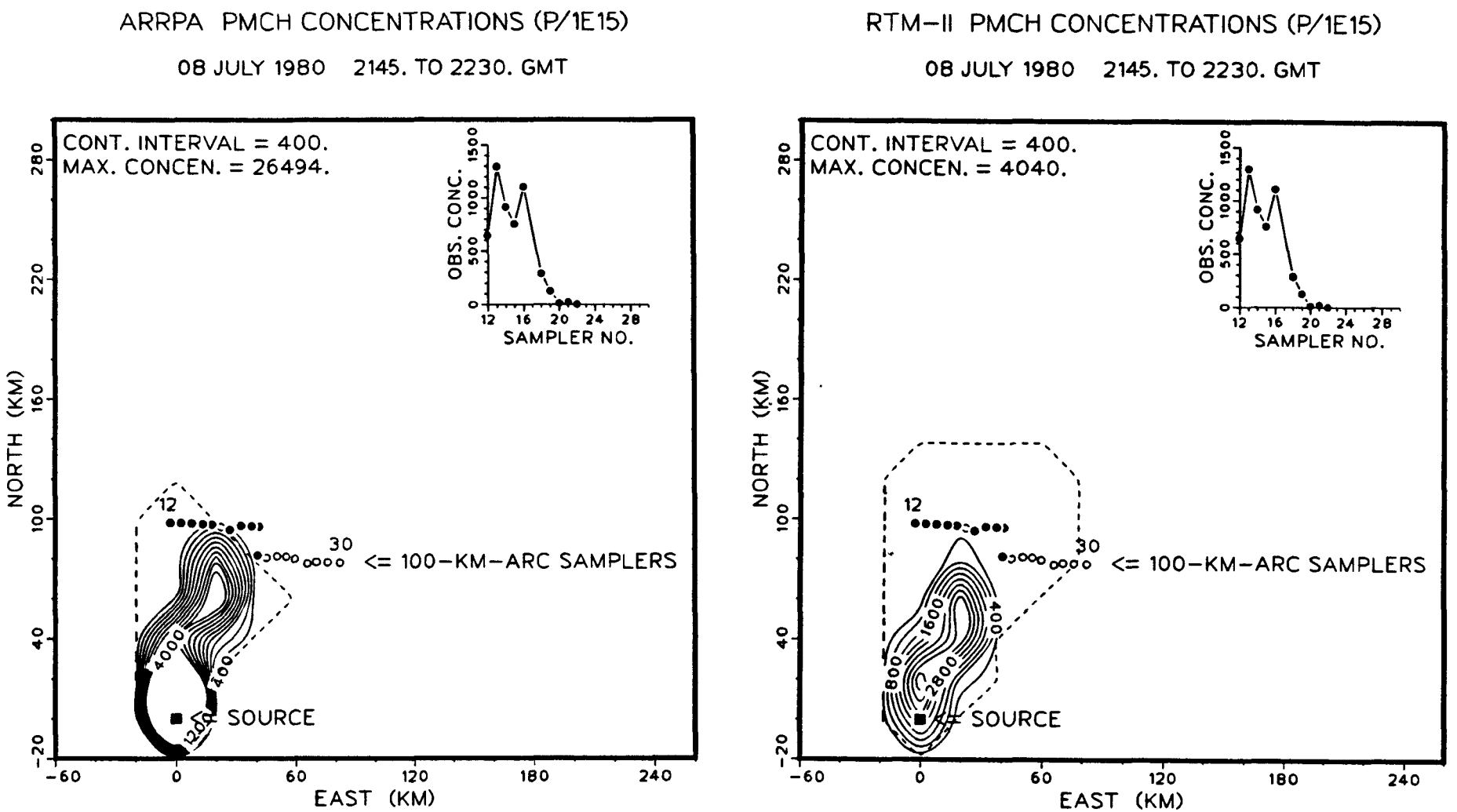

Figure E-18. Isopleth plot of ground-level concentrations for the Oklahoma experiment of July 8, 1980 (2145 to 2230 GMT) ... (left) ARRPA predictions, (right) RTM-II predictions.

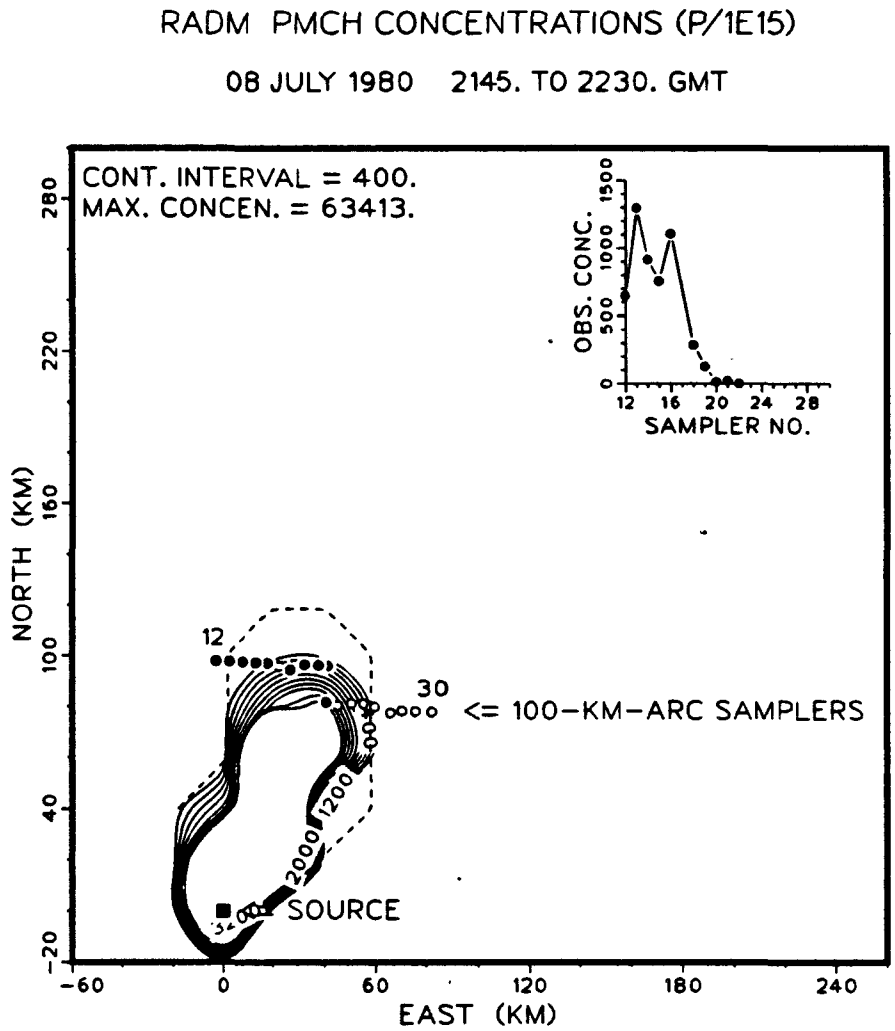

Figure E-19. Isopleth plot of ground-level concentrations for the Oklahoma experiment of July 8, 1980 (2145 to 2230 GMT) ... RADM predictions.

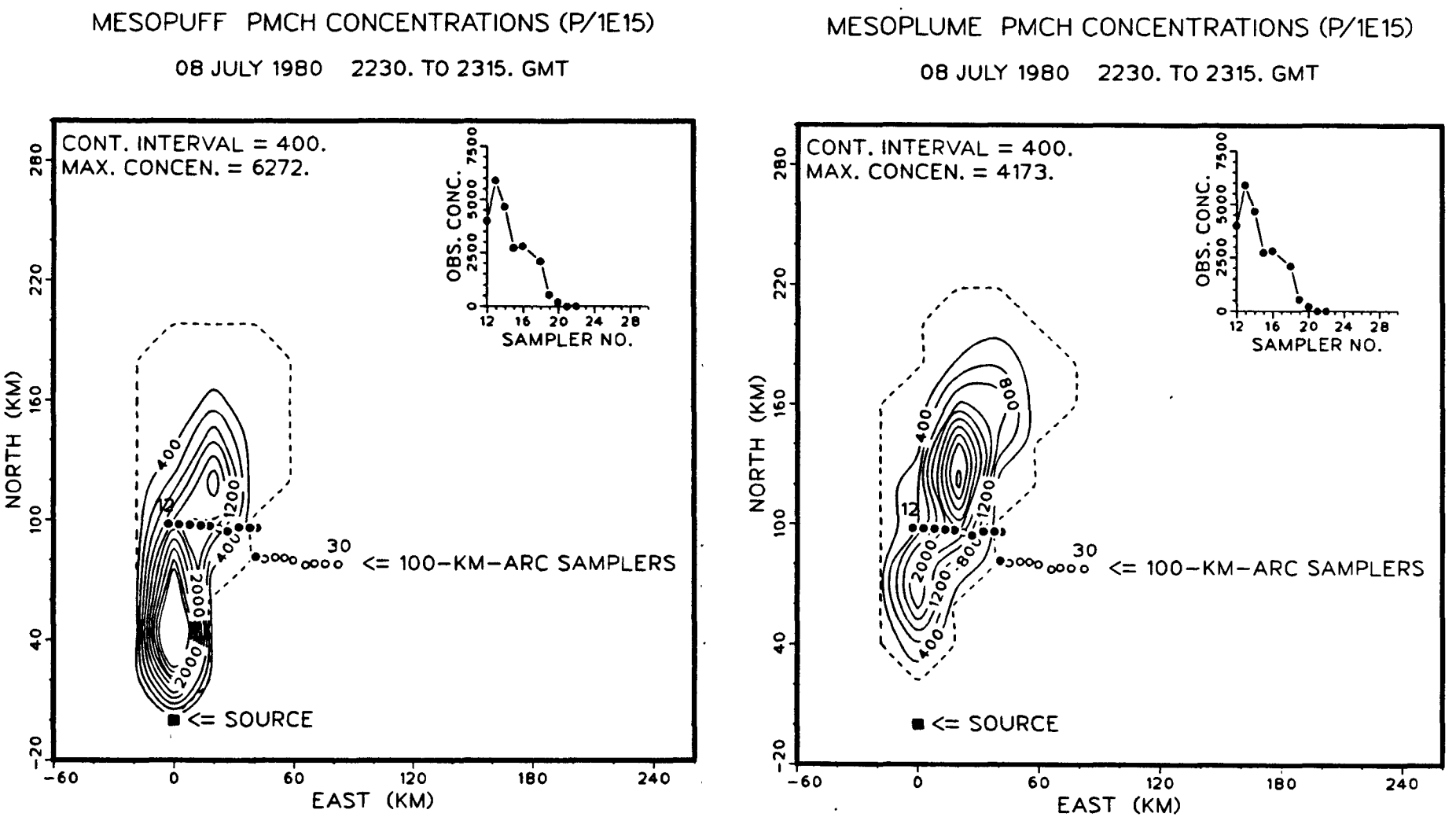

Figure E-20. Isopleth plot of ground-level concentrations for the Oklahoma experiment of July 8, 1980 (2230 to 2315 GMT) ... (left) MESOPUFF predictions, (right) MESOPLUME predictions.

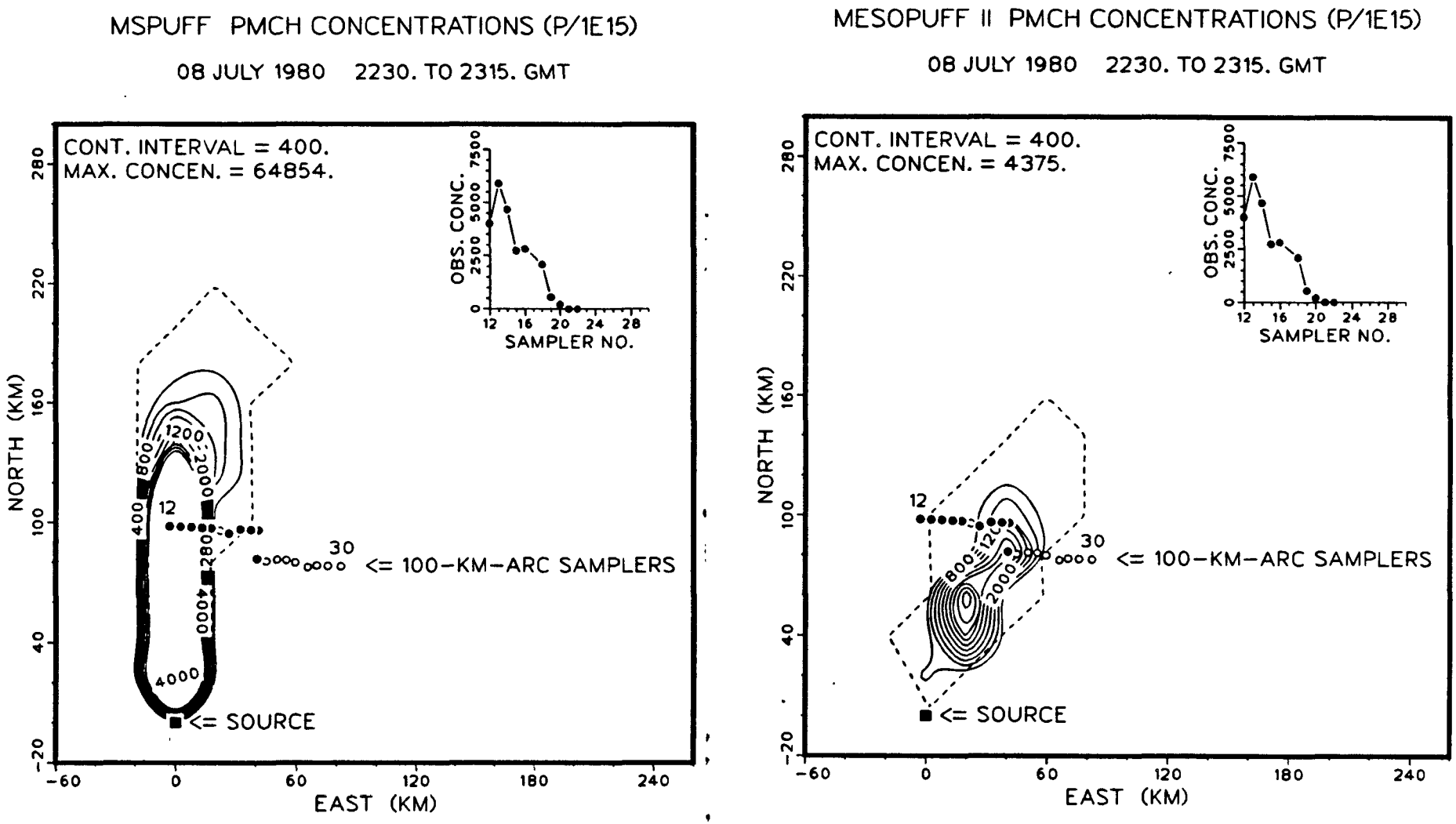

Figure E-21. Isopleth plot of ground-level concentrations for the Oklahoma experiment of July 8, 1980 (2230 to 2315 GMT) ... (left) MSPUFF predictions, (right) MESOPUFF II predictions.

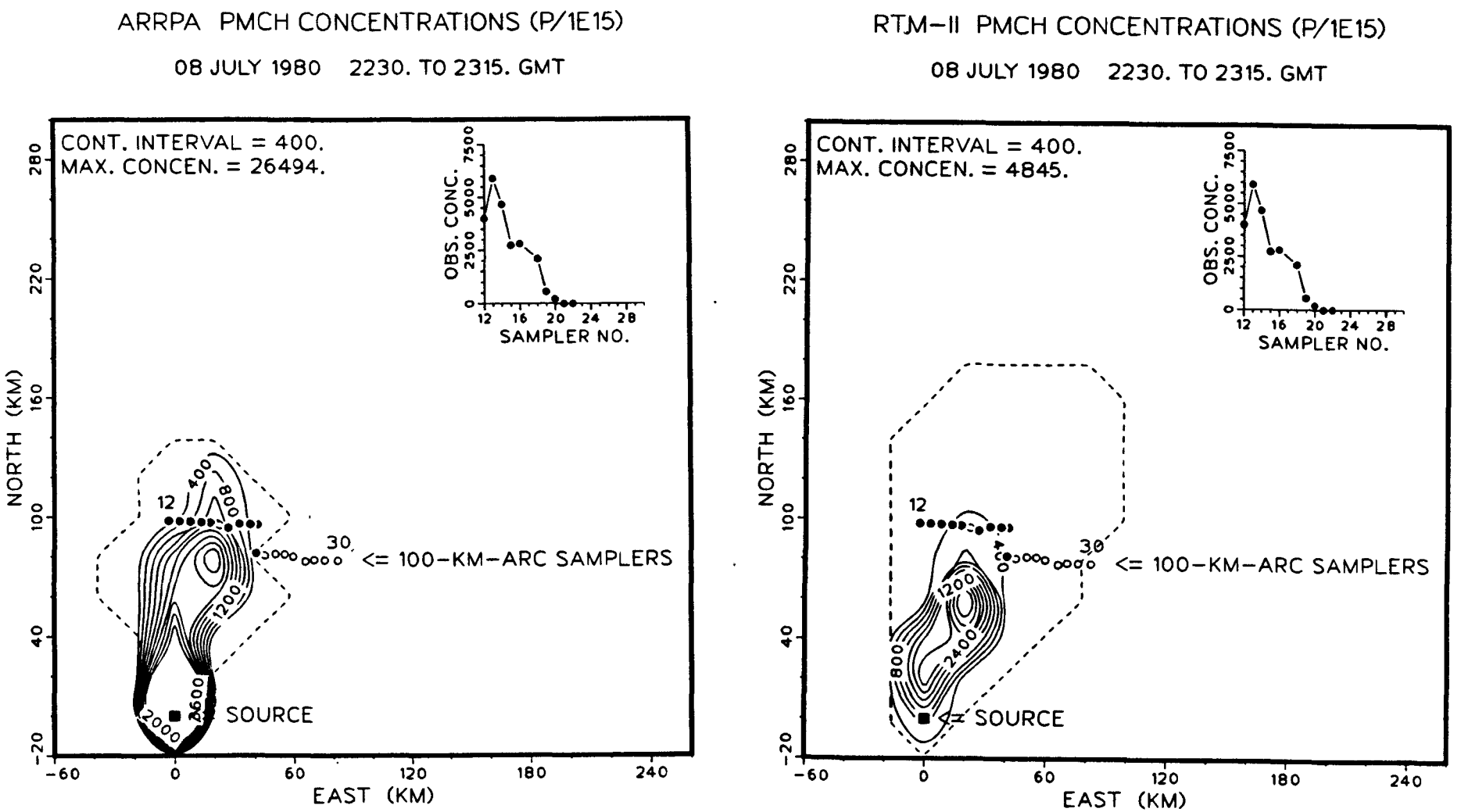

Figure E-22. Isopleth plot of ground-level concentrations for the Oklahoma experiment of July 8, 1980 (2230 to 2315 GMT) ... (left) ARRPA predictions, (right) RTM-II predictions.

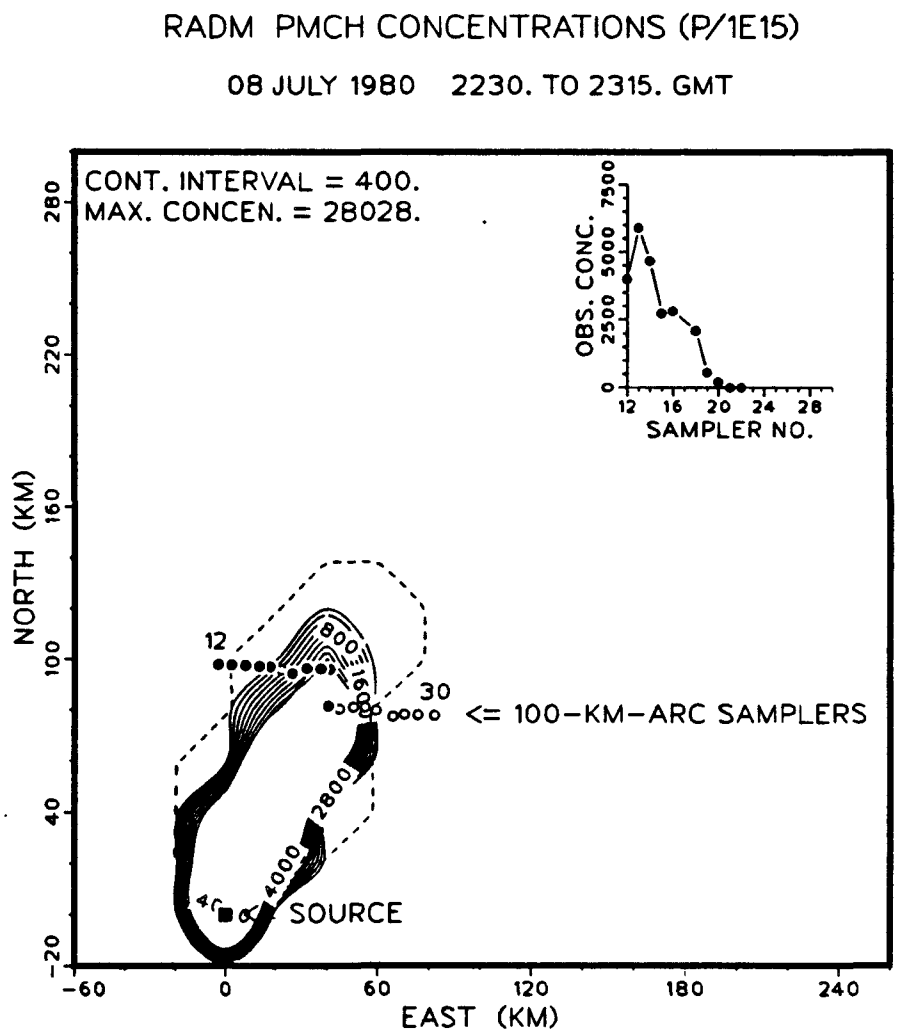

Figure E-23. Isopleth plot of ground-level concentrations for the Oklahoma experiment of July 8, 1980 (2230 to 2315 GMT) ... RADM predictions.

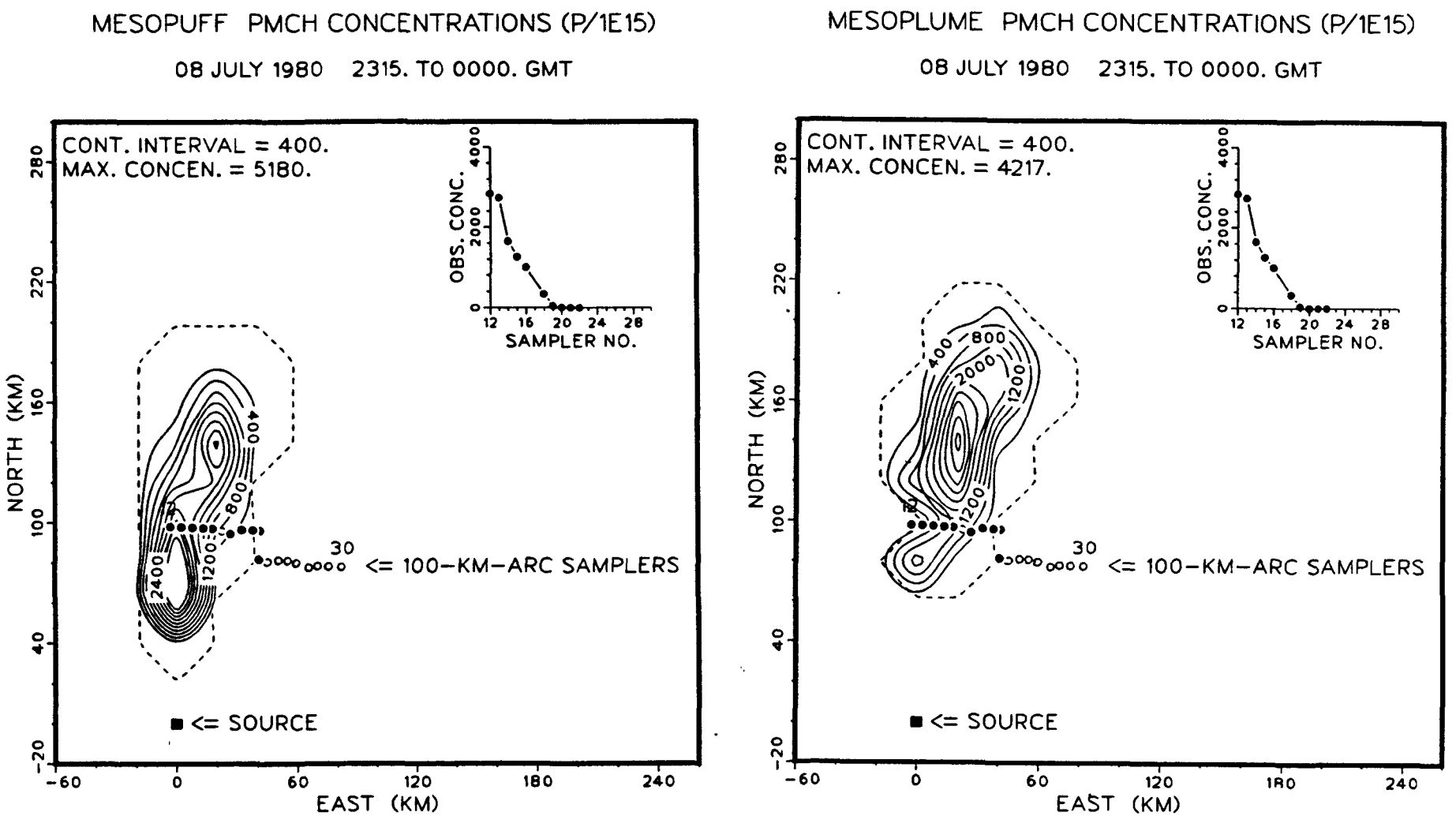

Figure E-24. Isopleth plot of ground-level concentrations for the Oklahoma experiment of July 8, 1980 (2315 to 0000 GMT) ... (left) MESOPUFF predictions, (right) MESOPLUME predictions.

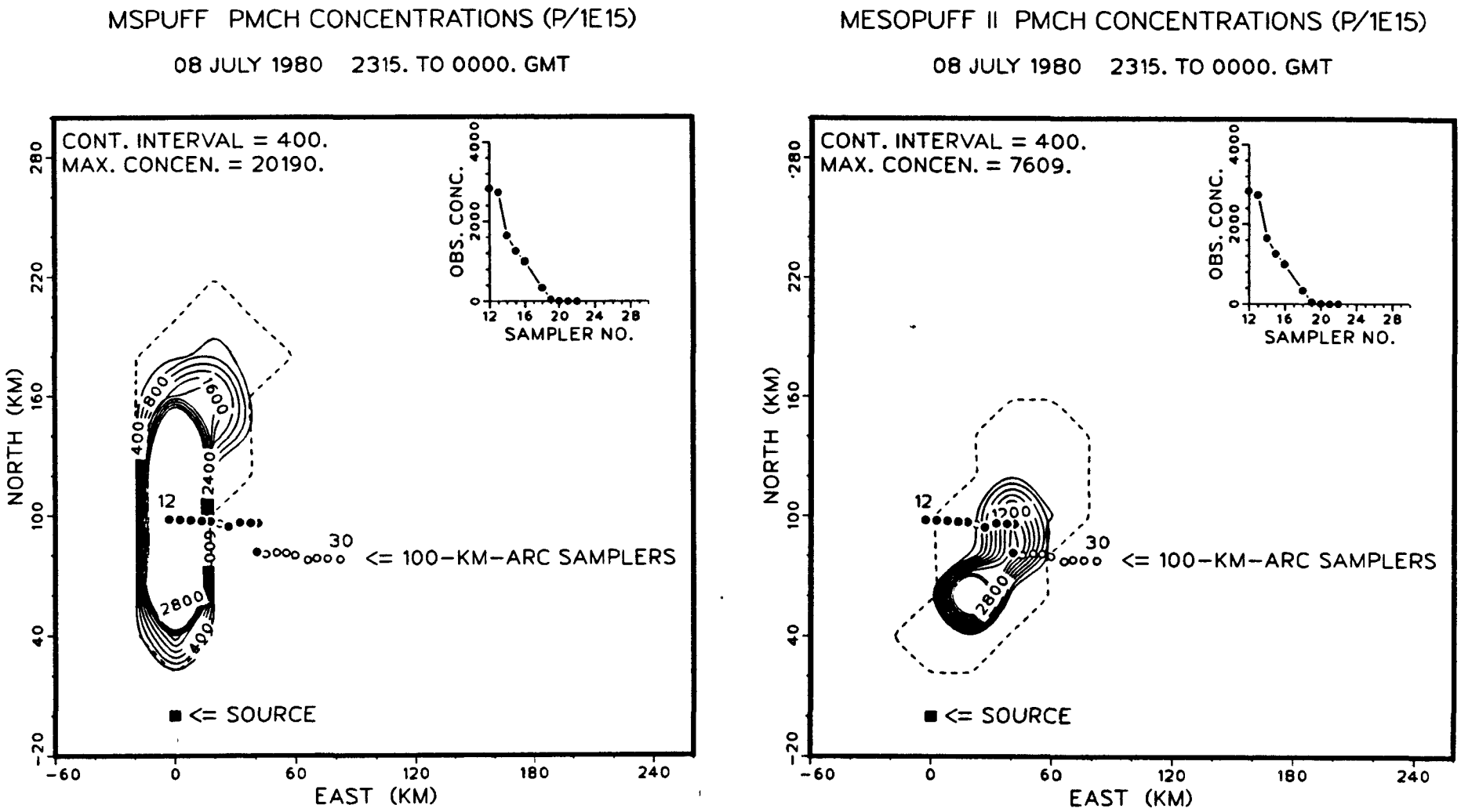

Figure E-25. Isopleth plot of ground-level concentrations for the Oklahoma experiment of July 8, 1980 (2315 to 0000 GMT) ... (left) MSPUFF predictions, (right) MESOPUFF II predictions.

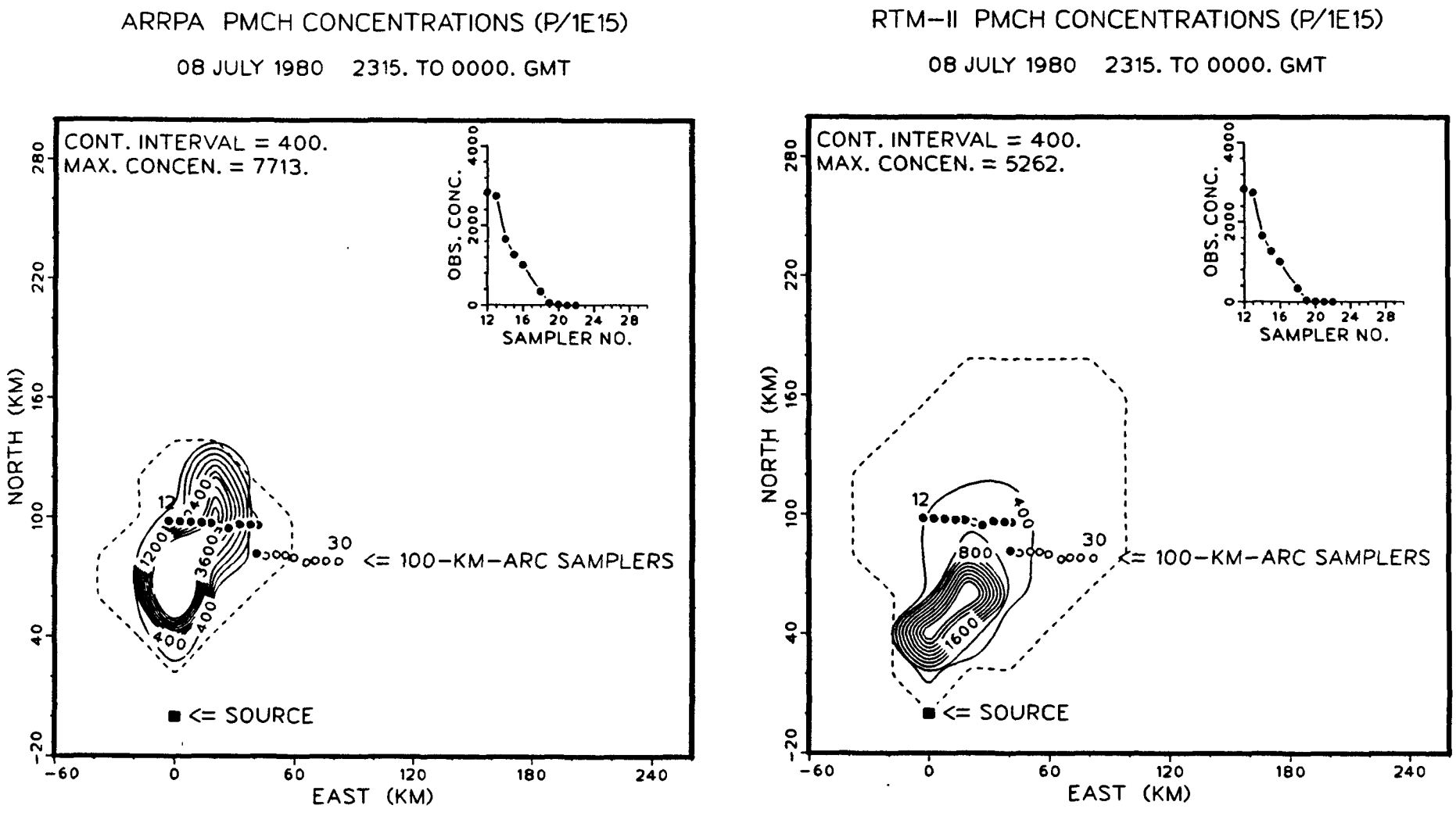

Figure E-26. Isopleth plot of ground-level concentrations for the Oklahoma experiment of July 8, 1980 (2315 to 0000 GMT) ... (left) ARRPA predictions, (right) RTM-II predictions.

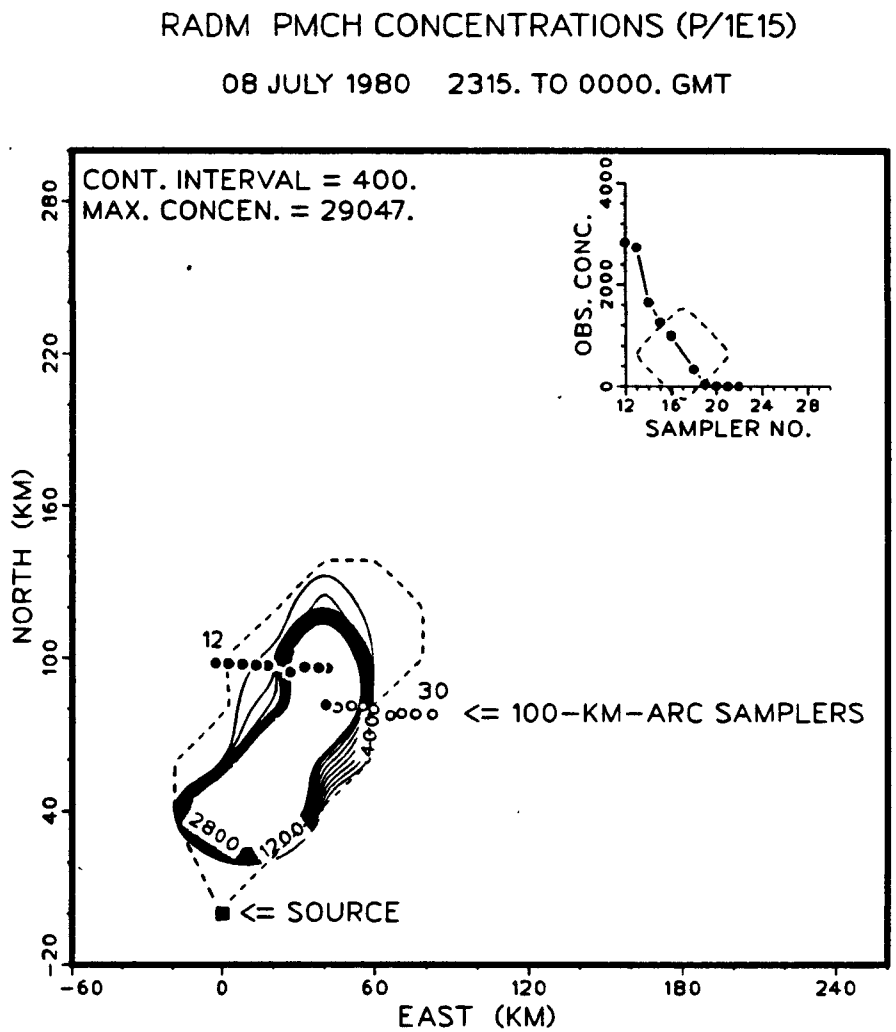

Figure E-27. Isopleth plot of ground-level concentrations for the Oklahoma experiment of July 8, 1980 (2315 to 0000 GMT) ... RADM predictions.

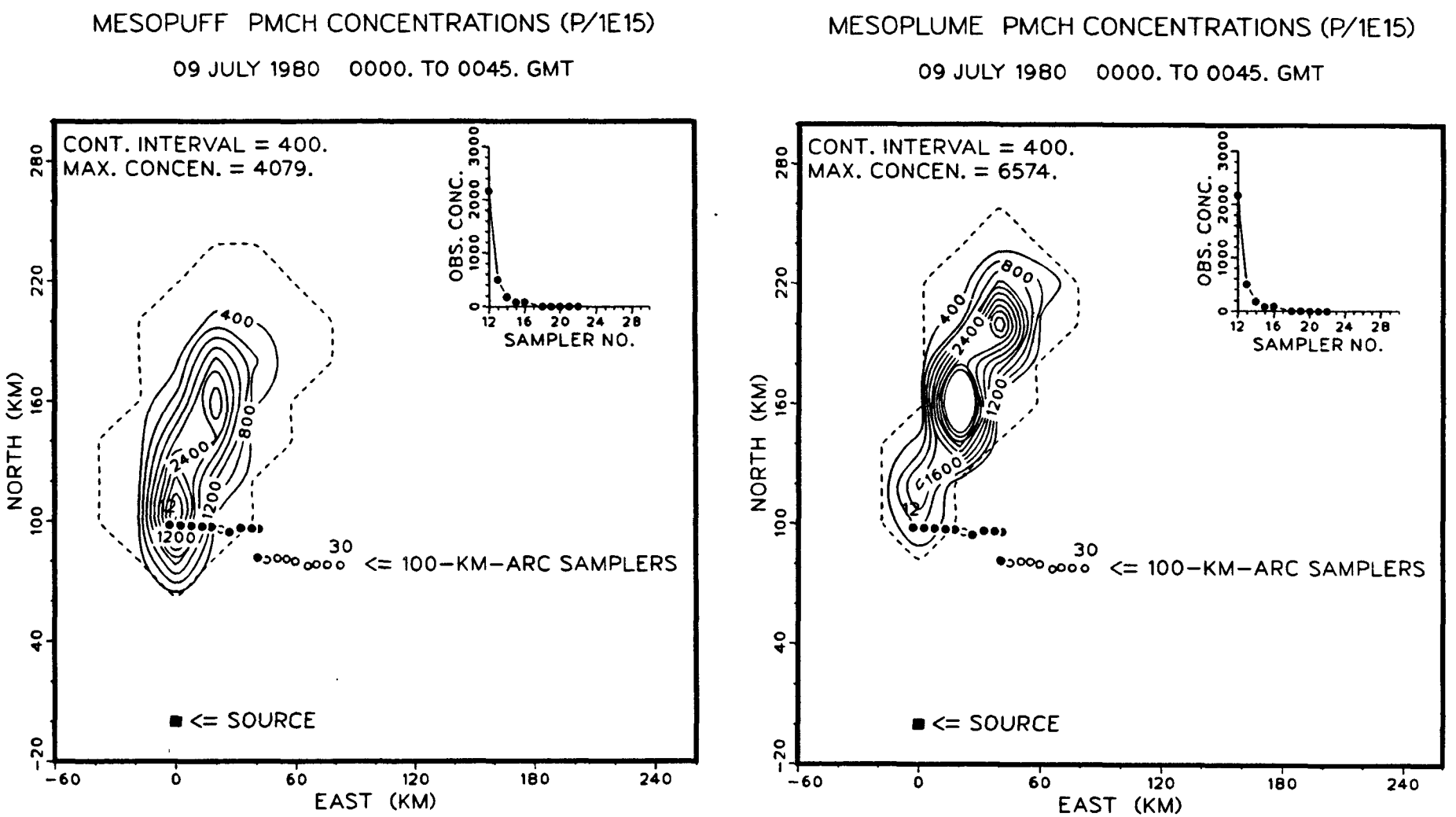

Figure E-28. Isopleth plot of ground-level concentrations for the Oklahoma experiment of July 9, 1980 (0000 to 0045 GMT) ... (left) MESOPUFF predictions, (right) MESOPLUME predictions.

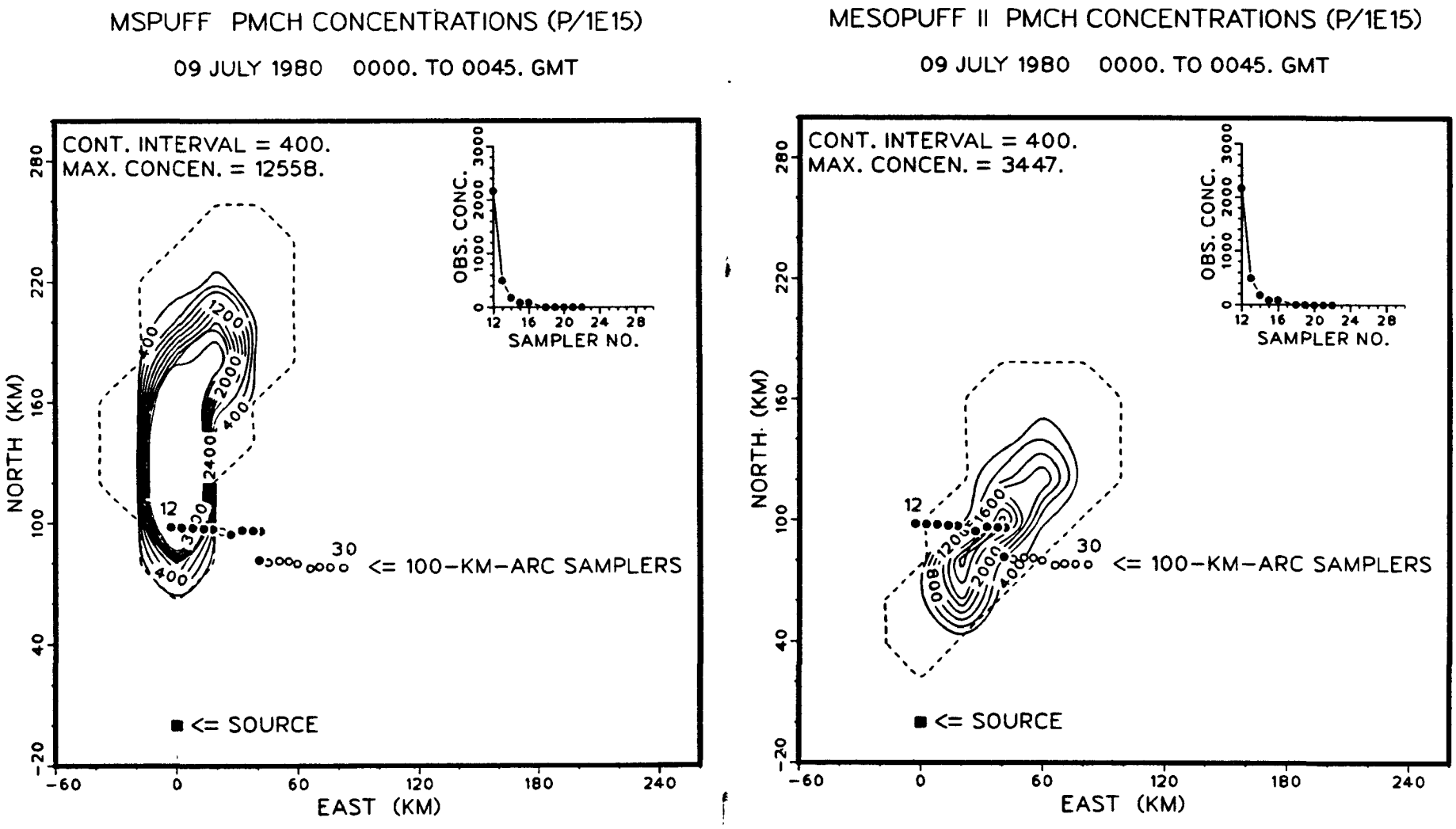

Figure E-29. Isopleth plot of ground-level concentrations for the Oklahoma experiment of July 9, 1980 (0000 to 0045 GMT) ... (left) MSPUFF predictions, (right) MESOPUFF II predictions.

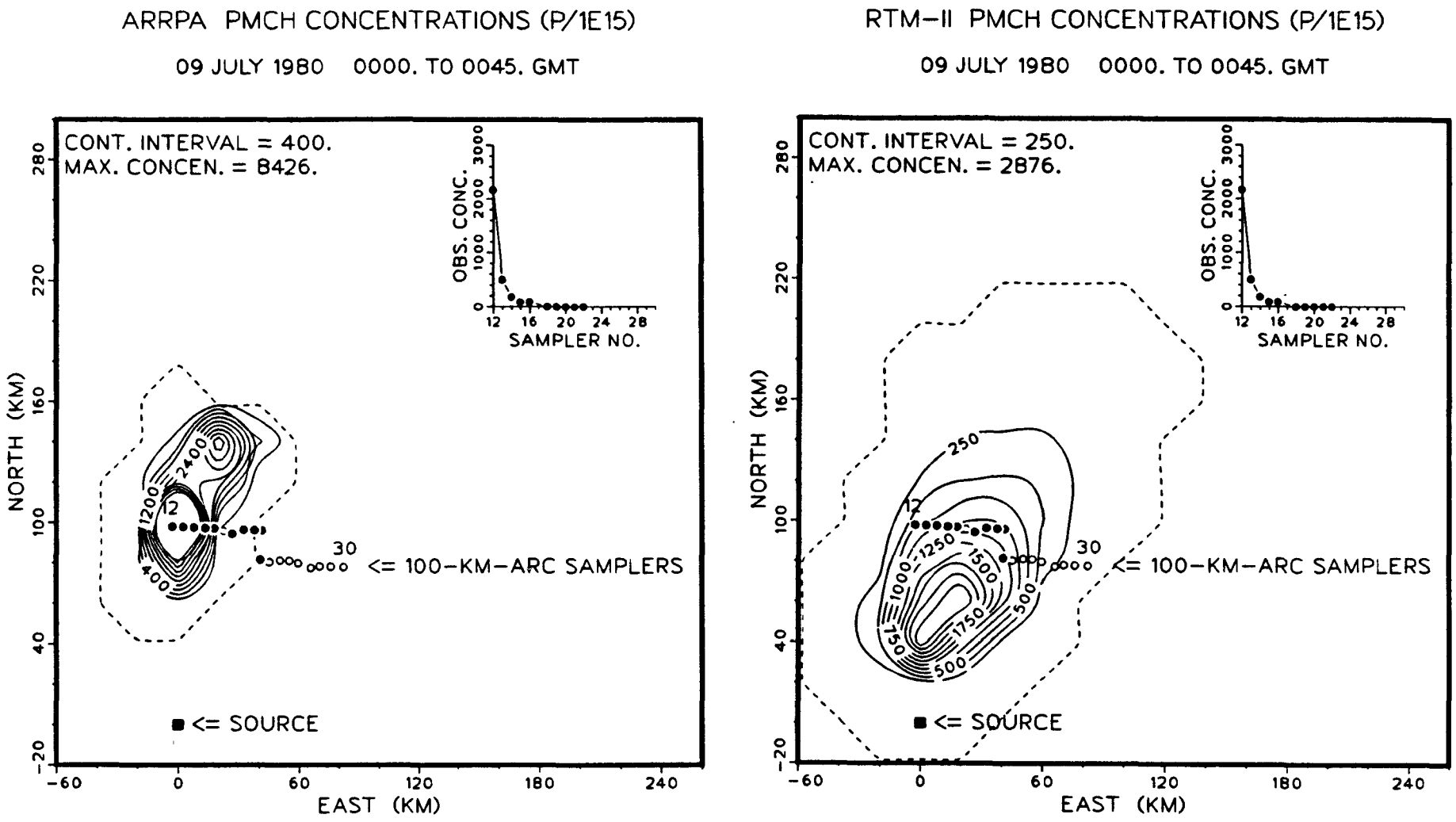

Figure E-30. Isopleth plot of ground-level concentrations for the Oklahoma experiment of July 9, 1980 (0000 to 0045 GMT) ... (left) ARRPA predictions, (right) RTM-II predictions.

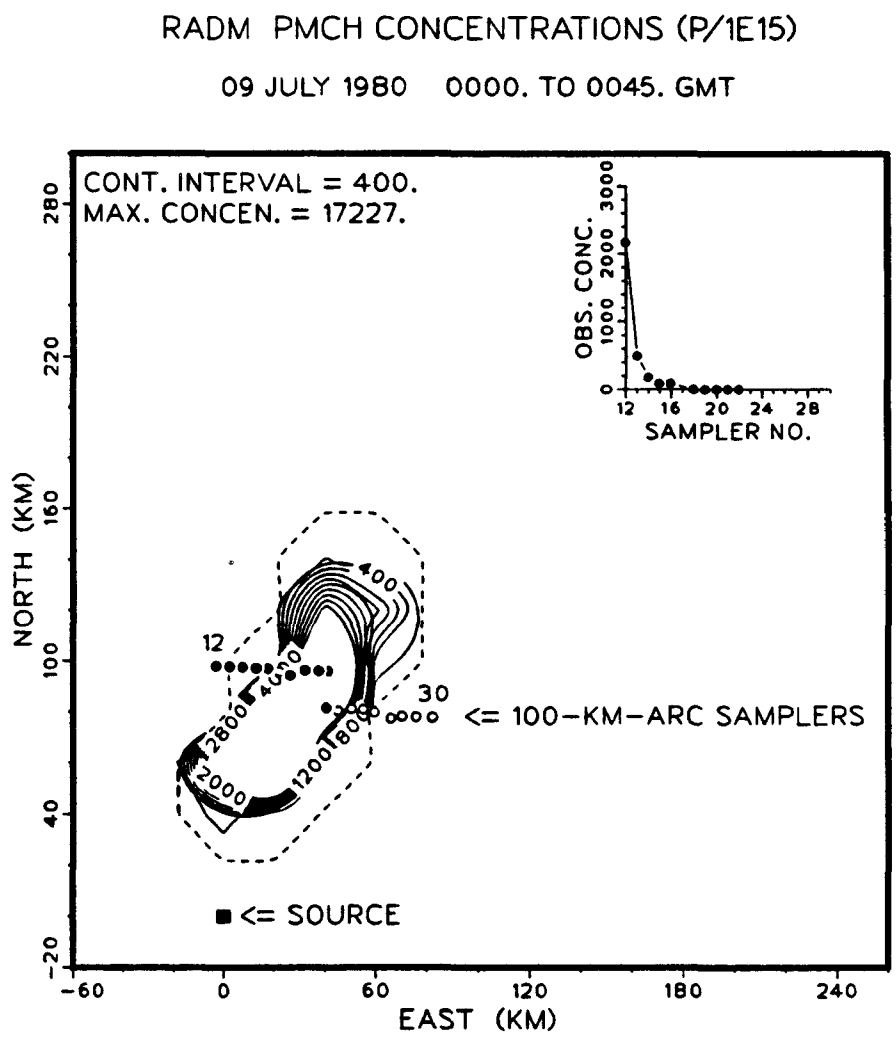

Figure E-31. Isopleth plot of ground-level concentrations for the Oklahoma experiment of July 9, 1980 (0000 to 0045 GMT) ... RADM predictions.

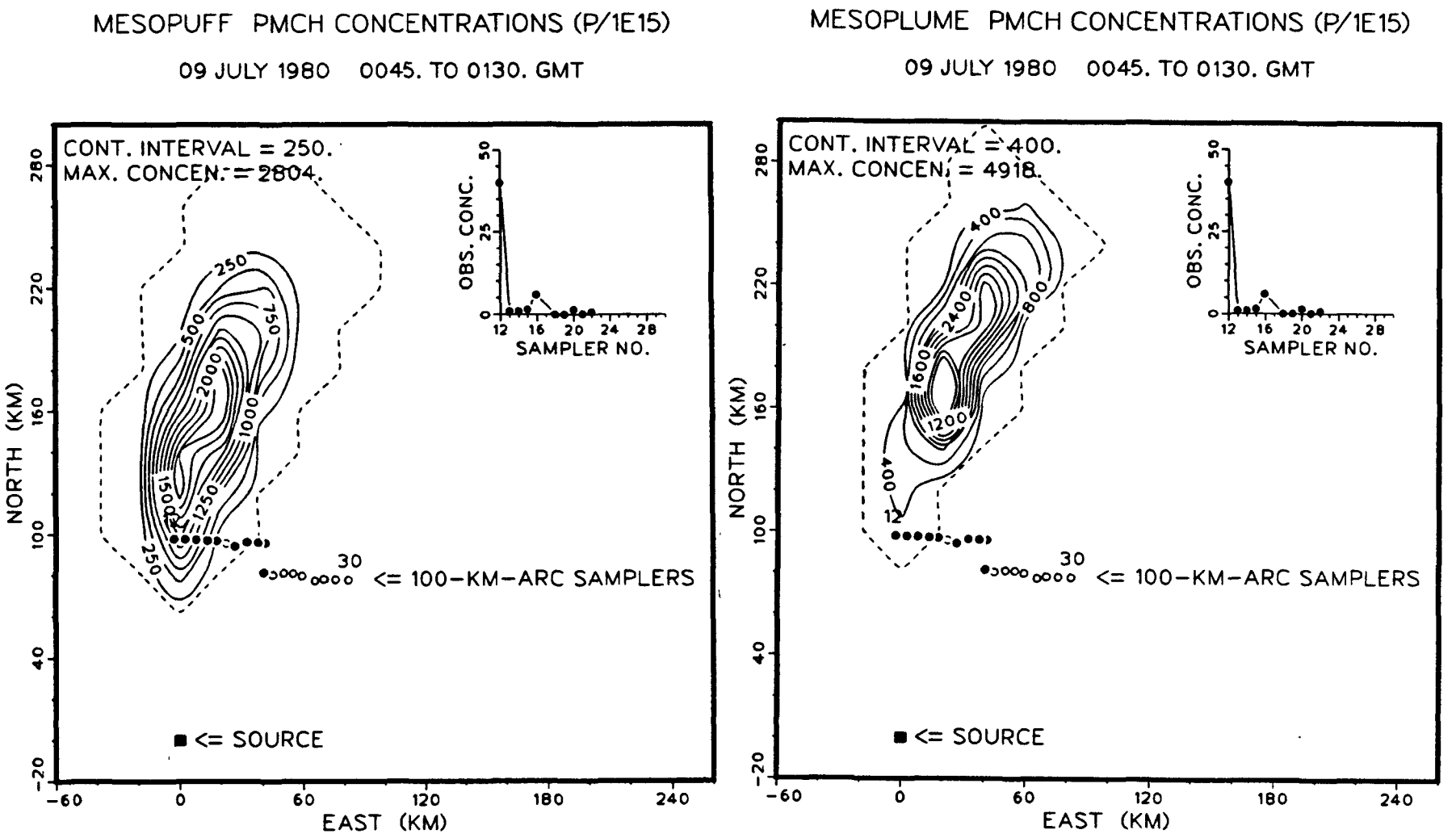

Figure E-32. Isopleth plot of ground-level concentrations for the Oklahoma experiment of July 9, 1980 (0045 to 0130 GMT) ... (left) MESOPUFF predictions, (right) MESOPLUME predictions.

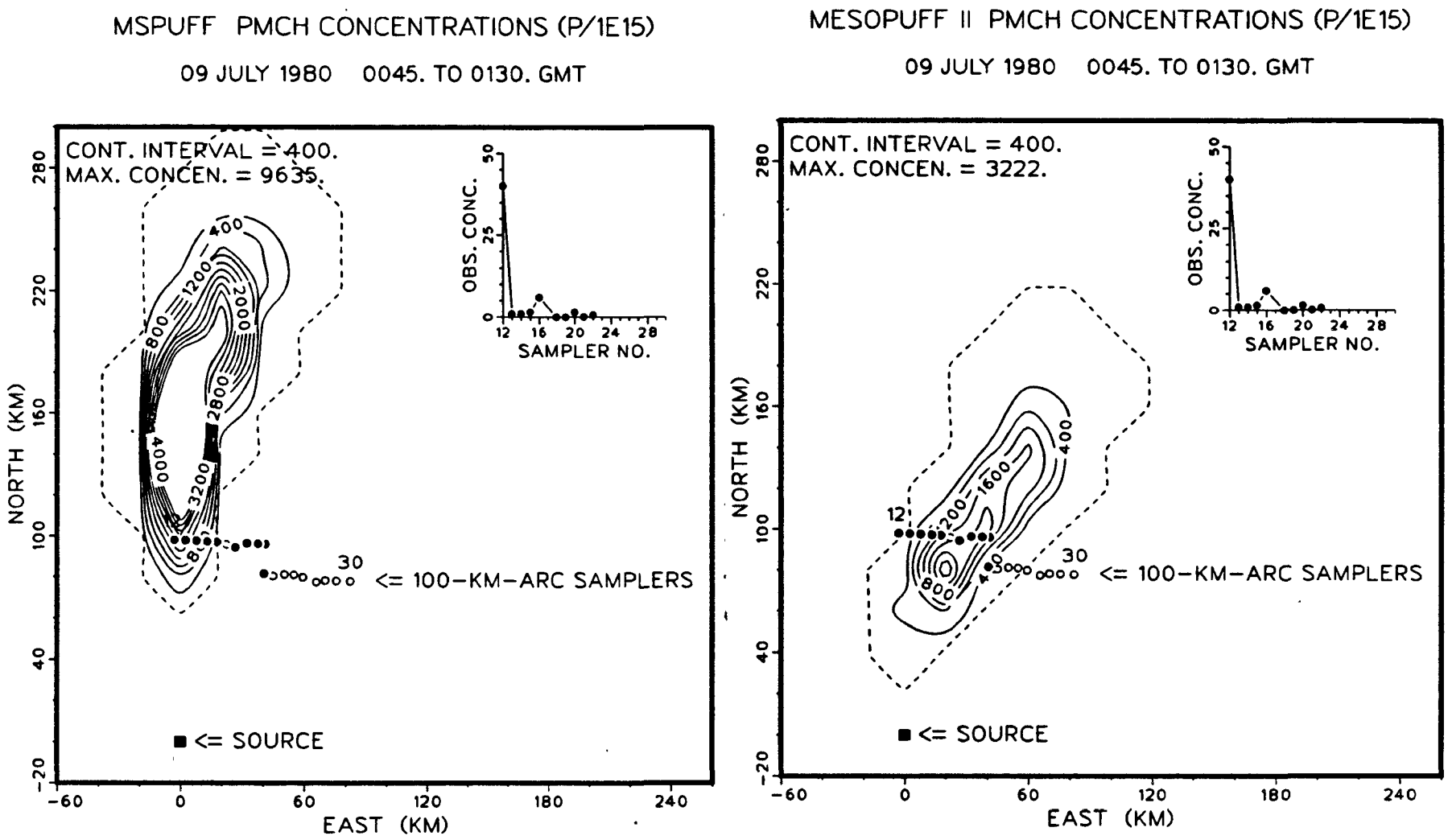

Figure E-33. Isopleth plot of ground-level concentrations for the Oklahoma experiment of July 9, 1980 (0045 to 0130 GMT) ... (left) MSPUFF predictions, (right) MESOPUFF II predictions.

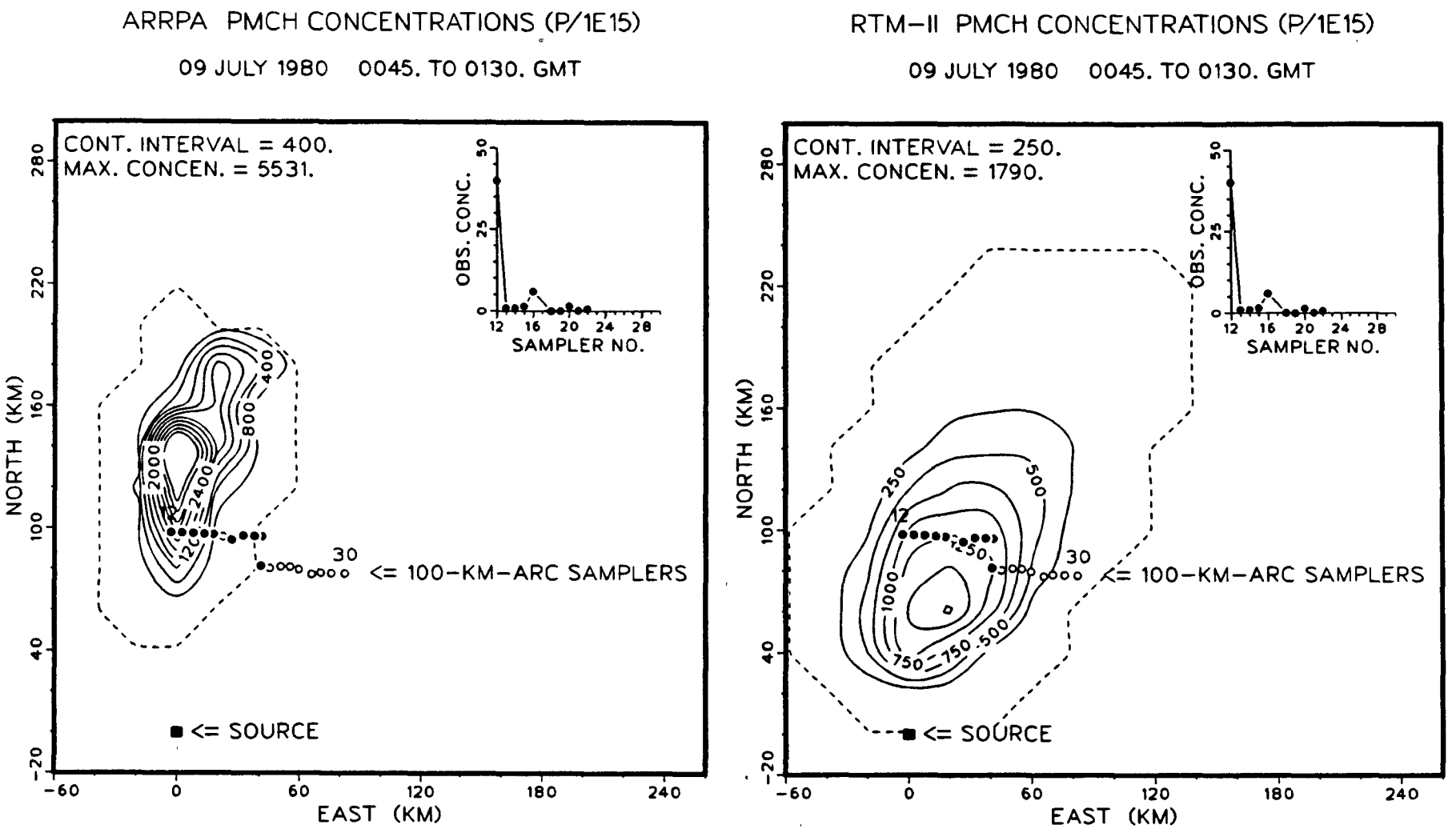

Figure E-34. Isopleth plot of ground-level concentrations for the Oklahoma experiment of July 9, 1980 (0045 to 0130 GMT) ... (left) ARRPA predictions, (right) RTM-II predictions.

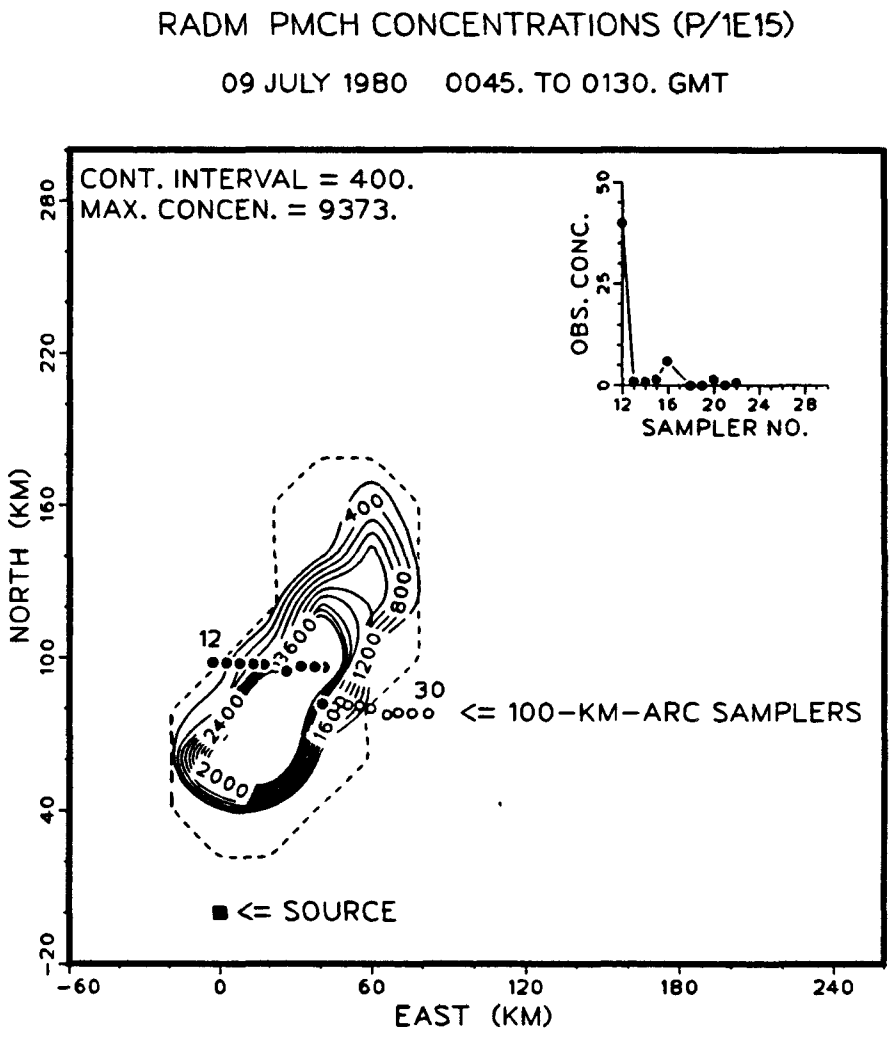

Figure E-35. Isopleth plot of ground-level concentrations for the Oklahoma experiment of July 9, 1980 (0045 to 0130 GMT) ... RADM predictions.

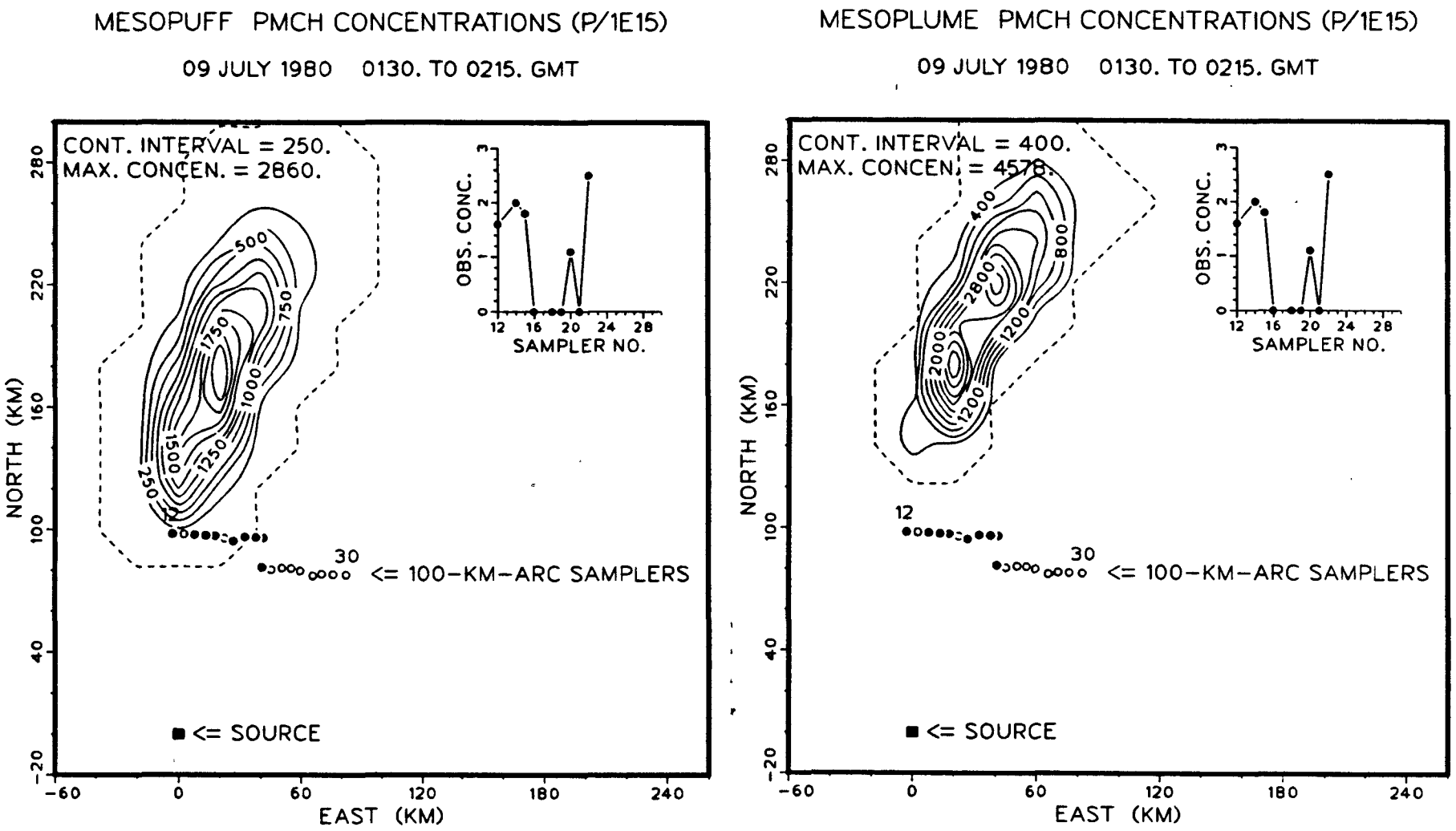

Figure E-36. Isopleth plot of ground-level concentrations for the Oklahoma experiment of July 9, 1980 (0130 to 0215 GMT) ... (left) MESOPUFF predictions, (right) MESOPLUME predictions.

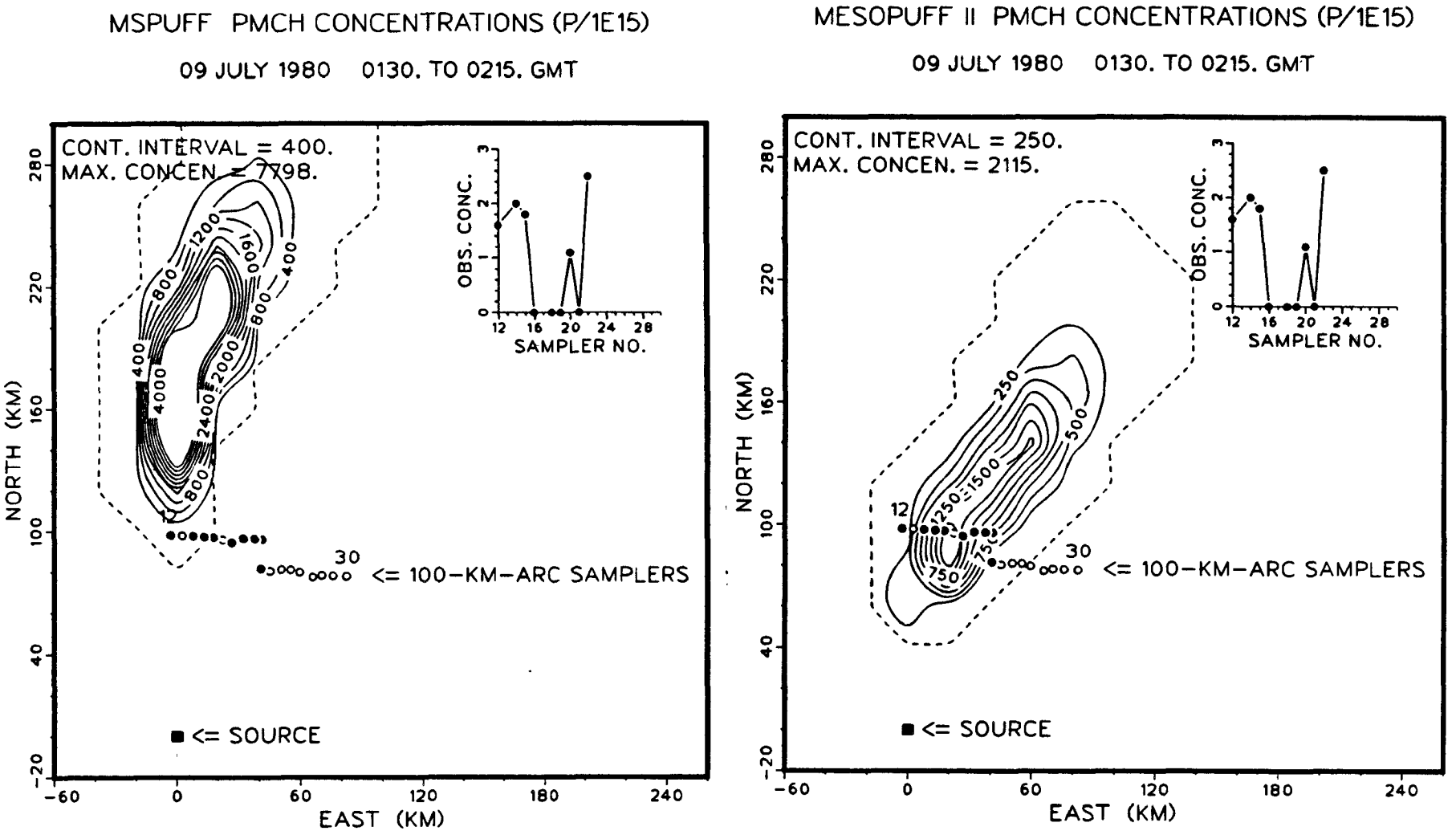

Figure E-37. Isopleth plot of ground-level concentrations for the Oklahoma experiment of July 9, 1980 (0130 to 0215 GMT) ... (left) MSPUFF predictions, (right) MESOPUFF II predictions.

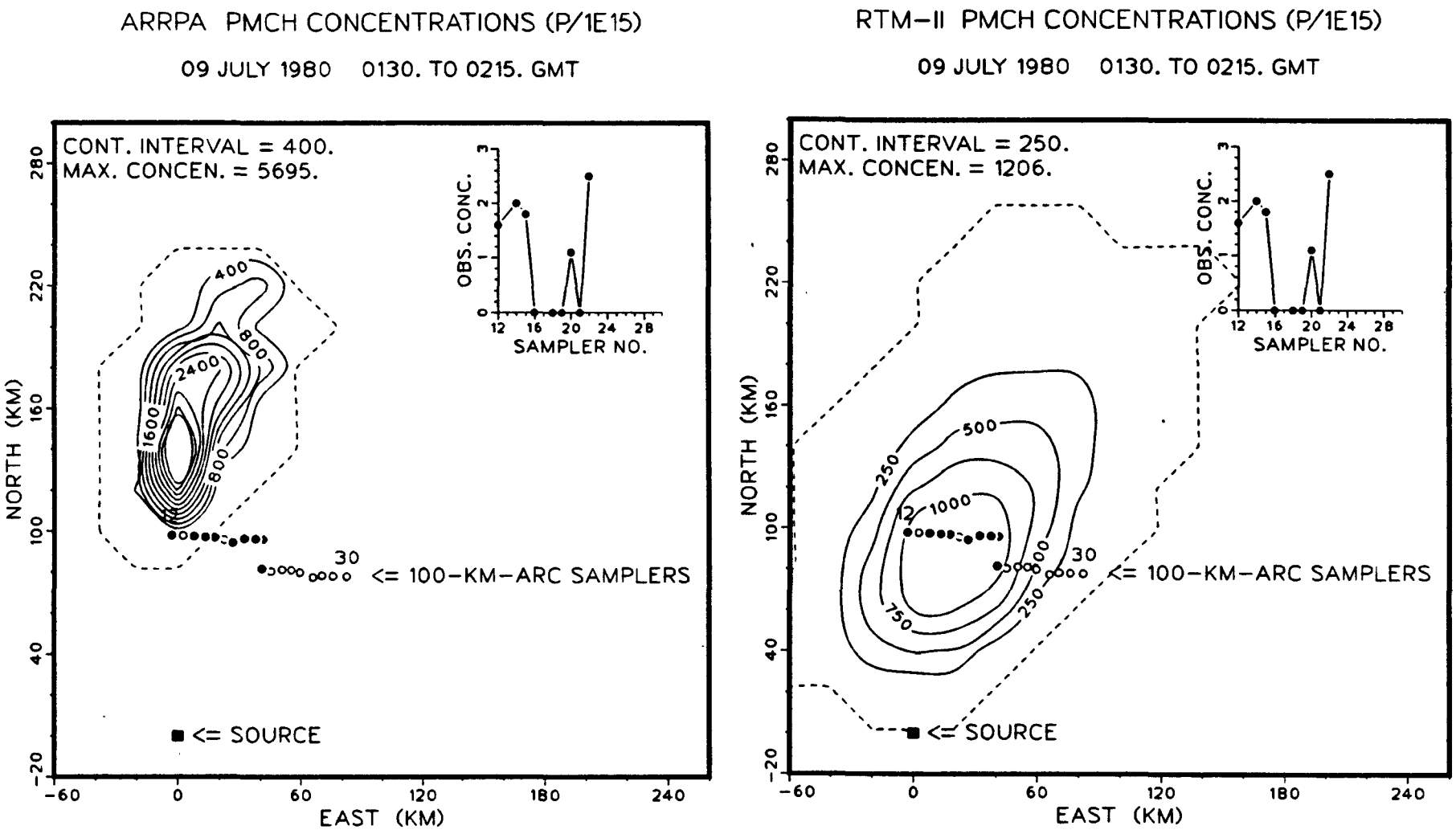

Figure E-38. Isopleth plot of ground-level concentrations for the Oklahoma experiment of July 9, 1980 (0130 to 0215 GMT) ... (left) ARRPA predictions, (right) RTM-II predictions.

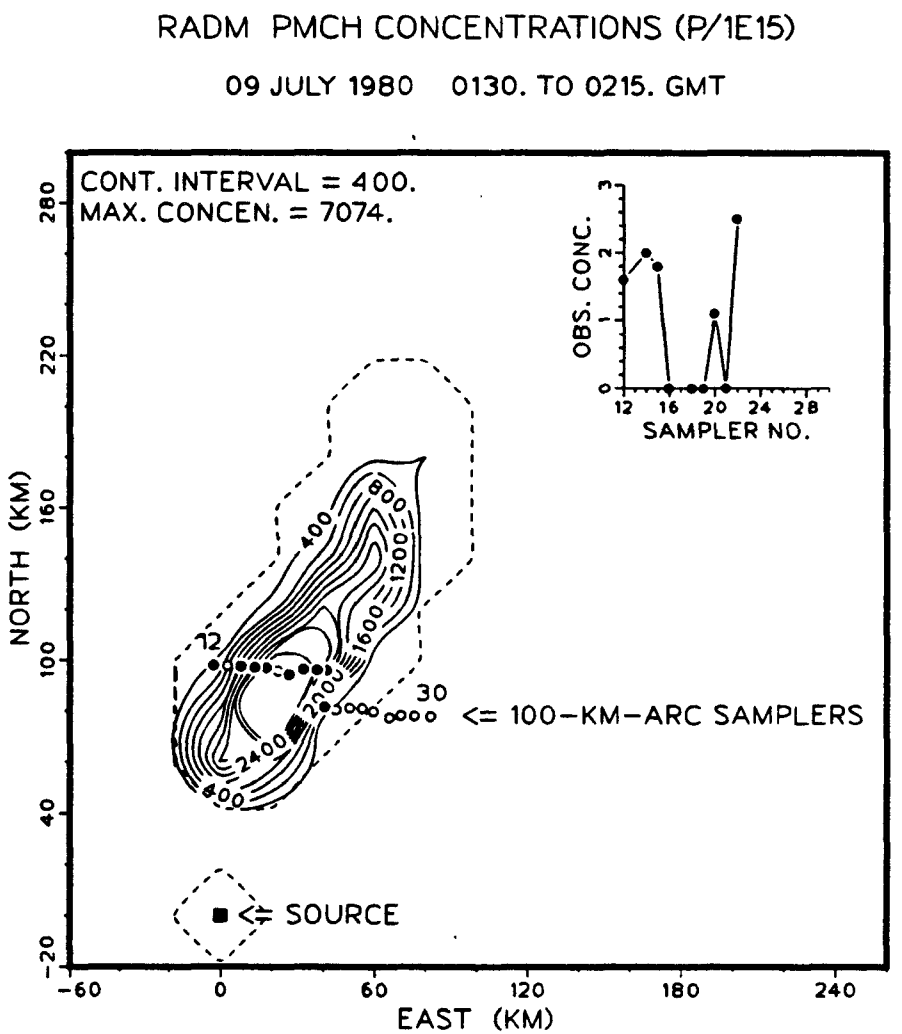

Figure E-39. Isopleth plot of ground-level concentrations for the Oklahoma experiment of July 9, 1980 (0130 to 0215 GMT) ... RADM predictions.

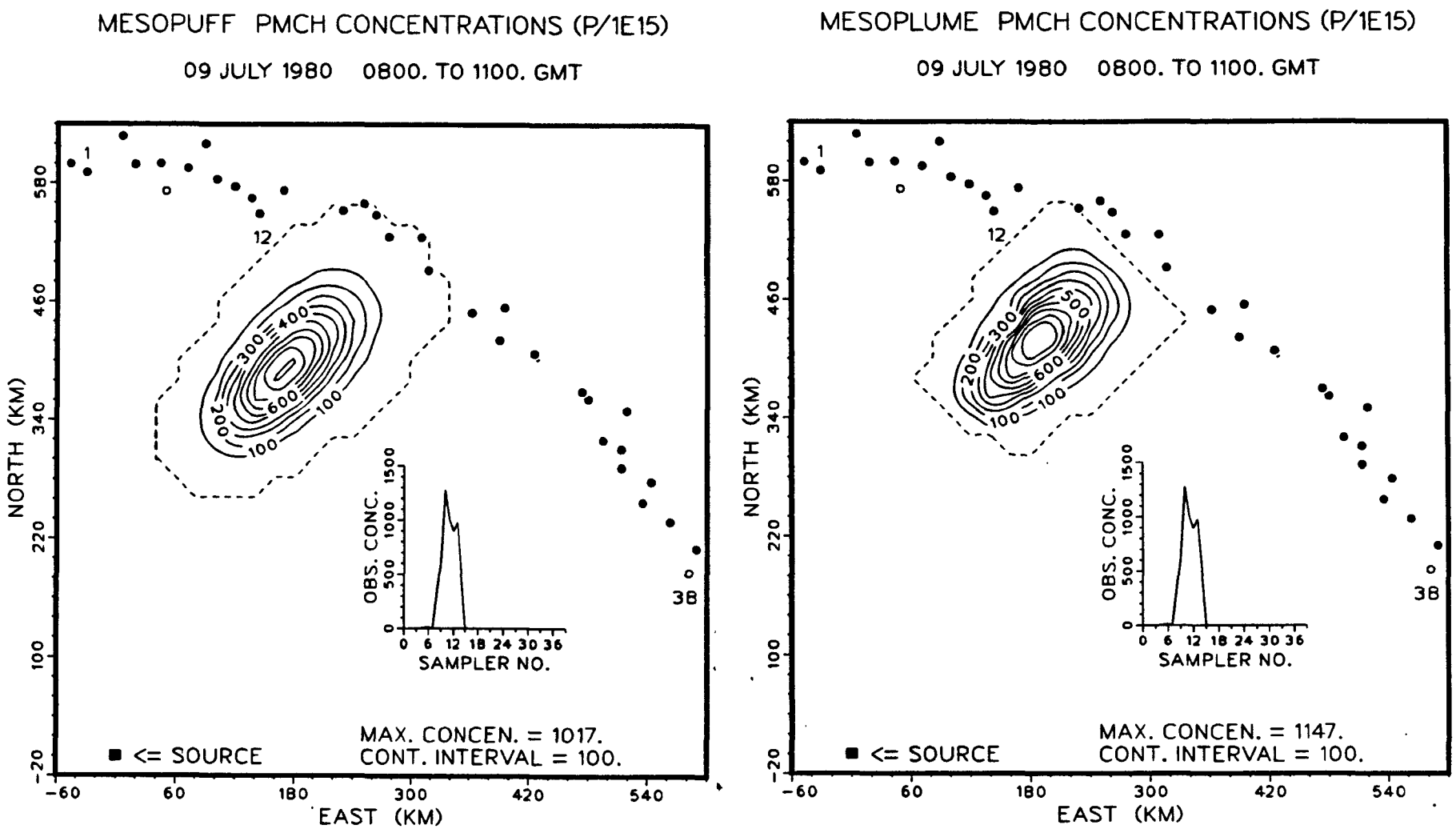

Figure E-40. Isopleth plot of ground-level concentrations for the Oklahoma experiment of July 9, 1980 (0800 to 1100 GMT) ... (left) MESOPUFF predictions, (right) MESOPLUME predictions.

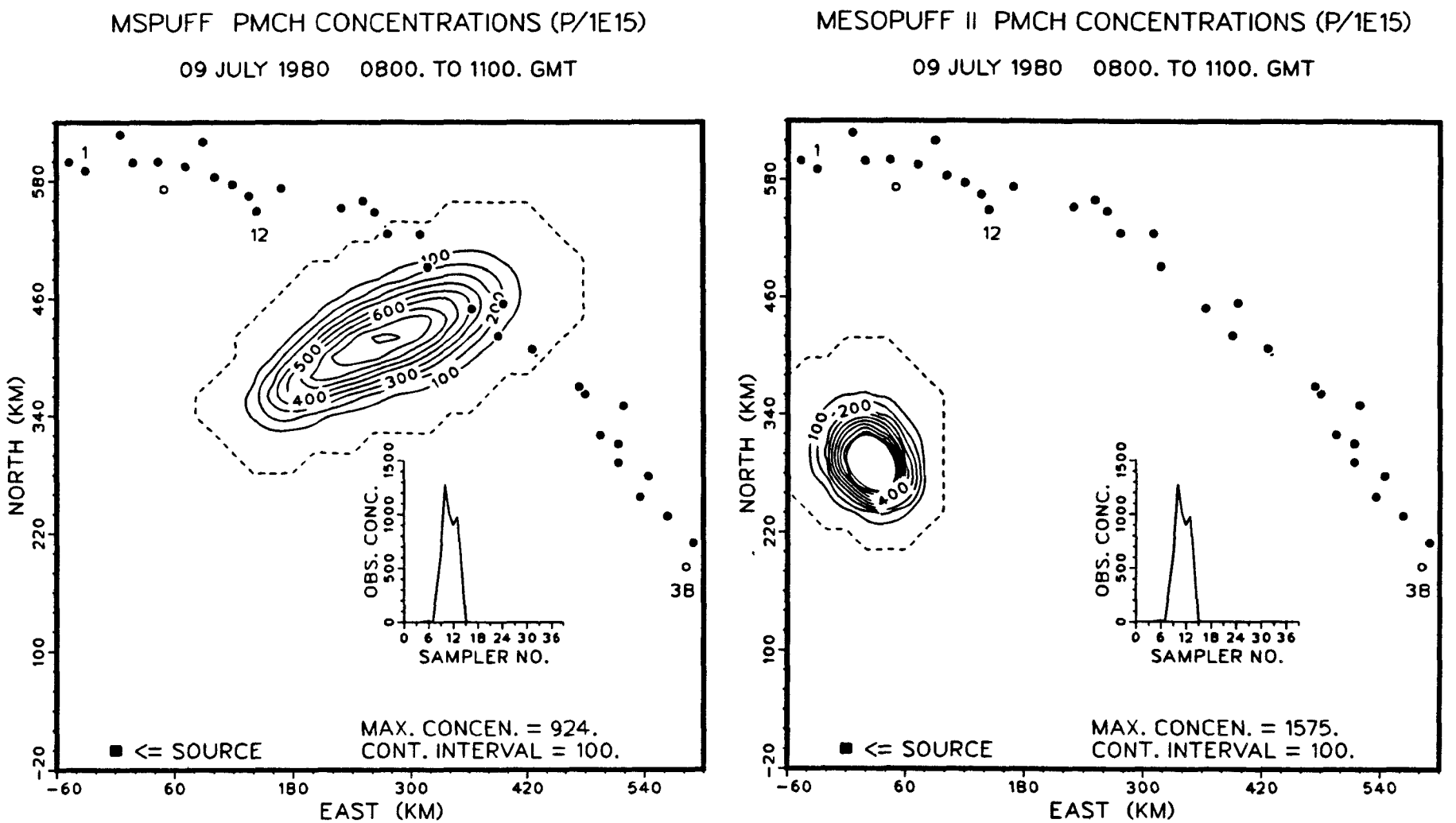

Figure E-41. Isopleth plot of ground-level concentrations for the Oklahoma experiment of July 9, 1980 (0800 to 1100 GMT) ... (left) MSPUFF predictions, (right) MESOPUFF II predictions.

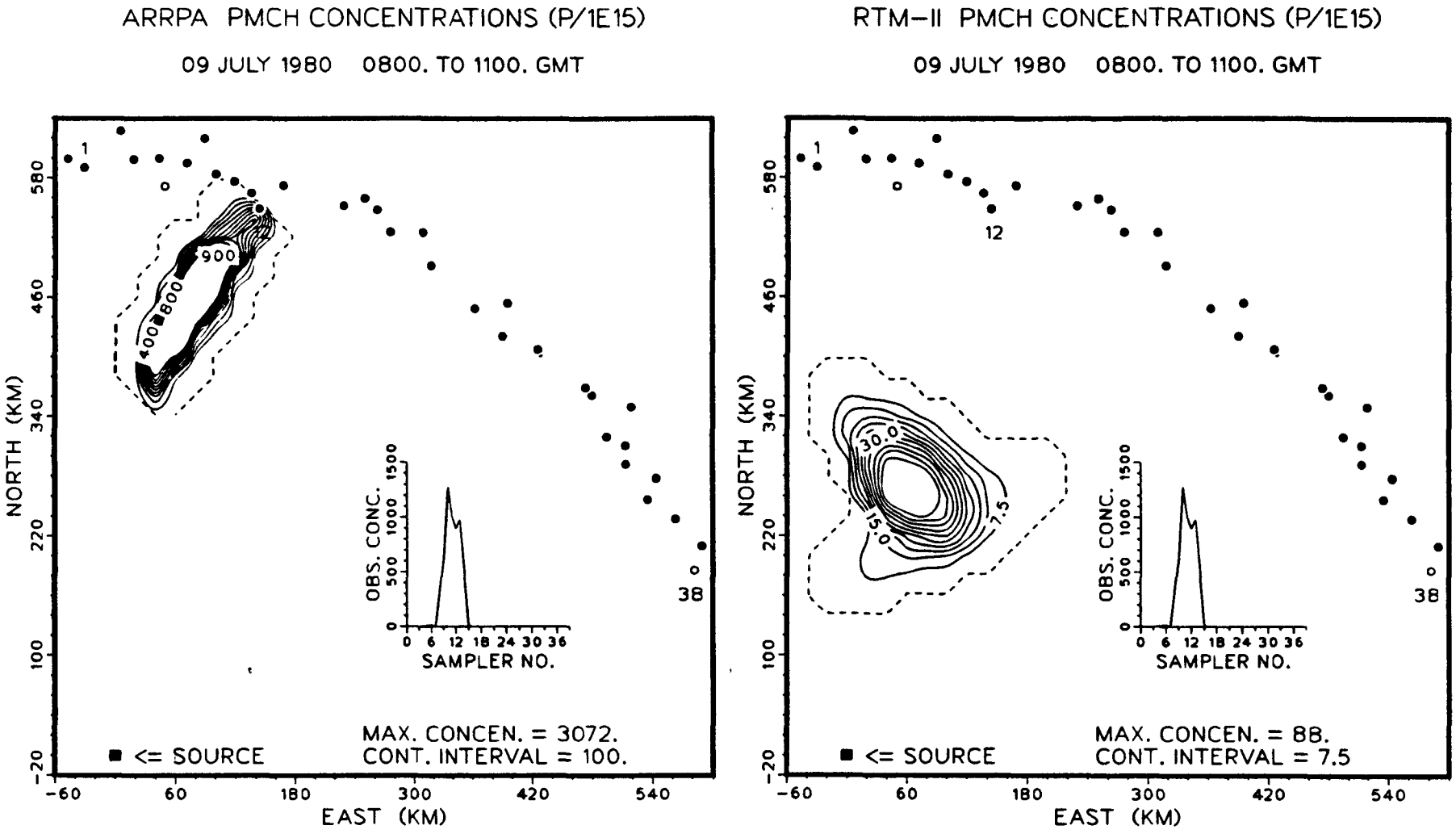

Figure E-42. Isopleth plot of ground-level concentrations for the Oklahoma experiment of July 9, 1980 (0800 to 1100 GMT) ... (left) ARRPA predictions, (right) RTM-II predictions.

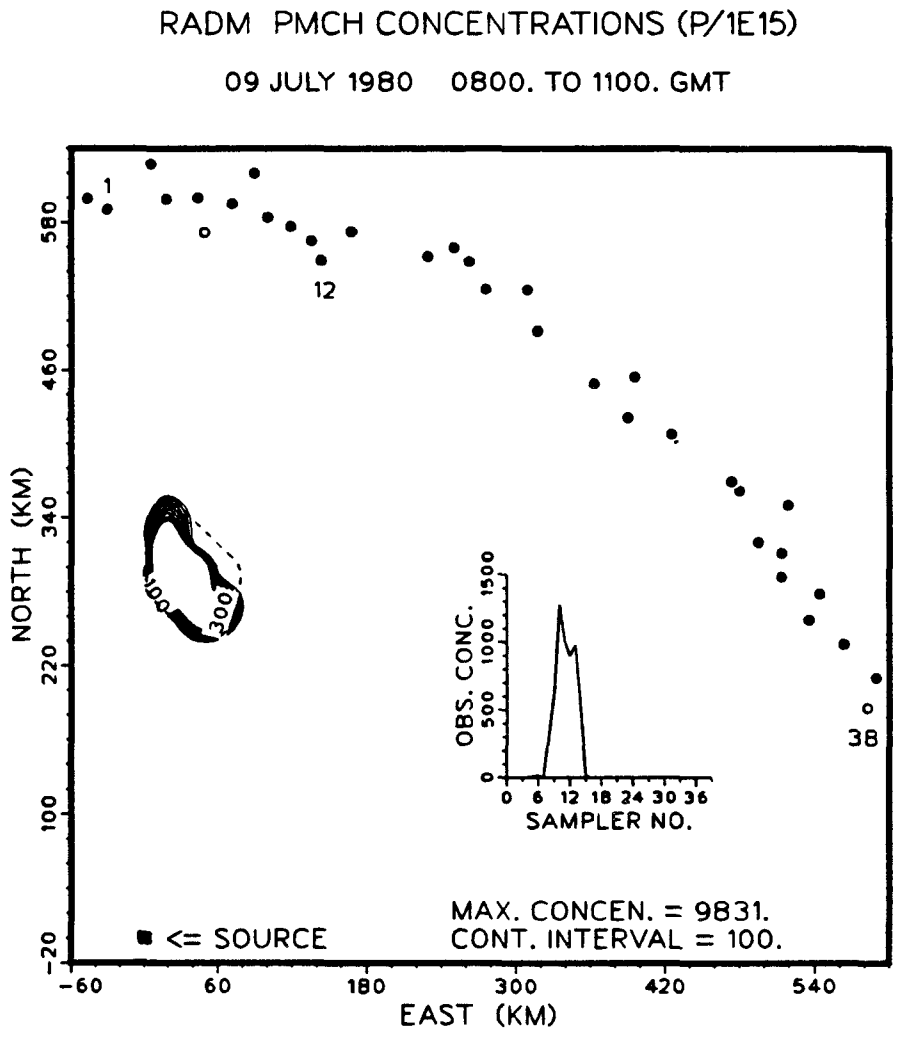

Figure E-43. Isopleth plot of ground-level concentrations for the Oklahoma experiment of July 9, 1980 (0800 to 1100 GMT) ... RADM predictions.

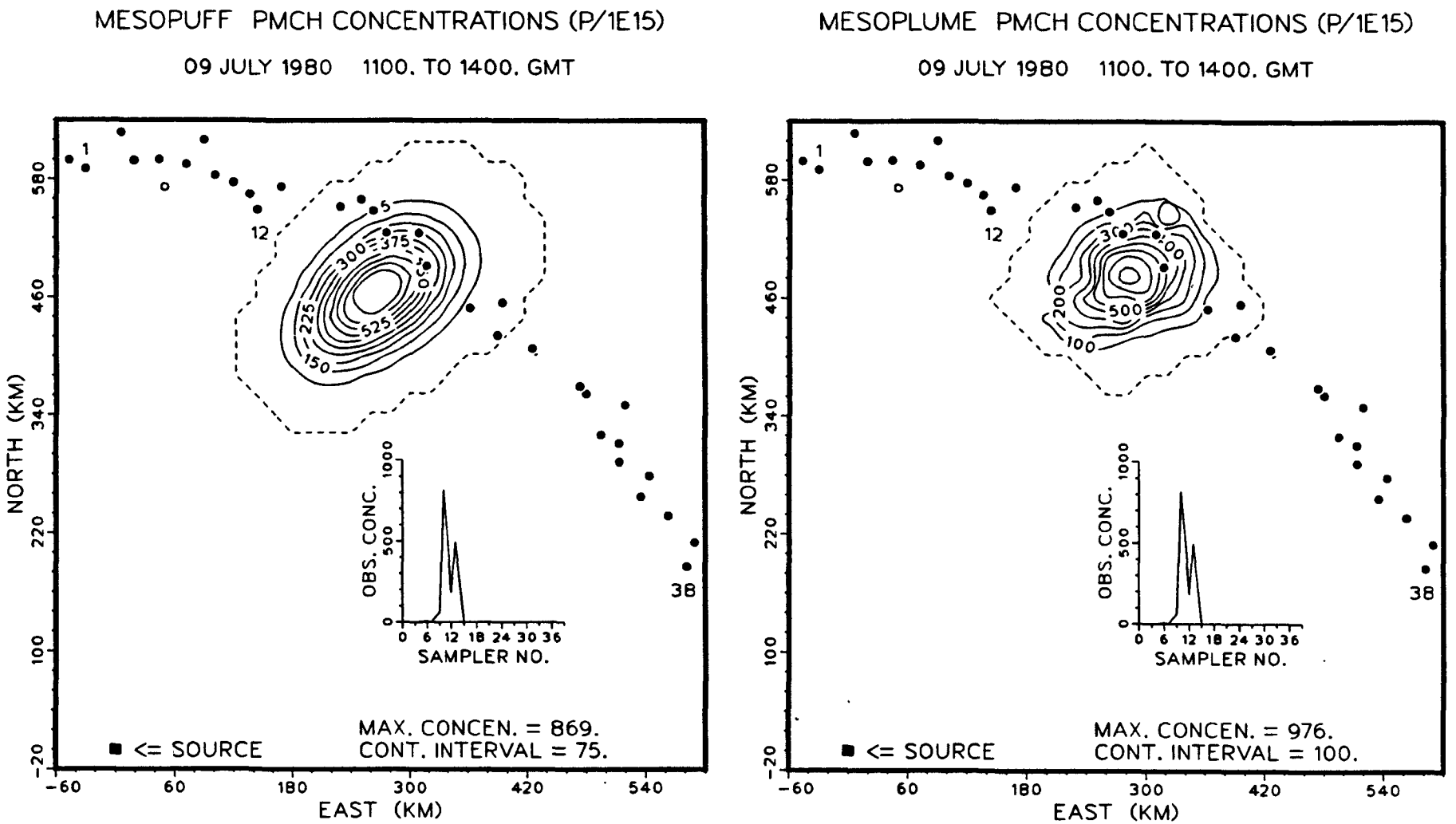

Figure E-44. Isopleth plot of ground-level concentrations for the Oklahoma experiment of July 9, 1980 (1100 to 1400 GMT) ... (left) MESOPUFF predictions, (right) MESOPLUME predictions.

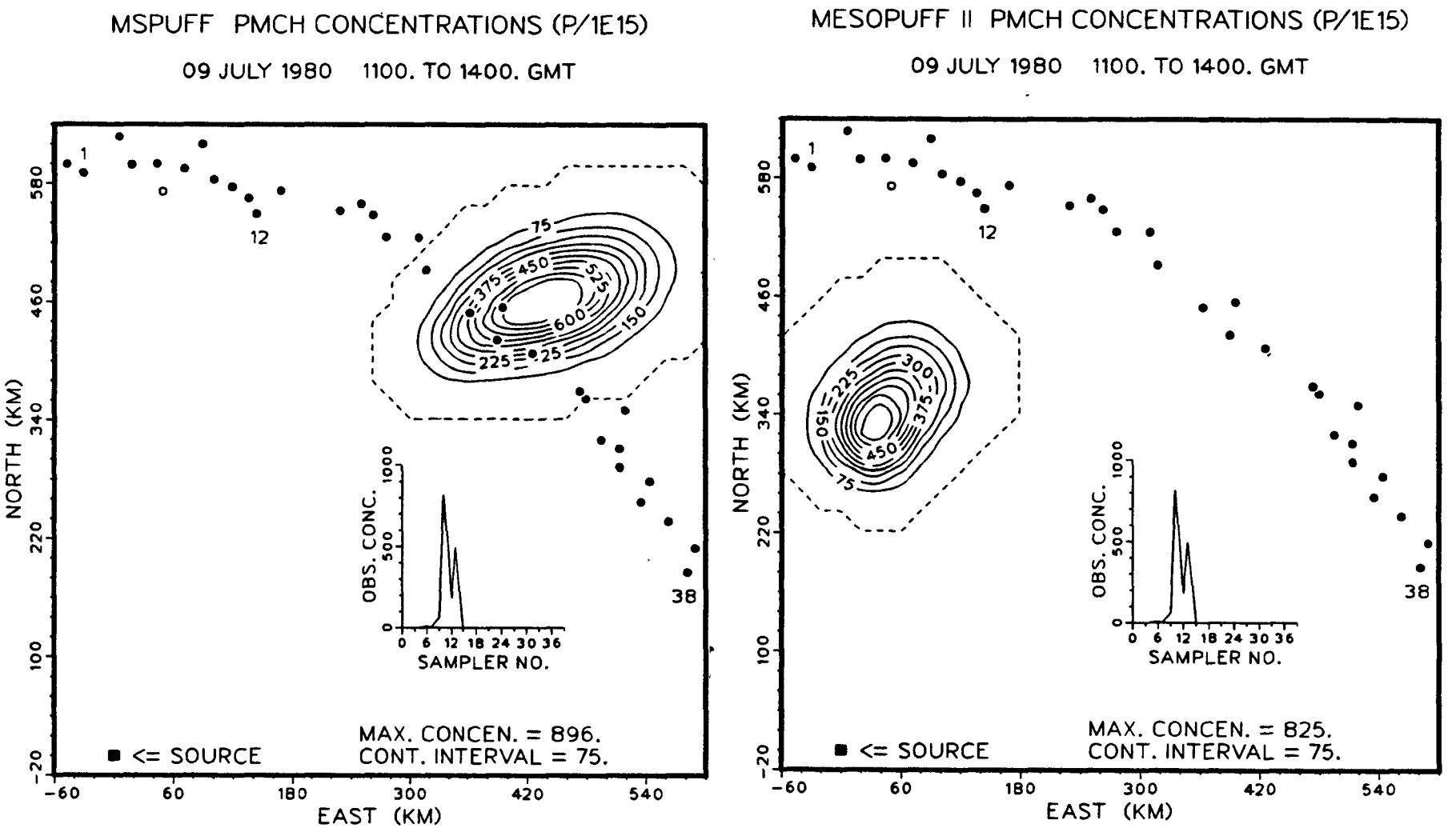

Figure E-45. Isopleth plot of ground-level concentrations for the Oklahoma experiment of July 9, 1980 (1100 to 1400 GMT) ... (left) MSPUFF predictions, (right) MESOPUFF II predictions.

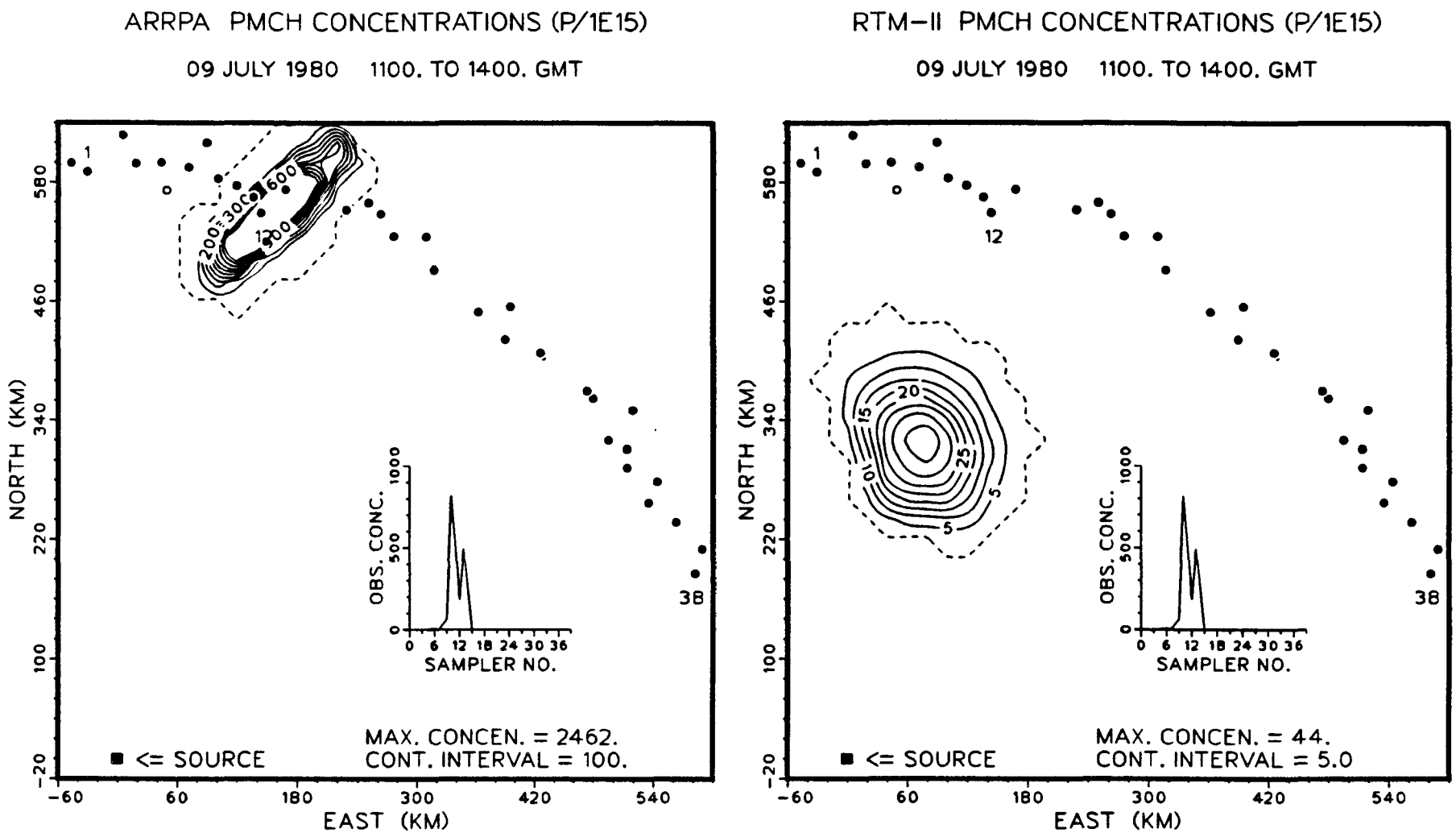

Figure E-46. Isopleth plot of ground-level concentrations for the Oklahoma experiment of July 9, 1980 (1100 to 1400 GMT) ... (left) ARRPA predictions, (right) RTM-II predictions.

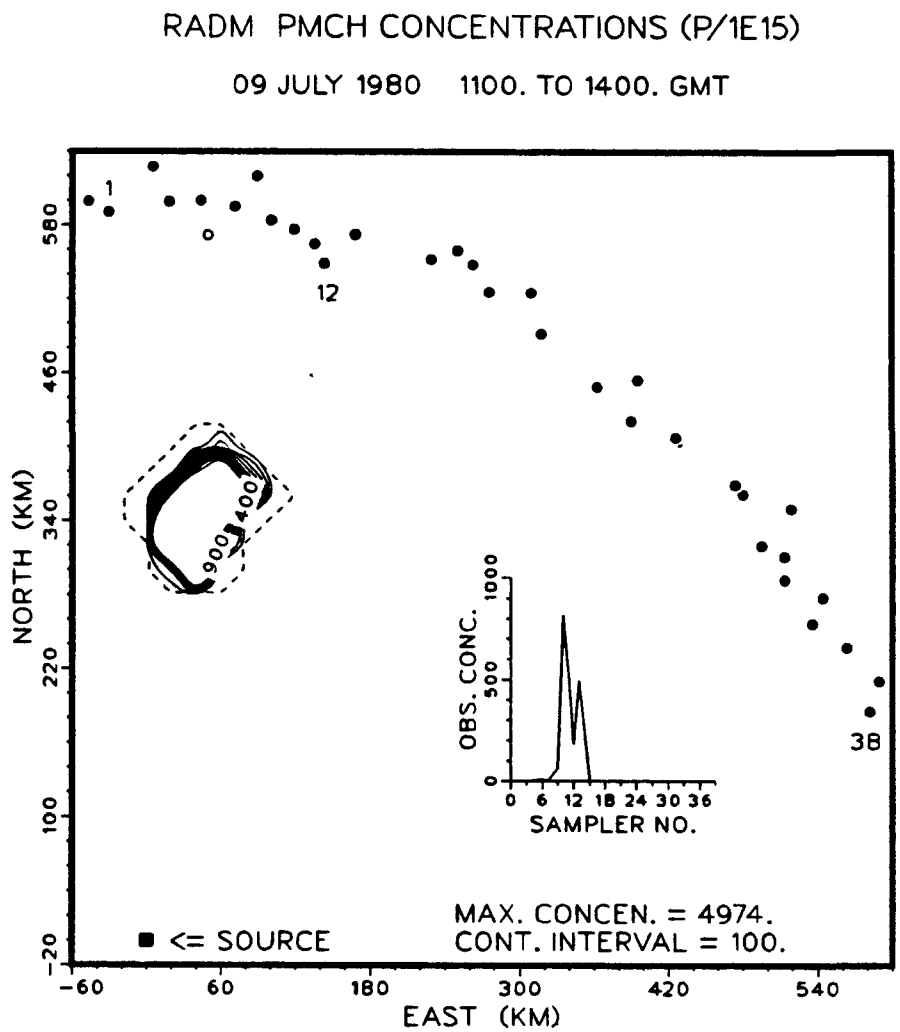

Figure E-47. Isopleth plot of ground-level concentrations for the Oklahoma experiment of July 9, 1980 (1100 to 1400 GMT) ... RADM predictions.

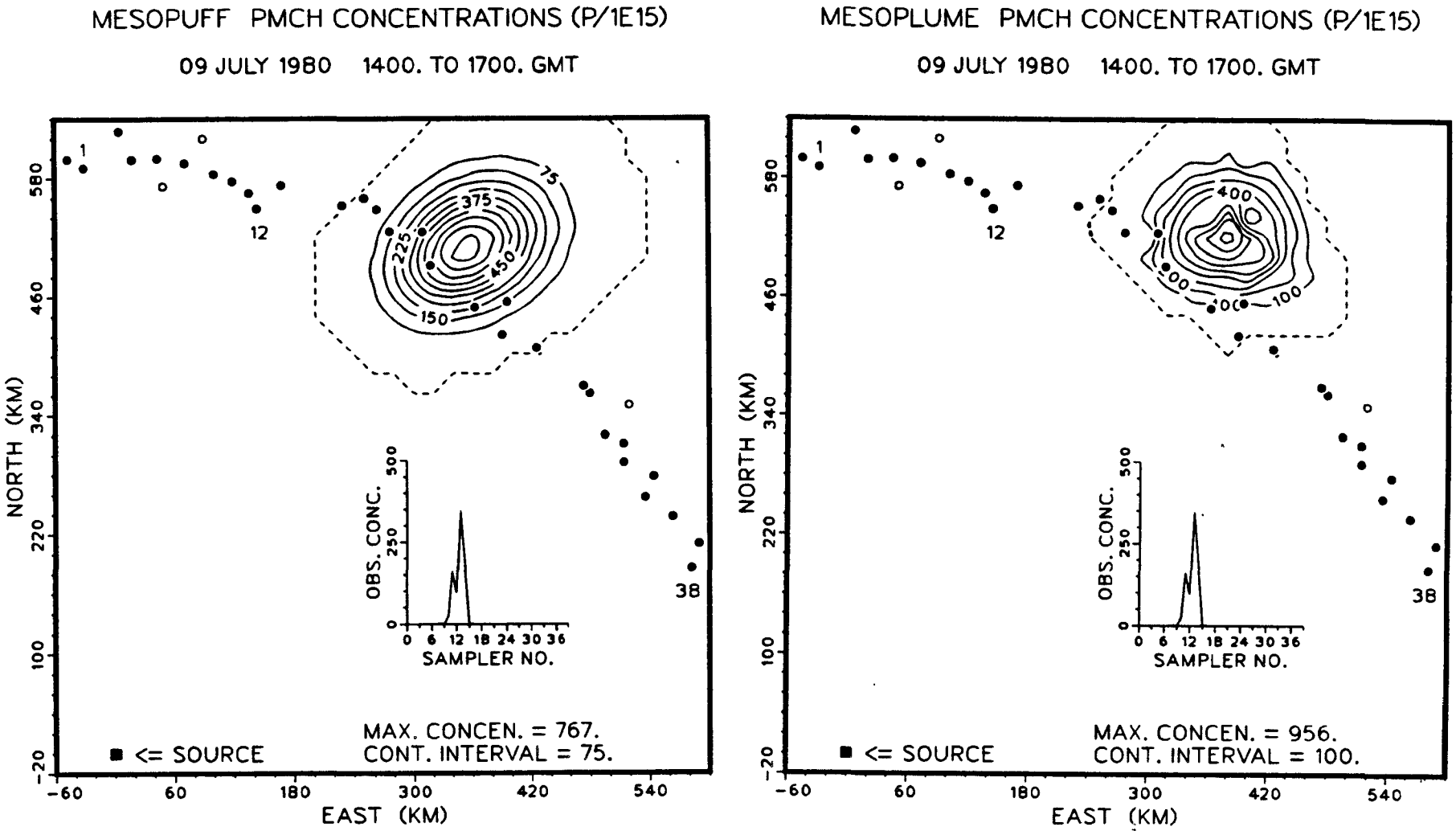

Figure E-48. Isopleth plot of ground-level concentrations for the Oklahoma experiment of July 9, 1980 (1400 to 1700 GMT) ... (left) MESOPUFF predictions, (right) MESOPLUME predictions.

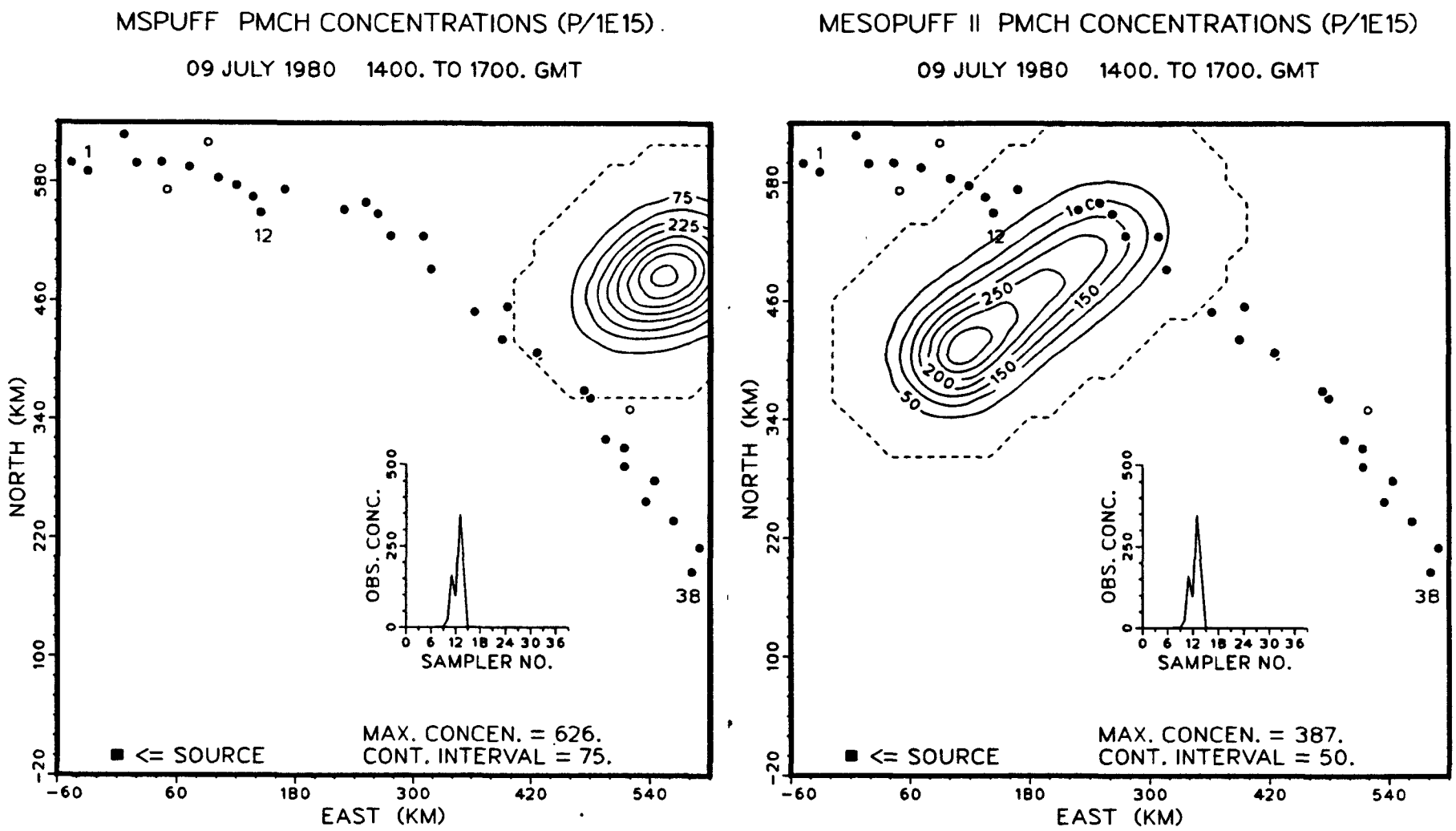

Figure E-49. Isopleth plot of ground-level concentrations for the Oklahoma experiment of July 9, 1980 (1400 to 1700 GMT) ... (left) MSPUFF predictions, (right) MESOPUFF II predictions.

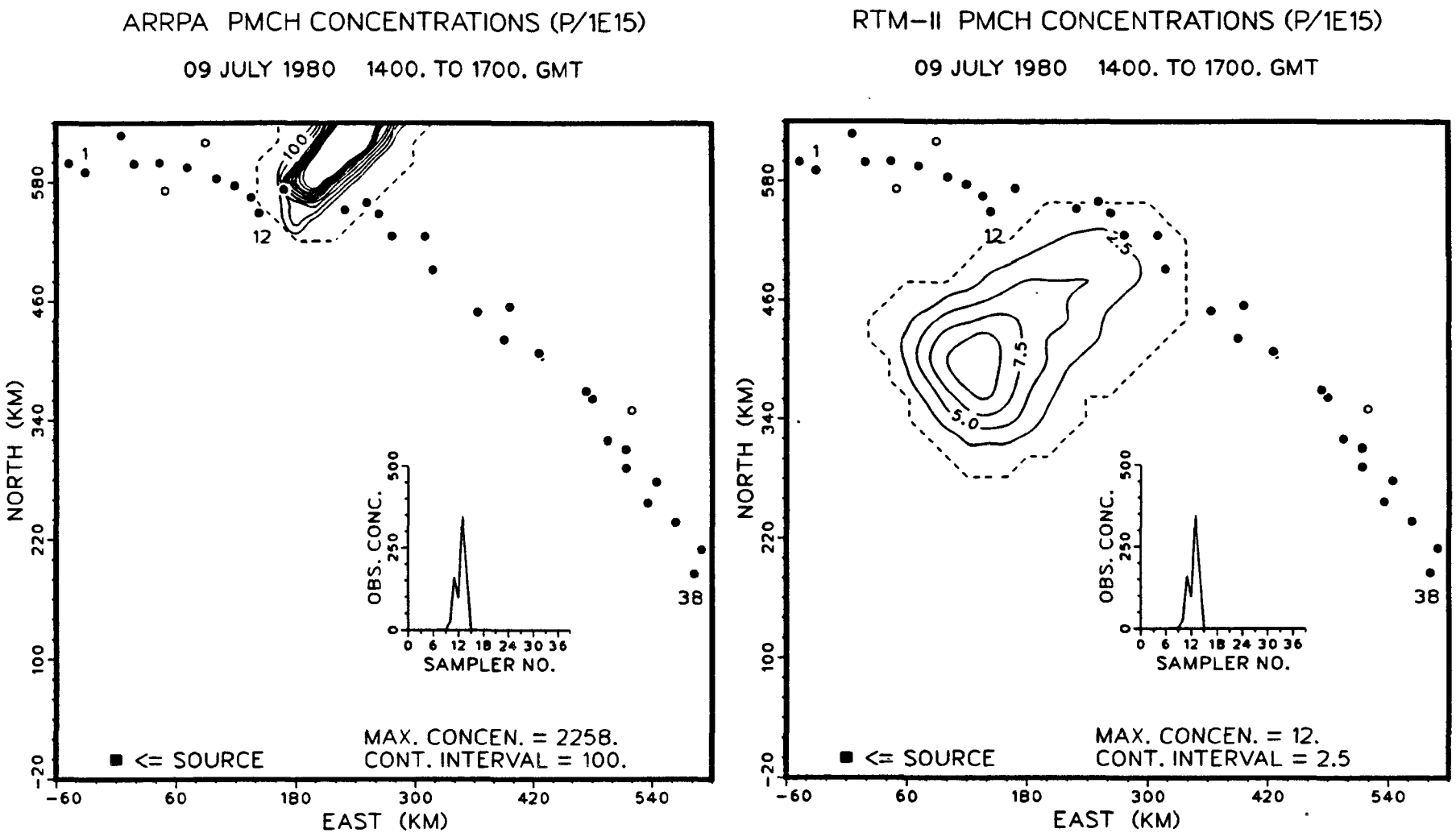

Figure E-50. Isopleth plot of ground-level concentrations for the Oklahoma experiment of July 9, 1980 (1400 to 1700 GMT) ... (left) ARRPA predictions, (right) RTM-II predictions.

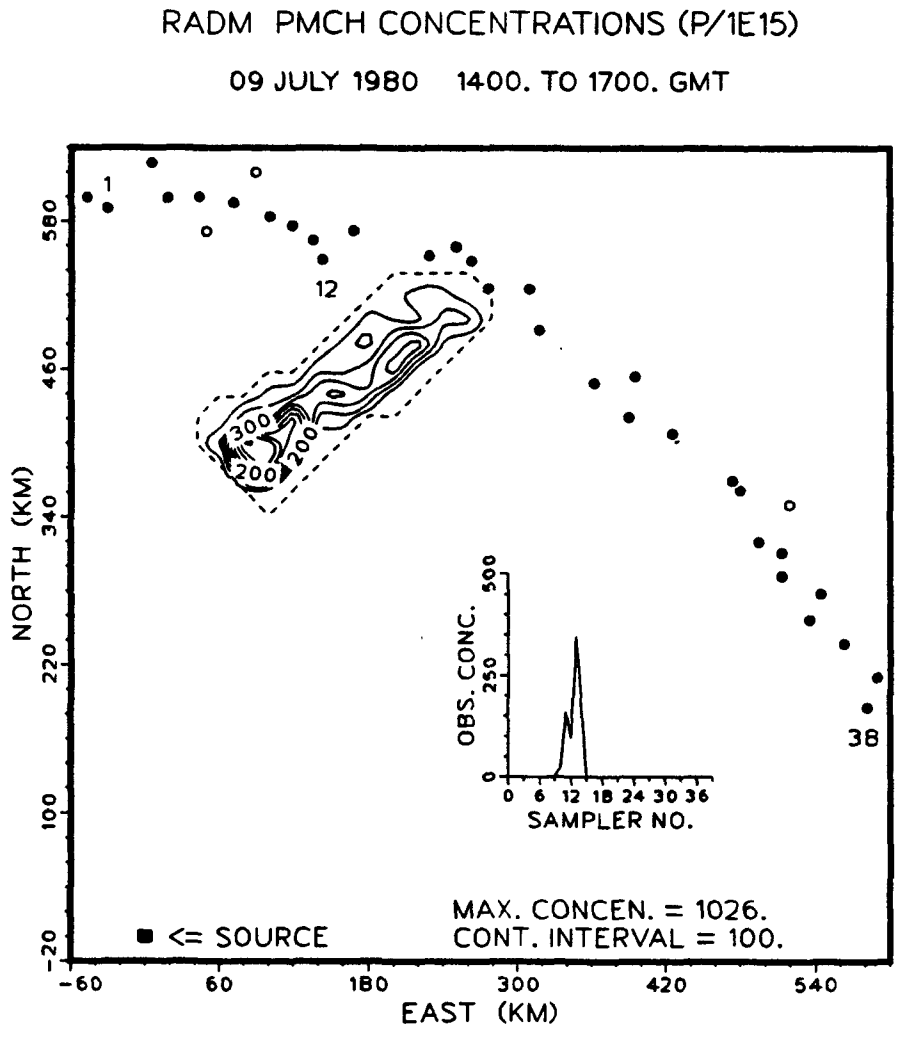

Figure E-51. Isopleth plot of ground-level concentrations for the Oklahoma experiment of July 9, 1980 (1400 to 1700 GMT) ... RADM predictions.

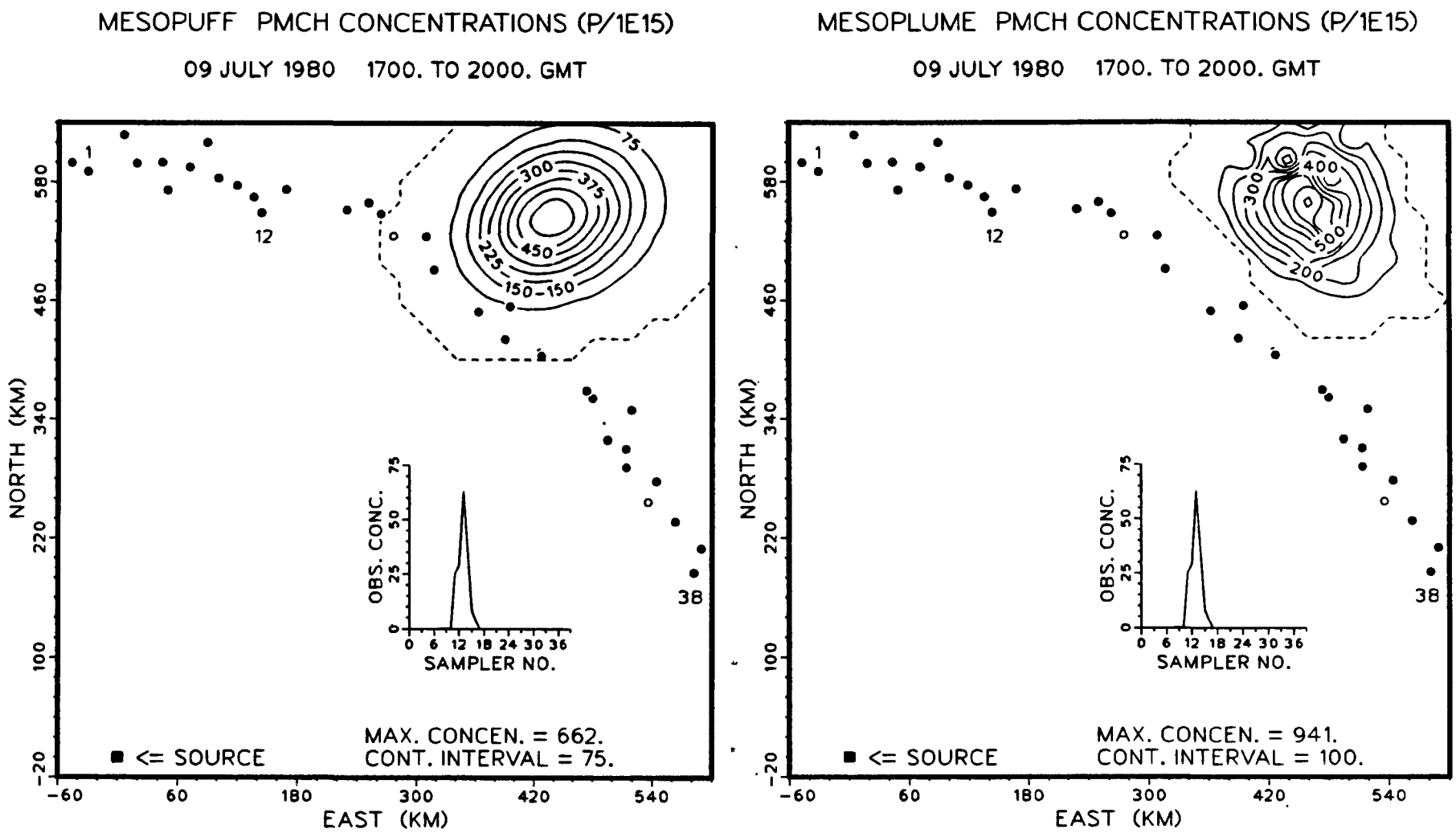

Figure E-52. Isopleth plot of ground-level concentrations for the Oklahoma experiment of July 9, 1980 (1700 to 2000 GMT) ... (left) MESOPUFF predictions, (right) MESOPLUME predictions.

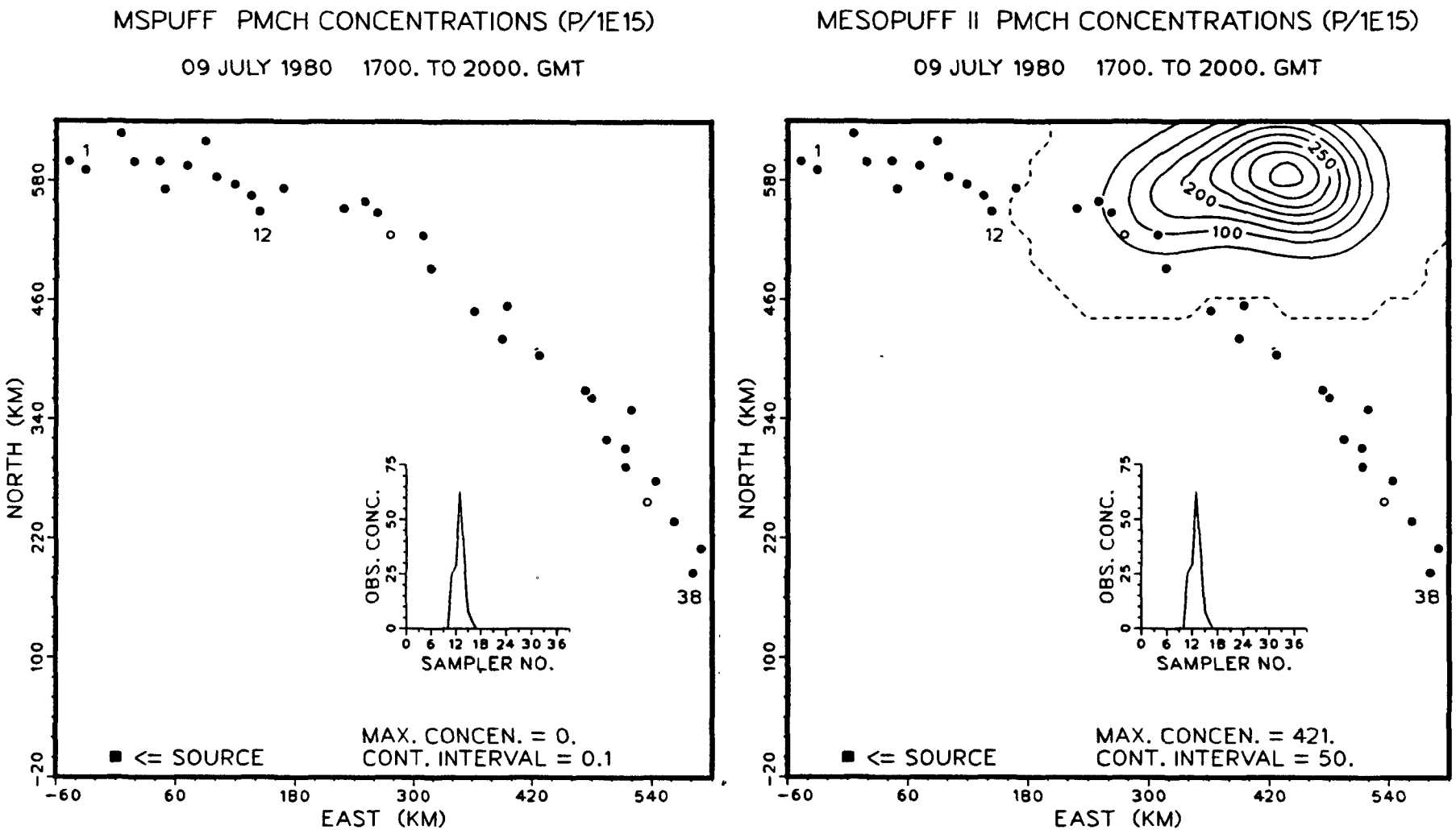

Figure E-53. Isopleth plot of ground-level concentrations for the Oklahoma experiment of July 9, 1980 (1700 to 2000 GMT) ... (left) MSPUFF predictions, (right) MESOPUFF II predictions.

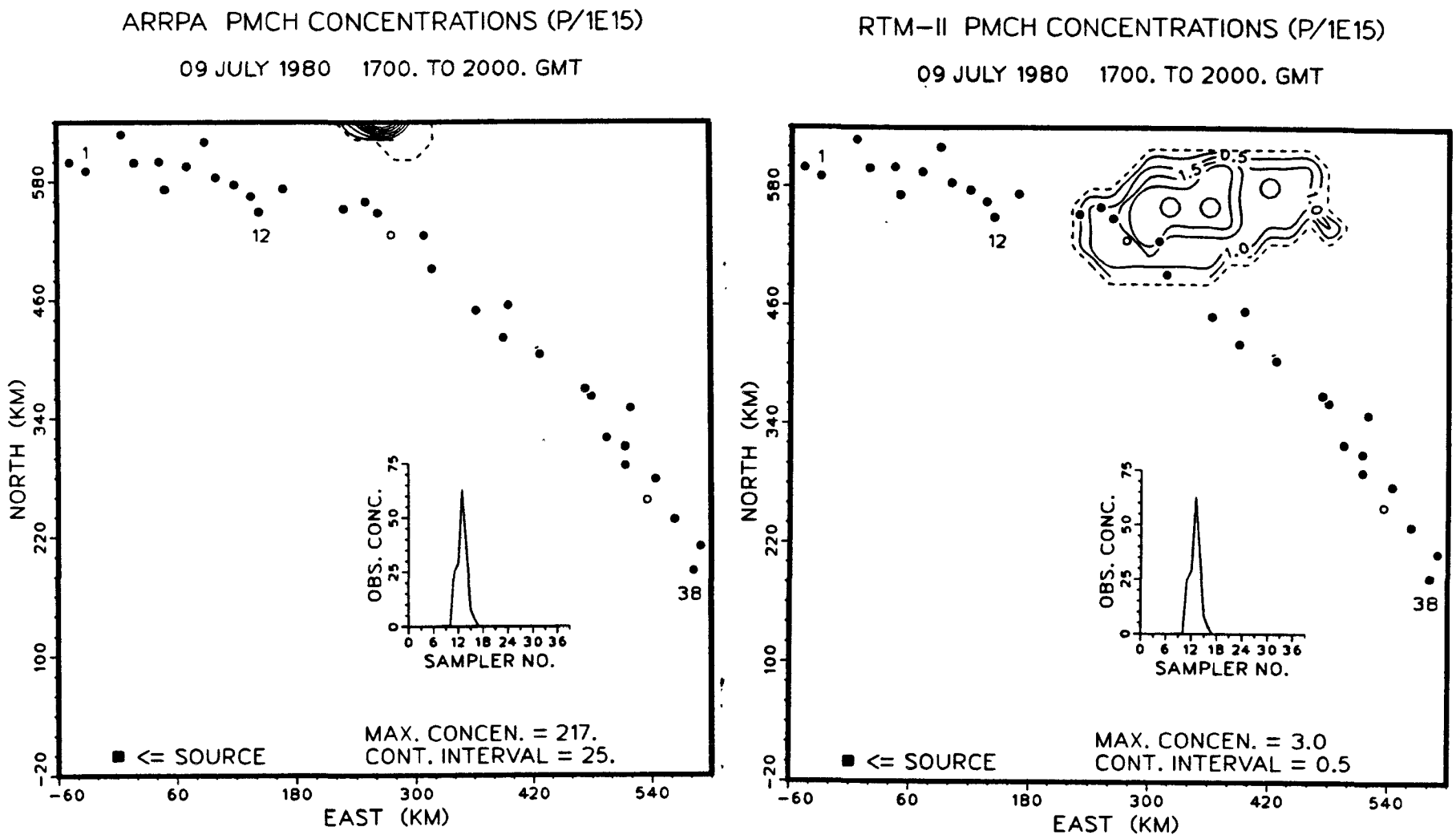

Figure E-54. Isopleth plot of ground-level concentrations for the Oklahoma experiment of July 9, 1980 (1700 to 2000 GMT) ... (left) ARRPA predictions, (right) RTM-II predictions.

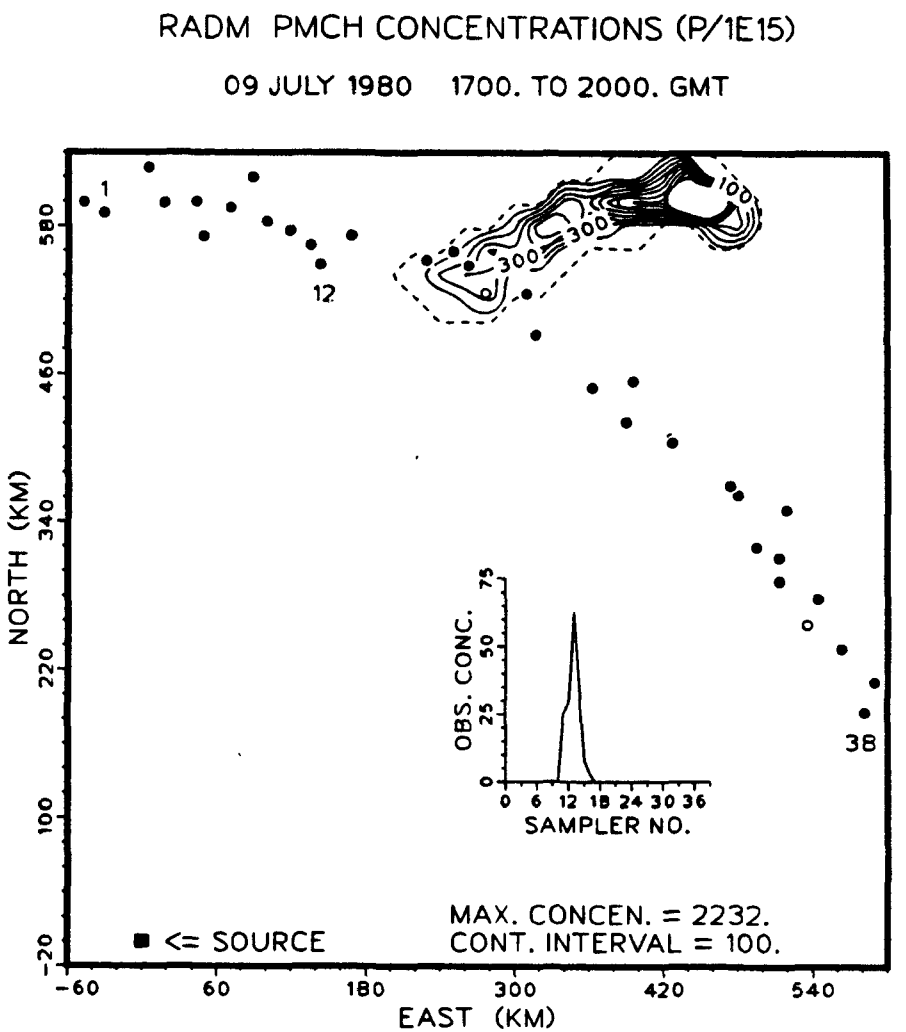

Figure E-55. Isopleth plot of ground-level concentrations for the Oklahoma experiment of July 9, 1980 (1700 to 2000 GMT) ... RADM predictions.

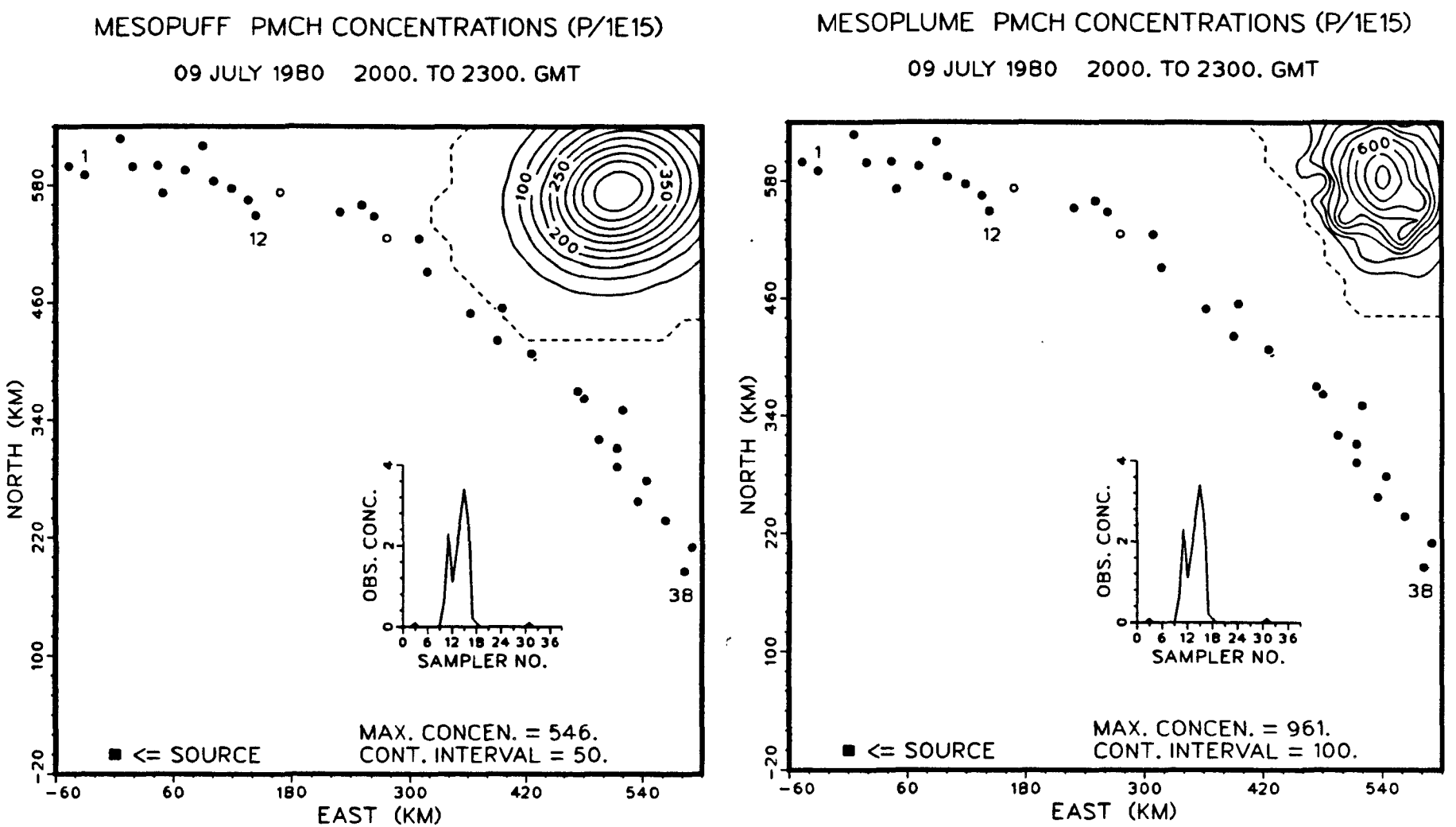

Figure E-56. Isopleth plot of ground-level concentrations for the Oklahoma experiment of July 9, 1980 (2000 to 2300 GMT) ... (left) MESOPUFF predictions, (right) MESOPLUME predictions.

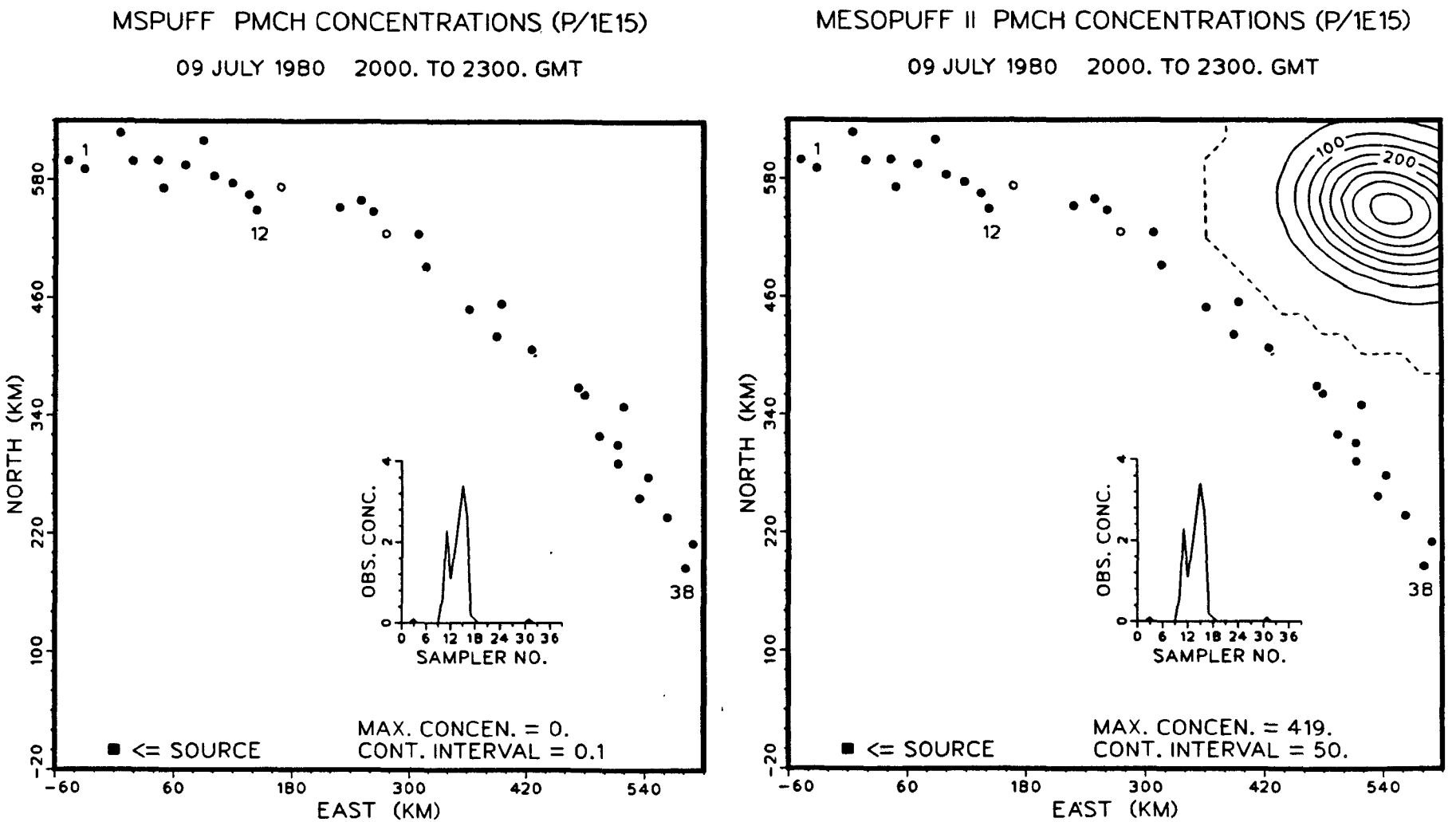

Figure E-57. Isopleth plot of ground-level concentrations for the Oklahoma experiment of July 9, 1980 (2000 to 2300 GMT) ... (left) MSPUFF predictions, (right) MESOPUFF II predictions.

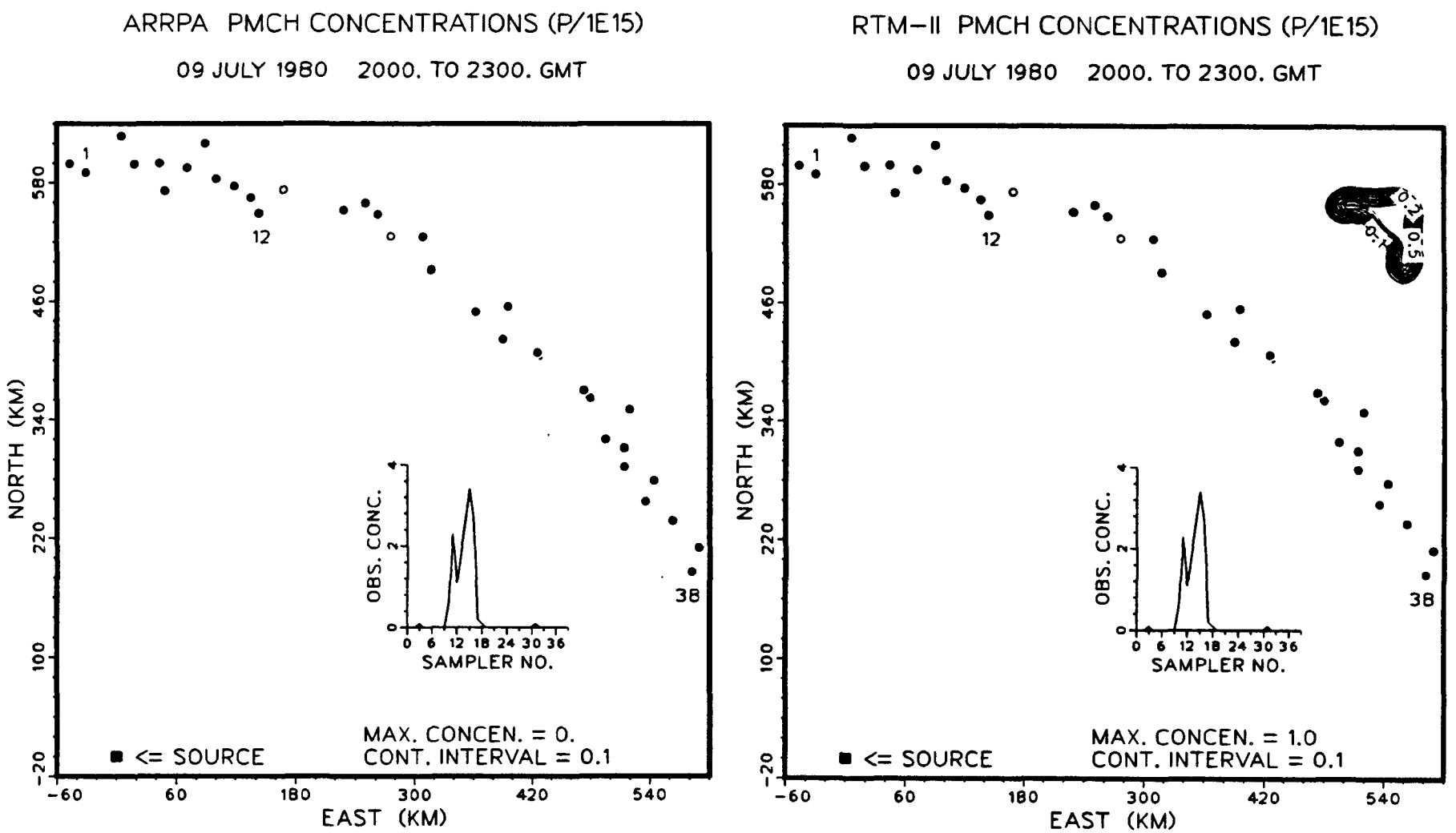

Figure E-58. Isopleth plot of ground-level concentrations for the Oklahoma experiment of July 9, 1980 (2000 to 2300 GMT) ... (left) ARRPA predictions, (right) RTM-II predictions.

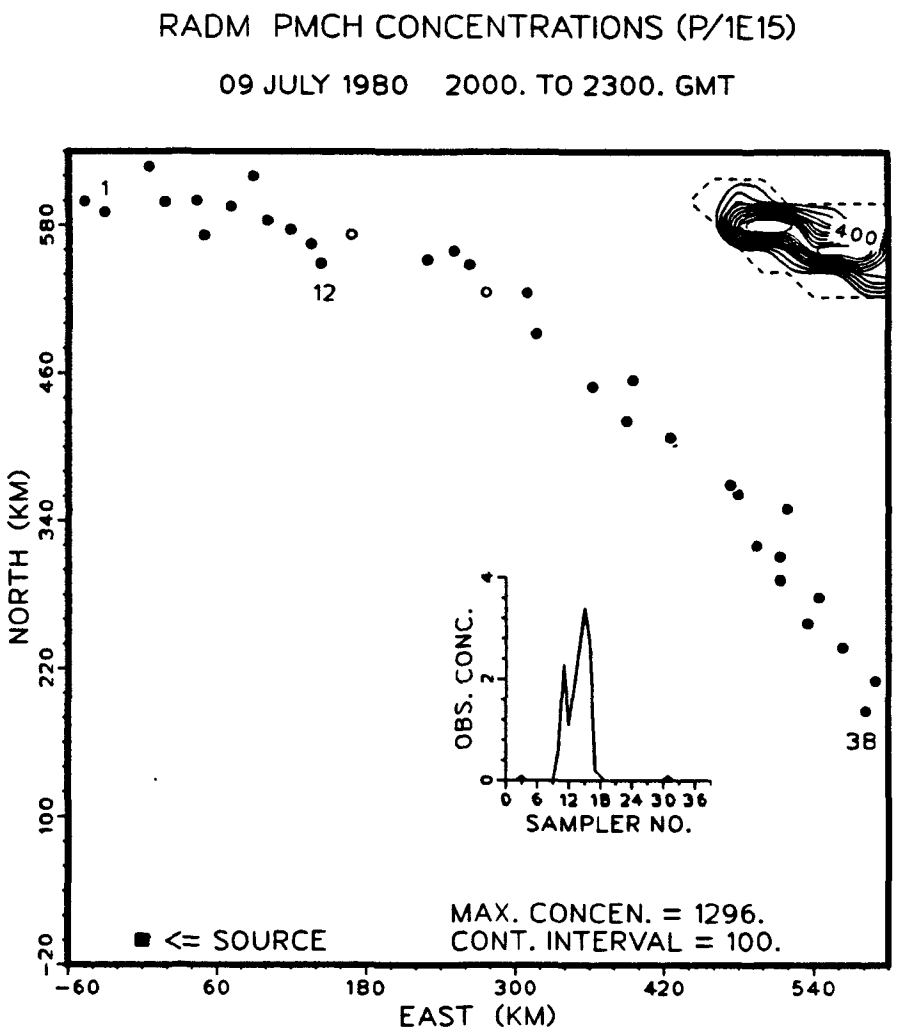

Figure E-59. Isopleth plot of ground-level concentrations for the Oklahoma experiment of July 9, 1980 (2000 to 2300 GMT) ... RADM predictions.

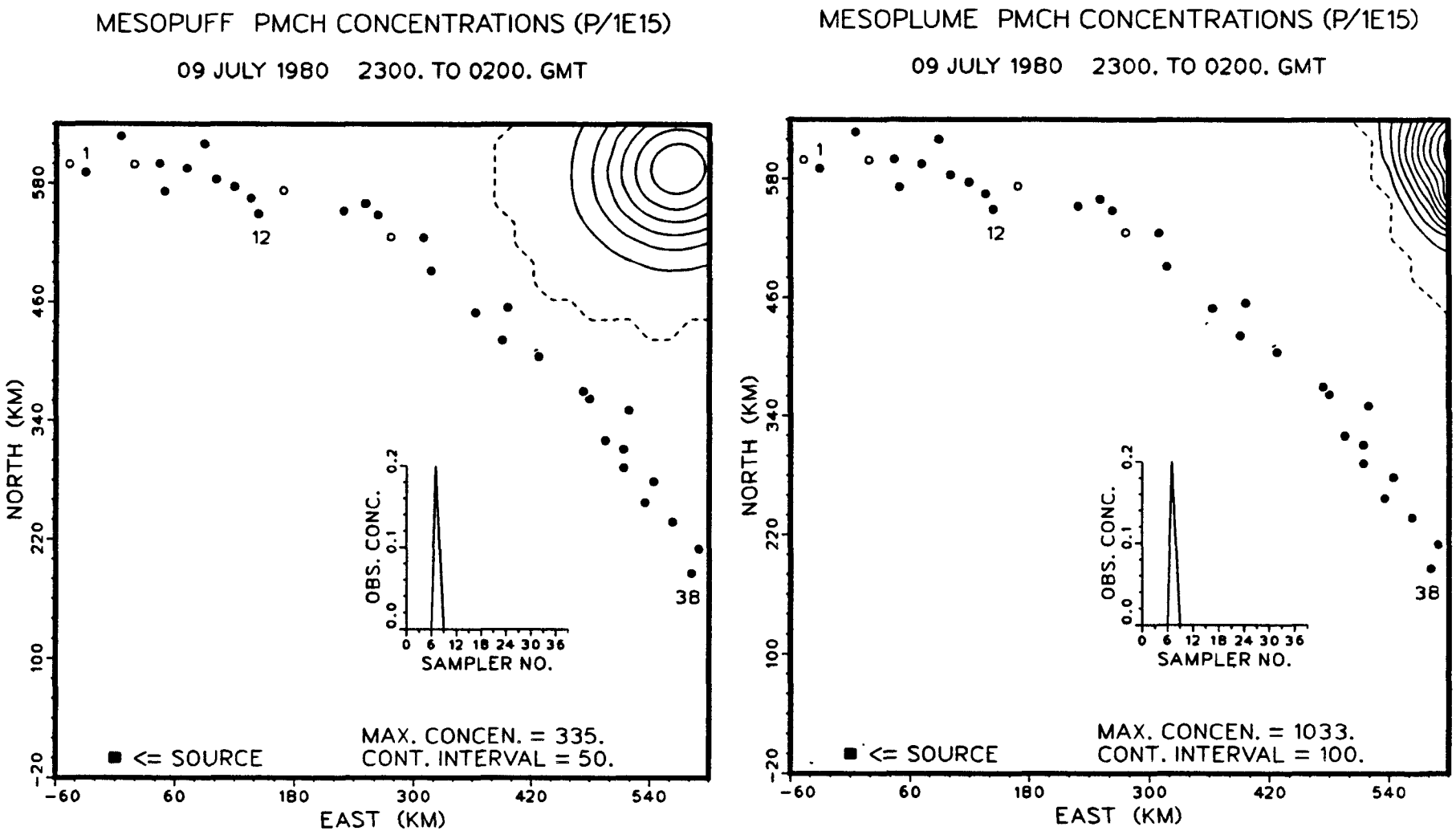

Figure E-60. Isopleth plot of ground-level concentrations for the Oklahoma experiment of July 9, 1980 (2300 to 0200 GMT) ... (left) MESOPUFF predictions, (right) MESOPLUME predictions.

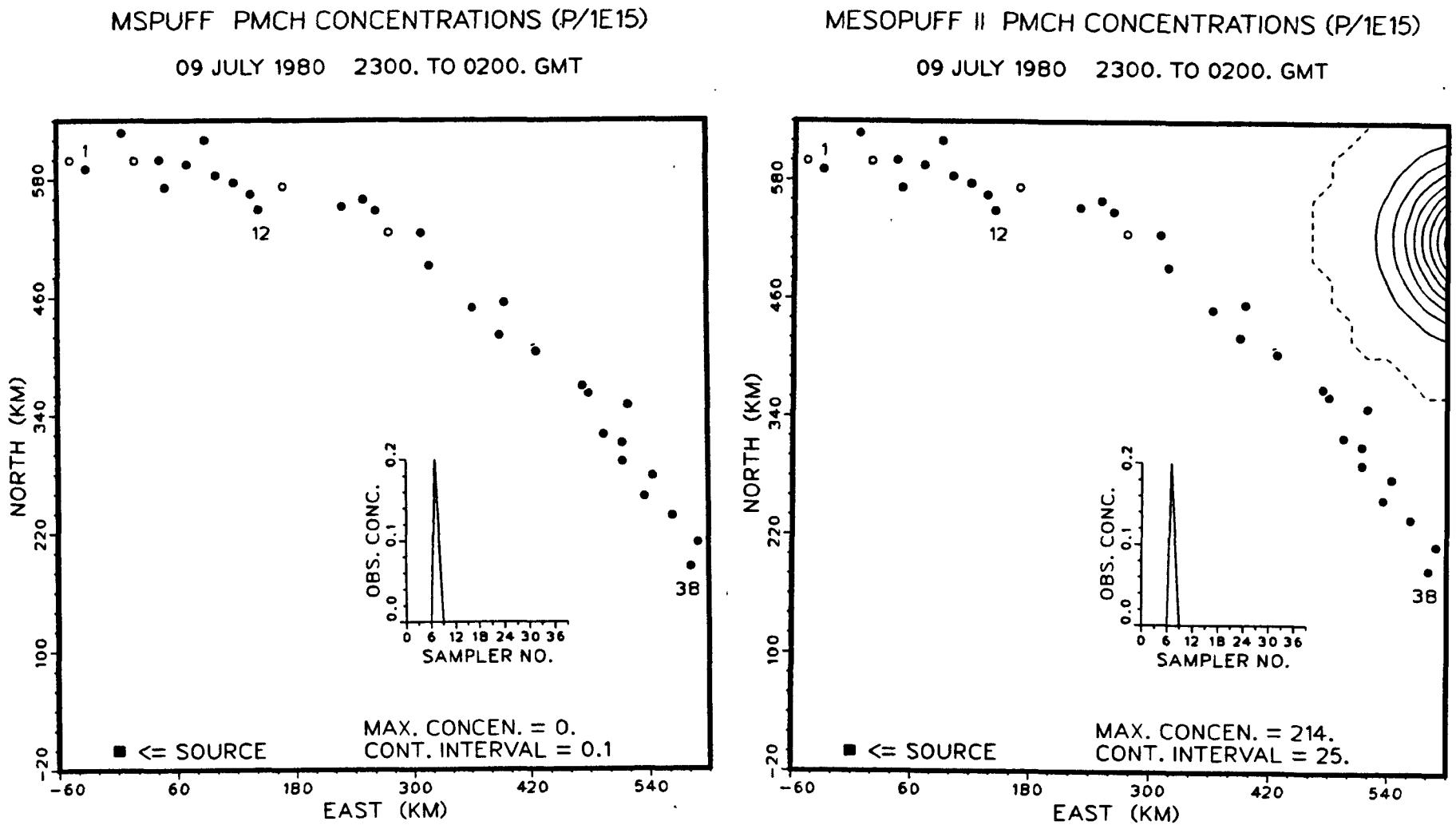

Figure E-61. Isopleth plot of ground-level concentrations for the Oklahoma experiment of July 9, 1980 (2300 to 0200 GMT) ... (left) MSPUFF predictions, (right) MESOPUFF II predictions.

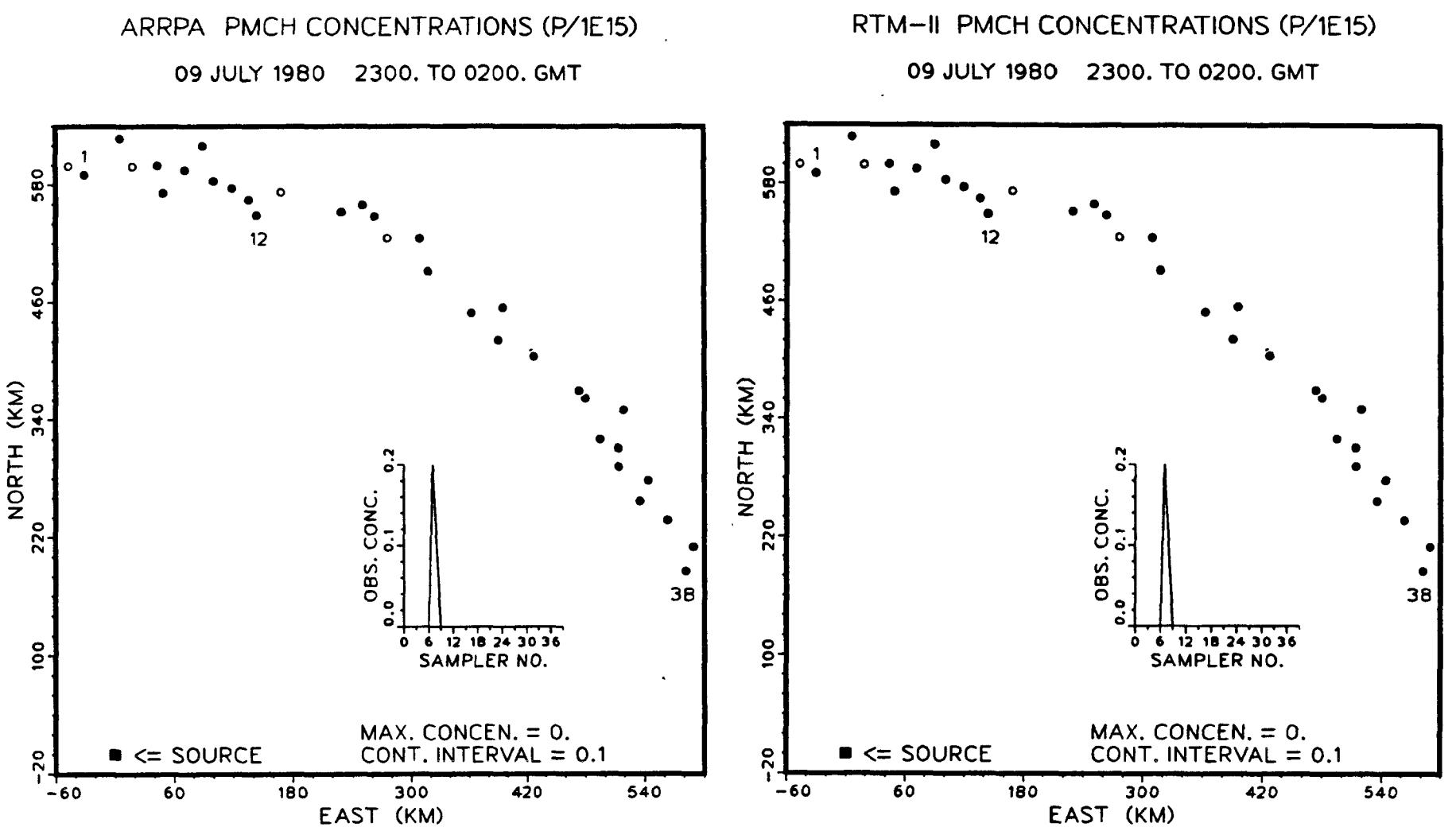

Figure E-62. Isopleth plot of ground-level concentrations for the Oklahoma experiment of July 9, 1980 (2300 to 0200 GMT) ... (left) ARRPA predictions, (right) RTM-II predictions.

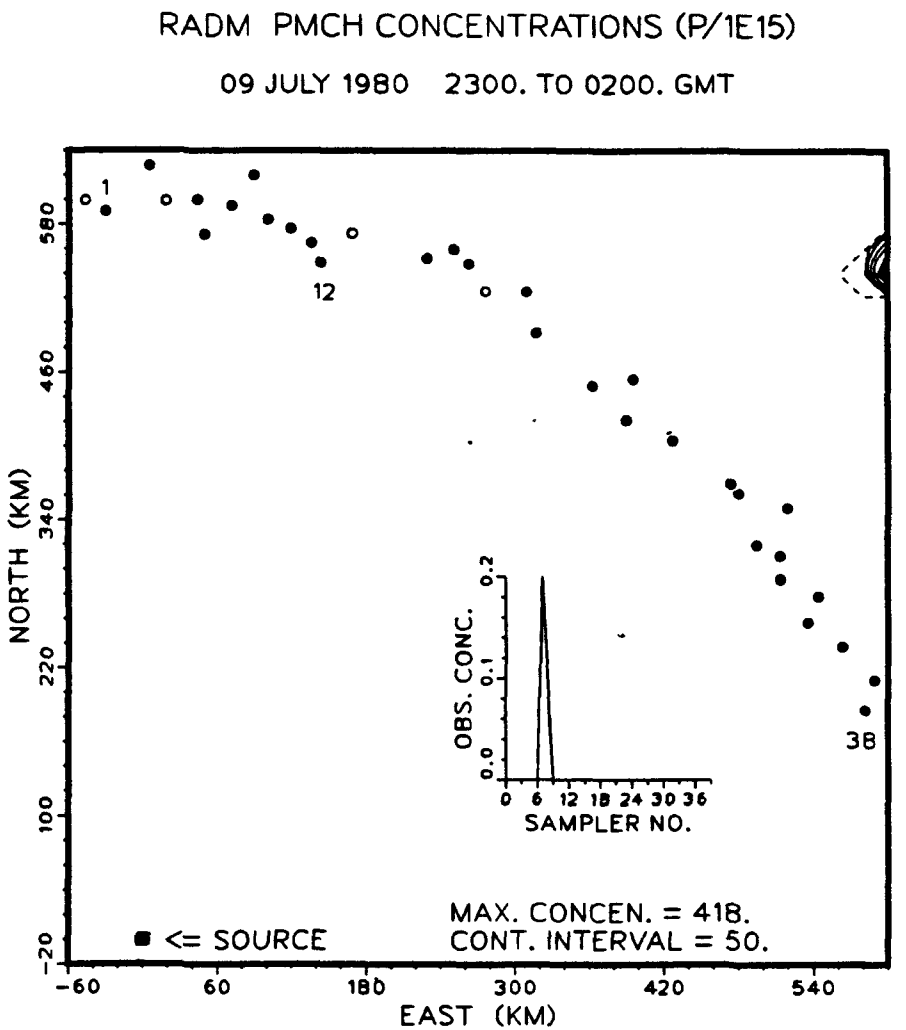

Figure E-63. Isopleth plot of ground-level concentrations for the Oklahoma experiment of July 9, 1980 (2300 to 0200 GMT) ... RADM predictions.

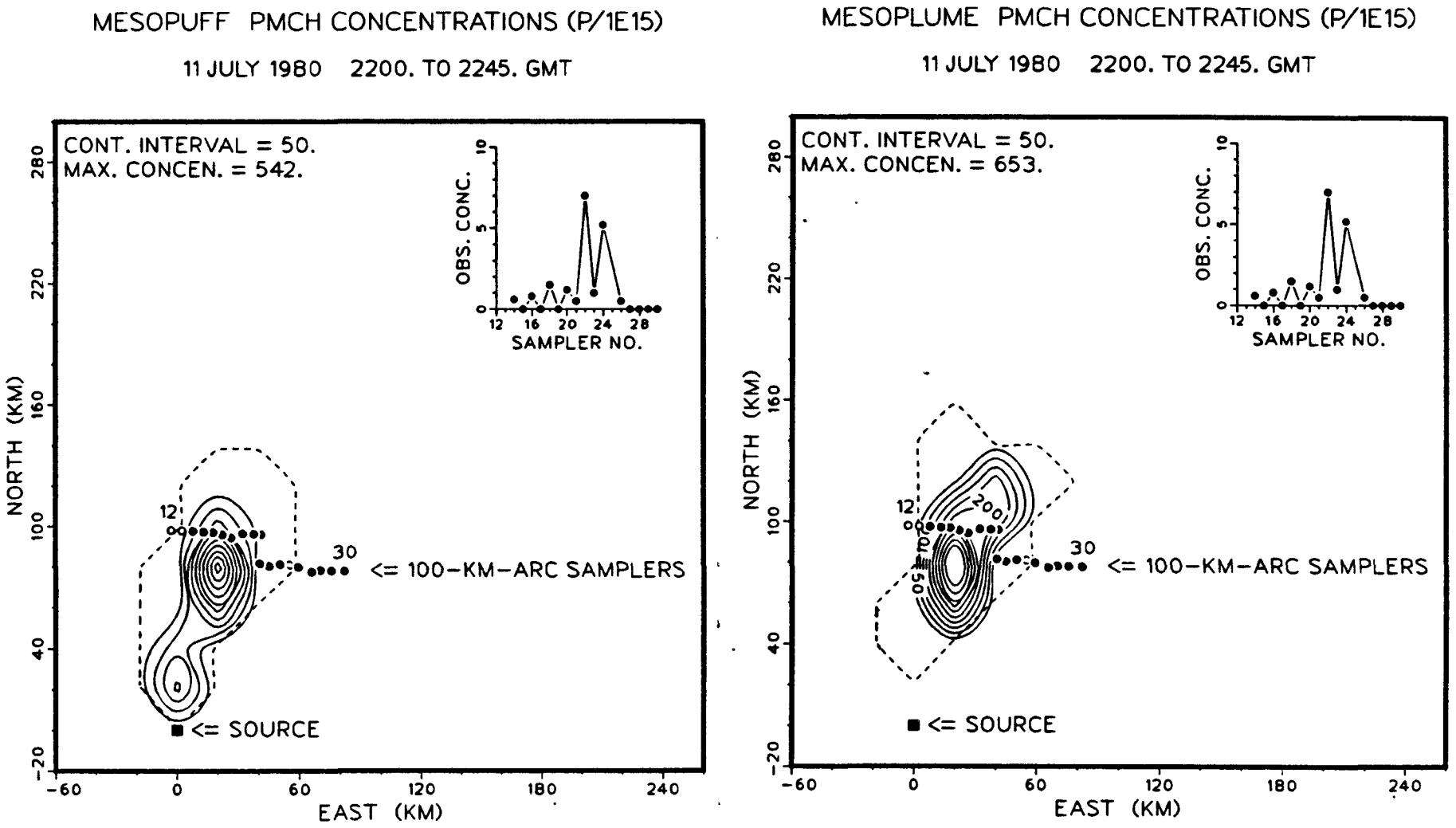

Figure E-64. Isopleth plot of ground-level concentrations for the Oklahoma experiment of July 11, 1980 (2200 to 2245 GMT) ... (left) MESOPUFF predictions, (right) MESOPLUME predictions.

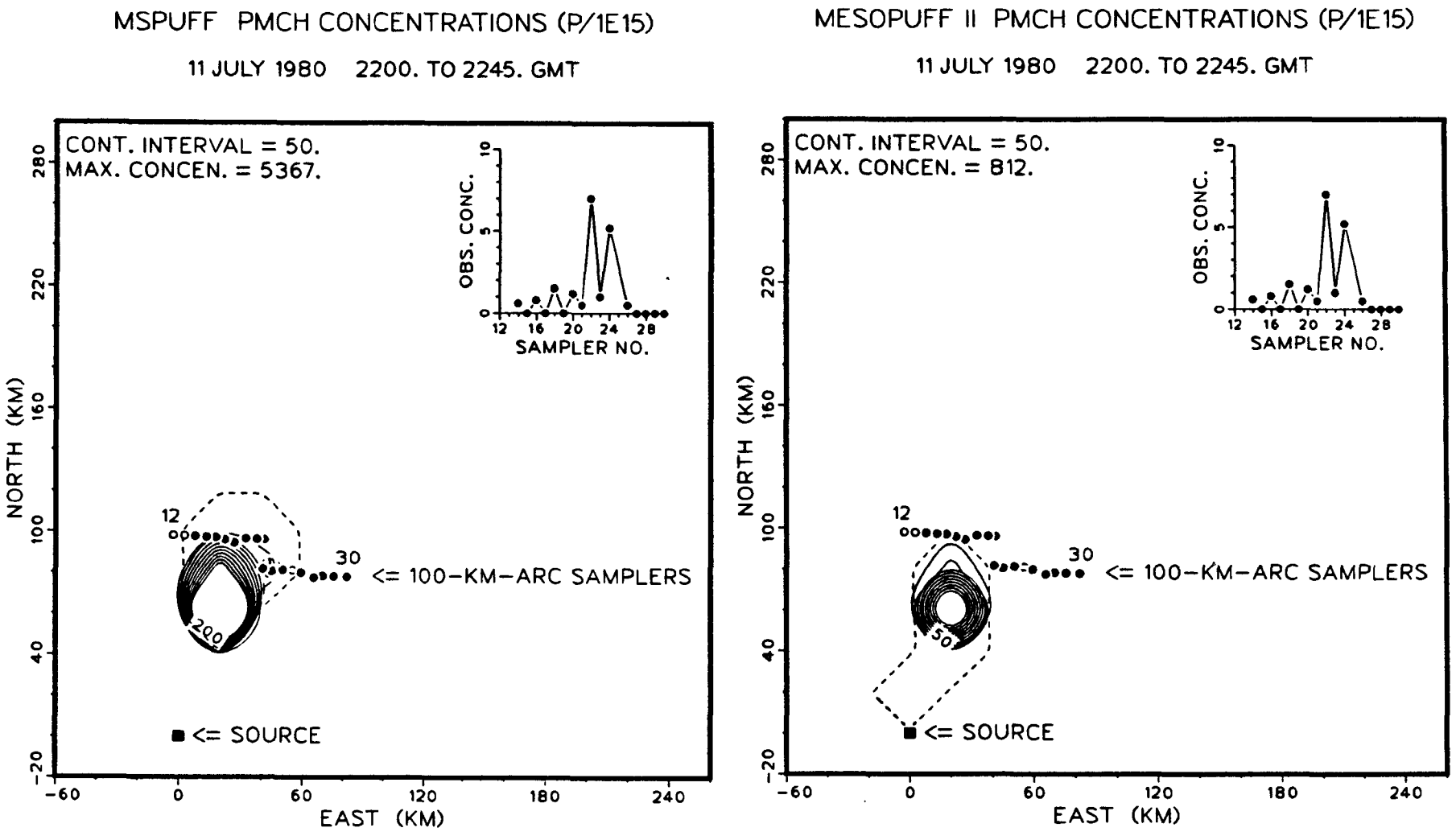

Figure E-65. Isopleth plot of ground-level concentrations for the Oklahoma experiment of July 11, 1980 (2200 to 2245 GMT) ... (left) MSPUFF predictions, (right) MESOPUFF II predictions.

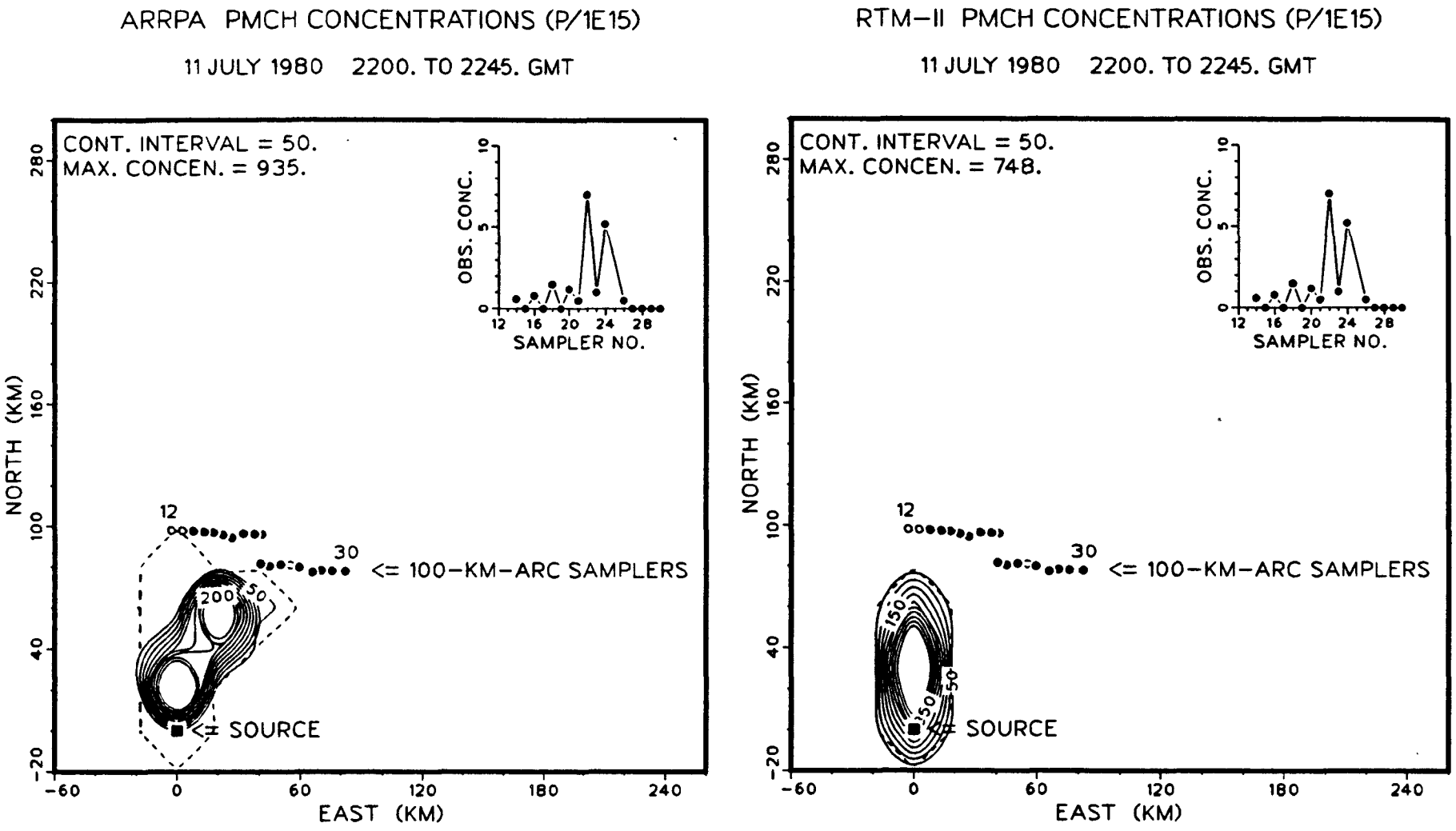

Figure E-66. Isopleth plot of ground-level concentrations for the Oklahoma experiment of July 11, 1980 (2200 to 2245 GMT) ... (left) ARRPA predictions, (right) RTM-II predictions.

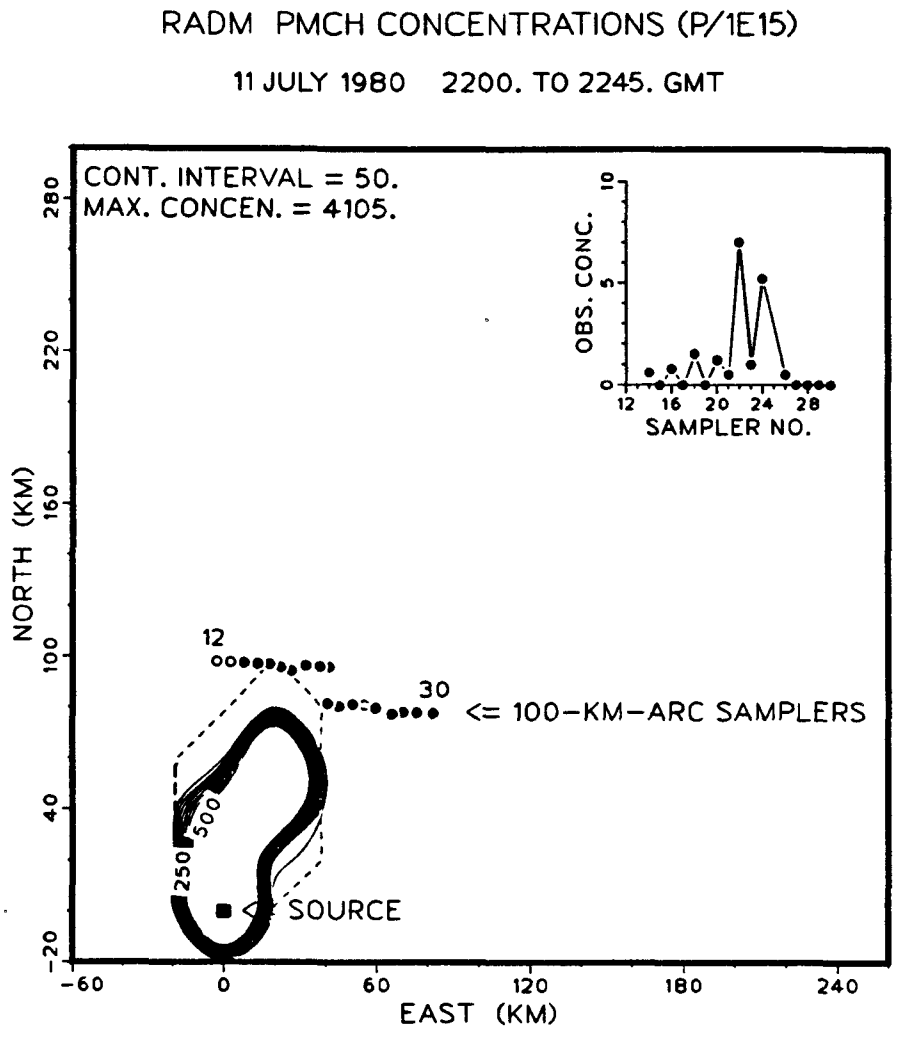

Figure E-67. Isopleth plot of ground-level concentrations for the Oklahoma experiment of July 11, 1980 (2200 to 2245 GMT) ... RADM predictions.

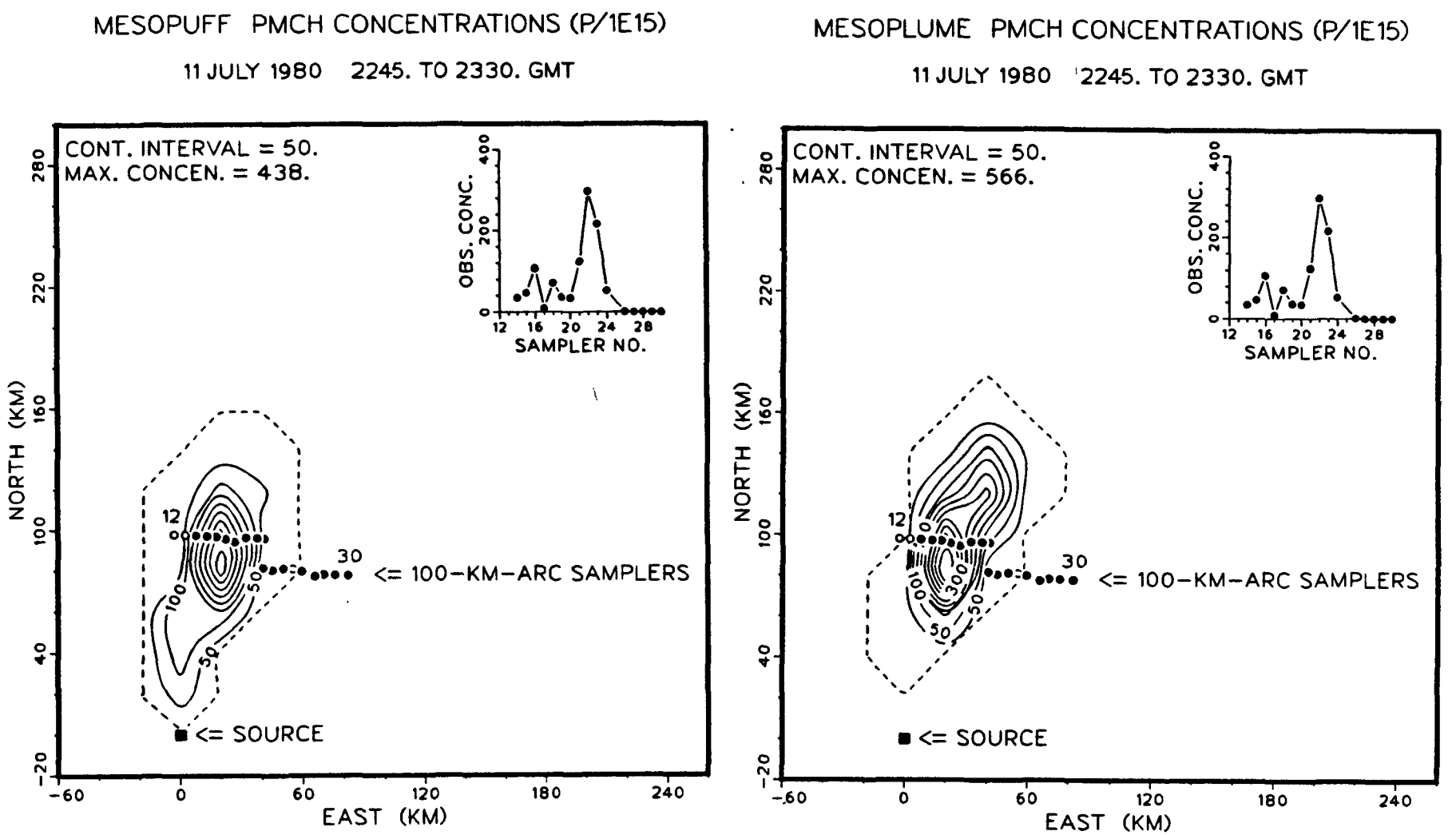

Figure E-68. Isopleth plot of ground-level concentrations for the Oklahoma experiment of July 11, 1980 (2245 to 2330 GMT) ... (left) MESOPUFF predictions, (right) MESOPLUME predictions.

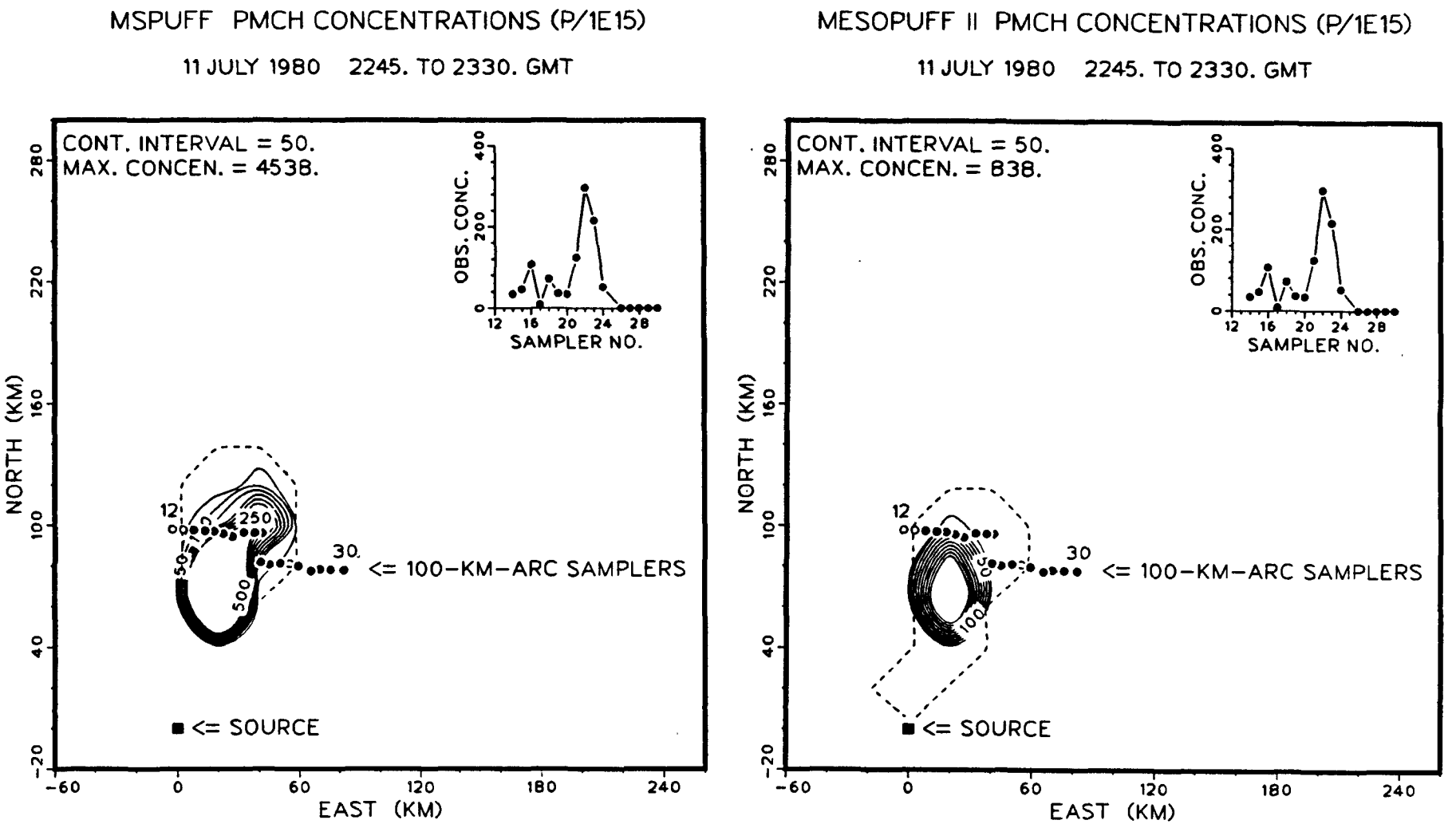

Figure E-69. Isopleth plot of ground-level concentrations for the Oklahoma experiment of July 11, 1980 (2245 to 2330 GMT) ... (left) MSPUFF predictions, (right) MESOPUFF II predictions.

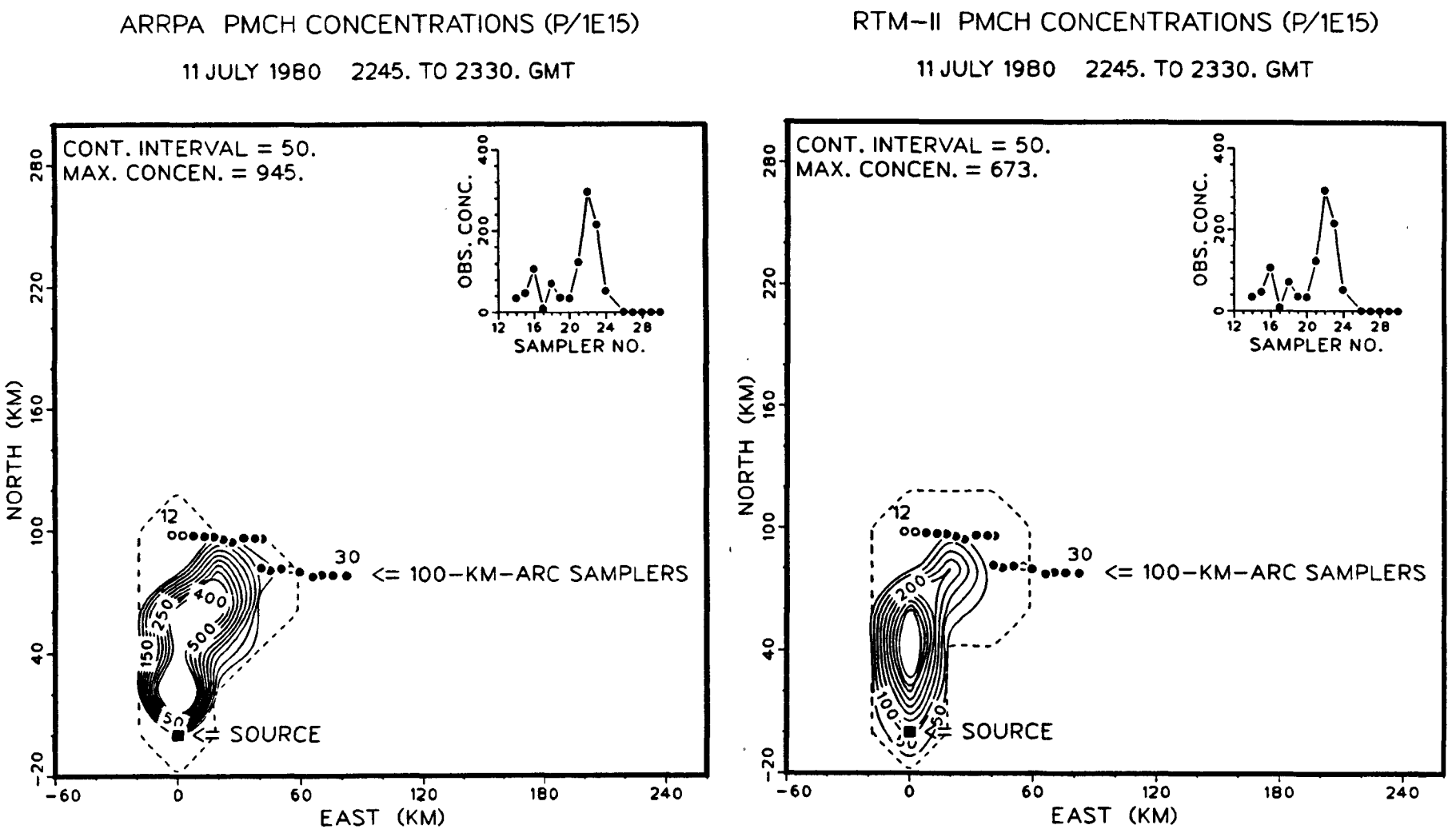

Figure E-70. Isopleth plot of ground-level concentrations for the Oklahoma experiment of July 11, 1980 (2245 to 2330 GMT) ... (left) ARRPA predictions, (right) RTM-II predictions.

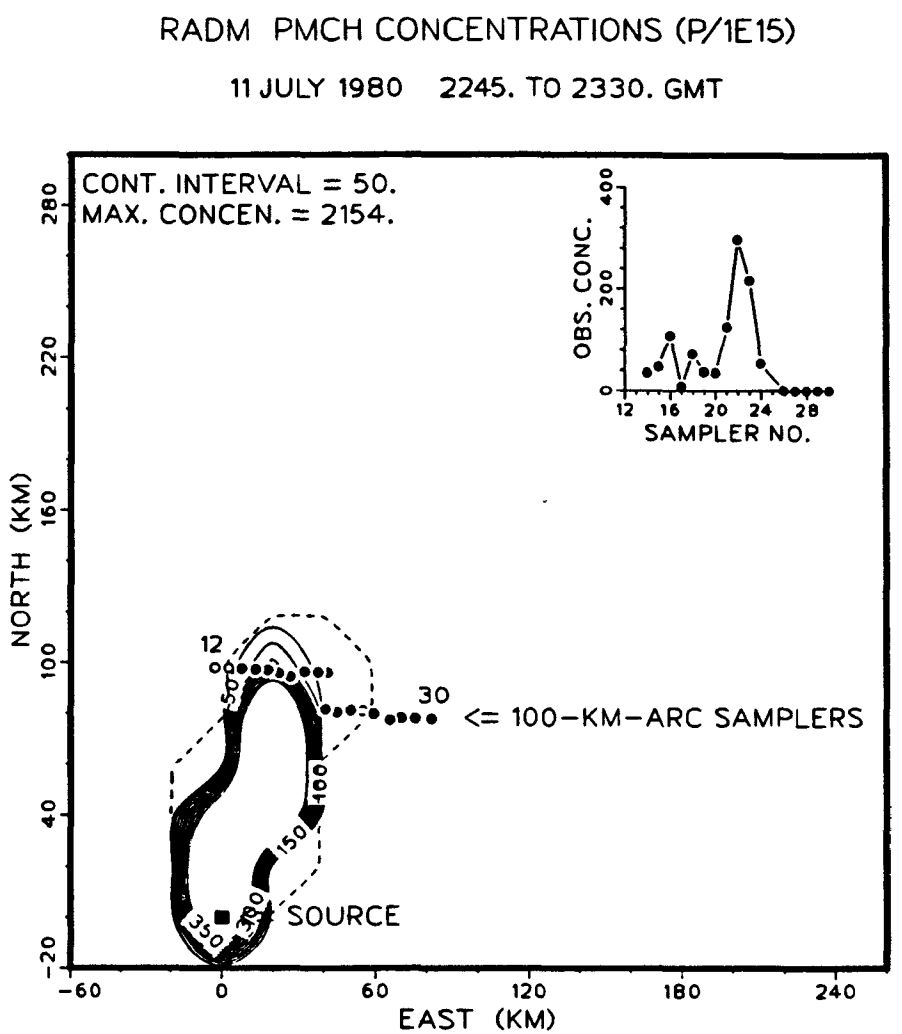

Figure E-71. Isopleth plot of ground-level concentrations for the Oklahoma experiment of July 11, 1980 (2245 to 2330 GMT) ... RADM predictions.

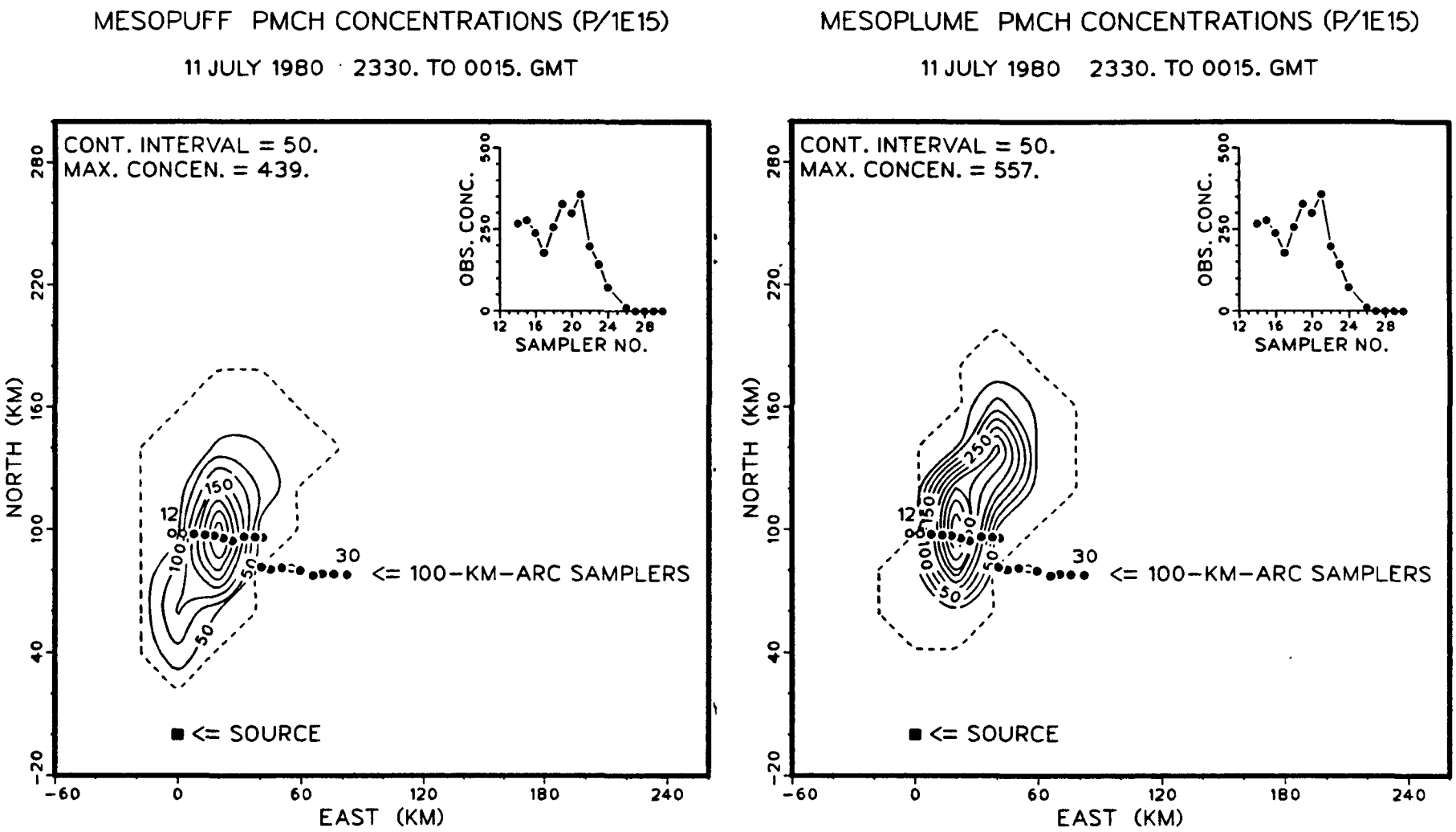

Figure E-72. Isopleth plot of ground-level concentrations for the Oklahoma experiment of July 11, 1980 (2330 to 0015 GMT) ... (left) MESOPUFF predictions, (right) MESOPLUME predictions.

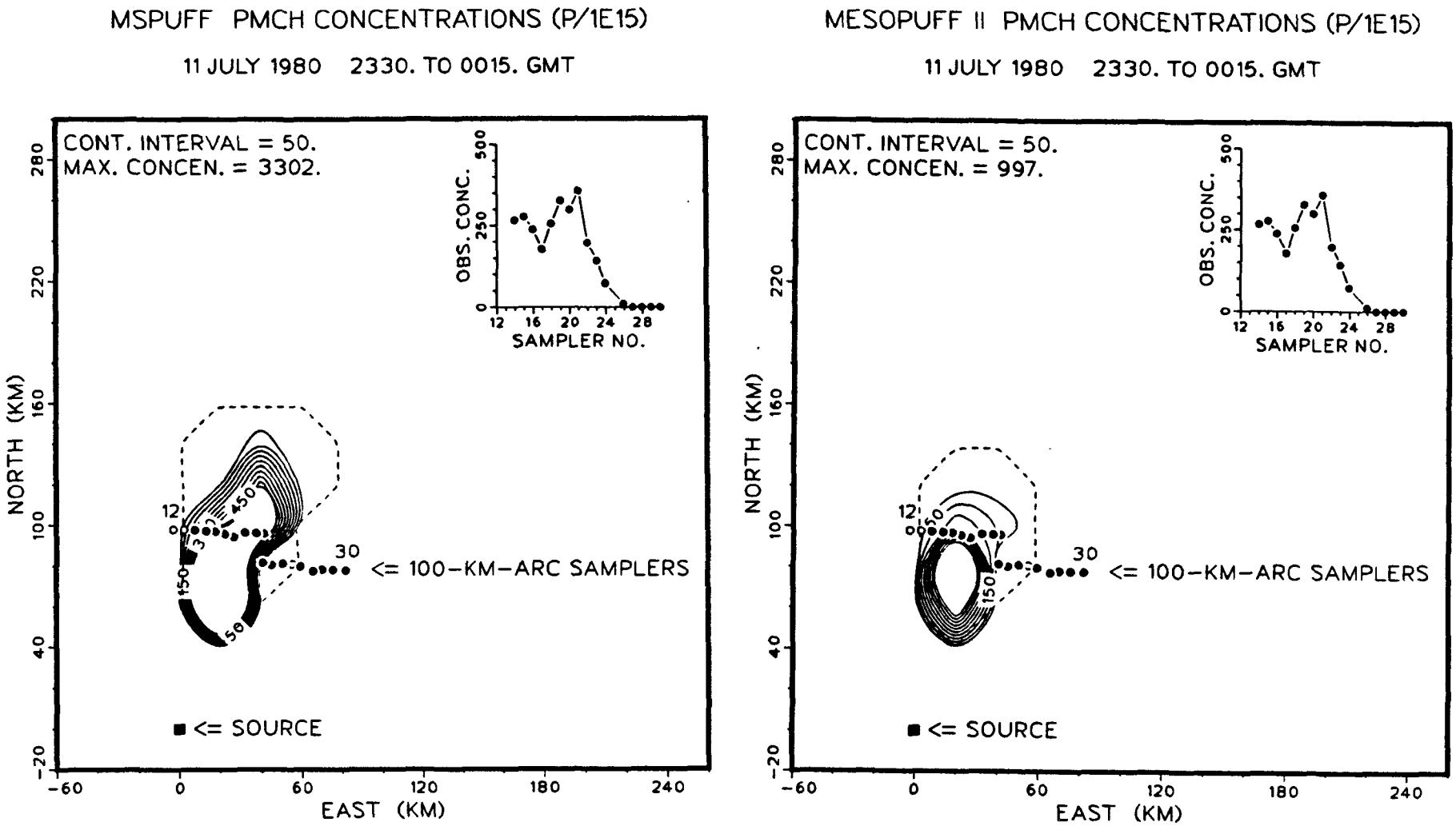

Figure E-73. Isopleth plot of ground-level concentrations for the Oklahoma experiment of July 11, 1980 (2330 to 0015 GMT) ... (left) MSPUFF predictions, (right) MESOPUFF II predictions.

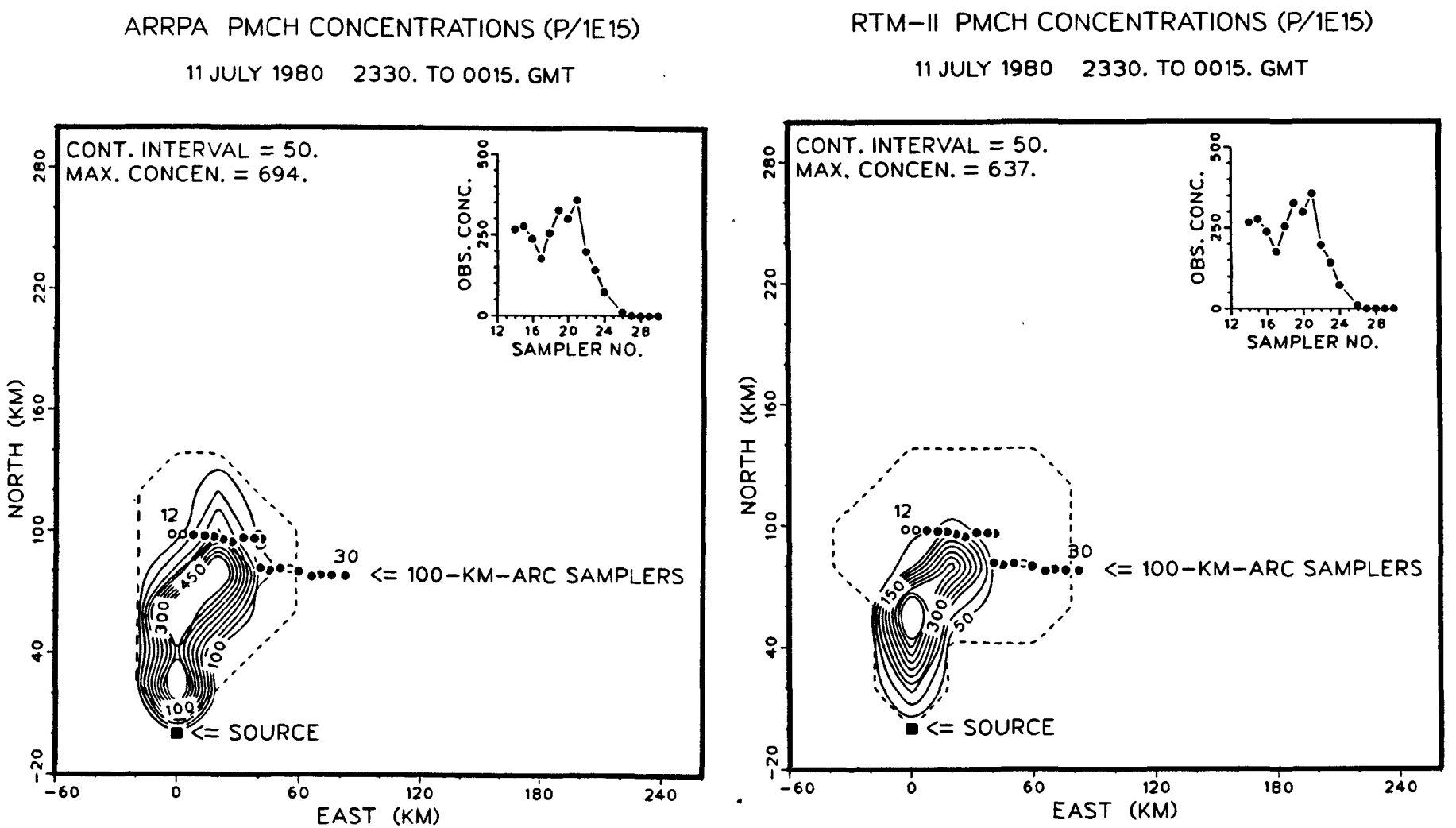

Figure E-74. Isopleth plot of ground-level concentrations for the Oklahoma experiment of July 11, 1980 (2330 to 0015 GMT) ... (left) ARRPA predictions, (right) RTM-II predictions.

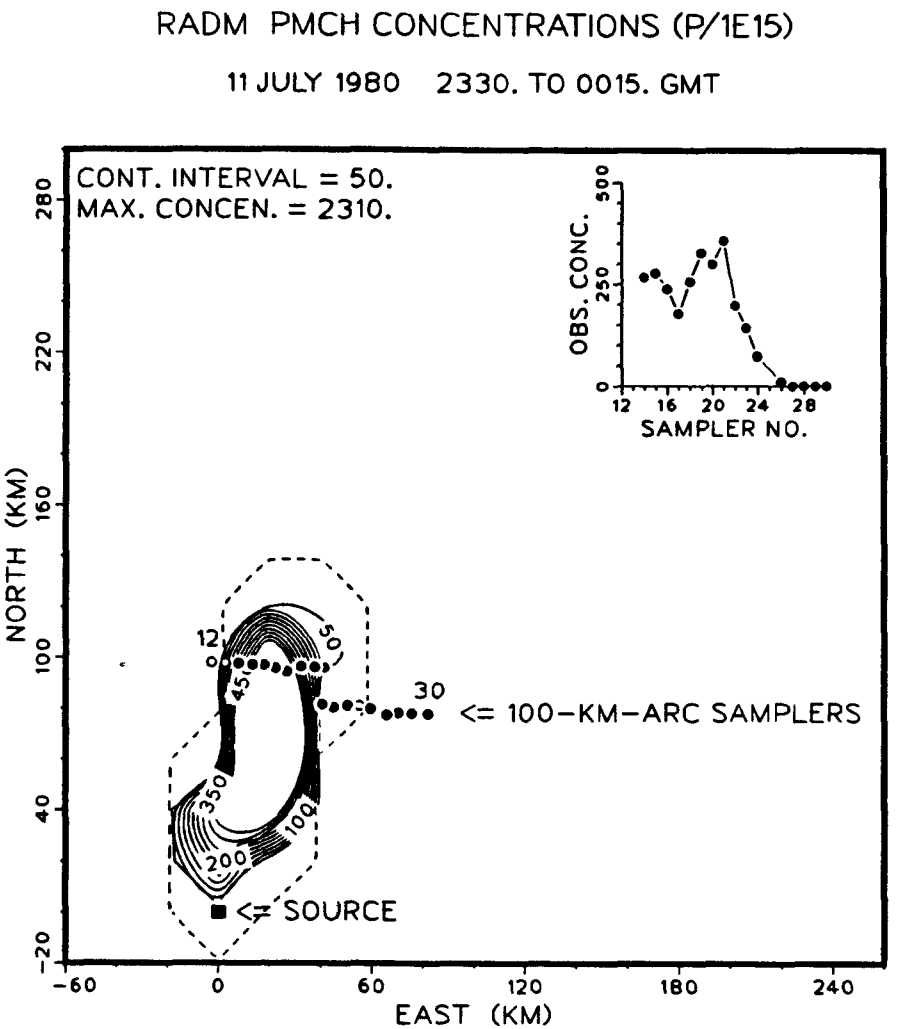

Figure E-75. Isopleth plot of ground-level concentrations for the Oklahoma experiment of July 11, 1980 (2330 to 0015 GMT) ... RADM predictions.

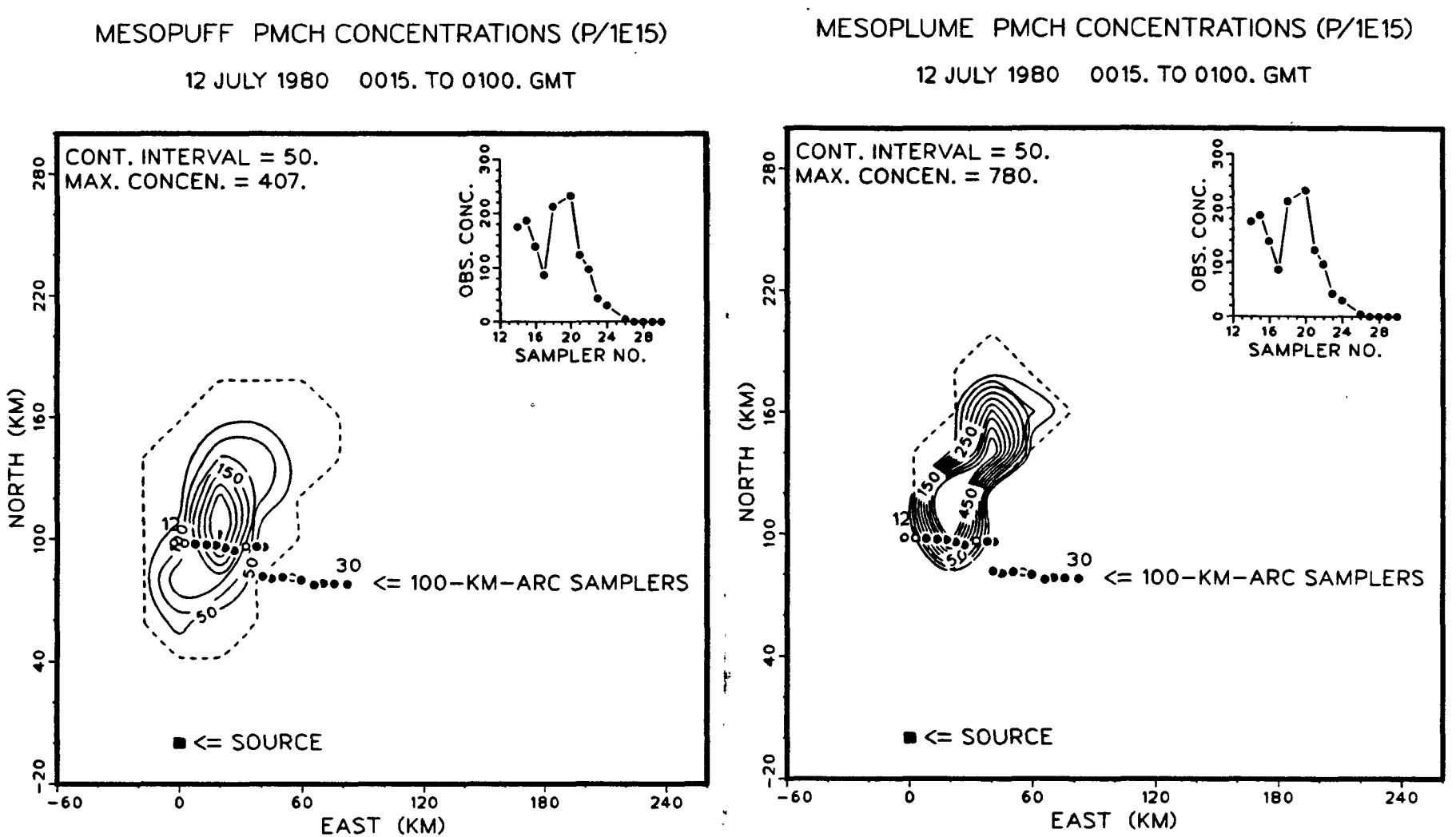

Figure E-76. Isopleth plot of ground-level concentrations for the Oklahoma experiment of July 12, 1980 (0015 to 0100 GMT) ... (left) MESOPUFF predictions, (right) MESOPLUME predictions.

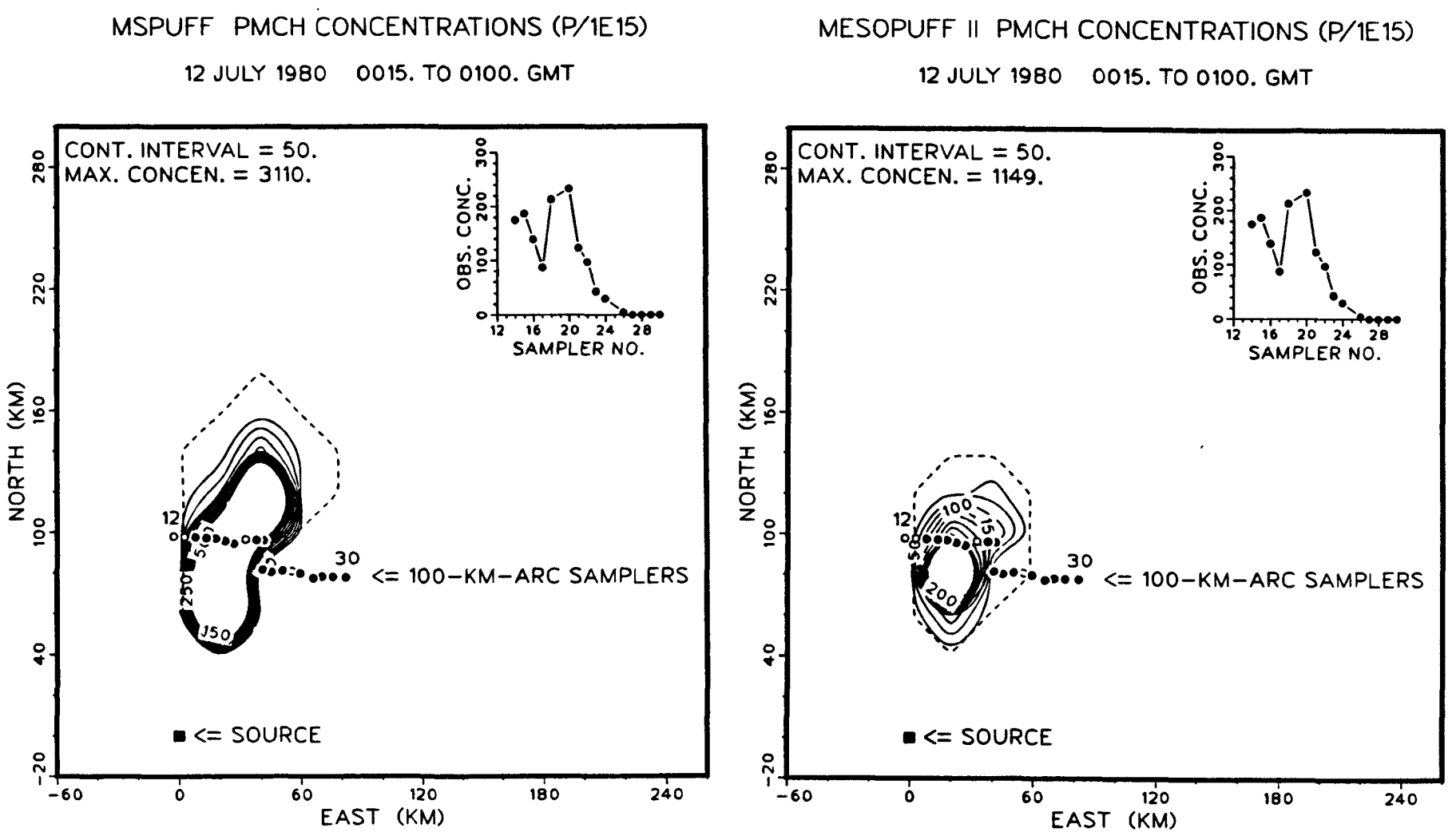

Figure E-77. Isopleth plot of ground-level concentrations for the Oklahoma experiment of July 12, 1980 (0015 to 0100 GMT) ... (left) MSPUFF predictions, (right) MESOPUFF II predictions.

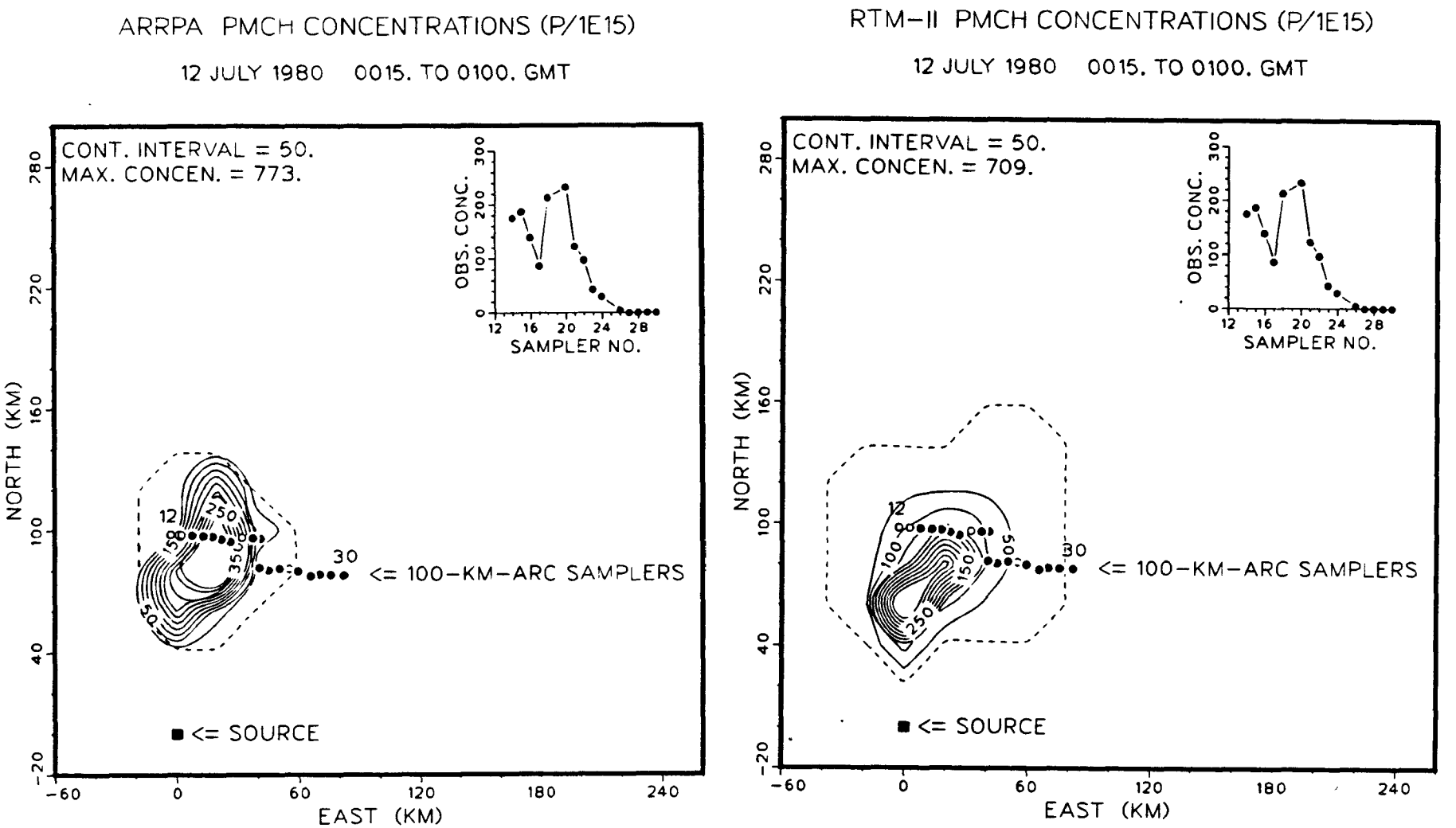

Figure E-78. Isopleth plot of ground-level concentrations for the Oklahoma experiment of July 12, 1980 (0015 to 0100 GMT) ... (left) ARRPA predictions, (right) RTM-II predictions.

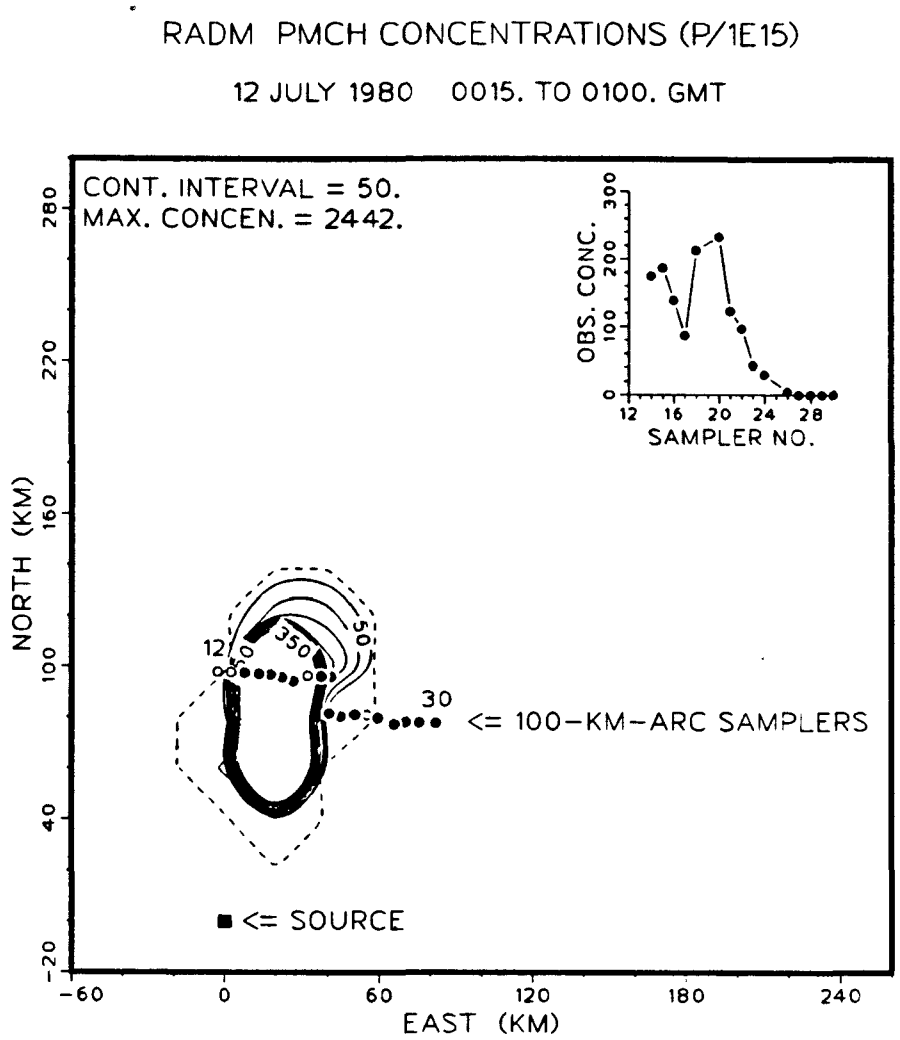

Figure E-79. Isopleth plot of ground-level concentrations for the Oklahoma experiment of July 12, 1980 (0015 to 0100 GMT) ... RADM predictions.

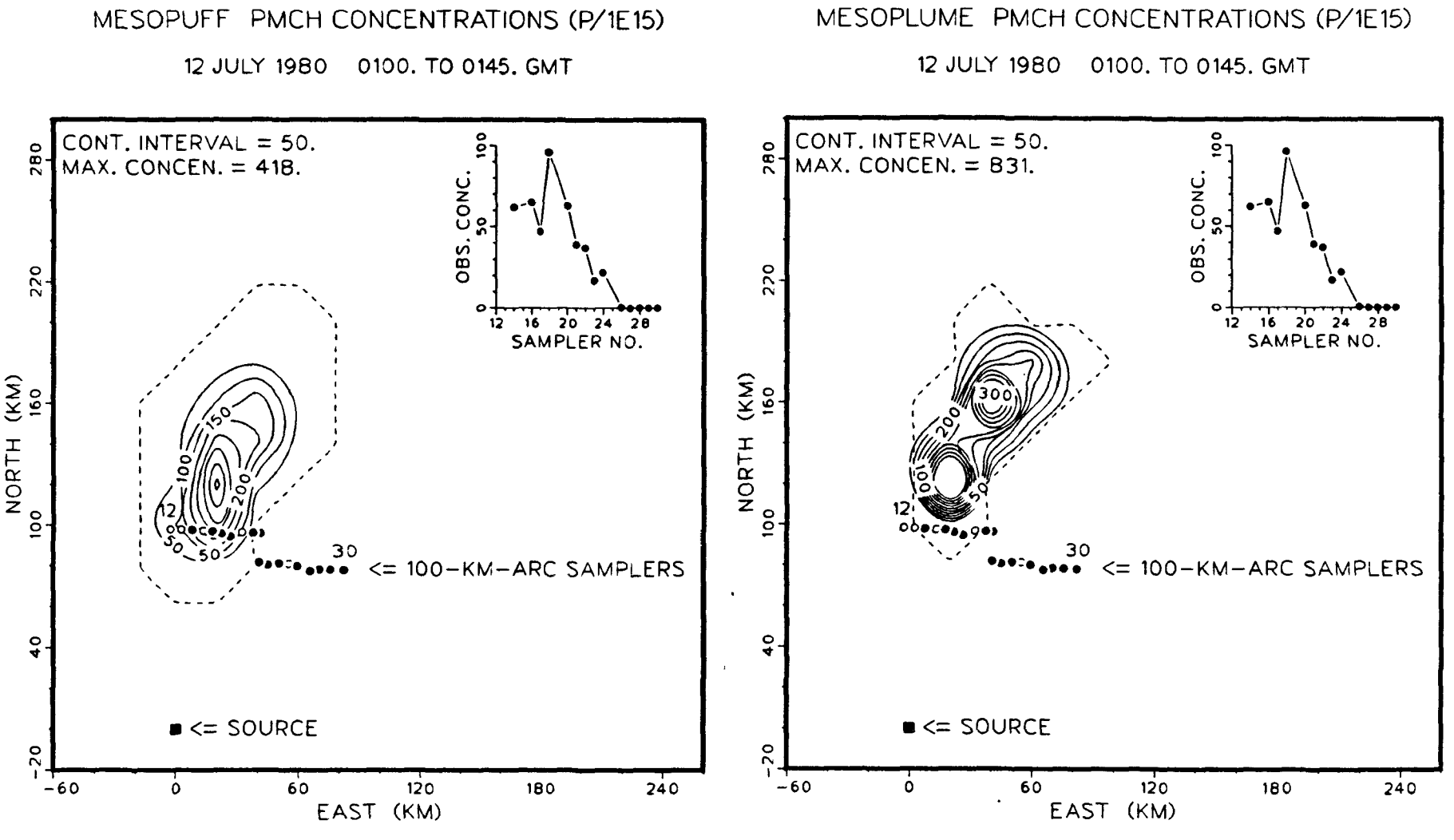

Figure E-80. Isopleth plot of ground-level concentrations for the Oklahoma experiment of July 12, 1980 (0100 to 0145 GMT) ... (left) MESOPUFF predictions, (right) MESOPLUME predictions.

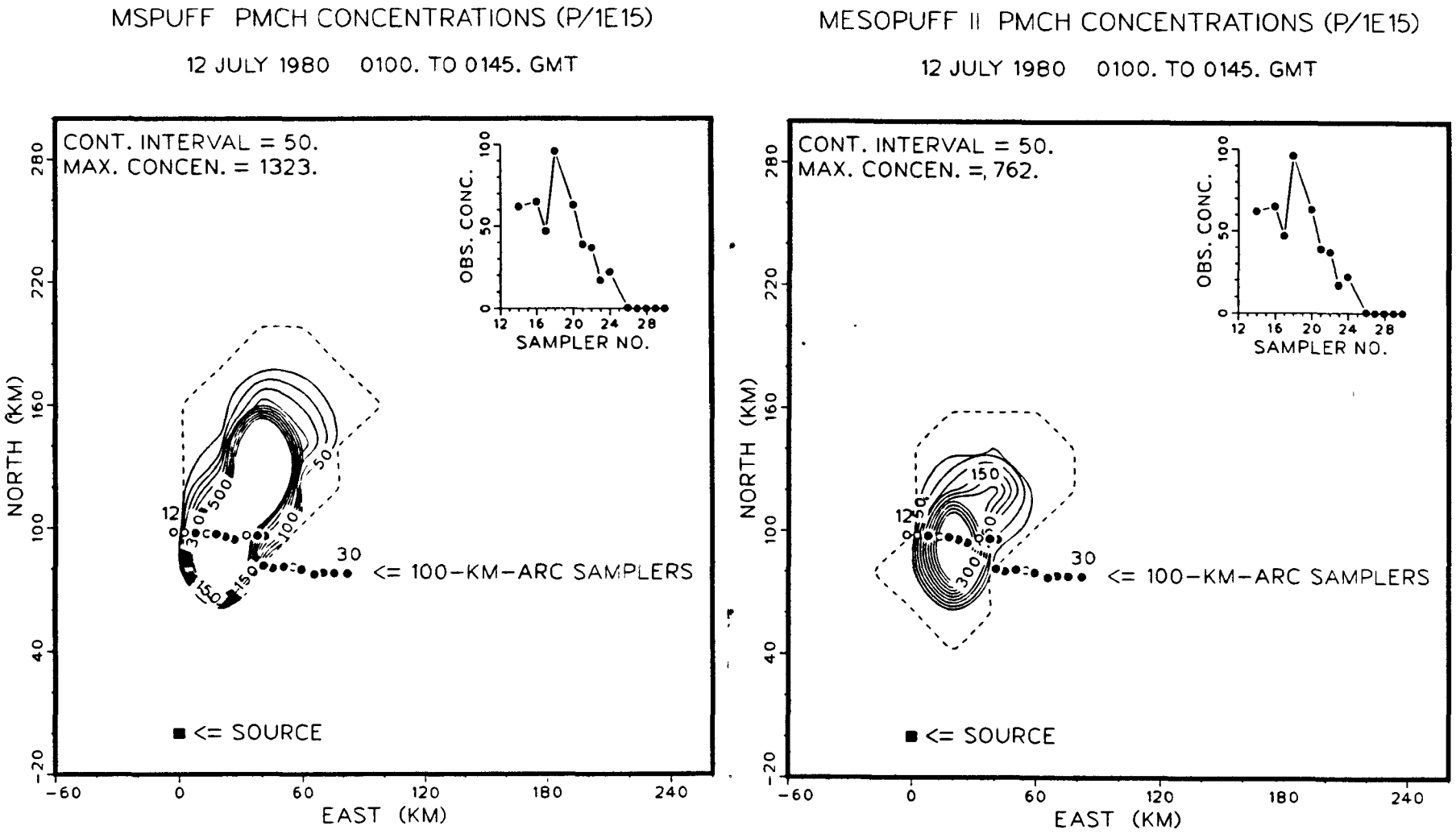

Figure E-81. Isopleth plot of ground-level concentrations for the Oklahoma experiment of July 12, 1980 (0100 to 0145 GMT) ... (left) MSPUFF predictions, (right) MESOPUFF II predictions.

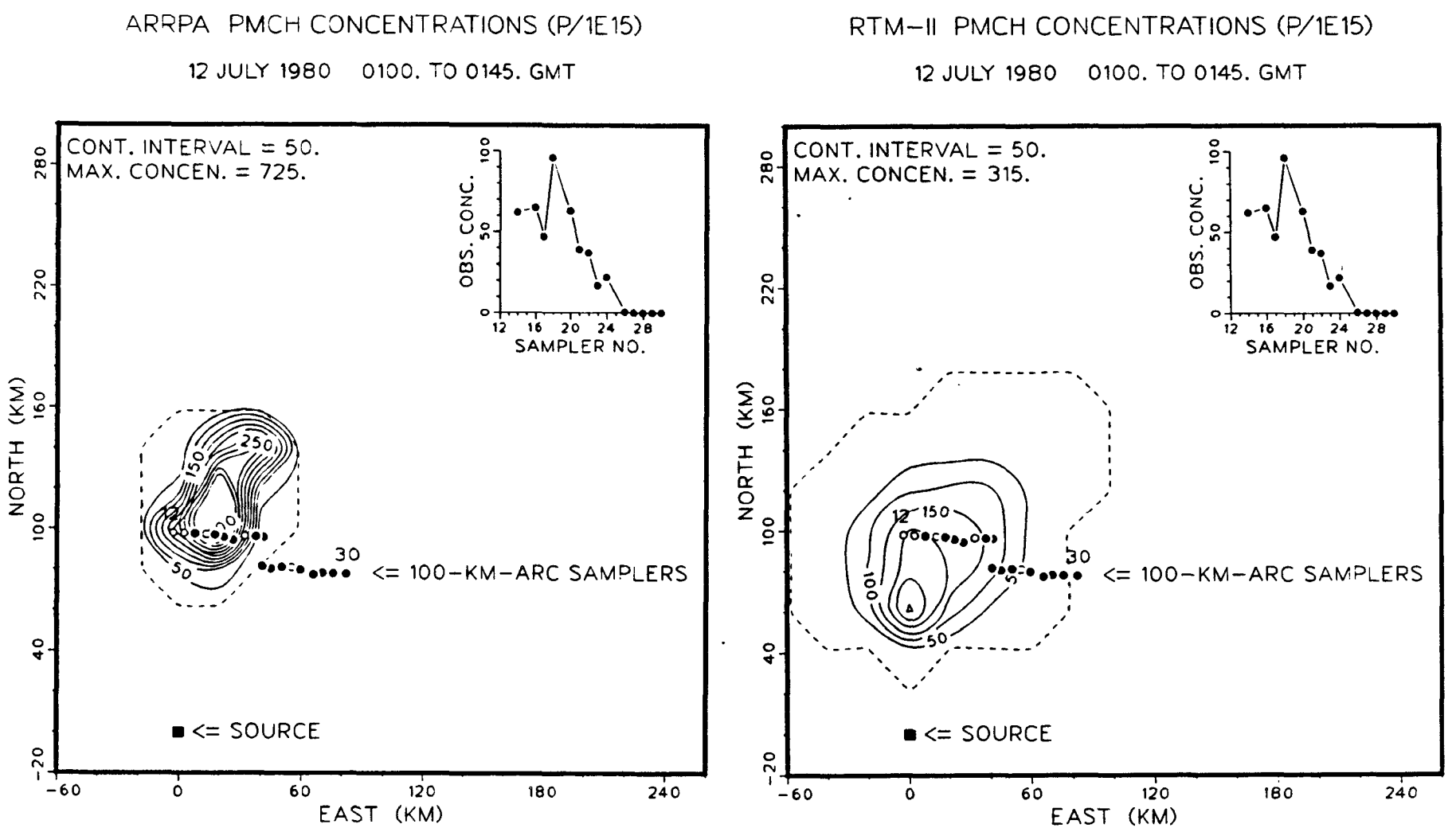

Figure E-82. Isopleth plot of ground-level concentrations for the Oklahoma experiment of July 12, 1980 (0100 to 0145 GMT) ... (left) ARRPA predictions, (right) RTM-II predictions.

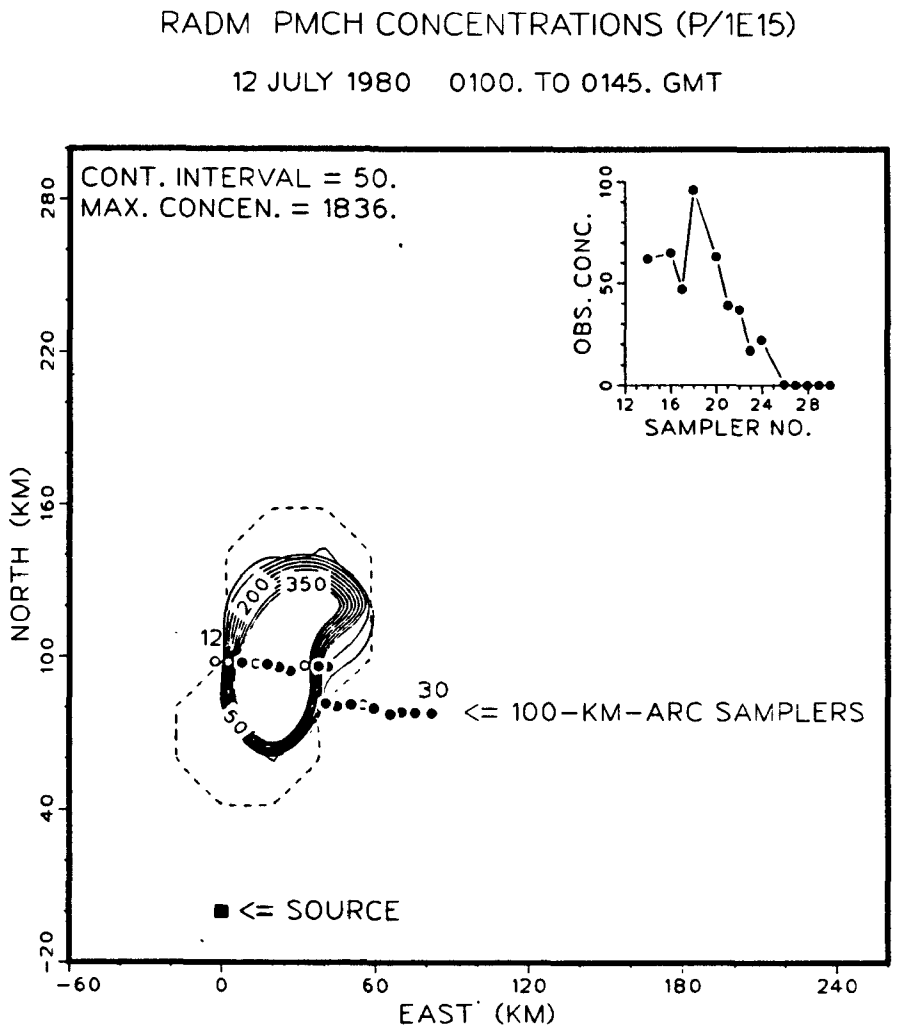

Figure E-83. Isopleth plot of ground-level concentrations for the Oklahoma experiment of July 12, 1980 (0100 to 0145 GMT) ... RADM predictions.

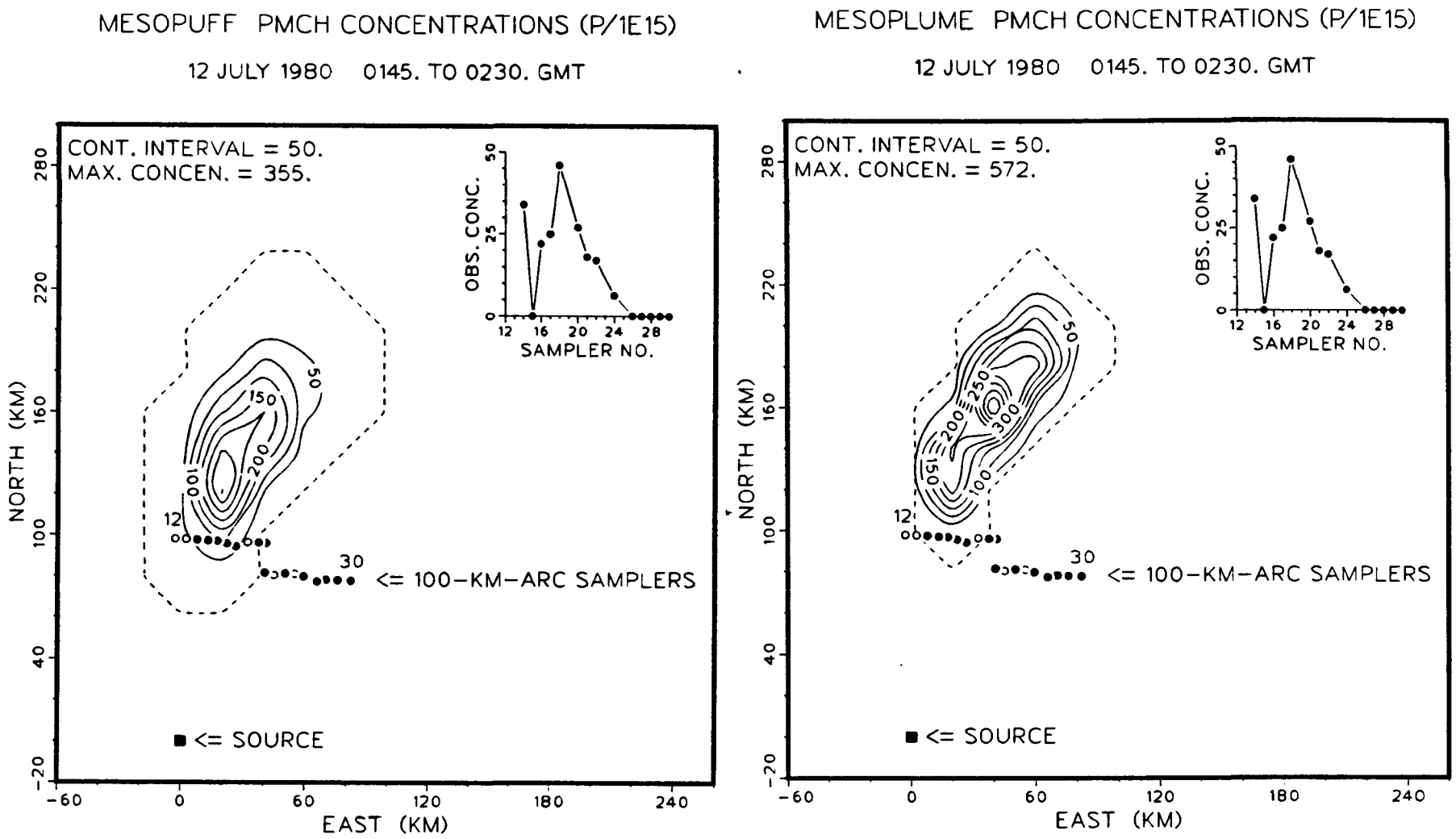

Figure E-84. Isopleth plot of ground-level concentrations for the Oklahoma experiment of July 12, 1980 (0145 to 0230 GMT) ... (left) MESOPUFF predictions, (right) MESOPLUME predictions.

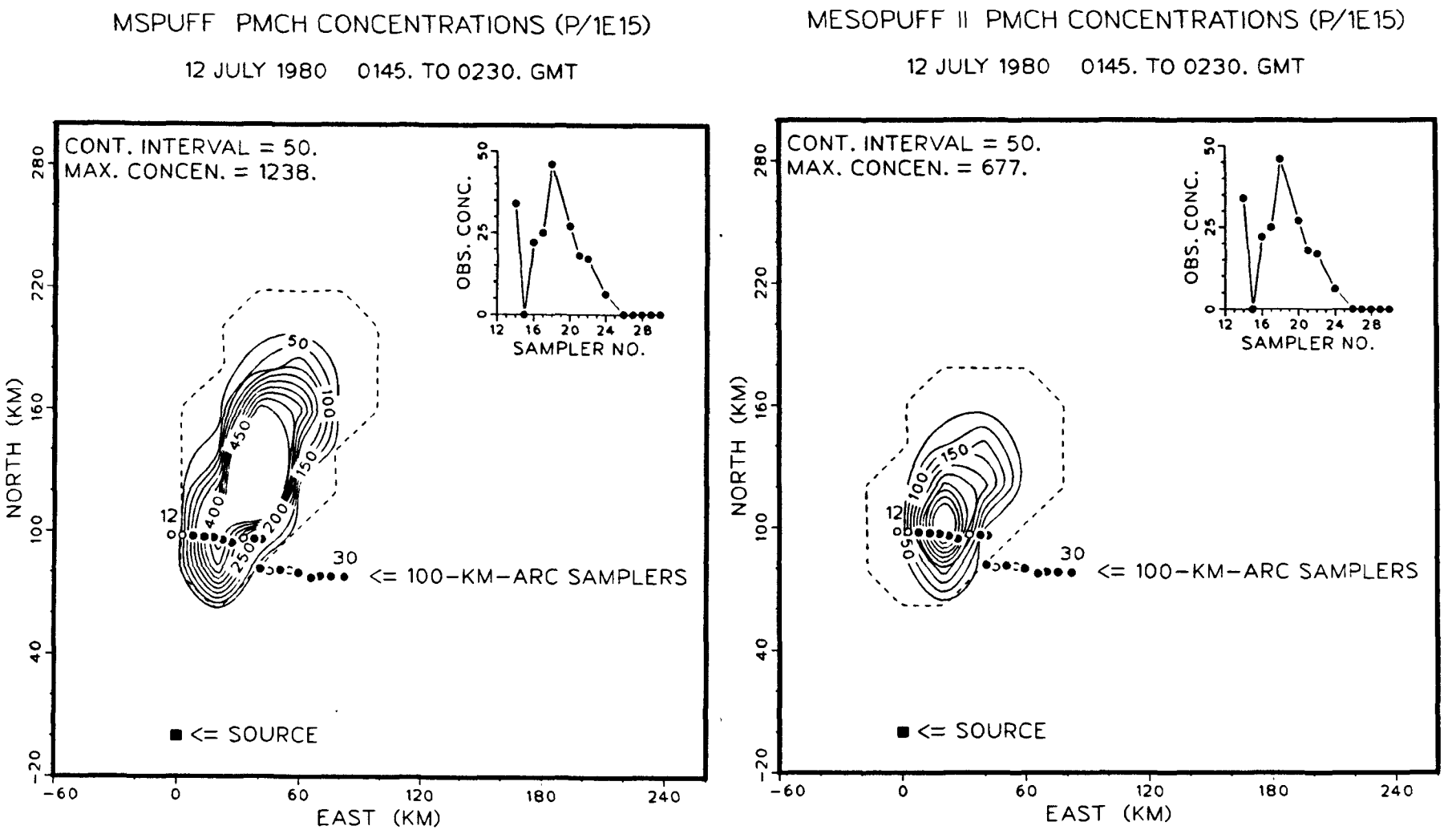

Figure E-85. Isopleth plot of ground-level concentrations for the Oklahoma experiment of July 12, 1980 (0145 to 0230 GMT) ... (left) MSPUFF predictions, (right) MESOPUFF II predictions.

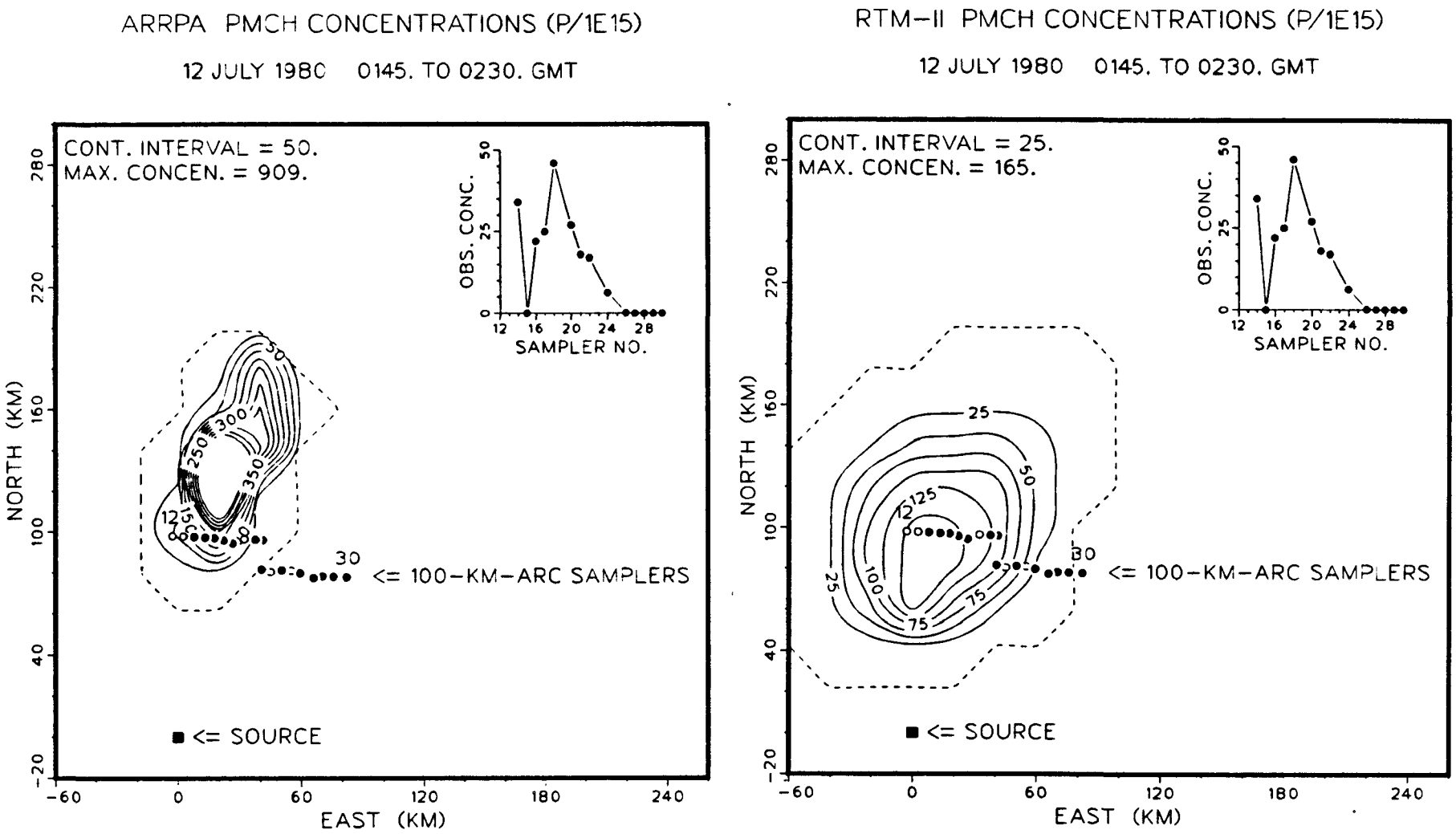

Figure E-86. Isopleth plot of ground-level concentrations for the Oklahoma experiment of July 12, 1980 (0145 to 0230 GMT) ... (left) ARRPA predictions, (right) RTM-II predictions.

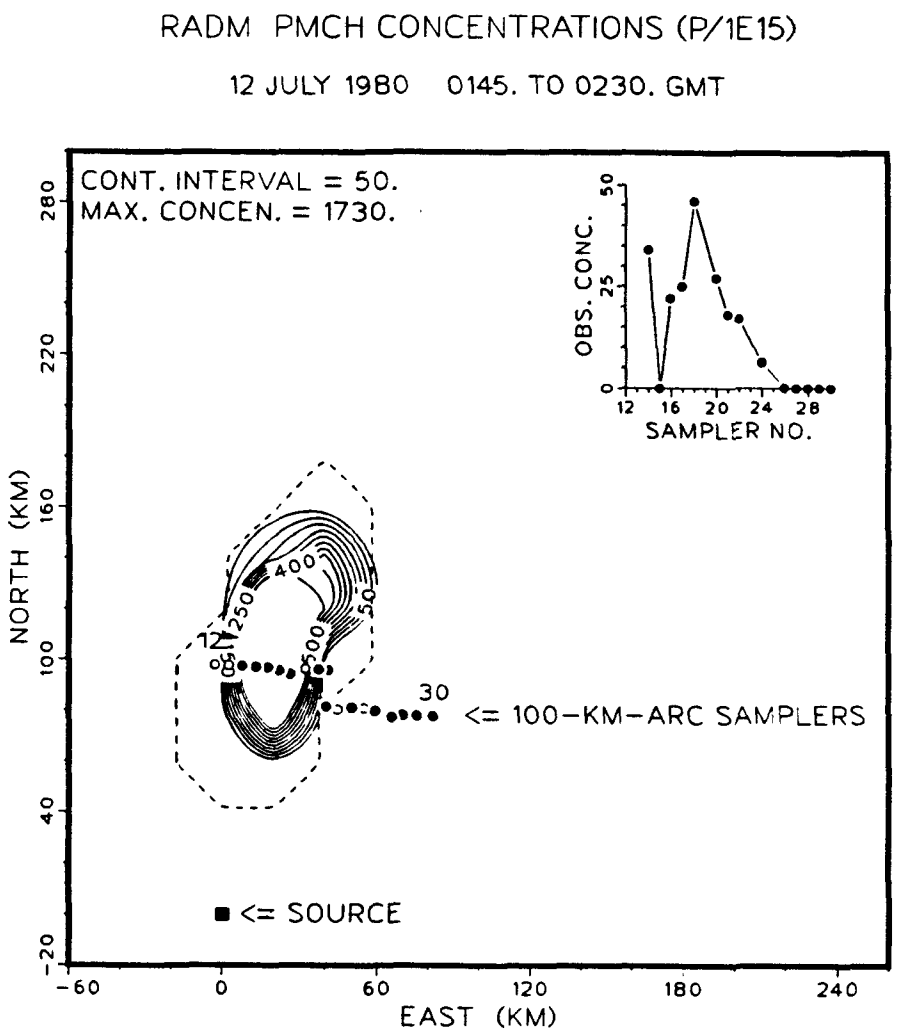

Figure E-87. Isopleth plot of ground-level concentrations for the Oklahoma experiment of July 12, 1980 (0145 to 0230 GMT) ... RADM predictions.

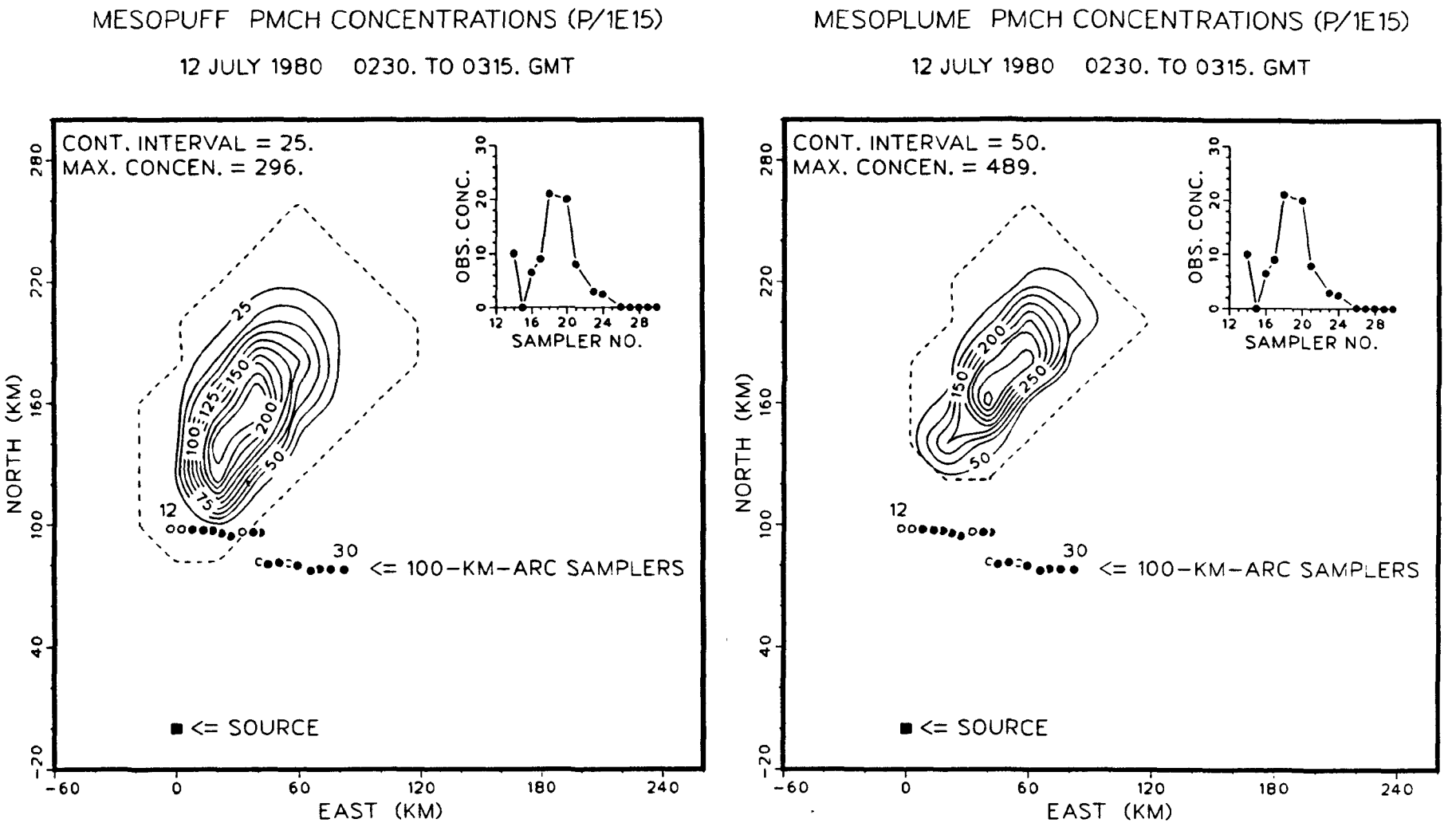

Figure E-88. Isopleth plot of ground-level concentrations for the Oklahoma experiment of July 12, 1980 (0230 to 0315 GMT) ... (left) MESOPUFF predictions, (right) MESOPLUME predictions.

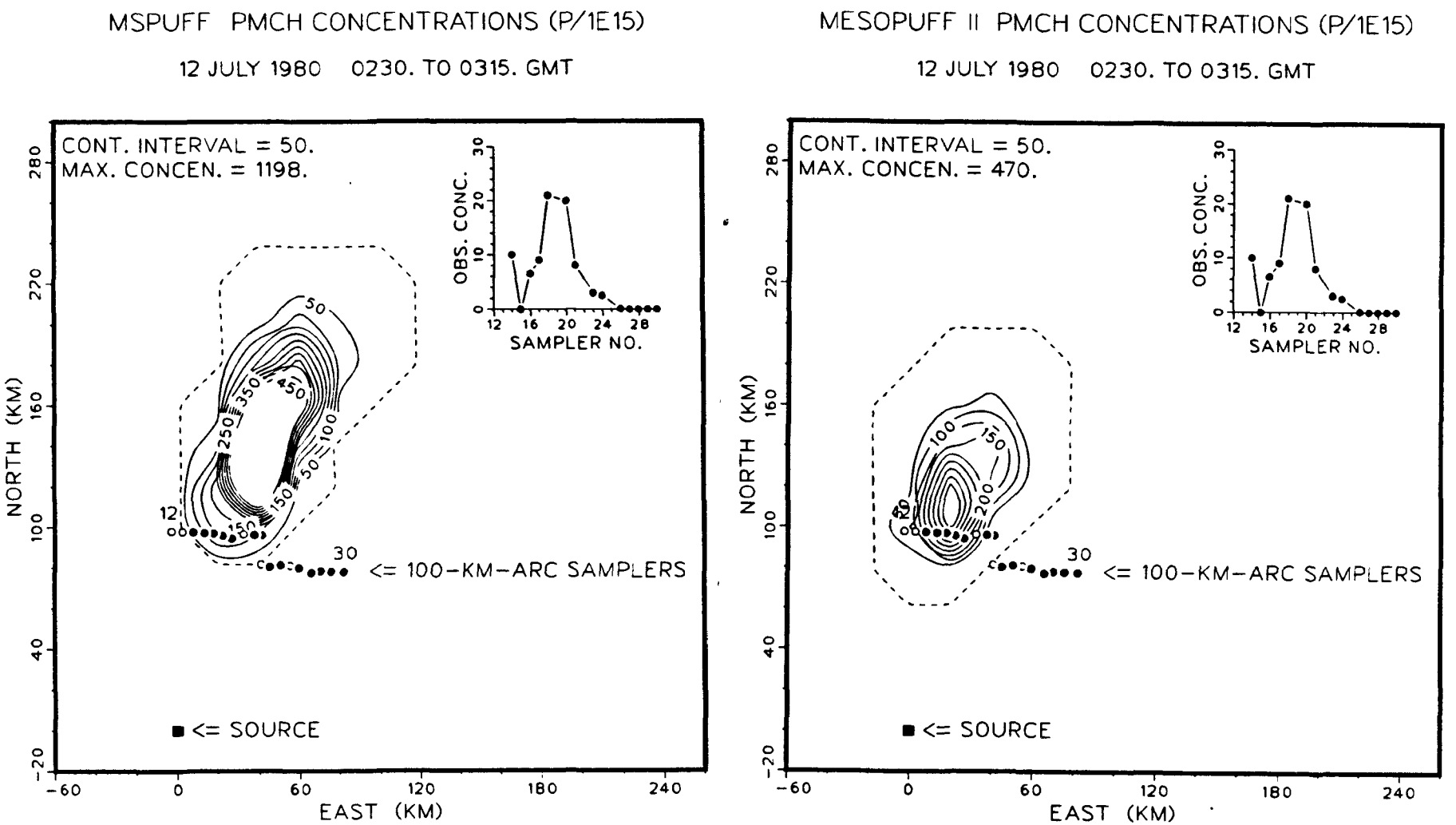

Figure E-89. Isopleth plot of ground-level concentrations for the Oklahoma experiment of July 12, 1980 (0230 to 0315 GMT) ... (left) MSPUFF predictions, (right) MESOPUFF II predictions.

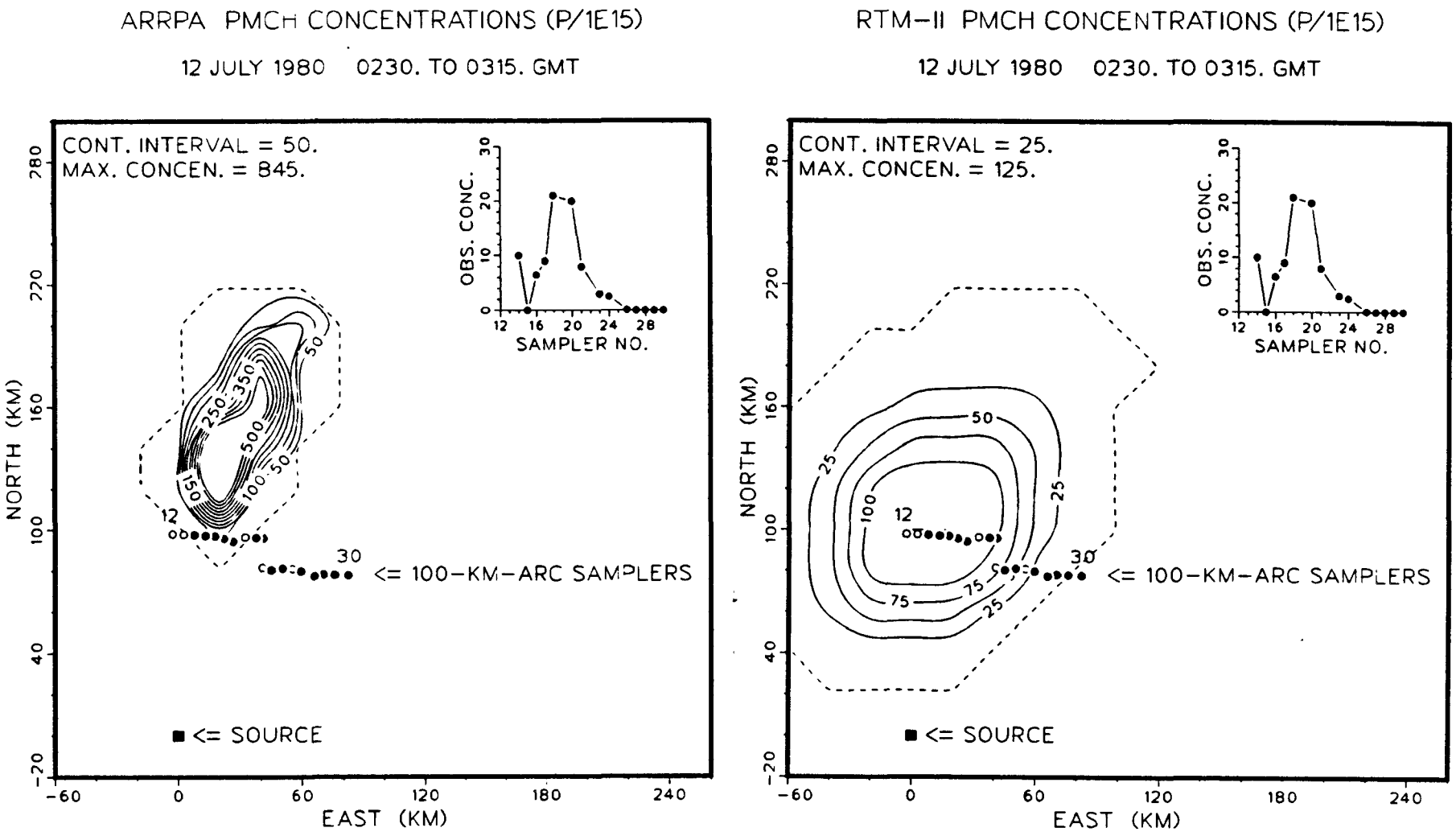

Figure E-90. Isopleth plot of ground-level concentrations for the Oklahoma experiment of July 12, 1980 (0230 to 0315 GMT) ... (left) ARRPA predictions, (right) RTM-II predictions.

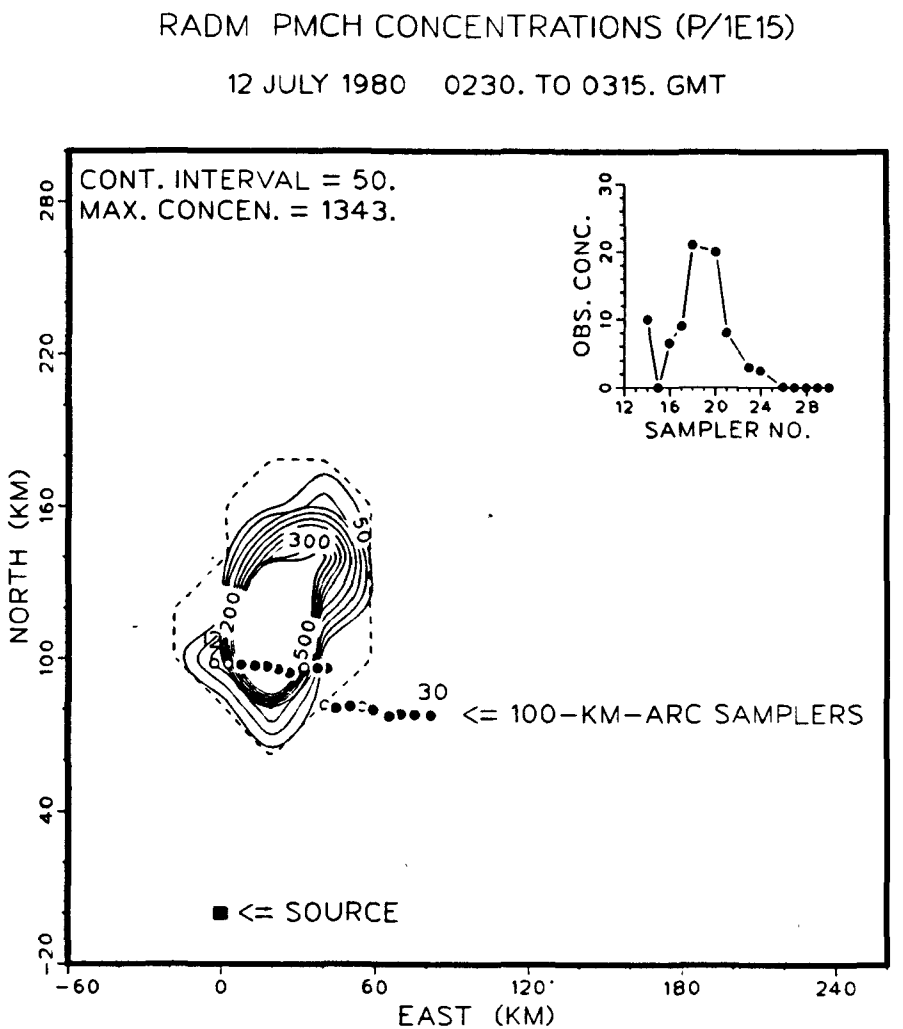

Figure E-91. Isopleth plot of ground-level concentrations for the Oklahoma experiment of July 12, 1980 (0230 to 0315 GMT) ... RADM predictions.

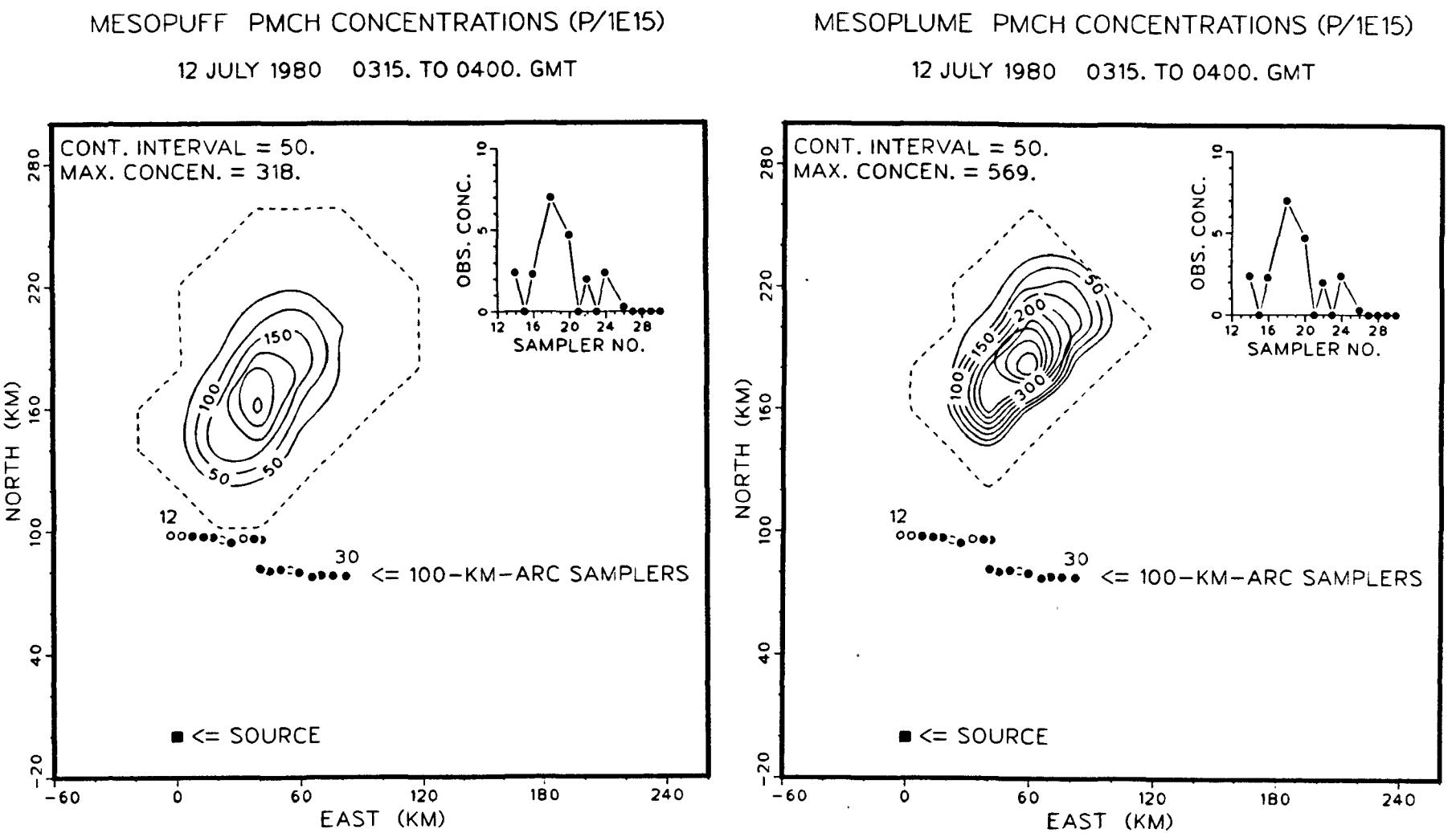

Figure E-92. Isopleth plot of ground-level concentrations for the Oklahoma experiment of July 12, 1980 (0315 to 0400 GMT) ... (left) MESOPUFF predictions, (right) MESOPLUME predictions.

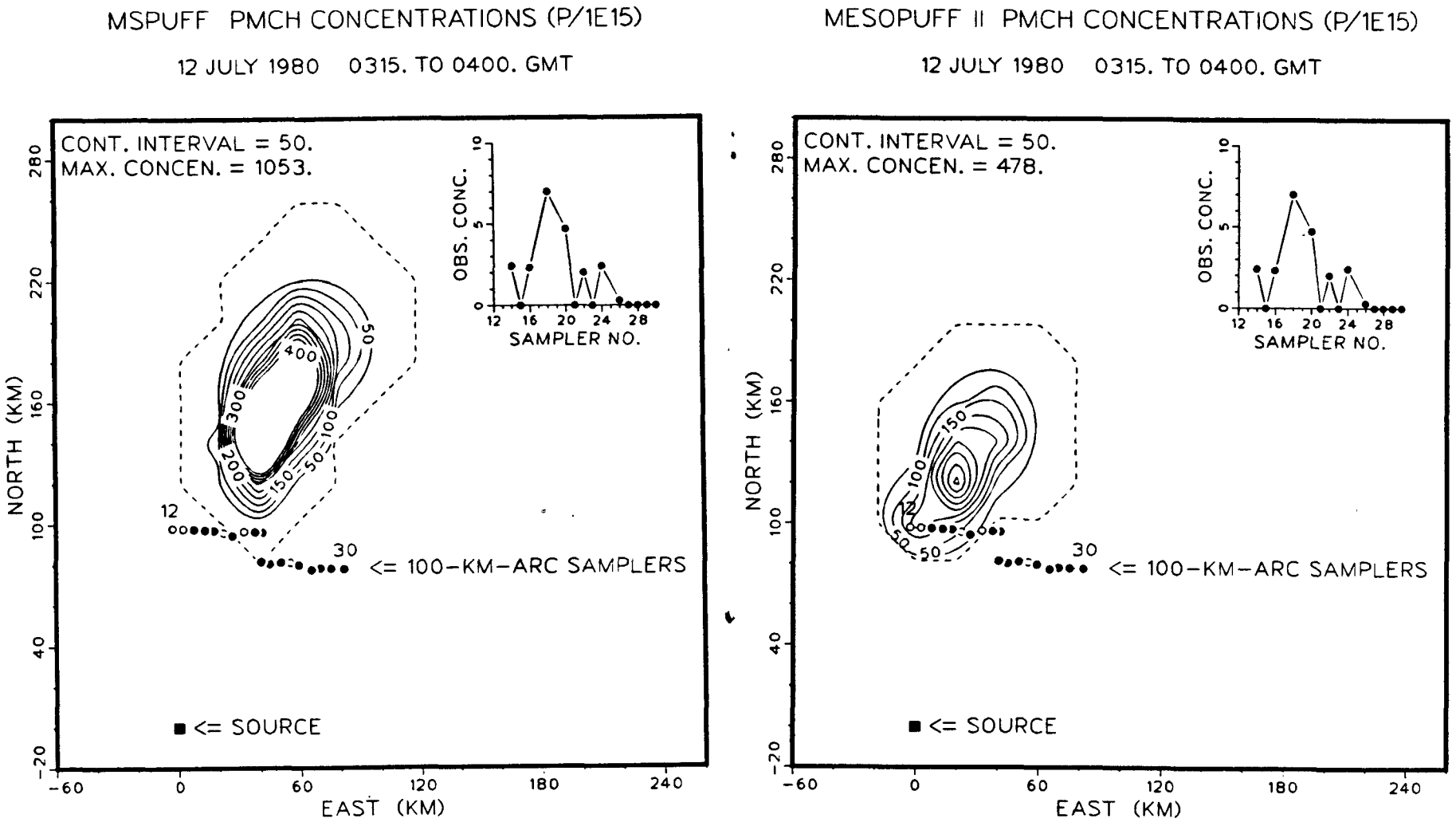

Figure E-93. Isopleth plot of ground-level concentrations for the Oklahoma experiment of July 12, 1980 (0315 to 0400 GMT) ... (left) MSPUFF predictions, (right) MESOPUFF II predictions.

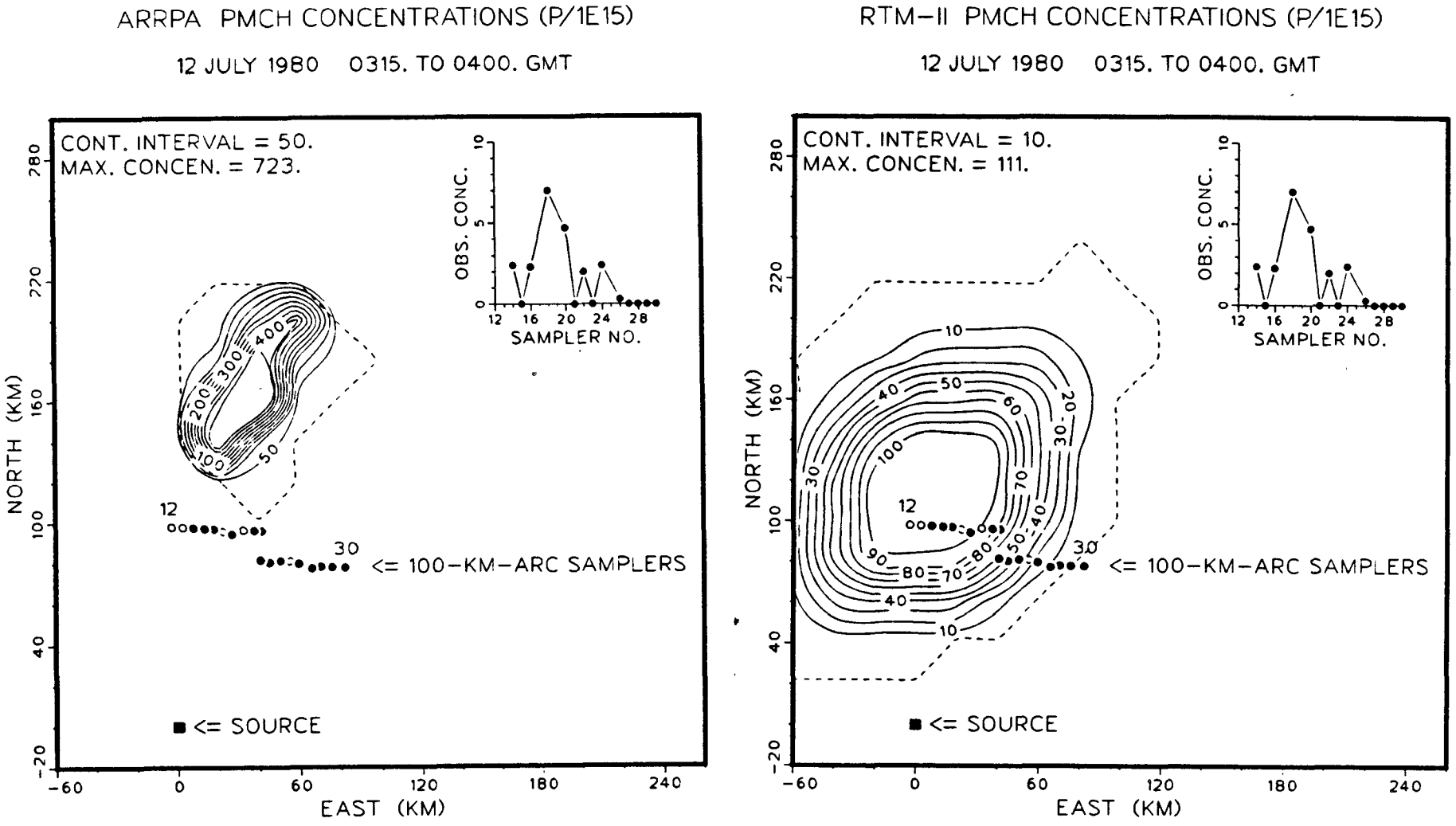

Figure E-94. Isopleth plot of ground-level concentrations for the Oklahoma experiment of July 12, 1980 (0315 to 0400 GMT) ... (left) ARRPA predictions, (right) RTM-II predictions.

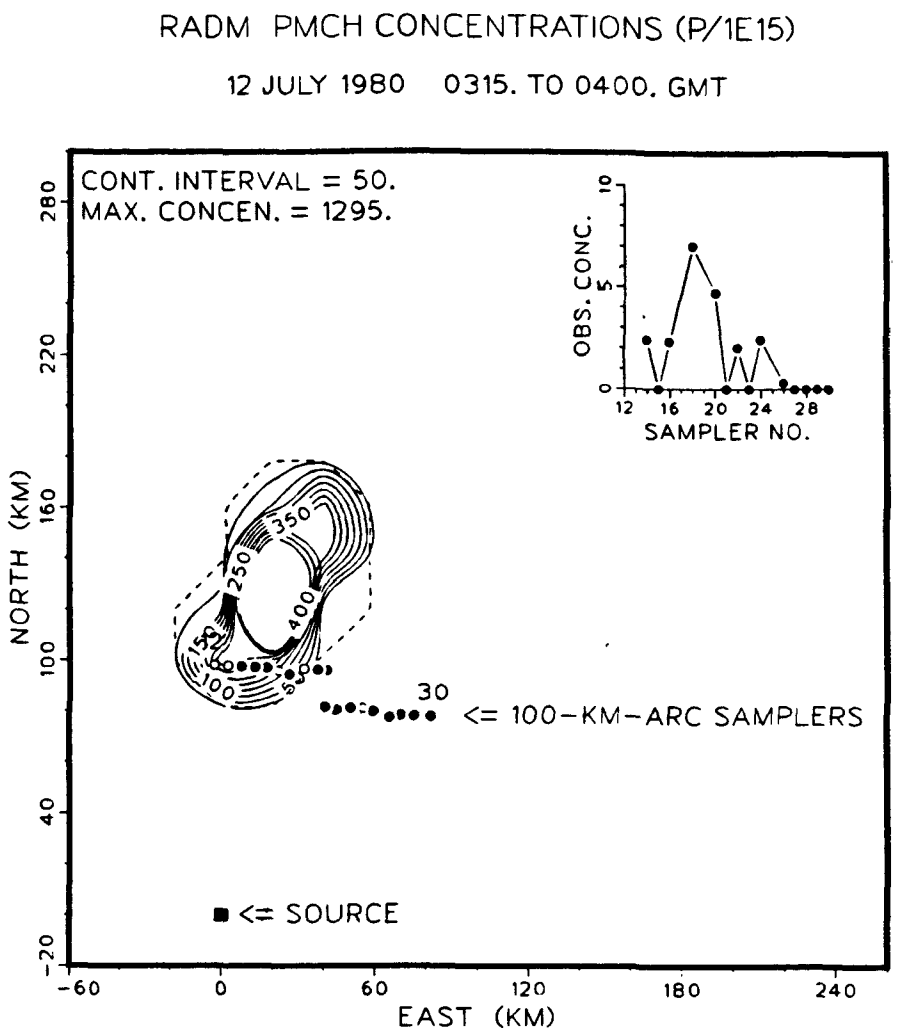

Figure E-95. Isopleth plot of ground-level concentrations for the Oklahoma experiment of July 12, 1980 (0315 to 0400 GMT) ... RADM predictions.

4. SUMMARY GRAPHICAL PLOTS COMPARING MODEL PREDICTIONS AND FIELD DATA AT OKLAHOMA

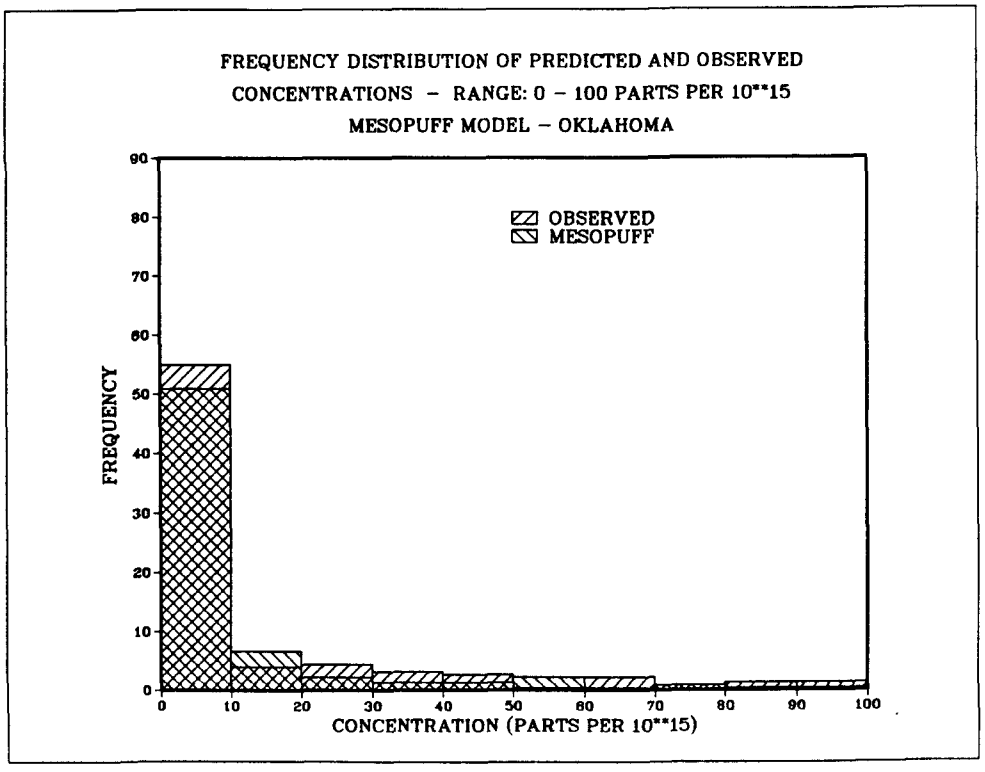

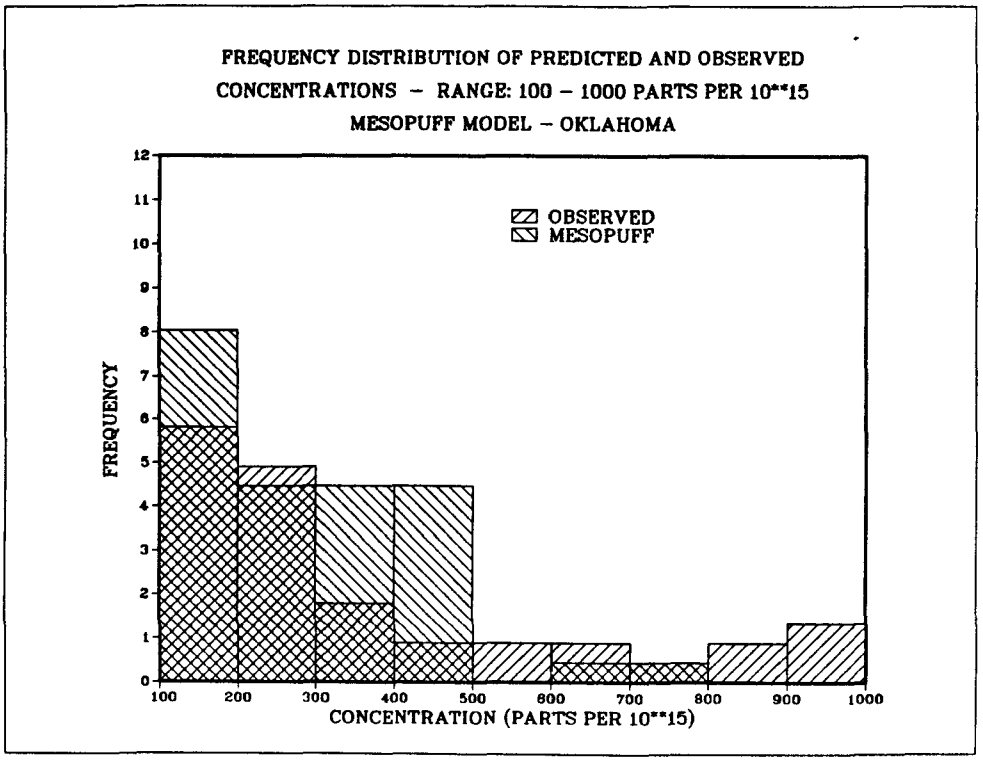

Figure E-96. Frequency distribution of predicted and observed concentrations at Oklahoma for MESOPUFF based on points paired in space and time ... (top) concentration range: 0 - 100 parts per 10^{15}, (bottom) concentration range: 100 - 1000 parts per 10^{15}.

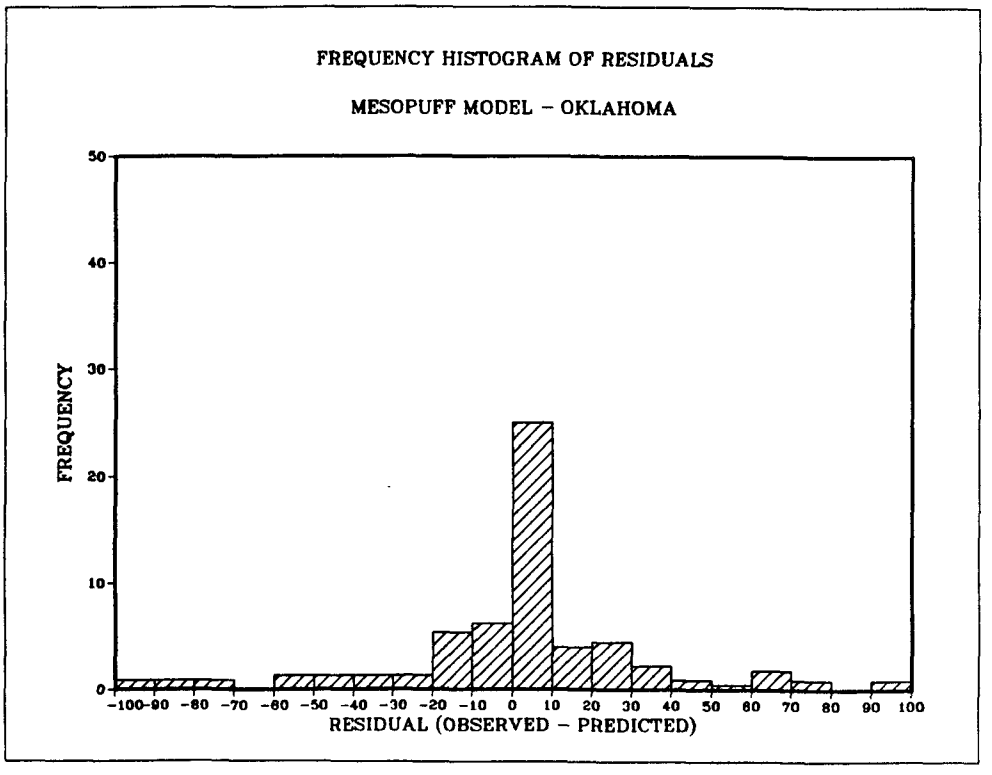

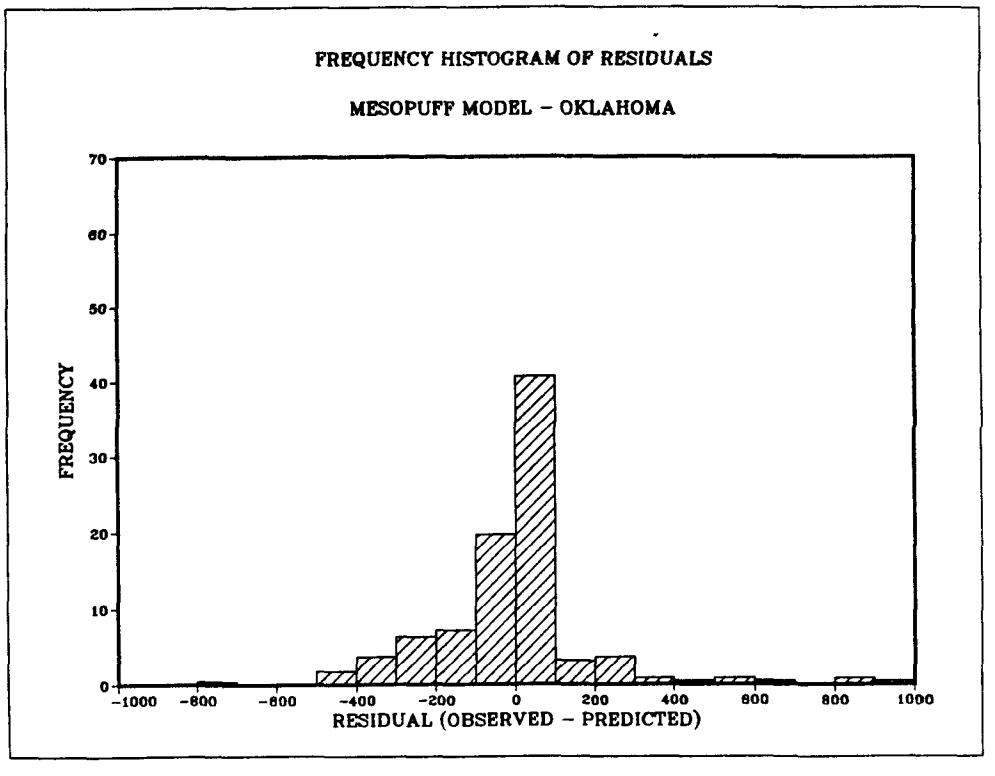

Figure E-97. Frequency distribution of residuals at Oklahoma for MESOPUFF based on points paired in space and time ...
(top) residual range: -100 to 100 parts per 10^{15},
(bottom) residual range· -1000 to 1000 parts per 10^{15}.

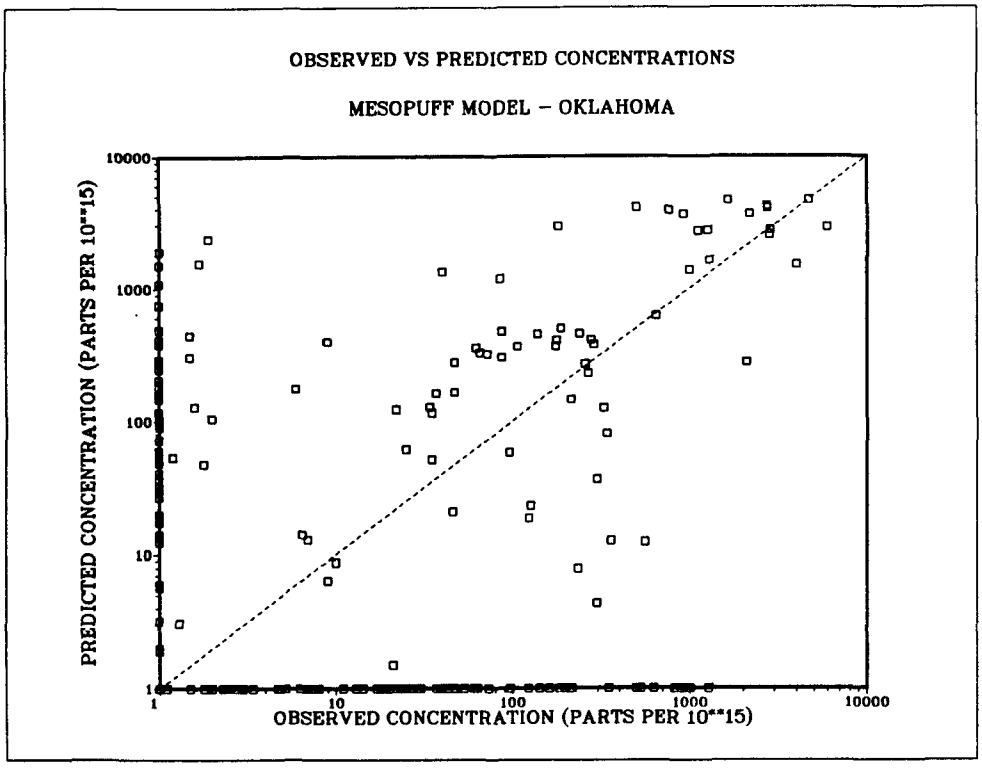

Figure E-98. Scatter plot of predicted and observed averaged concentrations at Oklahoma for MESOPUFF ... points paired in space and time.

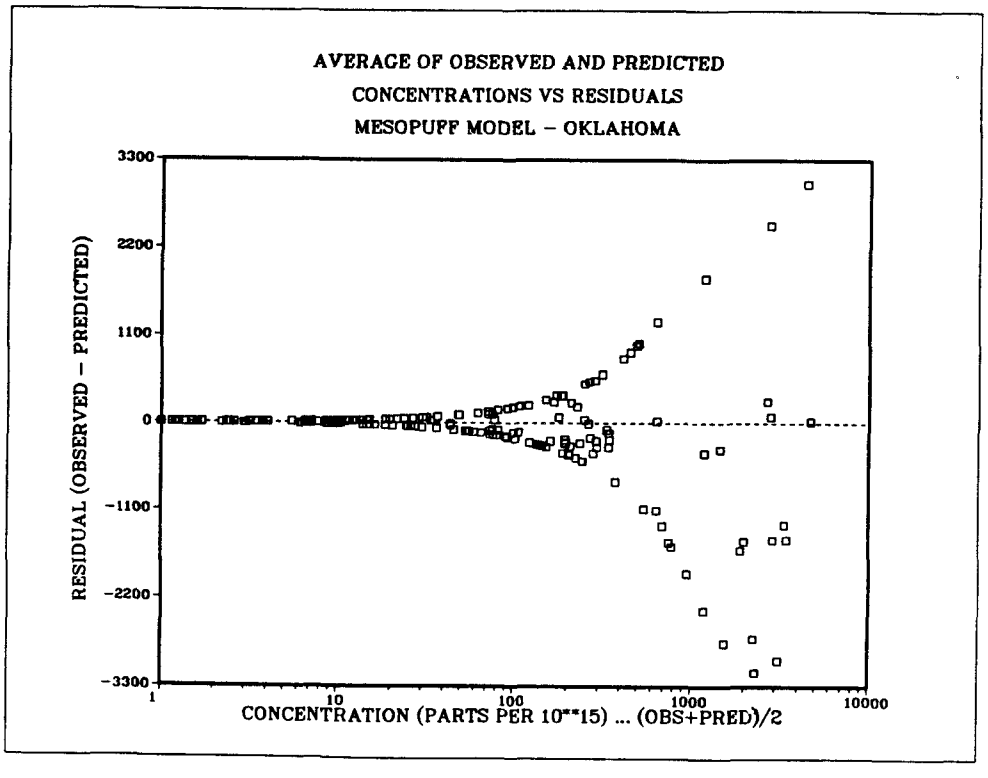

Figure E-99. Scatter plot of average of observed and predicted concentrations versus residuals at Oklahoma for MESOPUFF ... points paired in space and time.

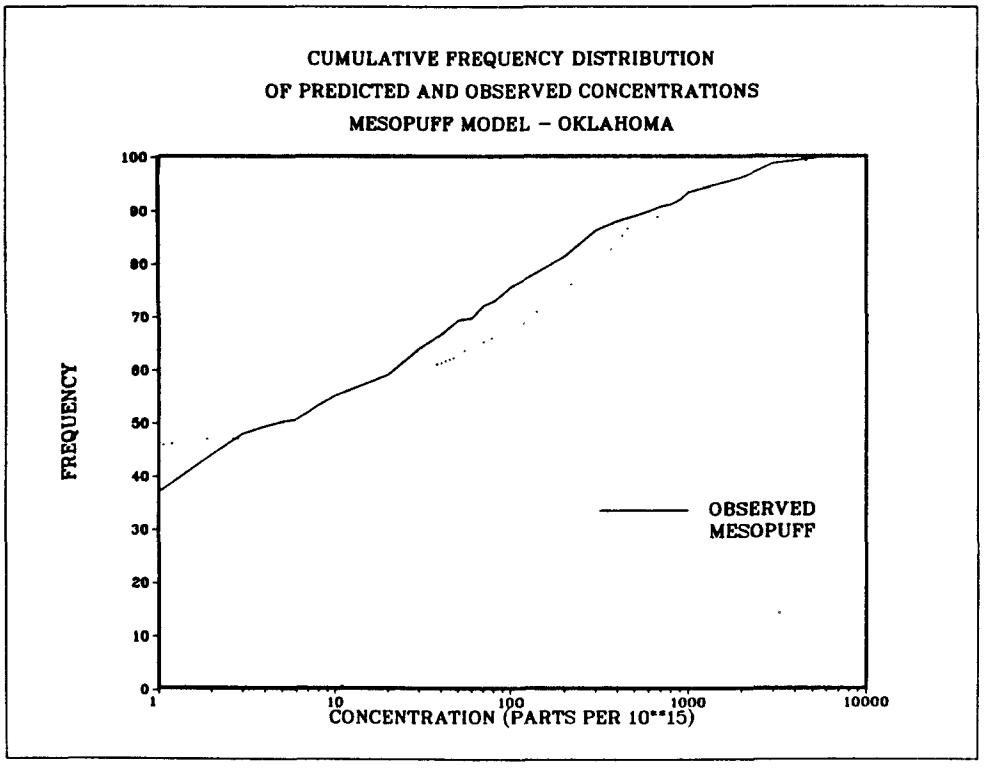

Figure E-100. Cumulative frequency distributions of MESOPUFF predictions and observed concentrations at Oklahoma based on points paired in space and time.

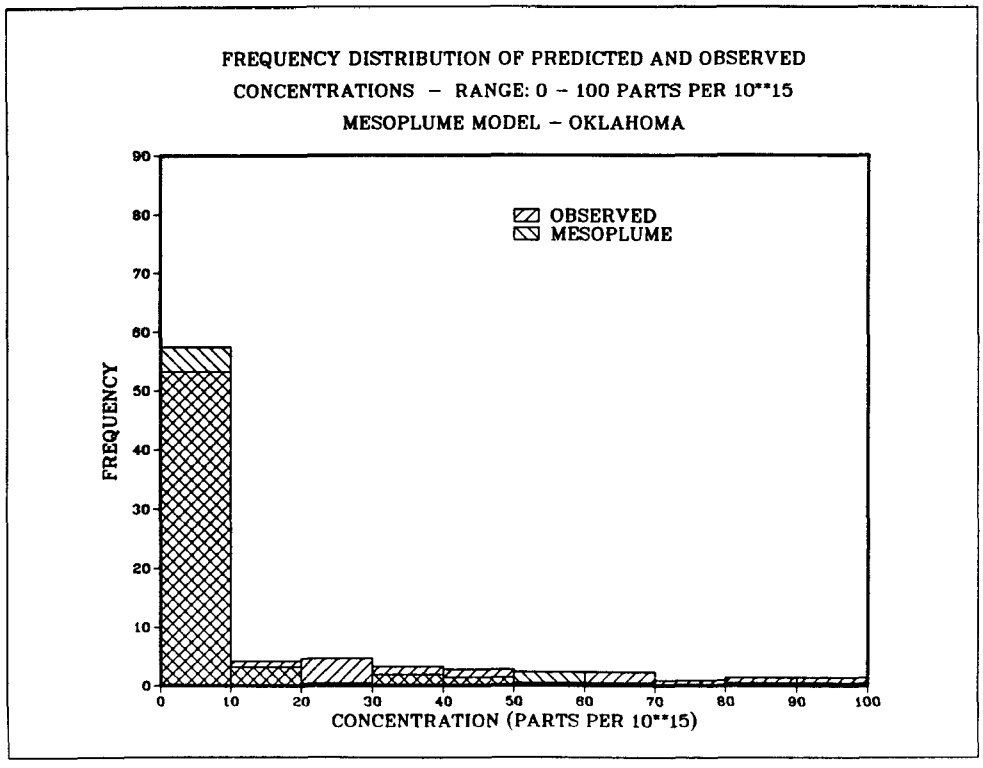

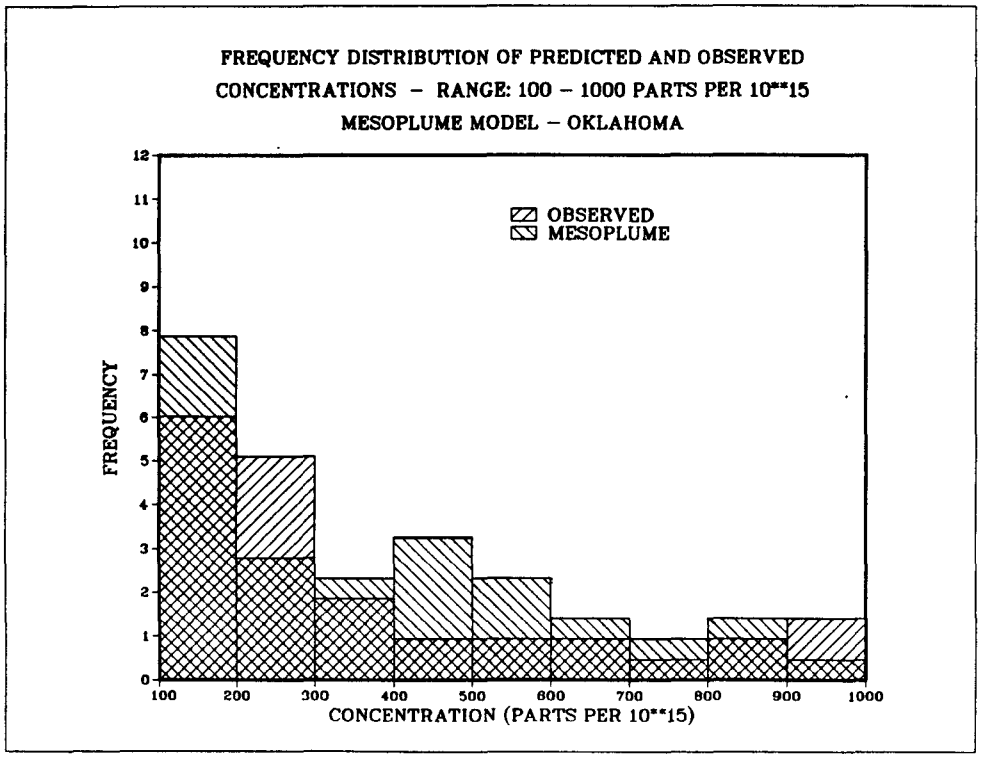

Figure E-101. Frequency distribution of predicted and observed concentrations at Oklahoma for MESOPLUME based on points paired in space and time ... (top) concentration range: 0 - 100 parts per 10^{15}, (bottom) concentration range: 100 - 1000 parts per 10^{15}.

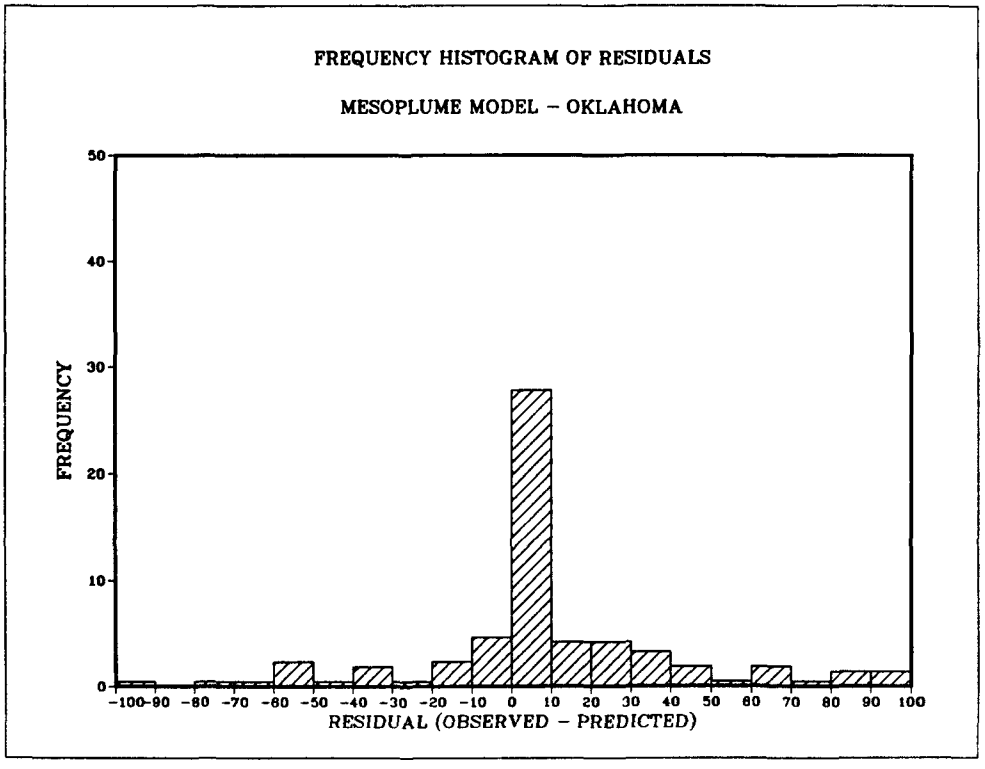

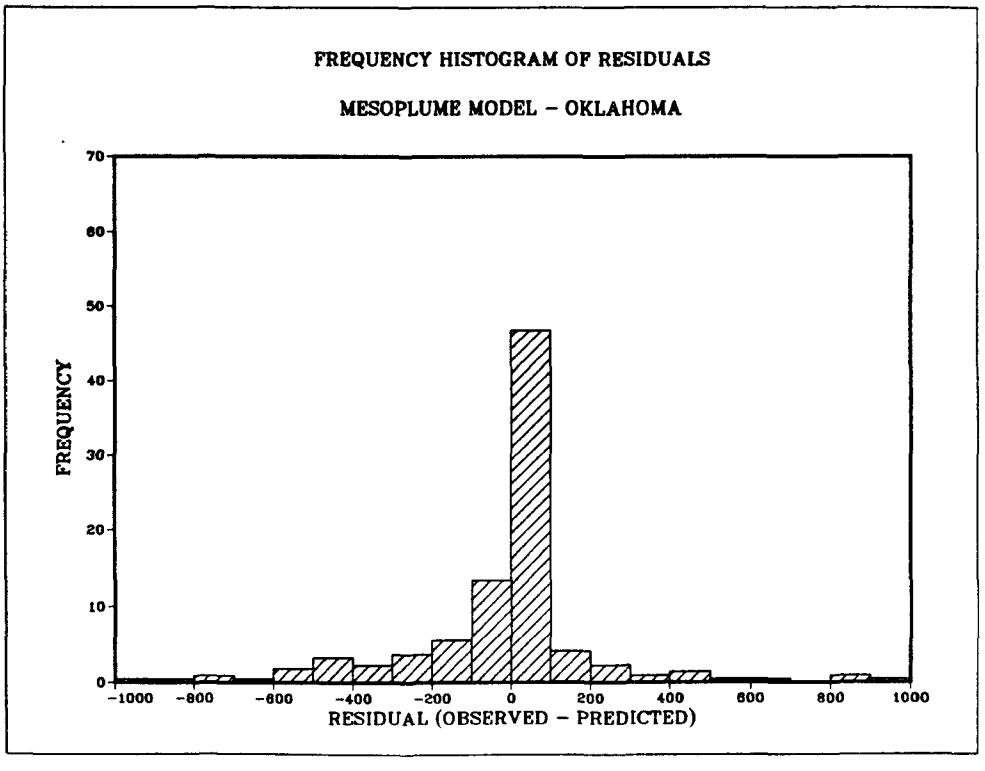

Figure E-102. Frequency distribution of residuals at Oklahoma for MESOPLUME based on points paired in space and time ...
(top) residual range: -100 to 100 parts per 10^{15},
(bottom) residual range: -1000 to 1000 parts per 10^{15}.

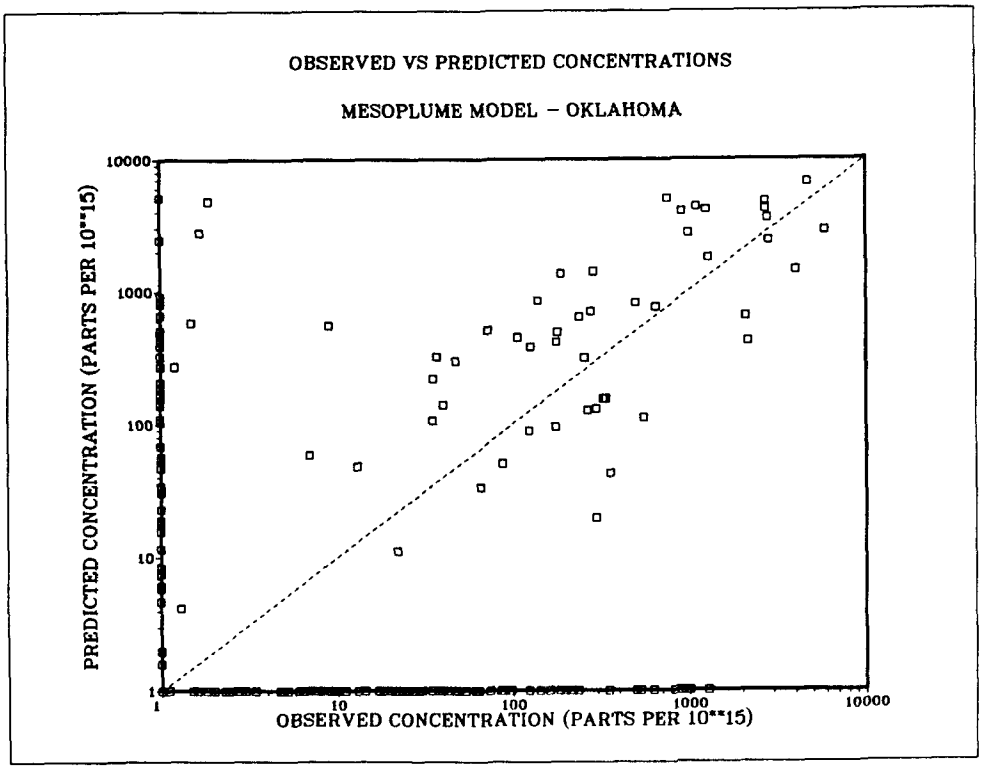

Figure E-103. Scatter plot of predicted and observed averaged concentrations at Oklahoma for MESOPLUME ... points paired in space and time.

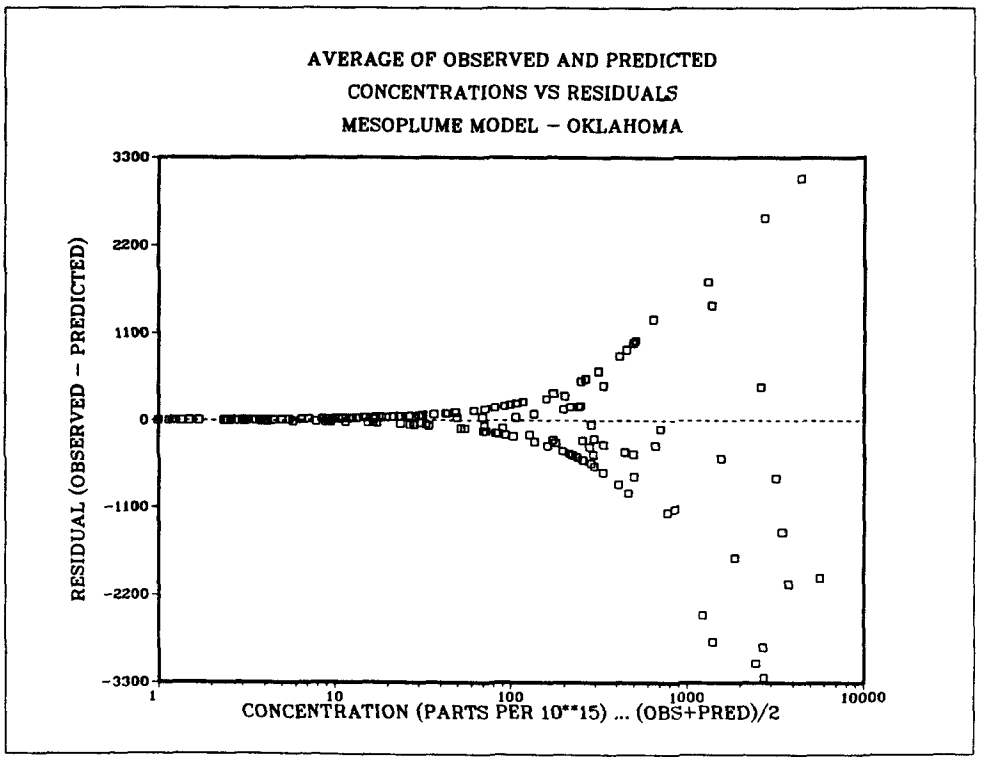

Figure E-104. Scatter plot of average of observed and predicted concentrations versus residuals at Oklahoma for MESOPLUME ... points paired in space and time.

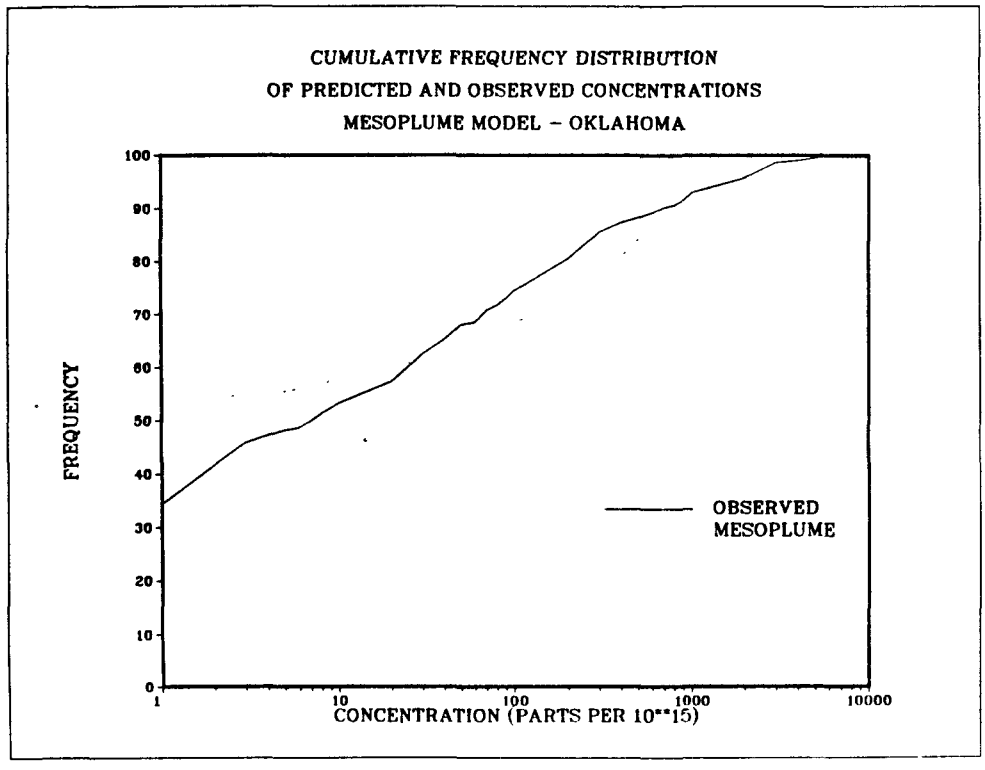

Figure E-105. Cumulative frequency distributions of MESOPLUME predictions and observed concentrations at Oklahoma based on points paired in space and time.

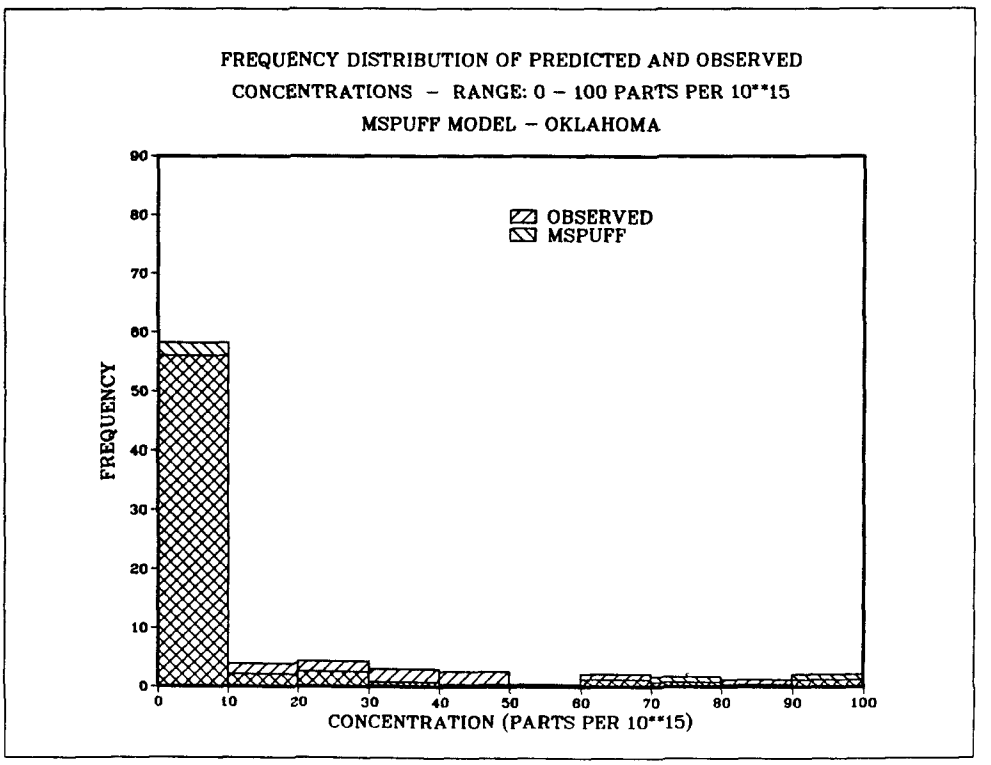

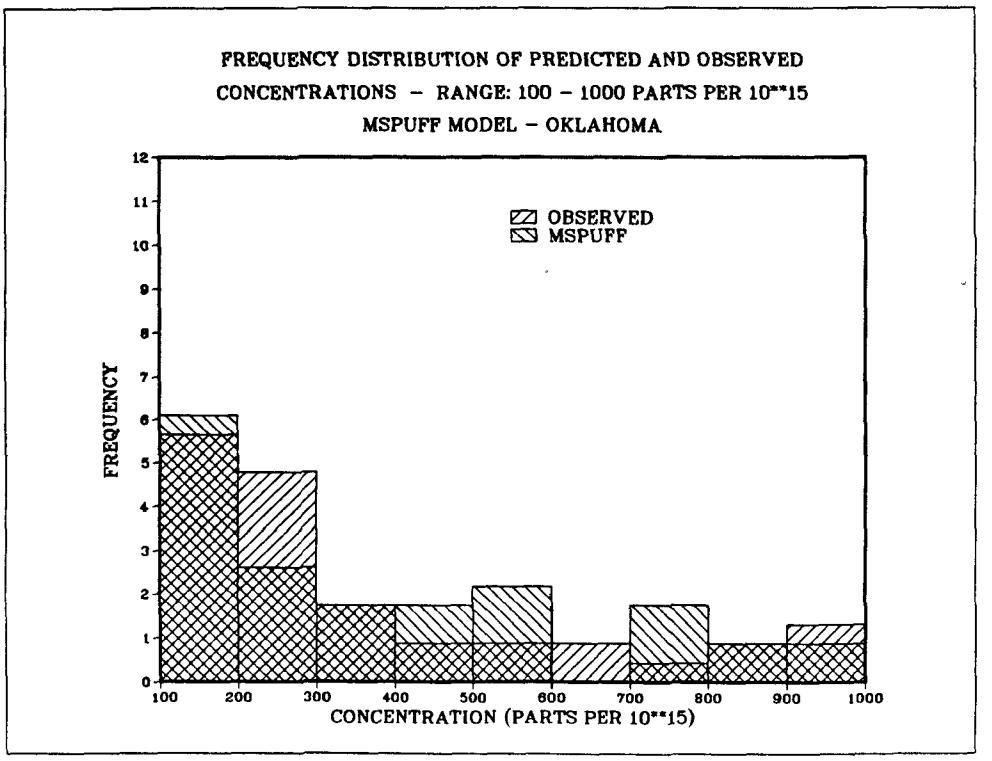

Figure E-106. Frequency distribution of predicted and observed concentrations at Oklahoma for MSPUFF based on points paired in space and time ... (top) concentration range: 0 - 100 parts per 10^{15}, (bottom) concentration range: 100 - 1000 parts per 10^{15}.

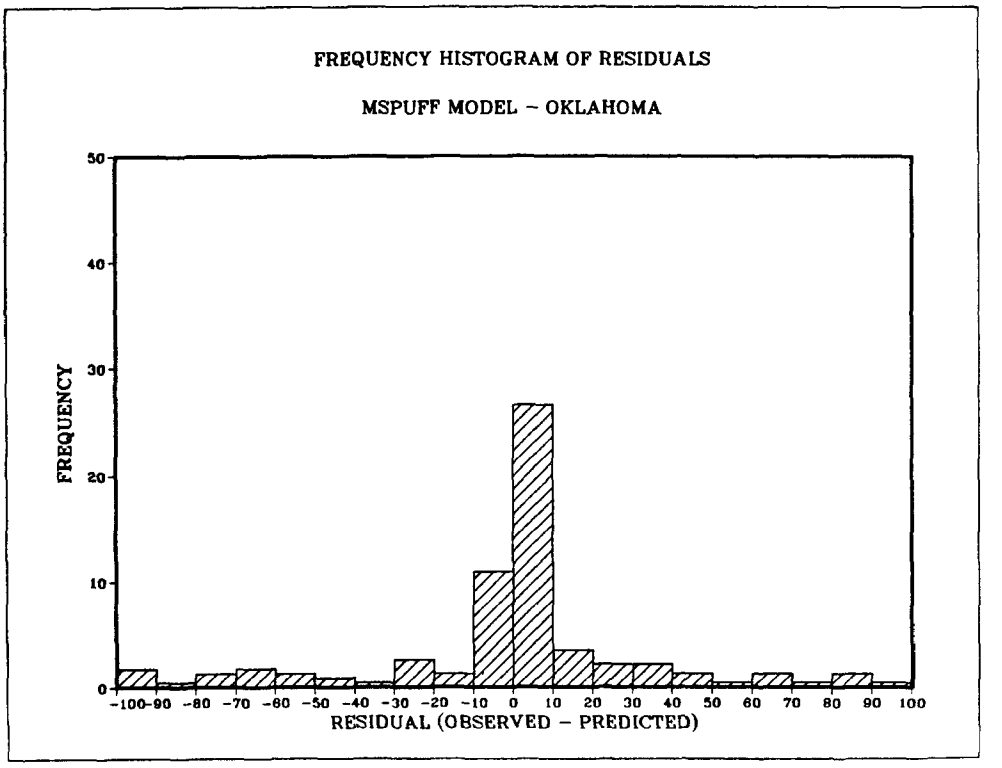

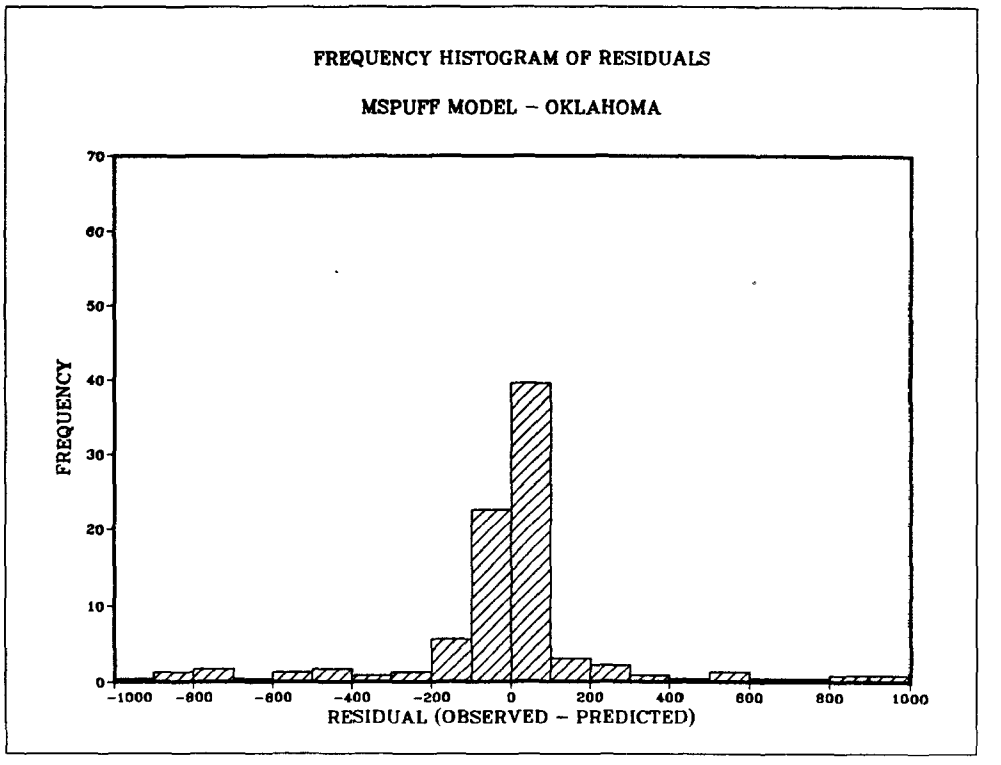

Figure E-107. Frequency distribution of residuals at Oklahoma for MSPUFF based on points paired in space and time ...
(top) residual range: -100 to 100 parts per 10^{15},
(bottom) residual range: -1000 to 1000 parts per 10^{15}.

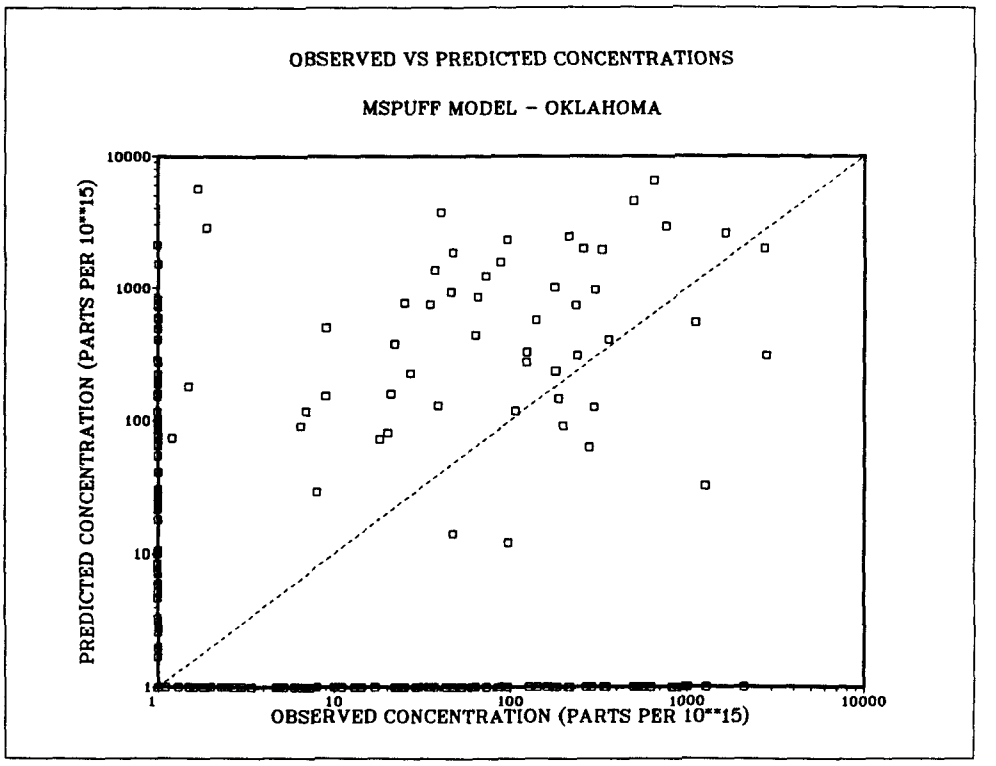

Figure E-108. Scatter plot of predicted and observed averaged concentrations at Oklahoma for MSPUFF ... points paired in space and time.

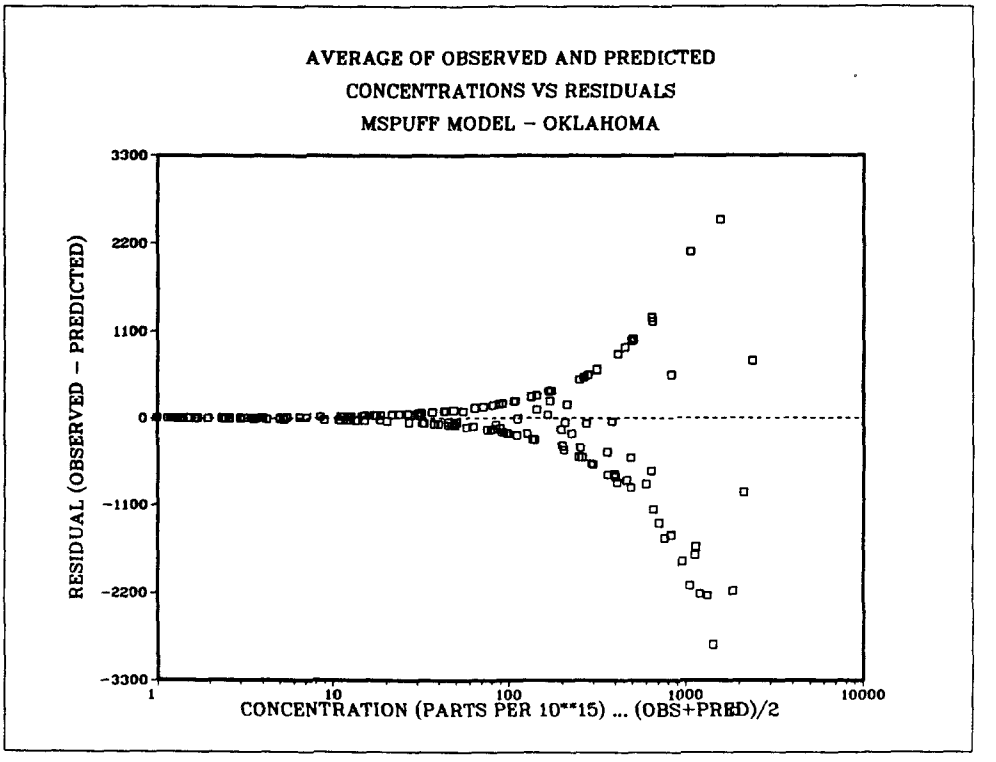

Figure E-109. Scatter plot of average of observed and predicted concentrations versus residuals at Oklahoma for MSPUFF ... points paired in space and time.

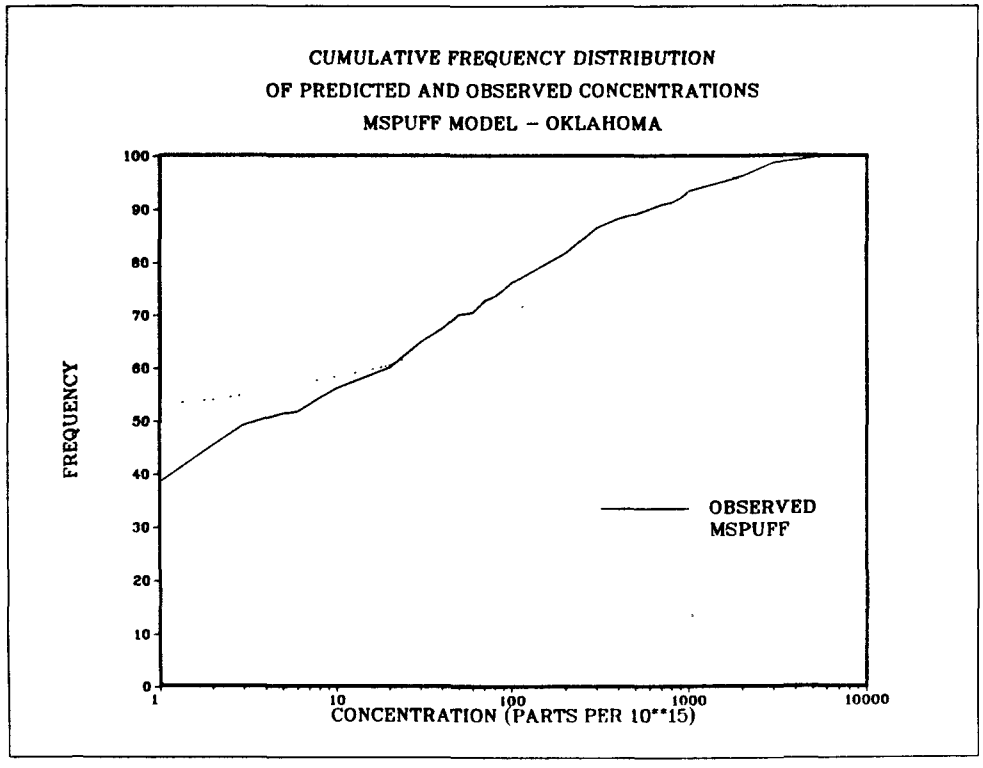

Figure E-110. Cumulative frequency distributions of MSPUFF predictions and observed concentrations at Oklahoma based on points paired in space and time.

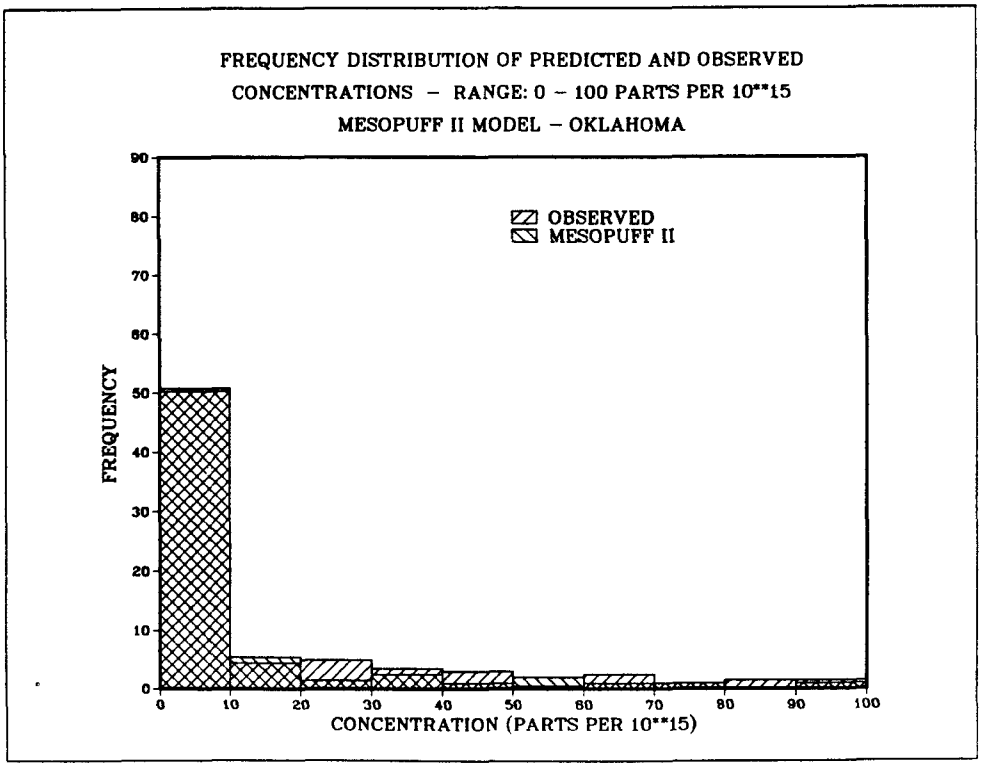

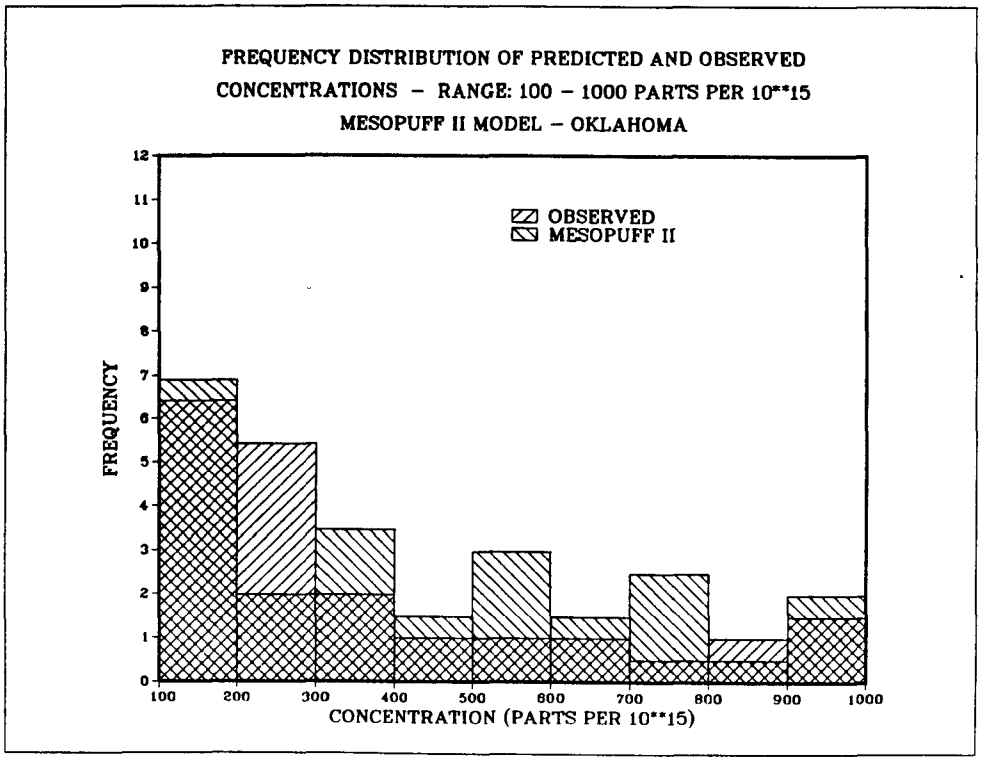

Figure E-111. Frequency distribution of predicted and observed concentrations at Oklahoma for MESOPUFF II based on points paired in space and time ... (top) concentration range: 0 - 100 parts per 10^{15}, (bottom) concentration range: 100 - 1000 parts per 10^{15}.

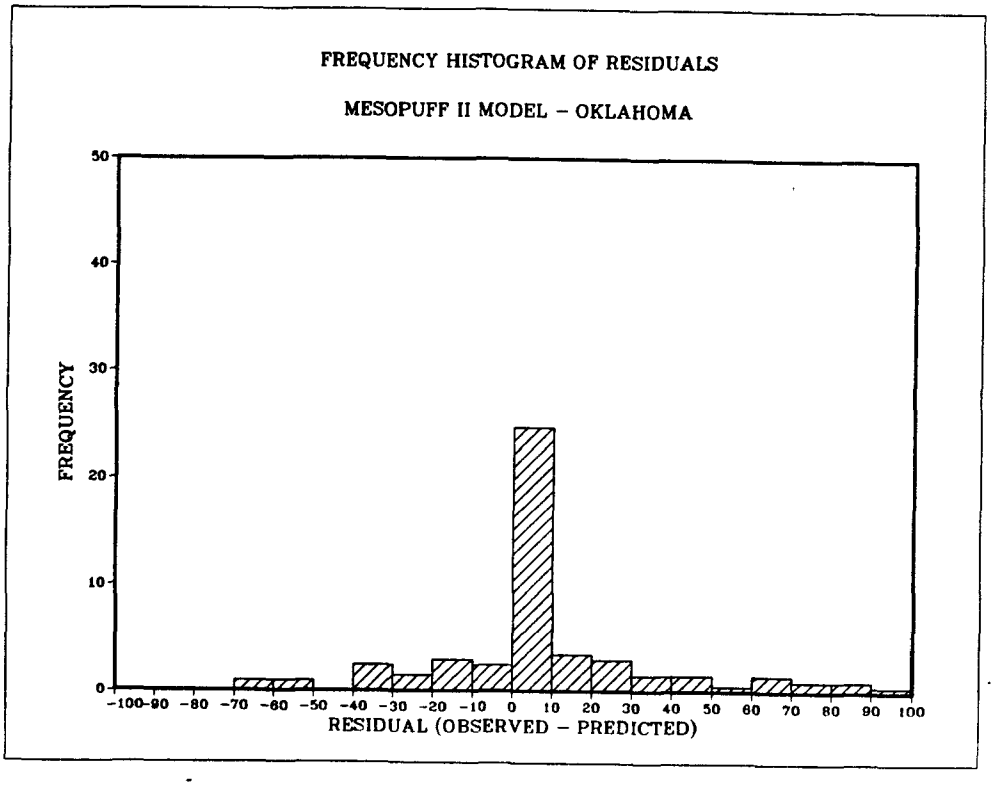

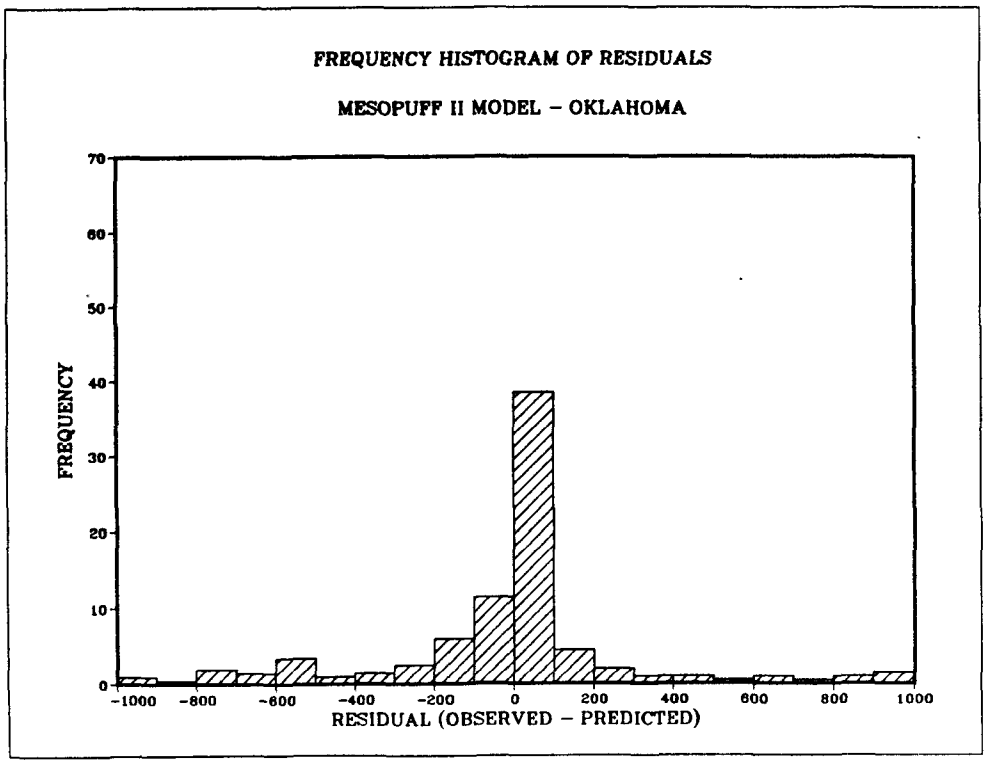

Figure E-112. Frequency distribution of residuals at Oklahoma for MESOPUFF II based on points paired in space and time ...
(top) residual range: -100 to 100 parts per 10^{15},
(bottom) residual range: -1000 to 1000 parts per 10^{15}.

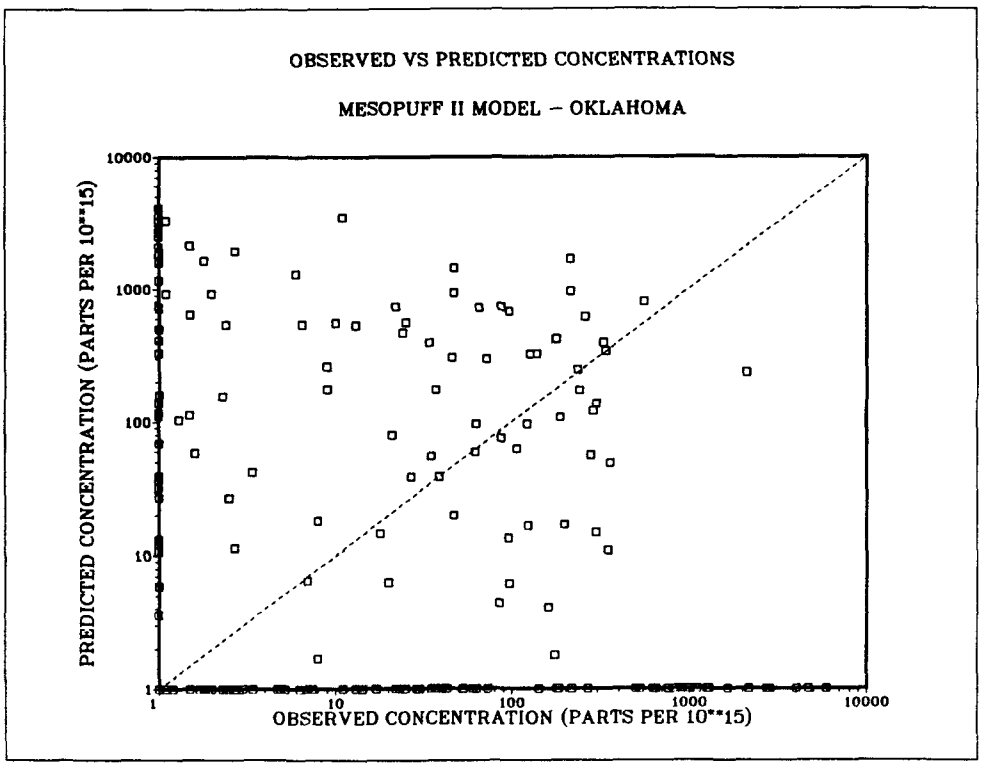

Figure E-113. Scatter plot of predicted and observed averaged concentrations at Oklahoma for MESOPUFF II ... points paired in space and time.

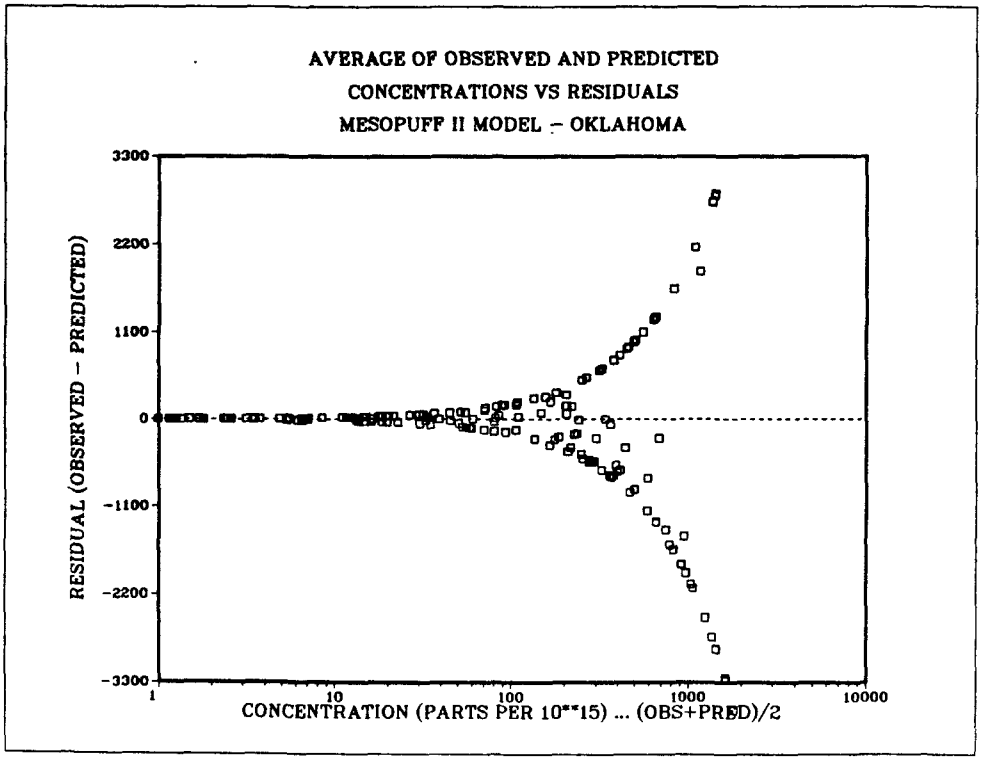

Figure E-114. Scatter plot of average of observed and predicted concentrations versus residuals at Oklahoma for MESOPUFF II ... points paired in space and time.

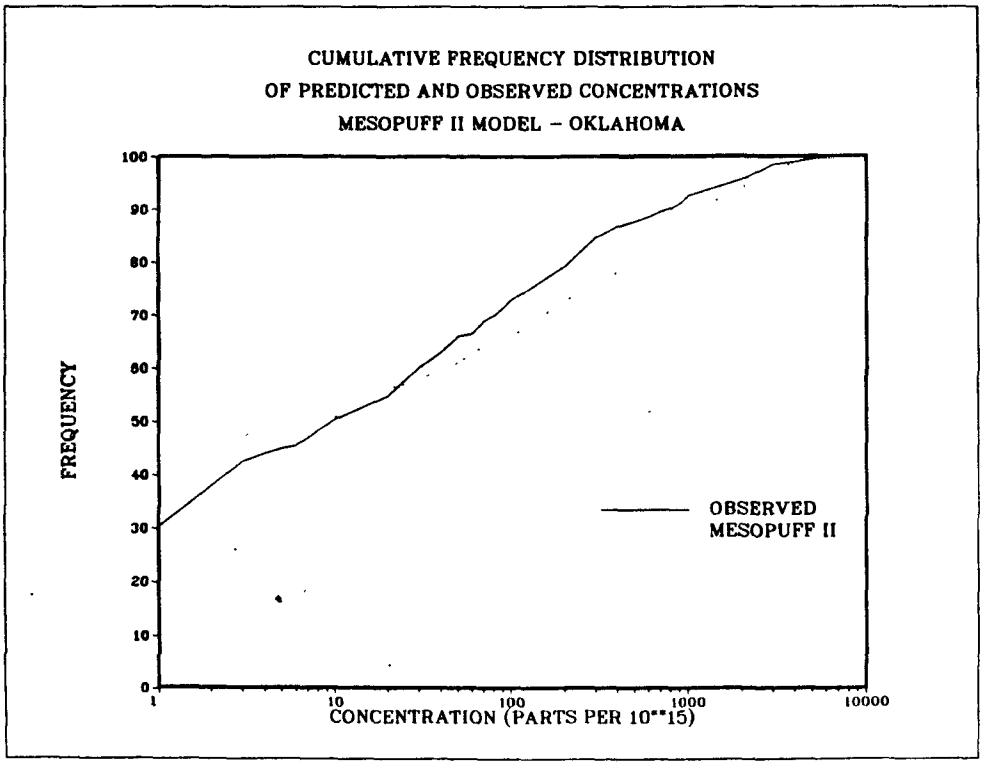

Figure E-115. Cumulative frequency distributions of MESOPUFF II predictions and observed concentrations at Oklahoma based on points paired in space and time.

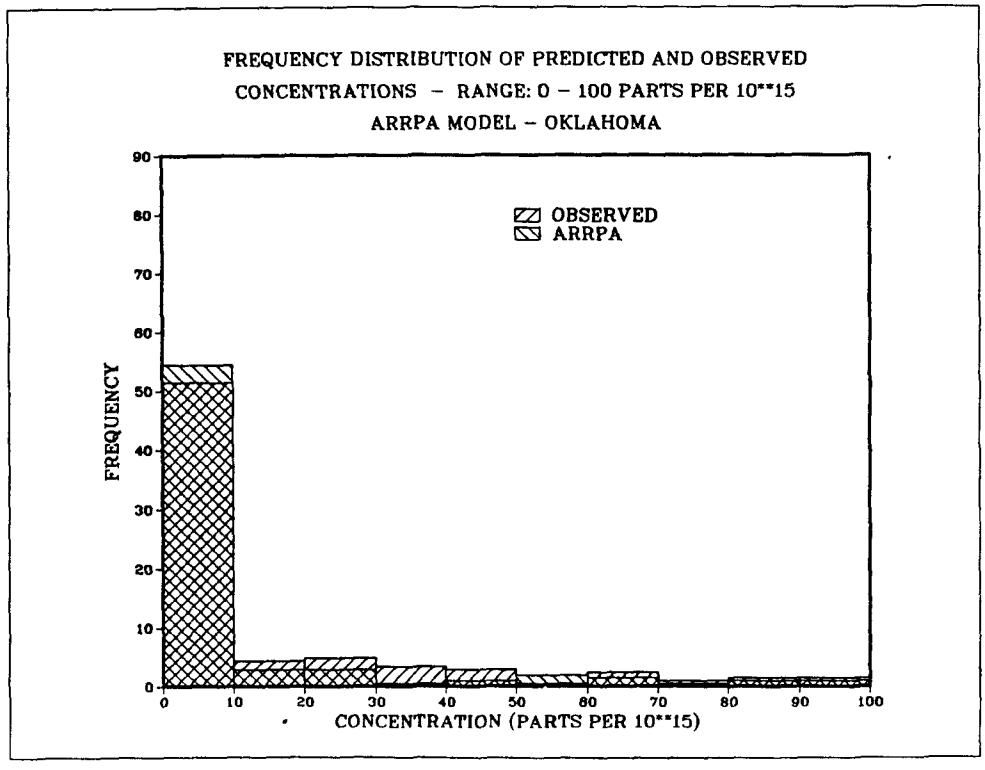

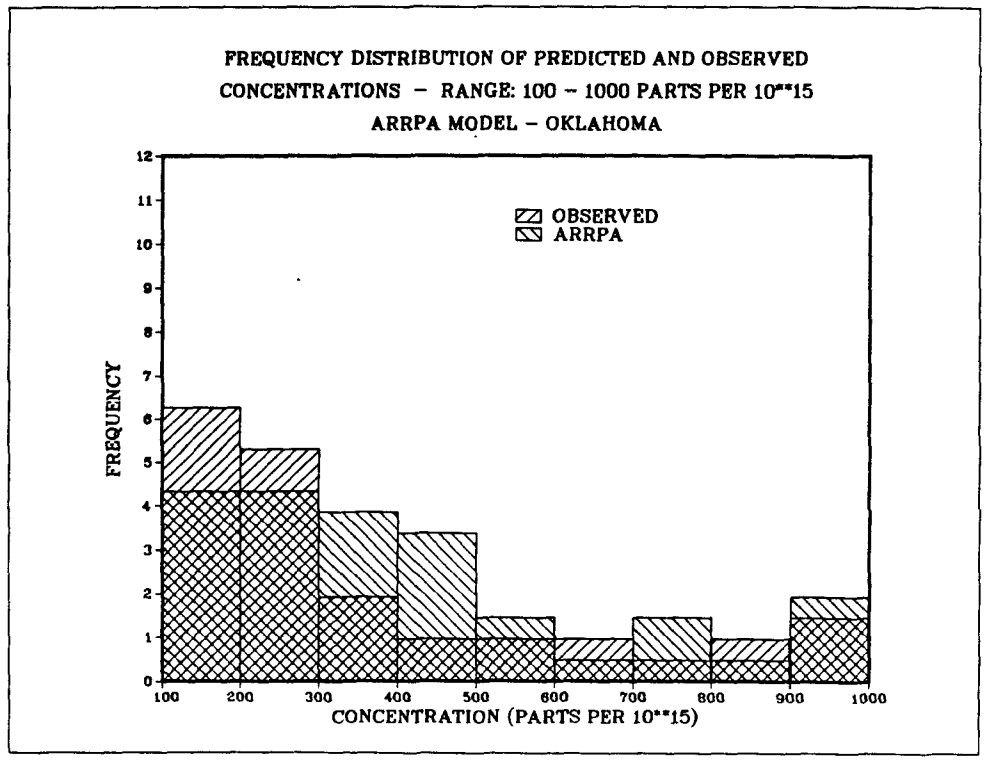

Figure E-116. Frequency distribution of predicted and observed concentrations at Oklahoma for ARRPA based on points paired in space and time ... (top) concentration range: 0 - 100 parts per 10^{15}, (bottom) concentration range: 100 - 1000 parts per 10^{15}.

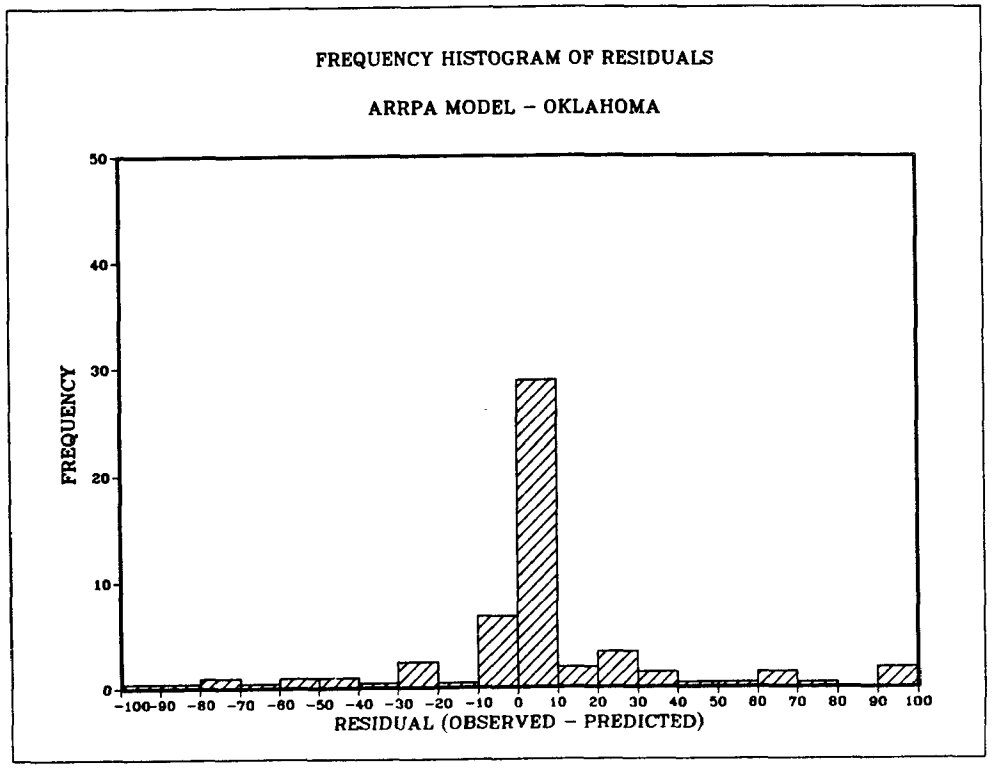

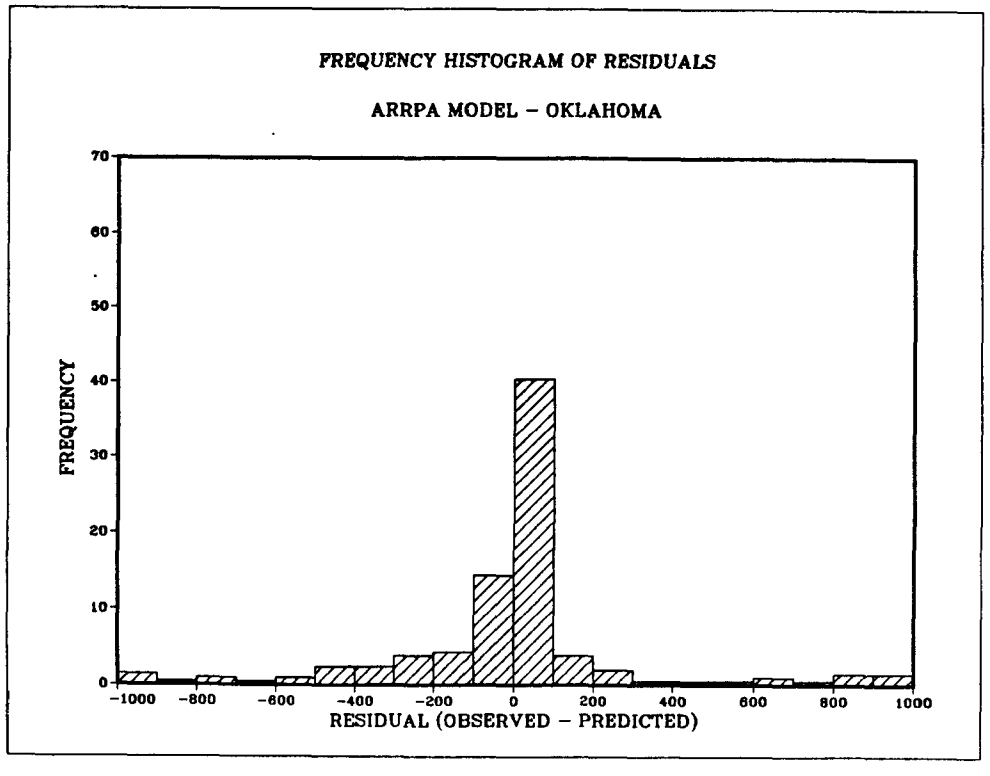

Figure E-117. Frequency distribution of residuals at Oklahoma for ARRPA based on points paired in space and time ...
(top) residual range: -100 to 100 parts per 10^{15},
(bottom) residual range: -1000 to 1000 parts per 10^{15}.

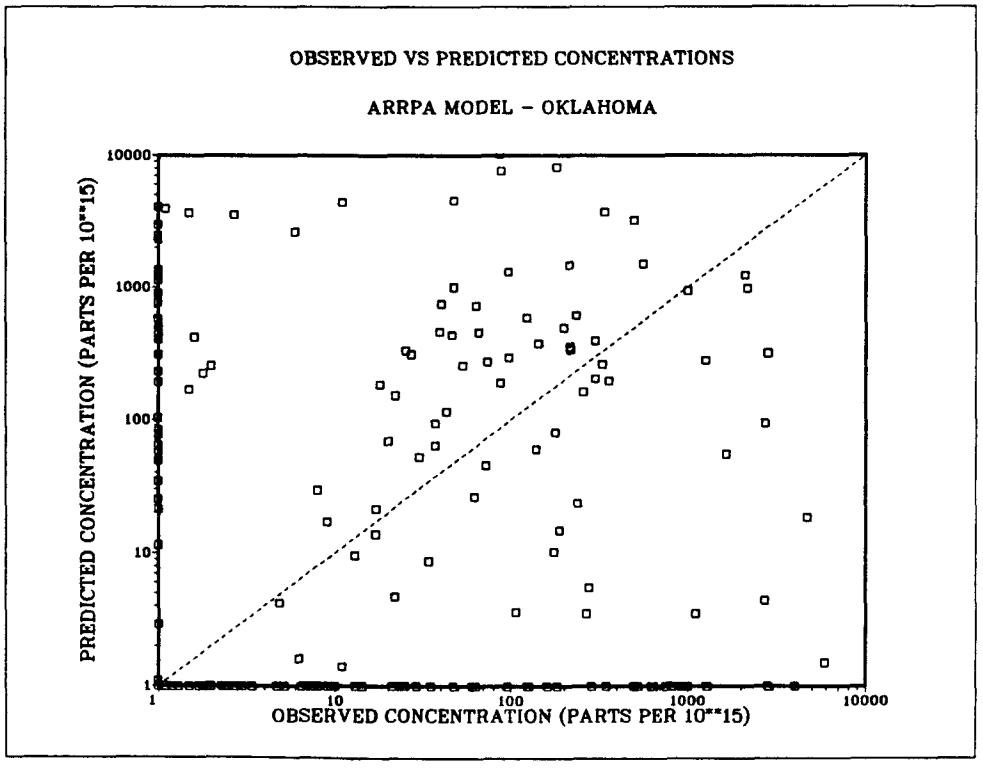

Figure E-118. Scatter plot of predicted and observed averaged concentrations at Oklahoma for ARRPA ... points paired in space and time.

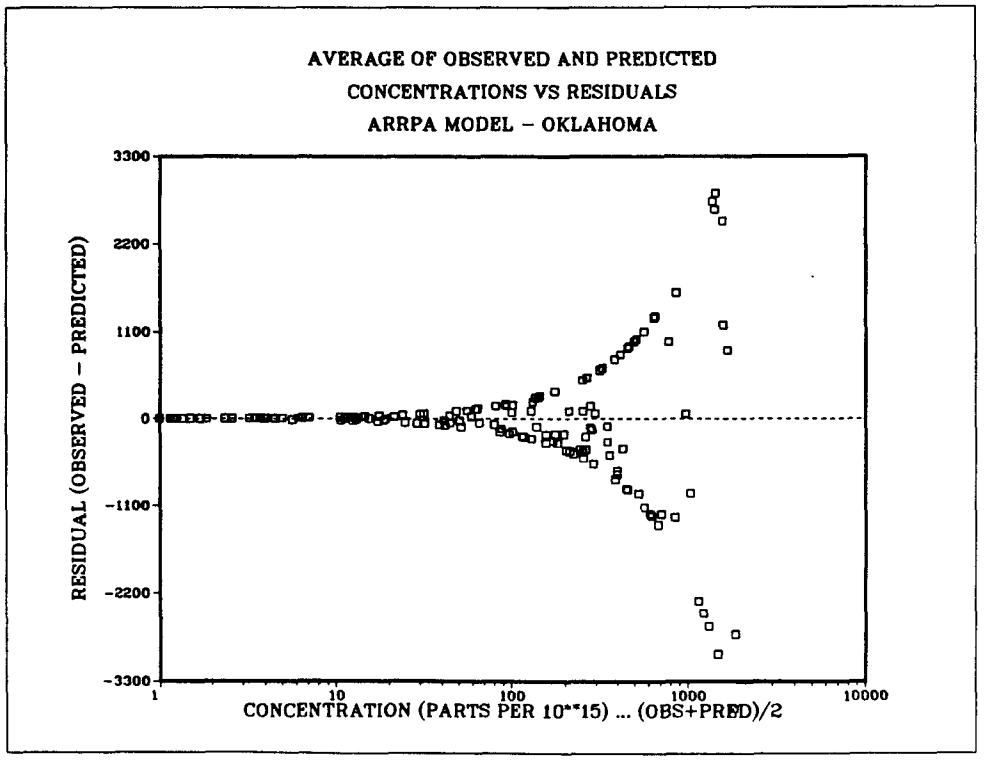

Figure E-119. Scatter plot of average of observed and predicted concentrations versus residuals at Oklahoma for ARRPA ... points paired in space and time.

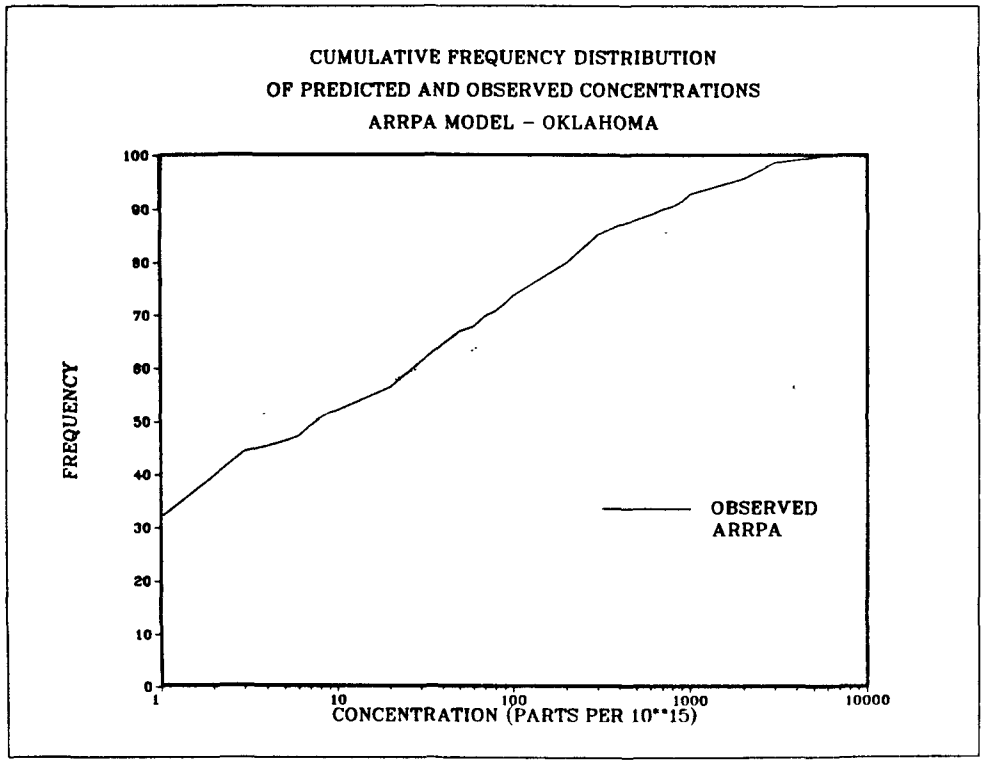

Figure E-120. Cumulative frequency distributions of ARRPA predictions and observed concentrations at Oklahoma based on points paired in space and time.

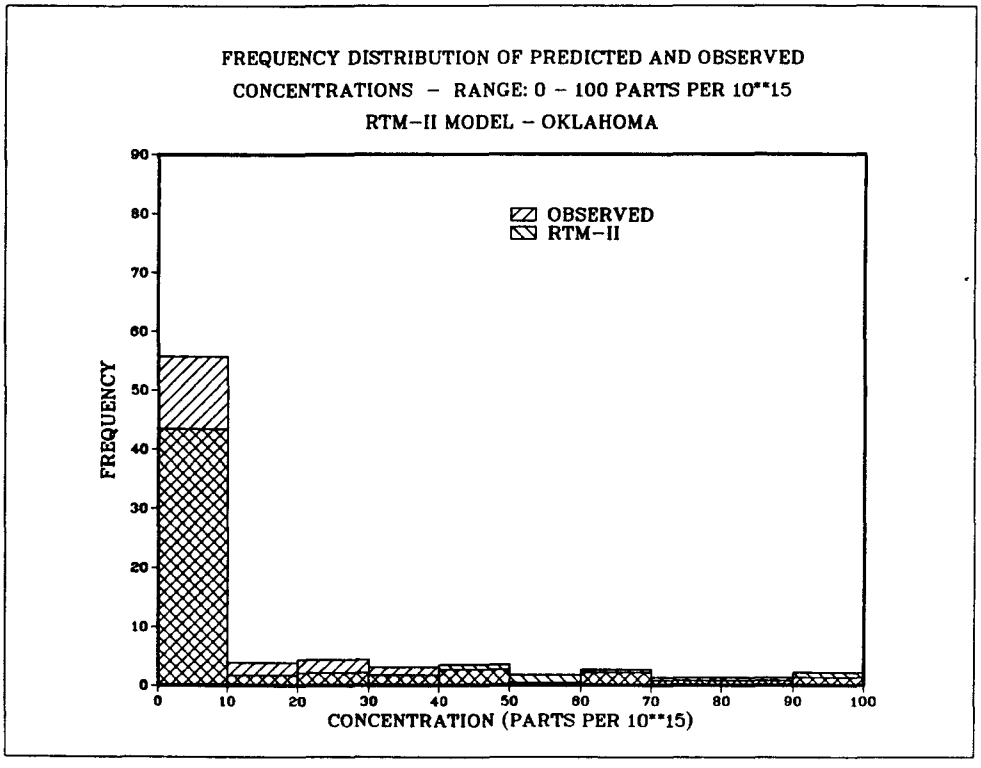

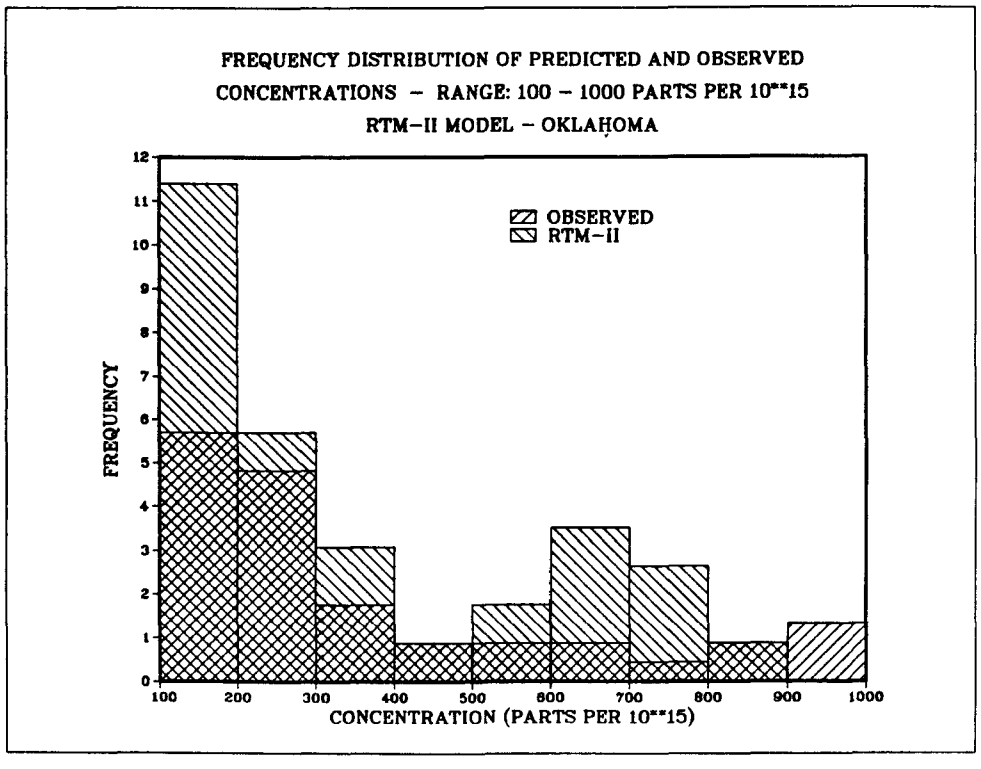

Figure E-121. Frequency distribution of predicted and observed concentrations at Oklahoma for RTM-II based on points paired in space and time ... (top) concentration range: 0 - 100 parts per 10^{15}, (bottom) concentration range: 100 - 1000 parts per 10^{15}.

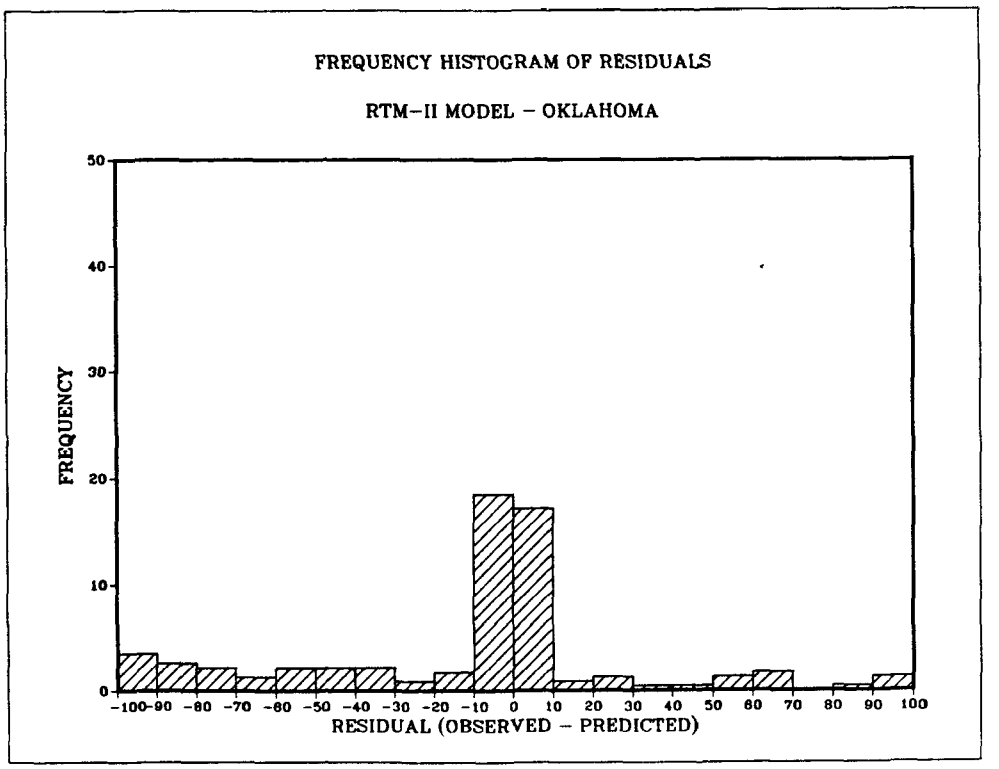

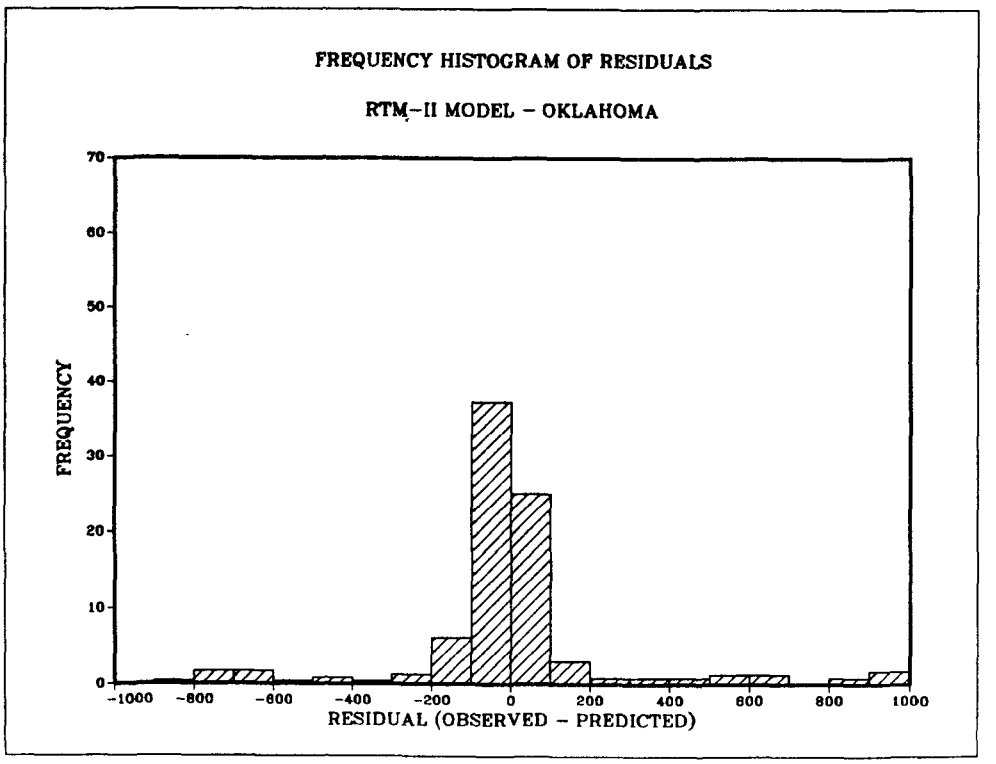

Figure E-122. Frequency distribution of residuals at Oklahoma for RTM-II based on points paired in space and time ...
(top) residual range: -100 to 100 parts per 10^{15},
(bottom) residual range: -1000 to 1000 parts per 10^{15}.

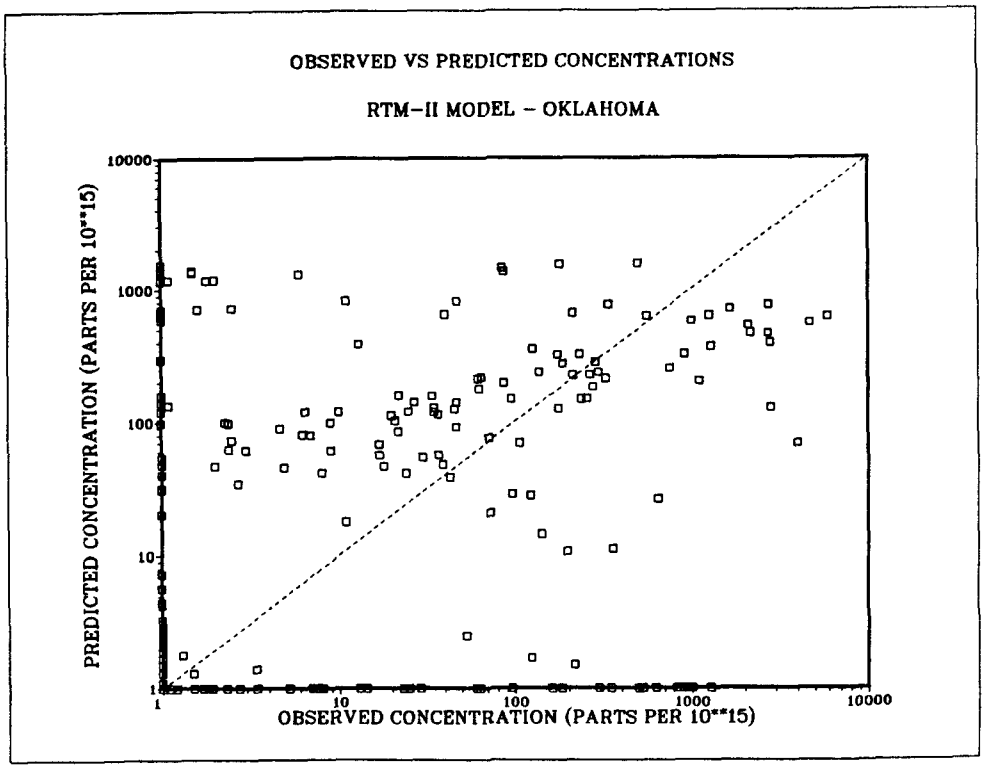

Figure E-123. Scatter plot of predicted and observed averaged concentrations at Oklahoma for RTM-II ... points paired in space and time.

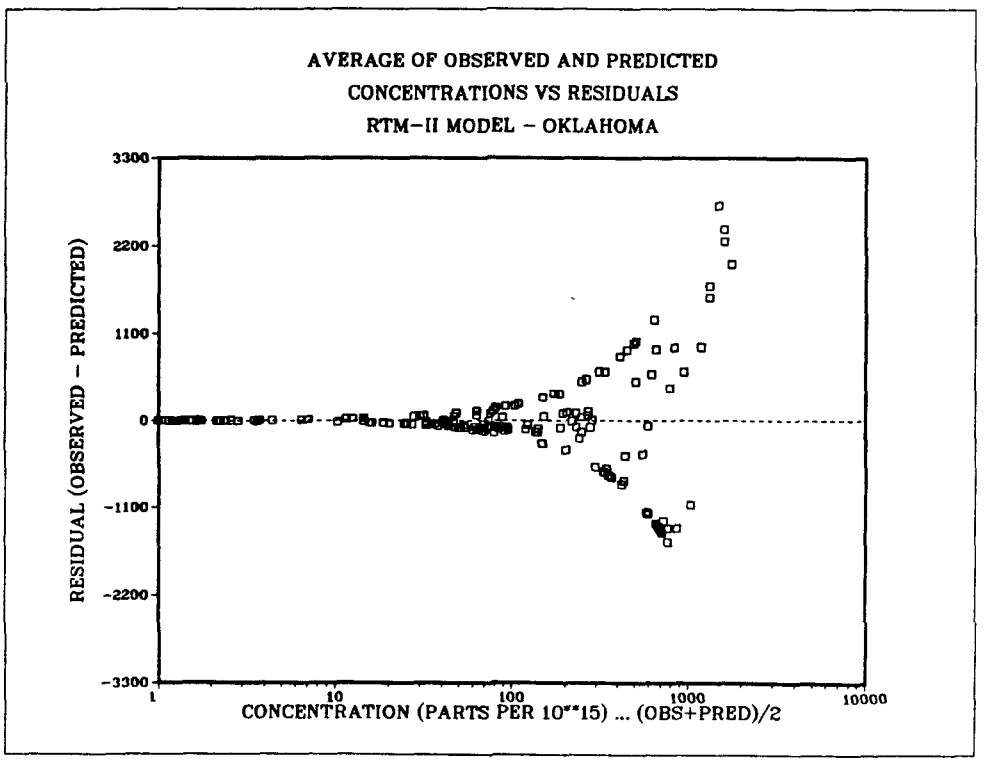

Figure E-124. Scatter plot of average of observed and predicted concentrations versus residuals at Oklahoma for RTM-II ... points paired in space and time.

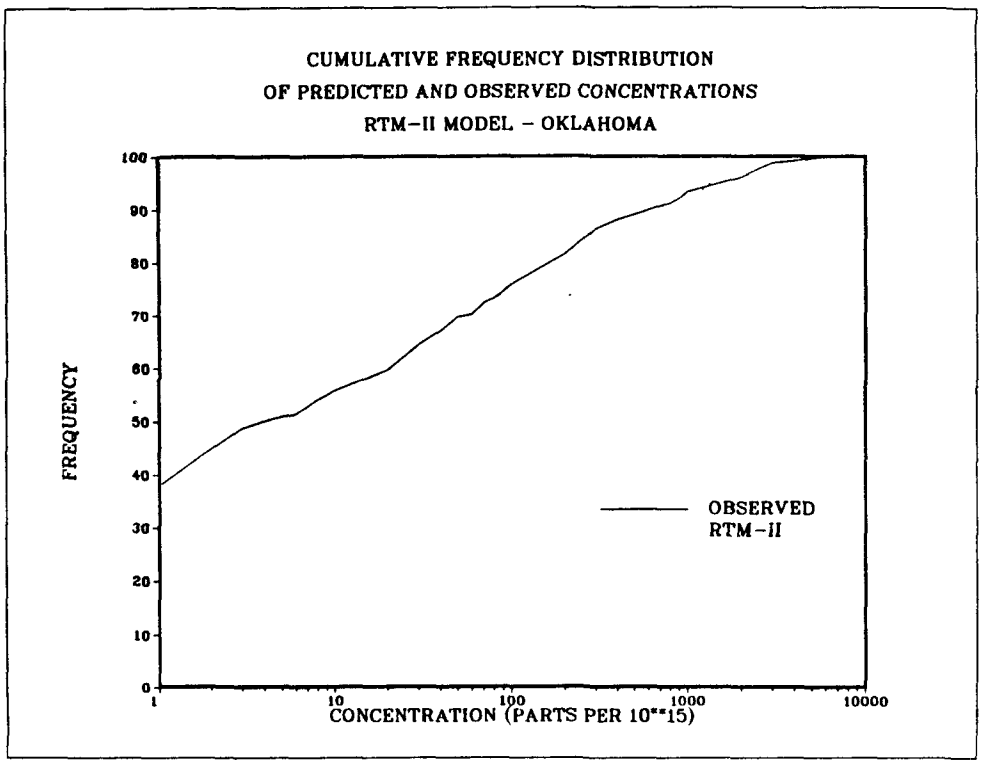

Figure E-125. Cumulative frequency distributions of RTM-II predictions and observed concentrations at Oklahoma based on points paired in space and time.

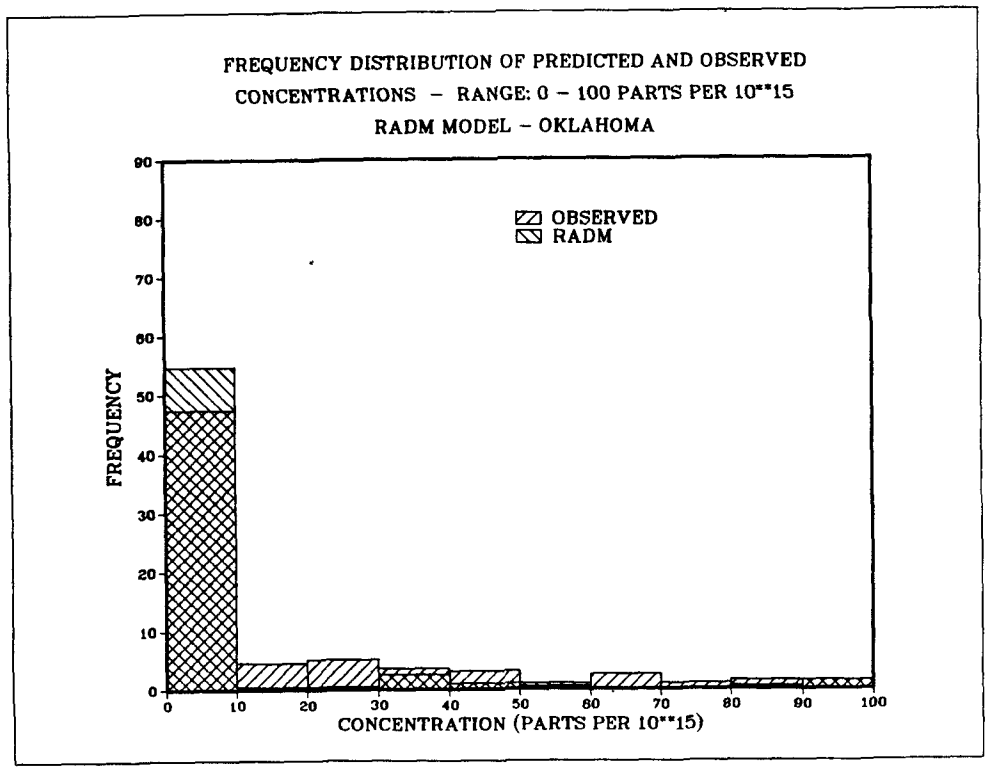

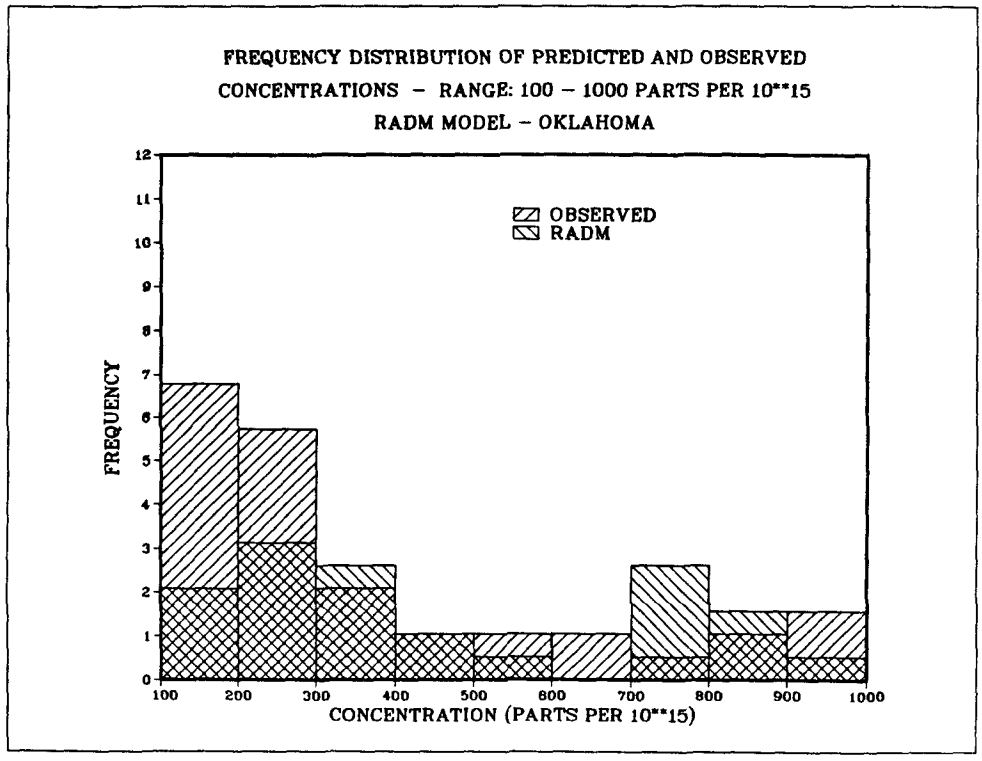

Figure E-126. Frequency distribution of predicted and observed concentrations at Oklahoma for RADM based on points paired in space and time ... (top) concentration range: 0 - 100 parts per 10^{15}, (bottom) concentration range: 100 - 1000 parts per 10^{15}.

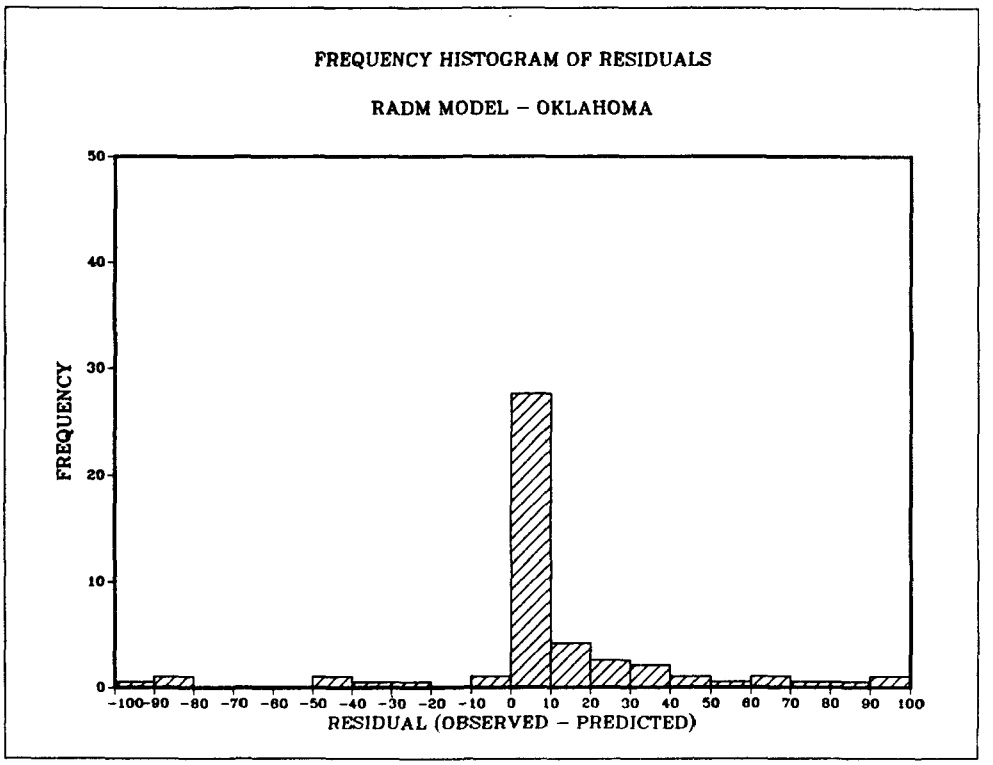

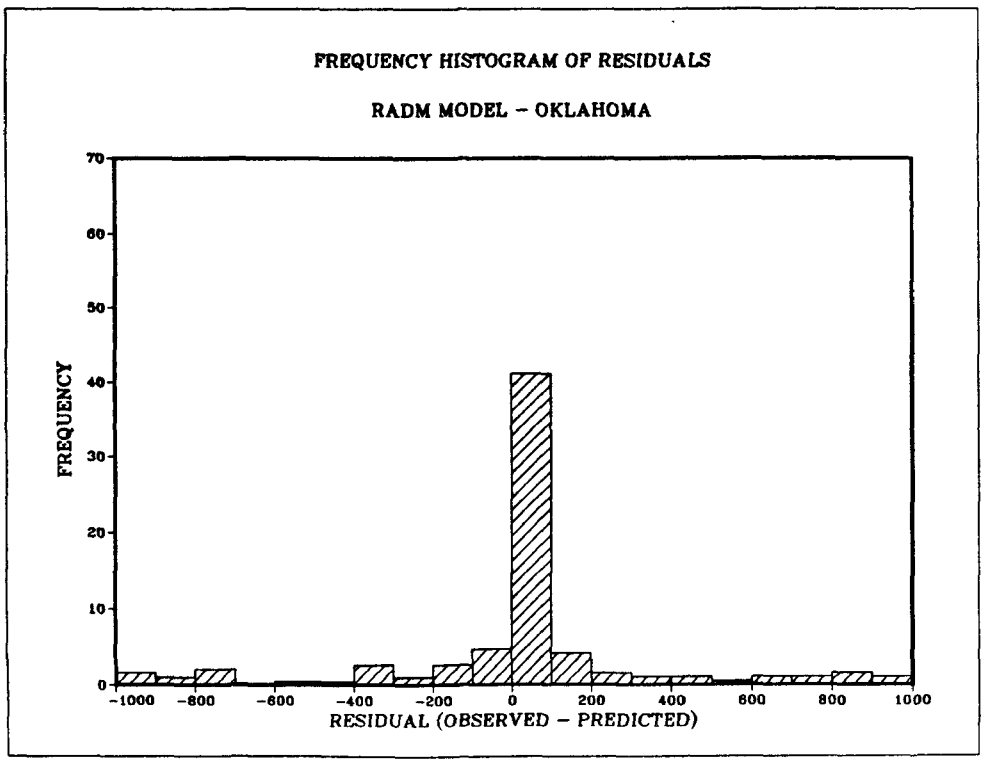

Figure E-127. Frequency distribution of residuals at Oklahoma for RADM based on points paired in space and time ...
(top) residual range: -100 to 100 parts per 10^{15},
(bottom) residual range: -1000 to 1000 parts per 10^{15}.

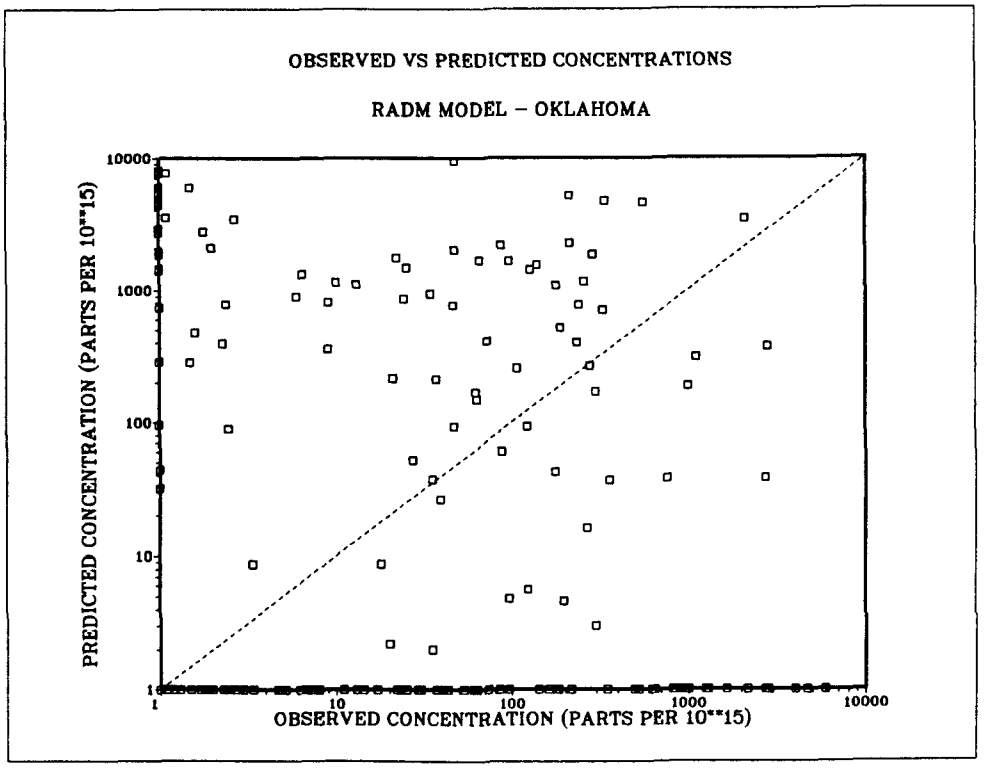

Figure E-128. Scatter plot of predicted and observed averaged concentrations at Oklahoma for RADM ... points paired in space and time.

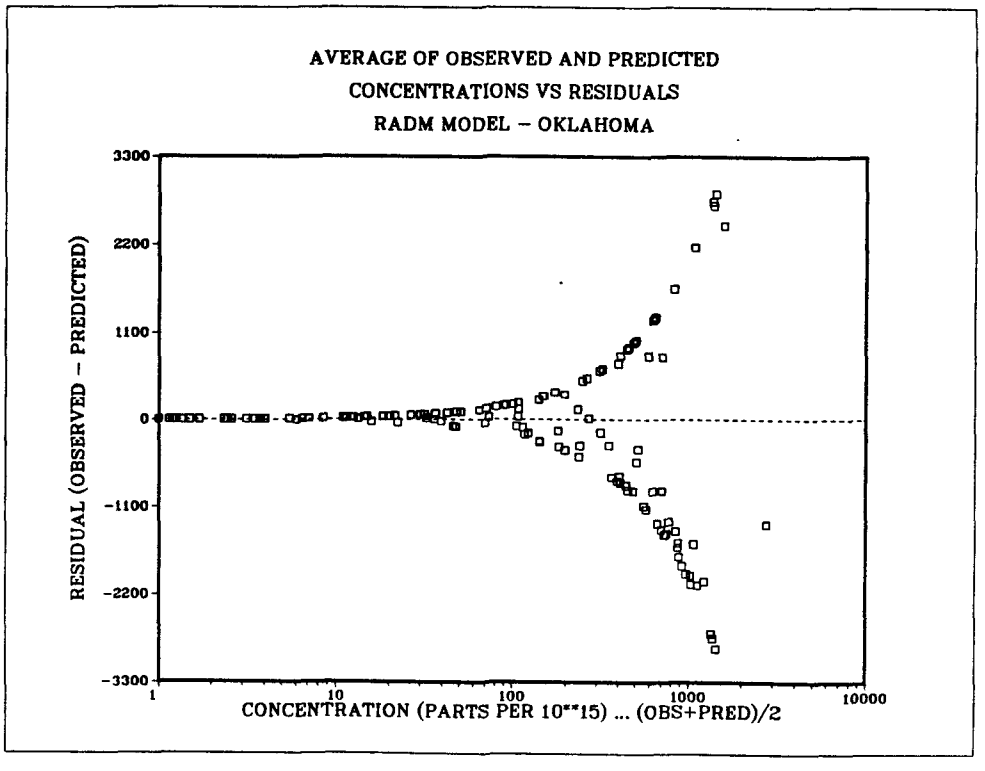

Figure E-129. Scatter plot of average of observed and predicted concentrations versus residuals at Oklahoma for RADM ... points paired in space and time.

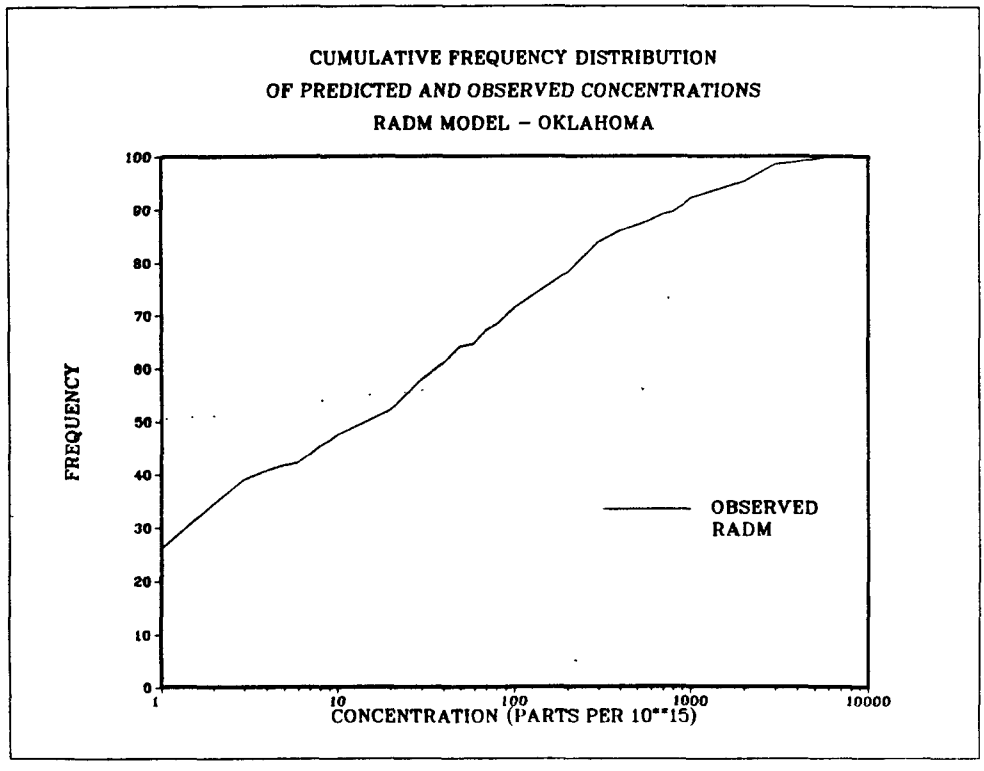

Figure E-130. Cumulative frequency distributions of RADM predictions and observed concentrations at Oklahoma based on points paired in space and time.

5. LOCATION OF AIR SAMPLERS AND SITE MAP FOR SAVANNAH RIVER PLANT EXPERIMENT

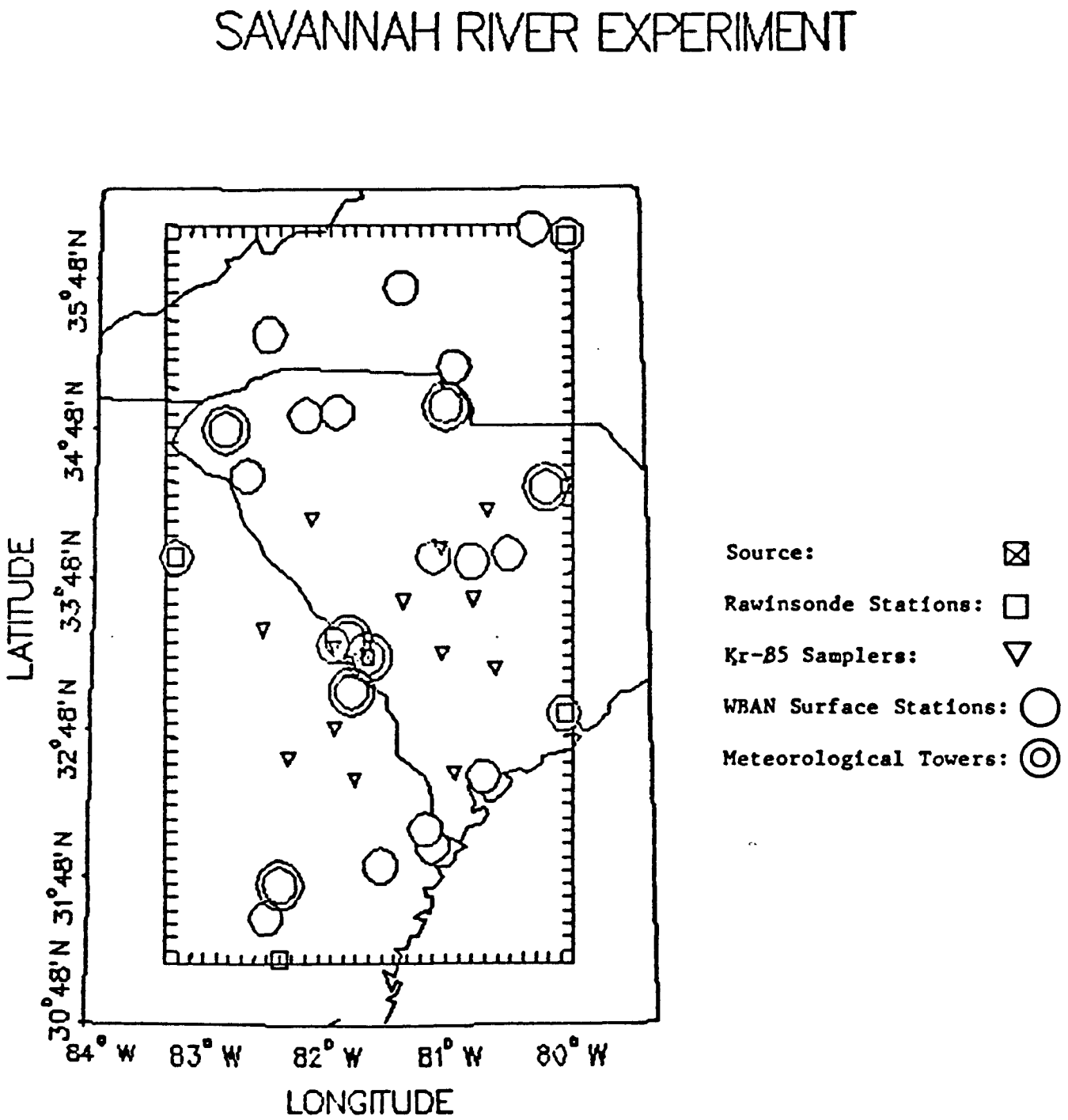

Figure E-131. Location of significant source, weather and receptors sites for Savannah River Plant Experiment.

6. SKETCHES OF PREDICTED AND OBSERVED GROUND LEVEL CONCENTRATIONS FOR TWO SAVANNAH RIVER PLANT EXPERIMENTS SUBCASES 4B AND 6C

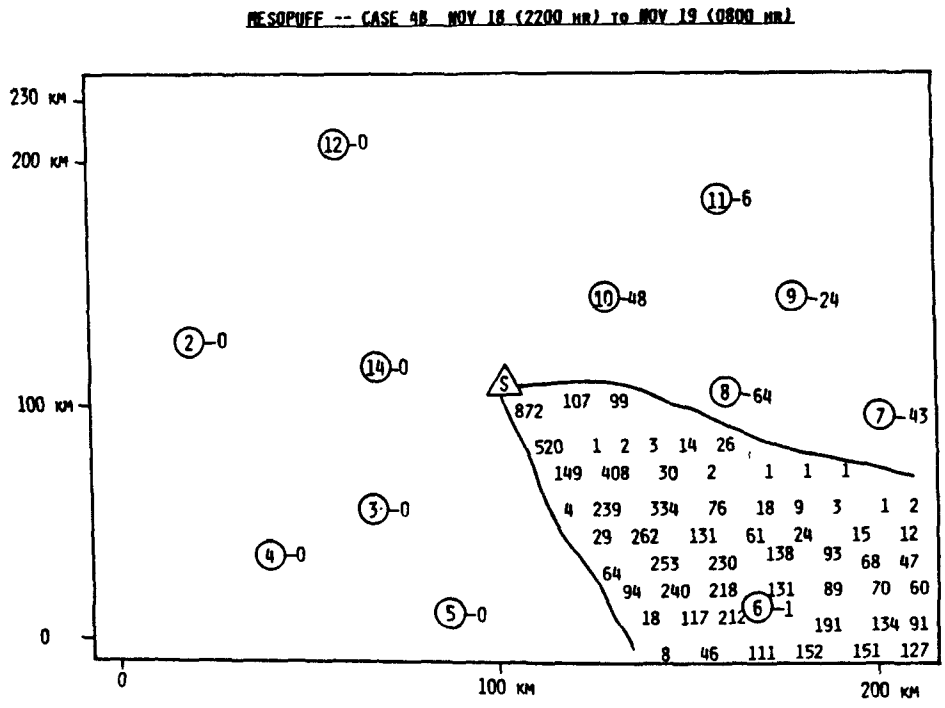

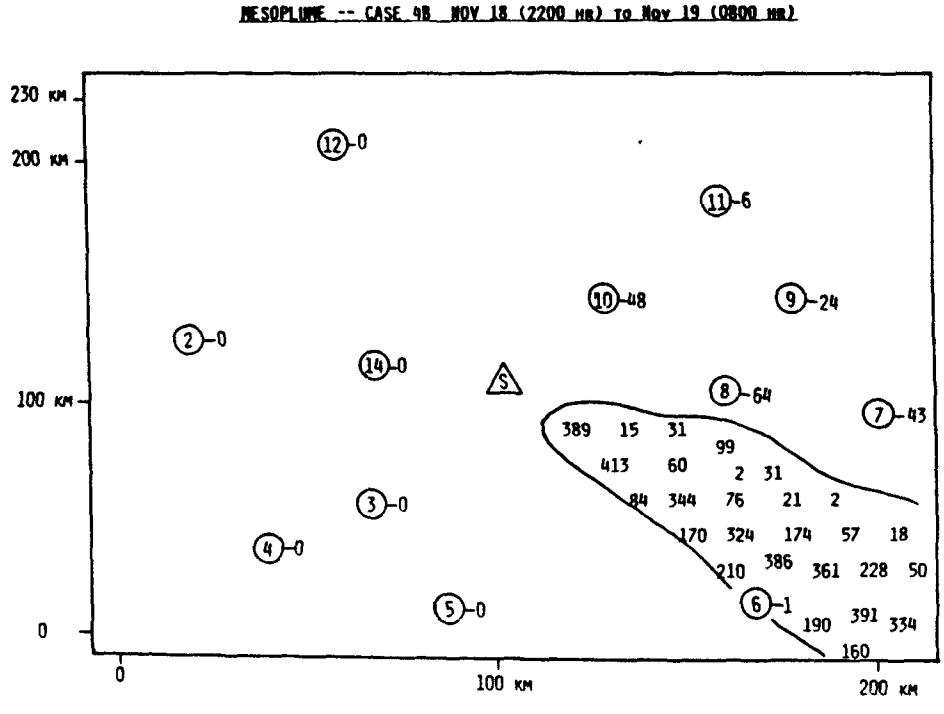

Figure E-132. Comparison of 10-hour averages of predicted plume and observed data (in pCi/m^3) for Savannah River Plant experiment of November 18-19, 1976 (2200 to 0800 GMT) ...
(top) MESOPUFF predictions, (bottom) MESOPLUME predictions.

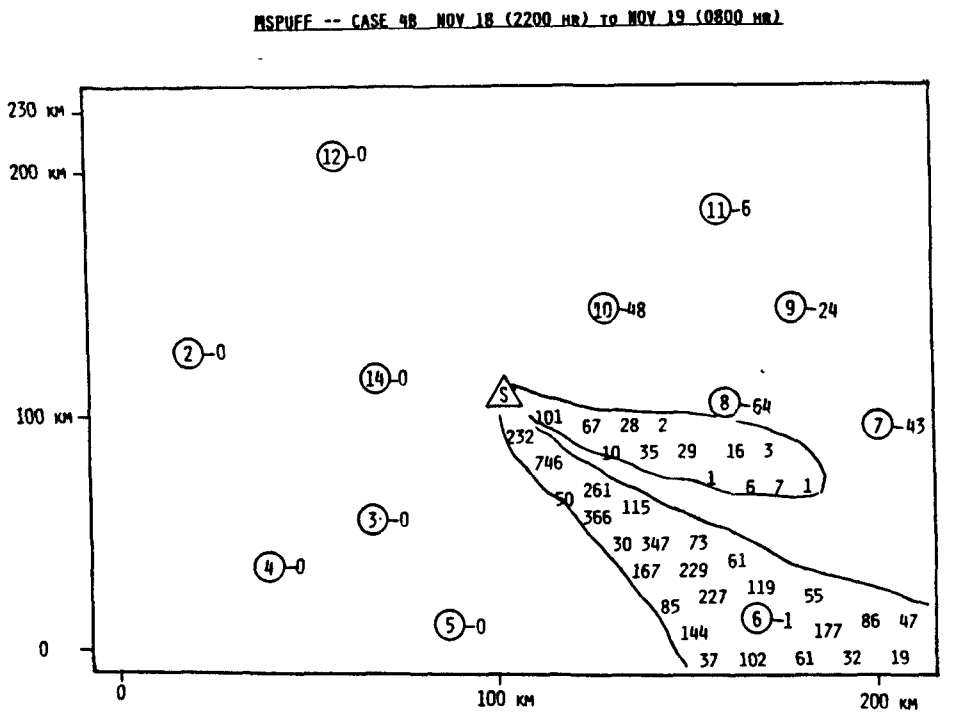

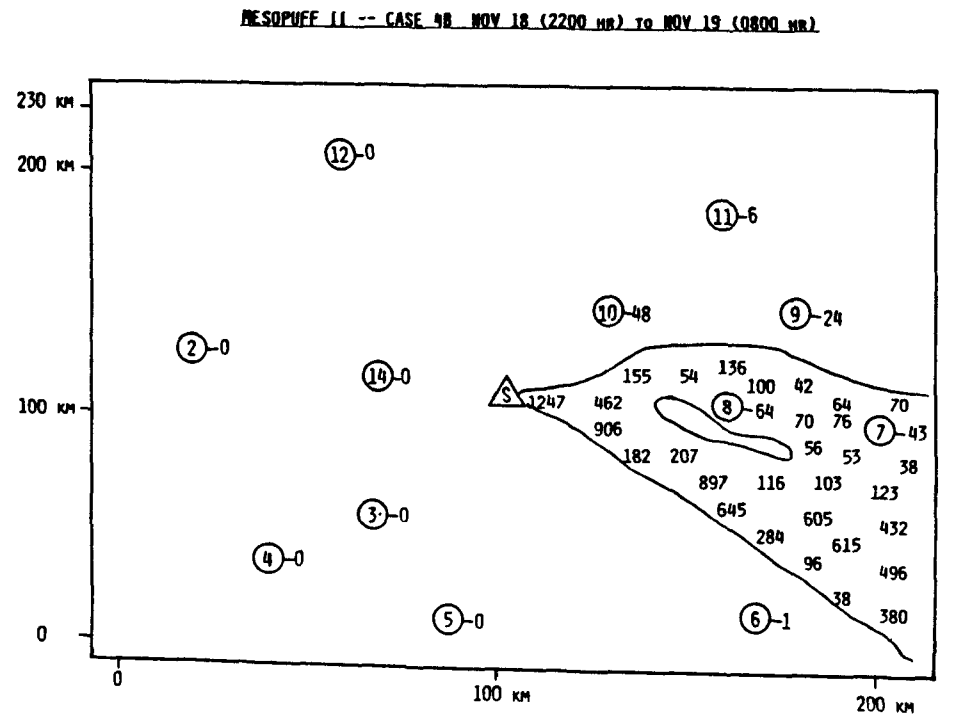

Figure E-133. Comparison of 10-hour averages of predicted plume and observed data (in pCi/m^3) for Savannah River Plant experiment of November 18-19, 1976 (2200 to 0800 GMT) ...
(top) MSPUFF predictions, (bottom) MESOPUFF II predictions.

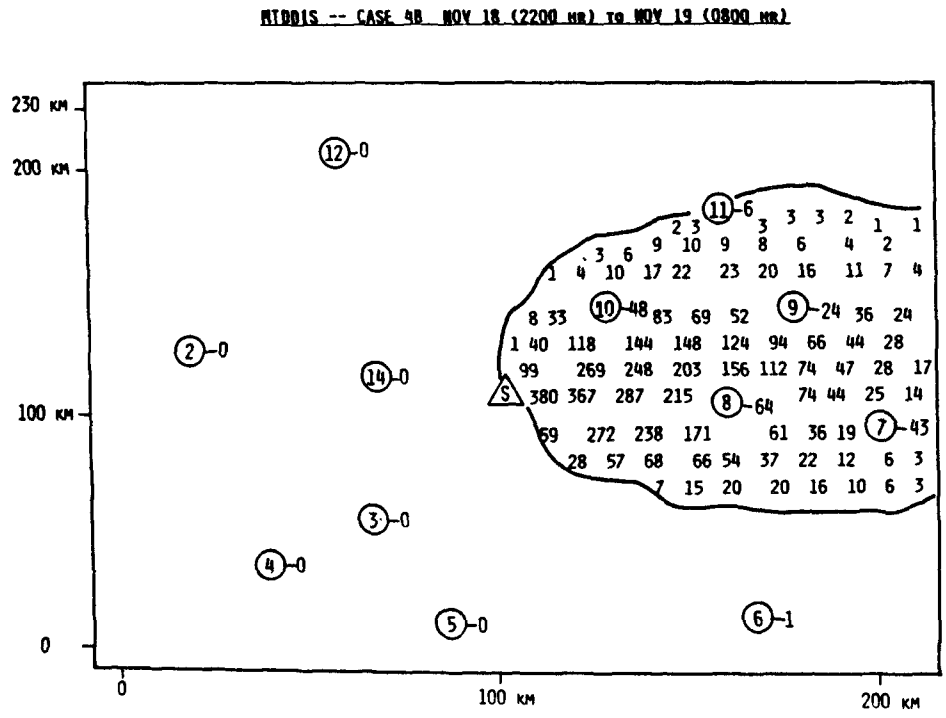

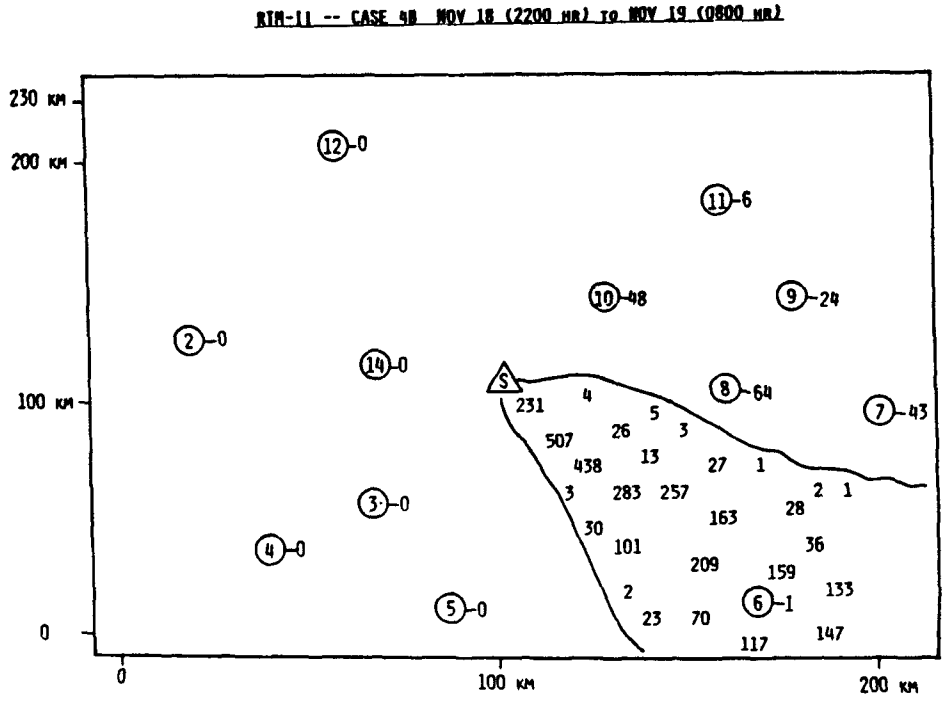

Figure E-134. Comparison of 10-hour averages of predicted plume and observed data (in pCi/m^3) for Savannah River Plant experiment of November 18-19, 1976 (2200 to 0800 GMT) ... (top) MTDDIS predictions, (bottom) RTM-II predictions.

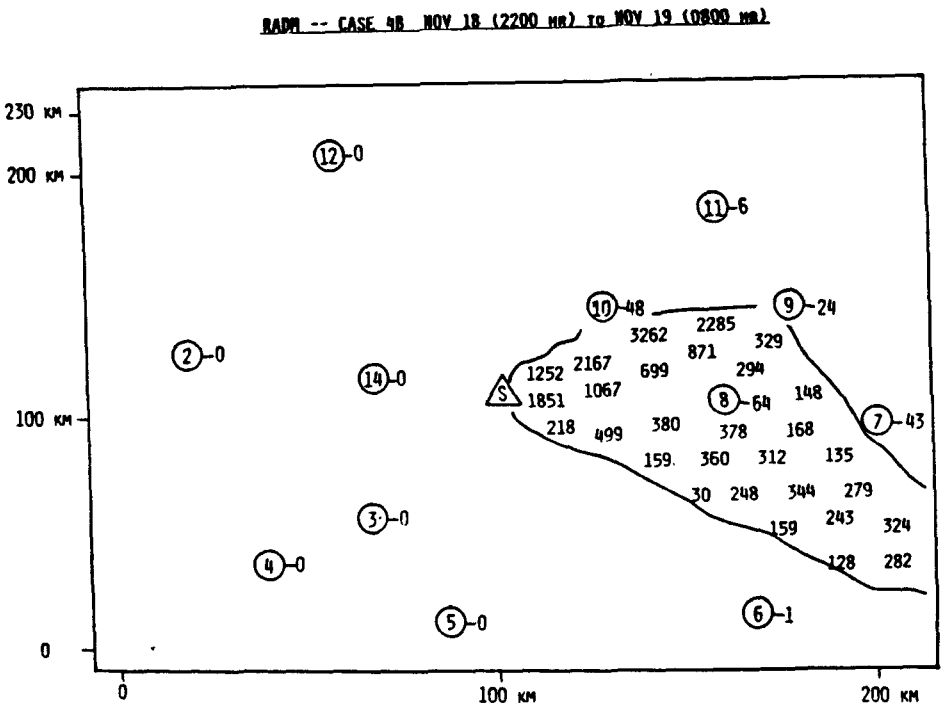

Figure E-135. Comparison of 10-hour averages of predicted plume and observed data (in pCi/m^3) for Savannah River Plant experiment of November 18-19, 1976 (2200 to 0800 GMT) ... RADM predictions.

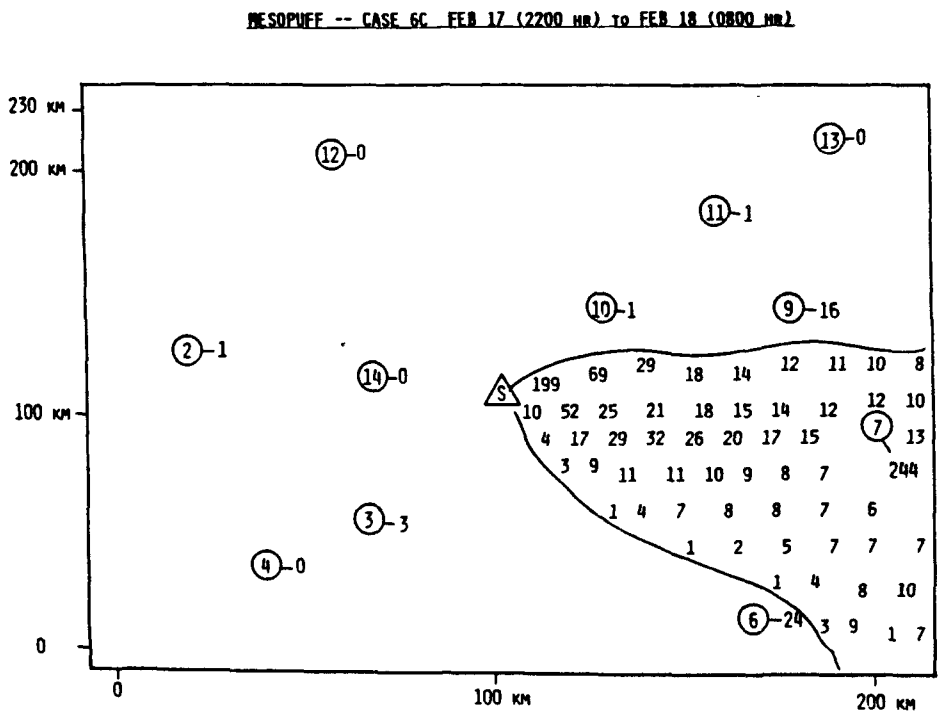

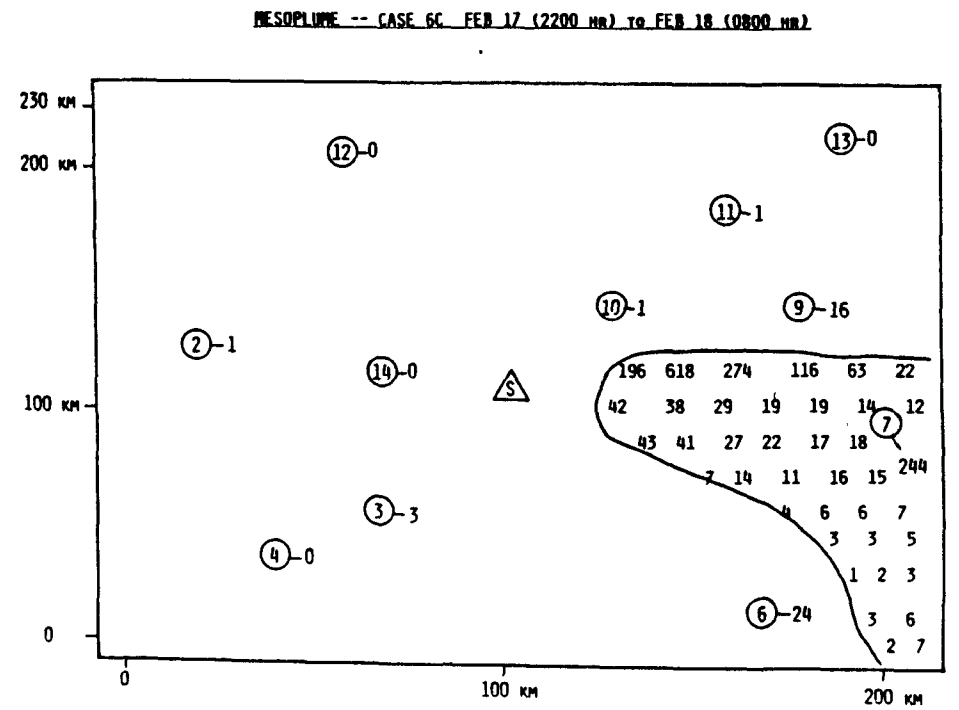

Figure E-136. Comparison of 10-hour averages of predicted plume and observed data (in pCi/m^3) for Savannah River Plant experiment of February 17-18, 1977 (2200 to 0800 GMT) ...
(top) MESOPUFF predictions, (bottom) MESOPLUME predictions.

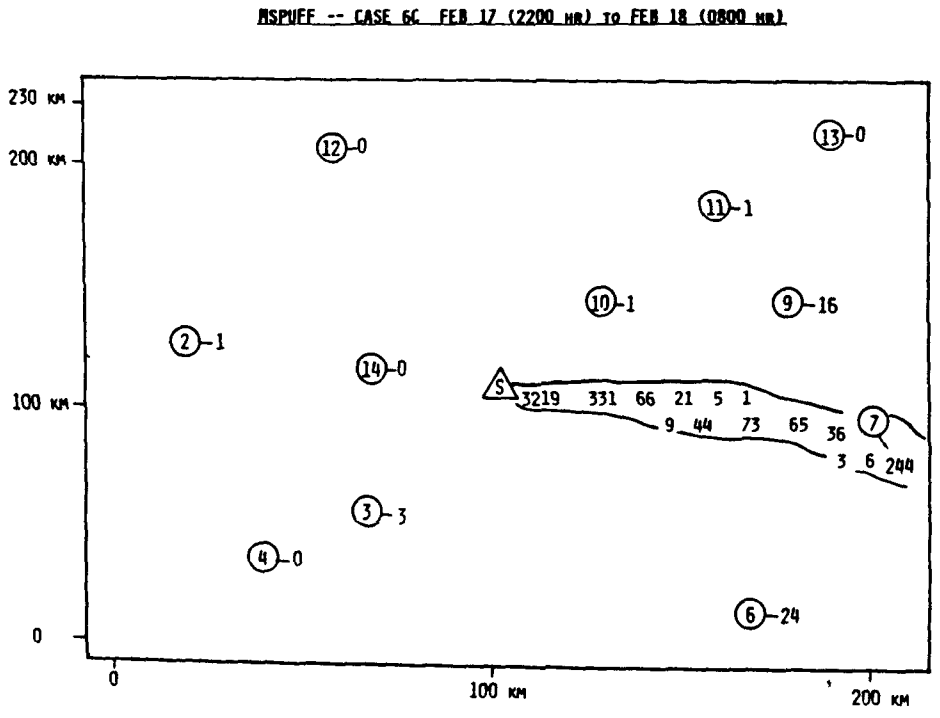

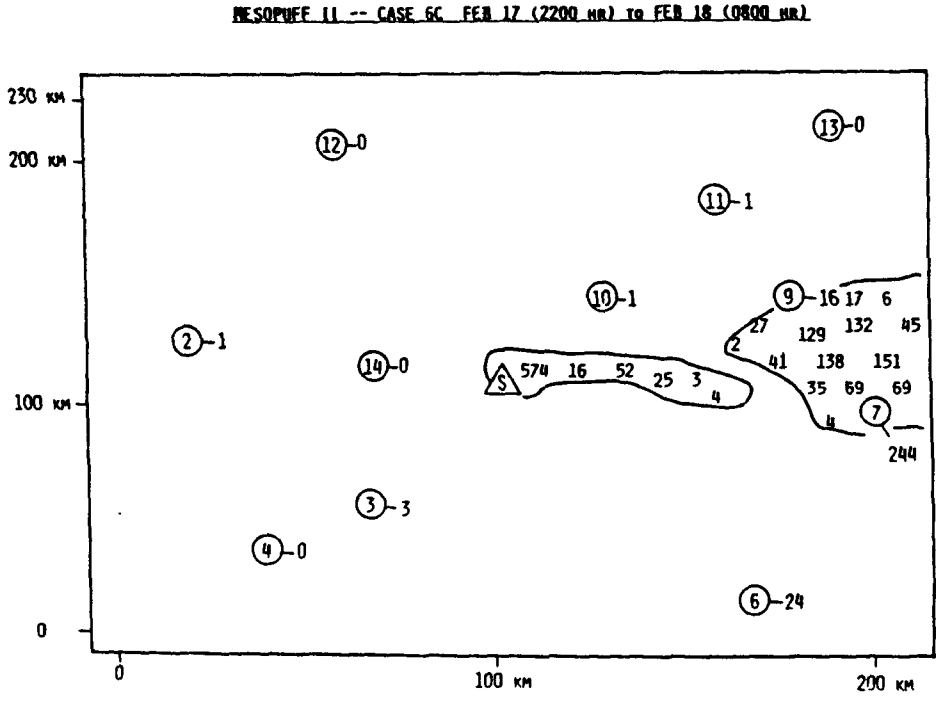

Figure E-137. Comparison of 10-hour averages of predicted plume and observed data (in pCi/m^3) for Savannah River Plant experiment of February 17-18, 1977 (2200 to 0800 GMT) ...
(top) MSPUFF predictions, (bottom) MESOPUFF II predictions.

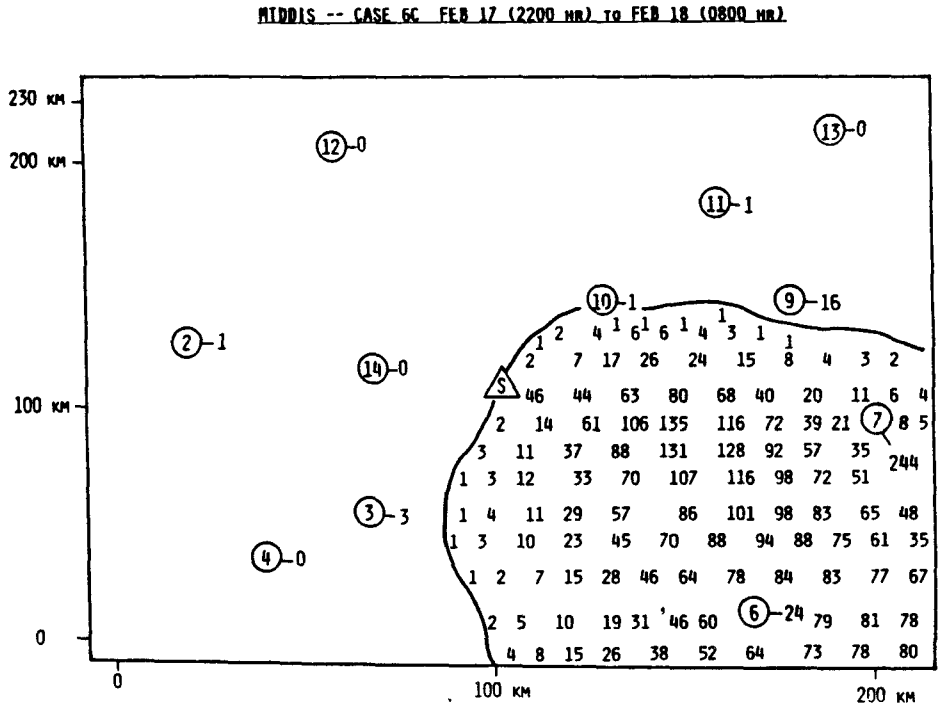

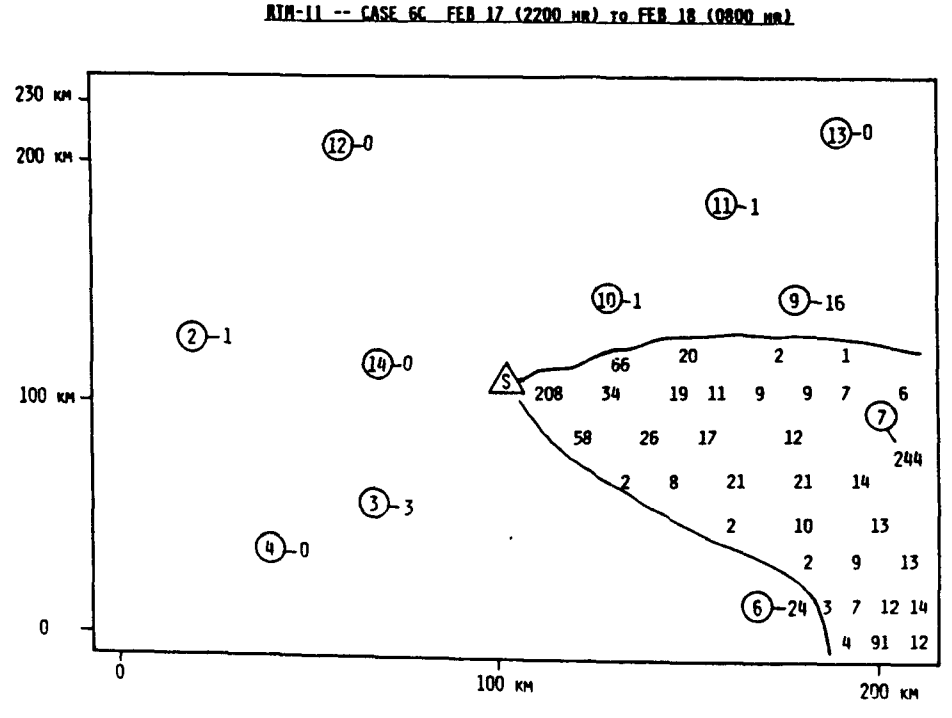

Figure E-138. Comparison of 10-hour averages of predicted plume and observed data (in pCi/m^3) for Savannah River Plant experiment of February 17-18, 1977 (2200 to 0800 GMT) ... (top) MTDDIS predictions, (bottom) RTM-II predictions.

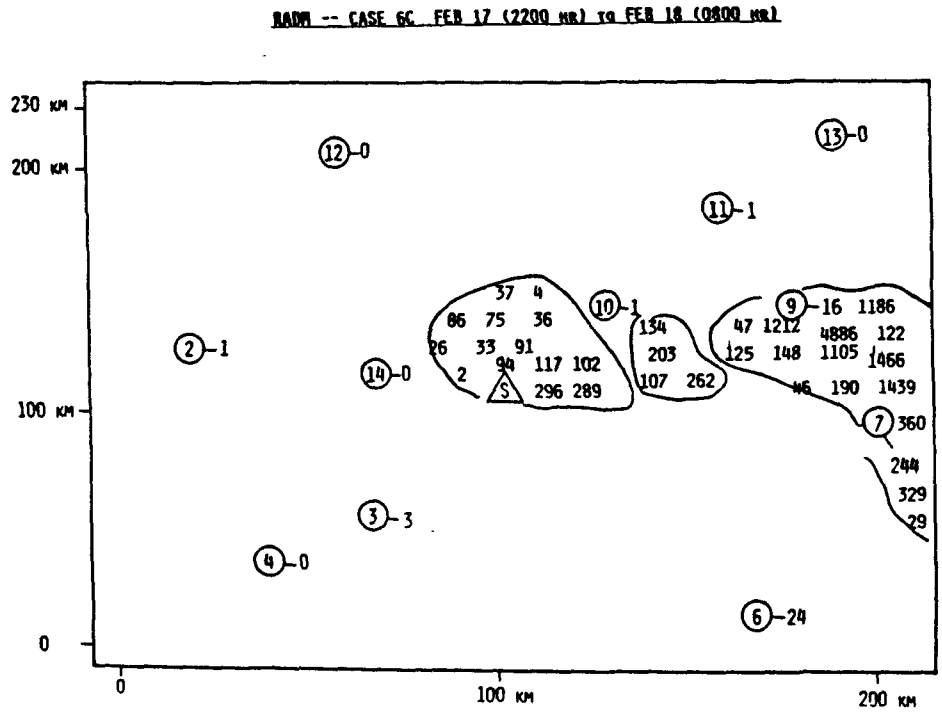

Figure E-139. Comparison of 10-hour averages of predicted plume and observed data (in pCi/m^3) for Savannah River Plant experiment of February 17-18, 1977 (2200 to 0800 GMT) ... RADM predictions.

7. SUMMARY GRAPHICAL PLOTS COMPARING MODEL PREDICTIONS AND FIELD DATA AT SAVANNAH RIVER PLANT

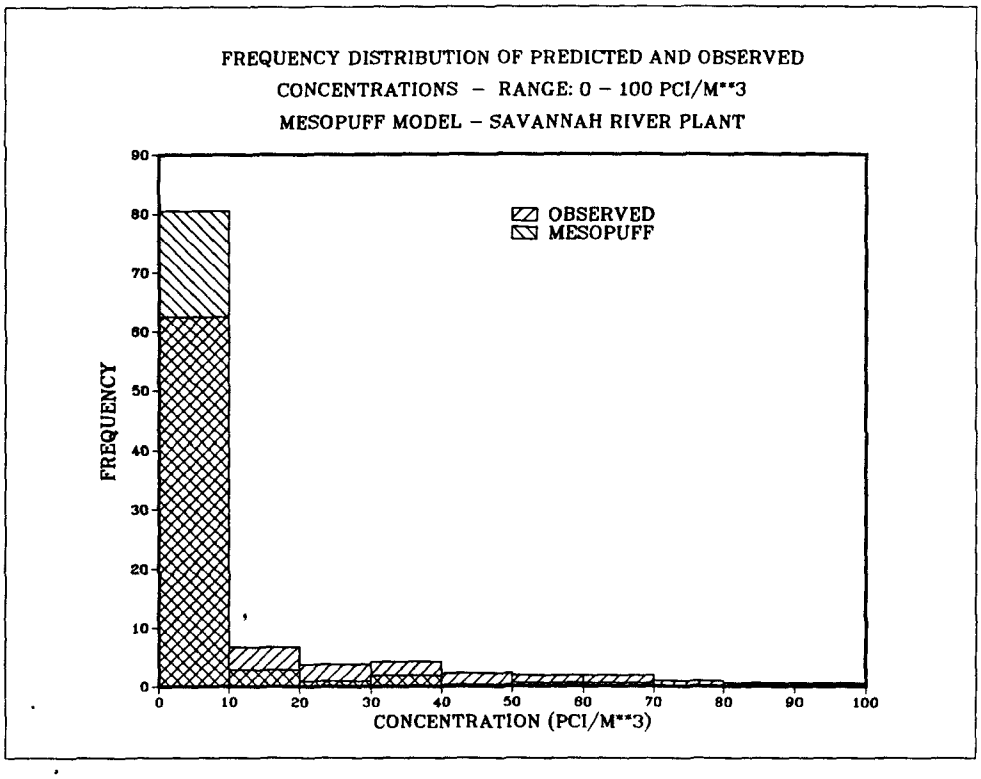

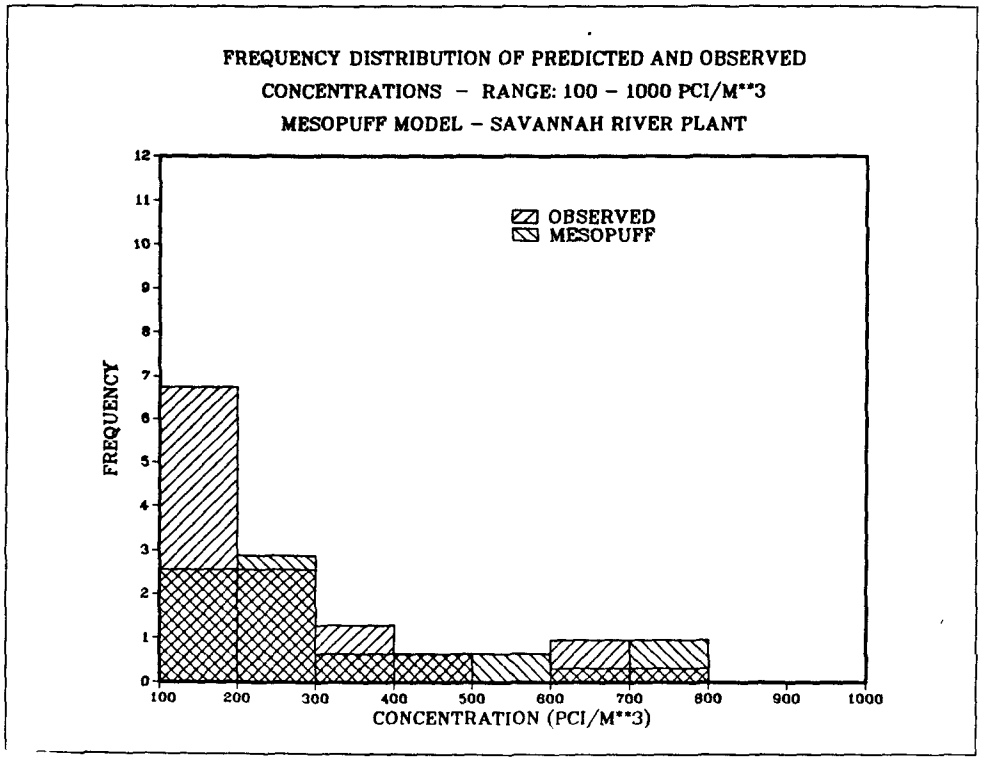

Figure E-140. Frequency distribution of predicted and observed concentrations at Savannah River Plant for MESOPUFF based on points paired in space and time ...
(top) concentration range: 0 - 100 pCi/m^3,
(bottom) concentration range: 100 - 1000 pCi/m^3.

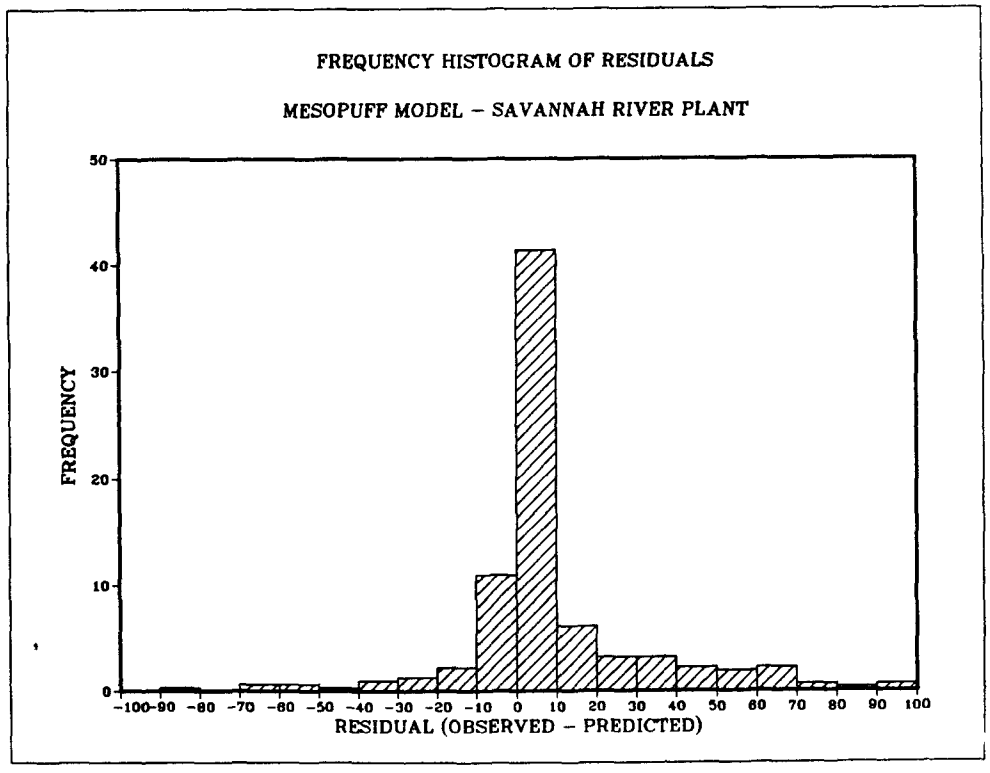

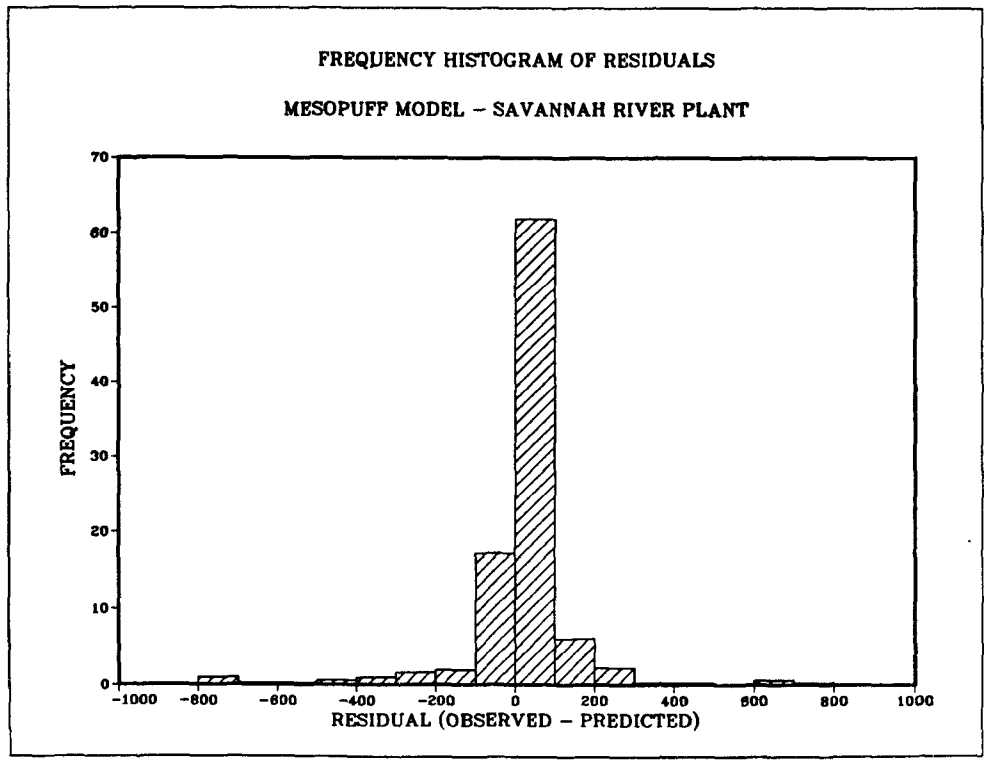

Figure E-141. Frequency distribution of residuals at Savannah River Plant for MESOPUFF based on points paired in space and time ...
(top) residual range: -100 to 100 pCi/m^3,
(bottom) residual range: -1000 to 1000 pCi/m^3.

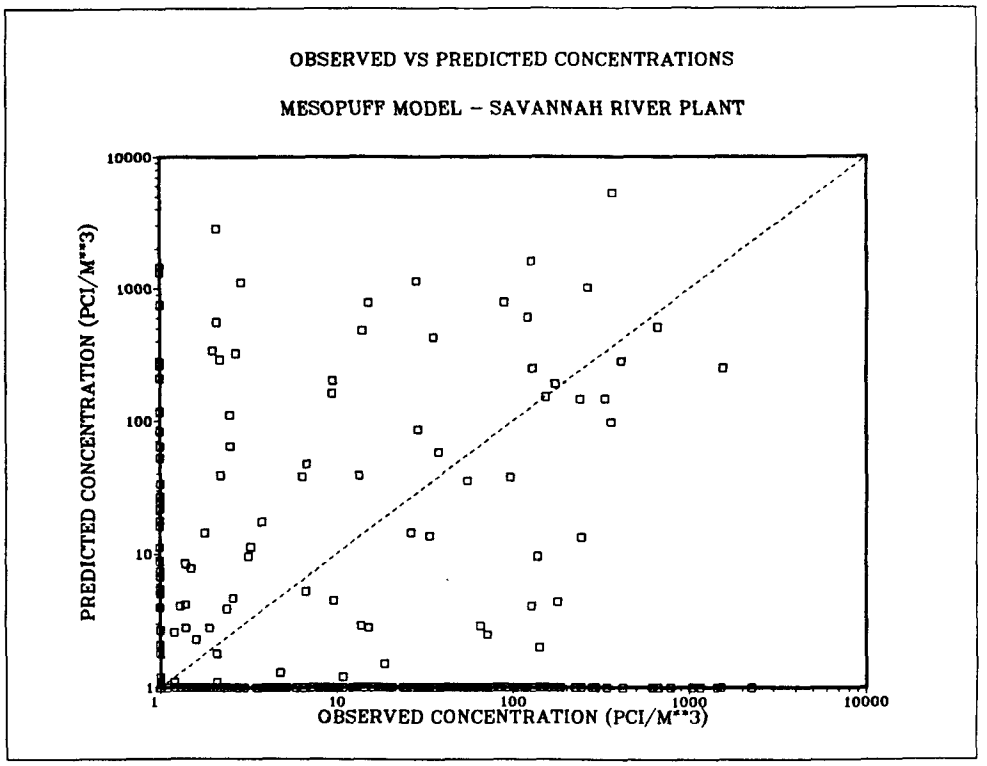

Figure E-142. Scatter plot of predicted and observed averaged concentrations at Savannah River Plant for MESOPUFF ... points paired in space and time.

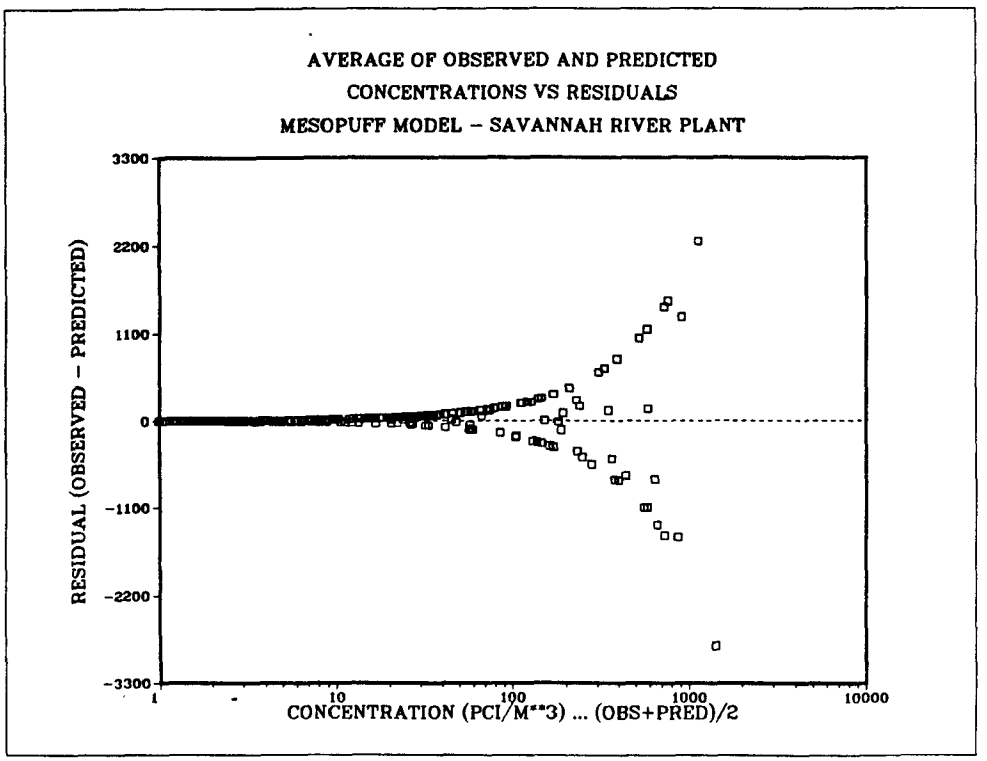

Figure E-143. Scatter plot of average of observed and predicted concentrations versus residuals at Savannah River Plant for MESOPUFF ... points paired in space and time.

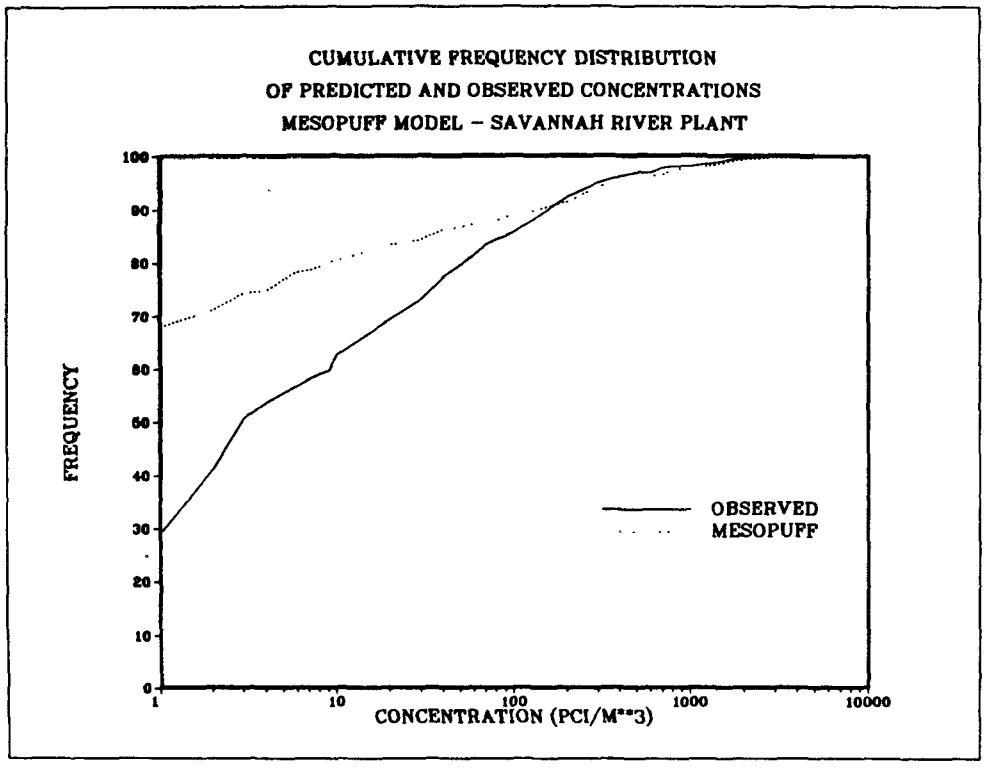

Figure E-144. Cumulative frequency distributions of MESOPUFF predictions and observed concentrations at Savannah River Plant based on points paired in space and time.

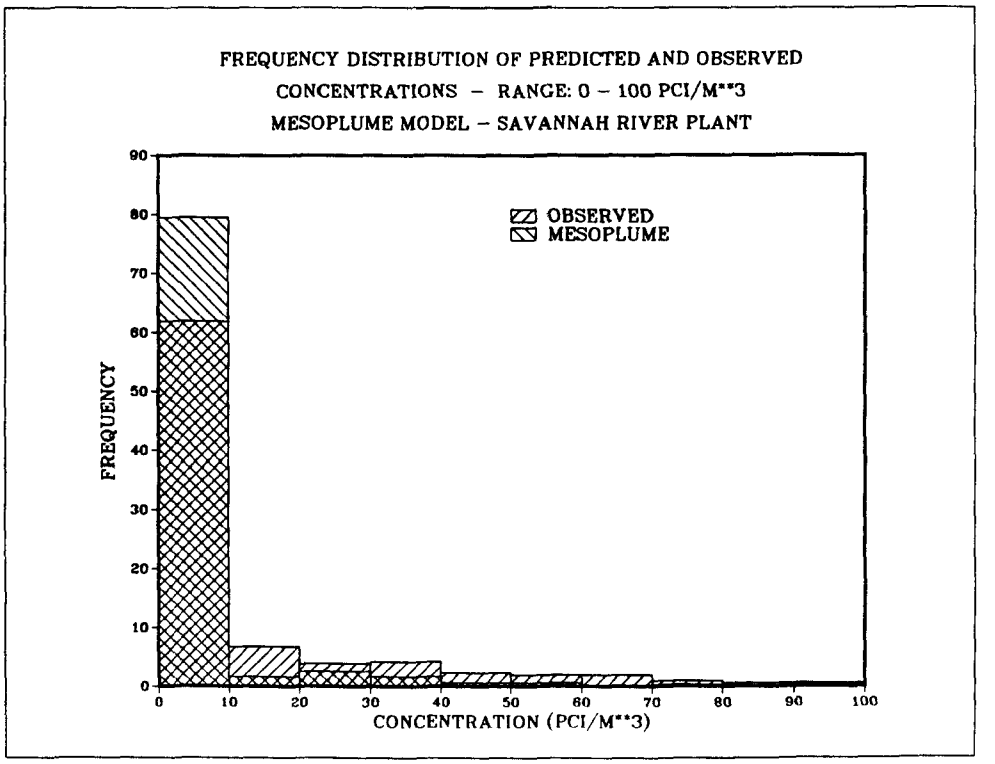

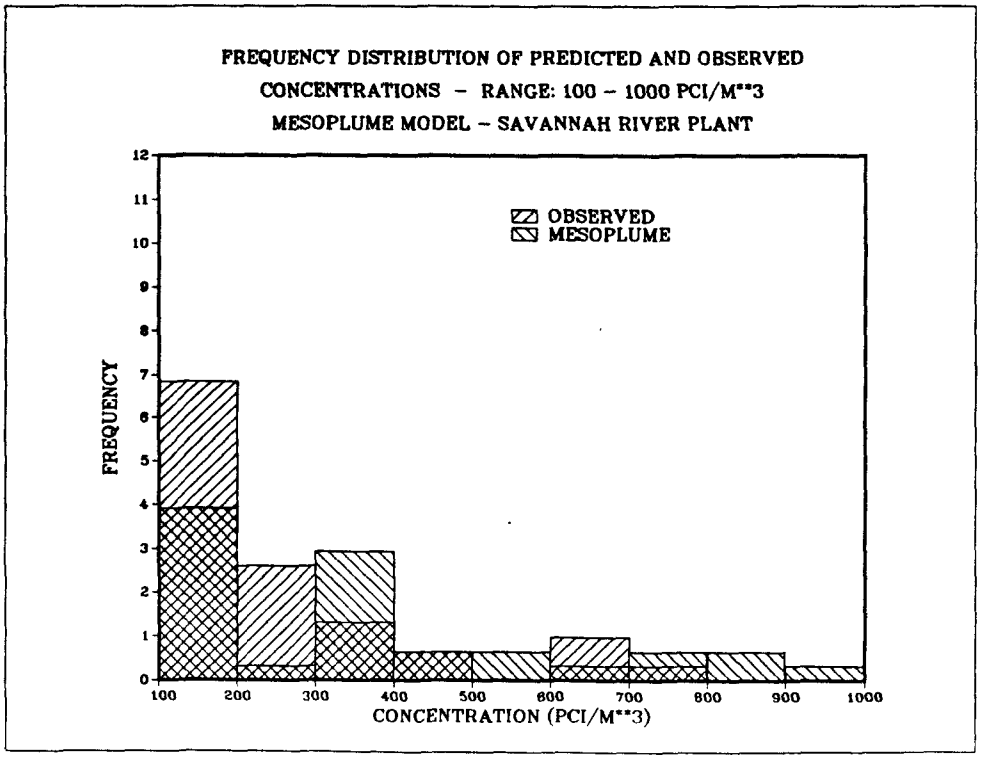

Figure E-145. Frequency distribution of predicted and observed concentrations at Savannah River Plant for MESOPLUME based on points paired in space and time ...
(top) concentration range: 0 - 100 pCi/m^3,
(bottom) concentration range: 100 - 1000 pCi/m^3.

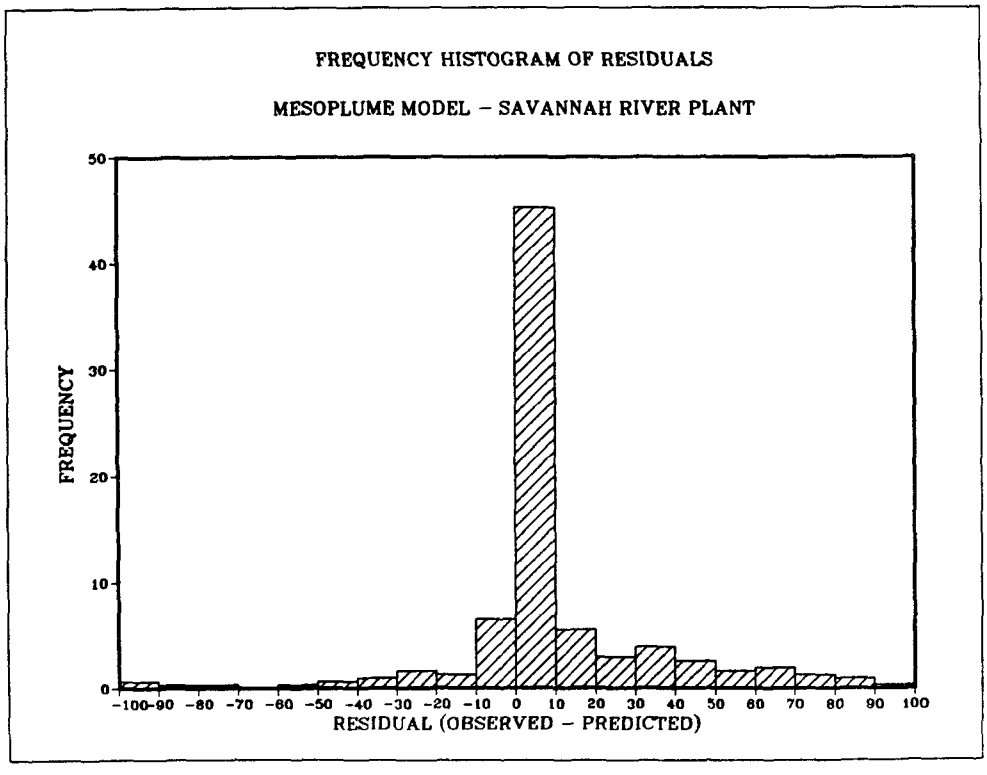

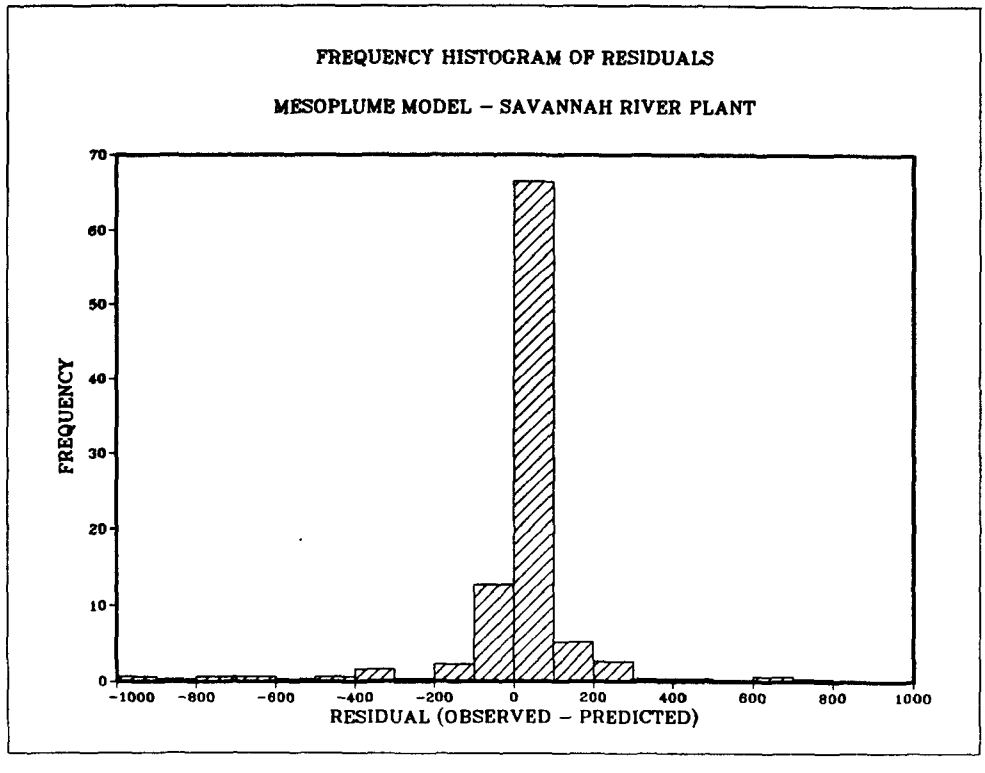

Figure E-146. Frequency distribution of residuals at Savannah River Plant for MESOPLUME based on points paired in space and time ...
(top) residual range: -100 to 100 pCi/m^3,
(bottom) residual range: -1000 to 1000 pCi/m^3.

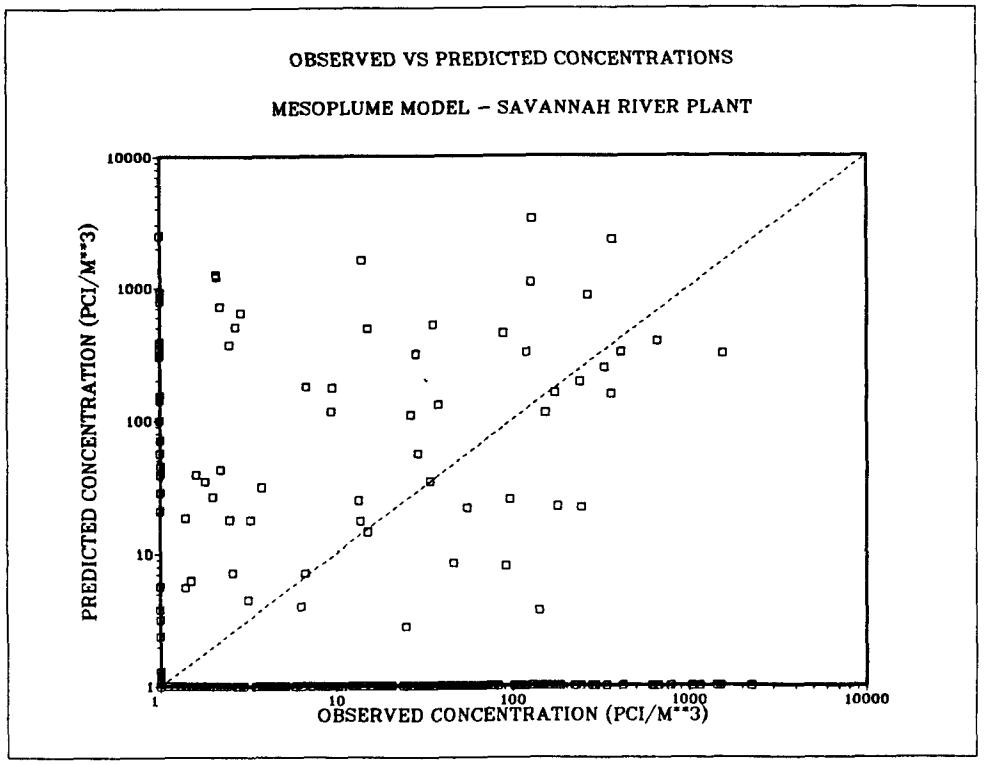

Figure E-147. Scatter plot of predicted and observed averaged concentrations at Savannah River Plant for MESOPLUME ... points paired in space and time.

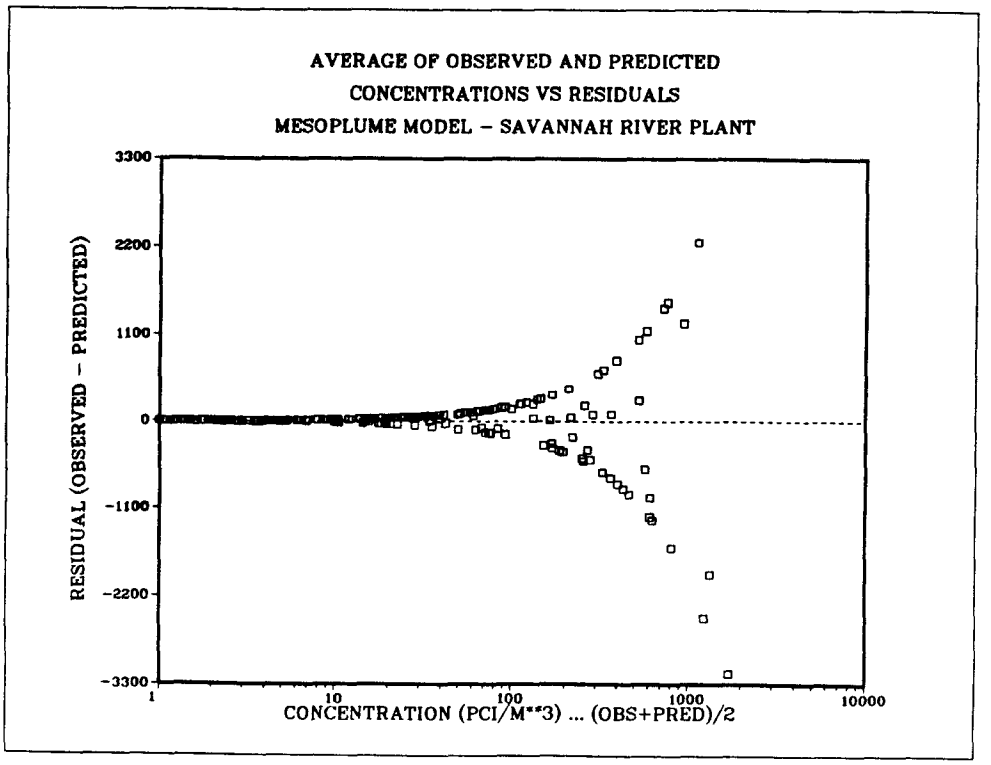

Figure E-148. Scatter plot of average of observed and predicted concentrations versus residuals at Savannah River Plant for MESOPLUME ... points paired in space and time.

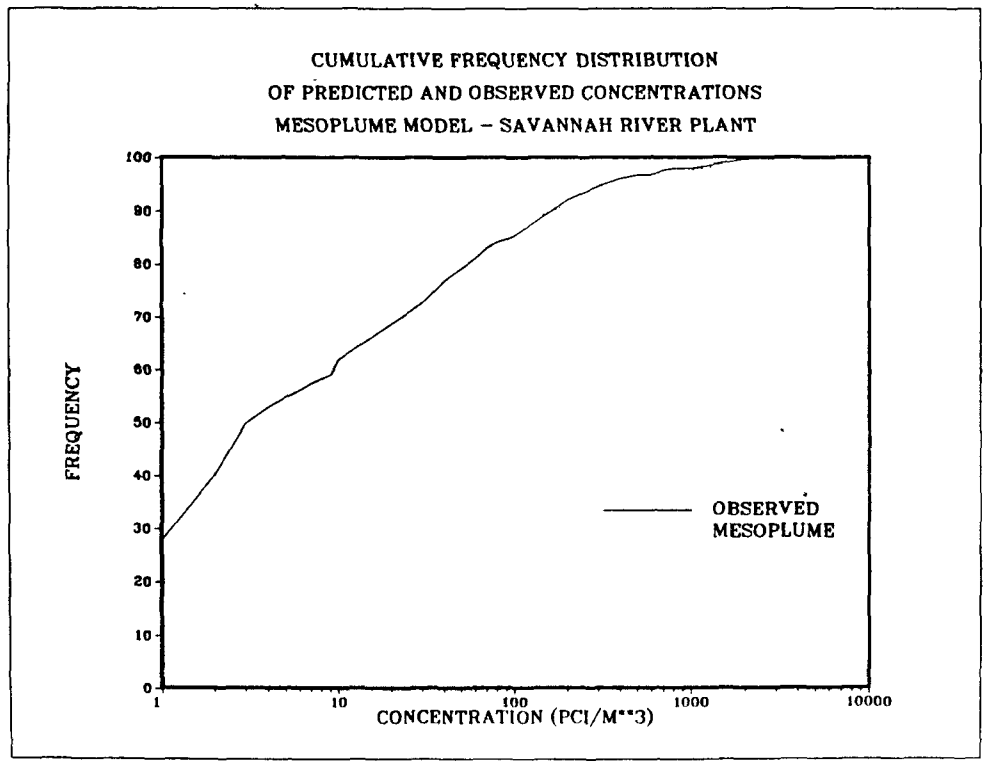

Figure E-149. Cumulative frequency distributions of MESOPLUME predictions and observed concentrations at Savannah River Plant based on points paired in space and time.

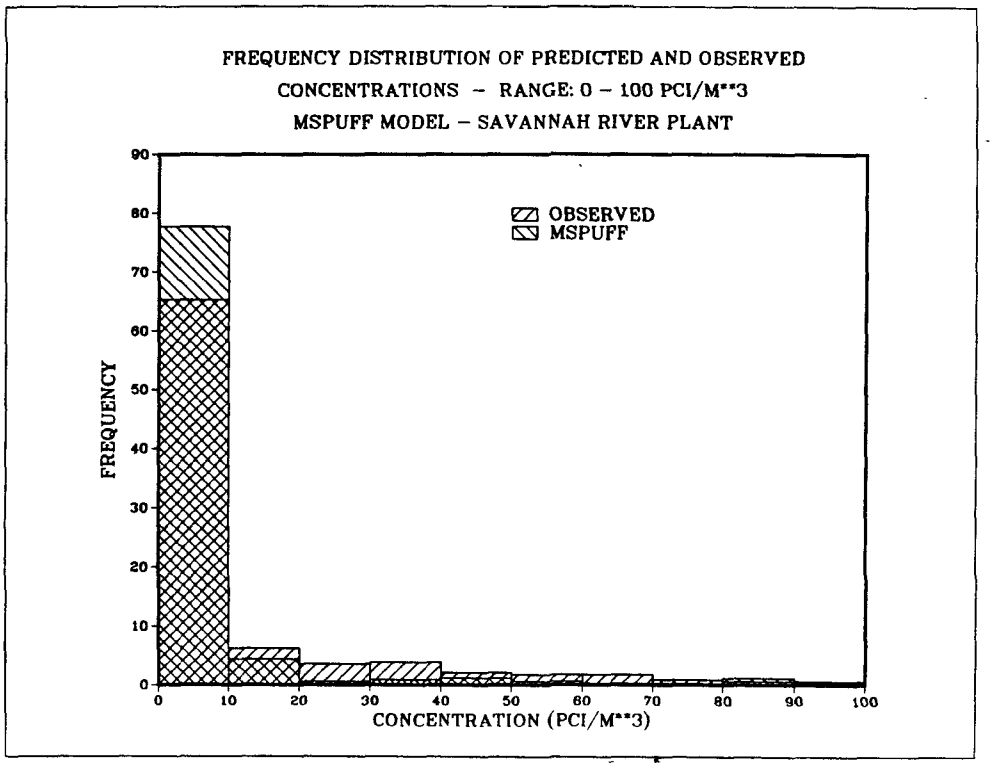

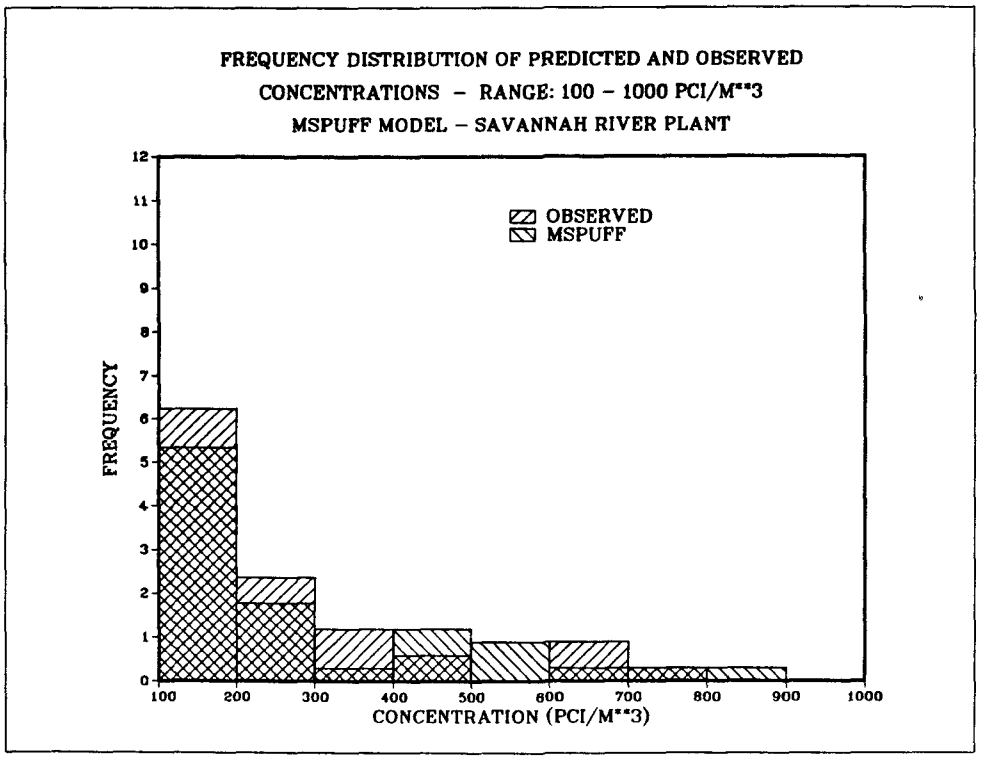

Figure E-150. Frequency distribution of predicted and observed concentrations at Savannah River Plant for MSPUFF based on points paired in space and time ...
(top) concentration range: 0 - 100 pCi/m^3,
(bottom) concentration range: 100 - 1000 pCi/m^3.

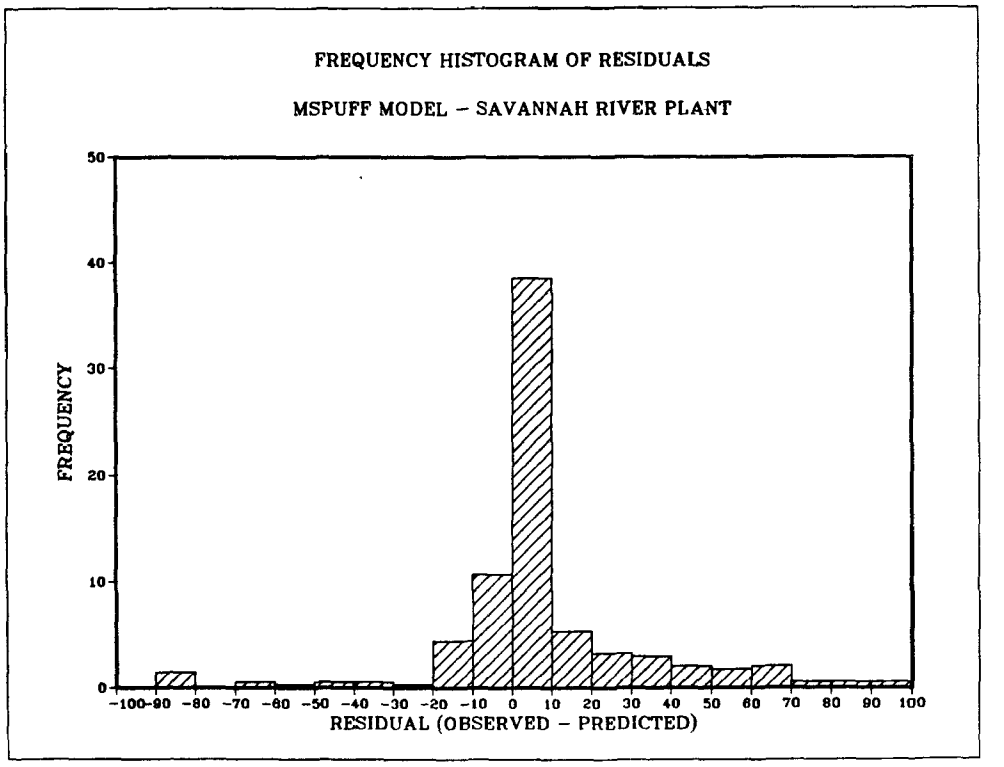

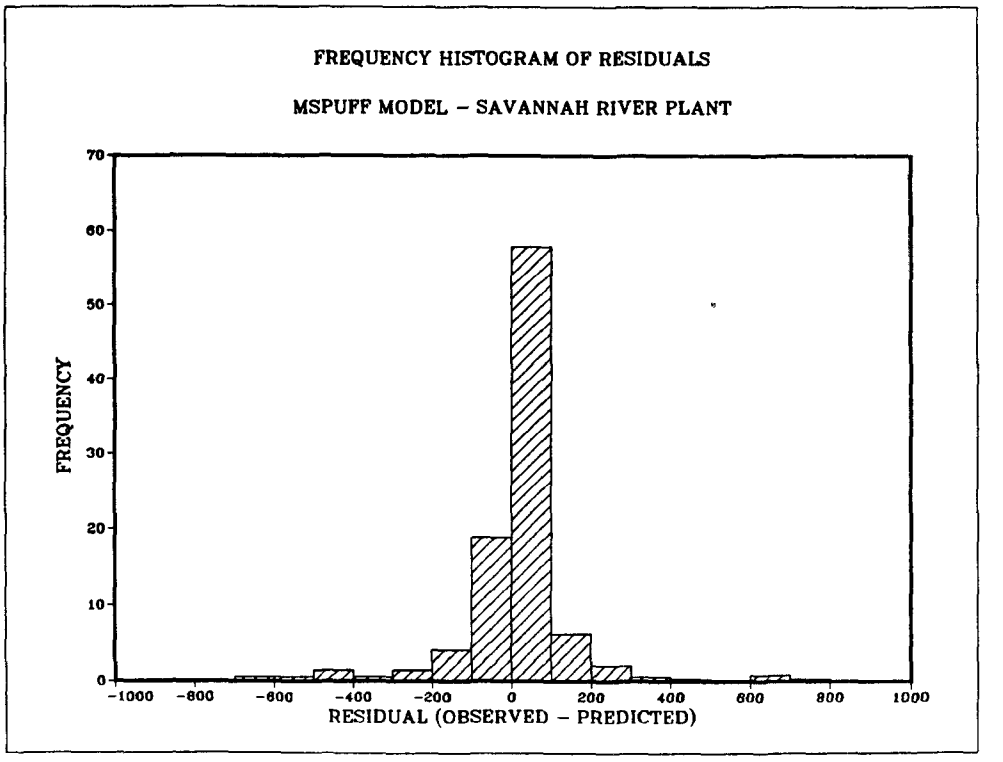

Figure E-151. Frequency distribution of residuals at Savannah River Plant for MSPUFF based on points paired in space and time ...
(top) residual range: -100 to 100 pCi/m^3,
(bottom) residual range: -1000 to 1000 pCi/m^3.

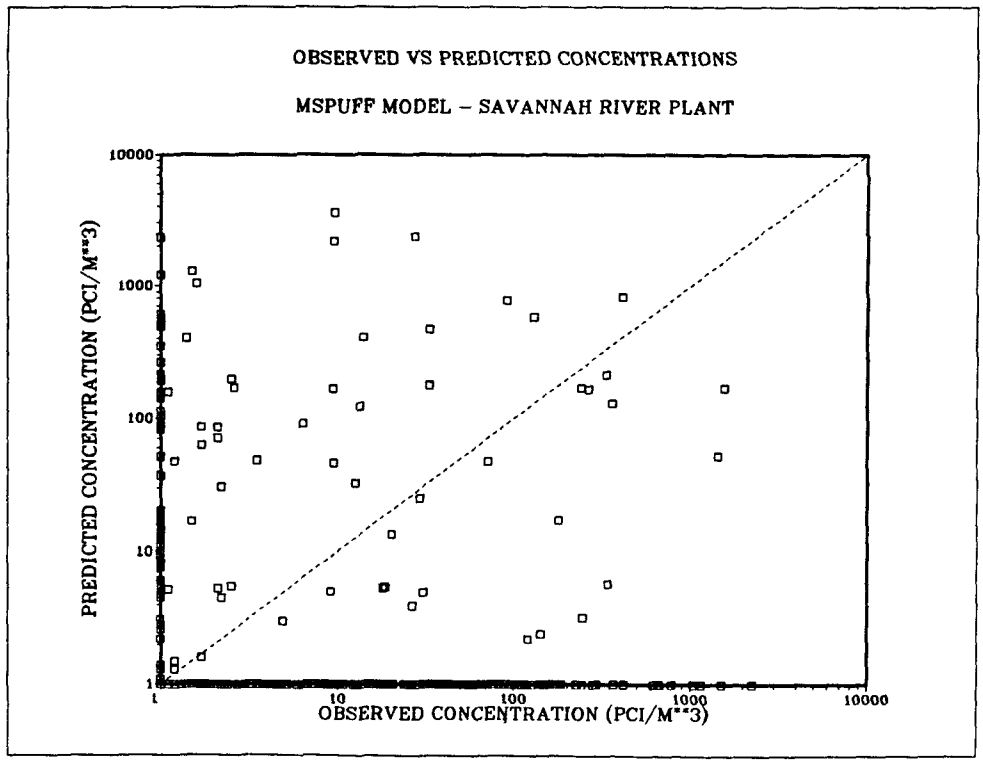

Figure E-152. Scatter plot of predicted and observed averaged concentrations at Savannah River Plant for MSPUFF ... points paired in space and time.

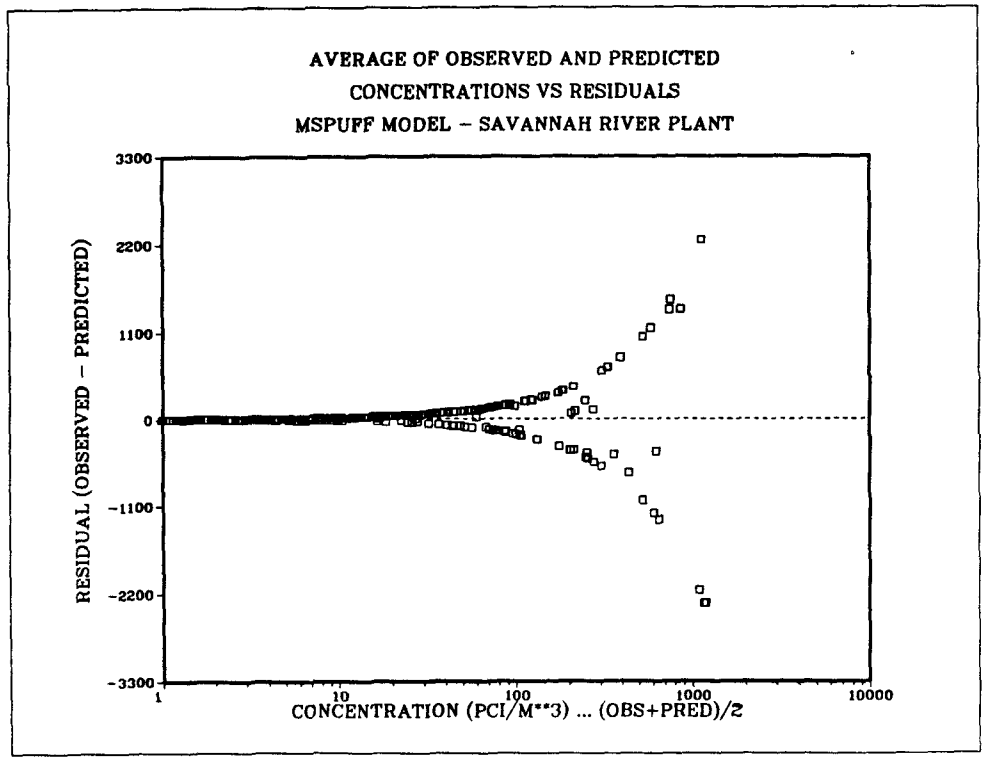

Figure E-153. Scatter plot of average of observed and predicted concentrations versus residuals at Savannah River Plant for MSPUFF ... points paired in space and time.

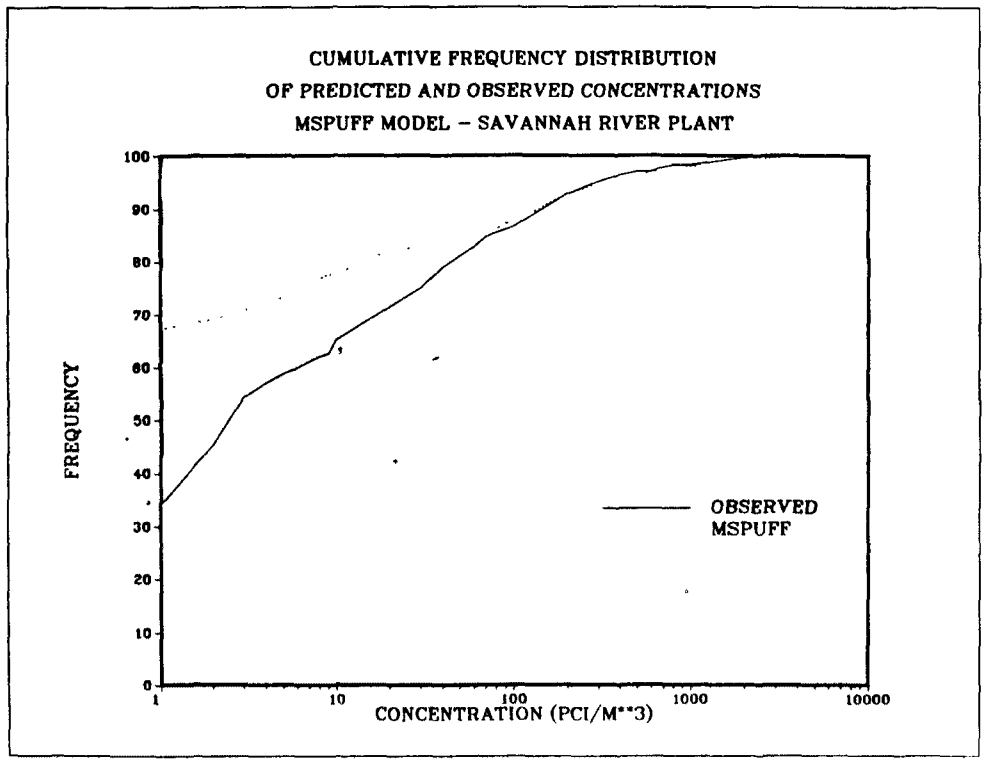

Figure E-154. Cumulative frequency distributions of MSPUFF predictions and observed concentrations at Savannah River Plant based on points paired in space and time.

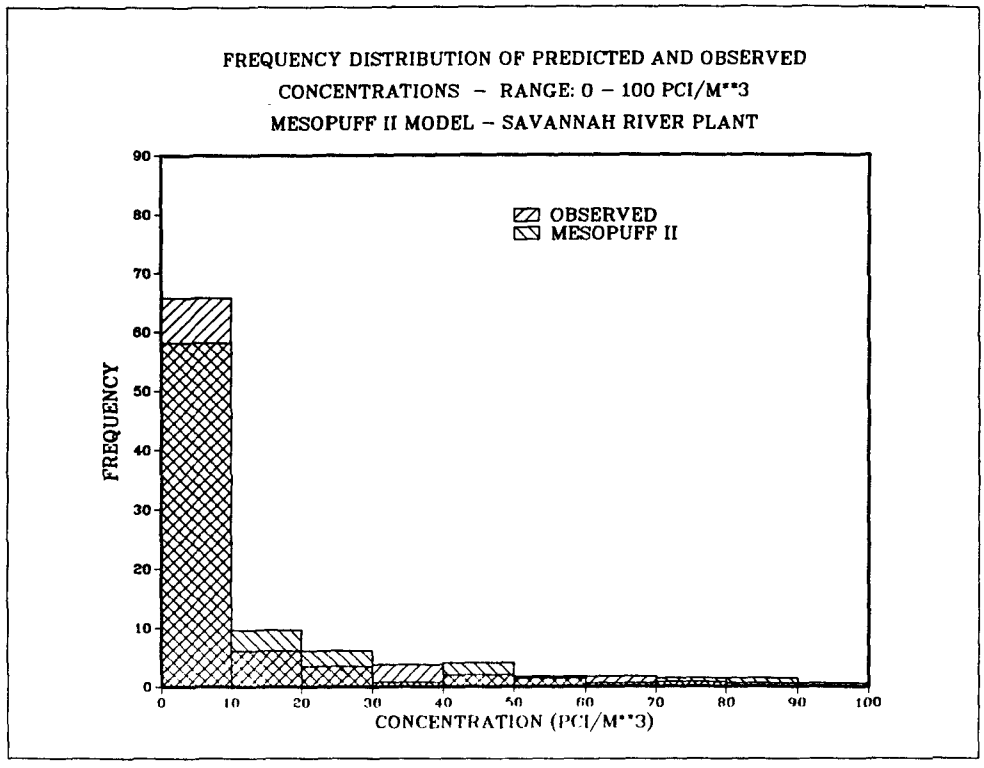

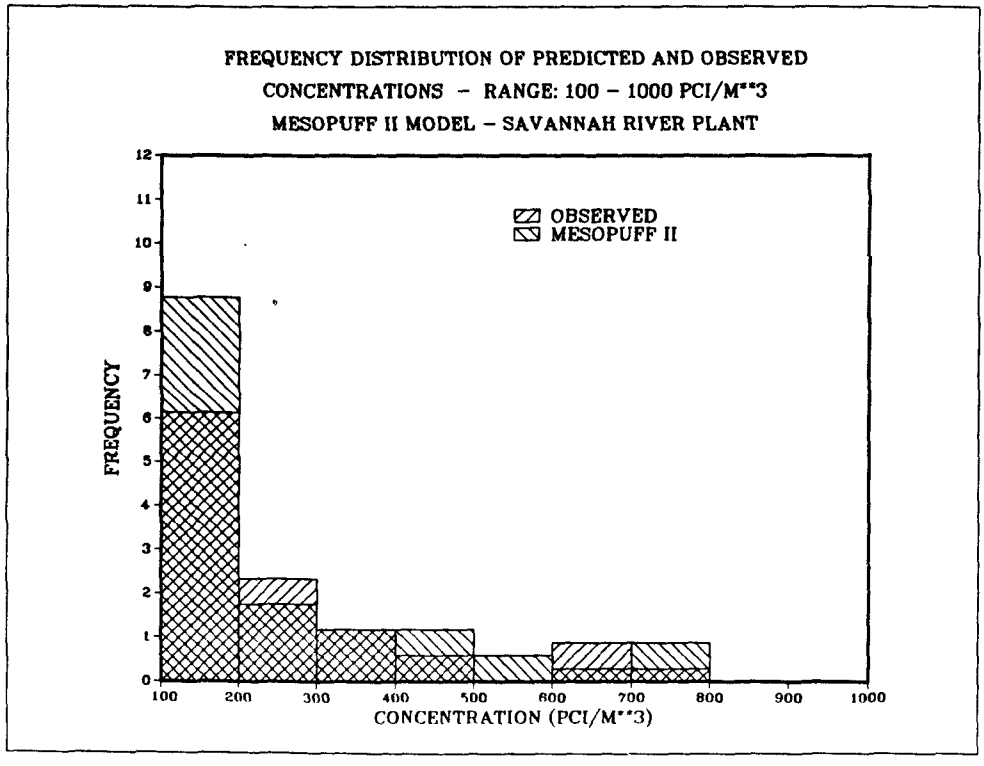

Figure E-155. Frequency distribution of predicted and observed concentrations at Savannah River Plant for MESOPUFF II based on points paired in space and time ...
(top) concentration range: 0 - 100 pCi/m^3,
(bottom) concentration range: 100 - 1000 pCi/m^3.

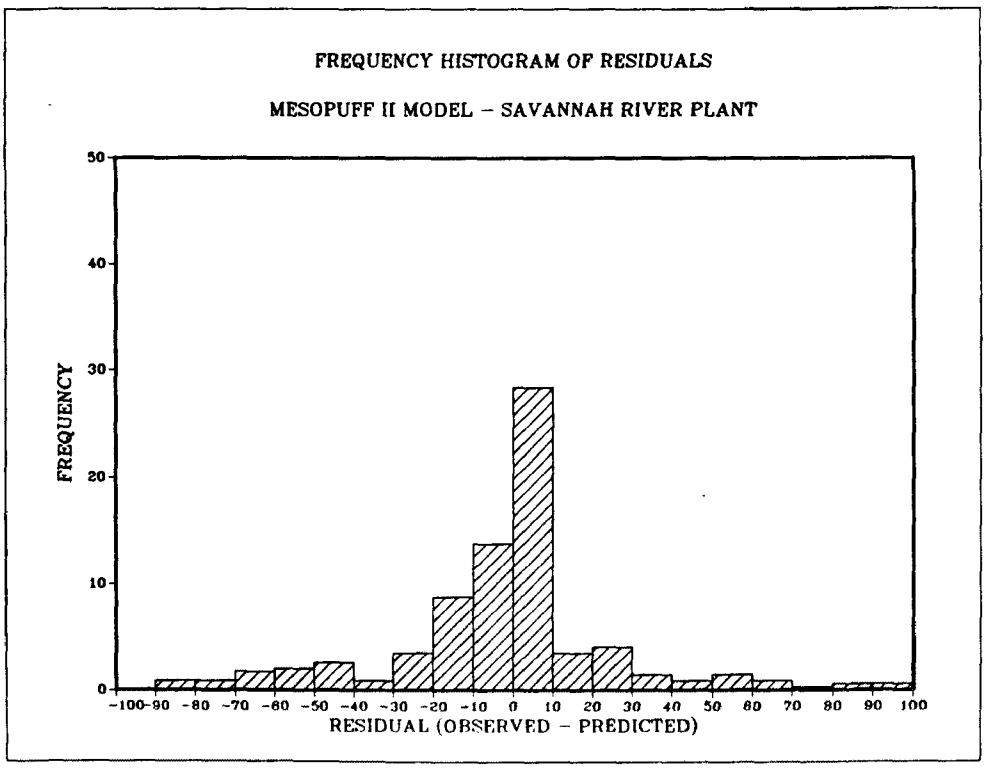

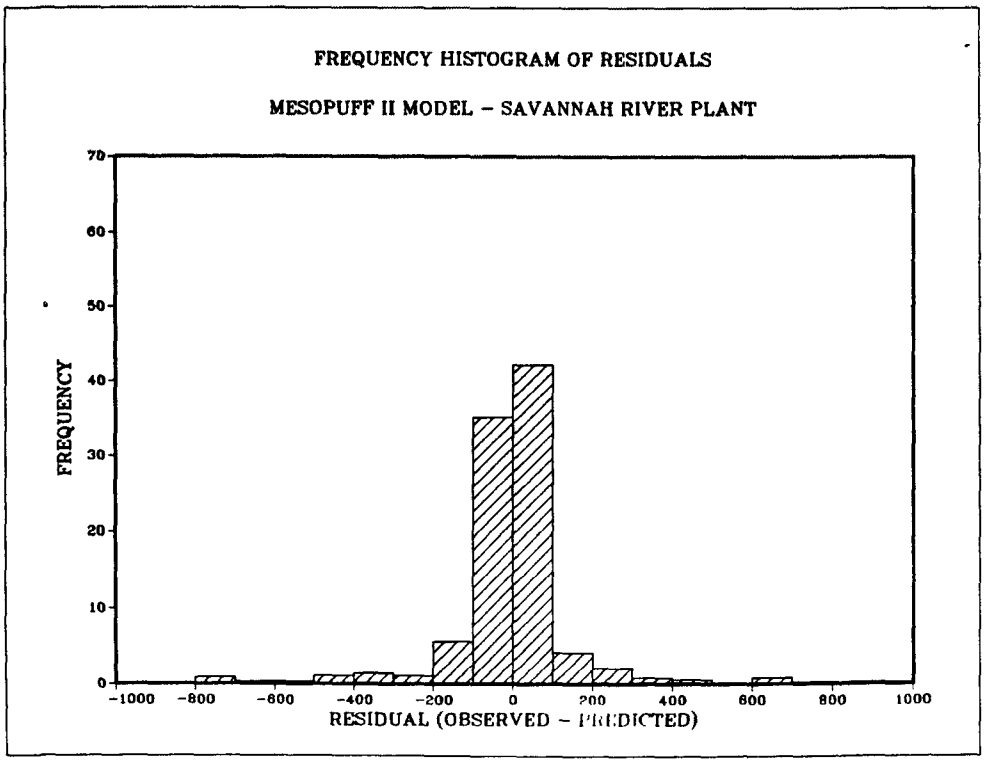

Figure E-156. Frequency distribution of residuals at Savannah River Plant for MESOPUFF II based on points paired in space and time ... (top) residual range: -100 to 100 pCi/m^3, (bottom) residual range: -1000 to 1000 pCi/m^3.

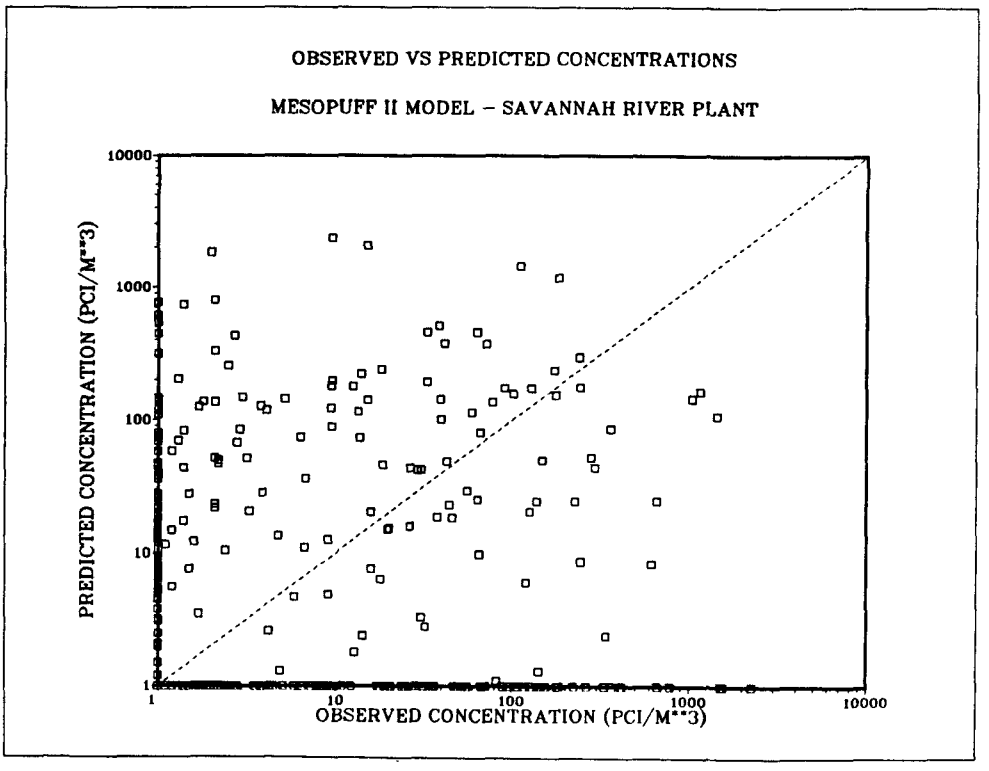

Figure E-157. Scatter plot of predicted and observed averaged concentrations at Savannah River Plant for MESOPUFF II ... points paired in space and time.

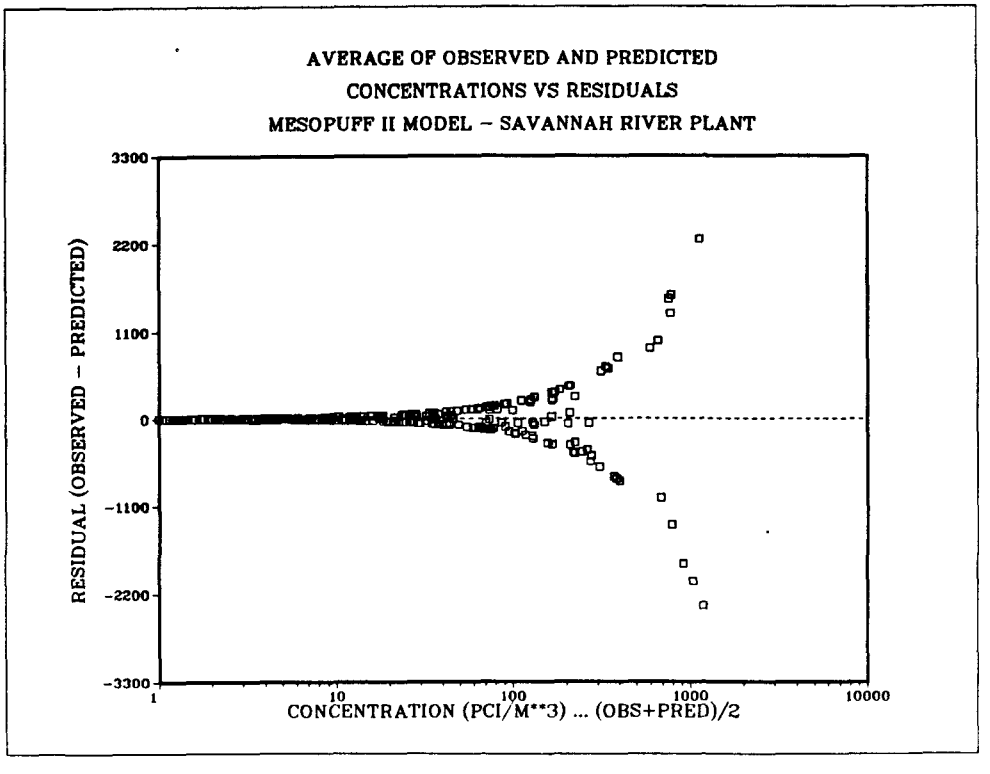

Figure E-158. Scatter plot of average of observed and predicted concentrations versus residuals at Savannah River Plant for MESOPUFF II ... points paired in space and time.

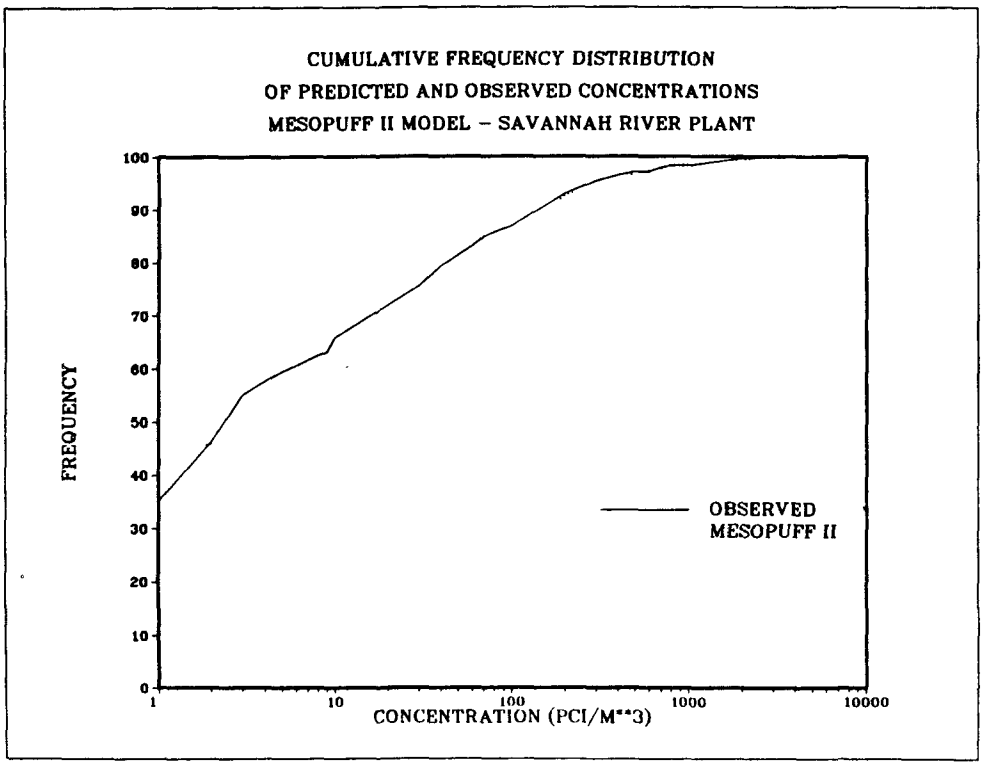

Figure E-159. Cumulative frequency distributions of MESOPUFF II predictions and observed concentrations at Savannah River Plant based on points paired in space and time.

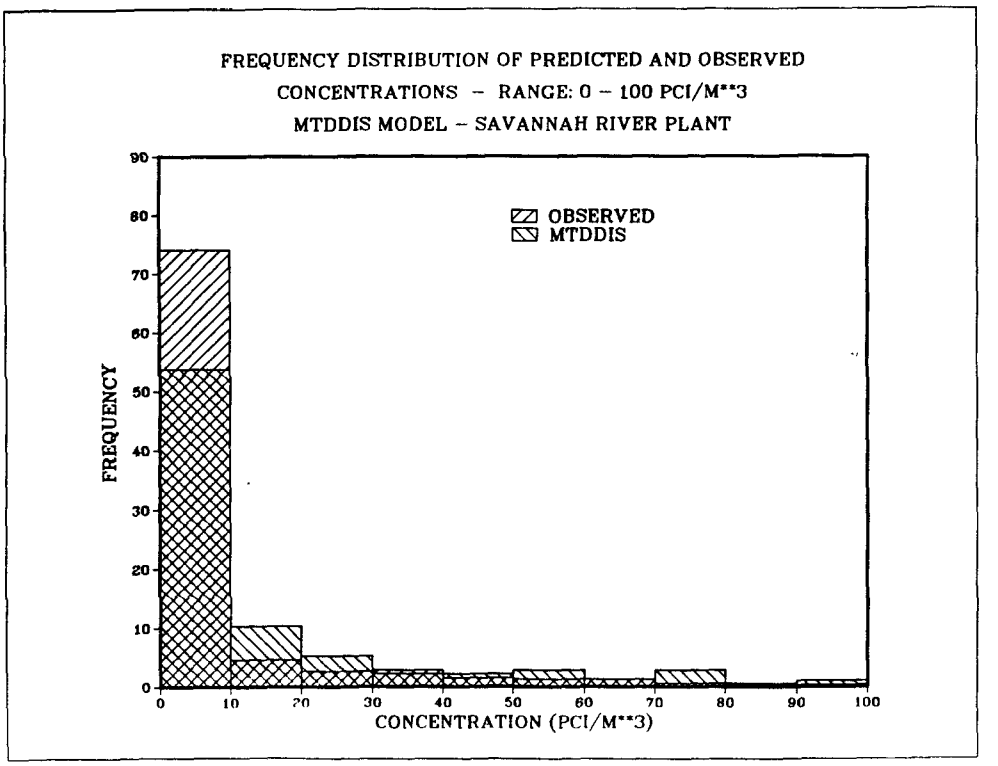

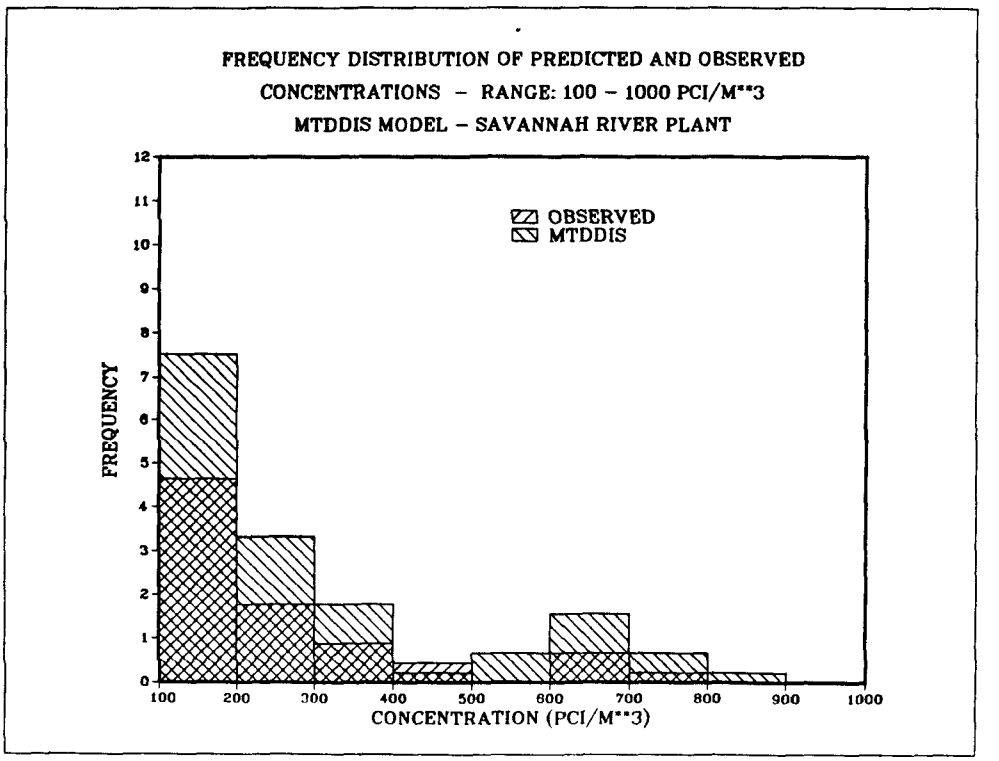

Figure E-160. Frequency distribution of predicted and observed concentrations at Savannah River Plant for MTDDIS based on points paired in space and time ...
(top) concentration range: 0 - 100 pCi/m^3,
(bottom) concentration range: 100 - 1000 pCi/m^3.

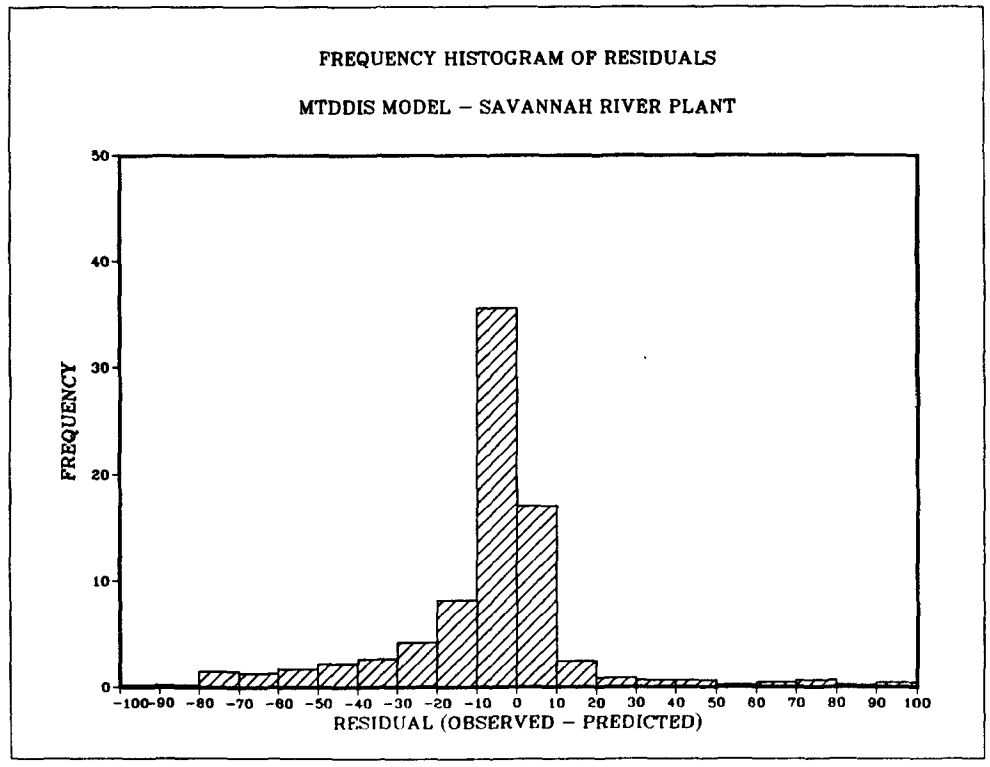

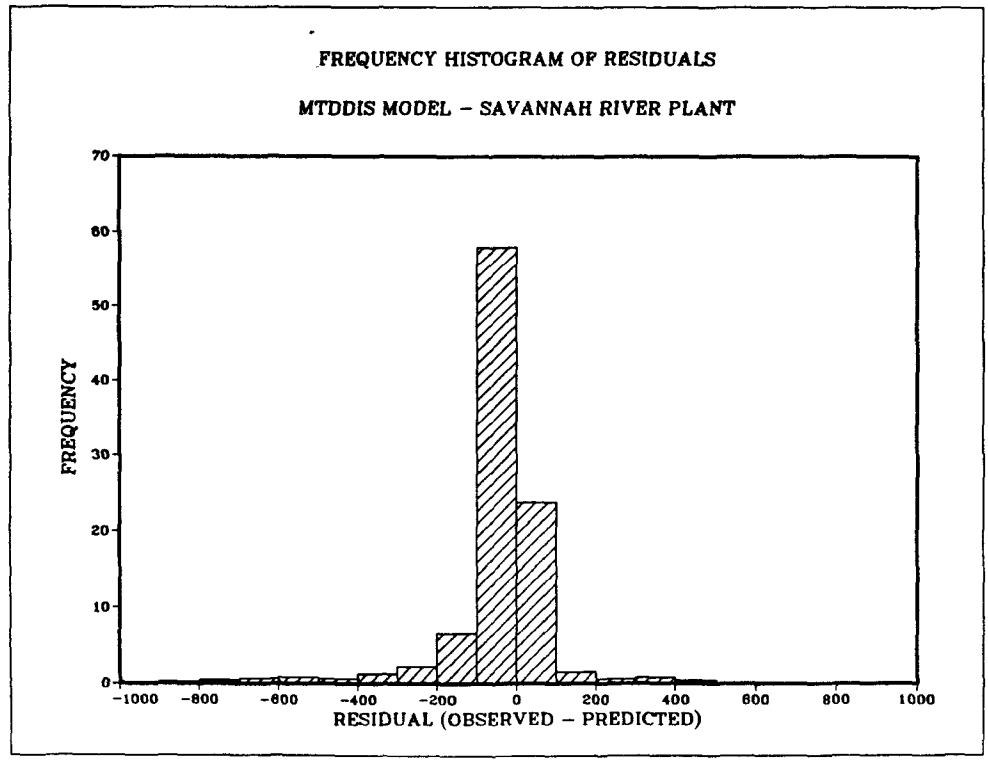

Figure E-161. Frequency distribution of residuals at Savannah River Plant for MTDDIS based on points paired in space and time ... (top) residual range: -100 to 100 pCi/m^3, (bottom) residual range: -1000 to 1000 pCi/m^3.

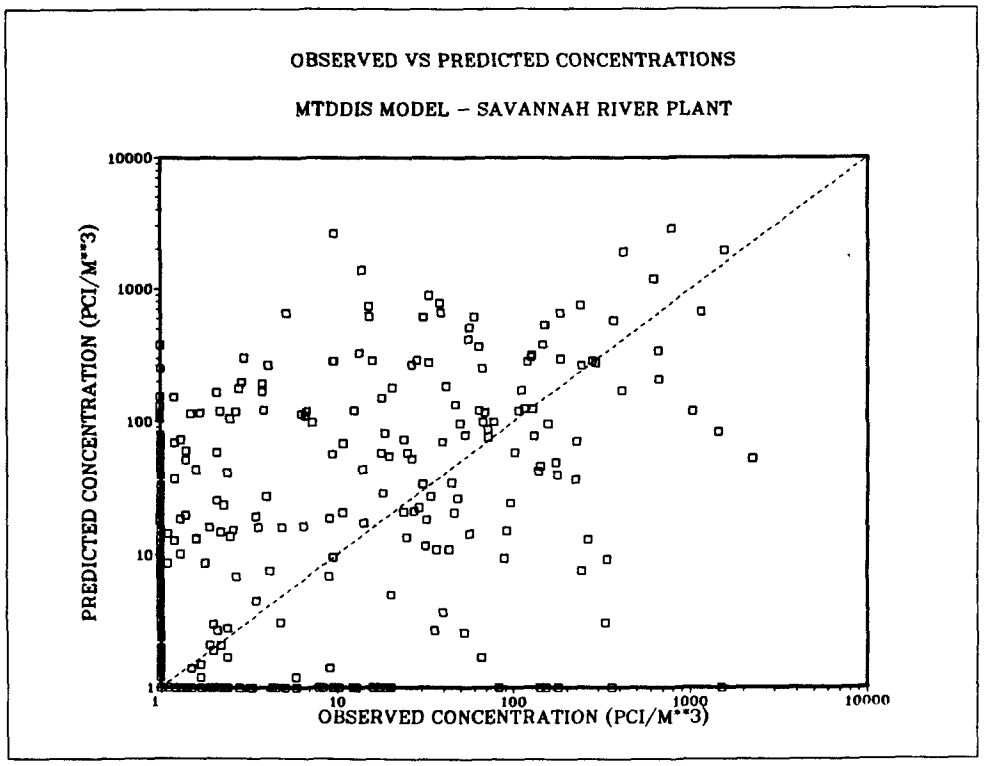

Figure E-162. Scatter plot of predicted and observed averaged concentrations at Savannah River Plant for MTDDIS ... points paired in space and time.

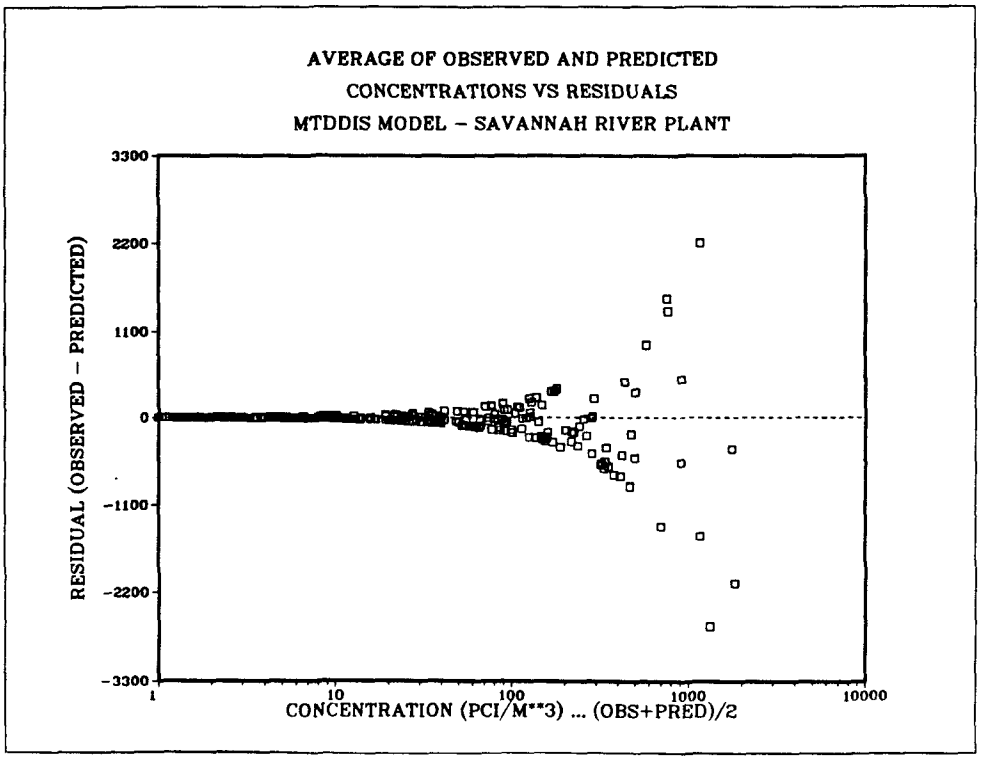

Figure E-163. Scatter plot of average of observed and predicted concentrations versus residuals at Savannah River Plant for MTDDIS ... points paired in space and time.

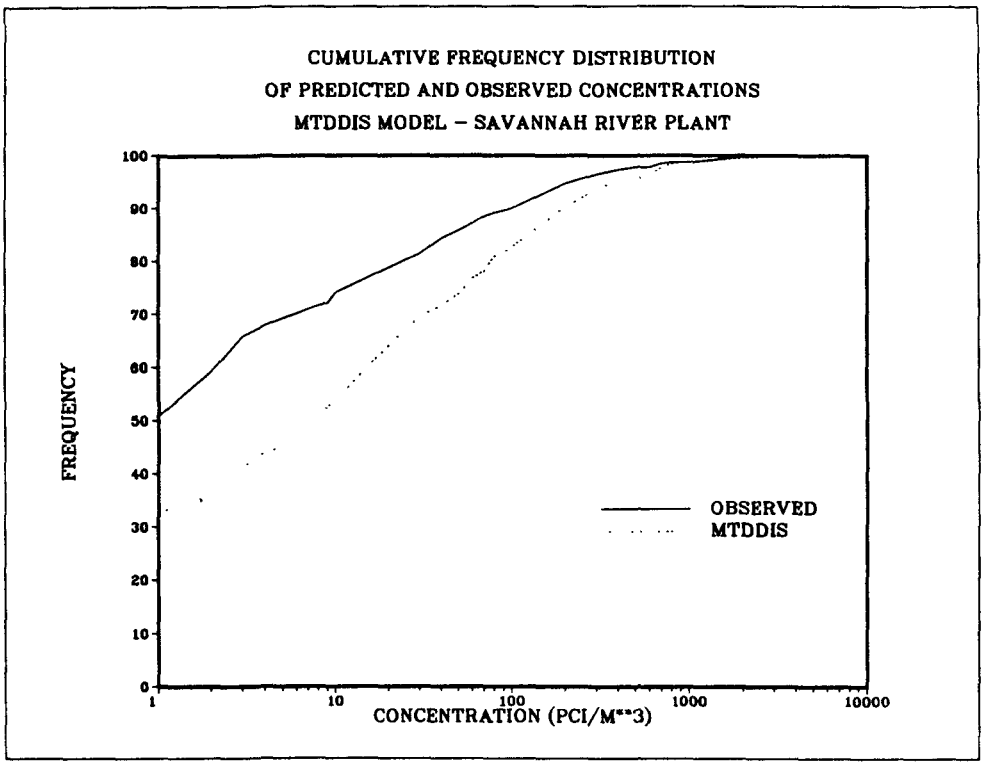

Figure E-164. Cumulative frequency distributions of MTDDIS predictions and observed concentrations at Savannah River Plant based on points paired in space and time.

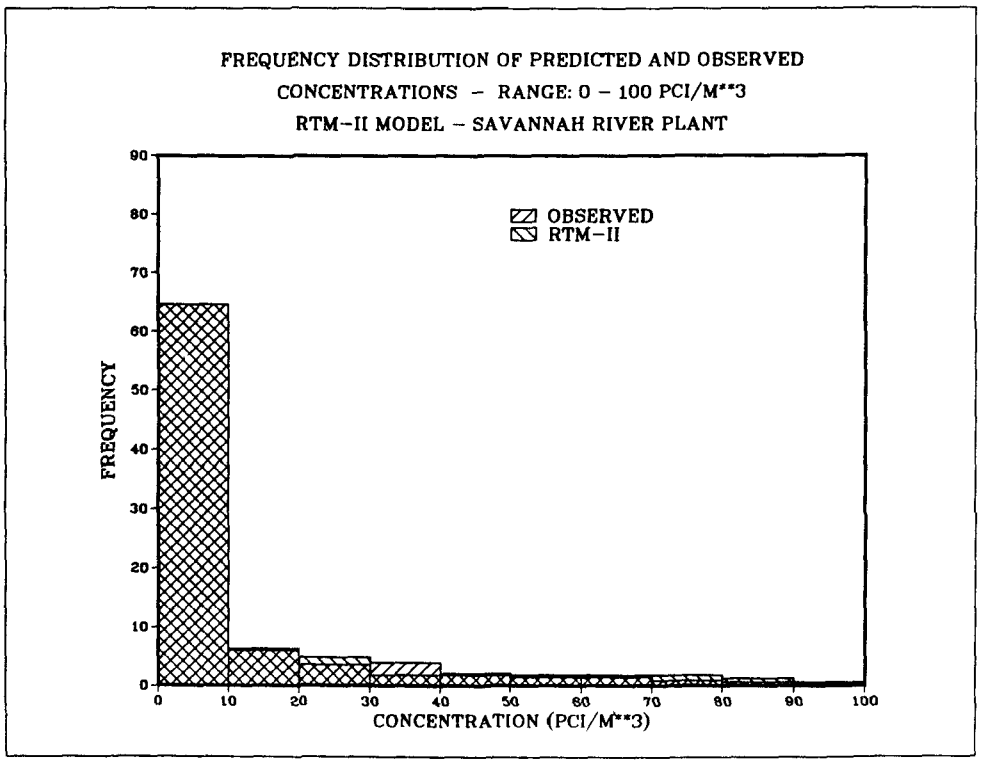

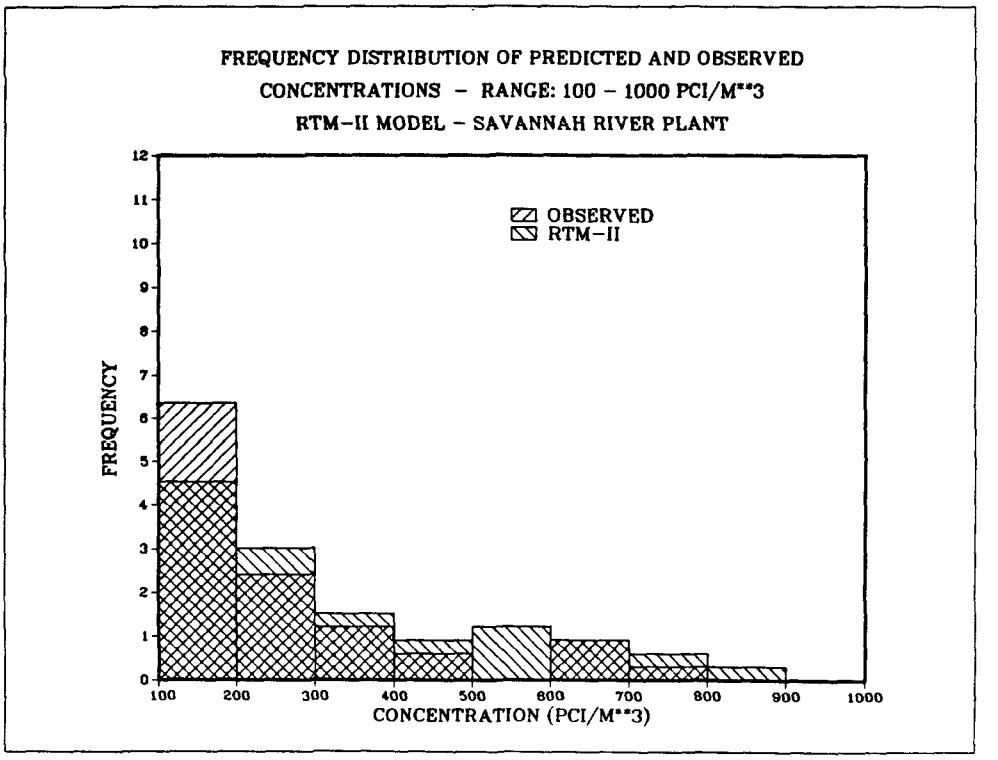

Figure E-165. Frequency distribution of predicted and observed concentrations at Savannah River Plant for RTM-II based on points paired in space and time ...
(top) concentration range: 0 - 100 pCi/m^3,
(bottom) concentration range: 100 - 1000 pCi/m^3.

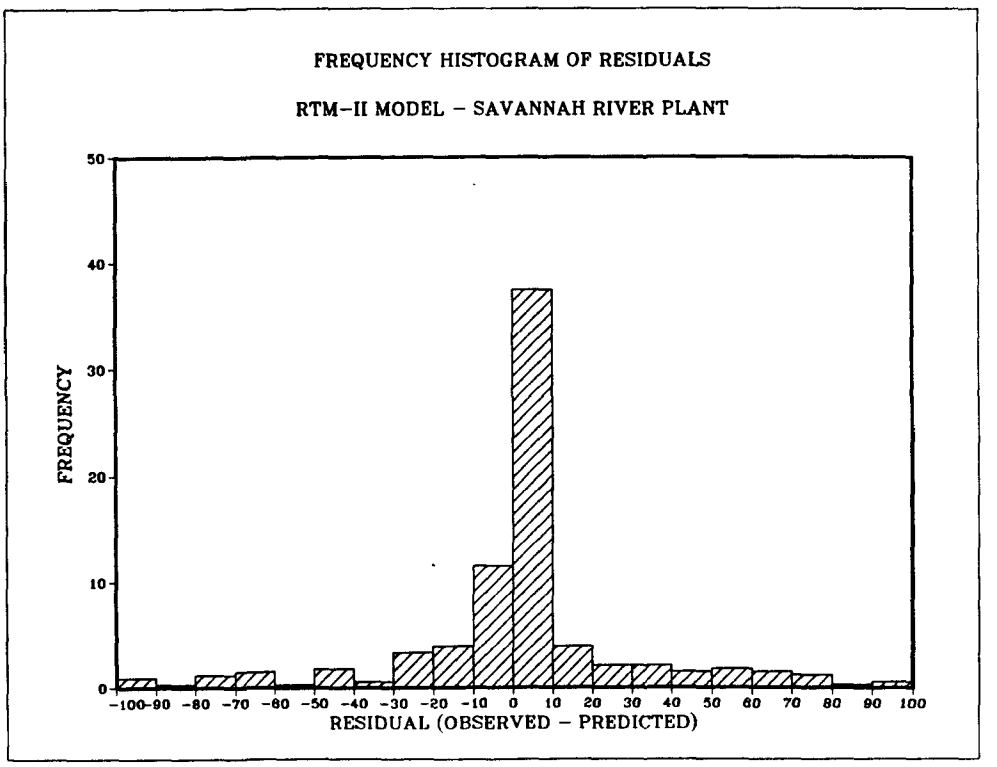

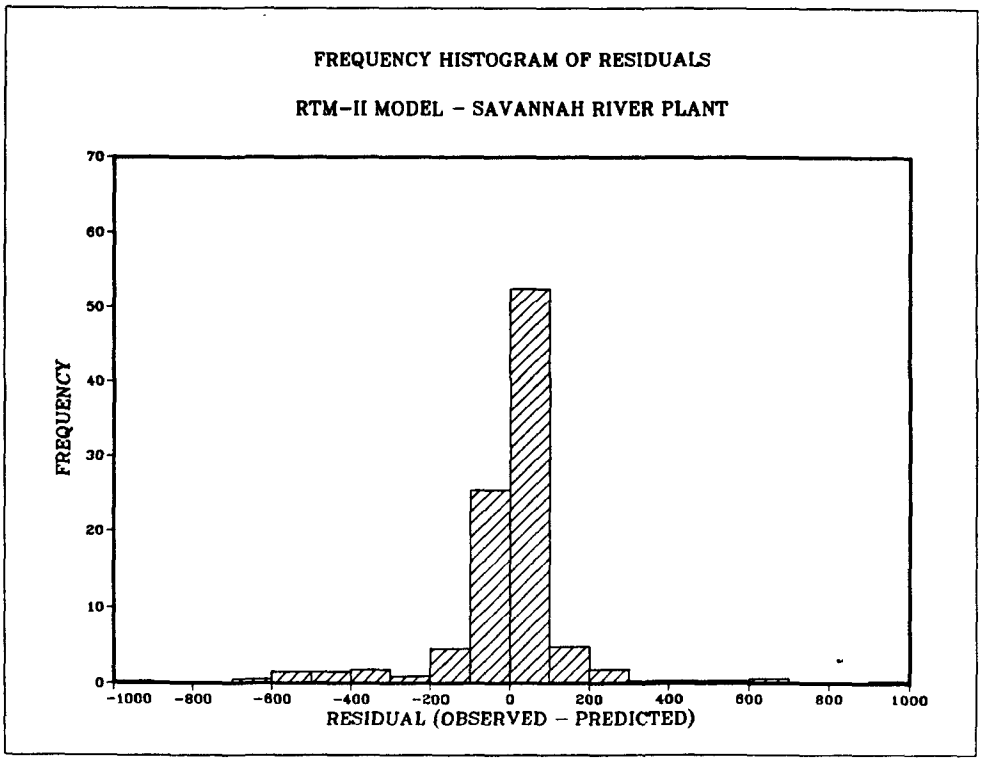

Figure E-166. Frequency distribution of residuals at Savannah River Plant for RTM-II based on points paired in space and time ... (top) residual range: -100 to 100 pCi/m^3, (bottom) residual range: -1000 to 1000 pCi/m^3.

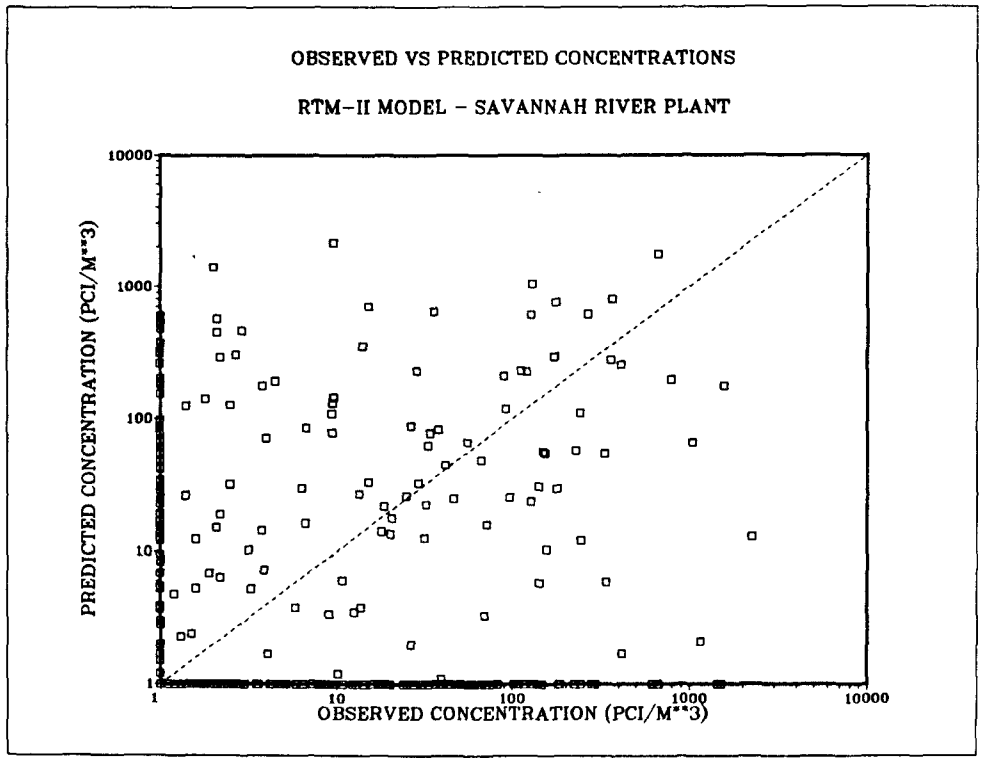

Figure E-167. Scatter plot of predicted and observed averaged concentrations at Savannah River Plant for RTM-II ... points paired in space and time.

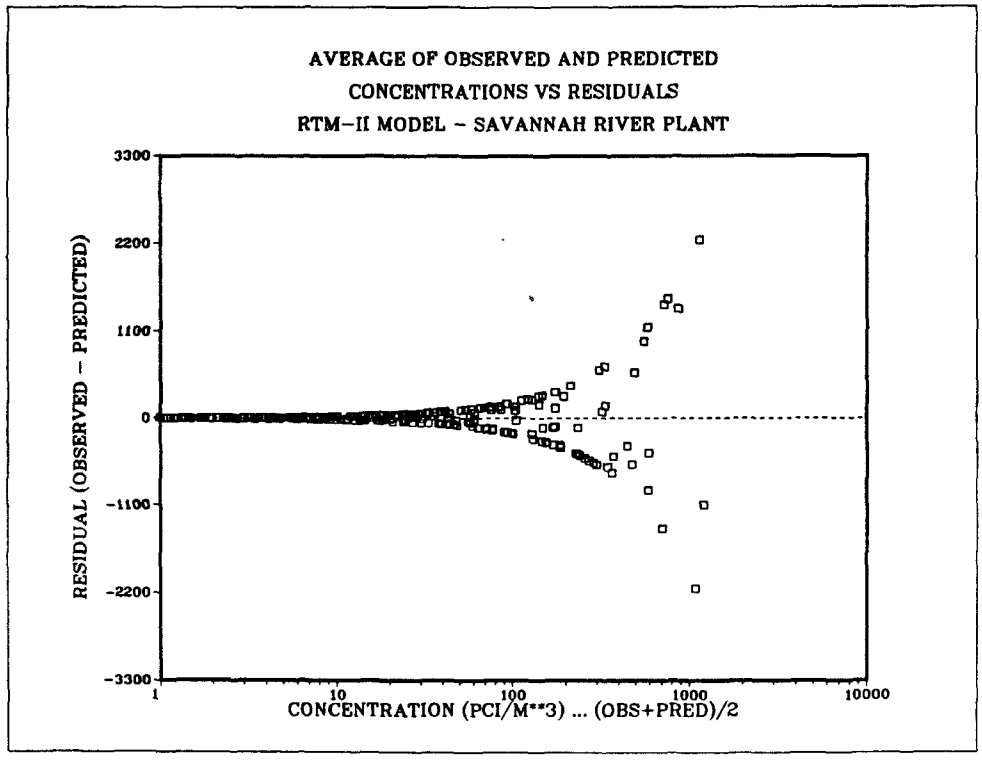

Figure E-168. Scatter plot of average of observed and predicted concentrations versus residuals at Savannah River Plant for RTM-II ... points paired in space and time.

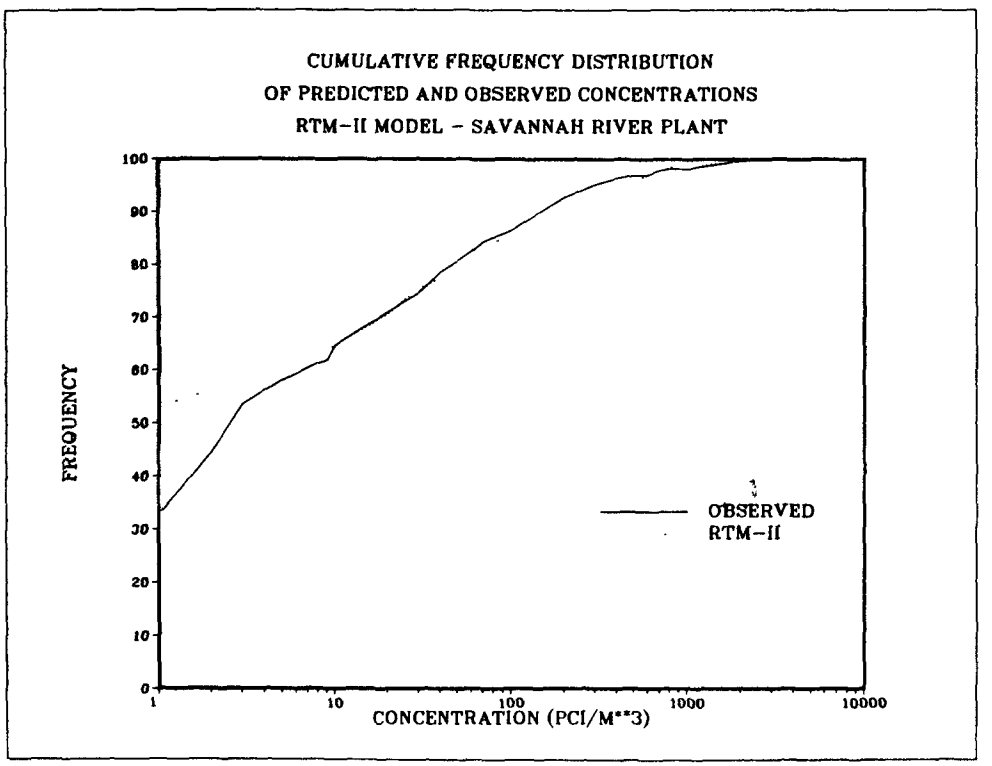

Figure E-169. Cumulative frequency distributions of RTM-II predictions and observed concentrations at Savannah River Plant based on points paired in space and time.

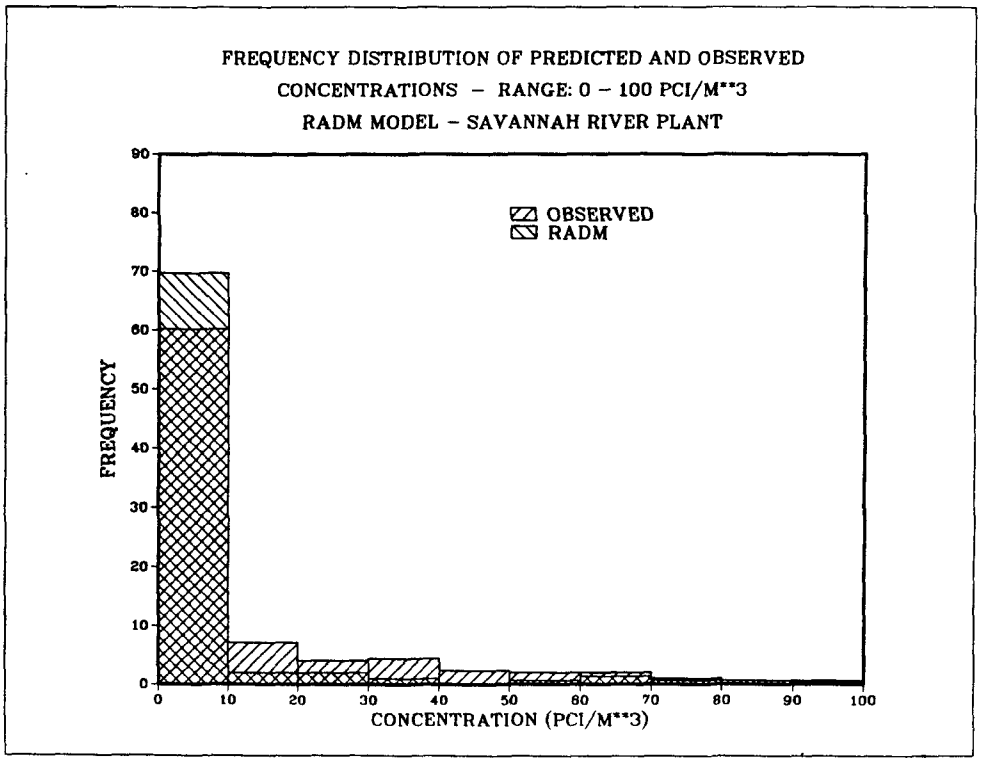

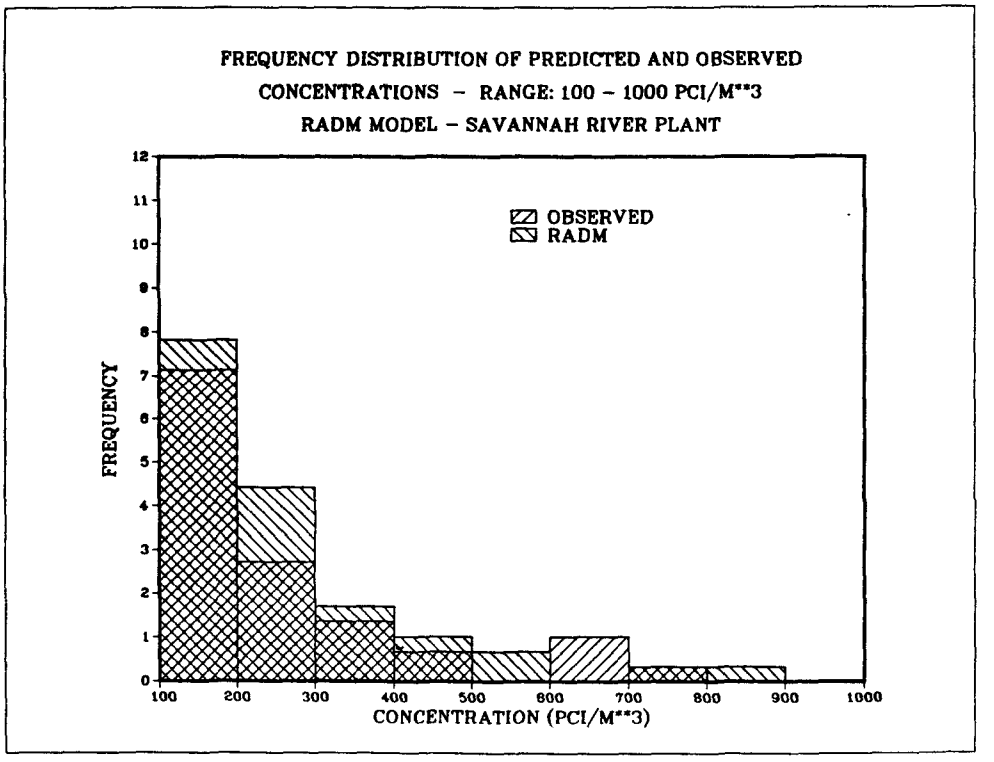

Figure E-170. Frequency distribution of predicted and observed concentrations at Savannah River Plant for RADM based on points paired in space and time ...
(top) concentration range: 0 - 100 pCi/m^3,
(bottom) concentration range: 100 - 1000 pCi/m^3.

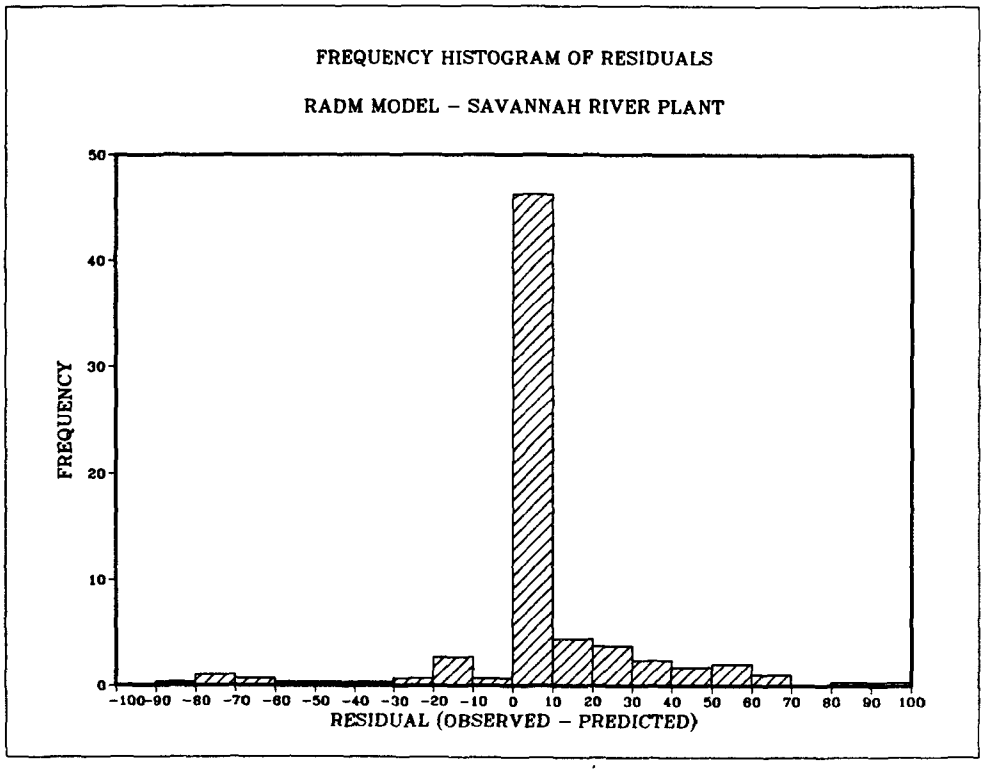

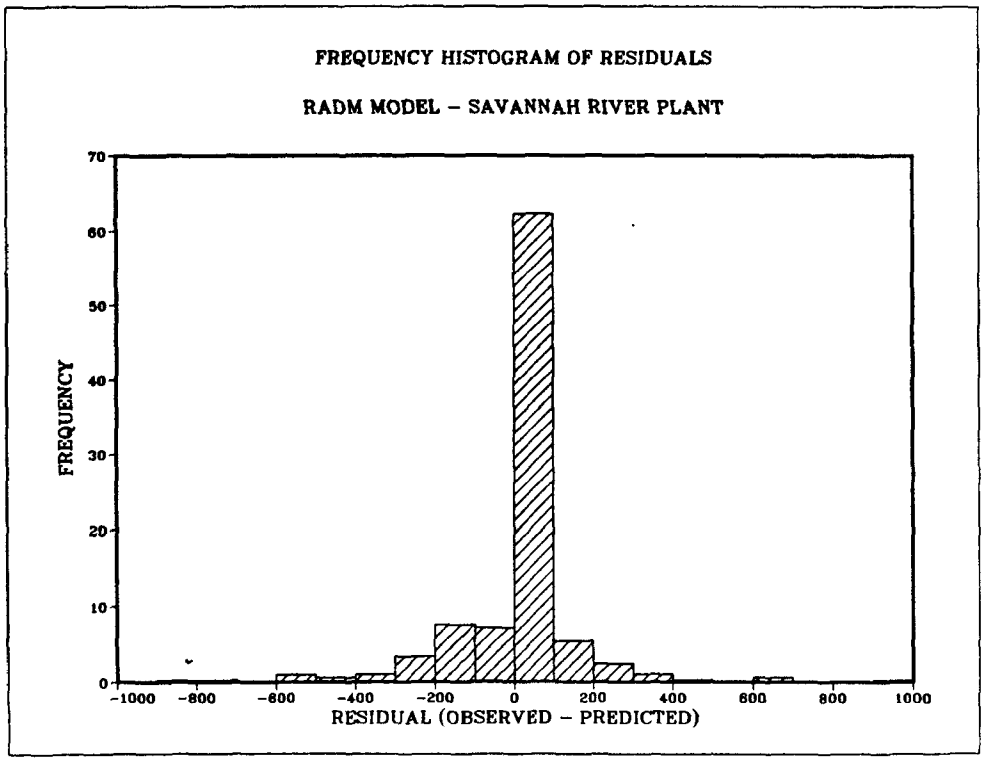

Figure E-171. Frequency distribution of residuals at Savannah River Plant for RADM based on points paired in space and time ...
(top) residual range: -100 to 100 pCi/m^3,
(bottom) residual range: -1000 to 1000 pCi/m^3.

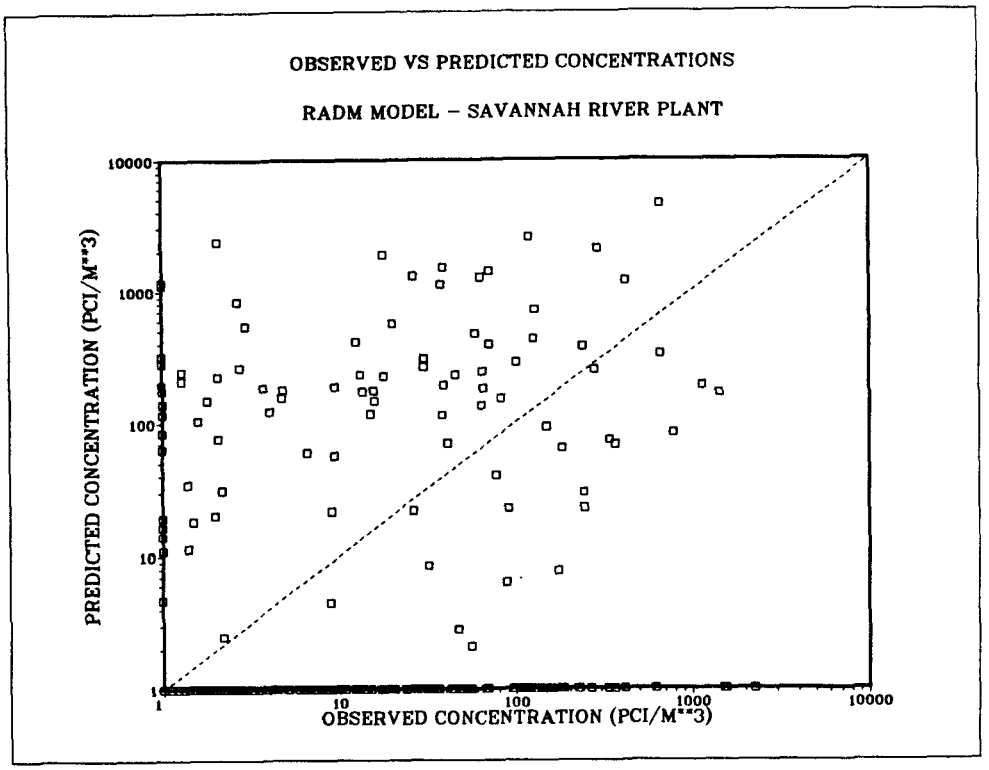

Figure E-172. Scatter plot of predicted and observed averaged concentrations at Savannah River Plant for RADM ... points paired in space and time.

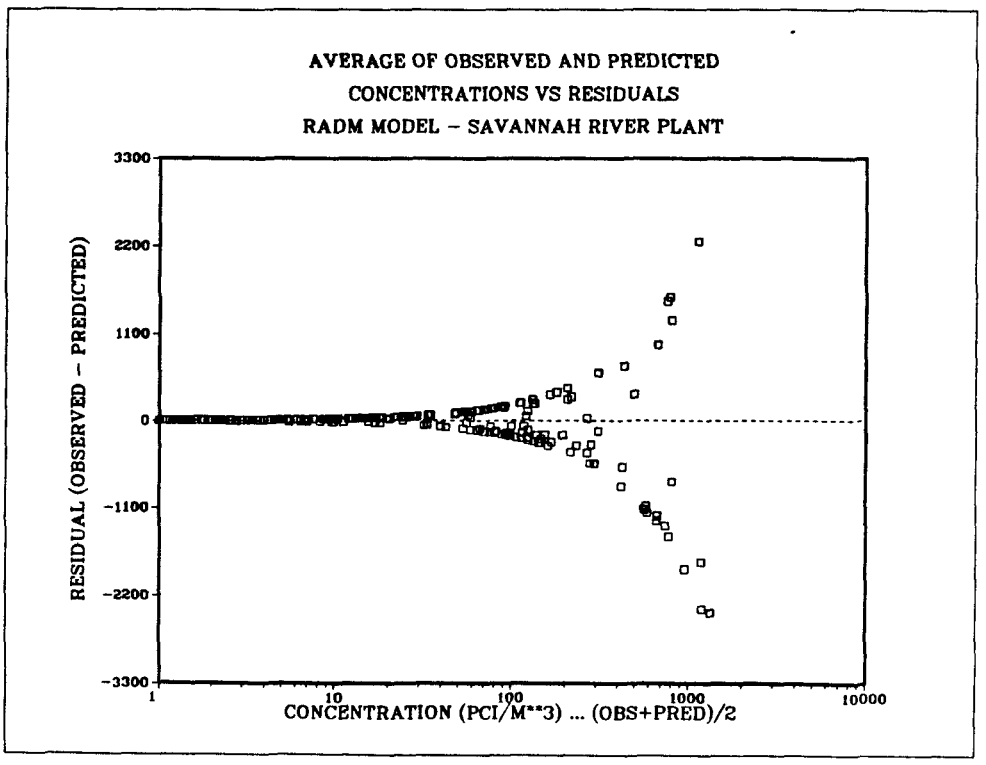

Figure E-173. Scatter plot of average of observed and predicted concentrations versus residuals at Savannah River Plant for RADM ... points paired in space and time.

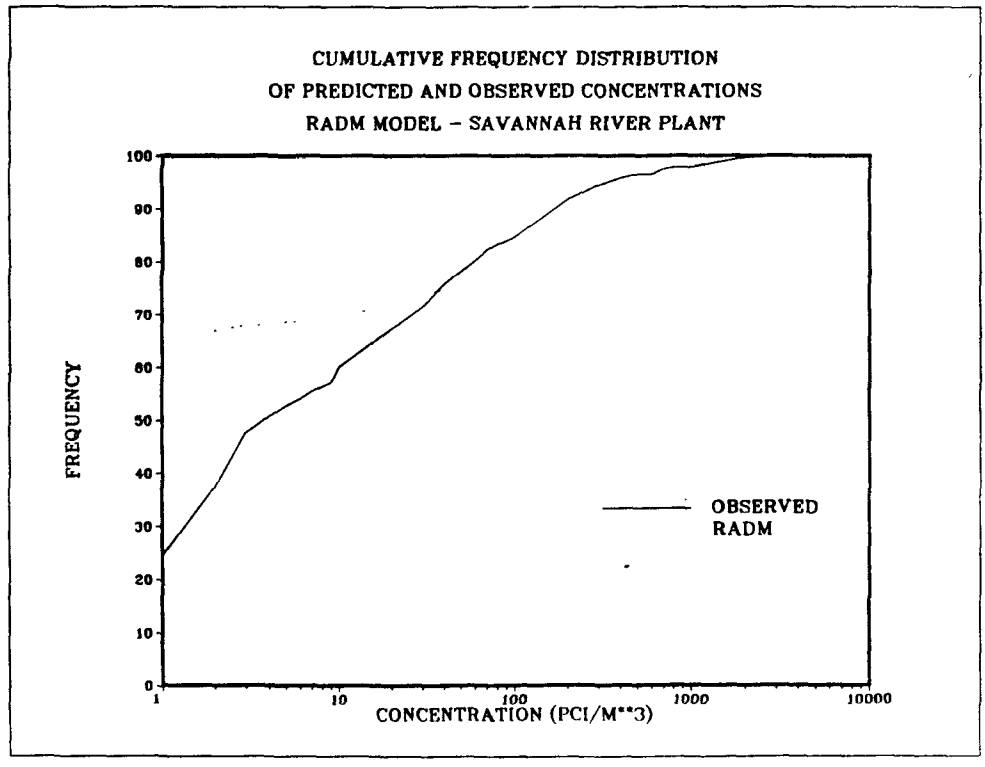

Figure E-174. Cumulative frequency distributions of RADM predictions and observed concentrations at Savannah River Plant based on points paired in space and time.

TECHNICAL REPORT DATA
(Please read Instructions on the reverse before completing)

1. REPORT NO. EPA-450/4-86-016b	2.	3. RECIPIENT'S ACCESSION NO.
4. TITLE AND SUBTITLE Evaluation of Short-Term Long-Range Transport Models--Volume II Appendices A-E		5. REPORT DATE date of preparation October 1986
		6. PERFORMING ORGANIZATION CODE
7. AUTHOR(S) A. J. Policastro, M. Wastag, L. Coke, R. A. Carhart, and W. E. Dunn		8. PERFORMING ORGANIZATION REPORT NO.
9. PERFORMING ORGANIZATION NAME AND ADDRESS Argonne National Lab. Argonne, Illinois 60439; U. of Illinois Chicago, Ill. 60680; U. of Illinois Urbana, Ill. 61801		10. PROGRAM ELEMENT NO. B24A2F
		11. CONTRACT/GRANT NO. DW89930807
12. SPONSORING AGENCY NAME AND ADDRESS U. S. Environmental Protection Agency Office of Air Quality Planning and Standards Research Triangle Park, NC 27711		13. TYPE OF REPORT AND PERIOD COVERED Final report
		14. SPONSORING AGENCY CODE
15. SUPPLEMENTARY NOTES		

16. ABSTRACT

Eight short-term long-range transport models (MESOPUFF, MESOPLUME, MSPUFF, MESOPUFF II, MTDDIS, ARRPA, RADM, and RTM-II) have been evaluated with field data from two data bases involving tracer releases. The primary quantitative means of evaluating model performance was the use of the American Meteorological Society statistics. Supplementary measures included the use of isopleth plots of ground-level concentrations, scatter plots, cumulative frequency distributions and frequency histograms of residuals. General features of the model performance included: (a) spatial offset of predicted and observed patterns, (b) a time difference between the arrival of the predicted and observed plumes at a particular receptor, and (c) an angular offset of as much as 20-45 degrees between predicted and observed plumes. The models also tended to underpredict horizontal spreading at ground level, along with overprediction of plume concentrations. As a result, predicted concentrations correlated poorly with concentrations observed at the same time and place. However, statistical comparisons of the peak values predicted by the models were significantly better. For example, the highest 25 averaged predictions and highest 25 averaged observations (unpaired in location and time) were within a factor or two of each other for six of the eight models tested (MESOPUFF, MESOPLUME, MESOPUFF II, MTDDIS, ARRPA, and RTM-II).

17. KEY WORDS AND DOCUMENT ANALYSIS

a. DESCRIPTORS	b. IDENTIFIERS/OPEN ENDED TERMS	c. COSATI Field/Group
Air Pollution Long Range Transport Models Meteorology Model Evaluation Statistics		

18. DISTRIBUTION STATEMENT Release unlimited	19. SECURITY CLASS *(This Report)* Unclassified	21. NO. OF PAGES 291
	20. SECURITY CLASS *(This page)* Unclassified	22. PRICE

EPA Form 2220-1 (Rev. 4-77) PREVIOUS EDITION IS OBSOLETE